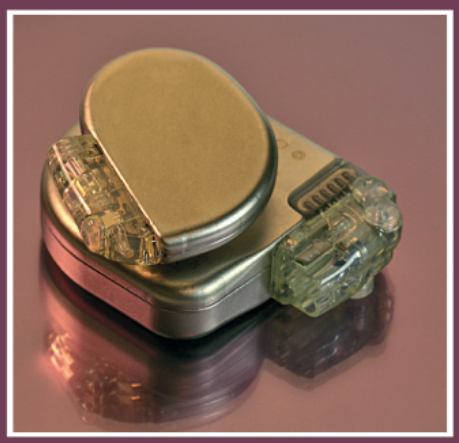
WOODHEAD PUBLISHING SERIES IN BIOMATERIALS



Joining and assembly of medical materials and devices

Edited by Y. (Norman) Zhou and Mark D. Breyen

WP
WOODHEAD PUBLISHING

Joining and assembly of medical materials and devices

© Woodhead Publishing Limited, 2013

Related titles:

Durability and reliability of medical polymers
(ISBN 978-1-84569-929-1)

Coatings for biomedical applications
(ISBN 978-1-84569-568-2)

Surface modification of biomaterials: Methods analysis and applications
(ISBN 978-1-84569-640-5)

Details of these books and a complete list of titles from Woodhead Publishing can be obtained by:

- visiting our web site at www.woodheadpublishing.com
- contacting Customer Services (e-mail: sales@woodheadpublishing.com; fax: +44 (0) 1223 832819; tel.: +44 (0) 1223 499140 ext. 130; address: Woodhead Publishing Limited, 80, High Street, Sawston, Cambridge CB22 3HJ, UK)
- in North America, contacting our US office (e-mail: usmarketing@woodheadpublishing.com; tel.: (215) 928 9112; address: Woodhead Publishing, 1518 Walnut Street, Suite 1100, Philadelphia, PA 19102-3406, USA)

If you would like e-versions of our content, please visit our online platform: www.woodheadpublishingonline.com. Please recommend it to your librarian so that everyone in your institution can benefit from the wealth of content on the site.

We are always happy to receive suggestions for new books from potential editors. To enquire about contributing to our Biomaterials series, please send your name, contact address and details of the topic/s you are interested in to laura.overend@woodheadpublishing.com. We look forward to hearing from you.

The team responsible for publishing this book:

Commissioning Editor: Laura Overend
Publications Coordinator: Steven Mathews
Project Editor: Cathryn Freear
Editorial and Production Manager: Mary Campbell
Production Editor: Mandy Kingsmill
Project Manager: Newgen Knowledge Works Pvt Ltd
Copyeditor: Newgen Knowledge Works Pvt Ltd
Proofreader: Newgen Knowledge Works Pvt Ltd
Cover Designer: Terry Callanan

© Woodhead Publishing Limited, 2013

Woodhead Publishing Series in Biomaterials: Number 54

Joining and assembly of medical materials and devices

Edited by
Y. (Norman) Zhou and
Mark D. Breyen



Oxford Cambridge Philadelphia New Delhi

© Woodhead Publishing Limited, 2013

Published by Woodhead Publishing Limited,
80 High Street, Sawston, Cambridge CB22 3HJ, UK
www.woodheadpublishing.com
www.woodheadpublishingonline.com

Woodhead Publishing, 1518 Walnut Street, Suite 1100, Philadelphia,
PA 19102–3406, USA

Woodhead Publishing India Private Limited, 303, Vardaan House, 7/28 Ansari Road,
Daryaganj, New Delhi - 110002, India
www.woodheadpublishingindia.com

First published 2013, Woodhead Publishing Limited
© Woodhead Publishing Limited, 2013. Note: the publisher has made every effort to ensure that permission for copyright material has been obtained by authors wishing to use such material. The authors and the publisher will be glad to hear from any copyright holder it has not been possible to contact.
The authors have asserted their moral rights.

This book contains information obtained from authentic and highly regarded sources. Reprinted material is quoted with permission, and sources are indicated. Reasonable efforts have been made to publish reliable data and information, but the authors and the publisher cannot assume responsibility for the validity of all materials. Neither the authors nor the publisher, nor anyone else associated with this publication, shall be liable for any loss, damage or liability directly or indirectly caused or alleged to be caused by this book.

Neither this book nor any part may be reproduced or transmitted in any form or by any means, electronic or mechanical, including photocopying, microfilming and recording, or by any information storage or retrieval system, without permission in writing from Woodhead Publishing Limited.

The consent of Woodhead Publishing Limited does not extend to copying for general distribution, for promotion, for creating new works, or for resale. Specific permission must be obtained in writing from Woodhead Publishing Limited for such copying.

Trademark notice: Product or corporate names may be trademarks or registered trademarks, and are used only for identification and explanation, without intent to infringe.

British Library Cataloguing in Publication Data
A catalogue record for this book is available from the British Library.

Library of Congress Control Number: 2013936018

ISBN 978-1-84569-577-4 (print)
ISBN 978-0-85709-642-5 (online)
ISSN 2049-9485 Woodhead Publishing Series in Biomaterials (print)
ISSN 2049-9493 Woodhead Publishing Series in Biomaterials (online)

The publisher's policy is to use permanent paper from mills that operate a sustainable forestry policy, and which has been manufactured from pulp which is processed using acid-free and elemental chlorine-free practices. Furthermore, the publisher ensures that the text paper and cover board used have met acceptable environmental accreditation standards.

Typeset by Newgen Knowledge Works Pvt Ltd, India
Printed by MPG Printgroup, UK

© Woodhead Publishing Limited, 2013

Contents

Contributor contact details *xiii*
Woodhead Publishing Series in Biomaterials *xvii*

Part I Fundamentals of joining and assembly in medical materials and devices 1

1 Introduction to medical materials and devices 3
J. J. Ramsden, Collegium Basilea, Switzerland

1.1 Introduction 3
1.2 The anatomy of interaction 10
1.3 Materials for drug delivery 20
1.4 The metrology of biocompatibility 21
1.5 Conclusion 23
1.6 Future trends 24
1.7 Sources of further information 24
1.8 References 24

2 Introduction to joining methods in medical applications 28
L. Quintino, Technical University of Lisbon, Portugal

2.1 Introduction 28
2.2 Welding processes 33
2.3 Adhesive bonding 41
2.4 Examples of applications 43
2.5 References 45

© Woodhead Publishing Limited, 2013

3 Microwelding methods in medical components and devices 47
K. J. Ely, GlaxoSmithKline Corporation, USA, P. Hall, Boston Scientic Corporation, USA and Y. Zhou, University of Waterloo, Canada

3.1 Introduction 47
3.2 Materials challenges 49
3.3 Medical components and devices 56
3.4 Joint design and process selection 65
3.5 Testing and verification 73
3.6 Conclusion and future trends 76
3.7 References 77

4 The effects of sterilization on medical materials and welded devices 79
W. J. Rogers, Consultant, USA

4.1 Introduction to sterilization 79
4.2 Sterilization methods 80
4.3 The effects of sterilizing on different materials 96
4.4 The effects of sterilizing on welded joints 121
4.5 Selecting a suitable sterilization method 126
4.6 Conclusions 127
4.7 Sources of further information 128
4.8 References 129

Part II Joining and assembly of medical metals 131

5 Micro-welding of shape-memory alloys 133
M. I. Khan, Smarter Alloys, Canada and Y. Zhou, University of Waterloo, Canada

5.1 Introduction 133
5.2 Fundamentals of Nitinol shape-memory alloys 134
5.3 Micro-welding of NiTi 138
5.4 Future trends 151
5.5 Conclusion 152
5.6 References 152

© Woodhead Publishing Limited, 2013

6 Joining of platinum (Pt) alloy wires to stainless steel wires for electronic medical devices 154
A. Pequegnat and Y. Zhou, University of Waterloo, Canada

6.1 Introduction 154
6.2 Material properties 155
6.3 Material challenges in joining 156
6.4 The crossed-wire joint 159
6.5 Joining processes 162
6.6 Future trends 174
6.7 Conclusions 174
6.8 References 175

7 Evaluating the corrosion performance of metal medical device welds 178
S. C. Kelley and D. F. Untereker, Medtronic, Inc., USA

7.1 Introduction 178
7.2 Measurements of corrosion 183
7.3 Direct measurements of corrosion current 188
7.4 Considerations when gathering corrosion data 196
7.5 Test sample preparation 198
7.6 Instrumentation and equipment 201
7.7 Interpretation of data 204
7.8 Mitigations for weld corrosion 205
7.9 Future trends 206
7.10 Sources of further information 207
7.11 References 207

8 Laser hermetic welding of implantable medical devices 211
J. Xie, Advanced Bionics, USA

8.1 Introduction 211
8.2 Hermetic-sealing techniques 212
8.3 Laser conduction welding 214
8.4 Focused laser beams 222
8.5 Laser welding parameters 225
8.6 Requirements for laser hermetic welds 228
8.7 Conclusion and future trends 233
8.8 References 235

© Woodhead Publishing Limited, 2013

9 Validating hermeticity in welded metallic implantable medical devices 236
K. J. Ely, GlaxoSmithKline Corporation, USA

9.1 Introduction 236
9.2 The physics of leak rates 237
9.3 Measurement of leak rates – testing and verification 249
9.4 Determining leak rate based on helium content 252
9.5 References 257

Part III Joining and assembly of medical plastics 259

10 Overview of welding methods for medical plastics 261
H. J. Yeh, Amgen Inc., USA

10.1 Introduction 261
10.2 Fundamental processes of plastics welding 263
10.3 Medical plastics and weldability 267
10.4 Part and joint design 269
10.5 Processes with external heating 271
10.6 Processes with internal heating 279
10.7 Processes with implant welding 283
10.8 Potential impacts from other manufacturing processes 286
10.9 Special applications for welding of medical plastics 287
10.10 References 295

11 Ultrasonic welding of medical plastics 296
H. J. Yeh, Amgen Inc., USA

11.1 Introduction 296
11.2 Ultrasonic-welding processes fundamentals 297
11.3 Ultrasonic-welding process parameters and control 302
11.4 Weldability 306
11.5 Horn design 309
11.6 Part and joint design 313
11.7 Process optimization 317
11.8 Other specific applications 318
11.9 Troubleshooting 320
11.10 Advantages and limitations 321
11.11 References 322

© Woodhead Publishing Limited, 2013

12 Radio frequency (RF)/dielectric welding of medical plastics 323
H. J. Yeh, Amgen Inc., USA

12.1 Introduction 323
12.2 Dielectric heating fundamentals 324
12.3 Dielectric welding/sealing process description and process parameters 327
12.4 Key factors affecting the sealing process and seal quality 333
12.5 Weldability 338
12.6 Testing approaches for seals and the dielectric sealing process 338
12.7 RF welding process advantages, limitations and future trends 341
12.8 Reference 343

13 Transmission laser welding strategies for medical plastics 344
I. Jones, TWI Ltd, UK

13.1 Introduction 344
13.2 Advantages and limitations of laser welding 344
13.3 Process description 345
13.4 Main welding parameters and effects 349
13.5 Forms of equipment 350
13.6 Weldable materials 356
13.7 Joint designs 359
13.8 Monitoring and quality control 360
13.9 Applications 360
13.10 References 368

14 Bonding strategies and adhesives for joining medical device components 370
K. Chaffin, C. Taylor and T. Grailer, Medtronic, Inc., USA

14.1 Introduction 370
14.2 Designing a joint with adhesive 371
14.3 Mechanisms of adhesion 388
14.4 Adhesion promotion 395
14.5 Types of adhesives used in medical devices 397
14.6 Conclusion 401
14.7 Sources of further information and advice 402
14.8 References 402

© Woodhead Publishing Limited, 2013

Part IV Joining and assembly of biomaterial and tissue implants 405

15 Advanced metal–ceramic joining techniques for orthopaedic applications 407
G. Sala, Aerospace Engineering Department, Italy

15.1 Introduction 407
15.2 The challenges of joining metals to ceramics 409
15.3 Mechanical joining techniques 415
15.4 Direct and indirect bonded joining techniques 418
15.5 Active brazing joining techniques 423
15.6 Future trends 443
15.7 Sources of further information and advice 445
15.8 References 446

16 Tissue adhesives and sealants for surgical applications 449
P. Jarrett, Ocular Therapeutix, USA and A. Coury, Coury Consulting Services, USA

16.1 Introduction 449
16.2 Principles of tissue adhesives and sealants 450
16.3 Definitions and general considerations 454
16.4 Mechanisms of bonding 454
16.5 Application methods 456
16.6 Synthetic bioresorbable sealants 457
16.7 Commercial resorbable synthetic sealants and adhesives 464
16.8 Commercial resorbable bio-derived sealants and adhesives 475
16.9 Commercial biostable bio-derived sealants and adhesives 477
16.10 Commercial biostable synthetic sealants and adhesives 479
16.11 Conclusion 480
16.12 Sources of further information and advice 480
16.13 References 486

17 Antibacterial adhesives for bone and tooth repair 491
E. A. Abou Neel, King Abdulaziz University, Saudi Arabia, Tanta University, Egypt and University College London, UK and A. M. Young, University College London, UK

17.1 Introduction to tooth repair 491
17.2 Introduction to bone repair 498

© Woodhead Publishing Limited, 2013

17.3 Future trends 506
17.4 Acknowledgment 507
17.5 References 507

18 Testing bond strength: the case of dental biomaterials 514
R. Van Noort, University of Sheffield, UK

18.1 Introduction 514
18.2 Rationale for bond strength testing 516
18.3 Classification of dental adhesive testing techniques 518
18.4 Behavioural adhesive tests 520
18.5 Structural adhesive tests 525
18.6 Future trends 529
18.7 Conclusion 530
18.8 References 530

Index *535*

© Woodhead Publishing Limited, 2013

Contributor contact details

(* = main contact)

Editors

Y. (Norman) Zhou*
Centre for Advanced Materials Joining
University of Waterloo
200 University Avenue West, Waterloo, Ontario
Canada N2L 3G1

E-mail: nzhou@uwaterloo.ca

Mark D. Breyen
Medtronic Inc.
710 Medtronic Parkway Northeast
Minneapolis
Minnesota 55432
USA

E-mail: mark.breyen@medtronic.com

Chapter 1

Jeremy J. Ramsden
Collegium Basilea (Institute of Advanced Study)
Basel
Switzerland

E-mail: J.Ramsden@colbas.org

Chapter 2

L. Quintino
Instituto Superior Técnico
Technical University of Lisbon
Departamento de Engenharia Mecânica
Av. Rovisco Pais
1049–001 Lisboa
Portugal

E-mail: lquintino@ist.utl.pt

Chapter 3

Kevin J. Ely
GlaxoSmithKline Corporation
Zebulon
North Carolina 27596
USA

E-mail: kevin.j.ely@gsk.com

P. Hall
Boston Scientific Corporation
St Paul, Minnesota
USA

Y. (Norman) Zhou*
Centre for Advanced Materials Joining
University of Waterloo
200 University Avenue West, Waterloo

© Woodhead Publishing Limited, 2013

Ontario
Canada N2L 3G1

E-mail: nzhou@uwaterloo.ca

Chapter 4

Wayne J. Rogers
Consultant
28482 Scenic Bay Cove
Menifee
California 92585
USA

E-mail: roger-wayne1@msn.com; roger-wayne1@hotmail.com

Chapter 5

Ibraheem Khan
Smarter Alloys
101 College Street
Toronto, Ontario
Canada M5G 1L7

E-mail: ibraheem@smarteralloys.com

Y. (Norman) Zhou*
Centre for Advanced Materials Joining
University of Waterloo
200 University Avenue West, Waterloo, Ontario
Canada N2L 3G1

E-mail: nzhou@uwaterloo.ca

Chapter 6

A. Pequegnat* and Y. (Norman) Zhou
Centre for Advanced Materials Joining
University of Waterloo
200 University Avenue West, Waterloo, Ontario
Canada N2L 3G1

E-mail: apequegn@uwaterloo.ca

Chapter 7

Shawn C. Kelley* and Darrel Untereker
Medtronic, Inc.
710 Medtronic Parkway Northeast
Minneapolis
Minnesota 55432
USA

E-mail: shawn.c.kelley@medtronic.com

Chapter 8

Jian Xie
Advanced Bionics
28515 Westinghouse Place
Valencia
California 91355
USA

E-mail: jian43026@yahoo.com

Chapter 9

Kevin J. Ely
GlaxoSmithKline Corporation
1011 North Arendell Ave
MS N232
Zebulon
North Carolina 27596
USA

E-mail: Kevin.j.ely@gsk.com

© Woodhead Publishing Limited, 2013

Chapters 10, 11 and 12

Hong Jun Yeh
Amgen Inc.
1 Amgen Center Drive
Thousand Oaks
California 91320
USA

E-mail: hyeh@amgen.com

Chapter 13

Ian Jones
TWI Ltd
Granta Park
Great Abington
Cambridge CB21 6AL
UK

E-mail: ian.jones@twi.co.uk

Chapter 14

Kimberly Chaffin*, Catherine Taylor and Thomas Grailer
Medtronic, Inc.
710 Medtronic Parkway Northeast
Minneapolis
Minnesota 55432, USA

E-mail: kim.chaffin@medtronic.com; kate.taylor@medtronic.com; tom.grailer@medtronic.com

Chapter 15

Giuseppe Sala
Aerospace Engineering Department
Politecnico di Milano
Via La Masa, 34
20156 Milano
Italy

E-mail: giuseppe.sala@polimi.it

Chapter 16

Peter Jarrett*
Ocular Therapeutix
36 Crosby Drive
Bedford
Massachusetts 01730
USA

E-mail: pjarrett@ocutx.com

Art Coury
Coury Consulting Services
154 Warren Ave #4
Boston
Massachusetts 02116
USA

E-mail: artjcoury@aol.com

Chapter 17

Ensanya A. Abou Neel*
King Abdulaziz University
Conservative Dental Science Department
Biomaterials Division
PO Box 80209
Jeddah, 21589
Saudi Arabia

Tanta University
Faculty of Dentistry
Biomaterials Department
Egypt

Biomaterials and Tissue Engineering Division
University College London
Eastman Dental Institute
256 Gray's Inn Road
London WC1X 8LD
UK

E-mail: eabouneel@kau.edu.sa; e.abouneel@ucl.ac.uk

© Woodhead Publishing Limited, 2013

Anne M. Young
Biomaterials and Tissue Engineering Division
University College London
Eastman Dental Institute
256 Gray's Inn Road
London WC1X 8LD
UK

E-mail: anne.young@ucl.ac.uk

Chapter 18

Professor Richard van Noort
Professor of Dental Materials Science
Academic Unit of Restorative Dentistry
School of Clinical Dentistry
University of Sheffield
Claremont Crescent
Sheffield S10 2TA
UK

E-mail: r.vannoort@shef.ac.uk

© Woodhead Publishing Limited, 2013

Woodhead Publishing Series in Biomaterials

1 **Sterilisation of tissues using ionising radiations**
Edited by J. F. Kennedy, G. O. Phillips and P. A. Williams
2 **Surfaces and interfaces for biomaterials**
Edited by P. Vadgama
3 **Molecular interfacial phenomena of polymers and biopolymers**
Edited by C. Chen
4 **Biomaterials, artificial organs and tissue engineering**
Edited by L. Hench and J. Jones
5 **Medical modelling**
R. Bibb
6 **Artificial cells, cell engineering and therapy**
Edited by S. Prakash
7 **Biomedical polymers**
Edited by M. Jenkins
8 **Tissue engineering using ceramics and polymers**
Edited by A. R. Boccaccini and J. Gough
9 **Bioceramics and their clinical applications**
Edited by T. Kokubo
10 **Dental biomaterials**
Edited by R. V. Curtis and T. F. Watson
11 **Joint replacement technology**
Edited by P. A. Revell
12 **Natural-based polymers for biomedical applications**
Edited by R. L. Reiss et al
13 **Degradation rate of bioresorbable materials**
Edited by F. J. Buchanan
14 **Orthopaedic bone cements**
Edited by S. Deb
15 **Shape memory alloys for biomedical applications**
Edited by T. Yoneyama and S. Miyazaki
16 **Cellular response to biomaterials**
Edited by L. Di Silvio

© Woodhead Publishing Limited, 2013

17 **Biomaterials for treating skin loss**
Edited by D. P. Orgill and C. Blanco
18 **Biomaterials and tissue engineering in urology**
Edited by J. Denstedt and A. Atala
19 **Materials science for dentistry**
B. W. Darvell
20 **Bone repair biomaterials**
Edited by J. A. Planell, S. M. Best, D. Lacroix and A. Merolli
21 **Biomedical composites**
Edited by L. Ambrosio
22 **Drug–device combination products**
Edited by A. Lewis
23 **Biomaterials and regenerative medicine in ophthalmology**
Edited by T. V. Chirila
24 **Regenerative medicine and biomaterials for the repair of connective tissues**
Edited by C. Archer and J. Ralphs
25 **Metals for biomedical devices**
Edited by M. Ninomi
26 **Biointegration of medical implant materials: science and design**
Edited by C. P. Sharma
27 **Biomaterials and devices for the circulatory system**
Edited by T. Gourlay and R. Black
28 **Surface modification of biomaterials: methods analysis and applications**
Edited by R. Williams
29 **Biomaterials for artificial organs**
Edited by M. Lysaght and T. Webster
30 **Injectable biomaterials: Science and applications**
Edited by B. Vernon
31 **Biomedical hydrogels: Biochemistry, manufacture and medical applications**
Edited by S. Rimmer
32 **Preprosthetic and maxillofacial surgery: Biomaterials, bone grafting and tissue engineering**
Edited by J. Ferri and E. Hunziker
33 **Bioactive materials in medicine: Design and applications**
Edited by X. Zhao, J. M. Courtney and H. Qian
34 **Advanced wound repair therapies**
Edited by D. Farrar
35 **Electrospinning for tissue regeneration**
Edited by L. Bosworth and S. Downes
36 **Bioactive glasses: Materials, properties and applications**
Edited by H. O. Ylänen

© Woodhead Publishing Limited, 2013

37 **Coatings for biomedical applications**
Edited by M. Driver
38 **Progenitor and stem cell technologies and therapies**
Edited by A. Atala
39 **Biomaterials for spinal surgery**
Edited by L. Ambrosio and E. Tanner
40 **Minimized cardiopulmonary bypass techniques and technologies**
Edited by T. Gourlay and S. Gunaydin
41 **Wear of orthopaedic implants and artificial joints**
Edited by S. Affatato
42 **Biomaterials in plastic surgery: Breast implants**
Edited by W. Peters, H. Brandon, K. L. Jerina, C. Wolf and V. L. Young
43 **MEMS for biomedical applications**
Edited by S. Bhansali and A. Vasudev
44 **Durability and reliability of medical polymers**
Edited by M. Jenkins and A. Stamboulis
45 **Biosensors for medical applications**
Edited by S. Higson
46 **Sterilisation of biomaterials and medical devices**
Edited by S. Lerouge and A. Simmons
47 **The hip resurfacing handbook: A practical guide to the use and management of modern hip resurfacings**
Edited by K. De Smet, P. Campbell and C. Van Der Straeten
48 **Developments in tissue engineered and regenerative medicine products**
J. Basu and J. W. Ludlow
49 **Nanomedicine: Technologies and applications**
Edited by T. J. Webster
50 **Biocompatibility and performance of medical devices**
Edited by J-P. Boutrand
51 **Medical robotics: Minimally invasive surgery**
Edited by P. Gomes
52 **Implantable sensor systems for medical applications**
Edited by A. Inmann and D. Hodgins
53 **Non-metallic biomaterials for tooth repair and replacement**
Edited by P. Vallittu
54 **Joining and assembly of medical materials and devices**
Edited by Y. (Norman) Zhou and M. D. Breyen
55 **Diamond-based materials for biomedical applications**
Edited by R.Narayan
56 **Nanomaterials in tissue engineering: Fabrication and applications**
Edited by A. K. Gaharwar, S. Sant, M. J. Hancock and S. A. Hacking
57 **Biomimetic biomaterials: Structure and applications**
Edited by A. Ruys

© Woodhead Publishing Limited, 2013

58 **Standardisation in cell and tissue engineering: Methods and protocols**
Edited by V. Salih
59 **Inhaler devices: Fundamentals, design and drug delivery**
Edited by P. Prokopovich
60 **Bio-tribocorrosion in biomaterials and medical implants**
Edited by Yu Yan
61 **Microfluidic devices for biomedical applications**
Edited by X-J. James Li and Y. Zhou
62 **Decontamination in hospitals and healthcare**
Edited by J. T. Walker
63 **Biomedical imaging: Applications and advances**
Edited by P. Morris
64 **Characterization of biomaterials**
Edited by M. Jaffe, W. Hammond, P. Tolias and T. Arinzeh
65 **Biomaterials and medical tribology**
Edited by J. Paolo Davim

© Woodhead Publishing Limited, 2013

1

Introduction to medical materials and devices

J. J. RAMSDEN, Collegium Basilea, Switzerland

DOI: 10.1533/9780857096425.1.3

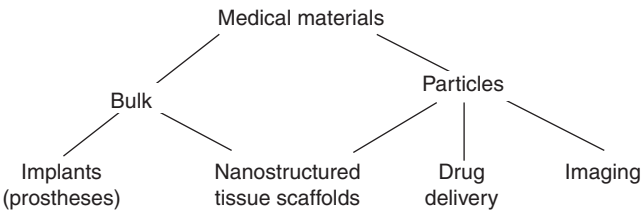
Abstract: This chapter introduces medical materials, especially from the viewpoint of their surface attributes and interactions with living matter, considered at various length scales ranging from molecular through cellular to tissular. The basic biophysical chemistry of interaction is covered in sufficient detail to allow the reader to estimate the interactions when appraising novel materials. Consideration is given to how welding and other forms of joining might affect the interactions. The metrology of biocompatibility is also covered in order to acquaint the reader with practical approaches to assessing the interactions, which are, of course, of crucial importance in determining the functional success of any artificial material in contact with living matter.

Key words: biocompatibility, interfacial energy, protein adsorption.

1.1 Introduction

Medical materials are defined as materials used in medicine. Since medicine itself is defined as 'the science and art concerned with the cure, alleviation, and prevention of disease, and with the restoration and preservation of health' (*Shorter Oxford English Dictionary*), the compass of medical materials would appear to be rather wide: even the material used for tubing in a food-processing factory would fall into the definition, the material being specially designed to prevent colonization by pathogenic bacteria. The scientific issues underlying the application of materials in medicine are, however, clearly circumscribed and can be grouped under the heading of biocompatibility, which in turn is typically defined as 'tolerant of life, or of biomolecular function' (PAS 132, 2007). Regardless of the specific use to which the material is put, it must be biocompatible. The bactericidal or, more generally, biocidal surfaces that play a valuable role in keeping the walls, floor, furniture, etc. of a hospital free from infectious agents are not, of course, biocompatible – rather just the opposite – but the same principles that provide a framework for understanding biocompatibility apply to the biocidal surfaces. These principles may be collectively described as the science of the bio/nonbio interface. Thus, regardless of properties such as density, stiffness, etc. required for a particular application, it is essential to

© Woodhead Publishing Limited, 2013



1.1 The upper part of a concept system for medical materials.

ensure that the *surface* of the material object is biocompatible. This implies that the special features of the science of medical materials are those associated with surfaces; properties such as density and stiffness are common to materials science as a whole. Hence, the specific focus of this chapter will be on the surface properties of materials relevant to medical applications that bring them into contact with biological matter.

Despite the acknowledgment above that materials used for production and packaging in the food and pharmaceutical industries and in water supply, etc. also have a bearing on health, in the remainder of this chapter medical materials will be defined more narrowly as the materials used for making medical devices. Nevertheless, it should be emphasized that the principles governing the bio/nonbio interface, which provide the theoretical framework for understanding biocompatibility, are also fully applicable to those other sectors.

1.1.1 An ontology for medical materials

Figure 1.1 gives the first three levels of a concept system for medical materials. From the viewpoint of surface properties, the division between the bulk materials and particles is of little consequence; particles are essentially all surface (Ramsden and Freeman, 2009). The key thing to note about the concepts appearing at the lowest level are that the objects constituting their extensions interact with both biofluids (e.g. blood) and tissues.

1.1.2 An ostensive definition of medical materials

Table 1.1 lists the 24 most abundant materials used in implanted medical devices. Note the dominance of titanium. Its surface is invariably coated with a thin film of titanium dioxide, which governs its biocompatibility. Titanium is attractive because of its combination of excellent biocompatibility (of its oxide) and mechanical properties (relatively lightweight and strong). Polymers of various kinds are also prominent. On the other hand, composites have as yet found little favour in clinical practice. This compilation does not include the (still mostly experimental) materials used to fabricate drug delivery particles.

© Woodhead Publishing Limited, 2013

Table 1.1 Relative importance (ranked by numbers of occurrences *N* of the listed words) of the materials used in implanted devices[a]

Rank	Material	*N*
1	Titanium	2492
2	Steel	607
3	Chromium	391
4	Polyethylene (PE), ultra-high molecular weight polyethylene (UHMWPE)	389
5	Silicone	375
6	Cobalt	235
7	Polytetrafluoroethylene (PTFE), Teflon, fluoroplastic	220
8	Molybdenum	216
9	Vitallium	198
10	Polypropylene (PP)	160
11	Polymethylmethacrylate (PMMA), acrylic	111
12	Polyester	107
13	NiTiNOL	101
14	Polyurethane (PU)	72
15	Platinum	58
16	Premilene (a lightweight polypropylene mesh)	55
17	Aluminium, alumina	52
18	Carbon	51
19	Rubber	49
20	Hydroxyapatite (HAp)	45
21	Silicon	42
22	Polylactic acid (PLLA)	39
23	Polyethyletherketone (PEEK)	32
24	Tantalum	18

[a] Words are from the *Prostheses List* of the Australian Health Insurance Association (AHIA), 2005.

1.1.3 Surface attributes of medical materials

As a general rule, it can be stated that materials in contact with the bloodstream should not interact with blood; that is, with its proteins and cells. Materials of devices such as hypodermic needles and surgical knives, intended for very transient contact with the living substance, form a subcategory of non-interacting materials. Conversely, materials intended to remain in contact with solid tissue (e.g. a bone implant) for an indefinite duration should become assimilated with it (Kutsevlyak *et al.*, 2008).

1.1.4 The nature of interaction

We are concerned with two materials, that of the artificial device (the medical material) and the biological tissue. They will sense each other's

© Woodhead Publishing Limited, 2013

presence through various forces. For example, if the materials have mass, the gravitational force will act between them (this is usually weak enough to be neglected, but even a single living cell will sediment when suspended in a fluid). Electrostatic forces are far stronger. Matter is, normally, electrostatically neutral but especially in a medium such as water, which has a high dielectric constant, atoms may separate from each other, becoming ions, as in

$$NaCl \rightleftharpoons Na^+ + Cl^- \quad [1.1]$$

and the ions may adsorb onto a neutral surface, electrifying it; water itself is also weakly ionized:

$$H_2O \rightleftharpoons H^+ + OH^- \quad [1.2]$$

but at neutral (physiological) pH the concentration of each ion is only 100 nM. The surfaces of metal oxides such as titanium dioxide are typically hydroxylated through reaction with water and the hydroxyl groups can themselves ionize:

$$-OH \rightleftharpoons -O^- + H^+ \quad [1.3]$$

The small, mobile hydrogen ions will tend to diffuse away (thermal motion competing with the electrostatic interaction pulling them back to the surface), electrifying the interface, a tendency which is exacerbated if the water is moving relative to the metal oxide.

'Ionization' means that an atom has lost or gained one or more electrons. Even if there is no ionization, atoms can interact electrodynamically because, being formed of a heavy, compact, positively charged nucleus and a light, extended, negatively charged electron 'cloud', they have a transiently dipolar character and these dipoles can interact (engendering the van der Waals, London and Keesom forces, collectively called the Lifshitz–van der Waals (LW) force (van Oss, 2006)). This provides a universal attractive force between all materials, which suffices to enable creatures such as the gecko to climb vertical walls and cross ceilings upside down. A corollary of the existence of this universal force means that it is not possible to make a truly non-interacting material. Fortunately there is another set of forces, also based on electrodynamics, which depends on the fact that when atoms combine to create chemical compounds, the electrons are not usually equally shared and, hence, some compounds are electron donors (they have a slight electron excess) and some compounds are electron acceptors (they have a slight electron deficiency). These are called Lewis bases and Lewis acids, respectively. Water, incidentally, is both a Lewis acid and a Lewis base. Two

© Woodhead Publishing Limited, 2013

monopolar surfaces (van Oss *et al.*, 1987) of the same polarity (e.g. two Lewis bases) will repel each other. Fortunately many natural materials, both biological and non-biological, have a pronounced electron-donating tendency and will, therefore, tend to repel each other. Hydrocarbon waxes and synthetic polymers such as polyethylene are essentially apolar – they can only interact with the LW force.

Materials of devices, such as stents, intended to remain in contact with the bloodstream for prolonged periods must strongly interact with macromolecular blood components – but repulsively. As will be covered in more detail in Section 1.2, this is achievable by more strongly interacting with the majority component of the blood, namely water, than anything else. This interaction is modified by the presence of small molecules (ions and osmolytes) dissolved in the biofluid (Cacace *et al.*, 1997). It follows that a material characterized as bioinert, defined as 'not evoking any significant response from the host organism or biological system' (PAS132, 2008), is not unreactive as are the gases helium, argon, etc., but must be strongly reactive – in the right sense.

Given that the characteristic time for macromolecular adsorption is typically of the order of tens of seconds (Ramsden, 1998), there is no need to consider such adsorption for the surfaces of devices (e.g. needles and knives) whose contact with the tissue is of the order of one second. Rather, the requirement here is to diminish the coefficient of friction as much as possible (see Section 1.2.4). Conversely, assimilation demands strong adhesion. Although from the viewpoint of the surgeon it is the cells that must strongly bond to the permanently implanted material, this in turn depends on macromolecules, mostly proteins and glycoproteins, expressed on the surface of the cell, which must be attracted to the artificial material's surface.

1.1.5 The concept of surface free energy

In order to make the notion of 'interaction' more precise and amenable to quantification, we introduce the concept of surface energy. If a solid substance (e.g. a block of titanium dioxide) is placed in a vessel containing a liquid substance (e.g. water) and then the block is cut in two, work must be done against the forces holding the atoms of the solid substance together, counteracted by the work arising through any attractive forces between the solid and the liquid. The net work can be expressed as the interfacial energy per unit area of interface created. Note that the units of interfacial energy per unit area are the same as that of surface tension (force divided by distance); these concepts are essentially interchangeable. This opens a convenient experimental route to the measurement of interfacial energy. At the beginning of the nineteenth century, Thomas Young established his famous

© Woodhead Publishing Limited, 2013

law, according to which the contact angle θ of a droplet of liquid 2 sitting on a planar surface of solid 1 is defined by the condition of stability of the droplet shape with respect to small perturbations or, equivalently, the fact that the droplet is stationary implies that, within the plane of the surface, the sum of the three forces meeting at the line at which the edge of the droplet contacts the surface is equal to zero, namely

$$\gamma_1 = \gamma_2 \cos\theta + \gamma_{12} \qquad [1.4]$$

where γ_{12} is the interfacial surface tension (or surface energy per unit area) between substances 1 and 2 and analogously for the other terms, neglecting the vapour phase surrounding the surface and the liquid droplet. The surface tension γ_2 of a liquid alone can be determined by measuring the shape of a hanging droplet of the liquid. Since γ_{12} can be considered to be the geometric mean of γ_1 and γ_2, we can then solve Equation [1.4] to find the unknown γ_2. If one wishes to determine the separate components of the surface tension (i.e. LW and Lewis acid/base) the measurement will have to be done three times with three different liquids to obtain three Young's equations, which can then be solved simultaneously to yield the LW component and the electron donor and electron acceptor components of the Lewis acid/base contribution. An exhaustive discussion is given by van Oss (2006), and some typical values are given in Table 1.2. Note that it is possible to prepare a protein (or other biomacromolecule) surface by repeatedly allowing droplets of a solution of the molecule to dry on a substrate.

The interfacial tensions can be considered to be the geometric means of the single-substance tensions of the two substances that come together to form the interface. This is straightforward for the LW interaction:

$$\gamma_{12}^{(\mathrm{LW})} = \left(\sqrt{\gamma_1^{(\mathrm{LW})}} - \sqrt{\gamma_2^{(\mathrm{LW})}}\right)^2 \qquad [1.5]$$

but more complicated for the Lewis acid/base (ab) interaction because this has both electron donor ($\gamma^{\ominus}$) and electron acceptor ($\gamma^{\oplus}$) components, and the mean therefore contains cross terms:

$$\gamma_{12}^{(\mathrm{ab})} = 2\left(\sqrt{\gamma_1^{\ominus}\gamma_1^{\oplus}} + \sqrt{\gamma_2^{\ominus}\gamma_2^{\oplus}} - \sqrt{\gamma_1^{\oplus}\gamma_2^{\ominus}} - \sqrt{\gamma_1^{\ominus}\gamma_2^{\oplus}}\right) \qquad [1.6]$$

The cross terms correspond, respectively (from left to right on the right-hand side of the equation), to the polar cohesive interaction energy between the electron donors and acceptors of the artificial surface, the polar cohesive interaction energy between the electron donors and acceptors of the aqueous medium in contact with the surface, the polar adhesive interaction energy

© Woodhead Publishing Limited, 2013

Table 1.2 Surface tension parameters of some artificial and biological materials[a]

Material	$\gamma^{(LW)}$/mJ m^{-2}	$\gamma^{\oplus}$/mJ m^{-2}	$\gamma^{\ominus}$/mJ m^{-2}
Synthetic polymers			
Nylon 6,6	36	0.02	22
Polyethylene	33	0	0
Polyethylene oxide	43	0	64
Polyvinyl chloride	43	0.04	3.5
Biological polymers			
Cellulose	44	1.6	17
Serum albumin, dry, pH 7	41	0.002	20
Human fibronectin	30	4.3	51.6
Metal oxides			
SiO_2	39	0.8	41
TiO_2	42	0.6	46
ZrO_2	35	1.3	3.6
Liquids			
Water[a]	22	25.5	25.5
Ethanol	19	0.02	68
Octane	22	0	0

[a] Data from van Oss (2006).

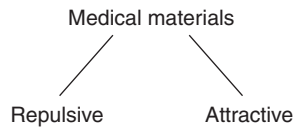
between the electron acceptors of the surface and the electron donors of the medium, and the polar adhesive interaction energy between the electron donors of the surface and the electron acceptors of the medium. Due to the presence of the cross terms, the Lewis acid/base interaction can be either repulsive or attractive (Fig. 1.2).

The sign of the interfacial free energy (ΔG) can be readily estimated using the concept of surface tension. A useful relation, derivable from Equations [1.5] and [1.6] and Dupré's convention that $\Delta G_{121}^{\parallel} = -2\gamma_{12}$ (Cacace *et al.*, 1997), is:

$$\Delta G_{123} = \Delta G_{22} + \Delta G_{13} - \Delta G_{12} - \Delta G_{32} \qquad [1.7]$$

This expression encapsulates the fact that the interfacial free energy depends positively on the cohesive energy ΔG_{22} of the liquid medium and the interfacial free energy ΔG_{13} of the artificial material and the biological material in the absence of intervening liquid, and negatively on the solvation free energies ΔG_{12} and ΔG_{32} of the artificial and biological materials. The superscript $\parallel$ denotes that the interfacial free energies are for plane parallel surfaces of infinite extent at the distance of closest approach ('contact distance'), which will be mentioned again in the next section. This equation clearly shows that the minimum requirement for attraction between an artificial and a biological material is the absence of any specific interactions

© Woodhead Publishing Limited, 2013



1.2 The division of medical materials into those that interact repulsively and those that interact attractively with the host organism – ultimately at the molecular level. The repulsive interaction is generally required for materials characterized as 'bioinert'.

(including solvation) – the cohesive energy of the solvent, which is large and negative in the case of water, will ensure that the interfacial free energy is attractive. Conversely, the only way to overcome attraction is to ensure that the artificial material or the biological material or both are well solvated, in which case either or both of the last two terms on the right will make significant positive contributions to ΔG_{123}. Note that the LW and ab contributions are simply added together.

Since the proteins present in the bloodstream and at the surfaces of living cells may undergo conformational change once present at the interface (Section 1.2.1), the overall behaviour is likely to be much more complicated than that suggested by Equation [1.7], which should therefore only be used to provide an initial indication.

1.1.6 How interactions are changed due to welding and other forms of joining

It is of course of relevance to understand how material processing may change biointeractions. This understanding may be achieved within the formalism of surface free energy; one needs to understand precisely how the surface energetic properties of the material have been changed. This can be investigated experimentally by *ex situ* experiments in which the material is subject to the same joining processes and then its surface morphology and energetics are measured. Welding is likely to involve heating of the material, and gluing involves the introduction of additional chemical species.

1.2 The anatomy of interaction

In the previous section we considered the rather idealized situation of plane parallel surfaces. In reality, the artificial medical material is typically hard relative to the biological material, which is conformal or soft. A liquid 'tissue' such as the blood represents the ultimate degree of condensed matter conformability. Even solid tissue (e.g. the epithelium) is mostly composed

© Woodhead Publishing Limited, 2013

of water. Nevertheless, small areas of the interface can still be considered to be plane parallel in nature. In any case, it should be emphasized that the most important aspect of the interfacial interaction, regardless of what kind of biological material is involved, concerns the behaviour of the proteins. For a medical material in contact with the blood, the adsorption of blood proteins is of primordial importance in determining the fate of the artificial material. But even cells are densely populated with proteins on their outer surface. Hence, understanding how proteins interact with artificial materials will take us a long way towards understanding the behaviour of medical materials in contact with biological tissue.

Let us consider a single protein molecule at a distance z from an artificial surface. At infinite distance from the surface, the molecule will not experience any force. In reality, given the relatively short range of the relevant forces (LW, Lewis acid/base and electrostatic), a molecule might only have to be a few tens of nanometres distant from the medical material in order not to experience any force of attraction to or repulsion from it. In order to compute the interfacial free energy, one integrates the force on moving from effectively infinite separation to the distance of closest approach (van Oss and Good, 1984) – about 1.5 Å. The free energies of interaction thereby obtained correspond to those discussed in the previous section (cf. Equation [1.7] and others). The free energy of interaction, ΔG_{123}, itself depends on z (Cacace *et al.*, 1997). A typical profile is shown in Fig. 1.3. Now, considering the adsorption event to be a reaction, and denoting the protein or other biomolecule as B and the medical material as M, we have for the transition from solution:

$$\mathrm{B_{soln}} + \mathrm{M} \rightleftharpoons \mathrm{B_{ads}} \qquad [1.8]$$

The forward rate constant k_f can be written as the quotient of the diffusivity of the protein D and the adsorption interaction length δ_a

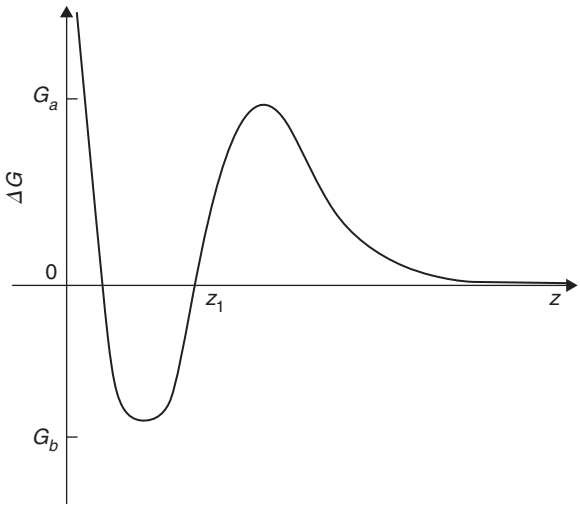
$$k_f = \frac{D}{\delta_a} \qquad [1.9]$$

where δ_a is in turn given by Spielman and Friedlander (1974)

$$\delta_a = \int_{z_1}^{\infty} \left[\mathrm{e}^{\Delta G_{123}(z)/k_B T} - 1 \right] \mathrm{d}z \qquad [1.10]$$

The lower limit z_1 of the integral can, practically speaking, be taken to be the point at which the curve of $\Delta G_{123}(z)$ first crosses the axis as z diminishes from infinity (Fig. 1.3). Expressions for the distance dependence of the

© Woodhead Publishing Limited, 2013



1.3 Sketch of the typical variation of interfacial free energy ΔG_{123} with separation *z*. The interface is, for example, that between a medical material and a biological fluid such as the blood, in which case the distance z is that between the surface of the medical material and a protein molecule. G_a is the height of the energy barrier hindering approach of the biological object to the surface of the artificial material, and G_b is the depth of the potential energy well in which a biological object, having arrived at the surface of the artificial material, finds itself.

components of ΔG_{123} can be found in van Oss (2006) or Cacace *et al*. (1997). The decay of the dominant ab interaction is exponential, that is,

$$\Delta G_{123}(z) = \frac{\Delta G_0 \mathrm{e}^{z}}{z_k} \qquad [1.11]$$

where ΔG_0 is the value of $\Delta G_{123}(z)$ for infinite parallel planar surfaces separated by the 'distance of closest approach' (van Oss, 2006) and z_d is the characteristic decay length for the interaction – typically of the order of 1 nm under physiological conditions.

The overall adsorption rate of a protein at a surface will be

$$\frac{\mathrm{d}\Gamma}{\mathrm{d}t} = k_f c^* \phi(\Gamma) \qquad [1.12]$$

where Γ is the surface excess (i.e. the number or mass of adsorbed proteins per unit area), c^* is the effective concentration of the proteins in the medium contacting the artificial material; it depends on the actual bulk

© Woodhead Publishing Limited, 2013

concentration (or activity) of the adsorbing species and the prevailing hydrodynamic regime, and ϕ is the available area function (which gives the probability that a molecule arriving at the surface finds space to adsorb). A good deal of the discussion about adsorption rates focuses on appropriate expressions for $c*$ and ϕ. For multilayer adsorption, ϕ always equals 1. Otherwise a random sequential addition (RSA) model might be appropriate (Ramsden, 1998), especially for small buoyant objects such as protein molecules. Cells sedimenting onto a horizontal substratum are best modelled as a ballistic deposition process (Lavalle *et al*., 1997). If the liquid medium in which proteins are dissolved is stagnant, their transport to the surface will be purely diffusive. Otherwise it will take place via convective diffusion, and it may be useful to characterize it with the Damköhler number Da, the quotient of reaction rate and convective mass transport rate, which here becomes, after cancelling $c*$ in both numerator and denominator:

$$\mathrm{Da} = \frac{k_f \phi}{D/\delta_h} = \frac{\phi \delta_h}{\delta_a} \qquad [1.13]$$

where δ_h is the thickness of the hydrodynamic boundary layer, which depends on the flow rate and geometry (Levich, 1962). If one is most interested in the initial events when the protein first comes into contact with the artificial material, ϕ may be taken as unity.

The desorption rate can be given, to a first approximation, as

$$\frac{\mathrm{d}\Gamma}{\mathrm{d}t} = -k_b \Gamma \qquad [1.14]$$

where k_b is the rate coefficient of desorption and Fig. 1.3 suggests that an Arrhenius expression

$$k_b = \exp[-(G_a - G_b)/(k_B T)] \qquad [1.15]$$

might be an acceptable first approximation to k_b. Due to *conformational* change (or even simple reorientation) k_b is, in reality, typically time-dependent (see Ramsden (2003) for more discussion).

1.2.1 Interactions of a protein molecule

The formalism developed in the previous section is still very rudimentary for use with real protein molecules. It has been tacitly assumed that the protein is a uniform sphere characterized by a particular value of single-substance surface tension parameters (Table 1.1), obtainable from contact angle

© Woodhead Publishing Limited, 2013

measurements with a layer of protein molecules deposited on a substrate. This kind of measurement averages out atomic detail. In reality, we know above all from protein crystallography that the surface of a protein is highly heterogeneous (Calonder *et al.*, 2001). The polypeptide backbone constituting the protein is itself rather polar, but the side chains ('residues') of the individual amino acids may be either polar or apolar. If this true nature of the protein surface is taken into account, the net interfacial free energy will be highly dependent on heterogeneity (especially of Lewis acid/base components) of the biomaterial. That the simple model averaging the various electron donating and accepting components is inadequate can already be seen by the behaviour of the abundant protein serum albumin, which according to the single-substance surface tension data should be repelled from pure silica, whereas it is a well-known experimental fact that it is strongly adsorbed. Similarly theoretically unexpected behaviour is observed with adsorption on heterogeneous materials (Aggarwal *et al.*, 2009).

Furthermore, it must be borne in mind that the native conformation of a protein is principally due to intramolecular hydrogen bonds between the backbone peptide bonds. Note that the hydrogen bond is a particular kind, the most important and ubiquitous in biology, of Lewis acid/base interaction. Since proteins are suspended in water (as are those parts of membrane proteins involved in adsorption to a medical material), which is itself a strong hydrogen bond donor and hydrogen bond acceptor, the main structural challenge that a protein has to meet is how to prevent denaturation through the attack of its intramolecular hydrogen bonds by water. Proteins have evolved a three-body structural motif in order to overcome the danger (Fernández and Scott, 2003), namely the intramolecular hydrogen bond with its donor and acceptor together with apolar residues to desolvate the hydrogen bond, thereby stabilizing it. An underdesolvated hydrogen bond (i.e. one with insufficient apolar residues in its vicinity) is called a dehydron, and the presence of dehydrons on the surface of a protein make it susceptible to bind to surfaces that can accomplish the missing desolvation. Artificial surfaces can be probed using atomic-force microscopy in order to ascertain their desolvation ability (Fernández, 2006).

Even if the adsorption of a protein on the surface is enthalpically neutral (i.e. any new bonds formed between the protein and the surface of the medical material would be compensated by breaking intramolecular bonds), there is nearly always the danger of an entropic penalty. Let us consider the representation of the three-dimensional conformation of a protein molecule by the two dihedral angles of successive peptide bonds. The Ramachandran diagram plots, for each amino acid, those combinations of the two angles corresponding to compact, native conformations and to extended, denatured conformations. Far more combinations are associated with extended states than with the native state. This means that there is inevitably an entropic

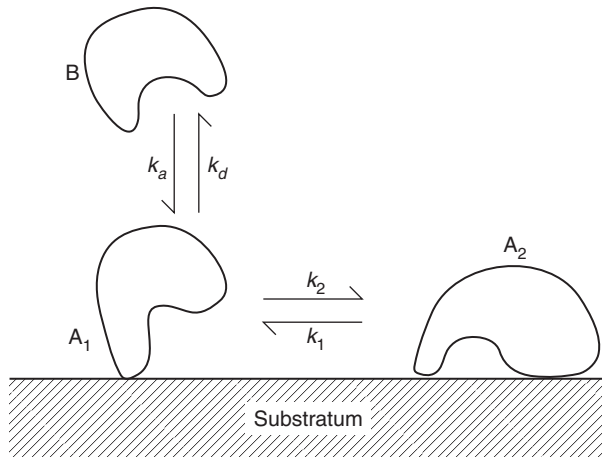
© Woodhead Publishing Limited, 2013

gain, hence a decrease of free energy, upon denaturation (Fernández and Ramsden, 2001). Hence, in order to obviate denaturation, it is essential to design the surface of a medical material to strongly repel the protein.

Most globular proteins have more than one stable compact conformation. This feature is usually an essential part of their operation as enzymes, motors, channels, etc. (Blumenfeld, 1981). Under some given condition (such as in a protein crystal), one would expect that one of the several possible compact confirmations is predominant. It is an unfortunate feature of the main source of structural information about proteins, namely X-ray crystallography, that the contributions of the minor structural component(s) to the X-ray diffractogram will be lost during computational refinement of the structure (Frauenfelder, 1984). It is highly likely that adsorption on a surface will cause a switch from one stable conformation to another. There is considerable evidence for such structural transitions upon adsorption (e.g. Ramsden, 1993) which, in the absence of definite knowledge about the different stable compact conformations, has sometimes been merely ascribed to reorientation (since globular proteins are rarely perfectly symmetrical but usually have some ellipsoidal character) or even to denaturation. Further evidence comes from observations of dramatic deceleration of enzyme operation, typically by many orders of magnitude, upon adsorption (e.g. Cacace and Ramsden, 2007). However, it is generally not possible to distinguish between deceleration due to the 'wrong' conformation being energetically favoured in the adsorbed state and the alternative explanation of a large fraction of the proteins being completely inactivated by denaturation and the remaining activity resulting from a few unchanged molecules. Figure 1.4 shows how a conformational change – or even merely an orientational change – can strongly change the affinity of a protein for a surface.

The final point we want to consider is the possibility of incorporating specific receptors into an artificial surface for certain motifs of amino acids present in the protein. Nature makes extensive use of such specificity. Examples are antigen–antibody interactions, the affinity of cell membrane-embedded integrins for the amino acid triplet arginine-glycine-aspartic acid (RGD), and so forth. Typically these specific interactions, even though they are themselves dependent on hydrogen bonds, are much stronger than the chance interactions between a randomly oriented protein and a more or less homogeneous artificial surface, since within a small area there is a large number of hydrogen bonds whose strength is assured by an appropriate geometry of binding. On the other hand, it is problematical to manufacture medical materials incorporating fragile biological components such as amino acids. Even if they survive processing and storage, they are likely to be quickly destroyed or altered in use. Therefore, there is considerable interest in mimicking such specificity. One way of achieving it using purely artificial materials is through molecular imprinting (Mosbach, 1992). A molecularly

© Woodhead Publishing Limited, 2013



1.4 Sketch of a protein (species B) dissolved in a biofluid in contact with some medical material ('Substratum'). The protein reaches the surface at a rate characterized by the rate coefficient k_a (which is related to the energy barrier G_a in Fig. 1.3). Immediately after arrival at the surface, the protein (species A_1) might differ very little from its dissolved counterpart, possibly being oriented in a fixed fashion and possibly retaining most of its native conformation while making some hydrogen bonds with the surface. While in residence (the duration of which will be proportional to the depth of the potential energy well, G_b in Fig. 1.3), it may undergo more extensive orientational and conformational changes, becoming transformed to species A_2 with a rate proportional to the coefficient k_2. In general, the reverse transformation would also be possible, with a rate proportional to the coefficient k_1. In this diagram it is supposed that A_2 is too strongly bound to the surface to be able to depart directly into the solution. Were it able to do so, it would very likely then be a different species from the original B.

imprinted material is prepared by mixing a precursor, which should be a polymer or polymerizable monomer with plenty of hydrogen bonding possibilities, together with the motif (e.g. the tripeptide RGD) to which it is desired to create affinity. The artificial material is polymerized around the guest, which is then washed out using a strongly hydrogen bond-breaking solution, leaving a material having cavities with highly specific affinity for the guest.

1.2.2 Interactions of living cells with medical materials

The classic mode of interaction of an isolated, suspended cell with a substratum on which it arrives is the transformation from a sphere to a segment ('cell spreading'). An extensive literature on the subject going back at least 50 years reveals that the nature of the spreading is highly dependent on the

© Woodhead Publishing Limited, 2013

cell type, the substratum and on the bathing medium (Li *et al*., 1994). This kind of approach has recently been updated, making use of experimental advances in nanofabrication, genomics and stem cells. The possibility of the creation of microscale and nanoscale features in a variety of materials has led to many studies of cell response (e.g. Curtis *et al*., 2001; Teixeira *et al*., 2004; Khor *et al*., 2007). Observations range from simple microscopical ones to immunochemistry for determining the presence of protein markers characteristic for certain cell types on the cell surface. The latter is of particular value when investigating the effect of substratum on stem-cell differentiation (e.g. Dalby *et al*., 2007). The relative ease, nowadays, of investigating gene expression has led to corresponding studies (e.g. Dalby *et al*., 2008). Despite the great volume of published work, it is difficult to draw general inferences. Knowledge of the effects of microscale and nanoscale topography, for example, is still limited to the fairly uninteresting observation that cells tend to align with parallel grooves. The difficulty of generalization is not least due to the fact that practically every experiment is carried out under different conditions, with different substrata or different cell types; particularly with stem cells, a very particular culture medium must generally be used for each type of cell, making it difficult to assess the effects of components in the medium on the behaviour. There is still a need for a far more extensive set of systematic studies coupled with rapid, quantitative cytometry (see also Section 1.4). Given that the number of possible combinations of variables is so vast, it is very necessary to develop testable hypotheses for the behaviour.

The native substrata of cells are, of course, the basement membranes constituted from extracellular matrix (ECM) proteins like laminin and tenascin (e.g. Bökel and Brown, 2002). It might therefore be supposed that the best medical materials are those that somehow mimic the ECM. On the other hand, it is known that if a cell comes into contact with an artificial material, it will secrete ECM proteins which coat the substratum (e.g. Li *et al*., 1994). This is somewhat discouraging for research into developing ideal material surface coatings, since it would appear that no matter how carefully the material is surface-engineered, its features will rapidly be obliterated by the cell carrying out its own engineering. A promising line of research is to attempt to artificially engineer surfaces such that the signals transmitted by the cell from its surface to its nucleus are controlled by the material. This represents a considerable challenge, on which very little work has hitherto been done, but not, hopefully, an insurmountable one.

Although the overall shape of the cell can be idealized as a sphere or a segment, in reality the cell is constantly creating protrusions (filopodia) with which to explore the surface (Aref *et al*., 2010). The tips of these filopodia are known to be rich in particular proteins, emphasizing the importance of

© Woodhead Publishing Limited, 2013

considering and understanding the interactions of proteins with medical materials as the foundation of knowledge of the field.

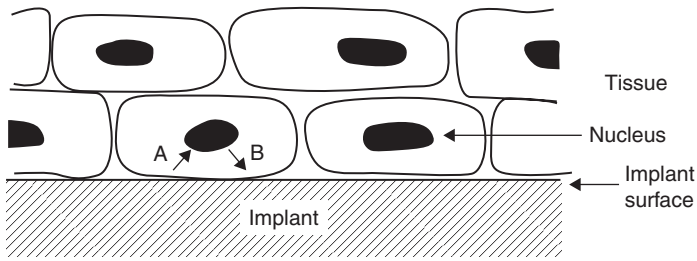
Overall, the interactions of cells with medical materials can be considered as an adaptive response taking place on different timescales and with correspondingly different mechanisms. Even if we just look at the spreading transition, phenomenologically there is the rapid spreading, taking place over tens of minutes (e.g. Aref *et al.*, 2010), and the classic or slow spreading, taking place over tens of hours (e.g. Li *et al.*, 1994). It might be supposed that the rapid spreading is a purely mechanical (viscoelastic) response of the cell to a constraint, whereas the slow spreading involves restructuring of the cytoskeleton, which requires internal signalling processes involving, for example, the phosphorylation and dephosphorylation of enzymes, which could take place without altered gene expression, but if ECM proteins have to be exuded, it is very likely that the enzymes involved in the synthesis and exudation would themselves have to be synthesized, hence involving the DNA of the cell. The differentiation of stem cells presumably results from considerable epigenetic activity. Once cells have differentiated, they typically cease to divide and, hence, there is no opportunity for investigating whether genotypes can be altered through residence on a substratum. Studies with bacteria have clearly shown changes in phenotype (e.g. Vilain *et al.*, 2004).

The majority of work appears to be carried out using eukaryotic cells, which are of course of immediate interest for the development of medical materials. Nevertheless, interactions with bacteria are also important and hopefully in the future more researchers will be attracted into that area. Certain parts of the human body, such as the colon, are rich in bacteria and devices intended for such parts need to interact appropriately with the bacterial population. For example, an implanted sensor should probably not become coated with a bacterial biofilm. Also of importance is the problem of persistent colonization of implants by bacteria. Very often they are resistant to antibiotics and act as a constant source of inflammatory irritation, which can often only be eliminated by removing the implant. The challenge is to create a material that is hostile to bacterial colonization, although, given the powerful capabilities of bacteria to modify their immediate environment (e.g. through biofilm formation) the challenge seems to be very great. As with the control of eukaryotic microexudates, influencing bacterial gene expression in a controlled fashion is a key goal.

1.2.3 Interactions with tissues

Tissues are of course made up of cells, the main difference between the topic of the previous section being that most of the laboratory research is carried

© Woodhead Publishing Limited, 2013



1.5 The interface between an artificial implant (hatched) and biological tissue represented by closely packed cells. Information characterizing the implant surface is transmitted (via signalling pathways) to the cell nucleus (arrow A), engendering changes in gene expression, resulting in fresh information being sent from the nucleus to the cell surface (arrow B), which might (for example) result in the excretion of some proteins to modify the implant surface.

out with individual cells, whereas in a tissue the cells are strongly mechanically constrained, which has a great effect on their behaviour (Nishihara, 2011). One implication is that the possibility of the implant to influence the cells within the tissue must principally work through influencing gene expression (Fig. 1.5).

1.2.4 Transient interactions: the tribology of medical materials

The two principal challenges in tribology are: (i) minimizing the coefficient of friction of surgical objects such as knives and needles; and (ii) minimizing the coefficient of friction of the materials in devices with rubbing surfaces, such as a ball-and-socket joint. Coefficients of friction depend on both material and morphology.

The purpose of (i) is to minimize collateral damage caused by a device as it passes through tissue. Similar considerations apply to permanently implanted devices that have to be passed through tissue in order to reach their final position. The purpose of (ii) is to minimize wear, which typically causes the release of particles. These particles may have significant deleterious biological effects (Revell, 2006), hence it is highly desirable to minimize their generation. The most common effect is inflammation caused by the adsorption of proteins (if the material is high density polyethylene, commonly used in prostheses, the hydrophobic nature of polyethylene – see Table 1.1 – promotes denaturation of proteins that come into contact with it, transforming them into non-self objects recognized as such by the immune system, which then works to eliminate them). One promising approach to minimizing wear is the introduction of ultra-hard materials such as

© Woodhead Publishing Limited, 2013

monocrystalline sapphire (Mamalis *et al.*, 2006, 2007). Sapphire–sapphire contacts have low coefficients of friction and the great hardness of the material means that it can be machined into very precise and stable shapes, which in itself minimizes wear. Nevertheless, some aspects of such novel materials still need further investigation. For example, the mass of ultra-hard material removed through wear during a given interval might indeed be one or more orders of magnitude less than in the case of traditional materials, but if the particles produced are very fine nanoparticles, they may engender a different set of biological responses, which might also be undesirable (Revell, 2006). Furthermore, if the particles are very small, they may be just as numerous as a much larger total mass of larger particles.

1.3 Materials for drug delivery

A very active area of research and development is the use of nanotechnology to engineer sophisticated small particles (as well as nanotubes and nanorods) for a variety of diagnostic and therapeutic applications (e.g. Arshady and Kono, 2006). The basic idea is to take a nanoparticle that is easy to image (e.g. a gold particle) and functionalize it with biomolecules having a specific affinity for some medically interesting cell or tissue (e.g. a tumour). The functionalization could be based on nucleic acids, peptides or oligosaccharides. In every case, the particles would be administered systemically. For diagnosis, one would then search (e.g. using X-rays) for any zone in which they have concentrated. It is easy to administer different particles (e.g. of different shape or size, each one being differently functionalized) simultaneously, thereby increasing the efficiency of diagnosis. By adding functionality, therapy can be carried out once the particles have reached the target. This might be achievable using external stimulation (e.g. radio frequency excitation, heating up the particles to locally destroy tissue, such as a tumour, by heating) or by arranging for the particles to release drugs from a reservoir (e.g. the particles could be hollow) in order to produce some therapeutic effect.

The main reservation of this kind of approach is that there is uncertainty over possibly adverse biological effects of the particles themselves (e.g. Revell, 2006). What is their fate after they have carried out their diagnostic or therapeutic mission? If they are rapidly excreted without causing any significant immune response, then there would appear to be little to worry about. At present, however, there is a great deal of uncertainty regarding the general health effects of nanoparticles (Hunt and Riediker, 2011).

Some of the most popular materials for nanoparticles used in biological research, such as the cadmium chalcogenides used as fluorescent markers, are highly chemically toxic and it is inconceivable that they would ever be diagnostically or therapeutically useful. But for the majority of materials

© Woodhead Publishing Limited, 2013

found in the research literature, present knowledge of their biological effects is simply inadequate. There are myriads of compounds that can be made into nanoparticles, nanoshells, nanotubes, nanorods and so forth, each of which can be made in a range of sizes covering the entire nanoscale (considered to be 1–100 nm).

Nevertheless, some of the diseases potentially treatable by this kind of nanomedicine are so life-threatening that one might be prepared to take some risks with toxicity. The main generic challenge is to prevent the nanoparticles, which are of course non-self and recognized as such by the immune system, from being rapidly eliminated before they have done anything of medical utility. This challenge brings us back to the issues discussed in the earlier sections devoted to the interaction of proteins with artificial materials. The nanoparticles need to be coated with strongly hydrated materials that will repel proteins, while at the same time retaining their specific affinity for their target. If the target is intracellular, the particles then need to be taken up by the cell, by endocytosis or pinocytosis (Maitra, 2010), which requires different surface properties from those that are needed to ensure their safe passage to the vicinity of the target.

The ultimate medical nanodevice is the nanoscale robot or 'nanobot' (Hogg, 2007), envisaged to be the size of a typical bacterium. Serious work on such devices has until now been confined to careful consideration of requirements concerning power, information reception, processing and transmission, the need for on-board sensors and, of course, the nature of the materials with which the device must be covered in order to prevent undue interference from the immune system. The principles governing the surface coating specification are, of course, those that have been already discussed.

1.4 The metrology of biocompatibility

From the above, it is clear that the main metrology challenge is to determine the degree of protein adsorption to a medical material. Many techniques for accomplishing this exist, and have been reviewed by Ramsden (1994). The most basic measurement is simply to determine the *quantity* of adsorbed biomolecules. A further step in sophistication can be achieved if information about the *structure* of the adsorbed biomolecules can be obtained. It may also be very illuminating to characterize the *kinetics* of adsorption and desorption.

Ideally the technique should be able to accomplish comprehensive characterization of the adsorption phenomenon *in situ* under conditions of use. No existing technique is able to achieve this. An implant can be inserted into the body, left for some time, and then removed and examined. Such tests are frequently carried out using animals, but given the subtlety of protein adsorption, when even the substitution of a single amino acid can

© Woodhead Publishing Limited, 2013

dramatically change the adsorption characteristics (e.g. Ramsden *et al.*, 1995), ultimately tests on human beings have to be carried out in order to have confidence in the results. To avoid, or minimize, the need for such *in vivo* experiments, it is highly desirable to develop laboratory simulations of the natural processes. In any case, the implant procedure cannot monitor the processes as they occur.

Fortunately, several optical techniques are now available that allow rather detailed quantitative, structural and kinetic characterization of the adsorption of proteins at the surface of a material. They are based on the phase shift of a beam of light totally internally reflected at the material/biofluid interface due to the accumulation of proteins (Ramsden, 1994). The most sensitive and informative technique (optical waveguide lightmode spectroscopy – OWLS) has the material in the form of an optical waveguide, which means that it is restricted to optically transparent substances. This is less of a restriction than might be imagined, since many ceramics used as medical materials (Table 1.1) are indeed transparent in practically useful regions of the optical spectrum, and most metals used for implants are coated with a layer of transparent oxide. If it is necessary to examine an opaque material, less sensitive techniques such as scanning angle reflectometry, ellipsometry or surface plasmon resonance (Ramsden, 1994) must be employed. The sensitivity of OWLS can be further augmented by configuring it as an interferometer (optical waveguide lightmode interferometry – OWLI), although fewer structural parameters can then be extracted from the measurements.

Chemical characterization of the adsorbed biomaterial can be achieved using vibrational spectroscopy in attenuated total internal reflexion mode, although this is less useful than in small-molecule chemistry because of the complexity of the absorption spectra of biomolecules.

In use, these techniques involve interrogation of the material in an appropriate form (e.g. a planar optical waveguide) while in contact with blood or any other relevant biofluid. Other techniques, useful for delivering complementary or corroborative data, include scanning probe microscopy and X-ray or neutron diffraction. The former is attractive because it allows high-resolution observation of the surface under biomimetic conditions, although the slow, raster-type interrogation of the surface generally precludes meaningful kinetic investigations. The latter techniques are generally only available for *ex situ* investigations of a preformed layer of adsorbed biomaterial.

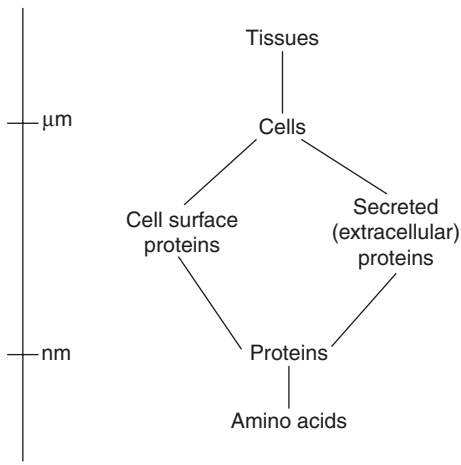
Some of these techniques can also be adapted to directly investigate the behaviour of living cells in contact with medical materials. The optical waveguide-based techniques are especially convenient in this regard (Ramsden and Horvath, 2009). The advanced application of OWLS enables successive slices of the cell parallel to the adsorbing substratum to be

© Woodhead Publishing Limited, 2013

interrogated in the fashion of confocal microscopy (Horvath *et al*., 2008). A significant advantage of these optical waveguide-based techniques is their ability to yield quantitative structural parameters *in situ* in real time, thus enabling rapid screening of the material for its compatibility with living cells (e.g. Aref *et al*., 2010). Scanning probe microscopies can also be adapted to observe living cells. In order to prevent the brutal contact of the scanning probe with the living cell in a conventional scanning probe microscope, the new technique of scanning ion conduction microscopy (SICM) has been developed (Gorelik *et al*., 2008). In this technique, the scanning probe is a miniature electrode. A large counter-electrode in the medium bathing the cells completes the circuit. When the miniature electrode is very close to the surface of a cell, the electrical resistance is high and this provides the information required to generate an accurate topography of cell surfaces without ever coming into actual content with them.

1.5 Conclusion

Considerations of the biological aspects of medical materials lead one to a hierarchy (Fig. 1.6): interactions between artificial material and biological matter mainly depend on interactions between the artificial material and proteins, which should therefore form the focus of research and development.



1.6 The hierarchy of interactions determining biocompatibility. Chemical functional groups (such as amino acid residues) determine the interfacial forces between proteins and artificial implants, and the ensemble of proteins expressed on the surface of cells determines the interaction between tissue and implant.

© Woodhead Publishing Limited, 2013

1.6 Future trends

The main development in recent years has been the opening of new possibilities in materials design and fabrication through nanotechnology. While we are still a long way from achieving such complete engineering control to enable any material of arbitrary shape and chemical composition to be created (but see Ly *et al*. (2011) for an encouraging sign of progress in this direction), there is already considerable fabrication capability in the submicrometre size domain, especially for regular structures, although whether their manufacture can be carried out cost-effectively at an appropriate scale remains to be seen. Above all, the problem is knowing *what* to make. There is a great need for more comprehensively systematic investigations of the responses of living cells and tissues to materials. Thanks to important advances in molecular biology, biological responses can be characterized in considerable detail and this capability, when coupled with comparable advances in creating precisely engineered material surfaces, should enable progress to be made. One difficulty seems to be the very large parameter space that is now available. It is, therefore, essential that more attention is paid to formulating hypotheses for the biological response to medical materials, which can then be rigorously tested.

1.7 Sources of further information

A basic introduction to biomedical surfaces is provided by Ramsden (2008). An encyclopaedic reference compendium for biomaterials is the work edited by Ratner *et al*. (2004). A good general work on materials is Ashby *et al*. (2007). For an overview of nanotechnology, including nanomaterials, one may consult the book by Ramsden (2011). The review by Ramsden *et al*. (2007) covers issues related to the fabrication of biomaterials.

1.8 References

Aggarwal, N., Lawson, K., Kershaw, M., Horvath, R. and Ramsden, J.J. (2009). Protein adsorption on heterogeneous surfaces. *Appl. Phys. Lett*. **94**, 083110.

Aref, A., Horvath, R. and Ramsden, J.J. (2010). Spreading kinetics as a means of quantifying cell state during stem cell differentiation. *J. Biol. Phys. Chem*. **10**, 53–54.

Arshady, R. and Kono, K. (eds) (2006). *Smart Nanoparticles in Nanomedicine*. London: Kentus.

Ashby, M., Shercliff, H. and Cebon, D. (2007). *Materials: Engineering, Science, Processing and Design*. Oxford: Elsevier.

Blumenfeld, L.A. (1981). *Problems of Biological Physics*. Berlin: Springer.

Bökel, C. and Brown, N.H. (2002). Integrins in development: moving on, responding to and sticking to the extracellular matrix. *Dev. Cell* **3**, 311–321.

© Woodhead Publishing Limited, 2013

Cacace, M.G. and Ramsden, J.J. (2007). In situ monitoring of adsorbed enzyme activity. *J. Biol. Phys. Chem*. **7**, 6568.

Cacace, M.G., Landau, E.M. and Ramsden, J.J. (1997). The Hofmeister series: salt and solvent effects on interfacial phenomena. *Q. Rev. Biophys*. **30**, 241–278.

Calonder, C., Talbot, J. and Ramsden, J.J. (2001). Mapping the electron 34 donor/acceptor potentials on protein surfaces. *J. Phys. Chem. B* **105**, 725–729.

Curtis, A.S.G., Casey, B., Gallagher, J.O., Pasqui, D., Wood, M.A. and Wilkinson, C.D.W. (2001). Substratum nanotopography and the adhesion of biological cells: are symmetry or regularity of nanotopography important? *Biophys. Chem*. **94**, 275–283.

Dalby, M.J., Gadegaard, N., Curtis, A.S.G. and Oreffo, R.O.C. (2007). Nanotopographical control of human osteoprogenitor differentiation. *Current Stem Cell Res. Therapy* **2**, 129–138.

Dalby, M.J., Andar, A., Nag, A., Affrossman, S., Tare, R., MacFarlane, S. and Oreffo, R.O.C. (2008). Genomic expression of mesenchymal stem cells to altered nanoscale topographies. *J. R. Soc. Interface* **5**, 1055–1965.

Fernández, A. (2006). Wrapping a hydrogen bond with a molecular force probe: the mechanical equivalent of dehydration propensity. *J. Biol. Phys. Chem*. **6**, 3–7.

Fernández, A. and Ramsden, J.J. (2001). On adsorption-induced denaturation of folded proteins. *J. Biol. Phys. Chem*. **1**, 81–84.

Fernández, A. and Scott, R. (2003). Dehydron: a structurally encoded signal for protein interaction. *Biophys. J*. **85**, 1914–1928.

Frauenfelder, H. (1984). From atoms to biomolecules. *Helv. Phys. Acta* **57**, 165–187.

Gorelik, J., Ali, N.N., Sheikh Abdul Kadir, S.H., Lab, M., Stojkovic, P., Armstrong, L., Sviderskaya, E.V., Negulyaev, Y.A., Klenerman, D., Bennett, D.C., Lako, M., Harding, S.E., Stojkovic, M. and Korchev, Y.E. (2008). Non-invasive imaging of stem cells by scanning ion conductance microscopy: future perspective. *Tissue Engng C* **14**, 311–318.

Hogg, T. (2007). Evaluating microscopic robots for medical diagnosis and treatment. *Nanotechnol. Perceptions* **3**, 63–73.

Horvath, R., Cottier, K., Pedersen, H.C. and Ramsden, J.J. (2008). Multi-depth screening of living cells using optical waveguides. *Biosens. Bioelectron.* **24**, 805–810.

Hunt, G. and Riediker, M. (2011). Building expert consensus on problems of uncertainty and complexity in nanomaterial safety. *Nanotechnol. Perceptions* **7**, 82–98.

Khor, H.L., Kuan, Y., Kukula, H., Tamada, K., Knoll, W., Moeller, M. and Hutmacher, D.W. (2007). Response of cells on surface-induced nanopatterns: fibroblasts and mesenchymal progenitor cells. *Biomacromolecules* **8**, 1530–1540.

Kutsevlyak, V.I., Starikova, S.L., Starikov, V.V., Mamalis, A.G., Lavrynenko, S.N. and Ramsden, J.J. (2008). Influence of implant surface modification on integration with bone tissue. *J. Biol. Phys. Chem*. **8**, 147–150.

Lavalle, P., Stoltz, J.-F., Senger, B., Voegel, J.-C. and Schaaf, P. (1997). Red blood cell adhesion on a solid/liquid interface: comparison of two models. *Clin. Hemorheol. Microcirc*. **17**, 307–313.

Levich, V.G. (1962). *Physicochemical Hydrodynamics*. Englewood Cliffs, NJ: Prentice Hall.

Li, S.-Y., Ramsden, J.J., Prenosil, J.E. and Heinzle, E. (1994). Measurement of adhesion and spreading kinetics of baby hamster kidney and hybridoma cells using an integrated optical method. *Biotechnology Progr*. **10**, 520–524.

© Woodhead Publishing Limited, 2013

Ly, D.Q., Paramonov, L., Davidson, C. Ramsden, J., Wright, H., Holliman N., Hagon, J., Heggie, M. and Makatsoris, C. (2011). The matter compiler – towards atomically precise engineering and manufacture. *Nanotechnol. Perceptions* **7**, 1–20.

Maitra, A. (2010). Nanotechnology and nanobiotechnology – are they children of the same father? *Nanotechnol. Perceptions* **6**, 197–204.

Mamalis, A.G., Ramsden, J.J., Grabchenko, A.I., Lytvynov, K.A., Filipenko, V.A. and Lavrynenko, S.N. (2006). A novel concept for the manufacture of individual sapphire-metallic hip joint endoprostheses. *J. Biol. Phys. Chem*. **6**, 113–117.

Mamalis, A.G., Lytvynov, K.A., Filipenko, V.A., Lavrynenko, S.N., Ramsden, J.J. and Soukakos, P.N. (2007). Perfection of contemporary hip joint endoprostheses by using a sapphire-sapphire friction pair. *J. Biol. Phys. Chem*. **7**, 3–5.

Mosbach, K. (1992). Preparation of synthetic enzymes and synthetic antibodies, and use of the thus prepared enzymes and antibodies. *US Patent* 5,110, 833.

van Oss, C.J. (2006). *Interfacial Forces in Aqueous Media*, 2nd edn. New York: Taylor & Francis.

van Oss, C.J. and Good, R.J. (1984). The 'equilibrium distance' between two bodies immersed in a liquid. *Colloids Surf*. **8**, 373–381.

van Oss, C.J., Chaudhury, M.K. and Good, R.J. (1987). Monopolar surfaces. *Adv. Colloid Interface Sci*. **28**, 35–64.

Nishihara, K. (2011). Great medical discoveries of the 21st century. Part I: Revitalizing stagnant medicine by establishing energy-based bioscience. Disclosure of the aetiological factors of three major intractable maladies at the subcellular level: immune diseases, carcinoma and mental illness. *J. Biol. Phys. Chem*. **11**, 63–85.

PAS (Publicly Available Specification) 132:2007. *Terminology for the Bio-nano Interface*. London: British Standards Institution.

Ramsden, J.J. (1993). Concentration scaling of protein deposition kinetics. *Phys. Rev. Lett*. **71**, 295–298.

Ramsden, J.J. (1994). Experimental methods for investigating protein adsorption kinetics at surfaces. *Q. Rev. Biophys*. **27**, 41–105.

Ramsden, J.J. (1998). Kinetics of protein adsorption. In: *Biopolymers at Interfaces* (ed. M. Malmsten), Chapter 10 (pp. 321–361). New York: Dekker.

Ramsden, J.J. (2003). Protein adsorption kinetics. In: *Biopolymers at Interfaces*, 2nd edn (ed. M. Malmsten), Chapter 8 (pp. 199–220). New York: Dekker.

Ramsden, J.J. (2008). *Biomedical Surfaces*. Norwood, MA: Artech House.

Ramsden, J.J. (2011). *Nanotechnology: An Introduction*. Oxford: Elsevier.

Ramsden, J.J. and Freeman, J. (2009). The nanoscale. *Nanotechnology Perceptions* **5**, 3–25.

Ramsden, J.J. and Horvath, R. (2009). Optical biosensors for cell adhesion. *J. Receptors Signal Transduction* **29**, 211–223.

Ramsden, J.J., Roush, D.J., Gill, D.S., Kurrat, R.G. and Willson R.C. (1995). Protein adsorption kinetics drastically altered by repositioning a single charge. *J. Am. Chem. Soc*. **117**, 8511–8516.

Ramsden, J.J., Allen, D.M., Stephenson, D.J., Alcock, J.R., Peggs, G.N., Fuller, G. and Goch, G. (2007). The design and manufacture of biomedical surfaces. *Annals CIRP* **56**/2, 687–711.

Ratner, B.D., Hoffman, A.S., Schoen, F.J. and Lemons, J.E. (eds) (2004). *Biomaterials Science: An Introduction to Materials in Medicine*. San Diego, CA: Academic Press.

© Woodhead Publishing Limited, 2013

Revell, P.A. (2006). The biological effects of nanoparticles. *Nanotechnol. Perceptions* **2**, 283–298.

Spielman, L.A. and Friedlander S.K. (1974). Role of the electrical double layer in particle deposition by convective diffusion. *J. Colloid Interface Sci*. **46**, 22–31.

Teixeira, A.I., Nealey, P.F. and Murphy, C.J. (2004). Responses of human keratinocytes to micro- and nanostructured substrates. *J. Biomed. Mater. Res*. **71A**, 369–376.

Vilain, S., Cosette, P., Zimmerlin, I., Dupont, J.P., Junter, G.A. and Jouenne, T. (2004). Bacterial proteome: homogeneity of versatility? *J. Proteome Res*. **3**, 132–136.

© Woodhead Publishing Limited, 2013

2

Introduction to joining methods in medical applications

L. QUINTINO, Technical University of Lisbon, Portugal

DOI: 10.1533/9780857096425.1.28

Abstract: The joining of materials has been used in manufacturing since the beginning of mankind and has become one of the key technologies in many manufacturing industries. This chapter begins with an introduction where general information is given about the joining techniques that are commonly used, followed by a description of some of the joining processes used in medical devices. The last section presents a few photographs of medical devices where welding has been employed.

Key words: joining technology, fusion welding, brazing, soldering, solid-state welding, adhesive bonding.

2.1 Introduction

The joining of materials has been used in manufacturing since the beginning of mankind and has become one of the key technologies in many manufacturing industries. With few exceptions, all products, machines or structures are assembled and fastened from parts. Joining is achieved through rivets, seaming, clamping, soldering, brazing, welding and the use of adhesives.

The medical-device industry is no exception. Medical devices are becoming more complicated, both in performance specifications and structural complexity. Medical devices typically consist of components and materials that must be joined in some way, whether used outside the body (in the form of instrumentation or surgical tools) or inside the body (for diagnostic monitoring or therapeutic purposes). Moreover, recently other joining methods besides stitching are also being applied for tissue bonding and skin closure.[1,2]

The ability to choose which joining process is appropriate at every step is critical in producing highly reliable devices, and the alternatives are diverse though all have advantages and limitations which ever application is targeted. The choice depends upon production economics as well as the mechanical properties desired in the final assembly. These properties go beyond just strength, covering issues such as vibration damping and

© Woodhead Publishing Limited, 2013

durability, corrosion or erosion resistance, as well as the ability to correct a defective final assembly.

Medical devices which are manufactured in a variety of materials such as metals, polymers and ceramics can be joined by mechanical fastening, welding and adhesive bonding. The complexity of the applications, the bio compatibility and the health-related legal requirements necessitate giving serious consideration to the joining processes used so that all requirements are met.

In this chapter a general overview of the joining technologies available is given, followed by a short description of the techniques more commonly used nowadays for medical devices. Joining processes are usually divided into three categories:

1. mechanical joining, where parts are joined through clamping and riveting, etc.;
2. welding, where parts are joined by fusion welding, brazing and soldering, and solid-state welding;
3. adhesive bonding, where parts are joint by applying an adhesive to the surfaces.

All three methods are used in medical devices though the material, size of the parts and application of the device imposes stringent limitations on the scope of processes with potential use.

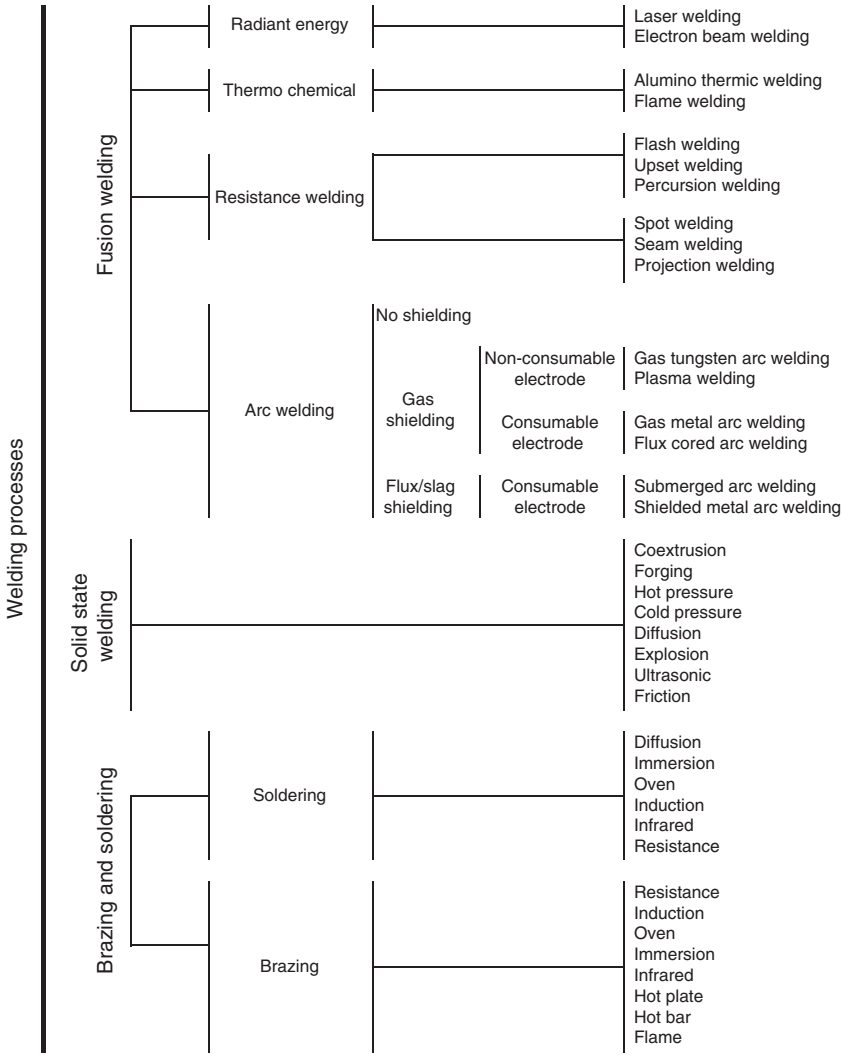
Joining the parts of surgical instruments which are not for invasive use has different requirements than joining prosthesis which are for invasive use and thus have special requirements in, for example, durability and corrosion resistance to cope with use inside the human body (see Chapter 14).

Mechanical joining is a process for joining parts through mechanical methods, which clamp or fasten the parts of the assembly together (e.g. nails, screws, bolts, rivets). Joining parts using screws or nuts and bolts are common examples of mechanical joining and can be found in many applications from simple chairs to sophisticated airplanes.

The advantages of mechanical joining include versatility, easiness to use and possible dismantling of the product, making it ideal for cases where periodic maintenance requires disassembly. The possibility of the joining of dissimilar materials is also an advantage. It allows movement of components relative to one another, for example by the use of hinges and bearings.

Mechanical joints also have disadvantages: the joint is achieved through discrete points thus not creating a continuous connection between the parts, while the holes employed for mechanical joining are vulnerable to fractures and galvanic corrosion.

© Woodhead Publishing Limited, 2013



2.1 Classification of welding processes.

Welding technology comprises three types of processes (Fig. 2.1):[1,3,4]

1. fusion welding, where there is melting and solidification of the zone being joined;
2. brazing and soldering, where joining is achieved by adding a melted filler material between the surfaces to be joined;
3. solid-state welding, where plastic deformation and diffusion are the main phenomena involved and there is no melting of base or filer materials.

© Woodhead Publishing Limited, 2013

Welding includes the joining process for metals and plastics where both the work pieces to be joined as well as the filler material used experience some melting. Examples include laser, electron beam, arc and resistance welding.

A common method for welding metals is arc welding, where an electric arc between an electrode and the work pieces to be welded together generates enough heat to melt the material under the arc. The joint is completed by solidification of the melted material from the parts being welded.

Arc-welding processes can use a consumable electrode from which the arc is generated, so that molten metal from the electrode and molten base metal from the work pieces all get mixed together, solidifying to form a strong joint upon cooling. In order to protect the molten material from contamination or the surrounding atmosphere a flux or a shielding gas are used.[5]

Most arc-welding processes are not used in medical applications since the related heat input, associated distortions and metallurgical transformations are inappropriate for the welding of small devices and, even in the cases where applicable, it would create defective welds. The required accuracy and quality are difficult to achieve.

High temperatures generated by the welding process alters microstructure in the welded areas, which creates a fusion zone associated with the molten metal and a heat affected zone (HAZ) that undergoes metallurgical transformations. This can change the mechanical behaviour of the material. The process of fusion and solidification also generates residual stresses that can lead to distortion. For these reasons the welding process must be optimized (heat input, metal composition and cooling rate) with a view to minimizing microstructural changes and residual stresses in welded joints. Post-weld heat treatments are often performed to relieve residual stresses and also for the purpose of changing the welded microstructure.

Resistance welding includes the fusion processes where heat is generated by the resistance of the work to the passage of electric current. Force is always applied during and after the application of current to create the weld.[5] The contacting surfaces in the region of current concentration are heated by a short time pulse of low-voltage, high-amperage current to form a fused weld nuget. When the flow of current ceases, the electrode force is maintained until full solidification of the weld metal.[1] Further information on these processes is given in Chapters 5 and 6.

Brazing is a process for joining two work pieces by the introduction of a filler metal that is melted between the two surfaces of the base material which is kept in a solid state.[5] The temperature at which brazing is done must be high enough to melt the filler material but not the base material. Materials used as fillers for brazing are those that melt above 450°C. Flux is also used during brazing for the purpose of eliminating oxide films from work-piece surfaces and avoiding oxidation. This ensures a good metallurgical bond

© Woodhead Publishing Limited, 2013

between the work pieces and the filler. Filler alloys used for brazing include copper–silver, zinc–copper and copper–nickel. The brazing material, once melted, fills up the spaces between the surfaces being joined, and flows into tight spaces by capillary action. A strong joint is thereby achieved after the brazing material has cooled down.

Soldering is a similar process to brazing, but performed at much lower temperatures. In soldering two work pieces are joined, so that only the filler metal undergoes melting; that is work pieces do not experience melting. Typically soldering materials melt at less than 450°C while brazing materials melt above this temperature. Common soldering materials include alloys in tin–lead, tin–zinc, lead–silver and cadmium–silver alloys. Like welding and brazing processes, soldering also employs materials (i.e. flux) to clean the surfaces being bonded. In the case of soldering flux, residues must be removed to reduce the risk of corrosion.

Solid-state welding includes the joining processes where pressure or temperature, or both, are used to achieve the joint.[5] No melting occurs in the base or filler material. In some cases a relative motion of the parts being joined is used to achieve the generation of heat. The application of pressure assures the plastic deformation or diffusion needed to accomplish joining. A filler metal may be inserted between the surfaces being welded.

Solid-state welding has the advantages of allowing to join similar and dissimilar metals and to obtain a continuous joint between the faying surfaces with minimal distortion. The disadvantages of these processes are that they cannot be adaptable to high production rates, surface preparation needs greater care than in fusion welding or brazing and soldering and the need of applying simultaneously heat and pressure leads to high equipment costs.

Adhesive bonding is a process for joining parts using bonding chemicals (materials known as adhesives).[6] This process is employed to join polymers and polymer–matrix composites, as well as polymers to metals, metals to metals and ceramics to metals. Adhesive-bonded joints have the characteristic that they can withstand shear, tensile and compressive stresses, but they do not exhibit good resistance against peeling. This last weakness of adhesive bonding requires a good design (i.e. the adhesion area must be maximized and mechanical interlocking is employed).

Maximum strength in adhesive bonding requires thoroughly cleaned surfaces. This, in essence, minimizes the interfacial gap between the adhesive and the adherent (material to be joined). Surface roughness improves mechanical interlocking and thus bond strength.

Medical devices which are manufactured in a variety of materials such as metals, polymers and ceramics can be joined by mechanical fastening, welding and adhesive bonding. The complexity of the applications, the bio compatibility and the health-related legal requirements necessitate giving serious consideration to the joining processes used so that all requirements

© Woodhead Publishing Limited, 2013

are assured. Not all the processes presented in Fig. 2.1 are used in medical devices.

Welding and adhesive bonding are the processes most widely used in medical devices. For metals the fusion welding process most often referred in the literature is laser welding while solid-state welding processes examples are ultrasonic, diffusion and friction welding. When considering polymers, hot-plate and hot-bar welding, ultrasonic and impulse welding are some of the techniques used, while adhesive bonding is possibly the most common joining method for this type of materials.

In the following chapters a description of the characteristics of the joining processes most often used in medical devices is presented. The list of processes addressed in not meant to include all joining processes that can be used in medical devices. It refers to joining processes frequently referred in the literature as giving good results in medical devices. Many more processes exist, some of which are variants of the referred ones and some based on different principles.

2.2 Welding processes

The welding process most commonly used in assembling metallic medical devices is laser welding. Other processes such as resistance welding,[7,8] and gas tungsten arc welding,[9] are described in the literature as achieving good results in the welding of NiTi parts or in particular applications like catheters and pacemakers. More recently the application of friction-stir welding (FSW) is increasing. For welding of polymers laser welding is also used and other processes include radio-frequency (RF) welding, ultrasonic welding (USW), diffusion welding, hot-plate and hot-bar welding.

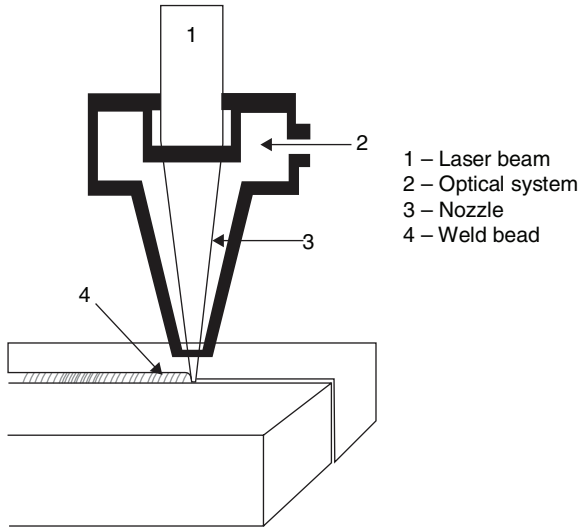
Selecting the best process for the welding of medical products involves a number of considerations which include the type of base material, the size of the part, the number of parts to be welded, the process capability and the cost.

The following chapters of this book detail the use of the different joining techniques for specific applications, while this chapter gives a brief explanation of the characteristics of the welding processes most often used in medical applications.

2.2.1 Laser welding

Laser-beam welding is a fusion welding process where radiant energy is used to produce the heat required to melt the materials being joined.[5,10–13] A concentrated beam of coherent, monochromatic light is directed by optical devices and focused to a small spot, for higher power density, on the abutting surfaces of the parts being joined (Fig. 2.2). Gas shielding is generally

© Woodhead Publishing Limited, 2013



2.2 Laser welding.

used to prevent oxidation of the melted material. It provides consistent joining and high flexibility. Different parts and even different metals can be joined in a non-contact process. The required accessibility to the work piece being from one side only and the opportunity to abandon filling material completely are the main advantages of laser-beam welding. Laser joining can be performed using either pulsed or continuous lasers. A pulsed laser can be used to create weld seams by means of overlapping pulses.

Lasers have played an important role in the joining of materials since the invention of high-power solid-state and gas lasers in 1964, especially for resistance trimming of electronic circuits, until the introduction of a reliable high-performance laser in the late 1970s, which allowed its application for welding of sheet-metal parts.

Several types of lasers can be used in materials processing though the most common have wavelengths of 10.6 μm – CO_2 lasers (gas lasers), or 1.06 μm – Nd-YAG lasers (solid-state lasers). The last decades have seen the rise of diode lasers and diode-pumped solid-state lasers. More recently high-power diode-pumped fibre lasers were developed. Fibre lasers are a serious alternative to solid-state and carbon-dioxide lasers for different materials-processing applications.

The CO_2 laser is a well-established materials-processing tool, available in power output up to 50 kW, and most commonly used for metal cutting.[14] CO_2 laser radiation (wavelength 10.6 μm) is readily absorbed by the surface layers of most metals and plastics. The CO_2 laser beam cannot be transmitted

© Woodhead Publishing Limited, 2013

down a silica fibre optic, but its path can be determined using mirrors, lenses in optical systems and wither gantry or robotic movement.

The Nd:YAG laser (Neodymium Yttrium Aluminum Garnet) is also well established for materials processing; it has a wave length of 1.06 μm and is a smaller laser available in powers up to 10 kW. The Nd:YAG laser beam can be transmitted down a silica fibre optic enabling easy, flexible operation with gantry or robot manipulation. However, the light from Nd:YAG lasers is absorbed far less readily in plastics than that of CO_2 lasers.

Small focus spots for CO_2 and Nd-YAG lasers are achieved through optical systems mounted in the arm of the robot or gantry systems.

High-power diode lasers (>100 W) have been available since the late nineties.[14] Recent developments have made available diode lasers up to 5 kW and competitively priced compared with CO_2 and Nd:YAG lasers. Diode lasers are energy efficient compared with other solid-state lasers (i.e. power input versus power output is 30 per cent, while for Nd:YAG laser it is 15 per cent). With diode lasers a rectangular beam shape is produced, which, while being preferential for some applications, limits the minimum spot size and maximum power density available. The diode laser source is small and light enough to be mounted on a gantry or robot for complex processing.

Excimer lasers are gas lasers which were first operated in 1975, some years after the CO_2 and Nd:YAG lasers.[14] The gases used to produce the laser beam are inert gas (e.g. Ar, Xe, Ne). They are available with average powers up to about 1 kW and focusable to very high-power densities. There is a family of wavelengths available by exciting different phases within the laser. These are all in the ultraviolet (0.15–0.35 μm), and lie in a photon energy range capable of breaking chemical bonds and splitting molecules. Excimer laser light is absorbed by molecules in the surface of plastics (<10 μm depth) and rapidly breaks the molecular bonds within the polymer structure. Consequently, this leads to a rapid increase in pressure and expulsion of material over a very precise region defined by the laser-beam size. Excimer laser beam is transmitted by mirrors and often focused through masks to give the required features on the material surface.

Fibre lasers were created in the early sixties and used widely at low-power levels throughout the 1980s and the 1990s as optical amplifiers. In 2000 the first 100 W fibre laser was launched. The first reports on the potential of these lasers in materials processing are very recent.[15,16] The multi-kilowatt range for materials processing with fibre laser is now possible with the recent commercialization of 7–10 kW power lasers.

These new lasers have multiple advantages: high efficiency, compared with the other types of lasers; a compact design, which simplifies its installation; a good beam quality, due to the use of thin fibres and thus a small beam focus diameter; and a robust set-up for mobile applications. The scaling of the

© Woodhead Publishing Limited, 2013

laser power is achieved by a modular design comprising several single-mode lasers. The lifetime of the pumping diodes exceeds the expected lifetime of other diode-pumped lasers, which leads to low costs of ownership.

The high-power lasers can be used for deep penetration welding in a diversity of materials and constructions as the low wavelength, similar to the one from the Nd-YAG lasers, that characterizes these lasers allows its absorption by almost all metals and alloys and the fibre delivery system provides the necessary flexibility on the positioning of the beam. Also high-speed welding of sheet-metal joints can surpass the productivities achieved with high-power CO_2 lasers. Due to the low wavelength its use on the welding of plastics presents the same limitations as Nd:YAG lasers.[16]

In general, the use of lasers to deliver the energy necessary for welding has the following advantages:

- high speed;
- no contact with a heated tool;
- highly automated and robotically manipulated;
- controlled heating for low thermal damage or distortion.

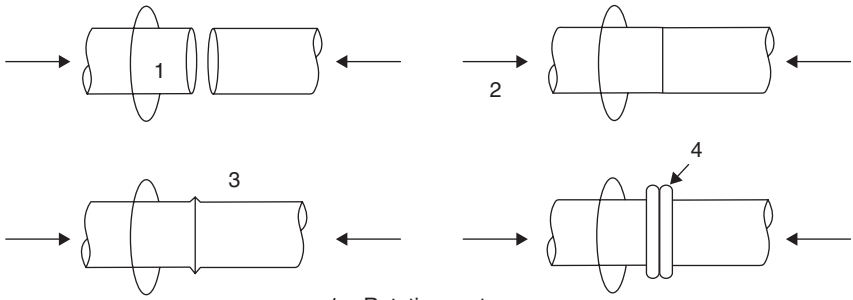
Laser techniques are also used for the welding of plastics in medical application as an alternative to vibration, ultrasonic, dielectric, hot-plate or hot-bar welding and adhesive bonding.[14]

Lasers are an attractive tool for processing of metals and also polymers as it allows a precise delivery of a controlled amount of energy precisely on the point where it is required (e.g starting point of a weld, spot welding). In addition, lasers are available with outputs covering a range of wavelengths, which has a large bearing on the interaction of the light with the plastic materials. An understanding of these absorption characteristics has led to the development of other novel applications in plastics processing. Common applications include end effector tools to tube bodies and hermetically sealing implantable devices.

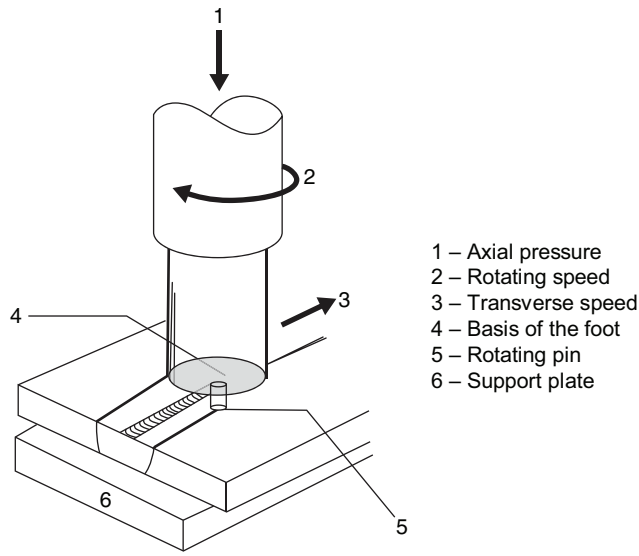
2.2.2 Friction welding

The heat necessary to induce plastic deformation in metals and to soften and melt some plastics can be achieved by simple friction when the two parts being joined are moved rapidly while in mutual contact (Fig. 2.3). This technique is most commonly used when two circular parts are welded, a circular part is being welded to a flat plate or a circular rod is being welded inside a hole. For maximum efficiency, the surfaces being friction welded should be relatively smooth and free of contamination. Very large surfaces are difficult to weld by this method because of

© Woodhead Publishing Limited, 2013



2.3 Friction welding.

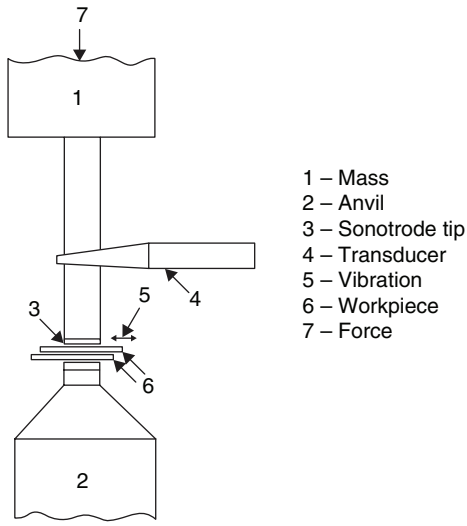


2.4 Friction-stir welding.

the large amount of energy that is required to melt or soften the entire surface simultaneously.

Friction-stir welding (FSW) is a solid-state welding process in which a spinning non-consumable tool is forced along the joint line, heating the abutting components by friction, and producing a weld joint by extrusion (around the tool pin), forging (under the tool shoulder and the base of the tool pin) and large-scale plastic flow mixing (stirring) of the material from the two components, in the vicinity of the tool (Fig. 2.4).[17]

© Woodhead Publishing Limited, 2013



2.5 Ultrasonic welding.

Friction-stir welding has been reported to be possible to use for joining parts in Nitinol, a shape-memory alloy, which is difficult to fusion weld to itself and to other metals.[18,19] One of the most common uses of Nitinol is in the production of biomedical devices such as arterial stents. The Nitinol retains its shape memory and superelastic properties following processing.

2.2.3 Ultrasonic welding

Ultrasonic welding (USW) is a solid-state welding process that produces a weld by local application of high-frequency vibratory energy while the work pieces are held together under pressure.[5] A sound metallurgical bond is produced without melting the base material.

Typical components of an ultrasonic-welding system are illustrated in Fig. 2.5; these include sonotrode, transducer and anvil. The ultrasonic vibration is generated in a transducer and the vibration is transmitted through a coupling system or sonotrode. The sonotrode tip makes direct contact with one of the work pieces there by transmitting the vibratory energy into it. The clamping force is applied axially through the sonotrode. The anvil supports the welding and opposes the clamping force.

Ultrasonic welding is used for applications involving both similar and dissimilar joints as well as the welding of polymers. The process is used to produce lap joints in metals, plastic sheets and plastic films in varied shapes as wires (crossed or parallel), ribbons and flat surfaces. For joining other types

© Woodhead Publishing Limited, 2013

of assembles that can be supported on an anvil, set-ups are designed for the material and the part shape required.

Next to fusion, the most important non-adhesive and non-mechanical method of joining plastics is ultrasonic welding.

2.2.4 Diffusion welding and brazing

Diffusion welding (DFW) is a solid-state welding process that produces a weld by the application of pressure at elevated temperature with no macroscopic deformation or relative motion of the work pieces.[20] A filler metal may be inserted between the faying surfaces.

Several kinds of metal combinations can be joined by diffusion welding:[18]

1. Similar metals may be joined directly to form a solid-state weld. The required pressures, temperatures and times are dependent only upon the characteristics of the base metals and their surface preparation.
2. Similar metals can be joined with a filler metal where this takes the form of a thin layer of a different metal which is situated between the metals to be joined. In this case one of the roles of the filler metal is to promote a more rapid diffusion and permit increased microdeformation at the joint to provide more complete contact between the surfaces. The filler metal may then be diffused into the base material by suitable heat treatment.
3. Two dissimilar metals may be joined directly where diffusion-controlled phenomena occur to form a metallic bond. The mechanisms are similar to those in category 1 above. In addition dissimilar metals may create added effects such as improved initial contact.
4. Dissimilar metals may be joined with a third metal; that is, a filler metal, between the faying surfaces to enhance weld formation either by accelerating diffusion or permitting more complete initial contact in a manner similar to category 2 above.

Diffusion brazing (DFB) is a process that forms liquid braze metal by diffusion between dissimilar base metals or between base metal and filler metal pre-placed at the faying surfaces. The process is used with the application of pressure. The filler metal may be diffused into the base metal to the extent that a distinct layer or brazing filler metal does not exist in the joint after the diffusion-brazing cycle is completed. The joint properties approach those of the base metal. The process is sometimes called liquid-phase diffusion-bonding eutectic bonding, or activated diffusion bonding.

© Woodhead Publishing Limited, 2013

2.2.5 Radio-frequency welding

Radio-frequency welding (RFW) has similarities to USW.[14,18] The main differences are that the frequency is higher and the power is lower. This process is mainly used for the welding of plastics. Some plastics are highly susceptible to induced vibrations in the radio-frequency range which produce an oscillation in the plastic molecules as the alternating current switches polarity. Some molecules attempt to align with these alternating signals and produce heat when radio-frequency energy is applied.

2.2.6 Induction welding

Induction welding relies on the heat generated by utilizing the property of some materials to vibrate in a magnetic field.[14,18] This process is mainly used for the welding of plastics. Induction welding is produced by generating electromagnetic heating in metal particles located inside a plastic matrix. That is, heat is generated by utilizing the property of metals to vibrate in a magnetic field inducing current. Heating in the plastic results from conduction of heat generated in the metallic particles.

One inductive welding technique is to place a thin metal shim between two plastic surfaces and apply an external electromagnetic field. The result is that heat generated in the shim wall causes local melting of the plastic which will lead to fusion. Another induction-welding technique is simply to place the plastic materials to be joined around a metal part (such as a rod) and then pass the rod and material through a magnetic field. Sufficient heat can be generated to fuse the plastic materials.

2.2.7 Hot-plate and hot-bar welding

Hot-plate welding is performed by pressing the parts being joined against a heated plate, and removing the parts when these are sufficiently melted and pressing them until the joint cools down.[14,18]

The plates are usually heated using resistance heaters and for most of the applications flat plates are used, though more complex shapes can be manufactured. The welding parameters are the temperature of the plates, the heating time, the welding pressure and the welding time. Thermoplastics can be welded using this technique and provided a good welding procedure is used the tensile strength of the joint equals the base material.

Hot-bar welding is a technique mainly used to join thermoplastic films, that is, materials having a thickness of less than 0.5 mm. It is based on the principle that if two thermoplastic films are pressed against a heated metal bar, they will soften and a joint can be made between them. Since the

© Woodhead Publishing Limited, 2013

technique relies on the conduction of heat through one of the films, this limits the thickness of material that can be welded. Some times two heated bars are employed, on either side of the films, and this has the effect of reducing the welding time.[11]

2.3 Adhesive bonding

Adhesive bonding is used to join metallic and non-metallic materials and is a technique used for medical devices both in plastic and in metals. The surfaces being joined are not melted although they may be heated.[6,18,21–24]

When two materials are joined together using adhesive bonding, those two materials are called the adherents, or substrates. The material that forms the bond between them is called the adhesive.

The first step in the joining process is the preparation of the adherent, by cleaning, etching or surface treatment to create the surface on which the adhesive is applied.[18] An adhesive is then applied in various ways where these include a liquid, a paste or a tacky solid each of which is to be placed between the faying surfaces of the joint. Liquid adhesives are commonly applied by brush, spatula, roller, flow gun, spray and dip coating. Some of these methods such as dip coating and spraying are especially useful for adherents that have complex shapes. Rolling and spatulas are better for flat surfaces. Film adhesives work best on flat panels but can be shaped into fairly complex forms by cutting and applying in strips (i.e. pressure is required to make sure that the adhesive flows to fill in gaps between the strips).

After application of the adhesive, the coated adherents are placed together and held until the adhesive becomes solid. A press can be used to hold the pieces together but jigs and fixtures that keep the alignment of the part and apply moderate pressure are also common. Most adhesives need to be pressurized during cure. If a press is not used, mechanical pressure devices like clamps or springs work well. Another way to exert pressure is with a vacuum bag.

When under pressure or in the jig/fixture, the adhesive solidifies. That step can be done by simply allowing the adhesive to cool (if it is a hot-melt adhesive) or by curing the adhesive (if it is a thermosetting material). During cure the important parameters are temperature and time. Ideally, the bond between the adherent and the adhesive will be so strong that if fracture occurs, it will be either within the adhesive itself or within the adherent itself rather than at the junction between them.

Typical examples of medical-grade adhesives are given below:

- Silicone adhesives: Organo-polysiloxanes, generally known as silicones, are semi-inorganic-based polymers with a molecular structure made up

© Woodhead Publishing Limited, 2013

Table 2.1 Summary of benefits, limitations and typical applications of common medical device adhesives

Adhesive type	Benefits	Limitations	Typical applications
Cyanoacrylate	Substrate versatility Rapid cure Adhesion to polyolefins with primers	Thermoplastic resin when cured Poor peel strength, rigid Refrigeration required	Catheter components Tube-set bonding Polyolefin bonding
Light-curable acrylic	Substrate versatility Good resistance properties Cure on demand	Capital expenditure for light-cure equipment	Needle assembly Anaesthesia masks Heat exchangers Oxygenators Tube-set bonding
Epoxy	Substrate versatility Superior thermal and chemical resistance Low shrinkage High gap filling	Poor peel strength, rigid Exothermic reaction Two-part systems require mixing	Needle assembly Deep section potting
Polyurethane	Substrate versatility High peel Good resistance properties	Moisture sensitivity Primers required for some substrates Two-part systems require mixing	Deep section potting Bonding of tips onto various components

of alternating silicon and oxygen atoms with organic side or end groups attached to some or all of the silicon atoms. Depending on the nature of side groups and the inter-chain cross-linking, silicones are available in the form of gels, liquids or elastomers.

- Epoxies: The epoxy resins are thermoset adhesives based on the epoxide group, a three-membered carbon, carbon and oxygen ring structure which is also known as oxirane group. The ability of this group to undergo a large variety of polymerization and cross-linking reactions leads to many different types of epoxy resins with a wide range of chemical and physical properties, molecular weight and molecular structures. Epoxies are one of the most widely used adhesives for both structural and non-structural applications. Epoxies have been used in a number of medical devices for bonding and sealing applications.

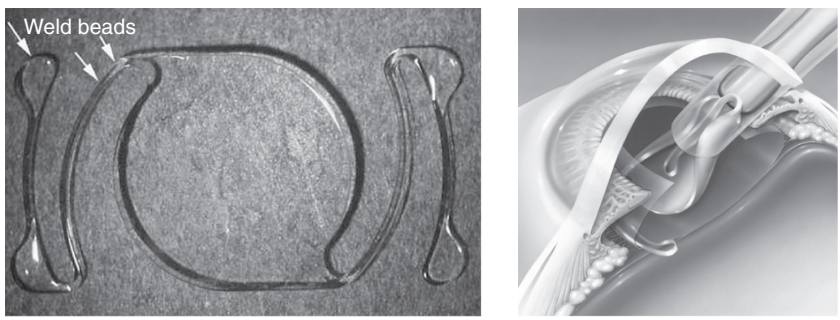
© Woodhead Publishing Limited, 2013

- Acrylics: There is a wide range of acrylic-based adhesives that have been used to join a variety of similar and dissimilar materials. The main types of acrylic-based adhesives are cyanoacrylates, anaerobics and modified acrylics. These adhesives are usually available as solvent-based liquids, emulsions or tapes, or as monomer–polymer mixtures (one- or two-part components), with liquid or powder curing agents. Acrylic-based adhesives may be polymerized or cured using moisture, catalysts, heat, ultraviolet (UV), visible light or other sources of radiation. These adhesives are of particular interest in the medical industry both for joining medical devices and as tissue bonding agents.
- Polyurethanes: Medical-grade polyurethanes are being used as adhesives, encapsulants or coatings in many medical devices. Most commercially available polyurethane systems are based on polyethers or polyesters with terminating hydroxyl functional groups. The reaction of alcohol and isocyanate results in the formation of urethane.

Table 2.1 presents a summary of the benefits and limitations of these adhesives and gives examples of applications.

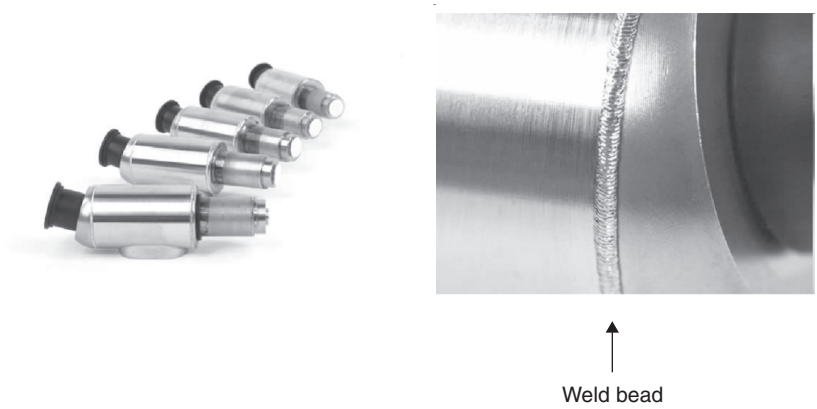
2.4 Examples of applications

Many examples of applications of joining techniques for medical devices can be found in the literature. Figures 2.6–2.9 depict a few of these applications where the welds are signalled. Many more will be found in the later chapters of this book.

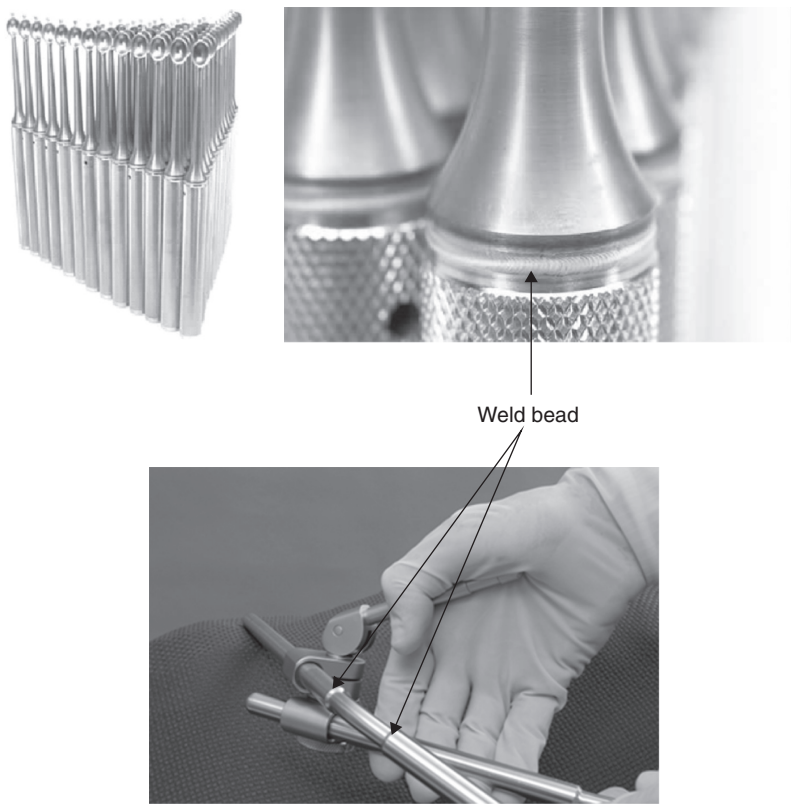


2.6 Laser welding of intraocular lenses.

© Woodhead Publishing Limited, 2013

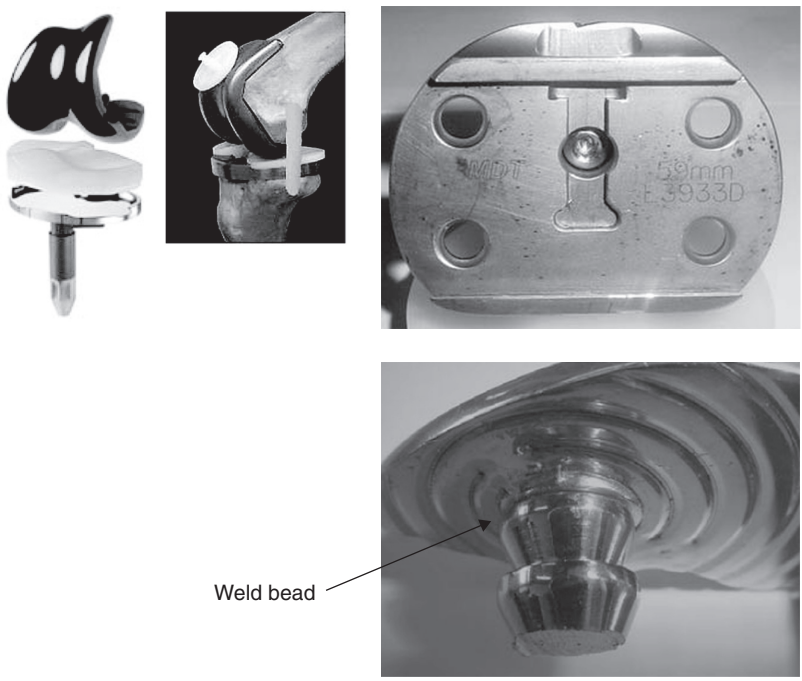


2.7 Laser welding of endoscopes.



2.8 Laser welding of surgical parts.

© Woodhead Publishing Limited, 2013



2.9 Laser welding of dissimilar joints in knee prostheses.

2.5 References

1. *ASM Handbook, Vol. 6: Welding, Brazing and Soldering*, ASM (American Society of Metals, ISBN: 9780871703828, 1993.
2. Y. Zhon, *Microjoining and Nanojoining*, Woodhead Publishing, 2008.
3. J.F. Oliveira Santos and L. Quintino, *Processos de soldadura*, Lisbon, Ed. ISQ, 1998.
4. I. G. Machado, *Soldagem e técnicas convexas: processos*, PortoAlegre, 1996.
5. *Welding Handbook: Welding Processes*, *Vol. 2*, 8th edn, American Welding Society (AWS), 1991.
6. A. B. Strong, *Plastics Materials and Processing*, 3rd edn, Prentice Hall, 2006.
7. B.H. Chang, M.V. Li and Y. Zhou, 'Comparative study of mall scale and "large scale" resistance spot welding', *Science and Technology of Welding & Joining*, vol. **6**, no. 5, pp. 273–280, Oct. 2011.
8. S. Fukumoto, K. Fujiwara, S. Toji and A. Yamamoto, 'Small-scale resistance spot welding of austenitic stainless steels', *Materials Science and Engineering: A*, vol. **492**, nos 1–2, pp. 243–249, Sept. 2008.
9. M. H. Wu, 'Fabrication of nitinol materials and components', *Materials Science Forum*, vols **394–395**, pp. 285–292, 2002.
10. F. Mian, G. Newaz, L. Vendra *et al*., 'Laser bonded microjoints between titanium and polyiide for applications in medical implants', *Journal of Material Science-Materials in Medicine*, vol. **16**, no. 3, pp. 229–237, Mar. 2005.

© Woodhead Publishing Limited, 2013

11. M. Tolinski, 'Lasers focus on medical devices – for small, delicate part applications, lasers deliver stable, accurate energy for cutting, marking and welding', *Manufacturing Engineering*, vol. **138**, no. 5, pp. LT1–LT7, May 2007.
12. Anon. 'Precision micro laser welding joins range of medical devices', *Advanced Materials & Processes*, vol. **164**, no. 1, p. 74, Jan. 2006.
13. M. I. Khan, S. K. Panda and Y. Zhou, 'Effects of welding parameters on the mechanical performance of laser welded nitinol', *Materials Transactions*, vol. **49**, no. 11, pp. 2702–2708, Nov. 2008.
14. S.B. Dunkerton and S.M. Tavakoli, 'Process developments enabling more effective joining of medical devices', ASM 2004 Materials & Processes for Medical Devices Conference, St. Paul, MN, 2004. Available from: www.twi.co.uk/content/spsbdaug2004.html.
15. P. Hill, 'Fiber laser hits 2kW record mark', *Opto and Laser Europe (OLE)*, p. 9, 2002.
16. L. Quintino, A. Costa, R. Miranda, D. Yapp, V. Kumar and C.J. Kong, 'Welding with high power fiber lasers – a preliminary study', *Materials & Design*, vol. **28**, no. 4, pp. 1231–1237. Included in *Science Direct* Top 25 Hottest Articles, October 2007. doi: 10.1016/j.matdes.2006.01.009.
17. N. Pépe, P. Vilaça and L. Quintino, 'Metallurgical and corrosion features of friction stir welding of AA5083-H111', *Welding in the World*, vol. **50**, no. 9/10, pp. 55–64, 2006.
18. F. F. Chipperfield and S. B. Dunkerton, 'Welding and joining techniques for polymeric medical devices', Medical Device Technology. Available from: http://www.twi.co.uk/content/spfamay2001.html, 2001.
19. B. London, J. Fino, A. Pelton, C. Fuller and M. Mahoney 'Friction stir processing of nitinol', The Minerals, Metals and Materials Society, 2005.
20. M.M. Schwartz and J.M. Gerken, 'Diffusion welding and brazing', *Welding Handbook*, chapter 26, pp. 814–837, American Welding Society (AWS), 1991.
21. T. Shah, 'Polyurethane thin-film welding for medical device applications', *Medical Device and Diagnostic Industry*, September 2002.
22. C. Salerni, 'Selecting engineering adhesives for medical device assembly', *Medical Device and Diagnostic Industry*, June 2000.
23. M. Tavakoli, 'A guide to adhesives in medical applications'. Available from: www.twi.co.uk.
24. L. Quintino and I. Pires, 'Overview of the technology of adhesive bonding in medical applications', *Business Briefing: Medical Devices Manufacturing and Technology, Materials/Biomaterials*, pp. 55–56, 2004.

© Woodhead Publishing Limited, 2013

3

Microwelding methods in medical components and devices

K. J. ELY, GlaxoSmithKline Corporation, USA,
P. HALL, Boston Scientific Corporation, USA and
Y. ZHOU, University of Waterloo, Canada

DOI: 10.1533/9780857096425.1.47

Abstract: Implantable cardiac rhythm devices, cochlear implants, and neurostimulators are some of the most complex medical devices. Not only do they comprise all of the materials of electronic assemblies, they require the biocompatibility and extreme reliability required for human use. The selection of the outer-case materials is typically driven by the ability to provide a hermetically sealed enclosure, and long-term corrosion resistance. Typical materials now in use include 316L stainless steels, MP35N, titanium, niobium, and alloys of platinum–iridium. Microjoining for these materials and applications includes the welding of pacing lead coils to terminal pins via resistance and laser-spot welding, laser-seam welding thin titanium housings, and spot welding of thin electrode rings to interconnect wires by various welding techniques. This chapter will review key aspects of material choices and the typical joining processes for medical devices.

Key words: medical devices, implantable, microjoining, biocompatibility, microwelding, hermetic sealing.

3.1 Introduction

The ageing of America and many of the industrialized countries has placed a burden on the healthcare industry. A key area within healthcare today is the burgeoning field of implantable medical devices and components. These devices include the now well-known pacemakers, but also include implantable defibrillators, heart failure cardiac care, neurostimulators, pumps, drug delivery, arterial stents, and other smart electronics or components.

All of these devices contain a wide variety of materials and joining processes. Due to the implant size and their intended purpose, the raw materials and assembly processes must be of the highest quality and reliability. Medical devices can be some of the most demanding applications due to the requirements for biocompatibility. The degree of compatibility required is driven by the type of application and the time requirement for interaction

© Woodhead Publishing Limited, 2013

with the human body. These applications are typically divided into three classes per FDA specification, with class I being minimal risk, such as a monitoring device or external pump, to a Class III device such as a permanently implanted arterial stent or pacemaker.[1] An additional requirement for medical devices is the need for extremely high reliability, to avoid any adverse risk to a patient. The combination of these two requirements, biocompatibility and reliability, makes medical devices a challenge to design and manufacture.

Some medical devices seem simple, yet have high degrees of complexity to predict final form and function. An example of this type of device is a bare metal stent. They are simple only in the sense that they are manufactured (laser cut) from a single tube of specialty metal, typically a cobalt bearing alloy, or other special alloys of nickel–titanium. These alloys can be fabricated with an optimal surface finish for the adhesion of supplemental polymer coatings that are doped with steroid drugs to control the normal inflammation response of the body and to control chronic restinosis.

Larger, more complex medical devices would include prostheses, including knee and hip replacements, polymer finger joints, and new vertebral disc implants. Many of these types of implants use multiple materials and forms of materials to enhance the human body's response to the material. The hip implant is an excellent example. The ball of the acetabular insert is covered in small cobalt alloy spheres, which yield a high surface area for bonding into the pelvic bone. An insert of high molecular weight polyethylene is used in the acetabular cup to provide a lubricious smooth surface for the mating ball socket of the hip implant. In this example the cobalt spheres are joined to the main body of the implant by sintering, while the high molecular weight polyethylene cup is ultrasonically staked through an opening in the metal housing.[2]

Implantable cardiac rhythm devices, cochlear implants, and neurostimulator devices are some of the most complex medical devices. Not only do they comprise all of the materials of electronic assemblies, they require the biocompatibility and extreme reliability required for human use. So the selection of the outer-case materials is typically driven by the ability to provide a hermetically sealed enclosure, and long-term corrosion resistance. Typical materials now in use include 316L stainless steels, MP35N, titanium, niobium, and alloys of platinum–iridium. Microjoining in this application includes the welding of pacing lead coils to terminal pins via resistance and laser-spot welding, laser-seam welding thin titanium housings, and spot welding of thin electrode rings to interconnect wires.

This chapter will review key aspects of material choices and the typical joining processes for medical devices.

© Woodhead Publishing Limited, 2013

3.2 Materials challenges

Implantable devices are approved for use by the FDA according to a device's ability to provide therapeutic value to the patient. Since the full device is approved in the process, individual materials alone are not approved for use. Therefore, most designs leverage off past proven designs where a material has been shown to perform well within a system.

Materials that have passed device-level approvals for a wide variety of implants are shown in Table 3.1. These materials all have the following key characteristics:

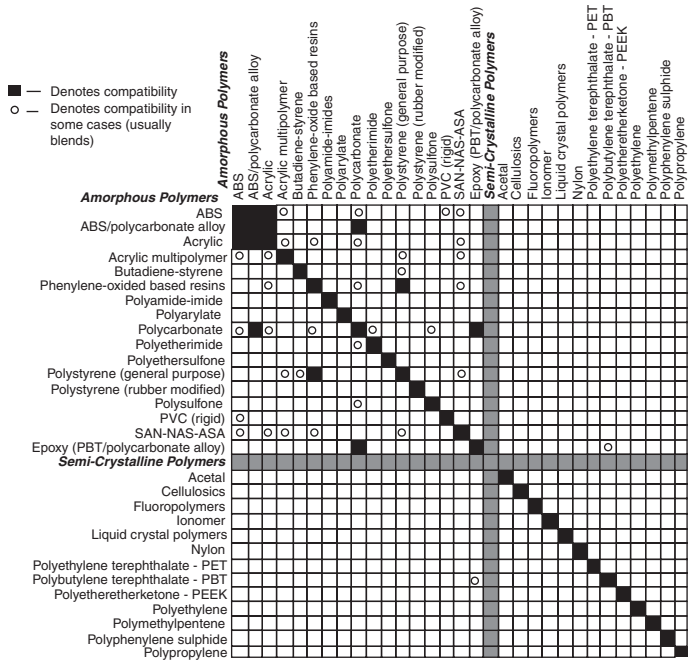
- biocompatible;
- corrosion resistant;
- consistent surface quality;
- amenable to welding and joining.

These materials are generally chosen at the beginning of design efforts due to their corrosion, electrical, and biocompatibility performance. However, that does not mean they can be joined in any combination using any methods. Further, while macroscopic size assemblies can often be joined, small-scale microscopic assemblies require more effort to maintain a tight joint during joining processes. Figures 3.1 and 3.2 highlight many common medical grade materials and their ability to be joined by various welding technologies. The tables assume a full fusion joint is developed between the parent materials. Many solid-state welds can be formed from combinations that under full fusion would develop unusable intermetallics. Similarly, the speed

Table 3.1 Implantable materials

Material	Application	Joining methods
Platinum	Wires, coils, electrodes, pins	Resistance, laser, ultrasonic
Pt/iridium	Wires, coils, electrodes	Resistance, laser, ultrasonic
Tantalum	Wire, coils	Resistance, laser, brazing
Titanium	Wires, coils, terminal pins, pulse generator (PG) cases	Resistance, laser, brazing
MP35N	Wires, coils, terminal pins PG cases, battery cases	Resistance, laser
Kovar	Standoffs, interconnect pads	Resistance, laser, brazing
316 SS	Wires, terminal, battery cases, capacitor cases	Resistance, laser, brazing
Lead free solders	Surface mount bumps, general soldering	Brazing, soldering, ultrasonics
Polyurethane	Tubings, seals	Laser, adhesive
Silicone	Tubings, seals, adhesives	Adhesives

© Woodhead Publishing Limited, 2013



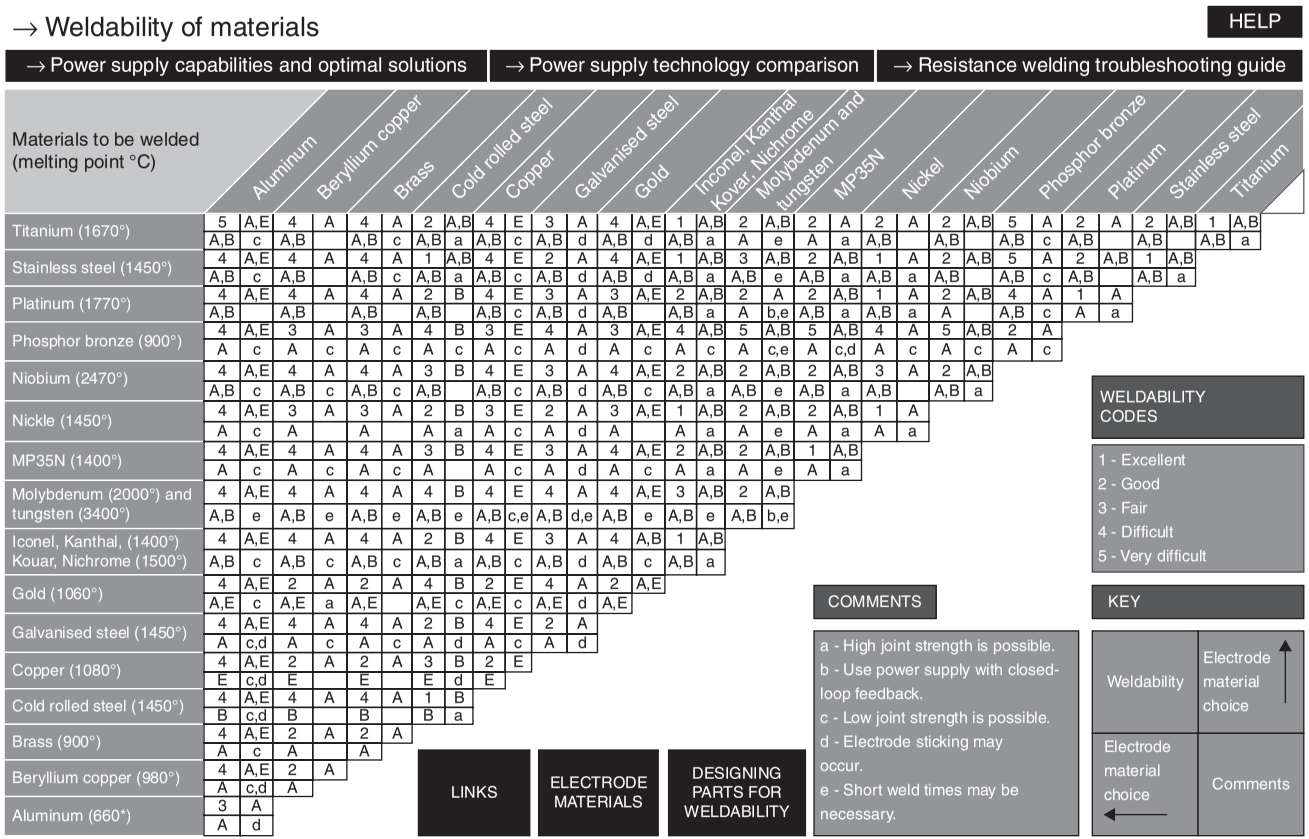
3.1 Weldability matrix for plastics (courtesy EWI). Note: this chart depicts compatibility as a complete mixing of materials resulting in a homogeneous bond. Other combinations of materials may be used to create mechanical or partial bonds.

of cooling in some small-scale laser welds allows the weld pool to freeze before bad microstructure can develop, allowing combinations of materials not allowed in the figure. Typical material properties for many common metals and alloys are shown in Table 3.2.[3,4]

Materials to be joined will be affected by all of the significant variables (process parameters, welding consumables, etc.). For example, the ductility of titanium welds can be greatly reduced through picking up interstitial elements, such as oxygen nitrogen and hydrogen, if shielding is inadequate during welding. A study of laser welding of titanium indicated that addition of oxygen in pure argon shielding gas (as in the case of shielding deficiency) caused further changes in weld microstructure (Fig. 3.3) and fracture morphology (Fig. 3.4).[5] Addition of oxygen in the shielding gas increased the amount of acicular and platelet alpha compared to equiaxed alpha in the base metal. As the oxygen content continued to increase (above 1.5–2.0%), weld microstructure was dominated by the acicular and platelet alpha. At very high oxygen content, the alpha platelets formed in colonies, giving a basketweave appearance (Fig. 3.3f). Accordingly, fracture surfaces during tensile testing changed from ductile manner with classical dimple

© Woodhead Publishing Limited, 2013

© Woodhead Publishing Limited, 2013



3.2 Weldability matrix for metals (courtesy Unitek Miyachi Corporation). (A and B refer to electrode material selections for resistance welding. Contact Unitek Miyachi Corporation for electrode materials.)

Table 3.2 Typical metallic material properties

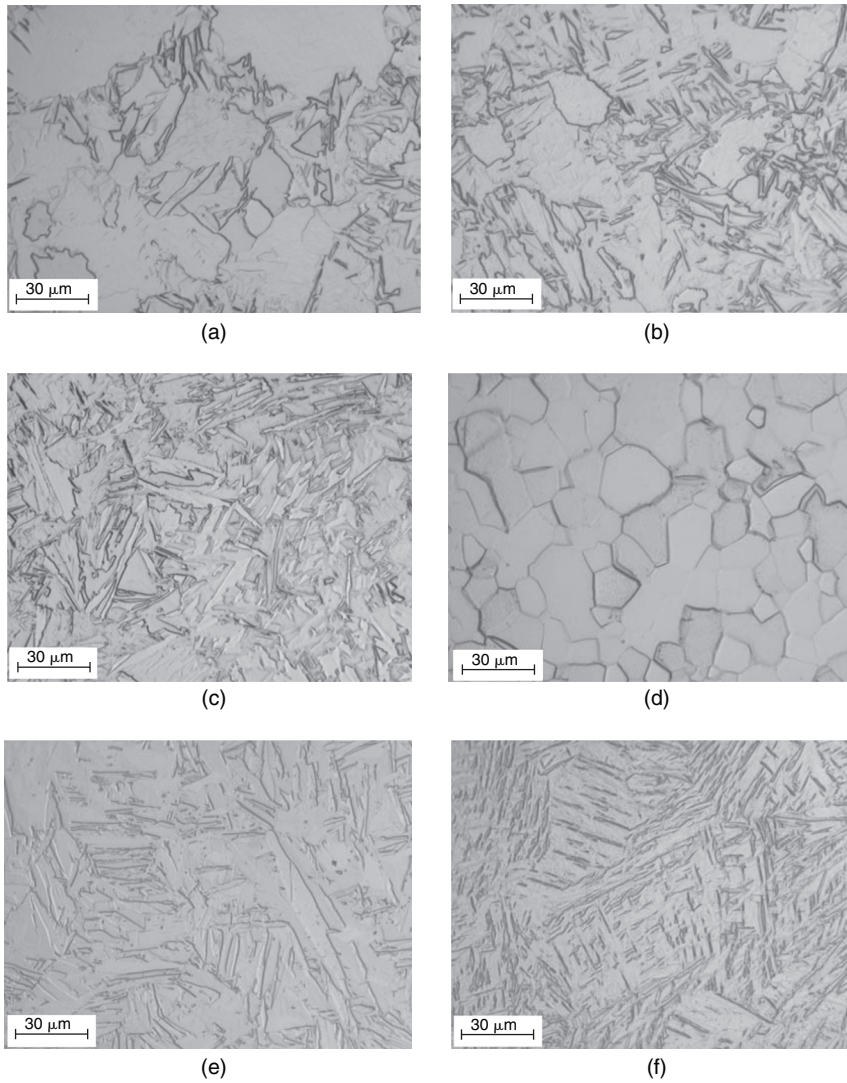
Metals	Melting point	Density	Thermal conductivity	Specific heat	Coefficient of expansion	Resistivity at 20°C	Elastic modulus	Poisson ratio
Pure	°C	g/cm^3	W/mK	cal/gramC	cm/cmC × 10^6	ohmscm 10^{-6}	GPa	
Aluminum	660	2.702	247	0.215	23.5	2.69	69	0.33
Beryllium	1278	1.848	210	0.436	12	4	288	—
Cadmium	321	8.642	97.5	0.0555	31	7.4	62	0.3
Chromium	1857	7.2	67	0.107	6.5	12.9	253	—
Cobalt	1495	8.9	69	0.107	12.5	6.24	—	—
Copper	1083	8.92	398	0.0922	17	1.67	125	0.33
Gold	1064	19.3	318	0.0308	14.1	2.3	77	0.42
Hafnium	2227	13.31	23	0.035	6	30.6	—	—
Indium	156	7.3	83	0.056	24.8	9	13.5	0.45
Iridium	2447	22.42	147	0.0312	6.8	5.3	517	0.26
Iron	1538	7.86	80	0.107	12.1	9.71	213	0.29
Magnesium	648	1.74	155	0.244	26	3.9	43	0.26
Molybdenum	2617	10.2	142	0.0598	5.1	5.7	330	0.37
Nickel	1453	8.9	83	0.106	13.3	6.84	202	0.28
Niobium	2468	8.57	52	0.064	7.2	14.5	106	0.38
Osmium	3045	22.48	—	0.0311	4.57	9.5	558	—
Palladium	1552	11.97	70	0.0584	11	10.8	115	0.39
Platinum	1772	21.45	71	0.0317	9	10.6	171	0.39
Rhenium	3180	20.53	71	0.0329	6.6	19.1	460	—
Rhodium	1966	12.4	150	0.0582	8.5	4.7	319	0.26

© Woodhead Publishing Limited, 2013

Silicon	1410	2.34	156	0.168	7.6	2.30E+11	163	0.22
Silver	962	10.5	428	0.564	19.1	1.6	74	0.37
Tantalum	2996	16.6	54	0.0334	6.5	13.5	186	0.35
Tin	232	7.28	63	0.0543	23.5	12.8	50	0.35
Titanium	1660	4.5	11	0.125	8.9	55	105	0.33
Tungsten	3410	19.35	160	0.032	4.5	5.5	398	0.28
Vanadium	1890	5.96	31	0.116	8.3	26	128	0.35
Zinc	419	7.14	113	0.0925	31	5.92	100	0.25
Zirconium	1852	6.49	21	0.0666	5.9	44.6	99	—
Metals								
Alloys								
Invar	1425	8.1	11.0	2.15	3.39		150	
304 SS	1450	8.0	16.2		17.2	720	193	0.33
316L SS	1400	8.0	16.3	2.09	16.2	740	193	0.29
MP35N	1315	8.43	11.2	0.0317		10.33	233	0.32
Ti-6V4Al	1660	4.43	6.5	2.20	8.6	178	114	0.33
Pt-Ir	1800	21.53	3.1		8.8	70–100		
NiTi	1300	6.45	10				21–110*	0.30

*21 = martensite; *110 = austenite.

© Woodhead Publishing Limited, 2013

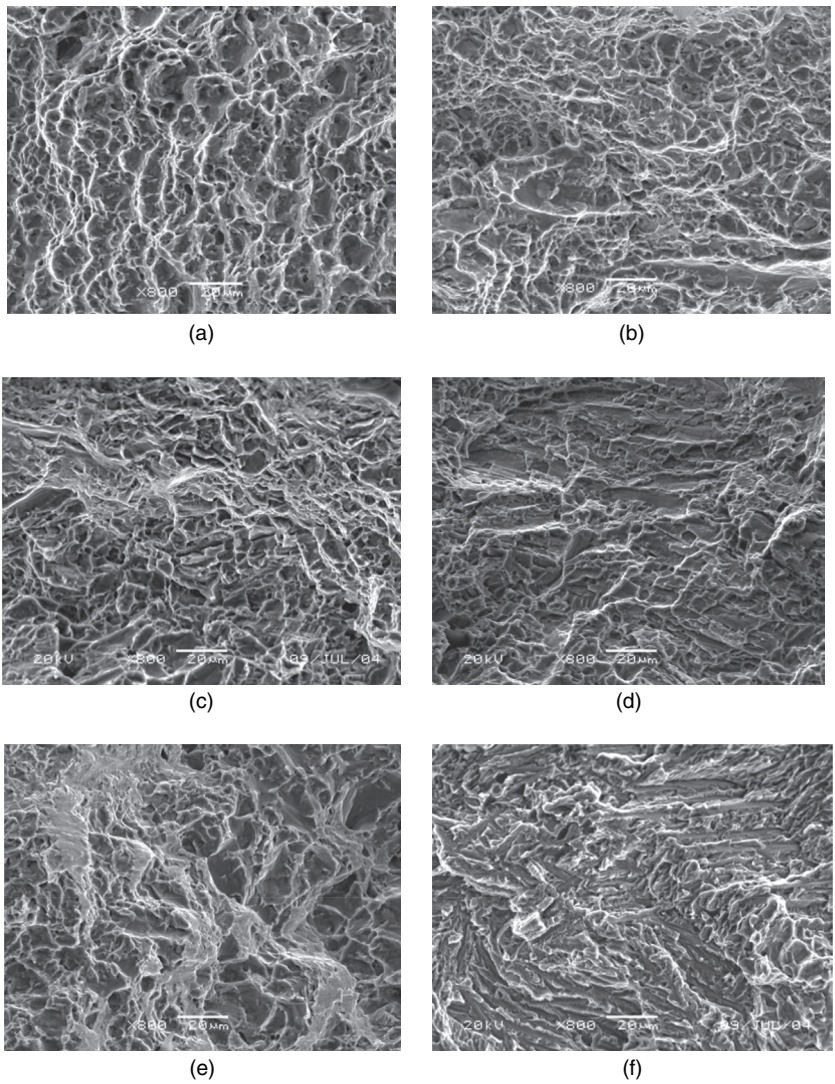


3.3 Micrographs of (a) base metal and (b–f) laser welds made with various oxygen contents in argon shielding gas: (b) 0%; (c) 0.5%; (d) 1.5%; (e) 3.0%; (f) 10.0%.[5]

morphology for the base metal to brittle appearance for welds made with oxygen addition. When the oxygen content was high (Fig. 3.4f), the weld fractures as intergranular along colony boundaries or cleavage across colonies, which indicates a complete brittle fracture.

The suitability (or weldability) of materials to be joined is greatly reduced for dissimilar material combinations, which are commonly required in medical-device manufacturing. For example, laser welds between dissimilar

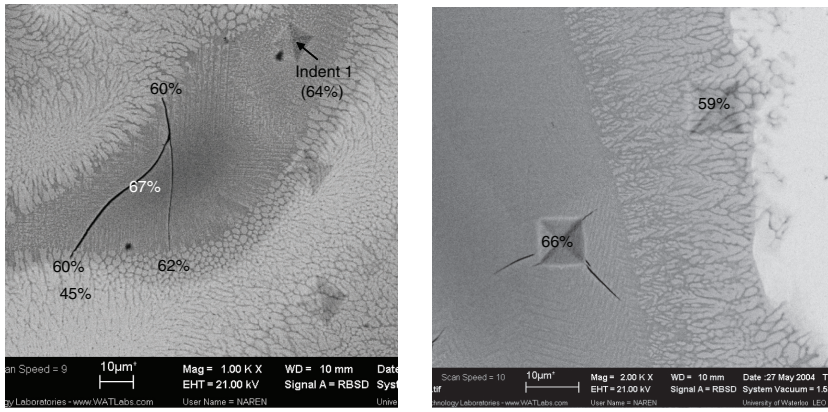
© Woodhead Publishing Limited, 2013



3.4 Fracture surfaces of (a) base metal and (b–f) laser welds made with various oxygen contents in argon shielding gas: (b) 0%; (c) 0.5%; (d) 1.5%; (e) 3.0%; (f) 10.0%.[5]

Pt and Ti alloys are susceptible to cracking.[6] In the welds, regions with 66–75% Ti, that is, consisting of primary Ti_3Pt and/or Ti_3Pt + TiPt eutectic, were found to have hardness above 700 VHN, while regions with 42–66% Ti, that is, consisting of primary TiPt, had hardness between 400 and 700 VHN. The regions consisting predominately of Ti_3Pt were very brittle, with cracks either formed during welding or hardness indentation (Fig. 3.5). It is believed that Ti_3Pt formed in the laser welds is the phase most susceptible to cracking.[6]

© Woodhead Publishing Limited, 2013



(a) (b)

3.5 SEM micrographs of laser weld between Ti and Pt alloys, with Ti percentages indicated, showing (a) cracks formed during welding in the regions predominantly consisting of Ti_3Pt but arrested in the regions predominantly consisting of TiPt and (b) cracks formed during hardness indentation in the regions consisting predominately of Ti_3Pt.[6]

While the obvious choice from a welding/joining standpoint is to make a design using one consistent material, practical design, cost, and machining ability often dictate the use of many materials within a design. This use of a combination of materials is also evident even within wires and coils now used in many catheters, pacing leads, and sensors. In many of these components the material is a cored wire, sometimes referred to as a drawn-filled-tube (DFT). Common wire and coil materials in this category include Tantalum cored MP35N, Silver cored MP35N, Platinum clad Tantalum, and Platinum clad Titanium.

Materials introduced into during welding and joining, such as filler metals during brazing, need to be biocompatible as well. For example, in brazing of Zirconia tube to Ti-6Al-4V ferrule in developing an implantable neuro-stimulator, existing brazing filler metals, such as Ag-Cu-Ti series, can not be used due the toxicity of the fillers.[7] Instead, a TiNi-clad braze, consisting of Ni/Ti/Ni laminated layers, is used since the braze becomes Nitinol, which is biocompatible, when the overall Ti/Ni ratio is 50:50.

A more thorough review of some medical devices and components, and the associated joining/processing challenges, is given in the next section.

3.3 Medical components and devices

Medical components and devices come in many shapes, sizes, and functions. The following section will highlight many current medical devices and the unique joining challenges they present.

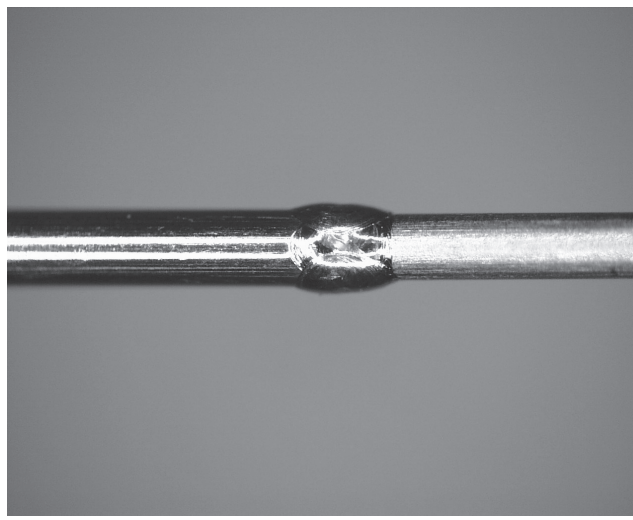
© Woodhead Publishing Limited, 2013

3.3.1 Vascular devices

Vascular devices cover a broad range of the medical-device industry from catheters and guidewires to balloon angioplasty and stents. While guidewires and catheters are generally single-use devices, stents are obviously permanent implants. For catheters the challenge is joining small diameter wires in a butt-weld configuration, often with subsequent sections having a smaller diameter. An additional challenge is that some sections may be made from unique materials. One such example is the joining of a 316L stainless-steel wire to a nitinol (nickel–titanium) end affecter. The nitinol can be formed or shaped to provide a certain function, while the 316L provides good torque transmission and lower cost for the long section of the wire. Alignment of the diameters to a center axis and control of the diameter in the weld zone can be difficult. An example of guidewire joining is shown in Fig. 3.6.

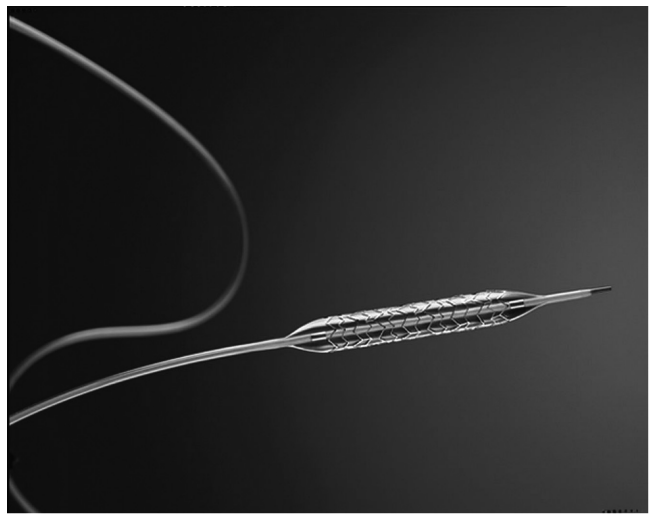
Balloon catheters require the joining of the polymer balloon to a polymer tube on a guidewire. This can be achieved via direct laser welding or adhesive bonding. Challenges are the consolidation of the thin weld zone to develop high strength, and control of the initial gap between the components during fixturing. An example of a balloon welded to a lumen is shown in Fig. 3.7.

Stents are complex devices, typically laser cut from tube stock or welded assemblies of small wires. The stent is collapsed and delivered to the precise



3.6 Guidewire for catheter applications. Note the change in diameter and smooth diameter across the joint zone (raw weld unpolished). The materials are NiTi and stainless steel.

© Woodhead Publishing Limited, 2013



3.7 Balloon catheter joined to lumen expanding a laser-cut stent. Photo courtesy of AngioTech Corporation.

arterial location via a catheter and fluoroscopy, and then deployed and expanded in place. These devices pose the challenges of excellent surface and edge finish, control of heat-affected-zones (HAZ), and extreme control of orientation and laser cutting path. A laser-cut stent is shown in Fig. 3.8.

3.3.2 Pumps and sensors

A wide variety of external and internal pumps and sensors are now in use and in development. Insulin pumps and left ventricular assist devices have been in place for many years, with recent years seeing the development smaller-scale silicon-based drug reservoirs, MEM-based pressure sensors, and implantable RFID tags. Challenges include the welding and joining of metal and plastic foils, bonding fragile semiconductor layers to each other, assembly of microscopic circuit assemblies, and wire or tab attachments for interconnects.

3.3.3 Cochlear implants

Hearing implants are growing in use and are complex multicomponent devices. These units require sub-miniature voice coil and electronic assemblies, in addition to implantable circuit cans, lead wires, and even RF transmit units. Small-scale joining of wires, hermetic seals of enclosures, and assembly of small-scale wire coil assemblies are unique challenges.

© Woodhead Publishing Limited, 2013



3.8 Laser-cut stent.

3.3.4 Neurostimulators, pacemakers and defribrillators

These devices, while providing unique therapy to the patient, are similar in that they are generally composed of a hermetic 'can' which encloses the critical electronics, and metal wire leads that provide sensing or therapy delivery. The cans are implanted in a pocket in the upper pectoral region, or low in the abdomen. Wire leads are then threaded through the vasculature to the point where therapy is to be delivered. In the case of cardiac care devices the heart lead is implanted directly inside the right atrium or right ventricle to pace or shock the heart into normal rhythm, as shown in Plate I(a) (see Plate I in colour section between pages 300 and 301). In neurostimulators, the lead tip is implanted near the spine, or deep in the brain to control electrical signals that signal pain or to control tremors, as shown in Plate I(b).

Table 3.3 lists typical microjoining processes used to manufacture an implantable pacing system, which includes mainly a pulse generator and leads. The pulse generator includes a battery to generate electricity and circuitry to generate, control, and deliver the pulses, which uses many of the

© Woodhead Publishing Limited, 2013

Table 3.3 Typical microjoining processes in pacemaker manufacturing

Interconnecting and attaching	Battery	Wire bonding, soldering, adhesive bonding, resistance and laser microwelding
	Circuitry	Wire bonding, soldering, adhesive bonding, ball grid array (BGA)
	Header	Brazing, laser and resistance microwelding, plastic joining
	Lead	Laser microwelding and adhesive bonding
Hermetical sealing	Pacemaker, battery cases	Laser welding
	Lead feedthrough	Ceramic/metal brazing

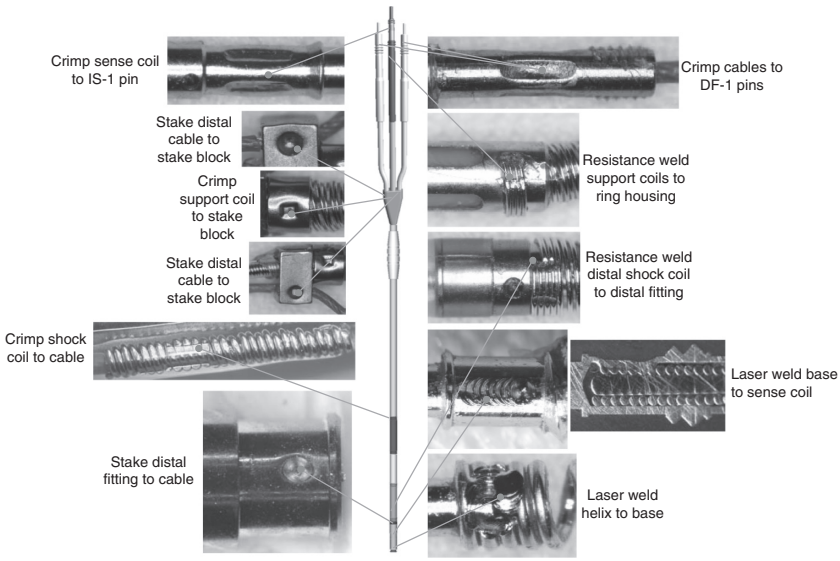
microelectronics packaging processes. The battery, however, is hermetically laser sealed to prevent leakage of chemicals (with a leak rate less than 1×10^{-9} atm-cc/s). Both the battery and circuitry are inside a titanium case that, again, is hermetically laser sealed to prevent human body fluids entering and causing corrosion. The internal circuits are connected through brazed joints such as Al_2O_3/Pt–Ir, to an outside connector block encapsulated in a biocompatible polymer such as polyurethane, and interconnected via Pt or Ti wires/ribbons using about 10–20 laser and resistance microwelds.

These hermetic cans are Class III devices and designed for long-term implant in the body. The cans are typically thin-walled titanium or MP35N, while the leads are straight wires or coils of MP35N, titanium, or platinum-clad cored wires of tantalum, MP35N, or titanium. Ensuring a hermetic seal of the thin-walled case is not trivial, as the designs require welding near feed throughs, pins, or ceramic inserts. The case halves must fit together with minimum gap, and the welding process must track a non-uniform shape or seam. The weld penetration must be carefully controlled so as to not overheat nearby structures or penetrate too deeply and damage internal components.

An example of neurostimulators is the BION® microstimulator: a RF powered single-channel ceramic-cased implantable stimulator, which weighing just 0.75 g with an overall volume of only 0.19 cm^3 (3×28 mm).[7] It includes a ceramic to metal case, where the ceramic provides a window for RF transmission. The case, 2.44 mm in diameter, is composed of an 11.28 mm long Zirconia tube brazed onto a 0.76 mm long Ti cap (cathode) and a 1.98 mm long Ti ferrule (anode). The wall of the ceramic tube and the ferrule is 0.28 mm thick. After the electronic module is inserted into this case, a Ti lid is laser welded to the ferrule for the final hermetic seal.

The wire leads, which often have several conductor pathways running the length of the lead for sensing as well as delivering therapy such as pacing

© Woodhead Publishing Limited, 2013



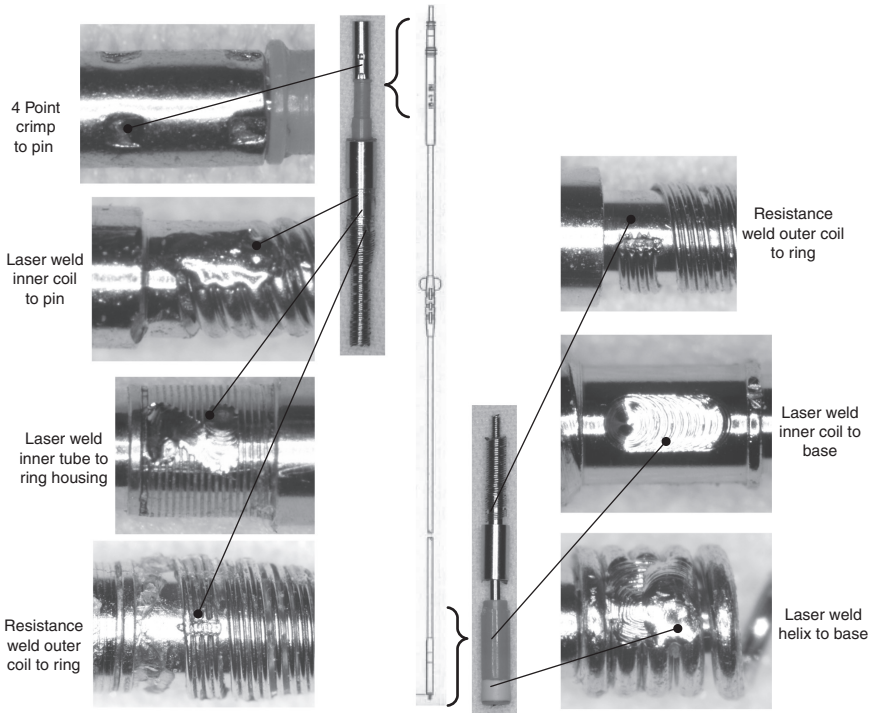
3.9 Typical welds and mechanical joints in a high-voltage tachycardia (shocking) lead which delivers both pacing and defibrillation therapy (courtesy of Boston Scientific).

pulses or defibrillation shocks in cardiac leads, also provide a multitude of challenges. Laser and resistance welding, and mechanical joining are generally used to assemble these conductors and the associated components, such as electrical contacts and electrodes (Figs 3.9 and 3.10). Most of these joints must provide some level of mechanical strength as well as electrical conductivity. Materials must be biocompatible and corrosion resistant since most of the lead is in direct contact with the body or body fluids.

The lead wires are often dual materials (clad cores), such as Pt–Ir coils coated with silicone rubber or MP35N-clad silver, and joined to pins, tubes, and other structures that are dissimilar material. An example is the termination of a coil wire for a heart pacing lead, in which the wire coil is MP35N-clad silver and the termination pin is 316SS. The weld is formed using a single laser-spot weld. Controlling the melt flow of the silver core can be a significant challenge if improper laser energy or poor targeting of the weld zone is used.

But, the most important consideration for any fusion weld between dissimilar metals is their metallurgical compatibility and the performance of the resulting weld deposit under service conditions. This is sometimes also referred to as weldability. The materials listed above are typically compatible with one another with the exception of the Titanium alloys. Titanium

© Woodhead Publishing Limited, 2013

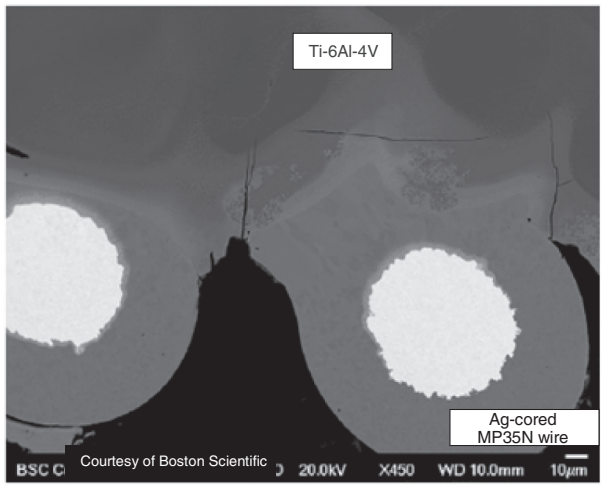


3.10 Typical welds and mechanical joints in a bradycardia or pacing lead (courtesy of Boston Scientific).

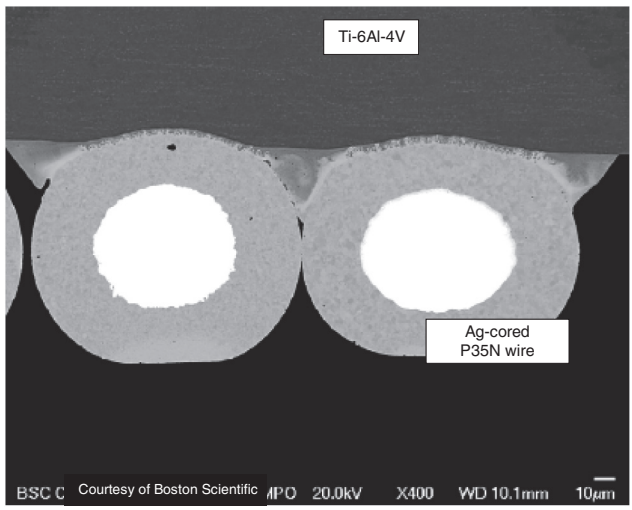
tends to form intermetallic compounds with many other transition metals such as Fe, Cr and Ni. These intermetallics are typically brittle and render the weld metal brittle. Often welds will crack immediately as a result of the thermal stresses generated during solidification and cooling. Figure 3.11 shows typical cracking in a resistance weld between a Ti-6Al-4V component and an MP35N wire.

Several methods have been explored to improve the weldability of Ti to other metals. One approach is to optimize the resistance welding process to get a solid-state weld as shown in Fig. 3.12, in which the amount of molten weld metal formation and subsequently the amount of intermetallic is minimized at the weld interface. This is very similar to the solid-state welds formed in resistance welding of crossed Ni wires where the initial molten metal is squeezed out from the weld interface.[8] Solid-state welding includes the forge-welding processes such as friction, magnetic pulse, and solid-state resistance welding. Friction welding has been successfully demonstrated for Ti to stainless-steel welding[9] and resistance welding for Nitinol to stainless-steel welding.[10]

© Woodhead Publishing Limited, 2013



3.11 Weld between Ti and MP35N showing significant weld metal cracking due to Ti intermetallic formation (courtesy of Boston Scientific).



3.12 Resistance weld between Ti and MP35N wire with minimal admixed weld metal and no weld cracking (courtesy of Boston Scientific).

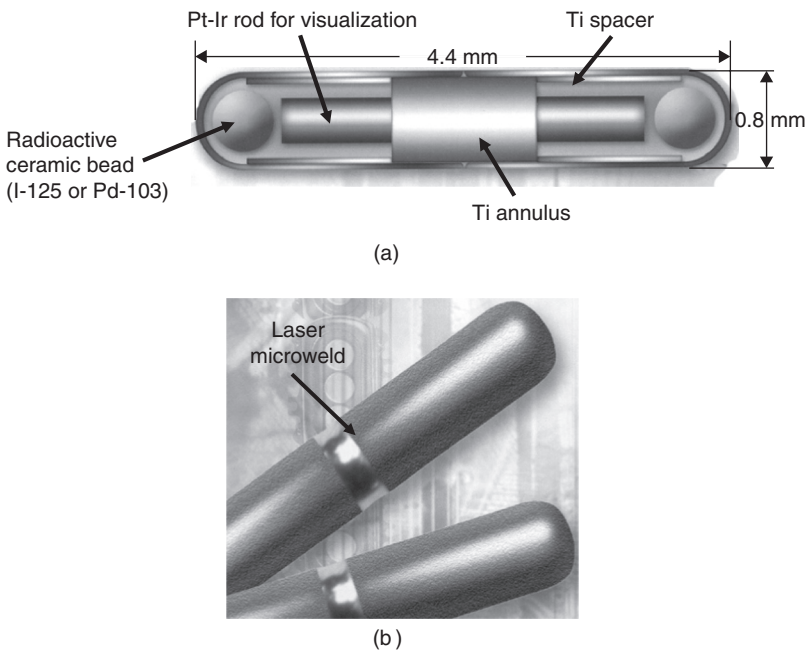
Another approach is to use more compatible metals. Niobium, Ta, and Mo all form solid solutions with Ti and therefore are not prone to forming brittle intermetallic phases. Alternatively, these materials can be used as an intermediate material, or interlayer, to allow welding of an incompatible metal to Ti. Yet another approach to welding Ti alloys to other metals is to add a filler

© Woodhead Publishing Limited, 2013

metal to intentionally manipulate the weld-metal chemistry and suppress the formation of intermetallic phases. One example is the addition of Ni to welds between NiTinol and stainless steel. Nickel enrichment of the weld metal suppresses the formation of the very brittle Fe_2Ti intermetallic phase and results in sound welds with comparatively good mechanical properties.[11]

3.3.5 Radioactive seed implants

Implant or internal radiation therapy, or brachytherapy, has been developed as an alternative to the traditional treatments such as radical surgery and external beam irradiation for cancer treatments. This technique uses a radioactive substance (e.g. in the form of pellets) sealed in needles, seeds or wires that are implanted directly inside or near the cancer. The cancer cells can be killed by the energy given off as the radioactive material decays. Figure 3.13a shows an example of such a seed implant developed for prostate cancer treatment. The radioactive substance is sealed inside Ti tubes by laser microwelding, as shown in Fig. 3.13b, in this case as the laser is well developed and suitable for such precision manufacturing.[12]



3.13 Radioactive seed implant: (a) schematic design and (b) laser welded assemblies.[8]

© Woodhead Publishing Limited, 2013

3.4 Joint design and process selection

As described in Sections 3.1 and 3.2, medical devices have unique requirements and use a specialized material set for biocompatibility and implant conditions. Many of the material and joint design configurations, however, are common across device types. The following sections will highlight specific assembly challenges and the selection of the microjoining processes best suited to achieve high-quality reliable assemblies.

3.4.1 Wire-to-wire assembly

Microjoining challenges manifest themselves at the assembly and joining stage. While small diameter wire and cable has been available for years, joining these small gauge wires to each other in either butt, overlap, or parallel (tipping as in a thermocouple) joint configurations and forming operational assemblies is a true challenge. Typical wire diameters may range from large at 0.100″ to small at 0.0005″ for the finest interconnect wires. Typical range for semi-automated assembly is 0.003–0.007″. Wire-to-wire assembly can be as simple as an overlap weld where both wire ends are flattened in the weld zone, to a uniform iso-diameter butt joint.

One of the best processes for joining butt-wire assemblies is percussive-arc welding. To form this type of weld, the following process steps are completed:

1. Cut the wire ends to form a tapered bullet or square face on the wire.
2. Straighten a short length of wire on each side of the joint. Careful axial alignment is required.
3. Accelerate the cut-wire faces toward each other, while simultaneously energizing the wires with opposing voltages; a current limit is also imposed. An alternative is to place a separate electrode between the wire faces with both wires opposite in charge to the center electrode. As the wire faces approach each other or the center electrode, an electric arc will form in the gap, and melt the opposing wire faces.
4. The wire faces are then allowed to forge together. Careful control of the force, the arc time, the closing velocity, and axial alignment are required.

Tipping of catheter wire, formation of thermocouples, and sensor wires can be completed in a similar manner. The heat source can be an electrical arc, or even the heat of the plasma formed at the tip of a micro-plasma torch. Laser energy can also be directed at the tip where a small portion of the wire end is melted. Natural surface tension causes the molten pool to pull back

© Woodhead Publishing Limited, 2013



3.14 Tip forming of a catheter wire. The formed end can be made using laser or arc processes followed by precision grinding to final shape.

and form a uniform sphere. This approach works best when the two wires are straight, parallel with each other, and form an isomorphous alloy in the melt zone. An example of catheter tipping is shown in Fig. 3.14.

For these types of small-scale wires, arc processes work very well. The small size of the wire helps direct or draw the arc only to the wire tip. Laser-weld spots are generally much larger in diameter than the wire. Because the laser can have a non-uniform energy distribution across the weld spot (Gaussian), the location of the wire to the beam can be non-optimum. Further, the laser welds and cools over a short timeframe, and minimizes the weld zone. In these types of assemblies this can lead to a marked gradient in grain size from the fusion ball to the parent material in the wire. Arc and plasma processes tend to add more heat, softening the grain transition from the welded ball to the parent wire. This improved gradient in microstructure can result in improved toughness and fatigue performance of the final assembly.

3.4.2 Wire-to-pin assemblies

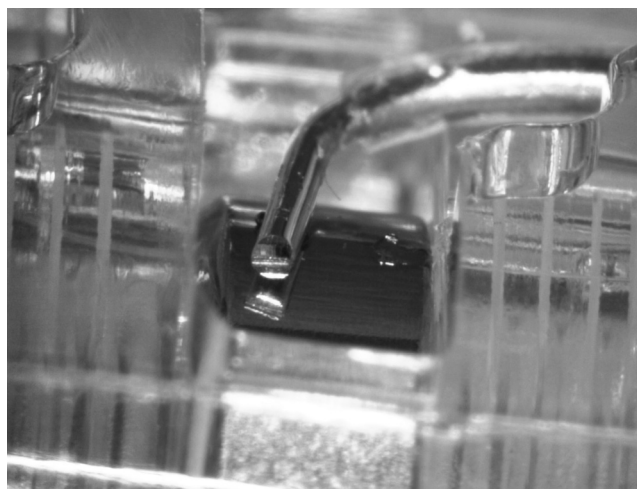
In this application the wire can be straight or in the form of a coil. The wire is then joined or terminated to a pin or other solid substrate, such as a jumper pad on a hybrid circuit or a header block where pacer leads are plugged in. The wire is often in the shape of a coil spring to improve flex fatigue and other mechanical performance attributes.

One of the best processes for this type of assembly is resistance welding. In this process oppositely charged electrodes are applied under force to the

© Woodhead Publishing Limited, 2013

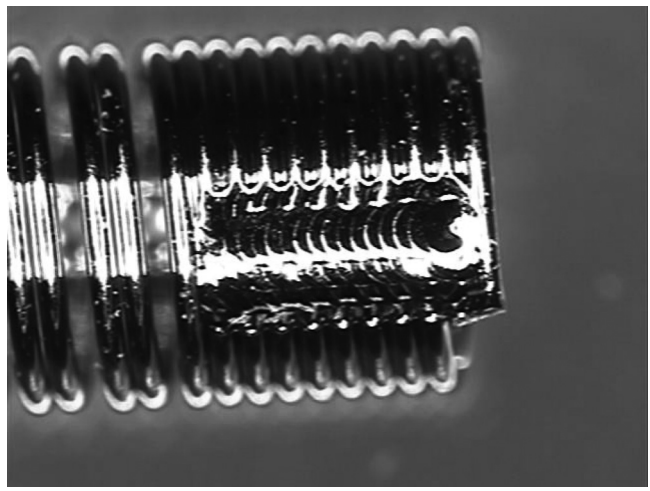
wire, and current is discharged through the wire to the interface. Resistance to the flow of current causes localized heating, resulting in weld formation where the resistance is highest (usually at the interface of the wire to the substrate). The clamping force used in resistance welding is a key advantage in that is directs the weld location, and consolidates the molten or softened metal to form a concise nugget. Gap is not such a problem as the forces used to clamp the electrode against the parts close any excessive gap. Further, as the materials are heated and soften during the first few milliseconds of the current application, additional joint consolidation occurs. Key challenges are the control of the current path in the often, small diameters, especially when direct access for the lower electrode is not possible. Electrode size, position, and force are also issues in that the electrode face often is larger than the wire to be joined. Careful construction of the electrode face and radiusing of the electrode corners can help define the precise weld zone to just a few wire diameters. Disadvantages are the development of small electrodes, electrode wear, and positioning the wire-substrate assembly prior to joining. An example of a titanium-wire resistance welded to a Ti-6/4 terminal block for a pacemaker application is shown in Fig. 3.15.

Laser welds are also used for wire to substrate bonds, as they are readily automated and simple to align and target. Both welds are used in the assembly of shocking coils used in defibrillation leads for implantable heart failure devices. A disadvantage of the laser-weld process is the lack of clamping force holding the wire in place against the surface. If the wire is not in good contact with the surface, there is no driving force to ensure



3.15 Resistance spot weld of 0.005″ titanium wire to Ti-6Al-4V terminal block in the header of an implantable pacemaker.

© Woodhead Publishing Limited, 2013



3.16 Laser welding of small diameter coil to seal the coil together and prevent unwinding (birdcage).

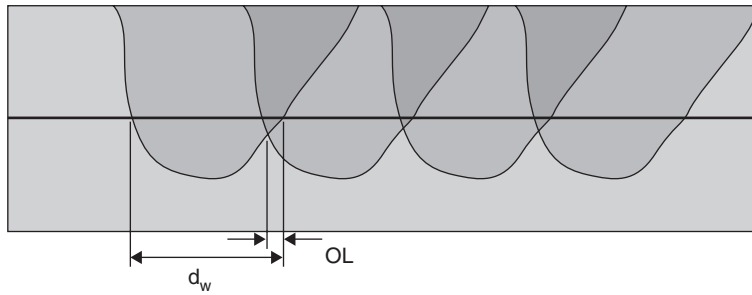
wetting and flow of the wire to the surface. Conversely, the driving force is surface tension in the molten wire, which pulls back from the surface, forming a balled end to the wire. An example of this common defect is shown in Fig. 3.16.

3.4.3 Hermetic sealing of electronic enclosures

A key similarity in many medical devices is the need for a small thin-walled can or container to hold the necessary electronics, power supply, batteries, capacitors, and other circuit functions. This package must be hermetic to at least moisture ingress, but is typically gas tight to even low volumes of helium. Typical housings in medical are MP35N, 316L, or, the most common, commercially pure titanium. Hermeticity is required to ensure moisture attack cannot cause corrosion and eventual shorts or opens of the circuits. Note that many hermetic enclosures in use today also incorporate getters for oxygen and moisture, to improve long-term reliability and quality. Regardless of the sealing technique, a minimum of 50% spot-to-spot overlap is recommended, with 75–80% overlap common practice. Also note that the important aspect is to achieve overlap of the weld zones at the interface of the joint. Overpenetration of individual spots detrimental and penetration does not correlate to hermeticity; it is the continuity of the seal at the interface. This is shown schematically in Fig. 3.17.

Three processes have been widely used to hermetically seal thin-walled medical cans:

© Woodhead Publishing Limited, 2013



3.17 Overlap condition (OL) requirement to achieve full hermetic weld at the interface of the weld joint. In general 50% overlap on the surface is the minimum to achieve uniformity at the interface. d_w – Weld diameter.

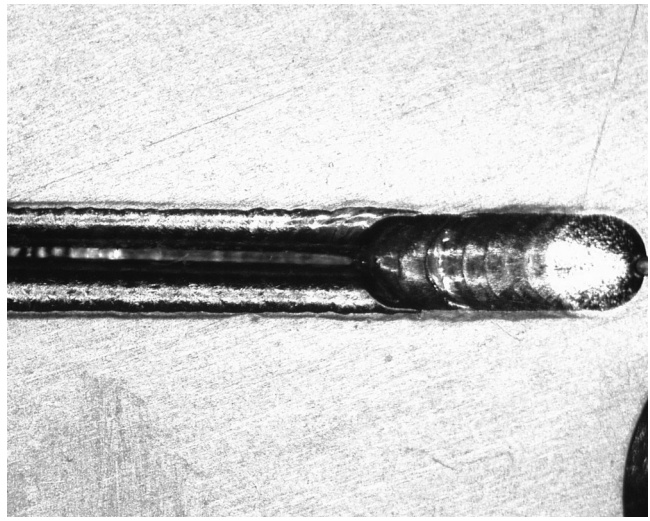
1. resistance-seam welding;
2. plasma-seam welding;
3. laser-seam welding.

Resistance welding is an excellent choice when the can materials are resistive as in the case of MP35N or 316L stainless steel. Opposed electrodes are clamped against a flange of the housing and slowly rotated to traverse the length of the package. Current and voltage is applied to form overlapping resistance weld spots. After the first pass along two parallel sides, the electrodes retract, the part rotates 90°, and the process is repeated along the two remaining sides. Circular packages can also be sealed with this technique. Disadvantages of the process are the requirements for a flanged cover, which is often nickel and gold plated. In this manner the resistance weld is actually a resistance braze, forming a eutectic alloy of gold–nickel at the interface. This allows the process to run somewhat faster and use less heat input than full fusion welding of the higher melting point MP35N or 316L stainless steel.

Plasma welding has hermetically sealed more medical pressure bellows than any other process. Pressure bellows are formed from a stack of preformed thin metal discs, sealed along their periphery. In a manner similar to arc processes for sealing wire tips, the arc is drawn to the sharp edge of the disc, melting and sealing the disc edge. The process produces a weld seam very similar to pulsed laser welding, but with slightly increased heat input. It is an excellent process for sealing flanged enclosures as well. Its disadvantage is the heat input for deeper penetration welds, and the close proximity of the torch face to the weld zone itself.

Laser welding is today the most popular and easy to implement for hermetic sealing. Advantages are the ease of "point-and-shoot" line of sight welding capability, and the ease with which automation can track odd

© Woodhead Publishing Limited, 2013



3.18 Laser welding application showing surface tension effects causing pull back of the weld zone opening a larger gap.

package shapes and configurations. Deeper penetration welds can be developed without overheating critical glass or ceramic feed-throughs, and weld cycle time is the shortest for laser welding. Disadvantages are often the initial start up capital cost, training and laser safety requirements, and the need for excellent part fit-up. A general rule of good laser welds is the joint fit-up must have a maximum joint gap of 10% of the thinner material. Excessive gaps cause the laser to punch through one layer causing a hole, or the edges of the seam pull back due to the molten material surface tension. An example of a seam weld with too much gap is shown in Fig. 3.18. Note the smooth-balled edges on each side of the seam. An example of a well-formed hermetic seam weld is shown for a pacemaker pulse generator in Fig. 3.19.

3.4.4 Cutting and drilling shapes and holes

The laser can also be used to cut and shape tubes for form unique scaffold like structures such as stents or abdominal aortic aneurysm (AAA) grafts. These lasers are unique configurations that develop very small spot sizes with extremely high peak powers. The small spot size minimizes the cut kerf and improves the cut-edge quality, while the high peak pulse power fully penetrates and ejects a plasma plume of material. The automation and computer control of the laser allows for the development of full 3-D structures. The cut-edge quality is critical in these applications, and post-cutting polishing and honing processes are often used to ensure smooth, burr-free edges.

© Woodhead Publishing Limited, 2013



3.19 Laser seam weld in a thin-walled titanium enclosure.

However, the proper selection of pulse rate, table feed rate, cover gas type, and cover gas pressure all contribute to cut-edge quality.

3.4.5 Ring-to-ring or tube-to-tube assembly

There are many instances in medical devices where the mating components are thin-walled tubes that slide into one another. Arthroscopic tools, catheters, and electrodes on pacing leads or terminals are examples of this application. Two joining processes are generally used to join these thin-wall structures. First and foremost is laser welding. The laser can be used to form single or overlapping spot-welds that join the outer tube to the inner tube. The wall thickness of the electrode can range from 40 to 75 μm. Here again the advantages of the laser are the ease of point-and-shoot process development, with the disadvantage of joint fit-up. If the inner ring is not in close contact to the outer tube, the laser will simply cut a hole in the outer layer, with little or no mating connection developed.

A newer process originally developed for larger-scale automotive applications is magnetic pulse welding. In this process magnetic fields are set up in the inner tube such that the repulsive force to an inner mandrel explosively forces the inner layer outward forming a solid-state bond to the outer layer. The larger-scale version of magnetic pulse welding has been used to form flares and expanded regions in cooling tubes and muffler components. The small-scale version is an excellent choice for bonding inner tube structures to outer electrode rings. An advantage of this process is the low heat input, rapid cycle time, and continuous weld over the entire mating surface.

© Woodhead Publishing Limited, 2013

Disadvantages are that the application works primarily for round conductive components and requires unique fixturing.

3.4.6 Polymer tube-to-tube assembly

Polymers are used throughout medical devices, especially for single-use disposable devices such as catheter sheaths, packaging, and insulators over wire components. One of the simplest and most widely used joining processes is adhesive bonding. Joint design challenges are especially evident where polymeric materials must be joined to metal components. Common practice is to clean and prepare the surface of the metal, and then join a tube over the metal and bond it in place with liquid adhesive. Here again the gap at the interface can define success or failure. In most cases the design extends the bond area to ensure adequate surface area for the bond to occur. Studies have shown that for optimal bonds, a uniform gap should exist to provide a uniform adhesive-layer thickness. Too thin an adhesive layer yields poor surface coverage and low strength. Similarly, too thick an adhesive layer yields low strength due to failure of the adhesive itself. Careful analysis of the bond failure is critical to development of the proper process and achievement of a robust design.

Balloon catheters are another example of polymer-to-polymer joints; this time joined using full fusion processes. A simple heated mandrel/clamp can be used to fuse the joint region, but newer methods using focused infrared light in the form of a laser or IR lamp are commonly used. The non-contact feature of the infrared welding process is an advantage for medical grade devices.[13] Cross-contamination of the heated tool approach is a serious defect, and careful tool and heat controls are required to keep the tool face clean and to avoid transfer to the next welded device. CO_2 laser systems are common in this application as most polymers have strong absorption bands near the 10.6 micron output of the CO_2 laser.[14] In CO_2 and some diode welding, the polymer itself absorbs the laser energy, causing the development of a fusion zone. Other wavelength diode lasers and standard ND:YAG systems can also be used, especially when welding onto metallic components.

3.4.7 Polymer tube-to-solid-pin assembly

When ND:YAG is used, its 1064 nm wavelength is usually transmitted through the polymer with very little absorption and heating. In this case the ND:YAG is focused on an internal metallic mandrel and heated with the laser. The thermal energy then conducts to the polymer layer forming a bond.[15] In this manner the process is referred to as through transmission infra red welding (TTIR). Additional research has been completed on

© Woodhead Publishing Limited, 2013

specific laser absorbing dyes that can be molded into the plastic parts or provided as a thin interlayer. In this application the laser is absorbed at the dye layer, and thermal conduction then heats the surrounding materials to form a weld zone. Note that in all polymer welds, the fusion zone must be held in compression while the nugget cools in order to achieve the best weld strength. The high expansivity and poor thermal conduction of polymers make this compression requirement vital to the development of good welds.

3.4.8 Polymer bags and enclosures

Numerous medical devices are fabricated using all polymer systems. These include intravenous fluid bags, drug delivery, microfluidic canisters, pumps, and filters. Sealing and welding of thin films to each other and to structural plastics is a common requirement. Early processes used simple heated bar or heated formed tools to compress the weld zone. However, cross-contamination from the tool face is a serious issue so non-contact methods were developed. Non-contact includes the aforementioned laser welding, but two of the most popular methods are radio-frequency (RF) dielectric welding and ultrasonic plastic welding.

In RF dielectric welding the process relies on the chemistry of the polymer itself. In this process an oscillating RF electric field is imposed on the weld joint. The polymer chains react to the imposed field, and the dipoles of the polymer attempt to align with the field. The polymer dipoles cannot oscillate in time with the applied field and this hysteresis loss causes rapid heating.[16] Benefits of the technology are fast cycle time, good weld-zone control with the applied clamping force, and the tool is cold so transfer and cross-contamination is eliminated. This process is commonly used for final packaging of devices prior to shipping.

Ultrasonic plastic welding uses a medium frequency transducer horn and clamping force to develop a weld zone. The ultrasonic energy is applied typically at 20 or 40 kHz depending on the component size, shape, and wall thickness. Similar to RF dielectric heating, the ultrasonic energy vibrates the polymer chains, causing rapid heating and development of a weld zone.[17] Here again the applied clamping force forges the molten zone together to form an excellent seal and weld. This process can be completed on virtually all thermoplastics.

3.5 Testing and verification

The first consideration is mechanical performance of the welded assembly. Although there are no standardized performance requirements for

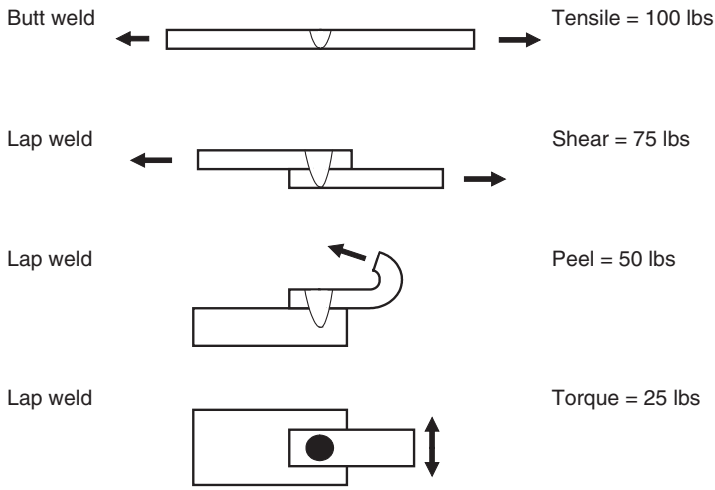
© Woodhead Publishing Limited, 2013

implantable joints, there are common performance considerations for all designs. For example, any joint must withstand any subsequent manufacturing steps and handling. The loads imposed during manufacture may in fact be far greater than loads seen during service. The loads imposed during the implant procedure are often more severe than those seen chronically. Handling by the physician as well as the interaction of the lead with delivery tools and/or the anatomy is largely uncontrolled and considerably variable. For example, on occasion, implantable leads must also be removed for various reasons. Perhaps some of the most extreme loads can be seen during an explant procedure when simple traction may be used to pull the lead out. Tissue ingrowth and encapsulation can anchor parts of the lead making them more difficult to remove. If a part of the lead was to break off during extraction a significantly more invasive surgery may be required to retrieve it. This puts the patient at a significantly higher risk of harm. All of these service conditions should be understood and considered when designing joints for implantable leads.

Implantable joints are often tested in manufacturing using small-scale tensile-testing equipment. During pull testing, the actual joint is often exposed to a complex stress state, resulting most often in tensile shear of the weld zone. It is important in small-scale welds to consider the effect of the weld process on the raw parent material strengths. As a general rule, full fusion welds yield approximately 60% of the raw parent material strength, in tension. In practice, the 'pull test' can apply off axis loads and stresses, leading to failure at lower than expected loads.[18] Peel testing is especially stressful, as the load is focused on a narrow zone of material, which tends to tear and unzip along the weld interface. Even though the weld-zone formation is the same, peel test samples may fail at 25% of the load applied in direct tension. A schematic of this effect is shown in Fig. 3.20. As the stresses are effectively applied to smaller and smaller areas of the joint or weld zone, the test strength decreases. The point here is to carefully document the testing procedure and provide adequate controls to apply the test force in a consistent and uniform manner.

In practice, small-scale joints typically have two failure modes. In the first, insufficient mixing across the interface leads to a small interface area to carry the applied load, so the joint fails. In this case the mating faces of the joint show very little transfer of material and it is obvious to the process and quality engineer that welding was insufficient. Overwelding is also an issue. Weldments generally exhibit a horseshoe form when plotted as strength versus power. At low power the weld has no strength due to lack of weld zone development at the interface. At some point, optimum welds will yield the highest strength. This occurs where the weld zone at the interface is optimized relative to the loss of parent material strength. With the application of too much power, the weld zone penetrates deeper and overheats the

© Woodhead Publishing Limited, 2013



3.20 Schematic of test conditions and the effect of loading condition on measured weld strength for a uniform area weld zone.

parent materials, causing parent material failure adjacent to the weld zone. This is often thought of as a "good" weld, even though the parent material has been seriously degraded from its original condition. The reader is encouraged to optimize the weld zone and parent material performance, and neither underweld or overweld these critical assemblies.

Another leading consideration for welds in implantable components and devices is corrosion performance. The corrosion performance of the weld metal should not degraded by the thermal cycle of welding. The primary concerns are excessive oxidation and/or dealloying due to weld-metal contamination. Excessive reaction between the molten weld metal and the welding atmosphere or surface contaminants can largely be avoided by using high-purity shielding gases and cleaning the joint surfaces thoroughly prior to welding. Polymeric materials such as silicone rubber, polyurethanes, and adhesives, which are commonly used in the construction of leads and other medical devices, are another potential source of weld contamination that should be considered and avoided.

Corrosion performance can be evaluated with a number of *in vitro*, or bench, testing approaches. ASTM F2129 is a potentiodynamic polarization test that evaluates the breakdown potential and pitting corrosion characteristics of a metal or assembly. ASTM F746 is a test for pitting and/or crevice attack. Simple soak testing in saline or simulated biological fluid can also be used to evaluate general and galvanic corrosion. ASTM G71 provides general guidance for galvanic testing. Current-induced corrosion testing specifically evaluates material and assembly performance under the service

© Woodhead Publishing Limited, 2013

conditions of delivering electrical stimulation therapy. For example, a cardiac lead may need to deliver chronic pacing therapy at 70 pulses per minute for 10 or more years. Under these conditions the cumulative corrosion could be significant for components or assemblies exposed to the pacing charge. The setup and duration of this testing should be sufficient to replicate the maximum cumulative charge that would be seen over the expected life of the implants.

As is the case for all implantable medical devices, *in vivo* testing is an important approach for evaluating the corrosion performance in the actual biological environment at the component, assembly, and complete lead level. It is highly recommended that any *in vitro* corrosion testing be supported with some level of in vivo testing.

3.6 Conclusion and future trends

Microjoining is a critical and enabling technology for manufacturing of medical implantable components and devices. The small scale of many emerging designs requires a deeper understanding of joining technologies and thin materials so that the proper joining method can be applied.

Lack of standardization in polymeric materials will slow the development of many new devices. Polymeric materials generally must meet a melt-flow index and density, but joining properties can be greatly affected by flow enhancers, regrind content, lubricants, etc. Material purchased to similar specifications from multiple vendors often do not perform with equal results. Polymeric materials must approach the compositional rigor imposed by metals standards to enhance their use in medical devices.

Joint designs for metals and plastics should also be developed and shared across the industry. Guidelines for joint-fitup, gap tolerance, weld penetration, and heat input would help improve overall quality and reliability of medical devices.

The weldability data given in Figs 3.1 and 3.2 should be expanded upon, especially for dissimilar material combinations. Further, that database should be driven by welding technology, as some small-scale laser welds cool so rapidly, the process can violate what the handbooks would indicate as weldable.

Biocompatibility and corrosion performance of joints should be studied and a database of performance presented to the medical industry. Many materials could be used for certain applications, but since compatibility is governed from a device level, some material choices are neglected because they must replicate what has been used in the past. This regulation limits the use of new materials until an overall design is approved.

Fatigue performance and testing of implantable devices is an area of increasing concern. Many devices see significant cyclic stresses associated

© Woodhead Publishing Limited, 2013

with cardiac/vascular or musculoskeletal motions. For example, the average person's heart beats approximately 400 million times during the 10-year expected life of many cardiac leads. Muscle contractions can be strong enough to crush a pacemaker or ICD pulse generator can and may repeat thousands of times depending on the activity level of the patient. As devices trend toward small and thinner designs the cyclic stresses on components and joints can become increasingly severe. This has been highlighted by several recent high-profile product recalls associated with fatigue failures of device components. Consequently, regulating bodies and standards will be increasingly focused on fatigue performance and testing.

Lastly, a key future trend in medical devices is a push toward more automated assembly processes. Current practice of manual assembly places high requirements on training and inspection processes. The use of automation has the potential to improve overall quality and reliability by removing the human element and inherent variability of manual processes.

3.7 References

1. FDA Classifications for Devices, www.fda.gov.
2. B.D. Ratner, A.S. Hoffman, F.J. Shoen, and J.E. Lemons, *Biomaterials Science*, Academic Press, 1996.
3. G.F. Carter, *Principles of Physical and Chemical Metallurgy*, American Society of Materials, 1979.
4. ASM Handbook, *Properties and Selection of Non-Ferrous Alloys and Special Purpose Materials*, Vol. 2, ASM International, 1990.
5. X. Li, J. Xie, and Y. Zhou, Effects of Oxygen Contamination in the Argon Shielding Gas in Laser Welding of Commercially Pure Titanium Thin Sheet, *J. Mater. Sci*., **40**, 3437–43, 2005.
6. N.J. Noolu, H.W. Kerr, Y. Zhou, and J. Xie, Laser Weldability of Pt and Ti Alloys, *Mater. Sci. Eng. A*, **397**, 8–15, 2005.
7. G. Jiang, D. Mishler, R. Davis, J.P. Mobley, and J.H. Schulman, *Biomed. Mater. Res. Part B: Appl. Boiomater*. **72B**, 316–21, 2005.
8. K.J. Ely and Y. Zhou, Microjoining in Medical Components and Devices, in *Microjoining and Nanojoining* (Ed. Y. Zhou), Woodhead Publishing, 2008.
9. S. Fukumoto and Y. Zhou, Metall. Mater. *Trans. A*, **35**, 3165–76, 2004.
10. A. Fuji, T.H. North, K. Ameyama, and M. Futamata, *Mater. Sci.*, *Technol*., **3**, 219, 1992.
11. G. Wang, "Welding of Nitinol to Stainless Steel" SMST-97, *Proceedings of the Second International Conference on Shape Memory and Superelastic Technologies*, eds. A. Pelton, T. Duerig, D. Hodgson, and S. Russell (Pacific Grove, CA: International Organization on SMST), p. 131.
12. P. Hall, "Laser Welding Nitinol to Stainless Steel" SMST-2003, *Proceedings of the International Conference on Shape Memory and Superelastic Technologies*, eds. A. Pelton and T. Duerig (Pacific Grove, CA: International Organization on SMST), p. 219.
13. Robert A. Grimm, *IR Welding of Polymers*, MDDI, May 2001.

© Woodhead Publishing Limited, 2013

14. P.C. Heimenz, *Polymer Chemistry*, Marcel Dekker Inc., 1984.
15. V.A. Kagan, R.G. Bray, and W.P. Kuhn, Laser Transmission Welding of Semicrystalline Thermoplastics, *Journal of Reinforced Plastics and Composites*, **21**, 1101, 2002.
16. K. Mistry, Plastic Welding Technology for Industry, *Journal Assembly Automation September*, **17**(3), 196–200, 1997.
17. *Ultrasonic Welding of Plastics Used in Medical Devices*, Welding Technology Institute of Australia, TGN-MS-04, Rev 0, April 2006.
18. G.E. Dieter, *Mechanical Metallurgy*, McGraw Hill Company, 1986.

© Woodhead Publishing Limited, 2013

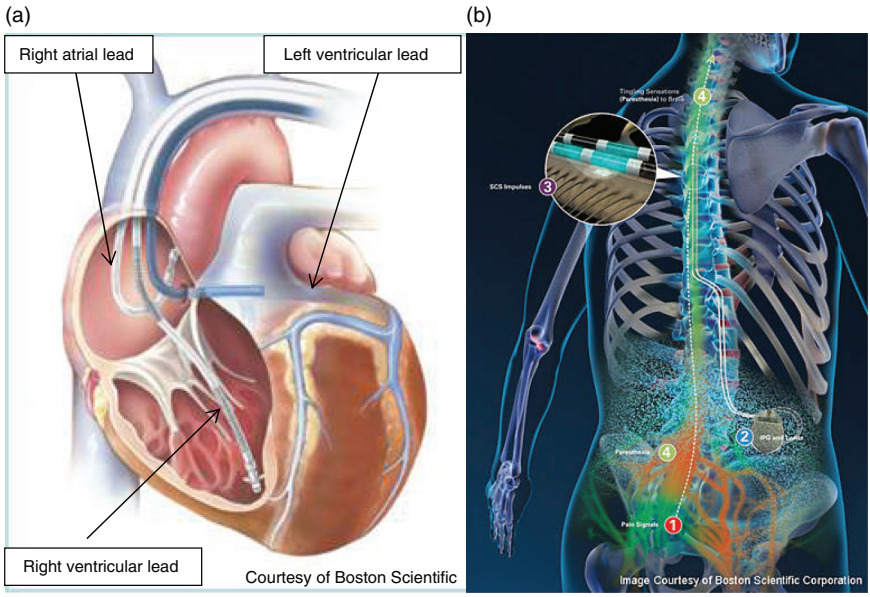


Plate I (Chapter 3) (a) Typical implanted cardiac leads and (b) spinal nerve stimulation implant (courtesy of Boston Scientific). (1) Pain signals; (2) IPG and leads; (3) SCS impulses and (4) (top) tingling sensations (parasthesia) to brain, (bottom) parasthesia.

© Woodhead Publishing Limited, 2013

4

The effects of sterilization on medical materials and welded devices

W. J. ROGERS, Consultant, USA

DOI: 10.1533/9780857096425.1.79

Abstract: The effects of a sterilization method on medical materials such as polymers are diverse. The number of sterilization agents is few without significant adverse effects to materials and polymers. Effects of sterilization methods consider not only chemical and physical effects, but also some effects on applications such as welding and device compatibility. Selecting the right method for a particular or specific product or procedure can be challenging in some situations, but beneficial and critical within other cases.

Key words: compatibility, dry heat, effects, ethylene oxide, hydrogen peroxide, ionizing radiation, materials, medical, plasma, moist heat(steam), polymers, ozone welding, effects, materials, medical, welding, sterilization.

Note: This chapter contains material previously published in *Sterilisation of biomaterials and medical devices*, eds. S. Lerouge and A. Simmons (Chapter 7 Sterilisation techniques for polymers by W. J. Rogers), Cambridge, Woodhead Publishing Limited, 2012, ISBN: 978-1-84569-932-1.

4.1 Introduction to sterilization

Sterilization is a like a magic wand that eliminates and removes all microbes and biological organisms from medical materials and medical devices. It inactivates extremely resistant bacteria spores that may have survived and recovered after thousands of years, since the pyramids.

Sterilization is used to create a germ-free environment and products, reducing the risk of microbial infections for the ultimate promotion or preservation of health. Sterilization is basic to the processing and manufacturing of sterile medical materials and medical devices.

'An ounce of prevention is worth a pound of cure.' Without sterilization, infectious disease would exist everywhere in a hospital or healthcare facilities, and it is debatable that antibiotics could ever control the onslaught of infections everywhere. Consequently, sterilization has tremendous value

© Woodhead Publishing Limited, 2013

to medicine surgery and healthcare facilities. Sterilization is typically performed by dry heat, ethylene oxide (EO) and hydrogen peroxide with and without plasma, irradiation, and ozone. The number of sterilization methods are few that are effective and efficacious without adverse effects to medical materials and devices, such as polymer degradation, melting, and oxidation of some metals.

The effect of sterilization on medical materials and devices can provide reasons why one method of sterilization is applied, employed and another is not, and why there is ultimately a sterilization method available and right for your medical material and device.

Heat sterilization (dry and moist) are traditional methods, but alter, corrode damage, distort, or melt many materials. Moist heat like steam can wet, distort, soften, expand and affect product functionality. Dry heat can melt and cannot sterilize aqueous exposed materials. Dry heat can sterilize some powders. Steam and dry heat have many similarities, including being easy to control and monitor, being inexpensive, and not having toxic residues or wastes as EO and gamma radiation may have. Ethylene oxide is a standard method that is able to sterilize many materials, but not liquids, and craze some materials, leaving toxic residues and by-products. Radiation is another standard method, but it can change molecular structure (cross-link or scissor), cause odors, change pH, discolor, embrittle, stiffen and degrade a few materials, or affect bond strengths and cause changes over shelf life. The development of sterilization has changed over the past few years. Hydrogen peroxide and ozone are two newer terminally accepted sterilizing methods. They can both oxidize some materials. Hydrogen peroxide cannot sterilize cellulosics. The potential disadvantages of oxidizing agents include their oxidizing reactivity with certain materials (e.g., rubber, celllulolistics, and polyurethanes). Neither hydrogen peroxide nor ozone have the penetration capability of traditional methods of dry heat, ethylene oxide, irradiation, or steam.

4.2 Sterilization methods

Sterilization is defined as killing or eliminating of 'all' types of biological organisms and is achieved by either physical or chemical processes. It is an absolute term as well as a probability function.

Processes that do not kill or eliminate all types of microbes are not deemed to be sterilization methods, but may be techniques such as antiseptics, decontamination agents, disinfection, germicides, high level disinfectants, or sanitizers. Current acceptable, available and recognized 'terminal' sterilization methods are dry heat, ethylene oxide, hydrogen peroxide with or without plasma, irradiation, steam, and ozone.

© Woodhead Publishing Limited, 2013

4.2.1 Dry-heat sterilization

Dry-heat sterilization is one of the oldest sterilization methods from the time of the ancient Egyptians, but it is infrequently applied in medical-device industry, except in the pharmaceutical area where it is used as part of aseptic processing.

It was originally used to preserve and sterilize items that were moisture sensitive. Today it is used to sterilize items such as powders, glass, non-aqueous materials, electronics, and silicone prosthesis. In hospitals high-temperature dry heat (e.g., 150–180°C) should only be used for materials that might be damaged by steam or impenetrable to steam. Dry heat has continued to be used in sterilizing dental instruments to minimize the corrosion of sharp items, and depyrogenation of pyrogens. It has been used more recently as the method of choice for spacecraft sterilization in the United States. The Russians used an EO/methyl bromide gas mixture, instead. With its further evolvement for sterilization of spacecraft component, etc. dry-heat sterilization became more useful. As a result it is used to sterilize silicone prosthesis (e.g., mammary glands).

Classically, dry heat has meant very high temperatures which have destroyed many items. In the pharmaceutical industry it is used to depyrogenate or inactivate pyrogens (typically cell walls of dead microbes that can elicit a febrile response from the patient).

Dry heat requires significantly more time or higher temperature to process and to inactivate resistant microbes (e.g., spores) on products than steam. Consequently dry-heat sterilization has been generally reserved for materials and products that cannot withstand steam (e.g., glass, powders, and depyrogenation) or penetrate with steam (e.g., silicone and prosthesis).

Dry-heat sterilization (Table 4.1) is as simple as baking in an oven. Dry-heat sterilization is a time- and temperature-dependent variable. With dry heat, the best sterilization occurs with elevated temperature (e.g., 105–190°C) and under dehydrated conditions. Typical dry heat (160–180°C) is the simplest, least expensive method, with fewer parameters and excellent penetration capabilities; however, it has long exposure:

- 6 min: 190°C
- 30 min: 180°C
- 60 min: 170°C
- 120 min: 160°C
- 150 min: 150°C
- Overnight: 105–135°C

Besides long exposure time it has a slow rate of heat penetration. New infrared can sterilize faster, but is not necessarily approved for hospitals.

© Woodhead Publishing Limited, 2013

Table 4.1 Dry-heat sterilization

Principal advantages

- simplicity (like baking), penetrating; and lack of consumables and toxic residuals
- generally reserved for materials and products that cannot withstand steam (e.g. powders, oils, hydration of certain polymers, corrosion of instruments, and dulling of sharps)
- dry-heat depyrogenates (deactivates pyrogens)
- sub-sterilization part of aseptic processing
- used as the method of choice for spacecraft sterilization in the United States
- sterilizing silicone implants that are cross-linked by radiation; impermeable to steam, peroxides; absorbable with EO
- sterilization of some electronics, which are inactivated by steam, high humidity EO/formaldehyde; irradiation
- may sterilize same polymers as steam sterilization, at lower temperatures but at much longer exposure times.

Principal disadvantages

- long processing (heat-up) times; high temperatures (160–190°C)
- fewer compatible polymers unless temperature is reduced (e.g., 105–135°C) but still cannot sterilize heat-sensitive materials like EO or irradiation
- minimizes corrosion and dulling of instruments as observed in steam sterilization, nevertheless this can occur if instruments are not pre-cleaned, treated and dried before dry heat sterilization
- heating is slow, unless using other means of transferring heat beyond convectional heated air
- longer sterilizing times compared to steam
- limited packaging to allow for heat transfer
- the transfer of heat by steam sterilization at 250°F (121°C) is 12 times greater than with hot air

Infrared, however, is used in the pharmaceutical industry for depyrogenating, sterilizing glass vials.

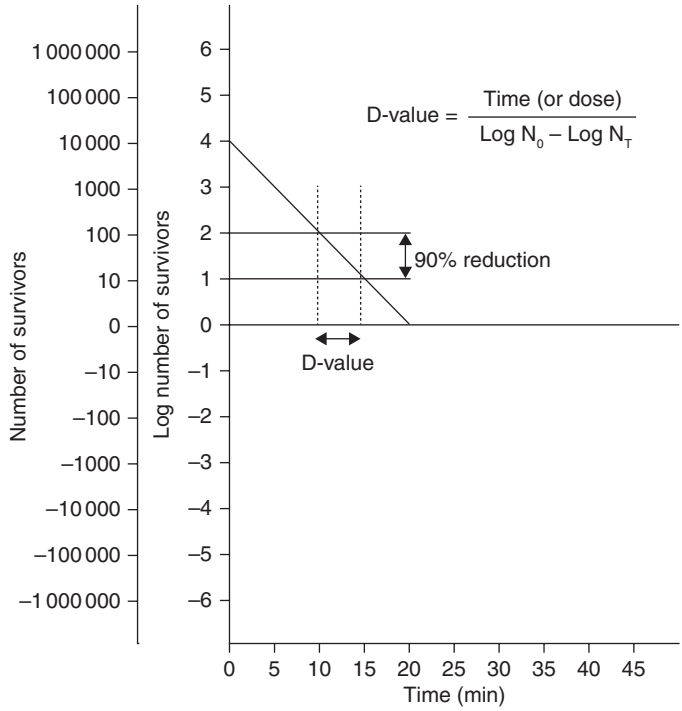
At a lower temperature (e.g., 105–135°C), more materials and devices become compatible. Lower sterilizing temperatures (e.g., <105°C) have been demonstrated with more than a day or year D-value. A D-value is defined as the time to kill one log or 90% of a population at a given temperature. The time to kill 90% of a *Bacillus atrophaeus* population at 120°C may be 1 h. Times also will vary depending upon the spore history, environment, substrate of the population, and heat-penetration needs of a product. The D-value (Fig. 4.1) is the backbone of microbial death kinetics.

The classical method is the Stumbo method, as follows:

$$\text{D-value} = \frac{\text{Exposure time or dose of sterilization}}{\text{Log } N_0 - \text{Log } N_T}$$

where N_0 is the initial number of organisms (the bioburden or biological indicator population) and N_T is the number of survivors after the exposure time or dose of the sterilant.

© Woodhead Publishing Limited, 2013



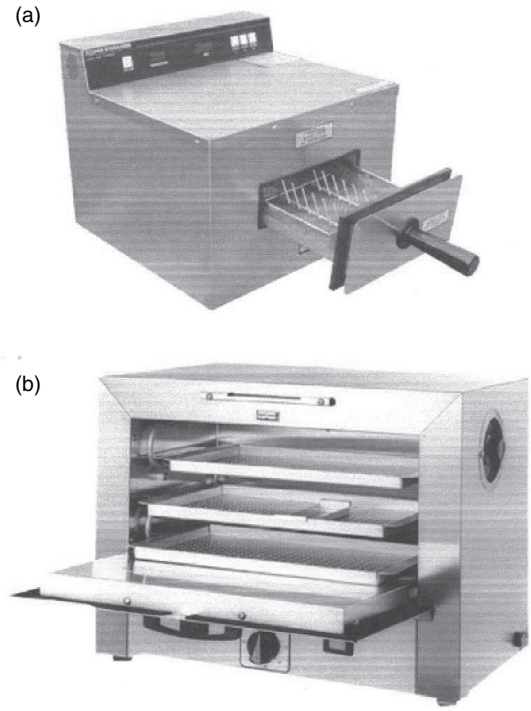
4.1 Microbial inactivation kinetics—death-value (D-value).

Bioburden is an estimate of what is on the product or item being sterilized. The biological indicator (BI) is a solution or carrier consisting of a known concentration (population) of spores (typically) that is highly resistant to and challenges the sterilization method (e.g., steam, EO, and dry heat).

Two typical commercial dry-heat sterilizers (Fig. 4.2) run exposure times of, for example, 6 min at 190°C and 30–120 min between 160°C and 180°C. At its highest temperatures (e.g., 330°C) dry heat becomes virtually an 'absolute method' and fastest (1.15 s) sterilization (Rhodes, 1966[1]) by breaking down all organic matter down to carbon. At its lowest possible temperatures (37°C or lower), dry heat can take the longest exposure time (~45 days D-value) of virtually any method to cause sterilization inactivation (12 × 45 days = 540 days). Theoretically at 0°C, under extreme dehydration, the dry heat D-value would be about four years. (Molin, 1977[2]). To achieve an overkill sterilization (e.g., 12 × D-value) this would require ~48 years.

Sterilization by dry heat, however, occurs primarily by dehydration and oxidation, but at temperatures typically at the same or higher than steam, which limits the types of heat-sensitive materials and polymers, unless there is a willingness to sterilize at lower temperatures and process for extremely long periods under dehydration conditions. So at its highest temperature

© Woodhead Publishing Limited, 2013



4.2 Two commercial dry-heat sterilizers: (a) Cox fastest dry-heat sterilizer (6 min unwrapped at 375°F (190°C) temperature; 12 min wrapped) and (b) Wayne S1000 dry-heat sterilizer (standard 160–180°C oven for instruments).

it could virtually destroy everything (and would even temper metals) that came in contact with it; however, at its theoretically lowest level it would take too much time to achieve sterility.

There is a chemical vapor dry-heat sterilizer that may sterilize in 20 min at 132°C. Its effects on polymers, however, is unknown. It does sterilize metal instruments without dulling, rusting, or corrosion, as steam sterilization may, and it is much faster than standard dry-heat sterilization with just heated air.

4.2.2 Ethylene oxide sterilization

Ethylene oxide (Table 4.2) is a mild sterilant to most medical materials and polymers. It is a long process with preconditioning and/or prehumidification, gas introduction, sterilization, evacuation air washes and aeration (Fig. 4.3) and the later step (aeration) is required to reduce EO

© Woodhead Publishing Limited, 2013

Table 4.2 Ethylene oxide sterilization

Principal advantages
- complex process but can be process controlled released through review and acceptable critical parameters, verification of validated sterilizer, product and packaging, and extra 'chemical' monitoring
- relatively simple to operate
- many safety systems
- can sterilize and is compatible with most polymers
- has been available and widely used
- sterilizes many reusables
- excellent penetration, penetrates many packaging and polymer materials, lumens, some mated surfaces as well as significant organic matter

Principal disadvantages
- can not sterilize liquids
- can leave toxic residues, which require aeration time
- lengthy cycle and aeration time
- EO is flammable, explosive without mixture
- EO is toxic and a carcinogen, etc.
- air can be a barrier to steam diffusion, for humidification
- can not sterilize oils
- there are significant regulations
- there are significant controls and safety required
- EO emissions must be controlled

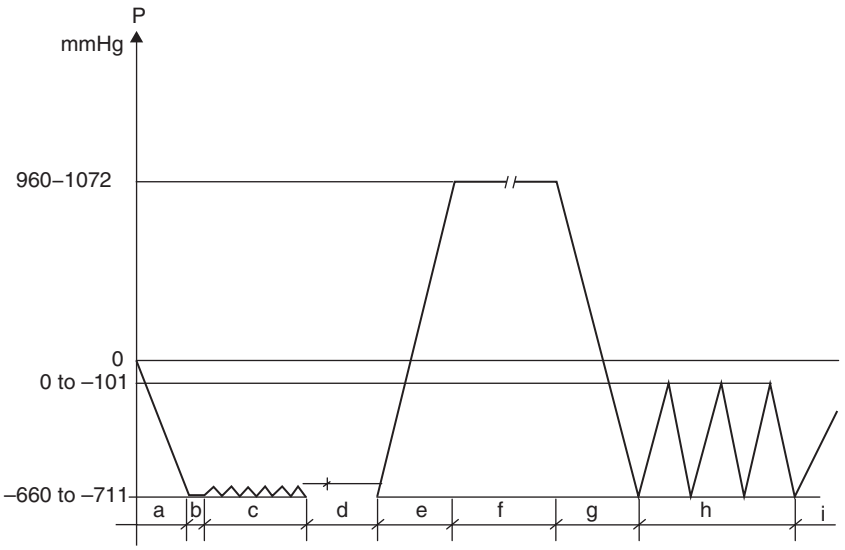
toxic residues, when necessary. Ethylene oxide requires typically temperature control such as +/– .5 C ambient to 63°C; relative humidity control within +/– 5% RH within a range of 40–80%, EO gas concentration typically higher than 400 mg/L. Lower EO concentrations have been used with expertise and specialized processing. Further control of evacuations and preconditioning to place moisture to the bacterial site and post-cycle vacuums to remove the toxic gas and reduce EO residuals within polymers. Because of the use of toxic gas, it requires post-sterilization aeration, special handling, control, scrubbers, and meeting a large number of regulations.

EO evolved for sterilizing heat-sensitive materials such as plastics, rubber, and metals upon continual exposure. EO was not meant as an alternative to steam sterilization, but as an alternative process for temperature-sensitive items. It is an ideal gaseous sterilant because of its characteristically high diffusivity, permeability, and gentleness to most medical materials and medical devices.

While EO sterilization probably has been the predominant method of gaseous chemical sterilization, it has remained second to steam sterilization in the hospitals, but not in the medical-device industry.

The EO process can be lengthy where medical materials and medical devices need to be preconditioned before sterilization and aerated after sterilization to remove toxic residues before using. While it can penetrate

© Woodhead Publishing Limited, 2013



4.3 A prehumidification EO sterilization cycle. Steps: (a) initial evacuation, (b) leak check, (c) prehumidifying, (d) humidity dwell, (e) ethylene oxide gas mixture injection, (f) ethylene oxide exposure, (g) post-evacuation, (h) 3 air washes, (i) final air inbleed to atmospheric pressure.

long lumens and (some) mated surfaces and sterilize papers or other materials that other methods such as hydrogen peroxide, steam, and ozone cannot, EO sterilization has been challenged by less dangerous, toxic and wasteful chemical methods, such as ozone and hydrogen-peroxide sterilization in hospitals, and irradiation in industry.

4.2.3 Hydrogen-peroxide sterilization

Hydrogen peroxide (Table 4.3) is relatively new and an alternative to EO for many materials and devices in the hospital.

Hydrogen peroxide (with plasma) sterilization provides a dry, low-temperature (e.g., 37–44°C) and nontoxic method, at the end of the process; however, extremely deep vacuums and a high concentration of H_2O_2 exists at the start of the process. It is not highly penetrable, but is increasingly used in hospitals for surface devices. With low temperature hydrogen peroxide gas plasma, the following process parameters need to be applied, considered and evaluated, such as H_2O_2 concentration (e.g. 6–18 mg/L), temperature (e.g. 37°–44°C, < 55°C), the presence and duration of plasma, and pressures (e.g. rate, level or both), vacuums (e.g. <50 Pa, <–0.5 Torr), exposure (time to sterilise). Exposure and

© Woodhead Publishing Limited, 2013

Table 4.3 Hydrogen peroxide and plasma

Principal advantages:
- relatively new as an alternative to ethylene oxide, with lots of technological breakthroughs and investigations
- it has been an expanding technique and is becoming a more available method
- it is ultimately environmentally safe; but uses a toxic consumable
- it is a relatively rapid process
- good candidate for many low-temperature moisture-sensitive materials that tend to be hydrophobic and chemically stable, which resist oxidation
- leaves no toxic residues
- simple to install
- sterilizes many medical devices, but not long lumens, or products with mated or hidden surfaces

Principal disadvantages:
- unlike EO, which is an alkalizing agent and penetrates through packaging and most devices, hydrogen peroxide gas plasma is an oxidizing agent
- it typically has only 'surface' contact capability, does not have diffusability like EO
- very deep vacuums are drawn
- requires special packaging
- number of materials compatible with H_2O_2 while extensive, has some notable exceptions, e.g., cellulose (includes paper, cellulose acetates), linens, natural rubber, polyamides, and liquids
- avoid absorbers (nylon, polyurethane, decomposers (silver, copper, copper alloys)
- small chamber size
- peroxide (H_2O_2) may be toxic at levels greater than time weighted average (1 ppm TWA)

process times continue to be reduced such as 73–52 min and further to a possible 32 min exposure with removal of most water from the H_2O_2.

With hydrogen peroxide with plasma, a very deep vacuum is drawn initially to vaporize the H_2O_2 and sterilize; then an electrical field is created by radio frequency to create a gas plasma; then the gases are removed and in the final stage vented to atmospheric pressure with-high efficiency filtered air. Newer and improved processes include consecutative sub-processes to improve penetration and inactivation.

Hydrogen peroxide with plasma and ozone are considered nontraditional sterilization methods yet are readily acceptable by regulatory agencies such as the FDA, because they do not have any toxic residuals *per se*.

Hydrogen peroxide (without plasma) can exist in vapor and liquid form. But the discussion here is of the vapor not liquid state. In the vapor phase it generally follows the ideal gas law.

Hydrogen peroxide has excellent antimicrobial properties against a wide range of microorganisms including bacterial endospores. Under carefully controlled process conditions hydrogen peroxide is also safe for use with

© Woodhead Publishing Limited, 2013

many materials. Hydrogen peroxide may be decomposed into water and oxygen rendering it environmentally safe.

Hydrogen peroxide is a strong oxidizing agent. Hydrogen peroxide primarily reacts with cysteine-containing proteins, creating disulfide crosslinks between proteins. This oxidation of amino-acid moieties within a given protein may cause secondary damage as the radicals modify other amino acids within that protein or other proteins. Another inactivation mechanism of damage may be through intracellular reactions. For example, reactions may occur when iron (II), present in heme groups or in other forms, reacts with peroxide forming hydroxyl radicals. Such hydroxyl radicals would be highly reactive and can oxidize most organic molecules within a cell.

While hydrogen peroxide with plasma may have additional excellent microbiocidal properties, it has poor penetration. And while highly toxic in form before sterilization it may be environmentally acceptable under process control. H_2O_2 is typically used in the vapor phase for medical materials and devices. While it is compatible with many polymers, there are some materials that are damaged (e.g., acrylics, cellulosics (includes paper), natural rubbers, and bioadsorbables such as polyglycolides and polyesters).

Due to the oxidative nature of hydrogen peroxide vapor, some materials are not recommended for instruments intended for this sterilization method. The low-temperature hydrogen peroxide gas plasma method uses the plasma phase to further eliminate residuals; therefore, most commonly used materials for medical instrument fabrication do not retain enough sterilant residuals to affect biocompatibility and post-sterilization aeration usually is not required, with plasma process; however, with straight H_2O_2 without plasma may require aeration.

4.2.4 Radiation sterilization

Radiation (Table 4.4) is an excellent sterilization method for many materials and single-use devices. There are typically no cleared hospital irradiators; because of its high cost in hospitals it has not been been favored. Large irradiators are used in industry (Fig. 4.4).

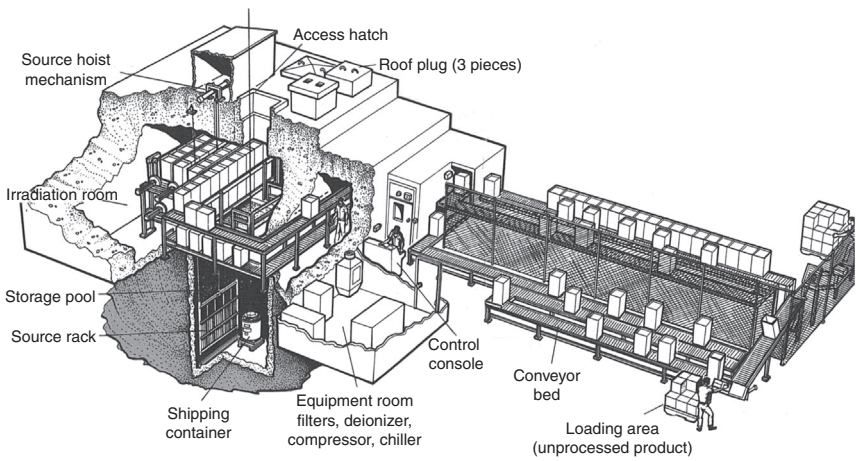
Ionizing radiation requires strong irradiation doses (e.g., 11–40 kGy), much higher than for body scanning. Radiation may be provided from gamma source (e.g., Co_{60}), electron beams or X-rays. It can be very quick (seconds–minutes) to hours. It can have deep penetration, except for dense materials, metals, and water. Irradiation is particularly available industrially, for manufacture of disposable, but not for sterilizing in hospitals. Because of Co_{60} radiation source, radioactive wastes, X-rays, or electron beams, expensive facilities, equipment, and special handling and control of the process are necessary.

© Woodhead Publishing Limited, 2013

Table 4.4 Irradiation

Principal advantages:
- radiation is an excellent sterilization method for many materials and devices
- no toxic agents used; deep penetration; dosimetric release; short exposure times, and simplicity of routine operation as compared with ethylene oxide
- has actually been demonstrated (1896) prior to ethylene oxide, ozone, hydrogen peroxide, but not before moist heat or dry heat
- sterilizes most medical devices, except reusables

Principal disadvantages:
- it requires expensive facilities and equipment; safety criteria
- it causes the generation of by-products (e.g., ozone, leachables, pH shifts), change in materials (e.g., odor, discoloration, stiffening, cracking), a few polymers unusable (natural polypropylene (PP), acetals or polyoxymethylene (POM), or teflon (e.g. polytetrafluoroethylene)); radical formation in water, liquid; limited tissue and drug irradiation
- qualification may require extended, time-consuming stability evaluations
- material validations can be expensive and lengthy
- gamma irradiation has toxic wastes
- exposure to irradiation can be a serious risk to health
- it is highly regulated



4.4 Automatic tote box irradiator.

Radiation has long been recognized as a means of sterilization since X-rays were first demonstrated in 1896 to inactivate microorganisms. However, its practical application followed the use of EO because of the continuous improvement of plastic materials and medical devices, the availability of improved electron-beam accelerators and radioactive materials, and increased regulations on the use of EO.

© Woodhead Publishing Limited, 2013

There are three major types:

1. Gamma irradiation provides protons with high penetration, longer exposure; but has toxic radioactive waste.
2. E-beam uses electrons which have limited penetration, are fast, and have no toxic waste.
3. X-ray delivers protons which have deep penetration, are moderately fast, and have no toxic waste.

Radiation can sterilize medical devices, pharmaceuticals, treat cosmetics, spices, biologics, foods, and consumer products. Radiation processes are very effective, but they are still very expensive and have not been put into use for general-hospital sterilization of supplies on site. Also, radiation would not be able to resterilize a number of polymer multiple resterilizations without effects on medical materials and polymers over exposures and time. Also, radiation is not typically useable in hospitals, due to costs and reusables.

Irradiation has been developed as means of sterilizing single-use (disposable) devices. It has tremendous penetration and 'killing' effectiveness, but it is costly for hospitals and not compatible with every product or material, multiple times.

4.2.5 Steam sterilization

Saturated steam (Table 4.5) is a simple, available, easy, environmental, and traditional sterilization process. In healthcare facilities, most medical materials and devices are made of materials that are heat stable for steam sterilization, but there are some medical materials and devices that are made of polymers which are heat and moisture sensitive.

Steam sterilization can inactivate all biological entities including prions, *Pyronema domesticatum*, and extremely small target viruses. With steam (moist-heat) sterilization, saturated moisture conditions elevated pressures, and elevated temperature (e.g., 104–138°C) are optimal for sterilization. The lower the temperature, the longer the exposure; however, more materials tolerate lower temperatures. Steam sterilization is available and traditional to healthcare facilities. Heat sterilization without steam or moisture is dry-heat sterilization.

Steam sterilization has long been recognized for its simplicity, efficiency, effectiveness, low cost, and speed of operation. In the 1880s Koch recognized that dry heat was relatively inefficient compared with moist heat; however, he did not rule out dry heat because of the need to decontaminate silk thread.

© Woodhead Publishing Limited, 2013

Table 4.5 Steam sterilization

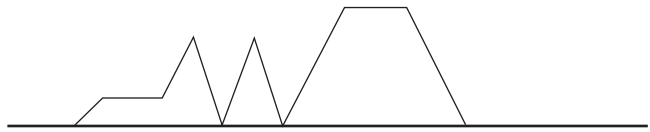
Principal advantages:
- simple process, can be process controlled released (through integration of lethality, from accumulation of temperature increments); relatively short exposure times; relatively inexpensive
- can sterilize many liquids
- available, widely used; sterilizes many reuseables
- lack of toxic residues
- can sterilize foods and many drugs
- efficient and fast (rapid cycle time)
- penetrates porous dense packs, medical packaging, lumens

Principal disadvantages:
- high temperature; incompatible with many heat- and moisture-sensitive polymers and materials
- can corrode and dull instruments, causing some instruments to rust
- not as penetrable as EO and irradiation
- air can be a barrier to steam diffusion
- can not sterilize powders and oils
- there is a potential for burns (e.g., for uncooled materials)

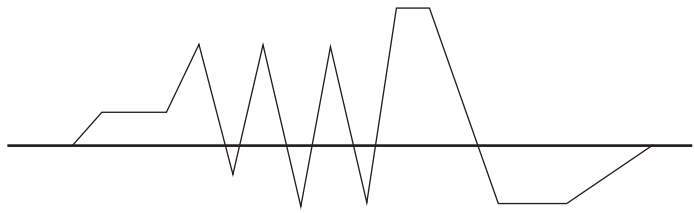
Steam sterilization is currently considered as a more ideal candidate because of its compatibility with the environment (not toxic agents or wastes) and health safety, and its capacity to sterilize the most resistant biological entity, the prion. But the number of plastic materials, chemicals, and some metals capable of tolerating its high temperature and moisture (corrosion and hydration) are few. In hospitals and laboratories where reusable materials are frequently used, steam sterilization is predominantly used. It is also widely used in decontamination of infectious waste materials. Now, however, with emphasis on the environment, there is renewed interest in this method of sterilization. Unlike most other sterilization methods, steam is compatible with most aqueous liquids. Steam can sterilize most metals, glass, and some heat-resistant plastic materials.

The number of plastic materials capable of being steam sterilized will vary considerably with the selected temperature of sterilization. Standard steam sterilization is generally carried out at 250°F (121°C) for 15–20 min. Faster or immediate to use (flash) sterilization is generally carried out at 270°F (134°C) and greater for 3–4 min, typically without wrap or packaging. Burns can occur from such a process if the product being sterilized is not cooled before use. Longer sterilization or lower steam sterilization is carried out at 240°F (115°C) (e.g., 30 min). Lower steam sterilization can be performed at approximately 212°F (100°C) (fractional) but lower-temperatures approaches are marginal and possibly questionable, unless other aspects are provided. Some alternative approaches to classical steam sterilization for lower temperatures are combination of steam and formaldehyde, and steam sterilization of liquids with acids, etc.

© Woodhead Publishing Limited, 2013



4.5 A dynamic gravity pulsing sterilization cycle curve. With a series of steam purge and pressure pulses with heat up phase to pressure, and a pressure hold period followed by cool down phase as shown above standard atmospheric pressure line. Simple gravity method will show only pressure displacement of air, hold period and cool down.



4.6 A dynamic evacuation pulsing sterilization cycle curve. With a series of steam purge and pressure/evacuation pulses with heat up phase to pressure, and pressure hold period followed by evacuation and drying period before returning back to the atmospheric standard pressure line. Simple high evacuation steam cycle would have neither the initial steam purge nor the pressure/evacuation series of pulses.

Steam sterilization 'overall' is more widely employed and available than other methods, but it can be deleterious to heat labile medical materials and healthcare products. It is the work horse in must hospitals. It has multiple processes for different situations. Low and high temperatures: removal of air by gravity or vacuum or pulsing. Gravity allows lighter steam to drive air out at the bottom of the chamber (Fig. 4.5). However, it may not remove all air which could result in failure to sterilize completely. The vacuum and steam pulsing processes are more ideal for removing air (Fig. 4.6).

Other processes typically not seen in hospitals are steam–air mixtures (SAM) and air overpressure (AOP). These are special processes adapted in pharmaceutical and medical-device industries to prevent certain products (containers) and packaging from bursting.

Steam autoclave is used today to eliminate and reduce outbreaks of the spore *Clostridium difficle* in hospital and other nosocomial contamination and infections. Because of its deleterious effects on heat-liable medical materials and medical devices it is frequently replaced by EO, hydrogen peroxide, irradiation, and ozone sterilization.

However, steam sterilization is both a classical and traditional method of sterilization, continuing today and into the future. Steam remains the

© Woodhead Publishing Limited, 2013

preferred method of sterilization in healthcare facilities, including the pharmaceutical industry, despite availability of low-temperature processes of increasing complexity for temperature-sensitive items. Steam remains a powerful weapon in the sterilization arsenal, including elimination or inactivation of prions.

There is a steam–formaldehyde process that will not be fully discussed here. It may be more compatible with heat-sensitive polymers than steam because it runs at 70–75°C cycles. However, it has toxic formaldehyde present which must be eliminated with aeration or neutralization, and it is a hotter cycle than other alternative heat-sensitive sterilization processes such as EO and hydrogen peroxide with plasma and ozone. It will not have the penetrating capability of EO sterilization.

4.2.6 Ozone sterilization

Ozone sterilization (Table 4.6) of medical devices has recently been introduced to healthcare facilities. It is a safe process by introducing the ozone *in situ* into a sterilizing chamber (Fig. 4.7). There are no toxic residues, and it may be more penetrable than hydrogen peroxide vapor (with plasma), but not as penetrable as EO, steam, dry heat, or irradiation.

In gaseous low-temperature ozone sterilization, the typical process variations or parameters required are vacuum, time, temperature, ozone concentration, humidity, and pressure (rate, level or both). The ozone concentration is typically at 85 mg/L for 15 min at a temperature of 30–36°C. The process temperatures are generally low, making it suitable for temperature-sensitive materials. Ozone sterilization can be achieved in water as well as gaseous form. Ozone is a very strong oxidizer, making it an efficient sterilizing agent. It is relatively new (gaseous) technique for medical devices, making it a nontraditional and acceptable process, although it has been traditionally used to sterilize water, etc.

This section relates only to ozone in the gaseous state. The sterilant must be able to penetrate all portions of a load and product areas intended to be sterilized. Materials must be resistant to oxidation. Gaseous ozone requires high humidity to be effective.

Ozone is produced by mean of an electrical discharge passing through oxygen (O_2). Due to its thermodynamic properties, ozone is a metastable product; it decomposes slowly (in minutes) at ambient temperatures and rapidly (in seconds) at higher temperatures.

Since ozone is a strong oxidizer it is an efficient sterilizing agent. But because ozone is a metastable product, it cannot be stored and is therefore produced *in situ*. Ozone-sterilization processes are particularly suited for sterilizing heat-sensitive materials because temperatures within the load currently do not exceed 36°C (97°F). The process is considered safe because

© Woodhead Publishing Limited, 2013

Table 4.6 Ozone sterilization

Principal advantages:
- ozone sterilization is environmentally friendly
- a replacement for EO and H_2O_2
- ozone sterilization is inexpensive
- leads to environmentally safe breakdown products—oxygen and water vapor
- ozone is easily prepared/produced on site, no transportation of toxic consumable as there is with H_2O_2.
- it has excellent microbial sterilizing capabilities
- it can sterilize many low temperature materials, as well as higher temperature materials (e.g., stainless steel, titanium anodized aluminum, ceramic, glass, silica, PVC, Teflon, silicone, polypropylene, polyethylene, and acrylic).
- it can potentially process some cellulosics, more so than H_2O_2
- it can sterilize many reusables
- it can penetrate longer lumens than H_2O_2
- can sterilize in larger chambers than H_2O_2

Principal disadvantages:
- may produce surface oxidation
- materials must be resistant to (strong) oxidation
- the shape of the materials as well as the design of a device is closely related to the longevity and resistance of the device to ozone sterilization
- polymeric components with large surface-to-mass ratios (e.g., fibrous material) will undergo fast oxidative degradation
- will not penetrate organic matter as well as EO
- ozone is unstable, half life is only 22 minutes at room temperature

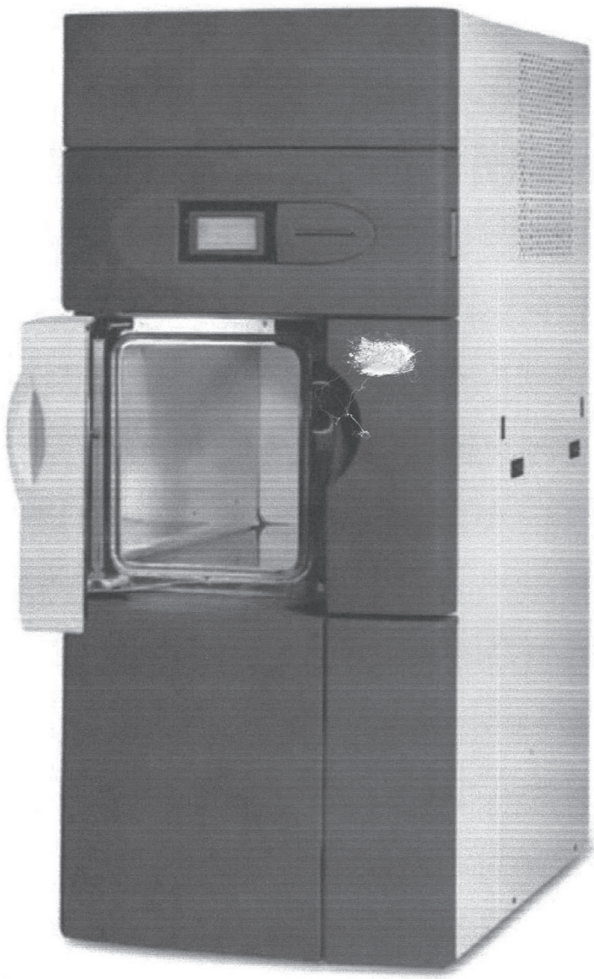
there are no toxic emissions (just O_2 and water), no residues to aerate, and a low processing time will not result in accidental burns.

Hydrogen peroxide (H_2O_2) and ozone (O_3)

There is a newer ozone process that combines ozone with hydrogen peroxide: the microbiocidal efficacy of the action of free radicals formed by the two sterilizing agents in this process, hydrogen peroxide (H_2O_2) and ozone (O_3). The mode of action for these two chemicals on microorganisms may be complex and specifically relates to the formation of free radicals such as $HO\bullet$, $O_2\bullet$-, $HO_2\bullet$, $HO_3\bullet$, $HO_4\bullet$ and other reactive species. In this oxidative-sterilization process, the radicals are formed first by the hydrogen peroxide and then by the reaction of ozone with the hydrogen peroxide, water, and radicals already present in the chamber. The combined process is fast, efficacious, low cost, has a large load capacity, and potentially higher material compatibility than just hydrogen peroxide vapor.

Ozone has a similar effect to plasma on the hydrogen-peroxide molecule in competitive technologies. However, the effect of ozone on hydrogen peroxide is not limited to only the accessible surface of devices, as in the case of plasma; ozone can penetrate lumens and hard-to-reach geometries.

© Woodhead Publishing Limited, 2013



4.7 A commercial ozone sterilizer

Vaporized hydrogen peroxide and ozone have been used as agents for sterilization and disinfection for many years. When mixed together, they become a very powerful oxidizing agent, often referred to in scientific literature as a peroxone or perozone process. During the combining process, highly reactive particles such as hydroxyl radicals (HO•) are formed. These radicals react by oxidizing a wide variety of organic compounds. These

© Woodhead Publishing Limited, 2013

processes are also called advanced oxidation processes. The advanced oxidative processes are characterized by the generation of hydroxyl radicals via various combinations of chemical and physical agents such as ozone, UV, and hydrogen peroxide. It will not be possible to fully discuss their effect on polymers until more information is acquired, but they may be more similar to just effects of ozone rather than hydrogen peroxide with plasma; however, the presence of ozone will allow for greater penetration of lumens than hydrogen peroxide with plasma. Nonetheless, this combination of peroxide and ozone may be more damaging to celluloses as hydrogen peroxide is.

Oxidizing agents such as ozone and hydrogen peroxide were evolved to replace EO that was extremely regulated, toxic, time consuming, and left toxic residues; however, oxidizing agents oxidize some materials, and they do not have the penetrating ability or capacity of EO.

4.3 The effects of sterilizing on different materials

Several types of materials are addressed within the following classes of materials: plastics and elastomers, metals, ceramics, and glass.

4.3.1 Plastics

The effects of sterilizing modalities on different plastics and elastomers are addressed for each sterilization modality (e.g., EO, heat, hydrogen peroxide, irradiation, ozone). In Section 4.3.2, the effects of different sterilization modalities on specific plastics are rated and described as excellent, good, poor to fair.

Effects of ethylene oxide on plastics

EO sterilization is compatible with nearly every polymer (Table 4.7), except those that may be particularly sensitive to humidity, low temperature, and high EO gas concentration EO sterilization is nearly always very gentle with most polymers, if used wisely. EO is compatible with nearly every polymer, and if there is a problem with the polymer because of the technique, there typically is an expert solution. EO has sterilized many polymers that could not be irradiated or heat sterilized. Some of the limitations related to EO may also relate to polymers' ethylene oxide absorptivity to accumulating residuals, but this will vary significantly depending upon humidity, EO gas concentration, temperatures, and aeration. There may be some sensitivity to humidity, such as hydrophilic coatings, but there are typically solutions to this type of problem. Users also need to be careful with EO sterilization when applying polymers as carriers for drug delivery, and its EO residues reactivity, temperature, and humidification. A drug applied through a plastic

© Woodhead Publishing Limited, 2013

Table 4.7 Polymers compatible with the ethylene oxide technique

Thermoplastics	Effects
Acrylic	Good. Some loss in tensile properties, no discoloration reported on multiple cycles with HCFC-124/EO blends There may be some crazing Excellent with low EO/CO_2 concentration gas mixture, except at high sterilizing temperature >63°C. Low EO cycle with EO/CO_2 gas mix had low absorbency and very short aeration
Acrylonitrile butadiene styrene copolymer (ABS)	Compatible High absorbance of EO and long aeration for desorption Excellent with low EO/CO_2 concentration Gas mixture with low EO concentration had low absorbance and short aeration
Nonplasticized polyvinyl chloride (PVC)	Compatible EO/CO_2 concentration Gas mixture with low EO concentration had very short aeration
Plasticized polyvinyl chloride (PVC)	Compatible Plasticized PVC absorbs more EO than non-plasticized PVC Excellent with low EO/CO_2 concentration Gas mixture with low EO concentration had very short aeration
Polyacetal	Compatible, no degradation Low EO concentration with EO/CO_2 gas mix had short aeration
Polyamide (Nylon, all classes)	Compatible Increased residuals with high humidities; but low residuals with low EO concentration with EO/CO_2 mix
Polyarylsulfone	Compatible
Polycarbonate	Compatible. Some formulations may be subject to stress cracking and some loss of tensile properties after multiple cycles and an extended time post-processing, no discoloration
Polyether sulfone	Compatible
Polyetheretherketone (PEEK)	Compatible
Polyethylene (PE, UHMWPE, LDPE, LLDPE, HDPE)	Generally compatible. HDPE may lose some tensile properties, no off-gassing Excellent with low EO/CO_2 gas concentration mix; absorbs and desorbs EO well, very short aeration EO is excellent with UHMWPE for hip and knee implantation
Polyethylene terephthalate glycol copolymer (PETG)	Compatible
Polymethyl methacrylate (PMMA)	Compatible, no discoloration; EO acceptable for contact lenses

(*Continued*)

© Woodhead Publishing Limited, 2013

Table 4.7 Continued

Thermoplastics	Effects
Polyphenylene oxide	Compatible
Polypropylene (PP)	Compatible. May be some long-term effect on tensile modulus. Excellent with 100% EO. Good with HCFC, no brittleness
	Can sterilize unstablized PP in syringes with no brittleness
	Excellent for 100% (pure) ethylene oxide gas. Good for HCFC-124 blend. Excellent with EO/CO_2 gas mixture
	Absorbs and desorbs EO well
Polystyrene	Typically poor. Some embrittlement and loss of tensile strength for some formulations has been reported
	However, polystyrene petri dishes have been easily sterilized (excellently) with EO/CO_2 gas mixtures and with moderate humidities; many European IV sets with styrene were compatibile with polystyrene parts
	Polystyrene tissue ware will absorb EO and will not desorb well enough
	For cell culture growth, unless low EO concentration in EO/CO_2 gas mix. No crazing and no residuals with low EO concentration with EO/CO_2 gas mix
Polysulfone	Compatible
Polytetrafluoroethylene (PTFE)	Compatible
Polyvinyl chloride	Compatible. Rigid PVC may decrease impact resistance after exposure. Medical-grade plasticized tubing may contain significant residual levels until aerated
	EO/CO_2 gas mixtures had little EO residuals with low EO concentration
	EO and CO_2 have the same molecular weight
Styrene acrylonitrile copolymer (SAN)	Generally OK for one cycle, but may embrittle and lose tensile properties on multiple cycles. May exhibit surface cracking and stress cracking on multiple cycles. Standard EO cycles have high EO absorbency and poor desorption, requiring long aeration
	Compatible with low EO/CO_2 gas concentration. Low EO concentration cycle with EO/CO_2 mix; had low EO absorbency and very short aeration
Styrenic block copolymer	Compatible
Polyester	Compatible
	With low EO concentration, EO/CO_2 mix had low EO absorbency and very short aeration time
Polyetherimide (PEI)	Depending on formulation and application. Very thin tubing may present compatibility issues. Bulk structural materials are generally compatible

(*Continued*)

© Woodhead Publishing Limited, 2013

Table 4.7 Continued

Thermoplastics	Effects
Polyurethane	Performance depends on formulation, cure conditions, material thickness and end use stresses. PU has high affinity for EO but releases with aeration
	Low EO concentration with EO/CO_2 gas mix had short aeration
Silicone (RTV)	Excellent; no cross-linking
Butyl rubber	Butyl is even stable in liquid EO
Ethylene propylene diene (EPDM)	Generally compatible, but changing curing method to sulfur cure from peroxide cure may result in formation of small amounts of polyethylene oxide inside the matrix of the material
Latex	Compatible, but may be limited to the number of repeat cycles
Neoprene®	Compatible
Polyvinylidene fluoride elastomer	Compatible
Silicone elastomer	Compatible; no cross-linking
	High absorbency or EO desorbs well for short aeration with low EO concentration
	EO/CO_2 mix had low EO absorbency, and very short aeration
	Nonelastomer prosthesis requires long aeration at high EO concentrations; but at very low EO concentrations with EO/CO_2 gas mixtures, EO residuals may be much lower
Teflons®	Good to excellent materials. There may be low EO absorbency, but very slow desorption in some types (e.g., PTFE), but not in PVDF. Low EO concentration in EO/CO_2 mix may result in very little EO absorbency

Notes: EO residuals will vary between polymer types, polymer designs, thickness, formulation changes, packaging, etc. Typical aerations vary between 2 and 7 days. The above very short aeration was <12 h at ~50°C with initial low EO concentration with EO/CO_2 gas mixture.
Sources: AAMI TIR 17[3] and references 4 and 5.

such as Taxol based-formulations cannot withstand high temperature and high humidity EO cycles.

EO will sterilize most polymers and materials for medical devices. However, because EO is deemed a potential human carcinogen and reproductive toxicant, its use is limited and controlled. It also has toxic byproducts such as ethylene glycol and ethylene chlorohydrin.

Post-sterilization evaluation for toxic residuals (ethylene oxide and ethylene chlorohydrin) must be performed before release or validation of

© Woodhead Publishing Limited, 2013

product. Long exposure times and post-sterilization aeration times as well as post-processing biological indicator testing may reduce the use of this process on a practical basis.

Effects of heat (dry-heat and steam) sterilization on polymers

Heat sterilization, weather by dry heat or by steam, can cause thermal degradation of polymers and this may be due to the oxidation mechanism. Thermal degradation of polymers is typically a molecular deterioration as a result of overheating. At high temperatures the components of the long chain backbone of the polymer begin to separate (molecular scission); and react with one another to change the properties of the polymer. Thermal degradation can present an upper limit to the service temperature of plastics as much as the possibility of mechanical property loss. Indeed, unless correctly prevented, significant thermal degradation of polymers can occur at temperatures much lower than those at which mechanical failure is likely to occur. Consequently, many plastics or polymers selected for possible heat sterilization should be reviewed for their transition temperatures. The chemical reactions involved in thermal degradation may lead to physical and optical property changes relative to the initially specified properties.

It is of interest to find out what the effects of heat cycles will have on properties of polymeric materials. Thermal degradation generally involves changes to the molecular weight (MW); and molecular weight distribution of the polymer and typical property changes include reduced ductility and embrittlement, chalking, color changes, cracking, and general reduction in most other desirable physical properties. Radiation can cause cross-linking, scissoring, oxidative, or combination effects in polymer changes, which may result in cracking, disintegration, embrittlement, discoloration, stiffening, leaching, and pH change. These may result in change in MW or MW distributions. Thermal decomposition by exothermic heat or polymer breakdown of polymers by heat is predominately oxidative, causing breakage in chemical bonds, with property changes such as discoloration, hardening, softening, warpage, and/or melting. Excessive heat, however, may cause some polymers to burn, char, and totally disintegrate. Steam may result in wetting, hydrating, and even degrading. Many of the polymer property changes due to heat may similarly occur in over-irradiation. Dry heat is essentially an oxidative process, but is also dehydration. The effect of the steam is both a hydrolytic as well as an oxidative process, but is also dehydrating. The effects of steam are both hydrolytic and oxidative. Steam may also corrode metals. With steam sterilization there is not only potential thermal degradation and decomposition of a polymer as with dry heat but also the potential of hydrolysis.

© Woodhead Publishing Limited, 2013

Some polymers will lose structural integrity at the temperatures used for autoclaving. Some products made from such polymers may need to be supported to prevent slumping and distortion of the product. Even some polymers where the softening temperature is higher than the autoclaving temperature may suffer from the release of molded-in stresses and subsequent distortion. Where steam sterilization is to be used, the effect of multiple sterilization cycles may nee to be considered to prevent cumulative effects of the treatment on the plastic, when the product is not deemed as a single-use disposable product. If the products are to be packaged before autoclaving then the packaging material and packaging method need to be carefully chosen. The suitability of a package for steam sterilization will depend on the polymer, the size of the package, the wall thickness of the package, and the contents including any sharp corners which may pierce the package.

It is of interest to know what effects heat processes will have on the properties of polymeric materials. The number of polymers capable of tolerating moderate temperature and moisture are more numerous than often considered or recognized (Table 4.8):

- Natural (isoprene) – EPDM, urethane, nitrile, butyl, styrene–butadiene.
- Fluor plastics (other than PTFE and FEP) – PVDF, PCTFE, PETFE.
- 'High-end' engineering – resins, PEK, PEEK, polyetherimide.
- Nylons(polyamides) – especially Aromatics, 12, 11, 6/12 and 6/10.
- Polyethylene HDPE, UHMWPE, but not low-density polyethylene.
- Polycarbonate (PC) and alloys.
- Polyesters (e.g., PET and PETG) and some polyesters are somewhat resistant to steam sterilization, but aliphatic forms are more vulnerable to hydrolysis than the aromatic form.
- Polysulfone (PSF) and polyphenyl sulfones may be virtually unaffected by thousands of autoclave cycles.
- Polyvinyl chloride (PVC); flexible and semi-rigid, color, plasticizer, and HCl creation. It may be corrected, where there is no load on them.
- Polystyrene (ABS, PS, etc.) typically melt with steam or dry-heat sterilization; however, syndiotactic polystyrene (S-PS) (where chemical groups are placed on one side of the polymer chain and then on the other side) is resistant and SAN can be heat resistant.
- Polyurethane (e.g., varieties) – some are very vulnerable to steam sterilization (e.g., moisture swelling); some vary with the hydrophobicity of the polyether segment of polyether urethanes.
- Polypropylenes (stabilized); and copolymers (PPCO); and polymethyl pentene – stabilized.

© Woodhead Publishing Limited, 2013

Table 4.8 Polymer compatibility for dry heat and steam sterilization techniques

Polymer	Comments (vary – consult authors or suppliers)
Acrylonitrile butadiene styrene (ABS)	Very unlikely, but some may be poor to possible, depending upon grade, filler Run low temperature process
Fluoropolymers	
Polytetrafluoroethylene (PTFE)	Compatible up to 170°C or higher Certain grades may allow for several cycles or long service; however, although PTFE has great thermal stability, once the activation energy for the rupture of the C-C bonds in the chain has been exceeded, it can unzip quantitatively releasing a potentially toxic monomer
Perfluoroalkoxy copolymer (PFA)	Working temperatures up to 204°C or higher Long term up to 170°C
Poly chlorotri-fluoroethylene (PCTFE)	Up to 150°C continuous
Polyvinyl fluoride (PVF)	Heat deflection temperature up to 134°C; limited use
Polyvinylidene fluoride (PVDF)	Per use temperature is 150°C (302°F); however, some grades may only go to 125°C Multiple, maximum operating temperature of 275°F/130°C
Ethylenechlorotri-fluorethylene	Compatible to 266°F (131°C); melt at 412°F (211°C)
Ethylene tetrafluoroethylene (ETFE)	Up to 150°C
Fluorinated ethylene propylene (FEP)	Up to 170°C or 200°C (392°F)
Polyoxymethylene (e.g., polyacetal)	Up to 121°C or higher; may degas May use up to 100 cycles at 121°C, but it may begin to degrade, emitting formaldehyde
Polyacrylic (e.g., PMMA)	Poor to fair; some highly resistant grades
Polyamide (e.g., Nylon)	Poor to excellent Absorbs moisture, some films will allow moisture to diffuse through
Polycarbonate	There are grades that can be sterilized at 134°C Some formulations only allow a few cycles; other formulations allow up to 200 repeat cycles
Polyester	Possible to excellent; depends upon type, grade, form and function Some good PET films at 240°F, PEN good Mylar resistant but will not allow steam penetration Aliphatic polyesters are sensitive to hydrolysis, while aromatic polyester (e.g., PET) may be less susceptible
Polyethylene (PE) – various densities; LDPE, LLDPE, HDPE, spun polyolefin®	Poor to fair HDPE fair and spun polyolefin fair High density better than low density Reinforcement of HDPE improves its temperature

(*Continued*)

© Woodhead Publishing Limited, 2013

Table 4.8 Continued

Polymer	Comments (vary – consult authors or suppliers)
Polyimides (PI)	Possible to excellent; depends upon grade, form and function PEI withstand up to 4000 cycles, 1000–2500 at 5 min at 134°C
Polymethylpentene (PMP)	Excellent up to 235°C; PMP withstands repeated autoclaving, up to 150°C
Poly (ether) Ketone	High-temperature resistance; PEEK has heat resistance Good up to 2000 h of steam Typically long service
Polypropylene	Depends upon grade, form and formula Use heat-resistant grade with heat stabilizer for multiple cycles
Polypropylene copolymer (PPCO)	It is autoclavable; provides properties of polypropylene and polyethylene PPO replaces polyallomer
Polystyrene	Standard polystyrene not autoclavable; but syndiotactic polystyrene (S-SPS) is excellent, as is styrene
Polyphenyloxides (PPO)	Good, 215°C; can be mixed with styrene
Polysulfones	Typically all types are excellent; however, polyether sulfone (PES) is less resistant Repeated autoclave cycle – PS up to 1500 cycles; but not PES
Polyurethane	Poor/possible, but some grades may be fair/good
Polyvinylacetates	Depends upon form, function, formulation and co-polymerization. Heat-stable PVA hot-melt adhesives used
Polyvinylchloride	Rigid PVC, not likely, unless PVC modified Plasticized (soft) PVC is good depending upon form, formulation and function
Styrene acrylonitrile copolymer (SAN)	Possible to fair; depends upon grade
Silicone	Has tremendous heat resistance, but is not a barrier to moisture vapor; dry heat may be better in some applications. If exposed to repeated steam, sterilization will eventually relax silicone and will become gummy Silicone is hydrophobic, it will resist moisture Diffusion, unless nano-channels exist
Thermoset polymers	
Epoxy reinforced plastics	Numerous types of reinforced epoxies Physical properties can vary. Heat distortion temperatures of up to 470°F
Phenolics	Autoclaving can lead to phenolic degradation and extractable into fluids
Polyester, unsaturated	There are a variety of unsaturated polyesters (e.g., vinyl esters). C better cross-linked. Possible to good Isophthalic acid-based polyester High-temperature resistance

(*Continued*)

© Woodhead Publishing Limited, 2013

Table 4.8 Continued

Polymer	Comments (vary – consult authors or suppliers)
Polyimides (e.g., BI maleimides (BMI) and acetylene terminated polyimide (ACTP))	BMIs and ACTP have use-service temperatures of 127–232°C and 316°C
Polyurethane (PU)	Typically possible; depends upon grade, form and function. There are heat-resistant cross-linked polyurethanes
Aliphatic	Radiation cross-linking increases its resistance
Aromatic	Aromatic thermoset PUR does not form 4,4′-methylenedianiline (MDA) in polyurethane
Adhesives	
Acrylic	Can tolerate autoclaving; depending upon grade and formulation, fair to good There is an acrylic adhesive film in a tape up to 280°F
Epoxy	Depending upon grade and formulation, deflection temperature from 200°F to 500°F Some can lose retention of initial strength on only five cycles
Fluoroepox(y)ies	Epoxy adhesives; depending upon cure and formulation, good to excellent Epoxy adhesives cured with heat are more heat resistant than those cured at room temperatures
Silicone adhesives	Typically good; depends upon form, formulation and function, good to excellent Some may be good for only up to 6–8 cycles
Elastomers	
Butyl	Good, depending upon type and grade Resistant to water and up to 120°C Multiple use – a halobutyl(halogenated poly (isobutylene))
Ethylene propylene diene monomer (EPDM)	Good up to 125°C in water; up to 134–150°C in air; continuous-use operation; temperature of 105°C
Natural rubber-latex (synthetic cis 1–4 polyisoprene)	Possible to fair There are autoclavable grades Plastomers enhance thermal stability. Possible to fair Hardens with use Withstands repeated autoclaving at 250°F for 20 min
Nitrile rubber (acrylonitrile butadiene)	Good resistance to moisture and water Tolerate temperatures of up to 120°C at lower processing conditions, below 230°F Better if hydrogenated nitrile rubber
Polyacrylic	Polyacrylate: it is a heat-resistant rubber; water resistance can be improved but with decrease in heat. Typically, resistance to water is poor.

(*Continued*)

© Woodhead Publishing Limited, 2013

Table 4.8 Continued

Polymer	Comments (vary – consult authors or suppliers)
Polychloroprene	Fair resistance to moisture, up to 230°F; intermittent to 250°F Fair to very good It is possible to resterilize at below 230°F
Silicone elastomer	There are some representative polymers for steam sterilization technique
Styrene block copolymers, SBR	Depends upon grade, type, form and formulation Possible to fair It is possible to resterilize up to 100°C
Thermal-based polyisocyanate, urethane (polyether/ polyester)	There are some heat-resistant grades; depends upon type, form and formulation With silicone there is increased heat resistance Not likely to be multiple sterilizations
Thermoplastic elastomer (TPE)	Polyolefin that can be molded into autoclavable parts
Urethane elastomer aliphatic	Typically possible; some up to 135°C. Steam autoclaving possible with selected grades
Urethane elastomer aromatic	Formation of 4,4′-methylenedianiline (MDA) with steam

Sources: AAMI TIR 17[3] and references 4, 5 and 6.

- Thermosets – epoxies, phenolic, polyimides, polyurethanes, and aromatic polyesters (aliphatic polyesters are more susceptible to hydrolysis attack).
- Silicones are heat stable, but more easily dry-heat sterilized, because moisture from steam cannot penetrate silicone prosthesis as dry heat can, for implantables.

A comparable number of polymers can be sterilized with dry heat without the adverse effects of moisture or hydrolysis (Table 4.9). Low-temperature dry heat may sterilize more polymers than steam, but the cycle or process times will be significantly longer (e.g., upwards to 12 times longer).

Effects of hydrogen-peroxide sterilization on polymers

Hydrogen peroxide and oxidizing agents can sterilize a multitude of polymers (Table 4.10). The numbers of polymers are more limited than with EO, because of the oxidizing effect of hydrogen peroxide; however, it is more attractive than EO sterilization because of its shorter process time and lack of residuals. Its very short processing time and no carcinogens make hydrogen peroxide very accessible. When designing for devices, it is best to avoid absorbers (such as silver, copper and copper alloys) and absorbers (such as polyurethane, nylon and cellulosic materials). Non-catalytic, non-absorbent

© Woodhead Publishing Limited, 2013

Table 4.9 Polymers and materials compatible with dry-heat sterilization technique (low and high temperatures)

Acetal (ACL), delrin, or polyoxymethylene up to 121°C (dry)
Aluminum up to 190°C (dry)
Cellulose acetate (non-load) up to 120°C
Cellulose acetate butyrate (non-load) up to 130°C
Cotton muslin up to 204°C
Glass >190°C
Grease (depends upon the type of grease) (dry)
Ethylene chlorotrifluoroethylene (ECTFE) up to 150°C
Epoxies (vary up to 177°C)
Ethylene propylene diene monomer (EPDM) up to 149°C
ETFE up to 150°C
Ethylene acrylic 149°C
Fluorocarbon rubber 199°C
Fluorinated ethylene propylene (FEP) up to 170°C
Fluoro silicone 232°C
High-density polyethylene (HDPE) up to 120°C
Hydrogenated nitrile rubber 149°C
Liquid crystal polymer (LCP) up to 275°C
Metals (note some metal temper may occur above 160°C) up to 190°C (dry)
Muslin up to 160°C
Natural rubber 104°C, but low heat aging resistance
Neoprene/chloroprene rubber 121°C
Nitrile rubber 100°C, and low heat aging resistance
Nylon 4/6 (polyamide heat-stabilized grades) up to 130°C
Nylon 6 <100°C
Paper (varies depending upon paper) up to 160°C (dry)
Perfluoroalkoxy (PFA) up to 170°C
Petrolatum gauze up to 160°C
Phenolics (vary) up to 150°C
Polyacrylate (ACM) 149°C
Polycarbonate (PC) up to 134°C
Polyetherimide up to 134°C
Polyetherketone (PEI, PEEK, etc.) up to 170°C
Polyethylene (vary per molecular weight (e.g., 80–142°C))
Polyethylene terephthalate copolymer (PETG) up to 170°C
Polyimide 232°C
Poly 4-methyl-pentene-1 (PMP) up to 170°C
Polypropylene (PP) up to 135°C, no stacking
Polyphenylene oxides (PPO) 100–148°C
Polypropylene copolymer (PPCO) up to 120°C
Polysulfone (PSF) up to 160°C
Polytetrafluoroethylene (PTPE) up to 170°C
Polyvinyl chloride tubing (flexible-non-load, varies) up to 120°C
Polyvinylidene fluoride (PVF) up to 125°C
Styrene-butadiene rubber 100°C, but heat aging resistance
Silicones up to 200/232°C
Teflons® up to 170°C
Select a polymer whose temperature transition or melting temperature is comfortably 'above' the required, selected or chosen dry-heat sterilization operating temperature. Melting and/or deflection/maximum temperature can vary with formulation changes.

Note: Polymer responses may vary with the length of exposure to a temperature.
Sources: AAMI TIR 17[3] and references 4, 5 and 6.

© Woodhead Publishing Limited, 2013

Table 4.10 Compatabilities of some polymers with hydrogen peroxide (with plasma*)

- ABS (excellent)
- Acetal – significant color changes or slight material changes after 10–100 cycles. Grade dependent
- Elastomers – silicones (excellent), thermoplastic polymer elastomer (TPE) (styrenic block copolymer compounds (SEBS), thermoplastic elastomer 'Q' polymer (TPQ)), natural (degrade), EPDM (fair to good), urethane (grade dependent), nitrile (good, grade dependent), butyl (excellent), styrene-butadiene (excellent), polyacrylic (good), polychloroprene (excellent)
- Fluoroplastics (PTFE and FEP, PVDF, PCTFE, PETFE) – excellent
- PEK, PEEK, polyetherimide (excellent, no change after 100 cycles)
- Nylons (polyamides), absorb, severe material degradation after 10–100 cycles. Grade dependent
- Polyethylene, LDPE < LLDPE, HDPE, UHMWPE (excellent, no change after 100 cycles)
- Polyesters (PE) and PETG – excellent
- Polycarbonate (PC) and alloys – excellent
- Polysulfone (PSF) – excellent
- Polyvinyl chloride (PVC) flexible and semi-rigid, color, plasticized (good no resterilization)
- PVC unplasticized (some color change or surface changes after 50 cycles)
- Polyurethane (8 chemical varieties) – some color change or loss of gloss after 100 cycles; however, polyurethane is a peroxide absorber and this can lead to decomposition of the peroxide needed for sterilization
- Polypropylene (unstabilized) – excellent
- Polypropylenes (stabilized) and copolymers (PPCO) and polymethyl pentene – excellent
- Polystyrene and copolymers, ABS, PS, SAN – excellent
- Polyacrylics (PA, PMA, PAN) – grade dependent; significant material changes or crazing after 10–50 cycles
- Silicone – excellent, no change
- Thermosets – epoxies, phenolics, polyimides, polyurethanes, polyesters (grade dependent)
- Acrylic – fair, resterilization not likely

Note: *Material compatibility with hydrogen peroxide vapor sterilization may not be the same as that with low-temperature hydrogen peroxide with plasma.
Sources: AAMI TIR 17[3] and references 5 and 6.

materials such as PTFE, polyethylene, stainless steel, or low copper–aluminum alloys are recommended. Adhesives that use large proportions of amines as curing or cross-linking agents tend to be incompatible.

Low-temperature hydrogen peroxide with plasma has less effect typically on polymers than hydrogen-peroxide vapor without plasma, because plasma destroys or gets rid of peroxide residual than with aeration.

Plasma and oxidizing agents are generally applied only to small niche and minimal-sized loads of devices. Its use is predominantly in the general

© Woodhead Publishing Limited, 2013

hospitals, and less in the medical-device manufacture industry. It is a surface sterilant and may not be used for implantables.

Effects of irradiation on polymers

Irradiation can cause deep changes in polymers that other methods will not, such as breaking bonds (scissoring), cross-linking or a combination of these ways, which may result in recombination. Radiation may cause odors, discolor, embrittle, and degrade a few materials, or affect bond strengths, which may cause changes to the life of a polymer during implantation.

Some polymers that may be particularly sensitive to radiation are unstabilized polypropylene, acetals, some Teflons (e.g., PTFE, PFA and FEP), polyglycolic acid and polylactide sutures, polymethylpentene, polyvinylidene fluoride, polymethyl methacrylate (PMMA), some acrylic adhesives, butyl rubber, some cellulose esters, natural liquid crystal polymer and cross-linking of silicone.

The effects of radiation on polymers may be influenced by:

- the chemical composition and formulation of the polymer;
- the morphology of the polymer (percentage of crystallinity, molecular weight, and density);
- radiation dose and dose rate that is applied;
- the temperature of the environment.

Understanding basic radiation chemistry may help to assess why a particular plastic is affected in a certain way. When a plastic is exposed to gamma radiation, in the case of Co_{60} with energy levels of 1.33 and 1.17 MeV, molecular bonds are broken. The polymer can either recombine into its original configuration or, if cross-scission occurs, the molecular weight of the molecules is reduced and the polymer is weakened. Conversely, where cross-linking occurs, a large three-dimensional matrix is formed and the polymer is strengthened.

The effects of radiation on polymers may also be influenced by the polymerization, molding, and process of plastics as well as the age and environment of the polymer.

- Some teflons (e.g., FEB and PTFE), despite their high heat resistance, are degraded by radiation, and generally not acceptable, although some thin films/coating and certain types of teflons have been demonstrated to be radiation compatible to low doses.
- ABS and polycarbonate are generally considered to be acceptable to one dose of radiation, but may be multiple sterilized up to 100 Mrad. Both may discolor; with ABS discoloring the most. ABS/Polycarbonate blend lose physical properties linearly with an increase in radiation dose.

© Woodhead Publishing Limited, 2013

- Acrylic polymers may be sensitive to radiation. The effect of scissoring of the ester chain is the main effect of radiation. Polymethylacrylate (PMMA) has been used for dosimeters, because it changes and is sensitive to irradiation. Radiation compatible acrylics, however, are available, but not typically for implantables or ophthalmic. Optical clarity of PMMA may be affected.
- Polyethylene is predominantly cross-linked, but may be acceptable to radiation, by sterilizing in nitrogen rather than in air (with oxygen). Slight odors may result, but they can be reduced through modification of the formulation. High-density polyethylene is more resistant than lower-density polyethylene.
- Polypropylene (unstabilized, natural) is both crosslinked and scissored. Embrittlement, breakage and discoloration can occur at sterilizing doses.
- Breakage of polypropylene syringe tips has been used for blood-borne-disease procedures to get rid of needles on tip.
- Radiation-stabilized polypropylene polymers, however, are available, using high molecular weights, co-polymerized and alloyed with polyethylene with additional stabilizers. Use of electron beam at high irradiation dose rate may further reduce the oxidative degradation of polypropylene.
- Polymethylpentene has similar effects as polypropylene, but using less irradiation improves possibilities.
- Polystyrene is very stable to radiation because of its benzene ring; however, it may begin to yellow above 50 kGy.
- ABS is much less resistant to radiation than polystyrene, but it may be suitable for a single dose of irradiation. High-impact grades are less radiation-resistant than standard grades.
- PVC can be compatible or tolerant to radiation, but may require squelching of HCl, prevention of discoloration and leaching of plasticizer(s). The addition of antioxidants and heat stabilizer help, as well as changing the plasticizer (DEHP or DOP) to one less toxic and non-carcinogenic.
- Resterilization with irradiation is not frequently used, as with other techniques. Single-use (irradiation) typically predominates. However, plasticized PVC may be resterilized. However, consideration of leaching of plasticizer should be made.
- Acetal or polyformaldehyde copolymers are sensitive to radiation and their chains are easily scissored (embrittlement); the material often changes from solid to dust, and the color changes from yellow to green.
- Polyamide or nylon are sensitive to radiation to cross-linking, but many are suitable for a single dose, and some for multiple doses. Nylon 10, 11, 12 and 6–6 are more stable than nylon 6. Nylon film and fiber are less resistant.

© Woodhead Publishing Limited, 2013

Table 4.11 Compatibilities of some polymers for irradiation

- ABS (excellent)
- Elastomers – silicones (peroxides and platinum cured), TPE (SEBS, TPO), natural (isoprene), EPDM, urethane, nitrile, butyl, styrene-butadiene
- Fluoroplastics (other than PTFE and FEP) – PVDF, PCTFE, PETFE
  PTFE and FEP may be adversely affected by irradiation
- 'High-end' engineering resins, PEK, PEEK, polyetherimide
- Acetal is adversely affected by irradiation
- Nylons (polyamides), especially aromatics, 12,11, 6/12, and 6/10
  Nylon may degrade oxidatively in applications that have large surface-to-mass ratios (e.g., films, fibers, adhesives)
- Polyethylene, LDPE < LLDPE, HDPE, UHMWPE
  (high-density PE is more radiation-resistant than low-density PE)
- Polyesters (PE) and PETG
- Polycarbonate (PC) and alloys
- Polysulfone (PSF)
- Polyvinyl chloride (PVC) flexible and semi-rigid are acceptable when color changes, plasticizer migration and HCl formation are corrected
- Polyurethane (8 chemical varieties). Aromatics may discolor somewhat
- Polypropylenes (stabilized) and copolymers (PPCO) and polymethyl pentene – radiation-stabilized are good
  (natural polypropylene (unstabilized) has little tolerance to irradiation)
- Polystyrene and copolymers, ABS, PS, SAN
- Polyacrylics (PA, PMA, PAN)
- Thermosets – epoxies, phenolics, polyimides, polyurethanes, polyesters

Sources: AAMI TIR 17[3] and references 5, 6 and 7.

- Despite difficulties with irradiation, the number of polymers that are sterilizable are numerous (Table 4.11).

Effects of ozone sterilization on polymers

It should be noted that during ozone sterilization, ozone breaks down into reactive species, including hydroxyl radicals and atomic oxygen. Because of the strong oxidizing nature of ozone, polymers must be resistant to oxidation. Further, polymers and medical devices should be resistant to high relative humidity levels (>80%), which are required for the ozone to be effective as a sterilant. Consequently, materials should be resistant or tolerable to oxidation and moisture. This method of sterilization cannot be used for fluids or woven textiles. Ozone sterilization is a surface-oxidative process. Although many polymers may be satisfactorily used in the manufacture of a device intended for single use, they might not be effective for use with a reusable or refurbished device. For gaseous ozone, compatible polymers for its low-temperature sterilization should be resistant to oxidation and moisture, for one or more multiple processes (see Table 4.12).

© Woodhead Publishing Limited, 2013

Table 4.12 Compatibility of some polymers with the ozone sterilization technique

Thermoplastics	Compatibility	Number of cycles that polymer may be compatible
Fluoropolymers		
Polytetrafluoroethylene (PTFE)	Excellent	No change after > 100 cycles
Perfluoro alkoxy (PFA)	Excellent	No change after > 100 cycles
Polychlorotri-fluoroethylene (PCTFE)	Excellent	No change after > 100 cycles
Polyvinylidene fluoride (PVDF)	Excellent	No change after > 100 cycles. PVDF is considered a polymer of choice for ozone
Ethylene tetrafluoroethylene (ETFE)	Excellent	No change after > 100 cycles
Fluorinated ethylene propylene (FEP)	Excellent	No change after > 100 cycles
Polyacetals	Good	Color change and loss of gloss. Slight to significant change may occur after > 100 cycles Contact equipment manufacturer
Polyacrylates (e.g., PMMA)	Good	Slight to significant material change may occur after 10–100 cycles Contact equipment manufacturer
Polyamides (e.g., Nylon)	Good	Color change and loss of gloss. Significant material change after 10–100 cycles
Polycarbonate (PC)	Excellent	Slight surface change and loss of gloss. No significant change after > 100 cycles
Polyesters, saturated	Excellent	
Polyethylene (PE), various densities	Good	Color change and loss of gloss. Significant material change may occur after 10–100 cycles
Polyimides (e.g., PEI)	Excellent	Slight surface change. No significant change after > 100 cycles
Polyketones (e.g., PEEK)	Excellent	Unfilled PEEK only – avoid sharp edges. Color change and loss of gloss. No significant change after > 100 cycles
Polypropylene (PP) natural stabilized	Good	Color change and loss of gloss. Significant material change may occur after 10–100 cycles Polypropylene may not be good for multiple reuse
Polystyrene	Poor	Significant material or surface change < 3 cycles
Polysulfones	Good	Slight surface change and loss of gloss. No significant change after > 100 cycles

(*Continued*)

© Woodhead Publishing Limited, 2013

Table 4.12 Continued

Thermoplastics	Compatibility	Number of cycles that polymer may be compatible
Polyurethane (PU)	Not likely	Significant material or surface change < 3 cycles
Polyvinylchloride (PVC) rigid	Excellent	Color change and loss of gloss. No significant change after > 100 cycles
Polyvinylchloride plasticised	Good	Surface change may occur after 5–25 cycles
Thermosets		
Epoxies	Variable	Significant material change may occur after 10–100 cycles, check reliability and stability
Phenolics	Excellent	Loss of gloss. No significant change after > 100 cycles
Polyester, unsaturated	Excellent	
Polyurethanes	Not likely	Significant material or surface change < 3 cycles; not good
Adhesives		
Acrylic	Good	Application specific. Contact equipment manufacturer
Epoxy	Variable	Application specific. Contact equipment manufacturer
Fluoroepoxy	Good	Application specific. Contact equipment manufacturer
Silicone	Good	Application specific. Contact equipment manufacturer
Elastomers		
Natural rubber	Not likely	Significant material or surface change < 3 cycles
Butyl rubber	Not likely	
Ethylene propylene dienemonomer (EPDM)	Fair	Significant material or surface change with < 3 cycles
Silicone	Excellent	Slight material change after > 100 cycles
Styrenic block copolymers	Not likely	Significant material or surface change < 3 cycles
Polychloroprene	Poor	While in an ozone normal environment, it is OK, but under sterilization significant material or surface change may occur with < 3 cycles
Urethane	Not likely	Significant material or surface change < 3 cycles

Sources: AAMI TIR 17[3] and reference 8.

© Woodhead Publishing Limited, 2013

Some polymers remain unknown in terms of compatibility to ozone at this time. Woven materials polystyrene, polyurethane, butyl and natural rubber, polychloroprene, nickel, and silver are not likely to be compatible. Some cellulosic, however, may be compatible. The shape of the device and material as well as the design of a device may be closely related to its stability and resistance of the device to sterilization. Device and polymeric parts with wide surface-to-mass ratios (e.g., fibrous material) can undergo faster oxidative degradation. While such device and materials can be adequate for single use or used in the manufacture of a device that has limited reuse, such a condition might not be satisfactorily used for a device with a longer expiration period.

Ozone and oxidizing agents are generally applied only to small niche and minimal-sized loads of devices polymer. Their use is predominantly in the hospitals, and may be limited in industry. While ozone and hydrogen peroxide are both oxidizing agents, their damage is different.

Ozone may sterilize some cellulosic better than hydrogen peroxide, but hydrogen peroxide may sterilize butyl rubber, urethanes, and natural rubber better than ozone. Silicone may be sterilized better by ozone than hydrogen peroxide. Hydrogen peroxide is typically a surface sterilant with some diffusion of small lumens, while ozone should have the capacity to diffuse and penetrate deeper than peroxide, but not EO, dry heat, steam, or irradiation.

4.3.2 Effects of sterilization modalities on various plastics

In this section, different plastics (e.g., olfines, styrenes, vinyls, fluorinated polymers), and other plastics and elastomers are compared to different sterilization modalities.

This comparison device provides medical applications with each sterilization modality.[5, 6] The following highlighted list incorporates a rating of effects (e.g., poor to excellent) of sterilizing different plastics and elastomers and their applications to different sterilization techniques.[3–6]

Olefin polymers

Polyethylene: radiation (good to excellent) – may 'off gas', low and moderately dense PE are more resistant and may be resterilized, but high-density PE can undergo oxidation (which has resulted in cracking under some circumstances); EO (excellent); moist heat (poor to good, high density more resistant); dry heat (poor to fair, but lower temperature improves for high density); hydrogen peroxide (excellent); ozone (excellent). Device

© Woodhead Publishing Limited, 2013

applications: orthopedics, replacements in joints, ankles, elbow, shoulder and toe, tubing.

Polypropylene: radiation (poor to good, stabilized, but single-use only); EO (good to excellent); moist heat (good, and excellent with heat-stabilized grades and can be resterilized); dry heat (good and excellent at low temperatures (up to 135°C), with heat-stabilized grades); hydrogen peroxide (excellent); ozone (excellent). Device applications: catheters, sutures, syringes, polypropylene surgical sutures, filaments, and mesh. Surgical meshes of this kind are used to reinforce soft tissue where weakness exists, such as in the repair of hernias and chest wall defects.

Poly methyl pentene: radiation (fair to good); EO (excellent); moist heat (good/excellent); dry heat (good/excellent up to 170°C); hydrogen peroxide (unknown); ozone (unknown). Device applications: containers, covers for medical instruments, TPX film.

Copolymers (e.g., polyethylene/poly propylene, polyallomer): radiation (poor to good, stabilized, but single-use only); EO (excellent); moist heat (good, and excellent with heat stabilised grades and can be resterilized); dry heat (good and excellent at low temperatures (up to 135°C); with heat-stabilized grades); hydrogen peroxide (excellent); ozone (excellent). Device applications: parenteral solution containers, containers for packaging applications; instrument, pneumatic and lubricant lines, tubes.

Styrene polymers

Polystyrene: radiation (excellent with benzene ring); EO (poor to good, but millions of parts and have been acceptably sterilized and some formulations can be resterilized 2–5 times); moist heat (poor to excellent, with *syndiotatic styrene*); dry heat (poor to excellent with *syndiotatic styrene*); hydrogen peroxide (excellent); ozone (fair). Device applications: containers, parts in IV sets, petri dishes, sputum cups.

Styrene acrylonitrile copolymers: radiation (good to excellent); EO (poor to good, but many parts are acceptable); moist heat (poor to fair); dry heat (poor to fair); hydrogen peroxide (excellent); ozone (may be unknown). Device applications: in dialysis devices, in IV connectors.

Acrylic polymers

Polymethyl methacrylate: radiation (fair to good); EO (good); moist heat (poor to fair at low temperatures but likely not resterilized); dry heat (poor to fair at low temperatures); hydrogen peroxide (fair); ozone (good). Device applications: bone cement, contact lenses, corneal prosthesis, grout for artificial joints, orthopedics, ophthalmology lenses, in membrane oxygenators.

© Woodhead Publishing Limited, 2013

Vinyl polymers

Polyvinyl acetate: radiation (good); EO (poor); moist heat (poor to fair); dry heat (poor to fair); hydrogen peroxide (excellent); ozone (unknown). Device application: film.

Polyvinyl chloride: radiation (good); EO (excellent); moist heat (poor to good up to 120°C – good if no load on polymer; moist heat hydrates the PVC, but dry heat removes with heated aeration); dry heat (poor to good up to 120°C*); hydrogen peroxide (excellent); ozone (good). Device applications: blood bags, catheters, containers, endotracheal tubes, films, hearing aid component, IV tubing, IV drip chambers, and packaging, shrink tubing, storage bags, in ventilation systems.

Vinyl chloride copolymers: radiation (good); EO (excellent); moist heat (poor to good (without load) up to 120°C); dry heat (poor to good up to 120°C); hydrogen peroxide and ozone unknown. Device applications: films, packaging, containers.

Polyvinylidene chloride: radiation (good); EO (excellent); moist heat (poor to fair up to 120°C); dry heat (poor to fair up to 120°C); hydrogen peroxide and ozone unknown. Device applications: PVDF syringe filters and PVDF membrane disc filters. Furthermore, PVDC is a thermoplastic that responds well to gas plasma treatment. Its inherently low surface energy and poor polarizability means the surface cannot provide enough energy to bond with adherents such as adhesives and inks, without gas plasma treatment.

Fluorinated polymers

Polytetrafluoroethylene (PTFE), PFA, PCTFE, PV, PVDF, ETFE, FEP: radiation has mixed results, some with poor compatibility (e.g., PFE, FEP, and PTFE); EO (excellent); moist heat (fair to excellent); dry heat (fair to excellent up to 170°C); hydrogen peroxide (excellent); ozone (excellent). Note: PFA has a low-temperature transition fluoropolymer without additives and may not be steam or dry heat sterilized. Device applications: artificial bone joints and vasculature, fiber optics, surface treatments, stop cocks, tubing.

Miscellaneous polymers

Polyamides (nylons): radiation (poor/fair to good, varies depending upon if aromatic or aliphatic); EO (excellent); moist heat (poor to excellent); dry heat (poor to excellent); hydrogen peroxide (good, but only one use); ozone (good). Note: Nylon is polar, and will absorb moisture. Device applications: bags, catheters, films, kidney dialysis, in laparoscopy devices, special packaging, and nylon spikes.

*Acceptable when there is no load on the polymer.

© Woodhead Publishing Limited, 2013

Polyester: radiation (fair to good); EO (excellent); moist heat (poor to excellent); dry heat (poor to fair); hydrogen peroxide (excellent); ozone (excellent cover). Device applications: covers, films, IV infusion fluid containers.

Polyketones, polyaryletherketone, polyetheretherketone (PEEK): radiation (excellent); dry heat (excellent); EO (excellent); moist heat (excellent); hydrogen peroxide (excellent); ozone (excellent). Device applications: cardiovascular, orthopedic, dental implants, and tubing.

Polysulfone (PSF), polyphenylsulfone: radiation (excellent); EO (excellent); moist heat (excellent); dry heat (good to excellent); hydrogen peroxide (excellent); ozone (good). Device applications: handles for dental instruments, ophthalmic scopes and lenses, endoscopic device, dialyzers, can be autoclaved thousands of times.

Poly terephthalate copolymer (PETG): radiation (good to excellent); EO (excellent); steam and dry heat (good to excellent up to 134°C); hydrogen peroxide and ozone (unknown). Device applications: packaging.

Poly terephthalate (PET): radiation (good to excellent); EO (excellent); steam and dry heat (good to excellent); hydrogen peroxide and ozone (unknown). Device applications: angioplasty balloons, woven vascular prostheses, vascular grafts of both large diameters.

Cellulosic, cellulose esters, cellulose acetate propionate, cellulose acetate butyrate, cellulose (paper, cardboard): radiation (fair to good (note: esters degrade less than other cellulosics); EO (excellent); moist heat (poor to good at low temperatures and depending upon the cycle, some may be good); dry heat (poor to good but higher temperatures will char); hydrogen peroxide (poor); ozone (poor to good). Device applications: films, filters, hemodialyser, membrane, IV burette champers, packaging.

Thermosets

Epoxy: radiation (excellent); EO (good to excellent); moist heat (fair to excellent); dry heat (fair to excellent); hydrogen peroxide (excellent); ozone (fair to excellent). Device applications: case by case, adhesives for parts, fiber optics, etc.

Phenolics: radiation (excellent); EO (good); moist heat (fair to excellent); dry heat (fair to excellent); hydrogen peroxide (good); ozone (excellent). Device applications: case by case, implantable vascular medical device, semiconductor device fabrication, casters.

Polyimide: radiation (excellent); EO (excellent); moist heat (excellent); dry heat (good to excellent); hydrogen peroxide (excellent); ozone (unknown). Device applications: case by case, tubing such as cardiovascular catheters, urological retrieval devices, coated wires.

© Woodhead Publishing Limited, 2013

Polyurethanes: radiation (good to excellent-aromatic better than aliphatic); EO (poor to good); moist heat (poor to fair, may create toxic residue); dry heat (poor to fair/good, at low temperature, likely has no toxic residue); hydrogen peroxide (good); ozone (poor). Device applications: blood pumps, catheters, connectors containers, enteral feeding tubes, lipid resistant stopcocks, needless syringes, vials, balloons, pacemaker leads.

Acetal: radiation (poor, embrittlement); EO (excellent); moist heat (fair to good up to 120°C); dry heat (good to excellent up to 120°C); hydrogen peroxide (excellent); ozone (good). Device applications: engineering plastic, structural keel for a prosthetic device, stop cock.

Polycarbonate: radiation (good to excellent); EO (excellent); moist heat (fair to good); dry heat (fair to good/excellent up to 134°C); hydrogen peroxide (excellent); ozone (excellent). Device applications: blood set, cases, covers, cardiotomy trocars, injection sites, in drug delivery devices, IV connectors, reservoirs, surgical instruments, safety syringes, valve occludes.

Acrylonitrile butadiene styrene (ABS): radiation (good); EO (excellent); moist heat (poor to fair); dry heat (poor to fair); hydrogen peroxide (excellent); ozone (fair). Device applications in administration IV sets (e.g. luers, roller clamps, Y connectors, etc.) and in dialysis units.

Elastomers (rubber)

Butyl: radiation (poor); EO (excellent); moist heat(fair to excellent); dry heat (poor to good); hydrogen peroxide (good, but only one cycle); ozone (poor). Device applications: tubing, butyl has been the most common choice for closures, but not implantable.

Ethylene propylene diene monomer (EPDM): radiation (good to excellent); EO (excellent); moist heat (good to excellent); dry heat (fair to good); hydrogen peroxide (fair to good); ozone (fair). Device applications: tubing, other uses, but not implantable.

Nitrile: radiation (good to excellent); EO (excellent); moist heat (fair to good); dry heat (poor to fair); hydrogen peroxide (fair); ozone (unknown). Device applications: gloves, including surgical gloves.

Polyacrylic: radiation (fair to good) (e.g., gamma radiation modifies the molecular weight of the PMMA while compression and bending strength may not affected by the sterilization process applied); EO (fair, but only one cycle); moist heat (poor, melts acrylic); dry heat (poor, melts acrylic); hydrogen peroxide (fair); ozone (good). Device applications: dental polymer, contact lens-methylacrylate.

© Woodhead Publishing Limited, 2013

Polychlorophrene: radiation (good); EO (good); moist heat (fair to good); dry heat (poor to fair); hydrogen peroxide (excellent); ozone (poor). Device applications: tubing.

Silicone: radiation (fair to good, can cross-link); EO (excellent); moist heat (fair to excellent); dry heat (fair to excellent up to 200°C, many prosthesis processed by dry heat); hydrogen peroxide (excellent, but surface sterilant); ozone (excellent but surface sterilant). Device applications: catheters, membranes, prostheses (prosthetics), tubing.

What may physically/chemically appear to be a compatible polymer may not be biocompatible. A polymer listing (as above) for a specific polymer is not an indication that the polymer is compatible biologically. Polymer degradation biologically and failure may occur individually with some polymers. It is the responsibility of the 'user' to determine the suitability and biocompatibility of a polymer for its specific application.[7]

Note: the presence of additives, plasticizers, and stabilizers can significantly affect the stability properties of many polymers, including their suitability for a specific sterilization. Additionally, under some conditions a material that is generally thought to be compatible with a technique will not be compatible when evaluated under another condition (e.g., irradiation of high-density polyethylene under air will be different when processed under nitrogen). This incompatibility is often due to oxidation, stability, formulation, and/or processing changes in the polymer.

4.3.3 Metals: the effects of different sterilization techniques on metals

The number of metals capable of tolerating moderate irradiation, oxidizing, temperature and moisture are more numerous than often considered. Most metals are compatible with different sterilization modalities, except with repetitive sterilizations and a few variations with different sterilization modalities. It should be noted that some oxidative processes occur in some sterilization processes.

Dry heat

Metals can be subjected to dry-heat sterilization typically without adverse effects. While metals can be subjected to dry heat sterilization some material fibers can be damaged

Ethylene oxide

Most metals are compatible with multiple sterilization cycles, except for acetylides in copper that may cause it to polymerize. EO may react with water vapor to form glycols on the surface of some metals.

© Woodhead Publishing Limited, 2013

Hydrogen peroxide

Metals may not retain measurable residual peroxide, but aluminum is attacked. With hydrogen peroxide, it is best to avoid decomposers (such as silver, copper, and copper alloys).

Irradiation

Metals are typically very stable under the influence of irradiation, but they may attenuate full penetration of a low dose. Metallic bonds result in minimal ionizations and thus no significant change in properties. They do not ionize as a result of the low-energy radiation used in medical product sterilization; however, electrical (e.g., circuit) systems may undergo significant changes in resistance owing to changes in the electrical potential of the circuit. The electrons in the valance band might shift to the conductive band and lower the resistance of the circuit, a condition that is not reversible. However, there have been circumstances where the circuit has not been adversely affected enough to observe a problem. This may be due to shielding from irradiation, or lower irradiation dose. Also radiation hardening, an act of making electronic components and systems resistant to damage or malfunctions caused by ionizing radiation, can be implemented or used.

With high doses such as E-beam and metals' low specific heats, localized elevated temperature rises might result. Also, in systems that use high-energy E-beam accelerators, neutron displacements and creation of measurable radioactive subspecies have been reported in some metals. Because of the very high rate of energy deposition in electron beam, care should be taken when product designs incorporate metals, as very large temperature gradients can develop. It is generally the case that metals are not negatively affected by radiation.

In general with gamma irradiation, the following metals response well with irradiation: aluminum, gold, brass, copper, magnesium, nickel, silver, stainless steel, and titanium, except in circuits. However, it should be noted that heavy metals may attenuate E-beam or electrons enough to prevent a 10^{-6} sterility assurance of some microbes.

Steam

Steam may sterilize many metals, but upon repeated reprocessing with, more than one, sterilization, oxidation and corrosion can occurs. Some metals (e.g., iron) may be subjected to steam corrosion but not all (e.g., stainless steel). If prudently applied (e.g., with inhibitors) and controlled (dry vs. wet steam), most metals may be sterilized. Moist heat may not corrode metals, except aluminum, copper, and iron, for example, but aluminum foil, when typically sterilized with single-use inhibitors, is acceptable. Corrosion may be limited if aluminum anodized. With brass it is used in steam traps. Copper

© Woodhead Publishing Limited, 2013

has no reaction when heated in steam, but surface blackens when heated strongly in air. Copper and brass are acceptable with corrosion inhibitors, including triazole. Gold has no reaction when heated in air and no reaction when heated in steam. Magnesium metal is autoclavable, as is titanium, but not magnesium powder per se. Nickel is used in autoclaves. Silver has virtually no reaction when heated in air and no reaction when heated in steam. Autoclaving does not remove activity. Stainless-steel response to steam will vary with the grade of the steel and content of other inhibitors. With chrome there may be stainless-steel pitting and dulling of cutting edges after several sterilization cycles. Iron will corrode with steam. Titanium resists corrosion. Nickel–titanium alloy improves against corrosion. Titanium molybdenum is acceptable. Many metals may be steam sterilized if generated with pure water without dissolved gases (e.g., oxygen, carbon dioxide, and sulfur dioxide).

Ozone

Ozone and humidity have some effects on a few metals, but at reduced temperatures and length of time most metals are compatible.

Nickle and silver have significant material or surface changes on them after only three ozone cycles.

4.3.4 Ceramics and glass: the effects of sterilizing on ceramics and glass

Ceramics are usually a compound of metallic and nonmetallic elements. They are poor conductors of heat, but are excellent at retaining heat once heated. They are very resistant to corrosion and are nontoxic. Due to their ability to retain heat, ceramic materials will keep warm longer than metallic counterparts of comparable shape and size.

A common problem with most ceramics is their tendency to crack due to thermal stress. Since they are such poor conductors of heat, there may be a large temperature difference between one side of the ceramic and the other. In such a case, the warmer side expands more than the other, causing the ceramic to crack. Ceramics are seldom used for quick heating for this reason; dry-heat ovens allow even heating from all sides, preventing large thermal gradients, which steam heat may not.

Ceramics in healthcare products may be sterilized by the following techniques:

- radiation (gamma, electron beam or X-ray);
- ethylene oxide (EO);
- moist heat (steam);
- dry heat;

© Woodhead Publishing Limited, 2013

- hydrogen peroxide vapor;
- ozone.

Some ceramic examples are aluminum oxides, silica, and zirconium oxide.[3]

Aluminum oxides are sterilized excellently with irradiation, EO, hydrogen peroxide, and ozone. Steam sterilizes aluminum oxides from good to excellent. Dry heat is good on aluminum oxide, but better at lower temperatures. Dry heat was selected for spacecraft sterilization because it could sterilize most ceramics between 105 and 135°C. Dry heat was run in large ovens.

The silica ceramic is sterilized easily by all techniques. It withstands thermal gradients better than ceramics such aluminum oxides and zirconium oxides

Zirconium oxides are easily sterilized by irradiation, EO, hydrogen peroxide, and ozone. Steam and dry heat sterilize zirconium oxides from fair to good; however, again spacecraft sterilize ceramics with dry heat.

Steam, EO, dry heat, hydrogen peroxide, and ozone can sterilize most glasses.

Irradiation, however, will affect glass. It will discolor glass, but this effect can be used for manufacturing colored glasses.

Steam will affect some types of glass, but dry heat will not. Dry heat is the better modalitie for sterilizing glass. It can also be used to depyrogenate any pyrogen contamination on glass.

4.4 The effects of sterilizing on welded joints

The first consideration in sterilizing welded joints is to determine that the medical materials or polymers are compatible with the sterilization technique. One of the major difficulties in sterilization of welded joints is how to determine if sterility occurred within possible welds, particularly for implantables. To determine this result, resistant spores are inoculated in joints that will be welded. After sterilization, the welded joint can be assessed with immersion in sterility-test media to determine if the inoculated spores are recoverable or not. Resistant spores will vary depending upon the sterilization techniques employed. For example:

Hydrogen peroxide, ozone and steam sterilization: thermophile spores (*Geobacillus sterothermophilus-ATCC 7953*) are more resistant than ambient or mesophile spores. These may also be used as biological indicators (BI).

Dry heat and EO sterilization: *Bacillus atrophaeus* ATCC 9372 or NCTC 10073.

However, new bead and crevice-free welding helps to eliminate bacteria build-up. Weld areas can be easily inspected in translucent polypropylene and PVDF.

© Woodhead Publishing Limited, 2013

In most cases the effects of sterilization on welds will be no different than their effects on materials, except for possible results from 'expansions' resulting from the sterilization, such as heat expansion, pressure/vacuum expansions of EO, hydrogen peroxide with vapor or ozone sterilization.

With dry-heat and steam sterilization, differences in expansion rates, which could cause damage to welded mated parts, should be evaluated. Even with irradiation, differences in expansion rates, which could affect the bond strengths of welded mated parts, should be evaluated.[7]

Welding materials will not eliminate the effects of sterilization on the materials being welded.

4.4.1 Laser welding of joints

One of the better techniques for welding joints is laser welding, it does not have any toxic effects on the joints and is therefore biocompatible. However, if the material being welded was already toxic before welding, it will remain toxic and not biocompatible.

Laser welding minimizes any heat effect. For dry-heat and steam sterilization, lasers create high-strength and helium leak-tight welds in metals and polymers with pore-free surfaces and in this way make this joining technique the ideal solution, against migration of microbes or impurities. Excellent beam quality, high pulse-to-pulse stability and flexible pulse shaping are the preconditions for the finest seam and spot welds. Thus, laser-welded joints can be used for high-temperature sterilization and exhibit pore-free surfaces even without finishing. This is a crucial requirement for sterilizable biocompatible components, particularly implant systems.

Gamma irradiation may not have little effect on the laser weld of a joint whether in the manufacture of sterilizable implant systems or in the manufacture of surgical instruments, endoscopes or other devices. The particular properties of laser welding joints and seams are further recognized here for their special ideal qualities:

- welding narrow seams with high strength;
- welding gas tight bonding of seams;
- welding that is corrosion resistant;
- welding porous free with smooth surface, suitable for high-temperature sterilization;
- biocompatibility in accordance with the basic material;
- material suitability in accordance with the basic material with effects from sterilization technique.

© Woodhead Publishing Limited, 2013

The welding can be carried out with or without filler wires, according to the properties of the basic material. Neither the biocompatibility, the strength, toxicity, nor the porous-free nature of the materials are typically affected by sterilization of laser welds.

4.4.2 Heat welding (sealing)

Heat is another type of welding that is frequently used on polymers (e.g., PE, polyolefins) instead of solvent bonding. For example, metallocene polyolefins are suitable for heat sealing but not for solvent bonding or RF sealing, which are required steps in assembling some products. However metallocene PE not may be autoclaved because of its low melting point (*Tm*).

Rigid PVC parts that have been molded are suitable for ultrasonic bonding, while flexible PVC extruded or calendered films can be EO sterilized when they have been sealed using heat.

The method of joining together the ends of melt processible fluoropolymers such as Teflon are characterized by a high degree of chemical inertness and a continuous service temperature in the range of 300 °F to 500°F. The joining of the ends together may be accomplished by the use of infrared heat emanating from an infrared heat source with temperatures in the range of 1250–2000°F. and spaced from the ends for a period of time approximately up to one minute which may be gauged by the appearance of the material end as it becomes visibly molten to a depth. The infrared heaters are then removed and the ends may be put together under almost no pressure and held briefly, in one form, for less than a minute, to quickly establish a joint that may become at least as strong and probably stronger than the original ends. Heat sterilization continues to be the idea technique for sterilization of the fluoropolymer family, except PFA which has heat deflection temperature of 164°F. The infrared fusion or thermal radiation heating is typically used as a substitute for hot-plate welding (contact heating) when the plate temperature has to rise above 260°C. Above this temperature, coatings to prevent adhesion of molten plastic to the hot plate can no longer be used. Therefore using infrared radiation heating instead of a hot plate at a temperature of 400 to 500°C or greater for fluorocarbons is preferred. Irradiation sterilization may be troublesome with some Teflon welding. The application of heat resistant fluoropolymers will likely continue to increase, providing more cost-effective solutions to the ever growing demands and diversity of joint-welding techniques and modern medical technology.

Infrared (IR) fusion is excellent toward welding PVDF and PP materials. PVDF may be a polymer of choice for steam and ozone. PP can be autoclaved up to about 121°C, while PVDF can be steam sterilized up to at least 127°C. PP, PVDF, and PVC may be H_2O_2 sterilized.

© Woodhead Publishing Limited, 2013

Thermal cycling can be particularly valuable in assessing designs that involve differentials in expansion coefficients, especially with welded joints.

4.4.3 Ultrasonic welding or bonding

Rigid PVC parts that have been molded are suitable for ultrasonic bonding, and may be EO, or irradiation sterilized.

Ultrasonic welding depends on materials softening not melting with increased temperature. Therefore, it is suitable only for thermoplastic polymers, not thermosets. For example, ABS, acrylic, polycarbonate, and PVC are amorphous polymers – with little or no crystalline structure, they are ideal for ultrasonic welding. Polyethylene, polypropylene, polyester and nylon are semi-crystalline – much more difficult to weld with ultrasonics. In general, best results are obtained when both components to be welded are made from identical material, but in some cases dissimilar materials can be welded using ultrasonics. For this to work the materials must be chemically compatible and have similar melting points (easier for amorphous materials – see the discussion of amorphous and crystalline materials above). One of the better combinations is acrylobutylstyrene (ABS) and acrylic (PMMA), though others are also possible to different degrees. Irradiation technique, however, may not work well with this joint because of the sensitivity of PMMA to irradiation. While polyethylene and polypropylene are both olefin the general consideration appears to be that these are chemically incompatible. Similarly, irradiation sterilization of these two materials would be disadvantageous.

4.4.4 Radiofrequency welding

Rigid flexible extruded or calendered PVC films can be sealed using radiofrequency (RF) sealing, and sterilizable with EO. Metallocene polyolefins (e.g., PE) are suitable for heat sealing but not for RF sealing. Metallocene (sealed) polyolefins may be heat sterilized.

RF welding can only occur between highly dipolar materials that are excited by an alternating magnetic field. The RF welding process uses radio frequency energy to produce molecular agitation in thermoplastic materials (e.g., thermoplastic polyurethane, PVC, PVDC, EVA, PET, nylon, and other customized resins) such that they melt and flow together, forming a bond that is as strong as the original materials. As long as the bond is as strong as the original materials the effects of sterilization of the original materials should continue to apply.

© Woodhead Publishing Limited, 2013

Variation, however, may occur with dissimilar materials, despite their both being highly polar. Dissimilar materials cannot be steam sterilized below their transitional temperature

4.4.5 Miscellaneous effects of sterilization on welded joints

With steam sterilization or other sterilization methods with pressure differentials (e.g., HO, EO and ozone), if the external pressure on a sealed soft bag or device space is greater than the internal pressure, the volume of the head-space will reduce due to compression of the air. In such a case, is difficult for a high-pressure differential in this direction to damage the bag because it does not stretch the material or compromise its welded joints. However, a low chamber pressure will cause the bag to inflate which, if it results in stretching beyond the elastic limit, may lead to nonrecoverable deformation or failure at a welded joint. Consequently, the ideal processing condition for this type of product is to always maintain the chamber pressure a little above the theoretical pressure inside the container, bag, or device space.

Thermal cycling is particularly valuable in assessing designs that involve differentials in expansion coefficients, especially with adhesive bonding

In the United States sterilizers are considered a medical device. Because sterilizers such as steam sterilizer have many welded parts and joints, there may be a number of standards required to evaluate these welded parts or joints by manufacturers. Some specific standards are provided as follows:

- BS 3970: 1990: Steam sterilizers.
- BS 2646: Autoclaves for sterilization in laboratories. Part 1: 1983; Part 2: 1990; Part 3: 1993; Part 4: 1991; Part 5: 1993.

Autoclave welds must be strong enough to withstand multiple changes in temperature and processing.

Radiation sterilization itself may be another possible means of welding materials. For example, incomplete cured silicone parts can be cross-linked together by irradiation.

Ultraviolet light can theoretically both sterilize and weld parts. UV is a limited sterilization technique because it cannot sterilize around corners nor penetrate many materials. Plastics are usually transparent in the visible spectrum, not UV. Ultraviolet light is both harmful to health and spatters. UV light range may occur from other welding techniques.

© Woodhead Publishing Limited, 2013

4.5 Selecting a suitable sterilization method

There are always tradeoffs when selecting a method of sterilization based on acceptable materials' inherent properties to welding and processing.[8]

4.5.1 Determining the appropriate method of sterilization

Some qualities to consider when selecting a sterilization method are:

- *Availability*: steam autoclave is most available in a hospital; for in-house or contract sterilization EO is available; and irradiation is very available by contract. Hydrogen peroxide is becoming more widely used in hospitals followed by ozone.
- *Cost*: dry heat is the least expensive method, next steam, then hydrogen peroxide and ozone, and then irradiation and EO sterilization. This cost includes equipment, facilities, and consumables.
- *Compatibility*: EO is the most compatible to polymer materials.
- *Disposability*: deals with disposal of polymers after use, and sterilant wastes (e.g., EO and used gamma sources).
- *Ease of control and monitoring*: dry heat and irradiation are the easiest to control, followed by steam, then hydrogen peroxide, ozone, and EO.
- *Environment*: ability to recycle, reuse, and disposal of polymers. Dry heat, moist heat, and ozone are the most environmental friendly; followed by E-beam and hydrogen peroxide.
- *In-house versus contract (external) sterilization*: dry heat and steam at re most easiest to use in-house; while radiation is used predominantly under contract basis; EO is used more often either in-house or by contract. Irradiation is typically used in contract with a few exceptions, such as for small gamma and E-beam facilities in industrial applications, but not in hospitals.
- *Lethality*: steam has the greatest lethality, which includes ineffectivity of resistant prions; irradiation has excellent penetration and consequently lethality; dry heat is able to depyrogenate pyrogens.
- *Packaging*: irradiation can penetrate virtually every type of package.
- *Regulatory*: EO is the most regulated sterilization process and sterilizing chemical.
- *Reusability*: steam is the easiest sterilant to reuse; EO can be reused.

Besides the above qualities the following 'steps' should be taken into consideration when selecting the sterilization method to be applied or used:

1. Identify the method(s) of sterilization that appear compatible with product design and materials and joining approaches.

© Woodhead Publishing Limited, 2013

2. List options: Cost, in-house vs contract; regulatory issues, local codes and environmental regulations.
3. Perform feasibility studies to determine gross compatibility with selected processes.
4. Perform detailed pre-validation studies to demonstrate product, component, joint compatibility with the selected process and attainment of required sterility assurance level (SAL).
5. Based upon the above qualities and steps select the most suitable sterilization method to be applied or used.

4.6 Conclusions

Every sterilization technique must be what their own characteristics and qualities determine. Control of sterilization must of necessity begin with its environment and material compatibility. The qualities of different sterilization techniques vary. Heat sterilization may melt and corrode some materials, while irradiation may create radicals and cause embrittlement and cross-linking of materials. Hydrogen peroxide and ozone sterilization both oxidize some materials and polymers. Sterilization of polymers continues to be an important challenge of medical materials and polymers in products.

Welding materials will not eliminate the effects of sterilization on the materials being welded. Different welding techniques have their individual qualities.

There are always tradeoffs when selecting a method of sterilization based on acceptable materials' inherent properties to welding and sterilization. Whatever the sterilizing technique, they must be able to (1) completely sterilize both surfaces and below surfaces or difficult to access locations; (2) the cost of heat sterilization is less costly, (3) there are more items being resterilizable by heat than by other means, (4) heat sterilization is more readily available and accessible in health care facilities than other techniques; (5) lower-temperature heat sterilization techniques will occur more easily in the future, allowing for more heat- sensitive polymers to be sterilizable (because the new sterilization techniques are more niche players, less penetrable, and are small sterilizers; (6) heat sterilization uses no toxic chemicals, or emits any toxic emissions or wastes, and is environmentally (green) safe; (7) polymers and packaging materials continue to be invented and improved to be heat stable, heat sterilizable, reusable, and less costly, paving the way to improved medical materials; (8) alternatives to EO sterilization continue to occur because of its toxicity and multiple regulations, inherent hazards and increasing costs; however, EO sterilization is likely the gentlest process on materials, polymers,

© Woodhead Publishing Limited, 2013

and welded joints, and it is able to penetrate and can sterilize many joints and welds.

Experience with real-world polymers and materials is showing a need for careful and thorough evaluations when it comes to the effects of sterilization on medical materials, polymers, and welded joints. In general, the trends point toward a need for more careful understanding of the interaction between design, material interaction, sterilization, biocompatibility, environment, and final polymer product and welded joint performance.

4.7 Sources of further information

Anand, V. P., Cogdill, C. P., Klausner, K. A., Lister, L., Barbolt, T., Page, B. F. J., Urbanski, P., Woss, Casimir J. and Boyce, J. (2003) 'Re-evaluation of EO hemolysis and irritation potential.' *Journal of Biomedical Materials Research*, **64A**, 648–654.

Anes, J., Nase, R. S. and White C. H. (1992) 'Use of plastics for parenteral packaging.' In: K.E. Avis, H.A. Lieberman, and L. Lachman (eds.), *Pharmaceutical dosage forms: Parenteral medication*, Vol. 1, 2nd edn, Munich: Marcel Dekker, pp. 387–444.

Berger, K. and Doriff, D. (2001) 'Efficacy and sterility in flexibile packaging', *Medical Device & Diagnostic Industry*, August, pp. 1–8.

Canon Communications (2004) *Modern plastics worldwide world encyclopedia: The global plastics magazine*, http://www.asiaing.com/modern-plastics-worldwide-free-subscription.html

Czuba, L. (1999) 'Medical plastics for PVC replacement in medical solution containers', *Medical Device & Diagnostic Industry*, April, pp. 1–5.

Czuba, L. (2004) 'Polymers: Paving the road of medical device progress', *Medical Device & Diagnostic Industry*, August, pp. 1–4.

Feldman L. A. and Hui H. K. (1997) 'Compatibility of medical devices and materials with low-temperature hydrogen peroxide gas plasma', *Medical Device & Diagnostic Industry*, 19, 57–62.896

Frissora, C. (2007) 'Trends in device design: Implications for materials selection', *Medical Device & Diagnostic Industry*, May, pp. 80–90.

Gil, F.J., Gnebra, M.P., Planell, J.A., Hermanson, N. and Wessel, T. (1998) 'Syndiotactic polystyrene: A new polymer for high performance', *Medical Applications*, July, pp. 1–4.

Hemmerich, K.J. (2002) 'Polymer materials selection for radiation-sterilised products', *Medical Device & Diagnostic Industry*, February.

www.devicelink.com/mddi/archive/00/02/006.html.

Lundy, Charles (1994) 'Selecting polymers for medical devices', *Medical Plastics and Biomaterials*, Summer, pp. 22–27.

Marino, F., Floyd, B., and Rogers, W. (technical assistance) (1992) 'Industrial sterilisation: A review of current principles and practices.' In: K.E. Avis, H.A. Lieberman and L. Lachman (eds.), *Pharmaceutical dosage forms: Parenteral medication*, Vol. 2. New York: Marcel Dekker, pp. 1–54.

Marczis, B. and Tibor, C., *Polymer Joints*, Department of Polymer Engineering and Textile Technology, Faculty of Mechanical Engineering, Budapest University of Technology and Economics.

© Woodhead Publishing Limited, 2013

Molin, G. (1977) 'Inactivation of bacillus spores in dry systems at low and high temperatures', *Journal of General Microbiology*, **101**(2): 227–231.
Modern Plastics (yearly) *Modern plastics world encyclopedia*, New York: Modern Plastics.
Perkins, J.J. (1970) *Principles and methods of sterilisation in health sciences*. Springfield, IL: Charles C. Thomas, pp. 54, 204, 261–262, 296–299, 301.
Plastics Design Library (1994) *The effect of sterilisation methods on plastics and elastomers.* Morris, NY: Plastics Design Laboratory.
Portnoy, R. (1997) 'Clear radiation, autoclavable polypropylene', *Medical Plastics and Biomaterials*, January, pp. 1–9.
Rhodes, A. and Fletcher, D. (1966) 'Principles of sterilisation, sterility tests and asepsis', Chapter 5 of *Principles of industrial microbiology*, Oxford: Pergamon, pp. 45–57.
Rogers, W. (2012) 'Steam (moist heat) and dry heat sterilization', Chapter 2 of *Sterilisation of biomaterials and medical devices*, eds. Sophie Lerouge and Anne Simmons, Cambridge: Woodhead Publishing.
Rogers, W. (2012) 'Sterilisation techniques for polymers', Chapter 7 of *Sterilisation of biomaterials and medical devices*, eds. Sophie Lerouge and Anne Simmons, Cambridge: Woodhead Publishing.
Rubin, I. (1990) *Handbook of plastic materials and technology*, New York: John Wiley & Sons.
Steward, R. (2005) 'New polymers offer advantages for medical devices and packaging', *Plastics Engineering*, October, pp. 20–27.
Sturdevant, M. (1998) Sterilisation compatibility of rigid thermoplastic materials. Dow Chemical Company report.
Szycher, M. (1991) *High performance biomaterials*, Lancaster, PA: Technomic Publishing.
Williams, D.F. (1987) 'Tissue-bio material interaction', *Journal of Material Science*, **22**, 3421–3445.
Woo, L. and Sherwin, S. (2000) 'Selecting materials for medical products', Chapter 38 of *Handbook of materials selection*, ed. Myer Kutz, New York: John Wiley, pp. 1195–1222.

4.8 References

1. Rhodes, A. and Fletcher, D. (1966). 'Principles of sterilisation, sterility tests and asepsis', Chapter 5 of *Principles of industrial microbiology*, Oxford: Pergamon, p. 50.
2. Molin, G. (1977). 'Inactivation of Bacillus spores in dry systems at low and high temperatures', *Journal of General Microbiology*, **101**, 227–231.
3. AAMI (2008). Technical Information Report 17, *Compatibility of materials subject to sterilisation,* Technical Information Report (TIR) 17, American Association of Medical Instrumentation.
4. Rogers W. (2006). 'Steam: uses and challenges for device sterilisation', *Medical Device & Diagnostic Industry*, Canon Communications, Los Angeles, CA, USA, pp. 80–87.
5. Rogers, W. (2005). *Sterilisation of polymer health care products*, RAPRA Technology, Shrewsbury, UK, pp. 26, 298–302.

© Woodhead Publishing Limited, 2013

6. Plastics Design Library (1994). *The effect of sterilization methods on plastics and elastomers*. Plastics Design Library, Morris, New York, pp. 1–338.
7. Tang, F.W., Lambert, B.J. and Rogers, W. J. (2001). *Polymers in medical applications,* RAPRA Technology, Shrewsbury, UK, pp. 1–15.
8. ANSI/AAMI/ISO 10993-7 (2001). *Biological evaluation of medical devices – part 7: ethylene oxide sterilisation residuals*, Association for the Advancement of Medical Instrumentation, Arlington, VA.
9. ANSI/AAMI (2003). *Biological evaluation of medical devices – part 1: evaluation and testing*, Association for the Advancement of Medical Instrumentation, Arlington, VA.
10. Kowalkski, J. B. (1993). 'Selecting a sterilization method', in *Sterilisation technology: a practical guide for manufacturers and users of health care products*, ed. Morrisey, Robert F. and Phillips, C. Briggs, Kluwer Academic Publishers, pp. 70–79.

© Woodhead Publishing Limited, 2013

5

Micro-welding of shape-memory alloys

M. I. KHAN, Smarter Alloys, Canada and
Y. ZHOU, University of Waterloo, Canada

DOI: 10.1533/9780857096425.2.133

Abstract: This chapter discusses the challenges in the joining of Nitinol (i.e. NiTi alloys) shape-memory alloys (SMAs) which are becoming increasingly popular in medical-device applications due to their unique shape-memory effect and pseudoelastic (i.e. superelastic) functional properties. The chapter starts by providing a brief introduction to the properties of SMAs followed by a review of how different micro-welding techniques affect the alloy microstructure and properties. Fundamentals for key micro-welding processes used in joining Nitinol SMAs are detailed, including resistance and laser micro-welding (i.e. RMW and LMW).

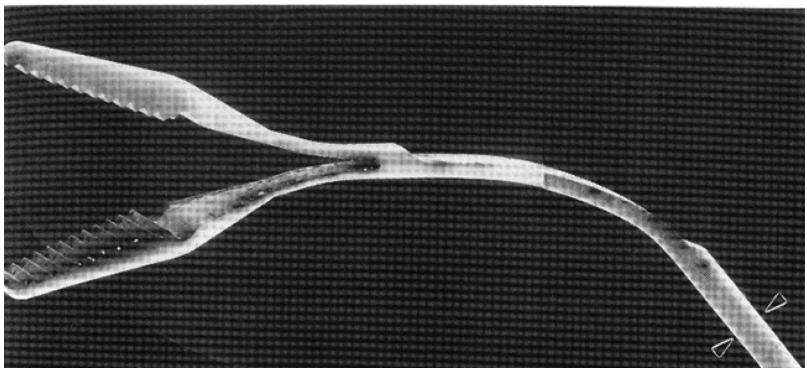
Key words: shape-memory alloys, Nitinol, laser micro-welding, resistance micro-welding, weld-material properties.

5.1 Introduction

The unique properties of shape-memory alloys (SMAs) have resulted in numerous applications, including fasteners, actuators, wear prevention and most importantly biomedical devices.[1] As the knowledge base and processing methods of these materials continue to evolve, many more potential applications can be realized. In particular, there is ever increasing interest and implementation of SMA in biomedical applications. Their excellent biocompatibility coupled with good strength and ductility has made them an ideal material for implantable medical devices. Temperature-dependent characteristics of their functional properties, which are disadvantageous in certain applications, are insignificant in implantable medical devices due to the temperature stability maintained by the human body (i.e. 37°C). Furthermore, specific surface treatments have shown to greatly improve SMA biocompatibility.[2]

In many cases, medical-device fabrication procedures require micro-welding techniques. An example of this is shown in Fig. 5.1 where microscopic forceps utilized in endoscopic brain surgery is connected to 0.63 mm wire using laser welding.[3] However, joining (i.e. welding, brazing and soldering) of Nitinol is generally difficult, which in turn limits flexibility in the

© Woodhead Publishing Limited, 2013



5.1 Laser-welded microforceps made from Nitinol. (Source: Reprinted with permission of ASM International. All rights reserved. www.asminternational.org.[3])

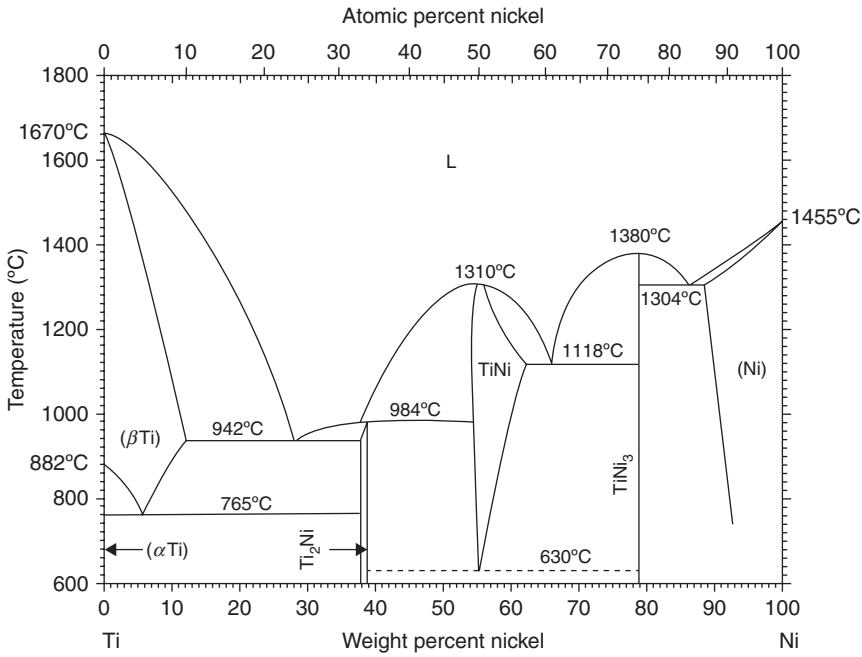
design and fabrication of Nitinol devices and hence impedes high-volume commercialization of the alloys. This is further complicated when working on small-scale products, such as those implemented in medical-device components. This chapter starts by providing a brief introduction to the properties of SMAs. Fundamentals for key micro-welding processes are detailed, including resistance and laser micro-welding. Finally (LMW), a review of current challenges faced with welding Nitinol is provided.

5.2 Fundamentals of Nitinol shape-memory alloys

The shape-memory and pseudoelastic properties of near equatomic Nitinol were discovered in 1963 by Beuhler *et al*.[5] Similar effects were discovered earlier in other alloys;[6,7] however, the superior mechanical and functional properties of NiTi alloys has led to greater popularity. As the fundamental understanding of Nitinol's mechanical behaviour improved, these alloys started to become commercially available in the 1970s. To date, Nitinol alloys provide the best combination of shape-memory material properties for commercial applications.[1] They particularly excel in the medical-device industry due to the excellent biocompatibility, where they are used for bone brackets, surgical staples, vascular stents, orthodontic arch wires and many more applications.[14]

The composition required to form Nitinol SMAs can be determined using a binary NiTi phase diagram, shown in Fig. 5.2.[8] The NiTi phase is restricted to the central region of the diagram between the Ti_2Ni and $TiNi_3$ phases, near equiatomic composition. Not shown on this diagram is the metastable Ti_3Ni_4 intermediate phase between NiTi and $TiNi_3$. This Ti_3Ni_4 phase is essential in altering the functional properties of the Nitinol SMA. At lower

© Woodhead Publishing Limited, 2013



5.2 NiTi phase diagram. (L in the figure refers to liquid.) (Source: Reprinted with permission of ASM International. All rights reserved. www.asminternational.org.[8])

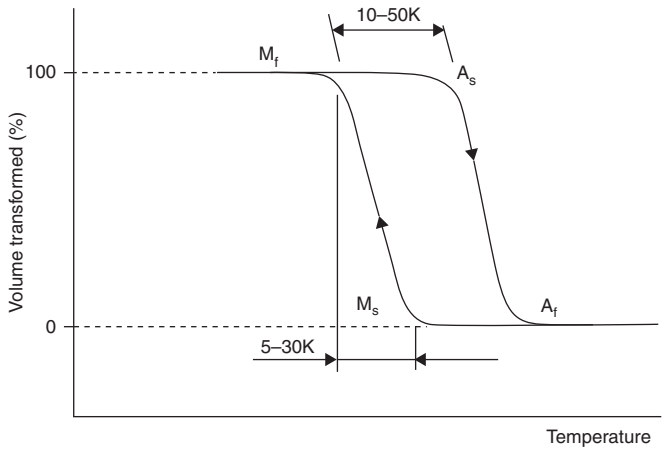
aging temperatures the Ti_3Ni_4 phase appears while at higher aging temperatures the $TiNi_3$ phase is more stable.[9]

Mechanisms responsible for Nitinol's functional properties are closely linked to diffusionless solid–solid martensitic phase transformations. SMA phase transformations typically occur in a metastable solid state. Phase transformations can be induced by either temperature change or mechanical deformation. During transformation the austenite (i.e. B2 phase) transforms into martensite (i.e. B19′). Temperatures and stresses required to induce phase transformation are largely dependent on the alloys' chemical composition and previous thermomechanical processing. The following sections describe the temperature- and stress-induced transformations and the associated shape memory and pseudoelastic properties, respectively.

5.2.1 Temperature-induced transformation

Temperature-induced transformation in SMAs are typically characterized by four distinct temperatures, including austenite start (A_s) and austenite finish (A_f) during heating and martensite start (M_s) and martensite finish (M_f) during cooling. A_s and A_f indicate the start and finish of martensite to

© Woodhead Publishing Limited, 2013



5.3 Schematic of the volume transformed as a function of temperature. (Source: Copyright (2001) Wiley. Used with permission from Van Humbeeck, J., Shape memory alloys: a material and a technology, *Advanced Engineering Materials*, John Wiley & Sons.[10])

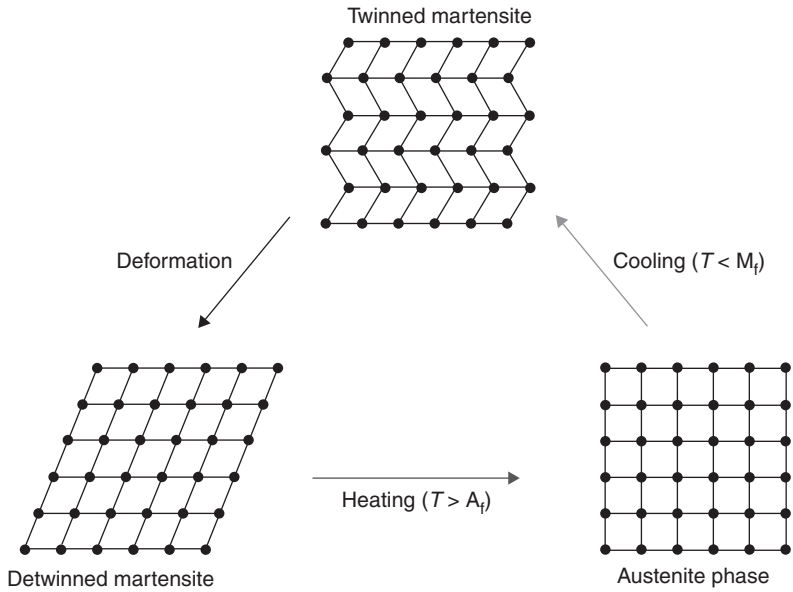
austenite phase transformation, while M_s and M_f describe the reverse austenite to martensite transformation. Temperatures are typically identified utilizing a differential scanning calorimeter which captures the endothermic and exothermic events during phase transformation. A schematic showing the volume fraction transformed as a function of temperature is shown in Fig. 5.3.[10] For Nitinol, transformation temperatures typically range from −150°C to 150°C, while the overall hysteresis of transformation are in the range of 10–50°C.

The ability Nitinol to undergo solid–solid phase transformation enables the material to exhibit a phenomenon known as shape-memory effect (SME). schematically detailed in Fig. 5.4. During this cycle the initial parent material is brought to a temperature below M_s. At this temperature detwinning of the martensite phase accommodates deformation and maintains the altered shape. Subsequent heating to above A_f would result in phase transformation and recovery of its original shape and hence its ability to remember a shape.

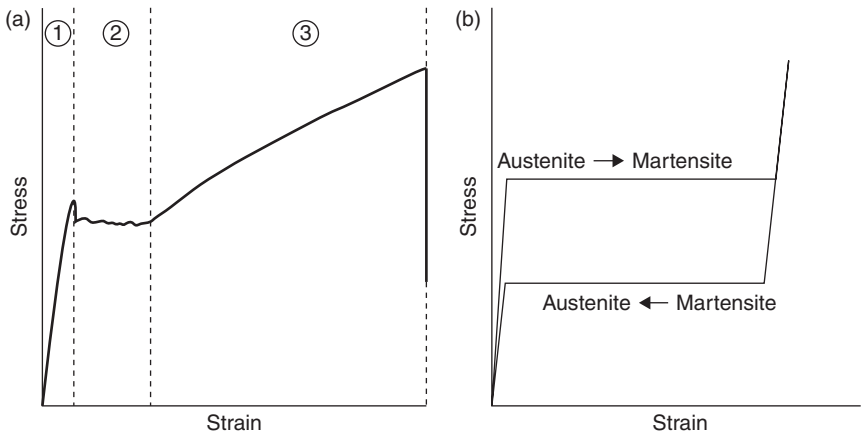
5.2.2 Stress–strain curve and pseudoelasticity

The non-linear stress–strain behaviour of SMAs is unlike other common metallic engineering materials. Figure 5.5a shows a typical pseudoelastic stress–strain curve where the sample is loaded to failure. This stress–strain curve consists of three distinct deformation zones: elastic (region 1), pseudoelastic (region 2) and plastic deformation (region 3). At

© Woodhead Publishing Limited, 2013



5.4 Schematic of the SME behaviour of Nitinol SMAs.



5.5 Schematic of a typical stress–strain curve for pseudoelastic NiTi alloy: (a) stress–strain curve until fracture and (b) loading–unloading curve.[10]

temperatures above A_f, the pseudoelastic properties of Nitinol enable it to be strained beyond the linear elastic (region 1) portion on a stress–strain curve while undergoing stress-induced phase transformation. The applied

© Woodhead Publishing Limited, 2013

stress transforms the austenite parent phase to martensite which is termed stress-induced martensite (SIM). Upon removal of stress within region 2 most of the mechanically induced martensite reverts back to austenite, as shown in Fig. 5.5b. The magnitude of near-perfect pseudoelastic strain for Nitinol can reach 8% in polycrystalline materials.[10] Straining beyond the pseudoelastic region results in the plastic deformation of martensite until full fracture occurs.

5.3 Micro-welding of NiTi

With increased demands for finer and more complex devices, advancement in effective processing methods becomes necessary. Hence, the development of effective micro-welding of NiTi is an integral part of the manufacturing of Nitinol-based devices. Welding processes commonly result in localized changes in the welded regions, yielding properties that differ from that of the original material. These changes become even more of a concern in SMAs because not only are their mechanical properties altered but also their functional properties. Strength reduction, inclusions of intermetallic compounds, altered pseudoelastic and SMEs are all examples of how Nitinol can be affected by welding.[5–13] Micro-resistance spot welding (MRSW) and LMW of crossed-wires are two commonly used welding processes for interconnection and component assembly for miniature medical devices, such as pacemakers.[14] Each of these processes can affect differently the aforementioned properties of Nitinol. Furthermore, their respective process parameters can greatly influence the extent of altered properties.[6] The following sections detail the effect of laser and resistance micro-welding (RMW) procedures on the mechanical and metallurgical behaviours of welded crossed Nitinol wires. Details on fundamentals for both welding procedures can be reviewed in Chapter 5 and Reference 11.

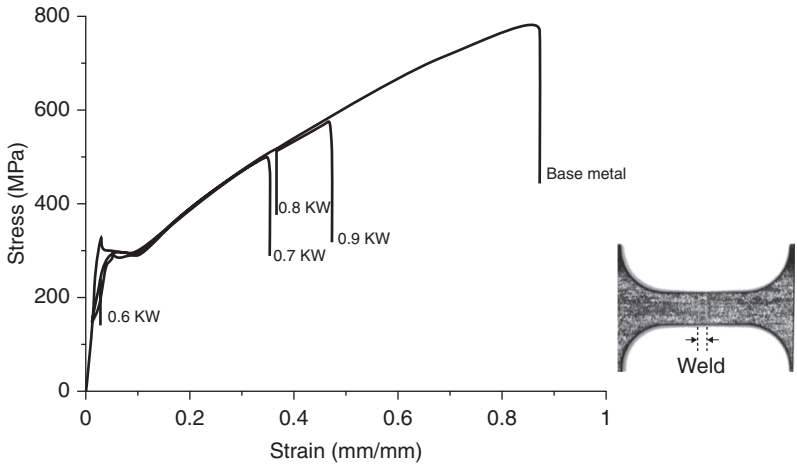
5.3.1 Laser micro-welding

During LMW peak temperatures in the weld metal typically surpass the material melting point resulting in a molten metal pool which subsequently solidifies upon removal of lasing energy. Often pulsing methods are implemented to aid in minimizing the heat-affected regions during the welding of miniature components. However, thermomechanical properties of the re-molten material can still greatly differ compared with the base material.

Effects of laser welding on mechanical performance

The majority of SMAs in application are subjected to loading to the pseudoelastic loading stress of the material. Therefore the failure stress

© Woodhead Publishing Limited, 2013

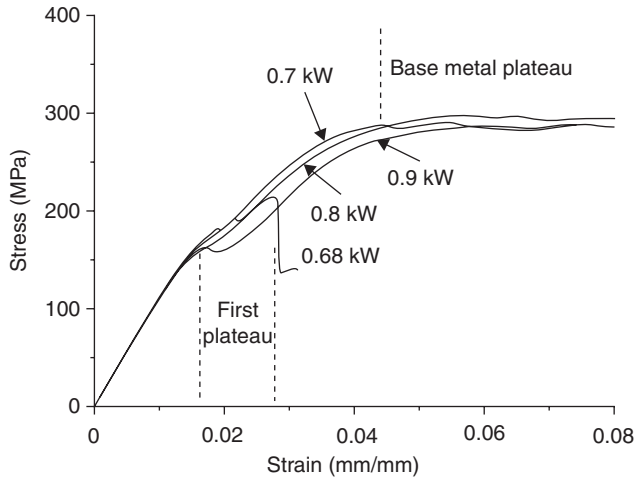


5.6 Representative tensile curves for varying peak power input for 10 pps frequency and 5 ms pulse time.[12]

is required to be above the pseudoelastic stress. However, depending on laser-welding processing parameters the maximum tensile stress can either be above or below the maximum strength. This process parameter dependence is shown in Fig. 5.6, which shows engineering stress–strain curves of traverse pulsed Nd:YAG laser-welded tensile specimens for varying peak power (0.6–0.9 kW) as compared to the Nitinol base material.[12] Typical pseudoelastic behaviour is indicated by a flat region (plateau) after linear elastic straining when a 290 MPa plateau stress is achieved. Beyond the plateau stress, plastic deformation of martensite occurs and load increases due to strain hardening followed by material failure. Laser-welded material often have reduced failure stress and ductility compared with the base metal. However, failure stresses obtained with high enough peak power surpass the pseudoelastic region and are acceptable for SMA applications (Fig. 5.6).

Although SIM transformation (austenite→ martensite) occurs in a traverse weld specimen,[1,9] the weld zones experience an irreversible initial yielding. This is shown in Fig. 5.7,[12] which details the elastic to pseudoelastic deformation. The initial plateau indicates yielding in the welded region, while the second plateau is the SIM transformation in the base metal (BM) stress–strain curve (Fig. 5.6). Furthermore, process parameters directly affect the magnitude of yielding, which became more pronounced with increasing peak power. Reasons for this change will be detailed in the following section. However, it is crucial that the mechanism of deformation and its correlation to process parameters is accounted for prior to implementation of a welded SMA device.

© Woodhead Publishing Limited, 2013



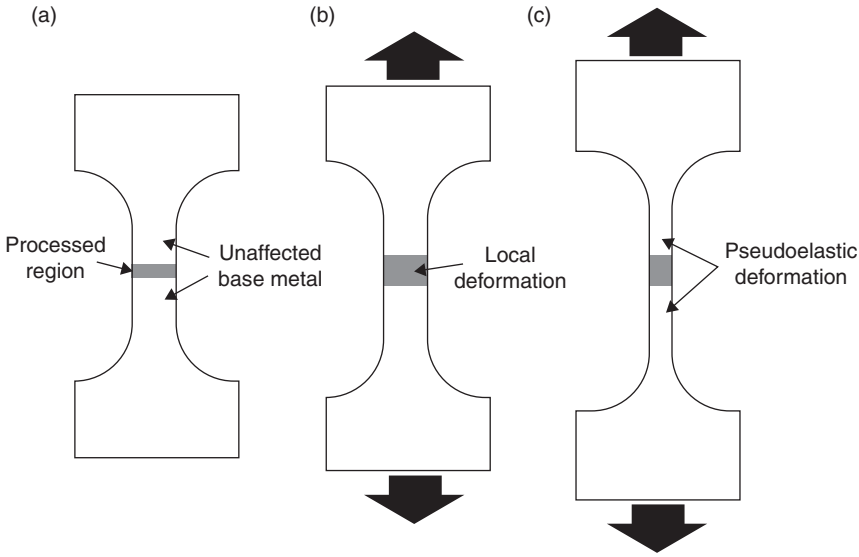
5.7 Detailed view of multiple plateaus in processed samples.[12]

For most welded SMA devices the weld metal only accounts for a fraction of total material. As such, it is more realistic to test weld tensile samples that consist of both unaffected base metal and weld metal. Figure 5.8 shows a schematic of such a sample that is at the different stages of deformation experienced during loading (i.e. see Fig. 5.7). During loading, the transverse tensile coupon induces stress in both the base and weld metal. Upon initial tensile loading, both regions experience elastic deformation until a critical stress is reached where the onset of the initial plateau occurs. Local yielding experienced within the welded region, illustrated in Fig. 5.8b, results in the formation of the initial plateau. Additional straining then induces further elastic deformation of the remaining unaffected gauge length followed by SIM transformation (Fig. 5.8c). Hence the presence of multiple plateaus results from different deformation mechanisms occurring in the weld and base metal. Amplification of the first plateau is directly related to the increasing peak power since increasing peak power results in a larger weld width. Accordingly, a larger volume within the gauge length undergoes local deformation. This altered mechanical performance must be accounted for during the design of welded SMA devices.

Effects of laser micro-welding on NiTi microstructure and phase transformation

Re-melting due to laser welding significantly alters base metal microstructure, which for most SMAs is responsible for the change in mechanical properties. Specifically, laser welding causes dendrite formation, grain coarsening and segregation of intermetallic (IMC) compound at grain

© Woodhead Publishing Limited, 2013

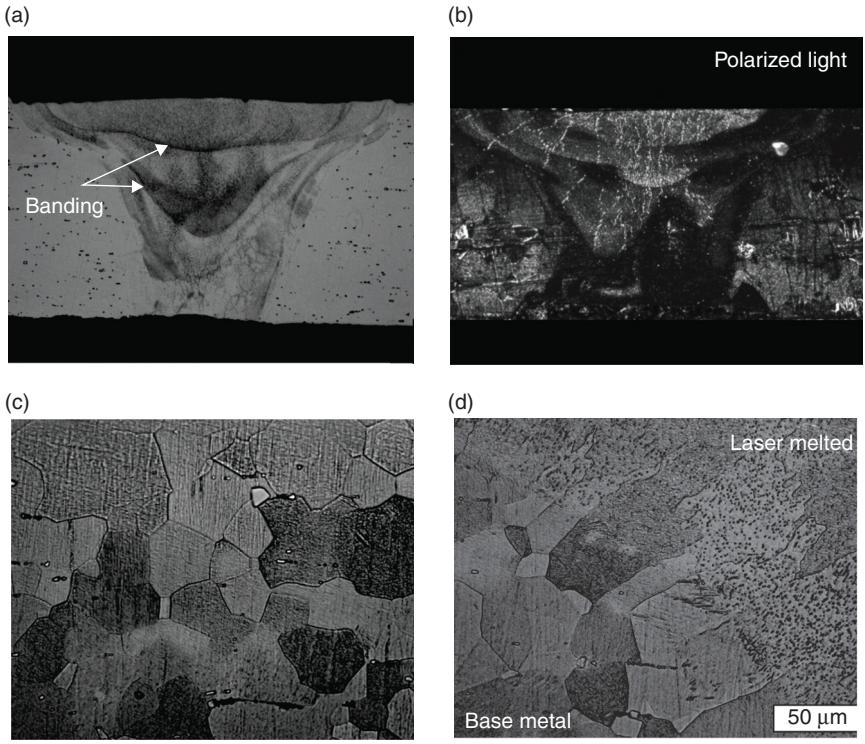


5.8 Schematic of deformation occurring in the tests presented in Fig. 5.7: (a) before straining; (b) initial plateau and (c) base metal plateau.

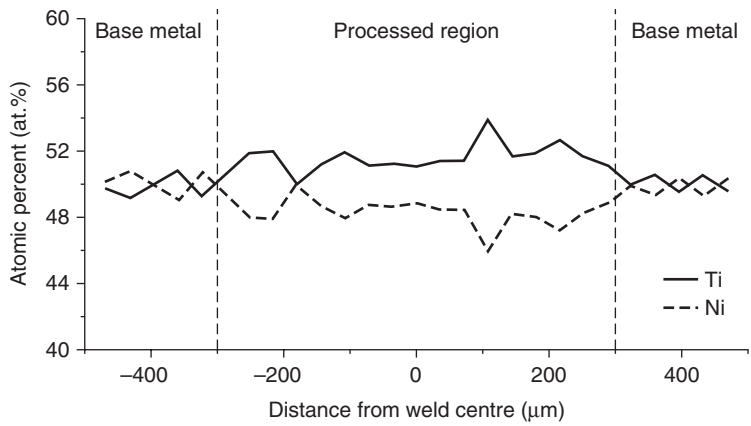
boundaries. These phenomena are observed in Fig. 5.9, which shows Optical micrographs for pulsed Nd:YAG laser-welded Nitinol. The base metal (Fig. 5.9b) consists of a homogeneous single-phase microstructure, with relatively large NiTi grains (about 20–40 μm). Similar base-metal microstructure is observed near the interface of the re-solidified fusion zone, shown in Fig. 5.9d. Columnar dendritic growth occurs along the solidification interface with finely dispersed IMC within the fusion zone. These IMCs are further defined in Fig. 5.9b where the use polarized light highlights their location.

Depending on the SMA alloy composition and welding parameters, IMCs in the weld material can be either Ti-rich (i.e. Ti_2Ni) or Ni-rich (Ni_3Ti). Ti_2Ni is an intermetallic present in the binary NiTi phase diagram (Fig. 5.2), it is most stable in Ti-rich alloys/regions. When the re-solidified material is in the Ni-rich domain, Ni-rich IMCs form (i.e. Ni_3Ti). However, the near equi-atomic composition of Nitinol coupled with ability of high power-density laser-welding processes to locally vaporize constituents, IMCs and composition in the weld metal can vary greatly. Furthermore, in NiTi alloys Ni is most susceptible to vaporization since it is most volatile, having the highest vapour pressure. An example of changes in Ni content is given in Fig. 5.10, where an energy dispersion spectrum (EDS) scan measures lower Ni concentrations in the weld metal. As such Ti-rich IMCs can become stable in Ni-rich alloys.

© Woodhead Publishing Limited, 2013

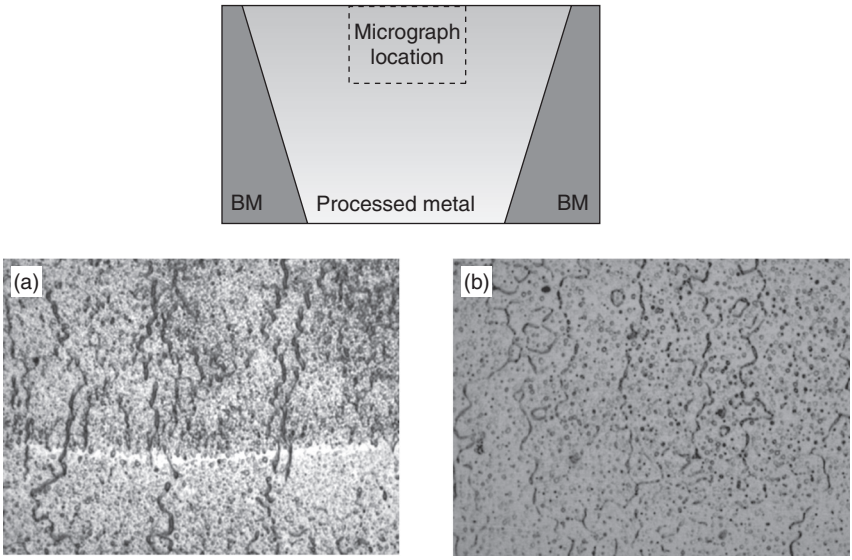


5.9 Cross-section of samples generated at 0.6 kW, 10 pps showing overall cross-section under (a) white and (b) polarized light and high magnification of (c) base material and (d) re-solidified interface.



5.10 EDS line scan across weld region.

© Woodhead Publishing Limited, 2013

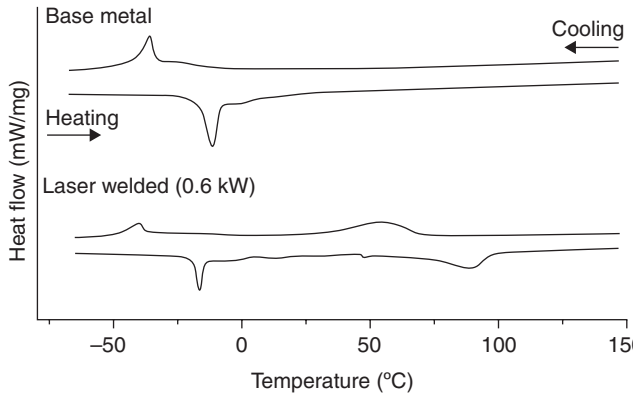


5.11 Fusion zone microstructure at the top of weld-fusion zone for (a) 0.6 kW and (b) 0.9 kW peak-power conditions. BM, base metal.

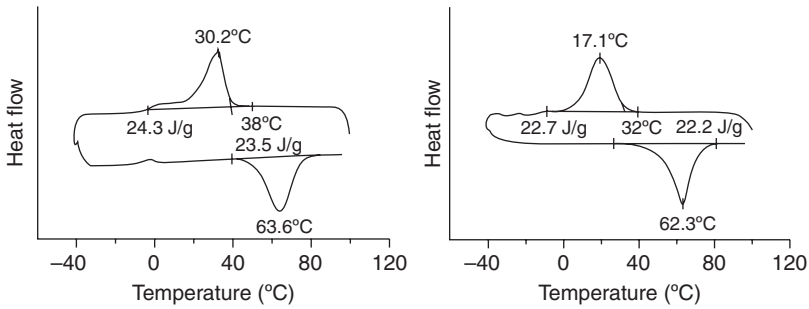
The concentration of IMC is greatly influenced by the laser-welding process parameters, which is also directly correlated to the mechanical performance. Specifically, it has been shown that high peak powers can result in reduced concentrations of IMC.[12] This can be observed in Fig. 5.11 which details the microstructures near the top of the welded region for 0.6 and 0.9 kW peak-power parameters. Each condition exhibits varying amounts of sub-micron Ti_2Ni segregation. The 0.6 kW weld shows a high density of continuous intergranular segregation compared to that of the 0.9 kW weld. These segregated phases act as preferential sites in the weld metal where failure initiates and/or propagates. As such, higher segregation concentrations may result in premature failure as observed for the 0.6 kW weld in Fig. 5.6. Specifically, the densely segregated condition observed with a peak laser power of 0.6 kW lead to premature failure, whereas with 0.9 kW the joint performed better and the weld strength surpassed the pseudoelastic plateau stress.

As a consequence of preferential Ni vaporization, the thermal properties of Nitinol are greatly affected. Sensitivity to composition change has been shown to be severe in the nickel-rich alloys, with changes of only 1 at% altering M_s temperature by as much as 250°C.[9] As Nitinol Ni content decreases with high power-density laser-welding processes, there is an increase transformation temperatures. This is observed in DSC curves shown in Fig. 5.12, where the laser-welded material exhibit a high temperature compared with base-metal phase transformation, which is primarily

© Woodhead Publishing Limited, 2013



5.12 Differential scanning calorimetry (DSC) scans for base and Nd:YAG laser-welded metal.



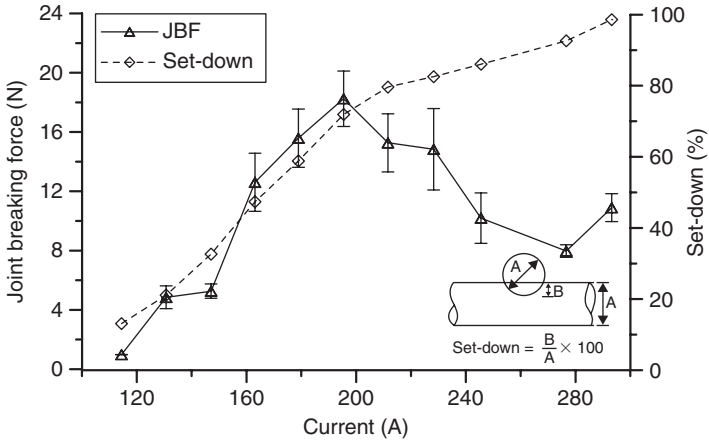
5.13 DSC scans for base (left) and CO_2 laser-welded metal (right) showing decrease in exothermic martensite phase transformation peak. (Source: With kind permission from Springer Science + Business Media: *Metallurgical Materials Transactions A*, Effects of CO_2 welding on the shape memory and corrosion characteristics of TiNI alloys, 32(3), 2001, p. 569, Hsu, Y. T., Wang, Y. R., Wu, S. K., Chen, C., Figure 4.[13])

induced by Ni vaporization. However, if power densities during laser welding are kept to a minimal and vaporization is not induced, then transformation temperature can decrease as shown in Fig. 5.13.[13] This decrease is due to the recrystallization of the microstructure, which removes transformation impeding dislocations. As such, change in weld transformation temperature must be considered in medical-device application.

5.3.2 Resistance micro-welding

Like laser welding, MRSW can affect the local functional properties of Nitinol. Modifications to base-metal transformation behaviours[15,16] and previous strengthening heat treatments[17,18] have been shown to occur during

© Woodhead Publishing Limited, 2013



5.14 Effects of welding current on joint breaking force (JBF) and set-down. (Source: With kind permission from Springer Science + Business Media: *Metallurgical Materials Transactions A*, Resistance microwelding of Ti-55.8 wt pct Ni Nitinol wires and the effects of pseudoelasticity, 43(8), 2012, p. 2969, Tam, B., Pequegnat, A., Khan, M.I., Zhou, Y., Figure 6.[14])

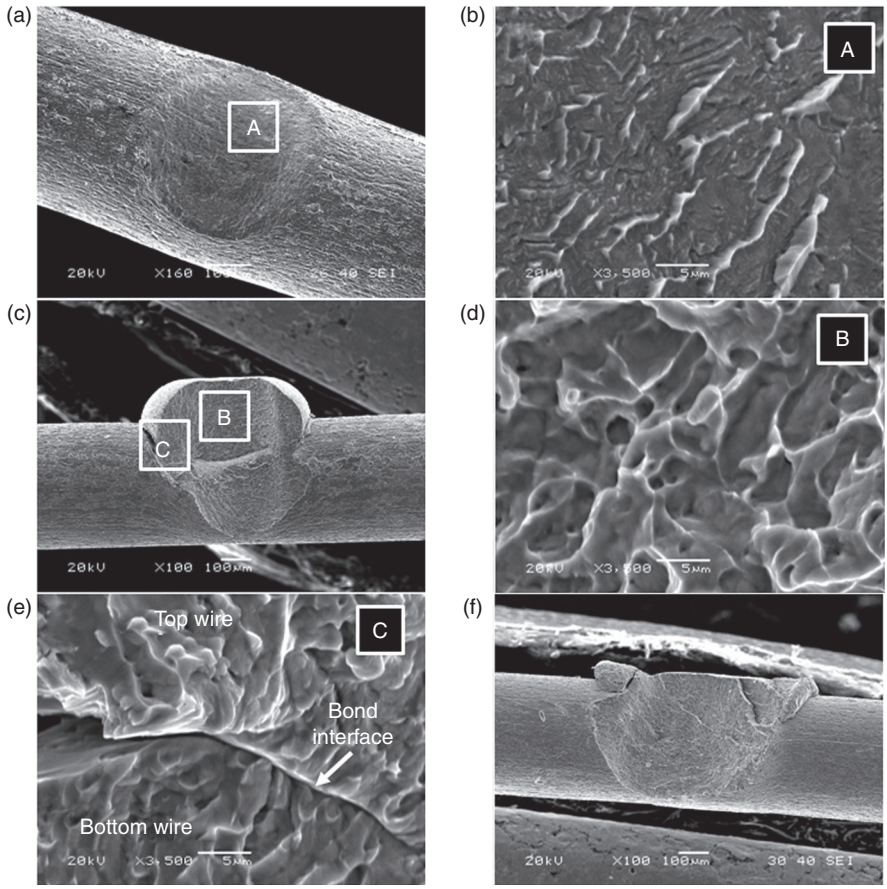
the application of thermomechanical processing. Similar thermomechanical processing is experienced during MRSW. During MRSW, metallurgical bonds form between two faying surfaces using heat generated by the resistance to passage of electric current through the workpieces. This involves the coordinated application of electric current and mechanical force of specified magnitude and duration.[19] The induced changes to Nitintol alloys must be thoroughly understood in order to refine the protocol for achieving functional welds. This section describes these effects on a crossed-wire configuration of fine Nitinol wire.

Mechanical properties and failure mechanism

Compared with the base-metal strength, MRSW welds have a considerably lower failure force, known as joint breaking force (JBF). Figure 5.14 shows the effects of welding current on JBF and set-down for MRSW of 400 μm diameter Nitinol wire.[14] Although Joint strength increases sharply with current, only a maximum JBF of 18 N was achieved with 200A current. The 18 N JBF is only a fraction of the 70 N breaking force of base metal. At higher currents, over welding and degradation to joint strength occur due to the introduction of weld defects.

Joint strength and fracture mechanism of MRSW of crossed NiTi strongly influence the weld morphology. Figure 5.15 shows the fracture surface of welds.[14] At low currents fracture occurs through the bond interface (Fig. 5.15a) in a brittle fracture mode, which is indicated by the relatively

© Woodhead Publishing Limited, 2013

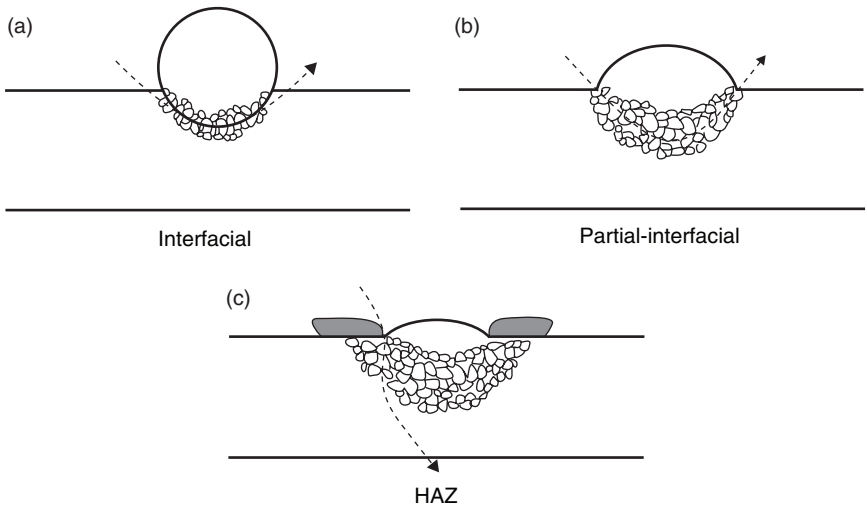


5.15 Fracture surfaces of joint welded at different welding currents: 145 A (a and b), 195 A (c to e) and 245 A (f). (Source: With kind permission from Springer Science + Business Media: *Metallurgical Materials Transactions A*, Resistance microwelding of Ti-55.8 wt pct Ni nitinol wires and the effects of pseudoelasticity, 43(8), 2012, p. 2969, Tam, B., Pequegnat, A., Khan, M.I., Zhou, Y., Figure 7.[14])

smooth surface (Fig. 5.15b). Joint strength gradually increases due to improved bond strength as set-down increases coupled with solid-state bonding. Higher currents also result in dimpled ductile fracture morphology (Fig. 5.15d). As the JBF increases due to the larger bond area the HAZ becomes increasingly softer due to recrystallization until eventually failure begins to occur in the HAZ.

Transition of fracture modes from interfacial at low currents to HAZ at high currents is schematically shown in Fig. 5.16.[14] Mixed-mode failure occurs at intermediate currents, also referred to as partial-interfacial. Increasing

© Woodhead Publishing Limited, 2013



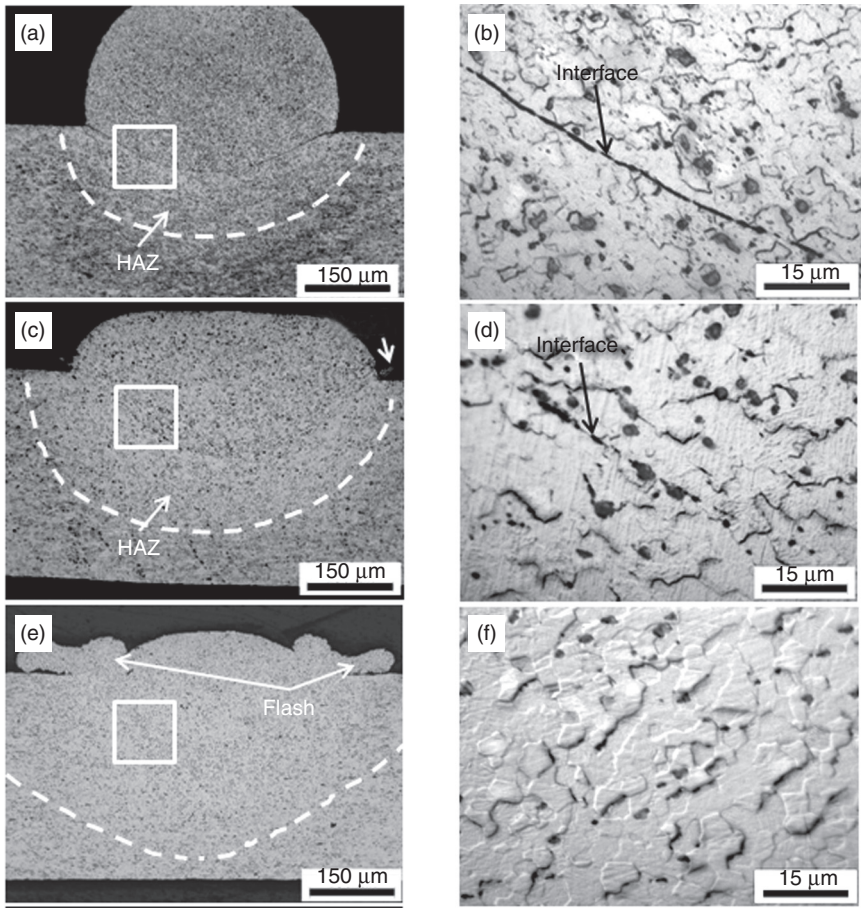
5.16 Schematic of failure modes with increasing weld current; interfacial (a), partial-interfacial (b) and HAZ (c). (Source: With kind permission from Springer Science + Business Media: *Metallurgical Materials Transactions A*, Resistance microwelding of Ti-55.8 wt pct Ni Nitinol wires and the effects of pseudoelasticity, 43(8), 2012, p. 2969, Tam, B., Pequegnat, A., Khan, M.I., Zhou, Y., Figure 9.[14])

welding current creates a competition between two counter-balancing behaviours, increased interfacial bond strength and wire softening, which improve and degrade joint strength, respectively. The sum of their effect determines the actual joint strength.[14] At low current, insufficient bonding leads to interfacial failure while at high currents; joints fail through the softer HAZ. Maximum JBFs can be achieved at intermediate welding currents when bond strength and wire softening are balanced. Although the severely reduced mechanical properties of Nitinol MRSW greatly impedes their use in structural application (i.e. stents), joint strengths are sufficient for non-load bearing applications such as electrical interconnects.

Effects of micro-resistance spot welding (MRSW) on NiTi microstructure and phase transformation

Nitinol alloys exhibiting pseudoelastic properties are thermomechanically manufactured to have a fine-grained base metal. However, heat generated at the weld interface during the initial application of current results in recrystallization and the onset of microstrcutral changes, as shown in Fig. 5.17a (HAZ outlined using dashed lines). At low currents, insufficient bonding (Fig. 5.17b) occurs due to the entrapment of surface oxides and contaminant.[14] Both base and weld metals of Nitinol often contains finely dispersed

© Woodhead Publishing Limited, 2013

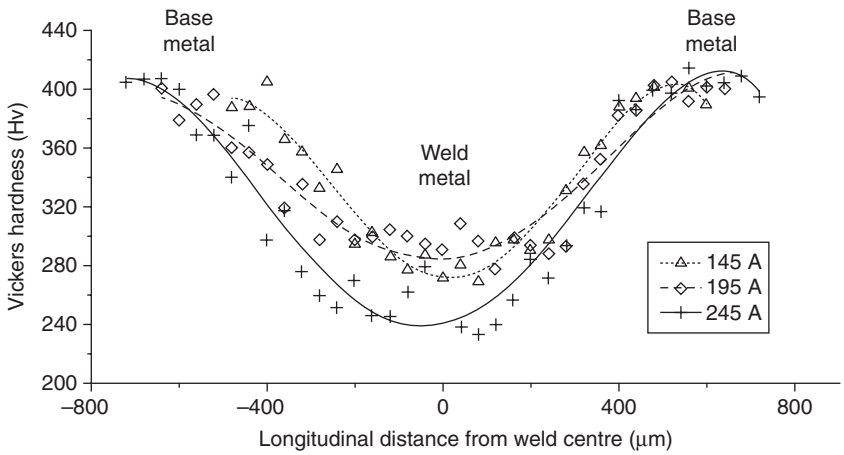


5.17 Cross-sections of joints welded at different welding currents; 145 A (a, b), 195 A (c, d) and 245 A (e, f). Heat-affected zone (HAZ) located between bond interface and dashed lines. (Source: With kind permission from Springer Science + Business Media: *Metallurgical Materials Transactions A*, Resistance microwelding of Ti-55.8 wt pct Ni Nitinol wires and the effects of pseudoelasticity, 43(8), 2012, p. 2969, Tam, B., Pequegnat, A., Khan, M.I., Zhou, Y., Figure 3.[14])

precipitates in the microstructure, which is often TiC compounds formed during the production of ingots.

As weld currents increase the HAZ widens (Fig. 5.17c). Weld microstructure undergoes grain growth at the faying surface, resulting in the partial disappearance of the bond interface (Fig. 5.17d). Squeezed out metal and surface contaminants, commonly referred to as 'flash material', is pushed to the joint periphery. This is facilitated by the combination of initial high resistance heating at the faying surface and electrode force, which melts

© Woodhead Publishing Limited, 2013



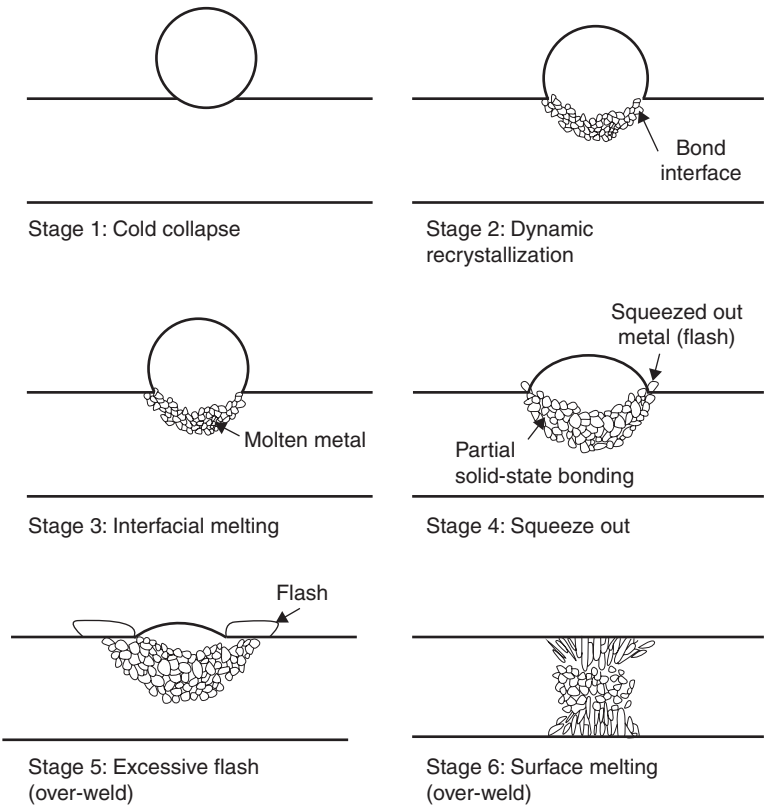
5.18 Hardness traces along cross-section of welds made using currents of 145 A, 195 A and 245 A. (Source: With kind permission from Springer Science + Business Media: *Metallurgical Materials Transactions A*, Resistance microwelding of Ti-55.8 wt pct Ni Nitinol wires and the effects of pseudoelasticity, 43(8), 2012, p. 2969, Tam, B., Pequegnat, A., Khan, M.I., Zhou, Y., Figure 5.[14])

the surface material and pushes molten surface material towards the joint periphery.[14] Weld microstructure at currents up to 245 A experience further widening of the HAZ and complete elimination of the bond interface while more flash material gets expelled (Fig. 5.17e and 5.17f).

Recrystallization and grain growth results in a drop of hardness values (softening) near the weld zones. The effects of current on weld hardness are shown in Fig. 5.18.[14] Softening become more pronounced at the interface as higher currents are applied and more heat is generated.

The primary joining mechanism for MRSW of crossed Nitinol wires is solid state, similar to Ni and 304 SS crossed-wires.[20,21] The MRSW of Nitinol process can be summarized in six main stages, shown schematically in Fig. 5.19.[14] The initial stage 1 'cold collapse' describes the mechanical deformation imposed by the electrode force, from which a larger contact area was formed. Subsequent application of welding current increases temperature at the interface, resulting in 'dynamic recrystallization' (stage 2) of the fine-grained base-metal microstructure and softening in the HAZ. As peak temperatures surpass the solidus temperature at the interface, 'interfacial melting' (stage 3) occurs, followed by stage 4 'squeeze out' where the electrode force pushes the partially molten metal towards the weld perimeter. This stage is necessary for good solid-state bonding as contaminants are removed from the junction, improving surface conditions for crystallographic matching and interdiffusion of atoms across the interface.[14] The large amount of expulsion with increasing welding currents is referred to

© Woodhead Publishing Limited, 2013



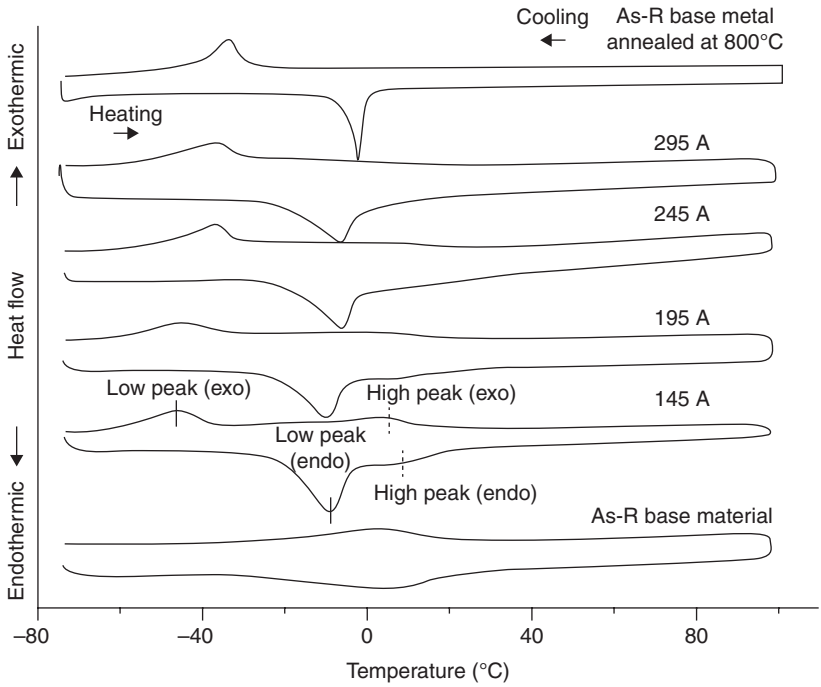
5.19 Main stages of the bonding mechanism of MRSW of crossed NiTi wires.

as stage 5 'excessive flash', which introduces undesired defects in the weld metal. Further increase in currents induces melting of the wire surfaces (stage 6 'surface melting') and sticking of welds to the electrodes, which can significantly affect weld quality and shorten electrode life.[19]

The intrinsic phase transformation behaviour of Nitinol is strongly influenced by thermomechanical processing. DSC curves for as-received, heat-treated base materials and welds produced at select weld currents are shown in Fig. 5.20.[14] Like LMW, RMW weld metal experiences different transformations. Residual base-metal accounts for the high-temperature peaks, which has similar transformation temperatures to the base material. On the other hand, weld-metal transformation occurs at lower temperatures, much like laser welds that have not experienced significant Ni vaporization. Increasing welding currents has little effect on the weld transformation temperatures.

Nitinol is known to exhibit broad temperature peaks when mechanically strained and narrow when fully annealed to its intrinsic state[15–18]

© Woodhead Publishing Limited, 2013



5.20 DSC heating and cooling curves of annealed wire, as-received wire (As-R) and weld made using various currents. (Source: With kind permission from Springer Science + Business Media: *Metallurgical Materials Transactions A*, Resistance microwelding of Ti-55.8 wt pct Ni Nitinol wires and the effects of pseudoelasticity, 43(8), 2012, p. 2969, Tam, B., Pequegnat, A., Khan, M.I., Zhou, Y., Figure 10.[14])

as observed in Fig. 5.20. Cold working results in higher transformation temperatures, since higher activation energy is required to overcome the internal stress induced by random dislocations.[15,17,18] Annealing previously thermomechanically processes base-metal reduces transformation temperatures. Similarly, during welding the high-temperature workpieces experience resetting of the effects of previous thermomechanical processing and return the material to near fully annealed state. A higher degree of base-metal annealing occurs at a higher welding current, which results in a more defined temperature peaks.

5.4 Future trends

Shape-memory alloys are complex materials which require a thorough understanding prior to being properly implemented in medical devices. Thus far, these alloys have been successfully applied in numerous medical devices and have been increasingly sought after due to their excellent

© Woodhead Publishing Limited, 2013

biocompatibility and unique functional properties. As the fundamental material knowledge base continues to spread, so will application in medical (and non-medical) devices. Welding has been a key restriction when implementing SMAs and, as joint complexity increases, these challenges will need to be resolved. Hence advances in SMA-welding techniques, such as refining process parameters and developing new filler materials, will continue for application-specific needs.

5.5 Conclusion

This chapter has shown that welding significantly impacts on the phase transformation behaviour of Nitinol. Specifically, two welding processes have been examined, including LMW and RMW. Local vaporization experienced during laser welding alters the local microstructure from austenite to martensite phase, reducing the mechanical strength. In contrast, resistance heating from the resistance-welding process anneals the original base metal, producing a HAZ that mimics solid-state solution treatment. These local modifications in the weld zones can adversely affect the functional properties of Nitinol and need to be considered in applications where RMW is implemented.

5.6 References

1. Lin, H.C. and Wu, S.K. (1994) Tensile behavior of a cold-rolled and reverse-transformed equiatomic TiNi alloy. *Acta Metallurgica et Materialia*. **42**(5): 1623.
2. Shabalovskaya, S.A. (1995) Proc. ICOMAT 95, *J. Phys. IV*. **C8**: 1199.
3. Shüßler, A. (1997) Micro-machining and joining of NiTi-alloys using Nd:YAG lasers: status and prospects. Proceedings of the second international conference on Shape Memory and Superelastic Technologies (SMST-97), Pacific Grove, CA.
4. Yan, X.J., Yang, D.Z. and Qi, M. (2006) Rotating–bending fatigue of a laser-welded superelastic NiTi alloy wire. *Mater. Charact*. **57**: 58.
5. Buehler, W.J., Gilfrich, J.W. and Wiley, R.C. (1963) Effect of low-temperature phase changes on the mechanical properties of alloys near composition NiTi. *J. Appl. Phys*. **34**: 1475.
6. Chang, L.C. and Read, T.A. (1951) Plastic deformation and diffusion-less phase changes in metals – the gold-cadmium beta phase. *Trans. AIME* **189**: 47.
7. Basinski, Z.S. and Christian, J.W. (1954) Crystallography of deformation by twin boundary movements in indium-thallium alloys. *Acta. Metall*. **2**: 101.
8. Massalski, T.B., Okamoto, H., Subramanian, P.R. and Kacprzak, L., eds (1990) *Binary Alloy Phase Diagrams*, 2nd edn, vol. 3. Materials Park, OH: ASM International, p. 2874.
9. Otsuka, K. and Ren, X. (2005) Physical metallurgy of Ti–Ni-based shape memory alloys. *Prog. Mater. Sci*. **50**(5): 511.

© Woodhead Publishing Limited, 2013

10. Van Humbeeck, J. (2001) Shape memory alloys: a material and a technology. *Adv. Eng. Mater*. **3**(11): 837.
11. Khan, M.I. and Zhou, Y. *Microjoining in Medical Components and Devices*. ASM Handbook, Volume 23, Materials for Medical Devices. 2012, ASM International, Materials Park, Ohio, USA.
12. Khan, M.I., Panda, S.K. and Zhou, Y. (2008) Effects of welding parameters on the mechanical performance of laser welded Nitinol. *Mater. Trans*. **49**(11): 2702.
13. Hsu, Y.T., Wang, Y.R., Wu, S.K. and Chen, C. (2001) Effects of CO_2 welding on the shape memory and corrosion characteristics of TiNI alloys. *Metal. Mater. Trans. A*. **32A**(3): 569.
14. Tam, B., Pequegnat, A., Khan, M.I. and Zhou, Y. (2012) Resistance microwelding of Ti-55.8 wt pct Ni Nitinol wires and the effects of pseudoelasticity. *Metal. Mater. Trans*. **43**(8): 2969.
15. Kuita, K., Matsumoto, H. and Abe, H. (2004) Transformation behavior in rolled Nitinol, *J. Alloys Comp*. **381**: 158.
16. Frick, C.P., Ortega, A.M., Tyber, J., Maksound, A.El.M., Maier, H.J., Liu, Y. and Gall, K. (2005) Thermal processing of polycrystalline Nitinol shape memory alloys. *Mater. Sci. Eng. A*. **405**: 34.
17. Miller, D.A. and Lagoudas, D.C. (2001) Influence of cold work and heat treatment on the shape memory effect and plastic strain development of NiTi. *Mater. Sci. Eng. A*. **308**: 161.
18. Matsumoto, H. (1993) Transformation behaviour of NiTi in relation to thermal cycling and deformation. *Physica B*. **190**: 115.
19. Thornton, P.H., Krause, A.R. and Davies, R.G. (1996) Contact resistances in spot welding. *Weld. Res. Suppl*. **75**(12): 402.
20. Fukumoto, S., Tsubakino, H. and Zhou, Y. (2006) Heat input and deformation control in resistance microwelding of fine nickel wires. *Weld. Int*. **20**(9): 692.
21. Fukumoto, S., Matsuo, T., Tsubakino, H. and Yamamoto, A. (2007) Resistance microwelding of SUS304 stainless steel fine wires. *Mater. Trans*. **48**(4): 813.

© Woodhead Publishing Limited, 2013

6

Joining of platinum (Pt) alloy wires to stainless steel wires for electronic medical devices

A. PEQUEGNAT and Y. ZHOU,
University of Waterloo, Canada

DOI: 10.1533/9780857096425.2.154

Abstract: The joining of dissimilar materials in medical-device applications is necessary to increase flexibility in design, enhance performance, and reduce material costs. This chapter will discuss the joining of platinum alloy wires to stainless steel wires in the crossed-wire joint configuration, providing a solid introduction to the challenges that accompany the joining of dissimilar materials in non-standard joint geometries. Example studies utilizing the resistance microwelding and laser microwelding processes are provided along with the process conditions required to produce sound joints.

Key words: dissimilar materials joining, platinum (Pt) alloy, stainless steel (SS) alloy, resistance microwelding (RMW), laser microwelding (LMW), crossed-wire joint configuration.

6.1 Introduction

The microwelding of dissimilar crossed-wire materials is becoming increasingly important for making electrical interconnections in medical devices.[1,2] Joining dissimilar materials allows for more flexibility in design, enhanced performance, and reduction in material costs. For example, the joining of platinum (Pt) alloys to stainless steel (SS) is necessary to reduce costs by using less Pt material as well as utilizing the excellent corrosion resistance, electrical properties, and biocompatibility of Pt alloys along with the superior mechanical properties of SS. Some common applications where Pt alloys require joining to SS alloys can be found in medical devices such as pacemakers, defibrillators, and cochlear implants, where Pt alloys are commonly used for electrodes and battery/capacitor feed through terminals which require joining to SS wire leads.[3,4] Dissimilar-materials joining and the crossed-wire configuration, however, pose several welding-related challenges, all of which are commonly experienced in the manufacturing of medical devices. Two of the most common microwelding processes used in the welding of medical

© Woodhead Publishing Limited, 2013

Table 6.1 Material properties (annealed condition)

Material	Ultimate tensile strength (MPa)	Melting point (K)	Thermal conductivity (W/(m·K))	Electrical resistivity (Ω·cm)
303 SS	620	1673–1693	16.2	7.2×10^{-5}
304 SS	505	1673–1728	16.2	7.2×10^{-5}
316 LVM SS	620	1643–1673	16.3	7.4×10^{-5}
Pt	125–165	2042	69.1	1.06×10^{-5}
Pt-10% Ir	380	2063	31	2.5×10^{-5}
Pt-20% Ir	690	2098	–	3.1×10^{-5}

LVM – low-carbon vacuum melted.

devices include resistance microwelding (RMW) and laser microwelding (LMW). In this chapter, both RMW and LMW of Pt alloy wires to stainless steel (SS) wires are discussed. Typical joint morphology with respect to welding parameters will be outlined along with the techniques and parameter sets used to obtain sound dissimilar crossed-wire joints.

6.2 Material properties

Materials used in medical-device applications are required to be tough, durable, corrosion resistant, and, most importantly, biocompatible. Failure to meet these requirements can cause serious harm to the patient, the need for corrective surgery, or even death. Pt alloys (i.e., commercially pure Pt, Pt-Ir, etc.) and SS alloys (i.e., 303, 304, 316, etc.) have been extensively used in the medical industry for many different applications ranging from microelectronic connections in pacemakers to surgical tools.[5,7,8] Material properties of the most common Pt and SS alloys used in the medical industry are given in Table 6.1 for aid in discussion.

Platinum and its alloys are well suited for medical applications due to excellent biocompatibility and mechanical properties. Platinum is classified as a noble metal, meaning it is resistant to both corrosion and oxidation. Hypoallergenic reactions to Pt alloys are rare and they have been long proven as passive-type biomaterials, making them ideal for both temporary and permanent implantation applications.[5,6] Platinum also has excellent processability where it can be easily fabricated into very small and complex components. Platinum is often alloyed with iridium (Ir) in order to improve the mechanical properties of the material such as tensile strength.[9] The major drawback to Pt alloys is high cost because Pt is a precious metal. For this reason many medical applications are exploring new biomaterials and designs to limit the amount of Pt used in order to reduce material costs.

Austenitic stainless-steel (SS) alloys are commonly used in medical applications and have been considered the baseline for implantable

© Woodhead Publishing Limited, 2013

medical-device materials. Stainless steel has a relatively low cost compared with other biocompatible metals, excellent mechanical properties, good corrosion resistance and excellent processability.[9] The corrosion and oxidation resistance of SS alloys are attributed to a passive Cr oxide layer on the surface of the material. Stainless steel does, however, still have the tendency to corrode in the human body due to being exposed to complicated aggressive fluids containing chloride ions and amino acids, as well as cells and proteins, causing the Cr oxide layer to locally break down.[9,10] The release of Ni ions into the body during the corrosion of SS alloys is undesirable since they are known to be toxic and can cause hypoallergenic reactions.[8,10]

6.3 Material challenges in joining

In materials joining the ultimate goal is to join two components where the joint has the same properties as the base material and the base-material properties are not affected by the joining process. This, however, would be an ideal situation and unfortunately is generally not feasible. In this section the effects of heat input on base-material properties along with the challenges associated with dissimilar material joining of Pt and SS alloys are discussed.

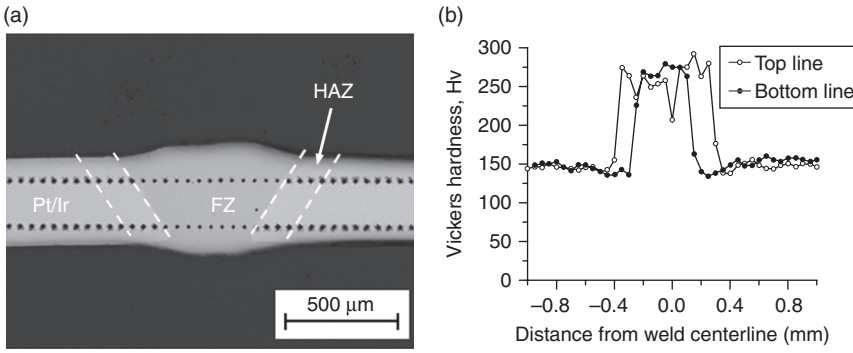
6.3.1 Effects of material properties on joint formation

The electrical and thermal properties of the dissimilar materials play a large role in the joint formation during microwelding. Pt alloys and SS alloys have significantly different thermal and electrical properties which lead to complications during both RMW and LMW, as will be discussed in more detail in subsequent sections. For example the difference in liquidous temperatures between Pt-10% Ir and 316 LVM SS is approximately 200–300 K and thermal conductivity of Pt-10% Ir is four times greater. This means the applied heat during welding will dissipate faster in the Pt alloy making the SS alloy even more susceptible to melting. Hence, these differences in material properties will play a large role in the bonding mechanism and must be taken into account prior to selecting joining process steps and joint geometry.

6.3.2 Thermal effects on base materials

Material properties can be altered during microwelding which can degrade the properties of the base material (BM) obtained through previous material-processing steps. Changes in material properties are attributed to the thermal cycles experienced during welding. Peak temperatures reached during the joining process can induce diffusion leading to the production of

© Woodhead Publishing Limited, 2013



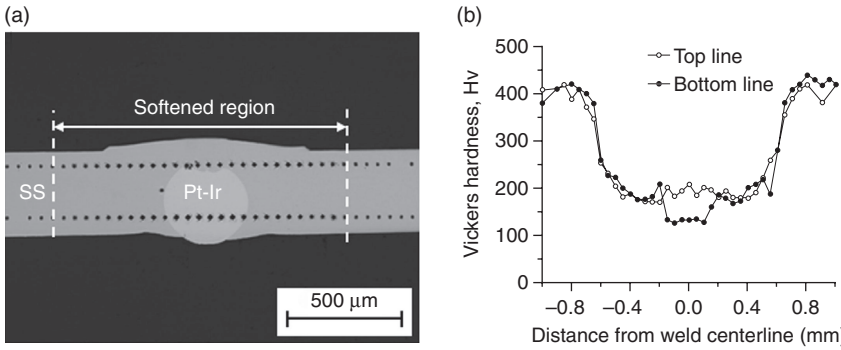
6.1 Microhardness tests performed on 0.39 kW LMW joint cross-sectioned along the Pt–Ir wire axis direction; (a) optical image of sample and (b) Vickers hardness results. With kind permission from Springer Science+Business Media: *Metallurgical Materials Transactions A*, Crossed-wire laser microwelding of Pt-10 pct Ir to 316 low-carbon vacuum melted stainless steel: Part I. Mechanism of joint formation, 43(4), 2012, p. 1223, G. S. Zou, Y. D. Huang, A. Pequegnat, X. G. Li, M. I. Khan, Y. Zhou, Figure 12.

different phases or cause recrystallization and growth of grains altering the prior base-metal microstructure. The final microstructure is usually softer and can have substantially different mechanical properties when compared with the unaffected BM. In joining Pt to SS crossed-wires changes in microstructure in the heat-affected zone (HAZ) adjacent to the crossed-wire joint can decrease the material strength by destroying the cold-worked structure obtained during the wire-drawing process. Khan *et al*.[11,12] showed a reduction in hardness and therefore strength in the HAZ of 316 LVM SS crossed-wire RMW and LMW welds. This reduction in strength leads to the fracture of the joint through the HAZ during tensile testing. Zou *et al*.[13] showed similar HAZ softening in the LMW of Pt-10% Ir to 316 LVM SS crossed-wires as shown in Figs 6.1 and 6.2. However, the Pt-10% Ir wire was in the annealed condition before welding therefore the decrease in Vickers hardness was not nearly as pronounced in the HAZ. Also, note the solidification structure in the fusion zone (FZ) which contains both Pt-Ir and SS has higher hardness than the Pt BM.

6.3.3 Effects of intermetallics formation

In joining dissimilar-materials, defects in the welded joint such as cracking, porosity, and intermetallic compounds (IMCs) are more likely to occur due to mixing of different elements either by diffusion or in the molten weld pool.[17] Intermetallics are notoriously brittle and are often cited as

© Woodhead Publishing Limited, 2013



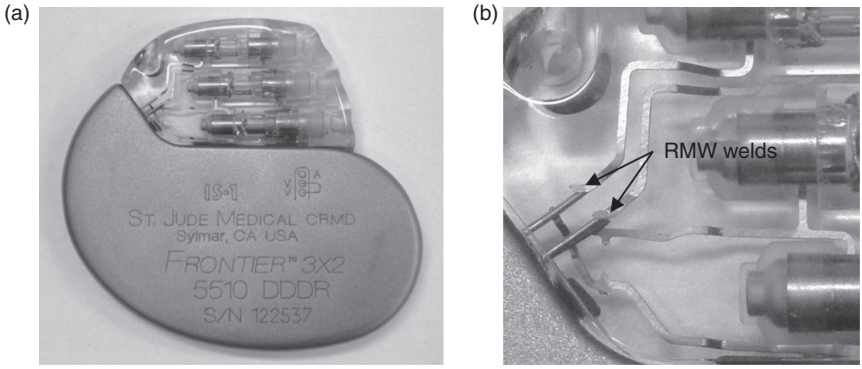
6.2 Microhardness tests performed on 0.35 kW LMW joint cross-sectioned along the SS wire axis direction; (a) optical image of sample and (b) Vickers hardness results. With kind permission from Springer Science+Business Media: *Metallurgical Materials Transactions A*, Crossed-wire laser microwelding of Pt-10 pct Ir to 316 low-carbon vacuum melted stainless steel: Part I. Mechanism of joint formation, 43(4), 2012, p. 1223, G. S. Zou, Y. D. Huang, A. Pequegnat, X. G. Li, M. I. Khan, Y. Zhou, Figure 13.

the limiting factor when considering maximum joint strength in dissimilar welds. For example, in laser welding dissimilar Pt and Ti materials, brittle IMCs (i.e., Ti_3Pt_5, $TiPt_3$ and Ti_3Pt) could not be avoided and were attributed to cracking in the joint.[17,18] In joining Pt to SS there are also several possible IMC compounds that can be identified from phase diagrams.[19] However, these IMCs were not found to play a large role in joint strength. Chen *et al.*[20] observed the RMW joint between 316L SS blocks and Pt wires failing in the Pt wire rather than through regions at the joint interface where IMC compounds reside. Also, in work by Zou *et al.*[13] and Huang *et al.*[15,16] LMW and RMW crossed-wire joints between Pt-10% Ir and 316 LVM SS wires were found to fail in the Pt-10% Ir wire at the maximum achievable JBF. Therefore, in the joining of Pt and SS alloys IMCs are likely present but do not significantly degrade joint strength.

6.3.4 Effects of welding on corrosion resistance

The corrosion-resistant properties of SS that are vital for implantable device applications can also be affected in the HAZ. Welding SS alloys increases the susceptibility of corrosion in Austenetic SS alloys by weld decay where the grain boundaries adjacent to the weld can become depleted of Cr and corrosion can occur more easily.[14] Therefore, the amount of heat produced in the joint must be limited in order not to alter the corrosion resistance of the SS base material. Low-carbon steels such as 316 LVM are often used in

© Woodhead Publishing Limited, 2013



6.3 Welded joints between feed through terminals and lead connector ribbons in pacemakers are shielded from the body using epoxy: (a) pacemaker and (b) welded joints covered in epoxy.

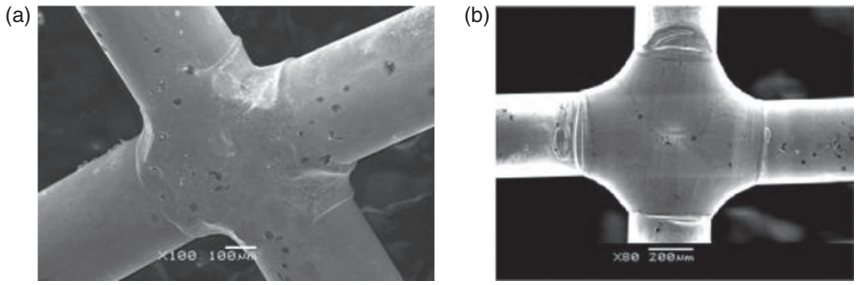
medical applications to reduce the susceptibility of forming Cr carbides and therefore weld decay.

In joining dissimilar materials such as Pt alloys to SS alloys a galvanic couple is also created at the joint. In an implantable medical device the joint must therefore be shielded from the corrosive environment in the body usually by encapsulation in epoxy or hermetic sealing in a titanium can. Figure 6.3 shows a pacemaker where epoxy is used to seal RMW joints between lead connector ribbons and feed through terminals. The galvanic couple between Pt-10% Ir and 316 LVM SS wires prevented etching of joint metallographic cross-sections in References 13, 15, and 16 where extensive pitting of the 316 LVM SS wire material could not be avoided. This further highlights the importance of considering corrosion resistance when joining dissimilar materials such as Pt and SS.

6.4 The crossed-wire joint

In medical applications many different joint geometries are necessary to achieve the required flexibility in design. The crossed-wire joint geometry is most commonly used for electrical connections in medical devices or for structural members including coronary stents.[1,21] Example RMW and LMW 316 LVM SS crossed-wire welds are shown in Fig. 6.4.[11,12] Several researchers have investigated the microwelding of thin (i.e., 200–500 μm) crossed-wires using both RMW[11,21–25] and LMW[12,26] for various different materials. However, the focus has been predominantly on joining similar materials with the exception of Zou *et al*.[13] and Huang *et al*.[15,16] who focus on the dissimilar crossed-wire joining of Pt-10% Ir and 316 LVM SS. A brief

© Woodhead Publishing Limited, 2013



6.4 (a) SEM image of 316 LVM crossed wire RMW joint (With kind permission from Springer Science+Business Media: *Metallurgical Materials Transactions A*, Bonding mechanisms in resistance microwelding of 316 low-carbon vacuum melted stainless steel wires, 40(A), 2009, p. 910, M. I. Khan, J. M. Kim, M. L. Kuntz, Y. Zhou, Figure 15a). (b) SEM image of 316 LVM crossed wire LMW joint. (Reprint with permission of ASM International. All rights reserved. www.asminternational.org.)

summary of several past crossed-wire microwelding studies is provided in Table 6.2.

6.4.1 Joint-quality characterization

The crossed-wire joint is characterized by its geometry, appearance, and strength. First the joint is inspected for defects such as surface pores, weld spatter, cracks, notches, contamination (i.e., by electrode in RMW), or necking. Poor surface quality is unacceptable in medical-device applications due to a reduction in joint reliability and the possibility of electrical shorts, uneven current transport through the joint, contamination, or even damage to living tissue. The surface quality is usually assessed by either optical microscopy or scanning electron microscopy (SEM). Weld cross-sections are also observed to identify hidden defects inside the joint itself. Some of these defects include internal pores and cracks.

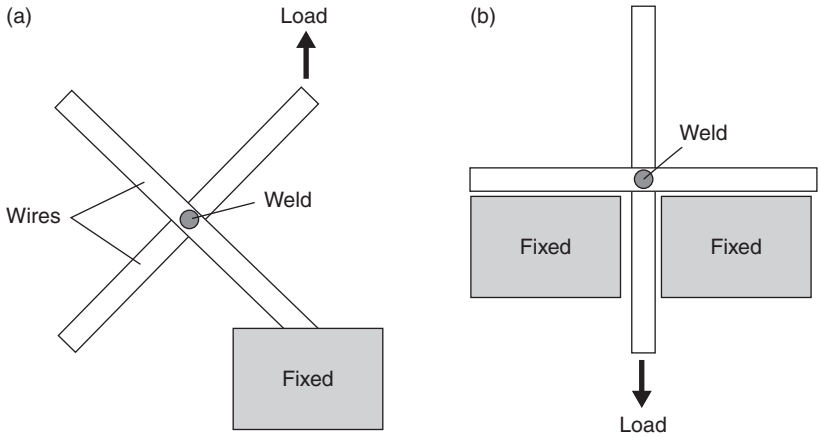
Defects such as porosity, cracks, necking, or notches reduce the integrity of the joint in both maximum strength and fatigue performance. The strength of crossed-wire joints is commonly measured by tensile testing where the joint is subject to a tensile shear loading condition until failure occurs. The force at which the crossed-wire joint fails has been termed joint breaking force (JBF). The two most common methods for measuring the JBF are illustrated in Fig. 6.5. The 45° tensile-test method is harsher since it adds a bending stress to the wires putting additional strain on the crossed-wire joint.

© Woodhead Publishing Limited, 2013

Table 6.2 Summary of previous crossed-wire microwelding studies

Materials	Process	Maximum JBF (N)	Bonding mechanisms	Notes	Reference
0.38 mm diameter 316 LVM SS wire	RMW	78.5	Solid state or fusion	• Bonding mechanism transitions from solid-state to fusion welding with increasing heat input	11
0.4 mm diameter 304SUS wire	RMW	~120	Solid state	• Transient liquid layer at interface expelled as flash leading to solid-state joint	23
0.4 mm diameter Ni200 wire	RMW	~57	Solid state	• Used lower firing force to cause surface melting • Higher welding force pushed liquid away from faying interface creating solid-state joint	21
0.4 mm diameter Au plated Ni200 wire	RMW	~59	Braze, braze + solid state or solid state + fusion	• Bonding mechanism transitions from braze to a combination of solid state and fusion with increasing current • Low melting point Au and Ni solution leads to braze	22
0.34 mm diameter NiTi wire	RMW	58.8	Solid state	• Melting at faying surface lead to production of flash and improved solid-state joining	24
0.41 mm diameter NiTi wire	RMW	18	Solid state	• Only solid-state welding was possible without severe electrode sticking • Heat input during welding alters base-material properties	25
0.38 mm diameter 316 LVM SS and Pt-10% Ir wire	RMW	37.4	Braze or braze + fusion	• Dissimilar-material joint • Bonding mechanism transitioned from braze to a braze/fusion combination with increasing heat input	16
0.41 mm diameter NiTi wire	LMW	120	Fusion	• Fusion-bonding mechanism was observed	26
0.38 mm diameter 316 LVM SS wire	LMW	70	Fusion	• Only fusion welding was possible • Heat input during welding alters base material	12
0.38 mm diameter 316 LVM SS and Pt-10% Ir wire	LMW	38.5	Braze, braze + fusion or fusion	• Dissimilar-material joint • Bonding mechanism transitioned from braze to fusion weld with increasing laser peak power	13

© Woodhead Publishing Limited, 2013



6.5 Most common methods for measuring JBF of crossed-wire welds using a tensile tester: (a) 45° method and (b) simple tensile shear method.[21,24]

6.5 Joining processes

As previously mentioned the most common welding processes used for joining metals in the medical industry are RMW and LMW. Both of these methods are capable of producing crossed-wire joints between the dissimilar Pt and SS alloys. In this section the RMW and LMW joining processes will be introduced and the specific challenges in joining Pt to SS crossed-wires will be addressed. The bonding mechanisms with respect to welding parameters will be outlined along with the techniques and parameter sets used to obtain sound dissimilar crossed-wire joints.

6.5.1 Resistance microwelding (RMW)

Resistance microwelding is widely used in the medical industry since it is an economical process that offers excellent reliability and productivity with relatively low capital costs.[2] There are major differences in RMW compared with large-scale resistance spot welding (LSRSW). Some of these differences include substantially lower welding forces and currents, non-ferrous materials are often welded, electrode cooling is not possible and much faster cooling rates exist.[2,27–29] Zhou *et al*.[27] and Ely and Zhou[29] were among the first to investigate the differences in RMW compared with LSRSW and outline the recommended process parameters to join thin Al, brass, Cu, Kovar, steel, and Ni sheets. Many investigations into the bonding mechanism and dynamic resistance during the RMW of similar non-ferrous thin sheets and fine wires have since been performed.[11–13,15,16,21–26,30–34]

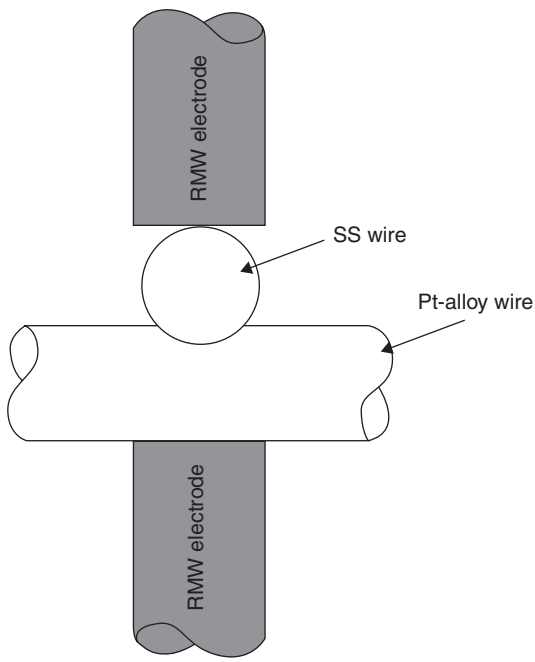
© Woodhead Publishing Limited, 2013

In the RMW process the heat required to form a joint between two metals is generated by resistive heating. The heat generated during the RMW process can be approximated by the following equation:

$$Q = I^2 Rt$$

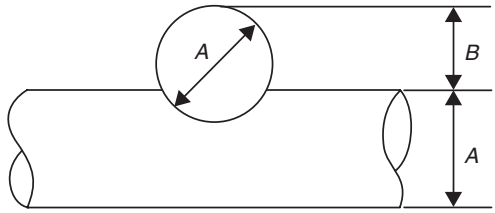
where the current (I) and the time (t) are controlled variables of the RMW process.[35] The resistance (R) is the sum of the contact resistance at the electrode/wire interfaces, the wire/wire interface and the bulk resistances of the base materials. A schematic illustration of RMW crossed-wire joining is shown in Fig. 6.6. Crossed-wire welding is often compared to projection welding since the contact area between the two wires is very dynamic, meaning it changes drastically throughout the welding process.[36] The balance between applied electrode force which directly influences the contact area at the faying interface and the welding current is therefore very critical in generating the correct amount of heat to create a sound joint. The increase in joint area during welding can be quantified by calculating the percent setdown with the following equation:

$$\text{Setdown} = \frac{A - B}{A} \times 100\%$$



6.6 Schematic illustration of the crossed-wire RMW process.[16]

© Woodhead Publishing Limited, 2013



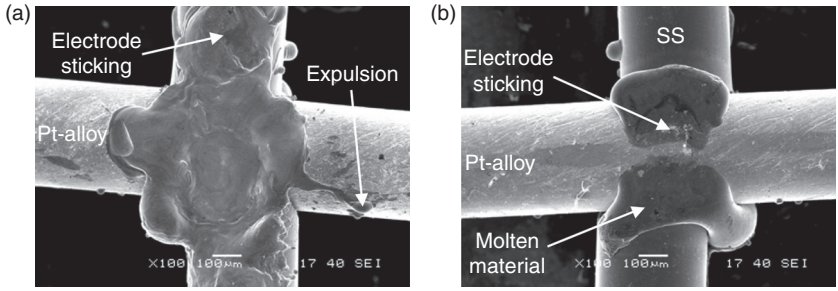
6.7 Schematic illustration of setdown in crossed-wire joining. (With kind permission from Springer Science+Business Media: *Metallurgical Materials Transactions A*, Mechanism of resistance microwelding of crossed fine Nickel wires, 35A, 2004, p. 3165, S. Fukumoto, Y. Zhou, Figure 3(b).)

where A and B are defined in Fig. 6.7.[21] In crossed-wire RMW the JBF increases with setdown because of an increase in joint area that results from higher heat input. However, once the heat input reaches a certain threshold a softening in the HAZ has been found to take over.[21] Therefore, increasing heat input leads to a competition between two counterbalancing phenomena, increasing interfacial bond strength and wire softening, which improve and degrade joint strength respectively. The sum of their effects determines the actual joint strength.[25]

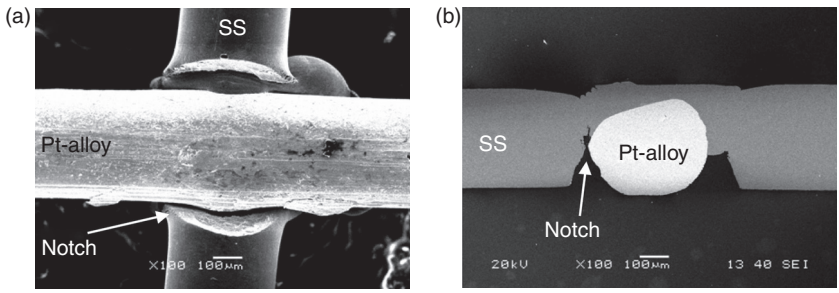
During RMW of dissimilar material crossed-wires the main challenges arise from the difference in electrical resistivity, melting temperature, and thermal conductivity.[12,16,20] Chen[20] found that the current required for melting Pt is approximately seven times greater than that required to melt SS. This means at a fixed weld current and weld time, the volume of melted SS produced is around seven times greater than that of melted Pt.[20] During the RMW welding of Pt-10% Ir and SS wire defects such as weld spatter, electrode sticking, and the formation of notches in the SS wire all result from the dissimilar material properties of the two wire materials leading to unbalanced heating. Unbalanced heating shifts the location of maximum heat generation away from the desired location, the faying interface between the two wires.

At low welding forces (i.e., <3 kgf) Huang *et al.*[16] observed excessive expulsion and electrode sticking when joining Pt-10% Ir and 316 LVM SS wires as shown in Fig. 6.8. The excessive melting of the SS wire at the electrode/wire interface causes this expulsion and electrode sticking. At higher electrode forces (i.e., >3 kgf) the process window for welding currents was found to increase as a result of cold deformation increasing the contact area of the faying and electrode/wire interfaces. Higher electrode forces help avoid expulsion and electrode sticking; however, due to the crossed-wire geometry, softening of the SS wire and high electrode force, a notch in the SS wire was formed as shown in Fig. 6.9a and 6.9b.[16] The JBF measured

© Woodhead Publishing Limited, 2013



6.8 Top (a) and bottom (b) view of RMW crossed-wire joints made between Pt-10% Ir and 316 LVM SS welded with electrode force of 1 kgf and current of 200 A. Electrode sticking and expulsion observed as a result of excessive melting of the SS wire.[16] Reproduced with permission of Maney Publishing, Science and Technology of Welding and Joining, www.maneypublishing.com/journals/stw.



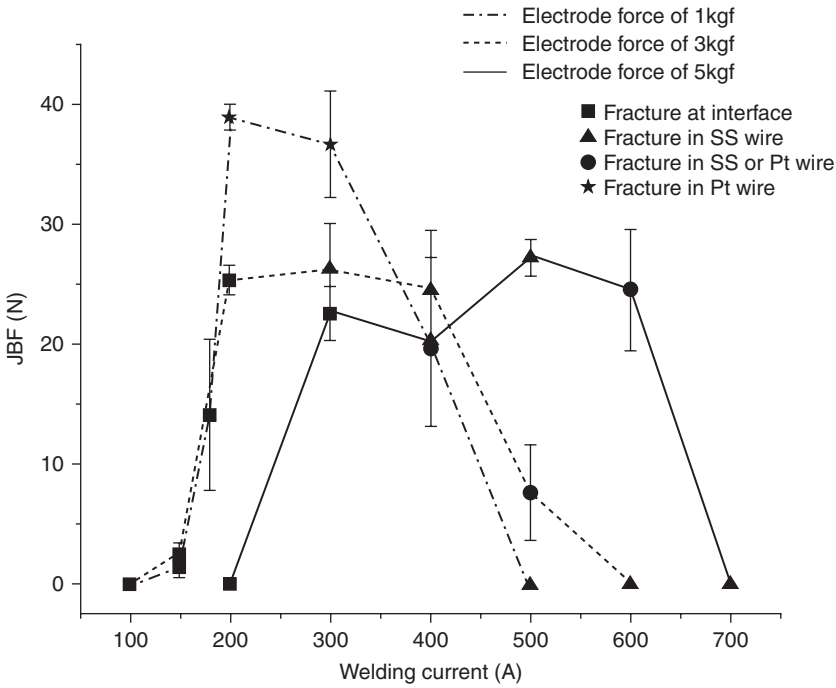
6.9 SEM images of RMW crossed-wire joints made between Pt-10% Ir and 316 LVM SS welded with electrode force of 5 kgf and current of 400 A. Bottom view (a) and weld cross-section (b) showing notch defect.[16] Reproduced with permission of Maney Publishing, Science and Technology of Welding and Joining, www.maneypublishing.com/journals/stw.

during single pulse RMW of Pt-10% Ir crossed wire welds are shown in Fig. 6.10.[16] At higher electrode forces (i.e., >3 kgf) the lower JBF values are attributed to a combination of insufficient heat input and notch defects. A maximum JBF of 38.8 N which is 90% of the 43 N (i.e., 379 MPa) tensile strength of the Pt-10% Ir wire was obtained with a 1 kgf electrode force and 200 A welding current. The weld geometry and excessive electrode sticking were, however, deemed unacceptable for all single-pulse RMW welds regardless of the maximum achievable JBF.[16]

Double pulse RMW

As discussed in the previous section, Huang *et al*.[16] found the traditional methods of balancing the electrode force and welding current to be insufficient in

© Woodhead Publishing Limited, 2013

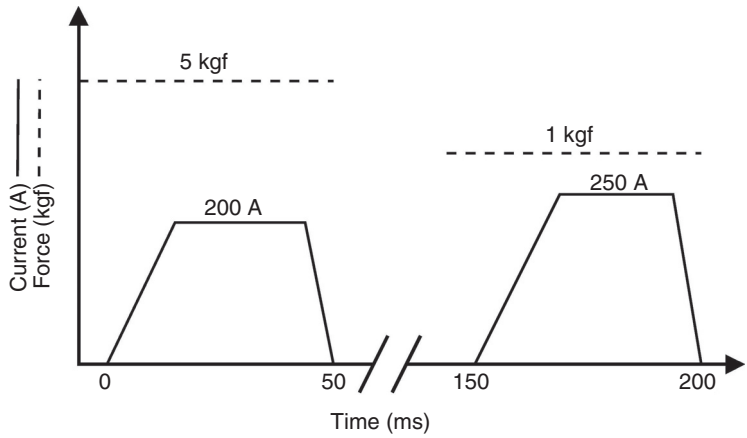


6.10 Joint breaking force for single-pulse RMW Pt-10% Ir to 316 LVM SS crossed-wire joints.[16] Reproduced with permission of Maney Publishing, Science and Technology of Welding and Joining, www.maneypublishing.com/journals/stw.

joining dissimilar Pt alloys to SS alloys in the crossed-wire configuration.[16] In LSRSW, several different techniques have been employed to shift the location of maximum heat input to the desired location at the faying interface when joining dissimilar materials or sheets of different thickness. The most common of these techniques include using electrodes with different geometries, water cooling one electrode,[37,38] using electrodes with different resistances,[37] or by modifying the welding schedule for example using multiple pulses.[39,40] Modifying the welding schedule is the most practical for the RMW process because using electrodes of different geometries or electrode cooling is not feasible,[2] and the significant difference in workpiece properties cannot be overcome by simply changing the resistance of the electrodes.[16]

Huang *et al.*[16] developed a double-pulse welding schedule capable of producing sound Pt-10% Ir to 316 LVM SS crossed-wire joints. The double-pulse welding schedule used is show in Fig. 6.11. The double-pulse welding schedule is designed to pre-deform the wires by hot deformation in the first pulse, where no melting occurs. This reduces contact resistance at the electrode/wire interface and causes the change in area at the faying surface to be

© Woodhead Publishing Limited, 2013



6.11 Double pulse RMW welding schedule for joining 0.38 mm dissimilar Pt-10% Ir to 316 LVM SS wires.

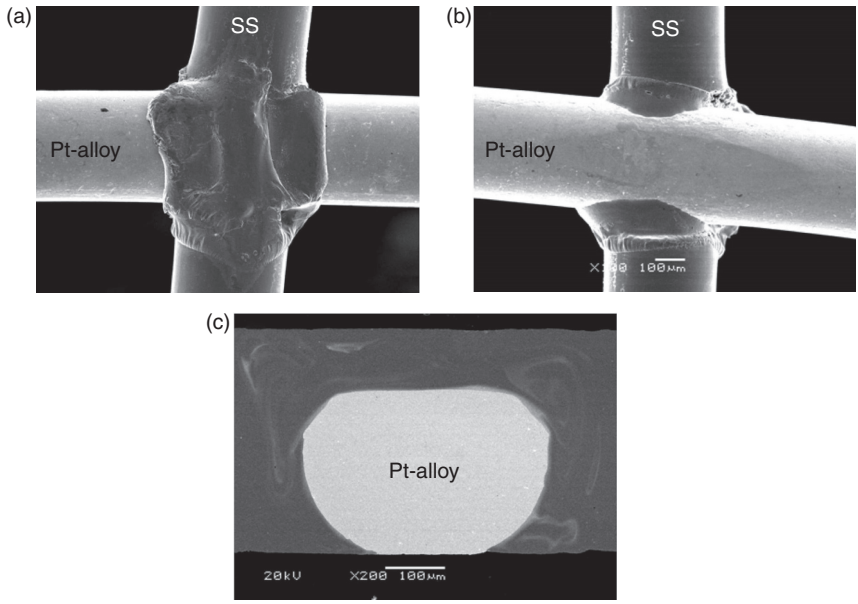
less dynamic as in sheet to sheet welding. The second pulse uses a lower weld force and higher welding current to cause sufficient melting to create a brazed joint at the faying surface and also heal any cracks or notches. Scanning electron micrograph images of double pulse RMW crossed-wire welds are shown in Fig. 6.12. No expulsion, cracks or notches are observed and excessive electrode sticking was avoided. A maximum JBF of 37.4 N, 87% of the tensile strength of Pt-10% wire was achieved.[16]

Bonding mechanism during RMW

When joining similar crossed-wire materials using the RMW process the joining mechanism predominantly transitions from solid-state to fusion with increasing heat input, as shown in References 11, 21, and 23–25. Resistive heating at the faying interface causes surface melting at the interface. The molten metal at the interface is squeezed out due to the electrode force. This cleans the interface by removing any surface contaminants, improving the surface conditions for crystallographic matching and interdiffusion of atoms across the interface, promoting quality solid-state bonding. With increasing heat input the solid-state bond increases in strength as the setdown increases and the bond area grows. This additional heat also promotes new grains to grow across the interface via recrystallization.[21] At even higher heat inputs fusion can occur. However, fusion welding in RMW crossed-wire bonding is often accompanied by expulsion, electrode sticking, and recrystallization and grain growth in the HAZ. Therefore, when fusion occurs it is usually considered overwelding which should be avoided.[21,25]

In joining dissimilar wire materials such as Pt-10% Ir to 316 LVM SS the bonding mechanism is predominantly brazing or a combination of brazing

© Woodhead Publishing Limited, 2013



6.12 SEM images of double pulsed RMW of Pt-10% Ir to 316 LVM SS crossed-wire joints: (a) top view, (b) bottom view, and (c) cross-section.[16] Reproduced with permission of Maney Publishing, Science and Technology of Welding and Joining, www.maneypublishing.com/journals/stw.

and fusion.[16] The brazing mechanism only occurs due to the large difference in melting temperatures between the two wire materials to be joined. For brazing only one of the materials becomes molten while the other remains a solid. In joining Pt-10% Ir and 316 LVM SS wires the 200–300 K lower melting point of the SS and the four times larger thermal conductivity leads to the SS material melting at a much lower heat input than the Pt-Ir wire causing wetting and the braze-type joint shown in Figs 6.8, 6.9 and 6.12.[16] Similar results were observed by Fukumoto *et al.*[22] in crossed-wire welding Au-coated Ni wires where, at low welding currents, insufficient heat was produced to melt the Ni wires but a brazed joint was created when the Au coating melted (i.e., >1064°C) at the interface. Also, a low melting point (i.e., >955°C) Ni–Au solution was also identified which acts as a braze melting at temperatures below that of pure Ni.

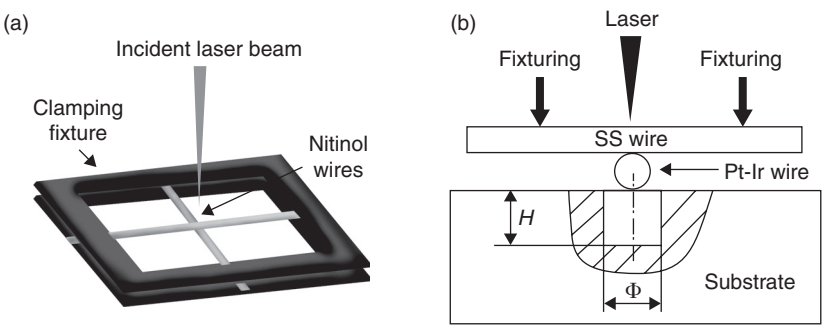
6.5.2 Laser microwelding (LMW)

Laser microwelding is a very attractive process in the medical industry having a number of advantages over RMW. Some of these advantages include high precision due to the small size of the laser spot, non-contact to

© Woodhead Publishing Limited, 2013

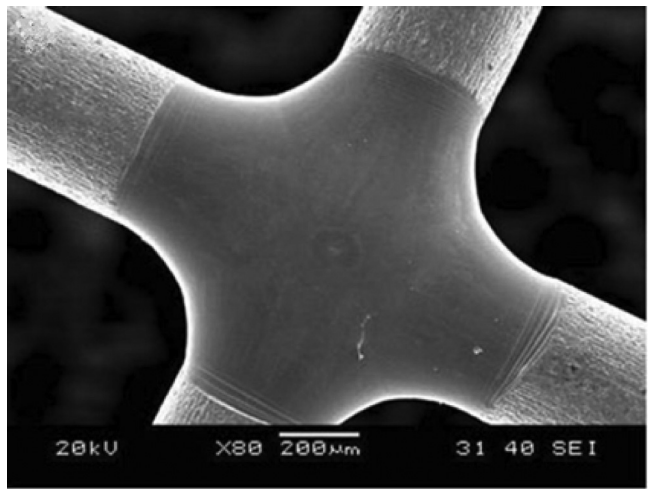
workpiece preventing contamination, excellent weld quality with low heat input and the laser process is easily automated.[17,41] Laser equipment is also a lot more affordable following a drop in cost over the last two decades.[17] Laser microwelding also has advantages when joining dissimilar materials as the difference in electrical resistance between the two different materials is not an issue and complete melting of only one material creating a braze-type joint is possible without expulsion and electrode sticking.[1,13] Pulsed neodymium-doped yttrium aluminum garnet (Nd:YAG) type lasers are commonly used in medical joining applications. Nd:YAG lasers have an average output power of 0.3–3 kW and a wavelength of 1064 nm, and can easily achieve a spot size of 200 μm.[17,42] Metals have a relatively low reflectivity at 1064 nm, therefore lower powers are required for welding due to the majority of laser energy being absorbed.[42]

In crossed-wire LMW a welding fixture is used to apply pressure on the top wire producing the intimate contact required for laser welding as well as promoting setdown. Examples fixture used for crossed-wire LMW are shown in Fig. 6.13a and 6.13b.[13,26] In the fixture shown in Fig. 6.13b used for crossed-wire joining of Pt-10% Ir to 316 LVM SS a hole in the fixture is located beneath the weld location is necessary to prevent welding of the wires to the fixture.[13] Zou *et al*.[13] found the optimized hole size to have a depth *H* of 1 mm and a diameter Φ of 1 mm in order to achieve acceptable joint geometries with acceptable setdown. Example LMW 316 LVM SS and NiTi alloy crossed-wire welds are shown in Figs 6.4b and 6.14, respectively.[12,26]



6.13 Example of LMW fixtures for crossed-wire welding. Two different types of crossed wire joining fixtures. (a) With kind permission from Springer Science+Business Media: *Metallurgical Materials Transactions A*, Mechanical and functional properties of laser-welded Ti-55.8 wt pct Ni Nitinol wires, 42(8), 2012, p. 2166, B. Tam, M. I. Khan, Y. Zhou, Figure 1. (b) With kind permission from Springer Science+Business Media: *Metallurgical Materials Transactions A*, Crossed-wire laser microwelding of Pt-10 pct Ir to 316 low-carbon vacuum melted stainless steel: Part I. Mechanism of joint formation, 43(4), 2012, p. 1223, G. S. Zou, Y. D. Huang, A. Pequegnat, X. G. Li, M. I. Khan, Y. Zhou, Figure 1.

© Woodhead Publishing Limited, 2013



6.14 Crossed-wire NiTi LMW. With kind permission from Springer Science+Business Media: *Metallurgical Materials Transactions A*, Mechanical and functional properties of laser-welded Ti-55.8 wt pct Ni Nitinol wires, 42(8), 2012, p. 2166, B. Tam, M. I. Khan, Y. Zhou, Figure 14(a).

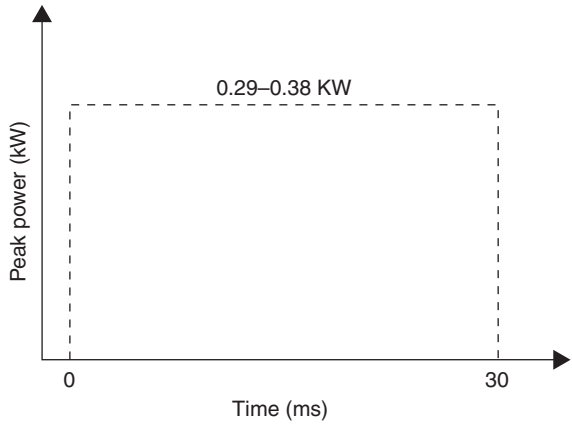
In laser welding dissimilar materials the best material combinations for weldability are materials that have good solubility and similar thermal properties. Materials combinations with large differences in thermal properties generally have poor weldability due to excessive vaporization of one of the materials and formation of brittle IMCs.[42] As mentioned previously, Pt alloys have a 200–300 K lower melting point and four times lager thermal conductivity compared with the SS alloys. Therefore, joining Pt alloys to SS alloys is expected to be challenging and a fusion-bonding mechanism may not be ideal.

When joining 0.38 mm diameter Pt-10% Ir and 316 LVM SS wires, Zou *et al*.[13] found a maximum JBF of 38.5 N could be achieved with peak laser powers between 0.29 and 0.38 kW, 30 ms pulse duration, and a square pulse profile as shown in Fig. 6.15. The JBF obtained at each peak power is shown in Fig. 6.16. This maximum JBF is 90% of the strength of the annealed Pt-10% Ir wire and the joint geometry and surface condition were considered to be excellent. Example welds made with a peak power of 0.35 kW are shown in Fig. 6.17.[13]

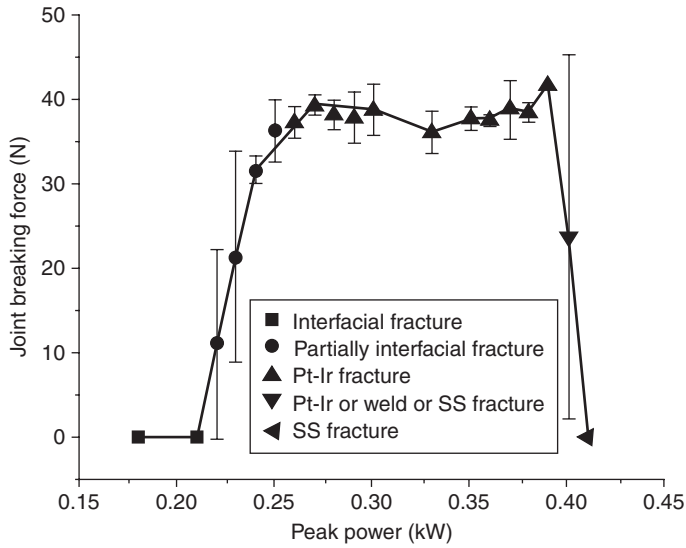
Bonding mechanism during LMW

As shown in Figs 6.4b and 6.14, for crossed-wire LMW of similar materials a fusion-type bonding mechanism is desirable, yielding excellent joint geometry and JBF.[12,26] However, in joining Pt alloys to SS alloys, complete fusion

© Woodhead Publishing Limited, 2013



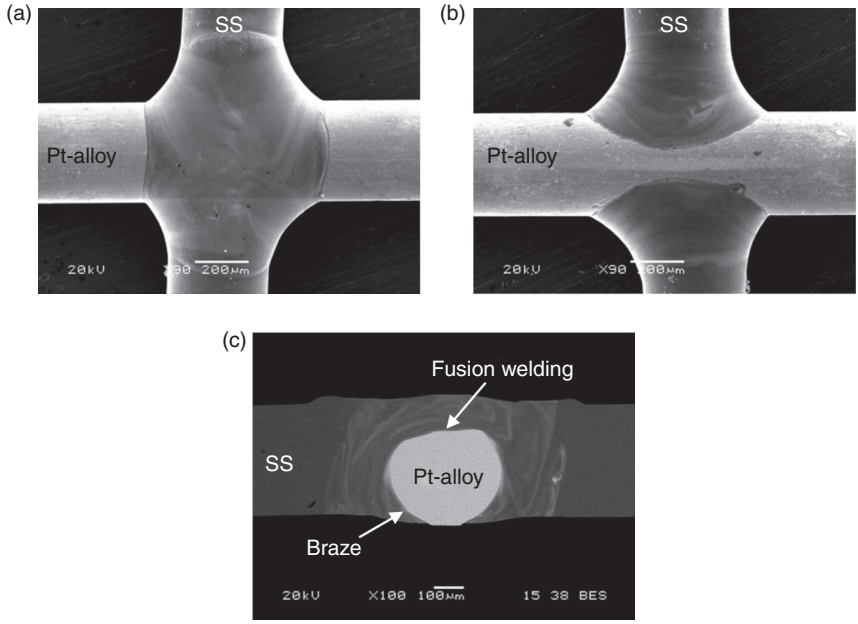
6.15 Pulse profile for LMW of Pt-10% Ir to 316 LVM SS crossed-wires.



6.16 JBF for LMW Pt-10% Ir to 316 LVM SS crossed-wire joints. With kind permission from Springer Science+Business Media: *Metallurgical Materials Transactions A*, Crossed-wire laser microwelding of Pt-10 pct Ir to 316 low-carbon vacuum melted stainless steel: Part I. Mechanism of joint formation, 43(4), 2012, p. 1223, G. S. Zou, Y. D. Huang, A. Pequegnat, X. G. Li, M. I. Khan, Y. Zhou, Figure 14(b).

welding must be avoided to prevent porosity and IMC formation due to the substantial differences in thermal properties of the two materials and solubility of the alloying elements. Complete fusion welding was considered overwelding when joining Pt-10% Ir to 316 LVM SS and pores are easily observed

© Woodhead Publishing Limited, 2013



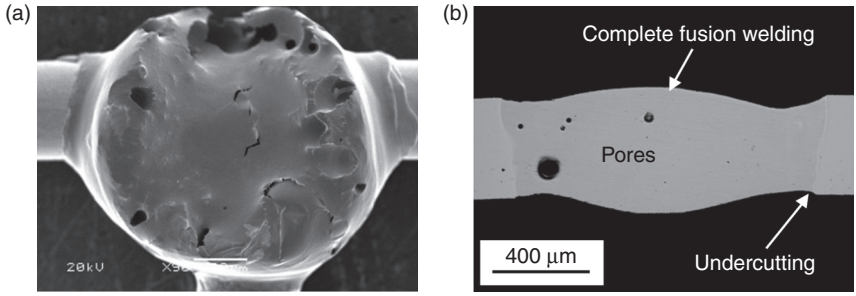
6.17 LMW Pt-10% Ir to 316 LVM SS crossed-wire joints made with 0.35 kW peak power: (a) top of joint; (b) bottom of joint and (c) joint cross-section. With kind permission from Springer Science+Business Media: *Metallurgical Materials Transactions A*, Crossed-wire laser microwelding of Pt-10 pct Ir to 316 low-carbon vacuum melted stainless steel: Part I. Mechanism of joint formation, 43(4), 2012, p. 1223, G. S. Zou, Y. D. Huang, A. Pequegnat, X. G. Li, M. I. Khan, Y. Zhou, Figures 4(c1,c2) and 10(a).

both on the surface and within welds made with peak laser powers above 0.4 kW as shown in Fig. 6.18a and 6.18b.[13] Zou *et al*. found that a braze-type bonding mechanism is to be desired.[13,15] In Fig. 6.17c it can be seen that there is limited mixing (i.e., fusion welding) between the Pt wire and the SS wire in the joint cross-section. A combination of fusion welding at the top of the Pt-Ir and brazing at the bottom of the Pt-Ir wire was found to be ideal.

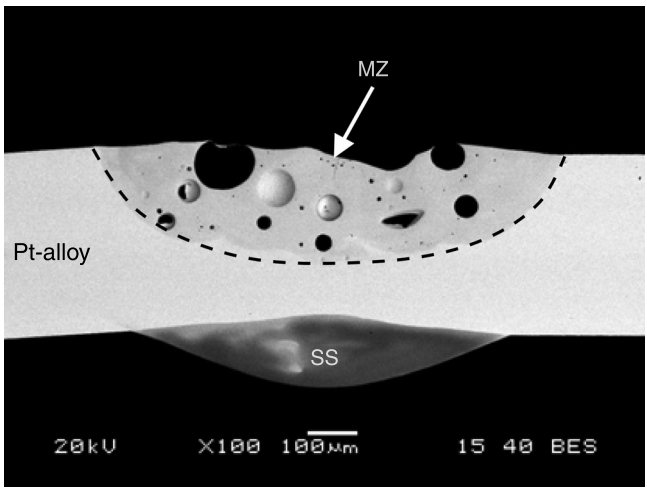
Importance of wire orientation in LMW

The joint formation for the dissimilar crossed-wire welds is greatly influenced by the temperature gradient in the joint during welding, as well as by the properties of the wire materials being joined. Since the material properties of Pt and SS are quite different, a large difference in joint morphology and quality can be realized by subjecting the higher melting point and larger thermal conductivity Pt wire to the incident laser beam (i.e., Pt wire on top). Huang *et al*.[15] were not able to produce a sound crossed-wire

© Woodhead Publishing Limited, 2013



6.18 Examples of overwelded LMW Pt-10% Ir to 316 LVM SS crossed-wire joints: (a) joint surface and (b) joint cross-section. With kind permission from Springer Science+Business Media: *Metallurgical Materials Transactions A*, Crossed-wire laser microwelding of Pt-10 pct Ir to 316 low-carbon vacuum melted stainless steel: Part I. Mechanism of joint formation, 43(4), 2012, p. 1223, G. S. Zou, Y. D. Huang, A. Pequegnat, X. G. Li, M. I. Khan, Y. Zhou, Figures 4(f1) and 11(b).



6.19 Cross-section of Pt-10% Ir to 316 LVM SS crossed-wire LMW joint where the Pt-Ir wire was subject to the incident laser beam. With kind permission from Springer Science+Business Media: *Metallurgical Materials Transactions A*, Crossed-wire laser microwelding of Pt-10 pct Ir to 316 low-carbon vacuum melted stainless steel: Part II. Effect of orientation on joining mechanism, 43(4), 2012, p. 1234, Y. D. Huang, A. Pequegnat, G. S. Zou, J. C. Feng, M. I. Khan, Y. Zhou, Figure 7(d).

joint between Pt-10% Ir and 316 LVM SS wire when the Pt-Ir wire was subject to the incident laser beam. A unique form of porosity was identified only in a mixed zone (MZ) where the molten SS material mixed with the molten Pt-Ir material as shown in Fig. 6.19.[15] The MZ forms due

© Woodhead Publishing Limited, 2013

to a combination of the wire orientation, geometry of the joint and the difference in thermal properties of the materials. The temperature gradient across the joint can be deduced by observing this unique sample cross-section and considering the three distinct regions, namely the MZ (top), the Pt-Ir region (middle), and the SS region (bottom). In the MZ the temperature must be the highest as the high melting point Pt-Ir wire is melted via direct interaction with the incident laser beam. In the middle of the weld the Pt-Ir wire does not reach a high enough temperature to melt. However, at the bottom of the weld, the lower melting point SS wire melts via thermal conduction through the wires causing it to wet the whole joint creating a braze-type joint and the MZ.

Huang *et al*.[15] attributed the porosity produced in the MZ to preferential vaporization of lower vapor pressure elements in the MZ which results from the wire orientation in the dissimilar material LMW process. This porosity defect leads to unacceptable joint geometries and considerably affects joint quality. This therefore highlights the importance of considering the joint geometry, material orientation, and material properties in joining dissimilar materials such as Pt to SS.

6.6 Future trends

With the population both growing and aging in the developed countries the demand for healthcare products will continue to grow.[5] With this increased demand for medical devices a need arises for better device design and technology as well as more cost effective manufacturing. It is therefore necessary to investigate manufacturing techniques such as dissimilar materials joining now in order to meet these future needs.

When considering the future of the RMW and LMW joining processes in the medical industry it is expected that they will still both be used for joining dissimilar materials. They are both capable of making quality dissimilar materials welds. The techniques used to achieve these dissimilar welds are, however, getting more complicated where an extensive knowledge in the process is required to achieve sound joints. The low cost and our excellent understanding of the RMW process will ensure its continuous application. However, due to the large advancement in our understanding of laser welding, the numerous advantages over RMW and the recent decrease in equipment costs, the use of LMW in the medical industry is expected to increase in future years.

6.7 Conclusions

The joining of dissimilar crossed-wire materials is becoming increasingly important in medical devices as it allows for more flexibility in design,

© Woodhead Publishing Limited, 2013

enhanced performance, and reduction in material costs. The crossed-wire Pt to SS welds discussed in this chapter provided a good introduction to the joining challenges that accompany the joining of dissimilar materials and non-standard joint geometries. It was shown that the RMW and LMW welding processes which are commonly used in the medical industry are capable of making dissimilar crossed-wire joints between Pt and SS alloys. In the RMW process traditional methods of balancing the electrode force and welding current parameters to cause localized melting at the faying surface were found to be insufficient. A novel RMW process such as a double-pulse process must be used to achieve high-strength joints that have acceptable surface quality and geometry. In the LMW process sound joints were easily produced; however, fusion welding was found not to be desired as one would expect when joining similar materials. A braze-type joint is preferred in order to prevent significant mixing of the two alloys which can lead to porosity and brittle IMCs when joining dissimilar materials. Overall, from this chapter it can be seen that an in-depth understanding of the fundamentals of the welding processes and metallurgy are essential in joining dissimilar materials in the crossed-wire geometry.

6.8 References

1. Y. Zhou, A. Hu, M. I. Khan, W. Wu, B. Tam, and M. Yavuz, Recent progress in micro and nano-joining, International Conference on Advanced Structural and Functional Materials Design 2008, *Journal of Physics: Conference Series* (2009), Vol. **165**, 012012.
2. Y. Zhou, *Microjoining and Nanojoining*, Woodhead Publishing Limited, Cambridge, UK, 2008.
3. J. Floyd, C. Genau, and K. W. Leyde, US Patent, US2010/0179627 A1, July 15, 2010.
4. S. M. Jones, A. A. Campbell, and J. L. Pennala, US Patent, 5844198, Dec. 1, 1998.
5. A. Cowley and B. Woodward, A healthy future: Platinum in medical applications, *Platinum Metals Review* (2011), Vol. **55**(2), pp. 98–107.
6. B. Brummer and M.J. Turner, Electrical stimulation of the nervous system: The principle of safe charge injection with noble metal electrodes, *Bioelectrochemistry and Bioenergetics* (1975), Vol. **2**, pp. 12–25.
7. G. Binyamin, B. M. Shafi, and C. M. Mery, Biomaterials: A primer for surgeons, *Seminars in Pediatric Surgery* (2006), Vol. **15**, pp. 276–283.
8. M. N. Helmus, D. F. Gibbons, and D. Cebon, Biocompatibility: Meeting a key functional requirement of next-generation medical devices, *Toxicologic Pathology* (2008), Vol. **36**, pp. 70–80.
9. B. D. Ratner, A. S. Hoffman, F. J. Schoen, and J. E. Lemons, *Biomaterials Science: An Introduction to Materials in Medicine*, Academic Press, London, 1996.
10. Y. Ren, K. Yang, and B. Zhang, In vitro study of platelet adhesion on medical nickel-free stainless steel surface, *Materials Letters* (2005), Vol. **59**, pp. 1785–1789.

© Woodhead Publishing Limited, 2013

11. M. I. Khan, J. M. Kim, M. L. Kuntz, and Y. Zhou, Bonding mechanisms in resistance microwelding of 316 low-carbon vacuum melted stainless steel wires, *Metallurgical and Materials Transactions A* (2009), Vol. **40A**, pp. 910–919.
12. I. Khan and Y. Zhou, Laser micro-welding (LMW) of crossed-316 LVM stainless steel wire, Proceedings in Material and Processes for Medical Devices Conference (MPMD), Palm Springs, CA, September 2007.
13. G. S. Zou, Y. D. Huang, A. Pequegnat, X. G. Li, M. I. Khan, and Y. Zhou, Crossed-wire laser microwelding of Pt-10 pct Ir to 316 low-carbon vacuum melted stainless steel: Part I. Mechanism of joint formation, *Metallurgical Materials Transactions A* (2012), Vol. **43**(4), pp. 1223–1233.
14. S. Kou, *Welding Metallurgy*, 2nd edn, John Wiley & Sons Inc., Hoboken, NJ, 2003.
15. Y. D. Huang, A. Pequegnat, G. S. Zou, J. C. Feng, M. I. Khan, and Y. Zhou, Crossed-wire laser microwelding of Pt-10 pct Ir to 316 low-carbon vacuum melted stainless steel: Part II. Effect of orientation on joining mechanism, *Metallurgical Materials Transactions A* (2012), Vol. **43**(4), pp. 1234–1243.
16. Y. D. Huang, A. Pequegnat, J. C. Feng, M. I. Khan, and Y. Zhou, Resistance microwelding of crossed Pt-10Ir and 316 LVM stainless steel wires, *Science and Technology of Welding and Joining* (2011), Vol. **16**(7), pp. 648–656.
17. J. Xie, S. Safarevich, Laser materials processing for medical devices, Proceedings from the Materials & Processes for Medical Devices Conference, Anaheim, CA, September 8–10, 2003, pp. 25–30.
18. N. J. Noolu, H. W. Kerr, Y. Zhou, and J. Xie, Laser weldability of Pt and Ti alloys, *Materials Science and Engineering A* (2005), Vol. **A397**, pp. 8–15.
19. T. B. Massalski, ed., *Binary Alloy Phase Diagrams*, ASM International, Materials Park, OH, 1990.
20. Z. Chen, Joint formation mechanism and strength in resistance microwelding of 316L stainless steel to Pt wire, *Journal of Materials Science* (2007), Vol. **42**, pp. 5756–5765.
21. S. Fukumoto and Y. Zhou, Mechanism of resistance microwelding of crossed fine Nickel wires, *Metallurgical Materials Transactions A* (2004), Vol. **35**, pp. 3165–3176.
22. S. Fukumoto, Z. Chen, and Y. Zhou, Interfacial phenomena and joint strength in resistance microwelding of crossed Au-plated Ni wires, *Metallurgical Materials Transactions A* (2005), Vol. **36A**, pp. 2717–2724.
23. S. Fukumoto, T. Matsuo, H. Tsubakino, and A. Yamamoto, Resistance microwelding of SUS304 stainless steel fine wire, *Materials Transactions* (2007), Vol. **48** (4), pp. 813–820.
24. S. Fukumoto, S. Morikawa, and A. Yamamoto, Small-scale resistance welding of crossed TiNi fine wire, *Materials Science Forum* (2008), Vol. **580**–582, pp. 225–228.
25. B. Tam, A. Pequegnat, M. I. Khan, and Y. Zhou, Resistance micro-welding of Ti-55.8 wt. % Ni Nitinol wires and the effects of pseudoelasticity, *Metallurgical Materials Transactions A* (2012), Vol. **43**(8), pp. 2969–2978.
26. B. Tam, M. I. Khan, and Y. Zhou, Mechanical and functional properties of laser-welded Ti-55.8 wt pct Ni Nitinol wires, *Metallurgical Materials Transactions A* (2011), Vol. **42**(8), pp. 2166–2175.

© Woodhead Publishing Limited, 2013

27. Y. Zhou, P. Gorman, W. Tan, and K.J. Ely, Weldability of thin sheet metals during small-scale resistance spot welding using an alternating-current power supply, *Journal of Electronic Materials* (2000), Vol. **29**(9), pp. 1090–1099.
28. S. Fukumoto, Small-scale resistance spot welding of bulk glassy alloys, *Welding International* (2011), Vol. **25**(7), pp. 501–504.
29. K. J. Ely and Y. Zhou, Micro resistance spot welding of Kovar, steel, and nickel, *Science and Technology of Welding and Joining* (2001), Vol. **6**(2), pp. 63–72.
30. K. S. Friis, M. I. Khan, N. Bay, and Y. Zhou, Resistance microwelding of 316L stainless steel wire to block, *Science and Technology of Welding and Joining* (2011), Vol. **16**(6), pp. 546–552.
31. Y. Zhou, P. Gorman, W. Tan, and K. J. Ely, Weldability of thin sheet metals by small-scale resistance spot welding using high-frequency inverter and capacitor-discharge power supplies, *Journal of Electronic Materials* (2001), Vol. **30**(8), pp. 1012–1020.
32. S. J. Dong, G. P. Kelkar, and Y. Zhou, Electrode sticking during micro-resistance welding of thin metal sheets, *IEEE Transactions on Electronics Packaging Manufacturing* (2002), Vol. **25**(4), pp. 355–361.
33. W. Tan, Y. Zhou, H. W. Kerr, and S. Lawson, A study of dynamic resistance during small scale resistance spot welding of thin Ni sheets, *Journal of Physics D: Applied Physics* (2004), Vol. **37**, pp. 1998–2008.
34. W. Tan, S. Lawson, and Y. Zhou, Effects of Au plating on dynamic resistance during small-scale resistance spot welding of thin Ni sheets, *Metallurgical Materials Transactions A* (2005), Vol. **36A**, pp. 1901–1910.
35. *Resistance Welders Manufacturers' Association (RWMA): Resistance Welding Manual*, 4th edn, George H. Buchanan Co., Philadelphia, PA, 1989, Sec. 1.
36. N. Scotchmer, The other resistance process: Cross wire welding, *Welding Journal*, December 2007, pp. 36–39.
37. W. R. Oates and A. M. Saitta, Welding Technology. *Welding Handbook*, 8th edn, Vol. 1, 1987. Miami, FL: American Welding Society.
38. T. W. Eagar, Resistance welding: a fast, inexpensive, and deceptively simple process, Proceedings of the 3rd International Conference on Trends in Welding Research, ASM International, Materials Park, OH, June, 1992.
39. L. Yi, L. Jinhe, X. Huibin, X. Chengzhi, and L. Lin, Regression modeling and process analysis of resistance spot welding on galvanized steel sheet, *Materials and Design* (2009), Vol. **30**, pp. 2547–2555.
40. S. Agashe and H. Zhang, Selection of schedules based on heat balance in resistance spot welding, *Welding Journal* (2003), Vol. **82**(7), pp. 179s–183s.
41. S. Safarevich, J. Xie, Peculiarities of micro laser welding of medical devices, Proceedings from the Materials & Processes for Medical Devices Conference, Anaheim, CA, September 8–10, 2003, pp. 31–36.
42. W. W. Duley, *Laser Welding*, John Wiley & Sons, Inc., New York, 1999.

© Woodhead Publishing Limited, 2013

7

Evaluating the corrosion performance of metal medical device welds

S. C. KELLEY and D. F. UNTEREKER, Medtronic, Inc., USA

DOI: 10.1533/9780857096425.2.178

Abstract: Corrosion is a ubiquitous process that affects nearly every aspect of our lives from large-scale structures like buildings and bridges to small intricate personal items like mechanical watches. Corrosion is also a concern for modern implantable medical devices such as pacemakers that have become synonymous with today's miracle medical technologies. Because the details of welds are less predictable than normal metallurgy, it is very important to be suspicious of weld corrosion and thus do a thorough assessment before marketing any implantable medical device. This chapter provides a practical guide for assessing the risk of weld corrosion from planning corrosion measurements to sample preparation, to data analysis and risk mitigation.

Key words: medical device, weld, corrosion, assessment, performance, electrochemistry.

7.1 Introduction

Corrosion is a ubiquitous process that affects nearly every aspect of our lives from large-scale structures like buildings and bridges to small intricate personal items like mechanical watches. Corrosion is also a concern for modern implantable medical devices such as pacemakers that have become synonymous with today's miracle medical technologies.

While we all recognize corrosion in the form of things like rust, the mechanisms leading to corrosion often appear mysterious and not well understood to the general population. When we talk about corrosion we are usually concerned with metals. In this chapter we are not only concerned with metals that may be complex alloys, but in particular we are focusing on metal welds in implantable medical devices.

Corrosion is an oxidative process. The material said to corrode is oxidized, which means it loses electrons and becomes a chemical compound that we refer to as the corrosion product. Rust, which is iron oxide, is an example of such a compound. What is sometimes overlooked is that corrosive oxidation cannot occur in isolation. There is always a second, corresponding reaction, called a reduction, which also occurs. In a majority of cases this

© Woodhead Publishing Limited, 2013

second reaction is the reduction of molecular oxygen to produce water or hydroxide ions. The laws of physics require that the amount of oxidation and the amount of reduction be equal. Thus, the overall corrosion reaction is said to be stoichiometric. It is this relationship that allows us to measure the amount and rate of corrosion by determining things like the amount of corrosion product formed, or the current associated with the transfer of electrons between the oxidized and reduced species.

In the sections below we will build upon these basics and discuss how some fairly simple methods can be used to estimate the instantaneous rate of corrosion, even if it is far too small to observe in real time. Even more, these same methods can help us to estimate the cumulative effect of corrosion over very long periods of more than a decade.

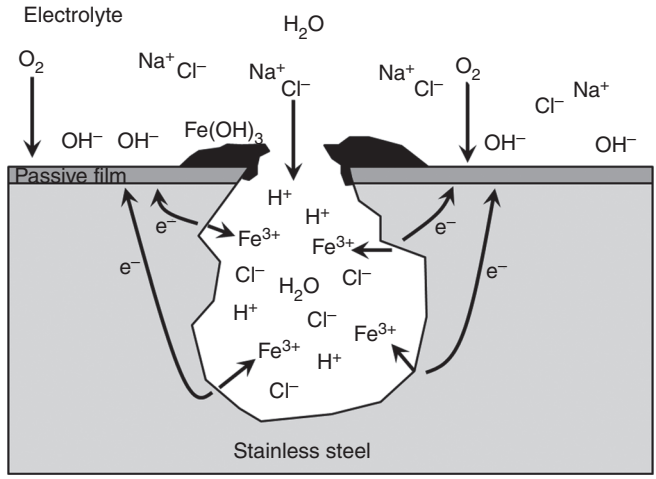
7.1.1 Types of corrosion

There are many ways to think about corrosion. Some of these are based on appearance and others on more scientific principles like the process that produces the corrosion. Probably the most useful way to begin classifying corrosion is by its general appearance. If the entire area of concern appears to be affected, the corrosion is said to be 'general' or uniform corrosion. The rusting of unpainted iron or steel left sitting out in the open is an example of uniform corrosion.

The second classification of corrosion by appearance is non-uniform corrosion. Such corrosion is readily recognized by its blotchy appearance. In many cases there are small heavily corroded areas in near proximity to relatively unaffected and maybe even pristine areas. Perhaps the most common example of non-uniform corrosion is pitting corrosion. Pitting corrosion is often observed as tiny spots, which are actually high aspect ratio pits, in an otherwise reasonable looking surface.

Another way to classify corrosion is by the process that causes it. In the vast majority of cases of interest here the driving force causing corrosion is thermodynamics; the corrosion reaction proceeds simply because the corrosion products are in a less energetic state than the starting surface and reducing species. Such a reaction is sometimes called a galvanic reaction because it is essentially a small, natural (unintended) battery. One of the things that make corrosion appear a little mysterious at first glance is that the metal being corroded and the reductant (usually oxygen) do not have to be in exactly the same physical location. The reason for this is that the metal being corroded serves as a conductor to move the electrons from the species being oxidized to the one being reduced. The other requirement is that an 'electrolyte', which is a solution containing conductive ions, bridges the area between where the oxidation and reduction takes place. This is illustrated in

© Woodhead Publishing Limited, 2013



7.1 Example of corrosion on a single metal piece (localized pitting corrosion).

Fig. 7.1. Notice that the charge exchanged is always perfectly balanced. On one side the charge is transferred by electrons moving through the metal, while on the other side the charge is passed via ions moving through a solution. This is exactly analogous to the operation of a battery.

There are many variations on galvanic reactions. Different concentrations of oxygen, or different electrolyte concentrations, or the electrical connection of different metals can all drive galvanic corrosion. Some of these will be described at the end of the chapter for those who are interested in more detail.

In order to understand how we can measure and make estimates of cumulative corrosion we need to look at two of the main equations governing corrosion. The first of these is Faraday's law which relates the amount of corrosion to the 'corrosion current', which is the rate electrons (or ions) are moving between the places where oxidation and reduction occur.

$$I = nFA\frac{\mathrm{d}N}{\mathrm{d}t} \qquad [7.1]$$

Here I is the corrosion current (as opposed to $i = I/A$, which refers to area normalized current or current density), n is the number of electrons transferred from the corroding species, F is a constant called the Faraday, A is the corroding area, and $\mathrm{d}N/\mathrm{d}t$ is the moles of the species corroding per area per second. The importance of this equation is that it states that if we can measure I and know the corrosion reaction and area, we know the instantaneous

© Woodhead Publishing Limited, 2013

rate of the corrosion. Integrating this value over time is the basis for estimating the cumulative amount of corrosion.

The second equation is the Butler–Volmer equation which relates current to the potential driving the reaction.

$$I = I_{\text{corr}}\left[\exp\left(\frac{\alpha_a nF\eta}{RT}\right) - \exp\left(\frac{-\alpha_c nF\eta}{RT}\right)\right] \quad [7.2]$$

$$\eta = \left(E - E_{\text{corr}}\right) \quad [7.3]$$

Here I_{corr} is the equilibrium corrosion current, R is the universal gas constant, α_a and α_c are the oxidation and reduction charge transfer coefficients, T is temperature, and η is overpotential (the potential relative to the equilibrium corrosion potential). Notice that in this equation the current is proportional to an exponential term involving the potential of the system with respect to the corrosion potential. The key features of this equation are the exponential dependence of I on E and the reciprocal involvement of temperature in the exponential. Later we will see that this equation also leads to our ability to measure corrosion rates by observing the slope of a log I vs E plot near where I approaches zero. These equations also tell us about ways to make accelerated estimates of corrosion.

The corrosion reactions discussed so far are termed 'spontaneous' because they are powered by thermodynamics and occur without external intervention. However, some implantable medical devices also incorporate a battery, which is a source of energy that may cause systems that would not otherwise corrode to corrode. A common example of this kind of corrosion is the bluish deposits that are often observed on the top of a car battery. This corrosion is caused by some of the energy in the battery being 'siphoned off' from its intended purpose of running the car. This process is called electrolysis when it is intended to occur and is the basis for many very important industrial processes such as the manufacture of chlorine gas and aluminum metal. There are a few instances where electrolysis can cause corrosion in some parts of a medical device.

7.1.2 Corrosion on medical device welds

While the corrosion associated with medical devices is technically the same as any other corrosion, it needs to be thought of in a somewhat different manner. One distinction is that medical devices are only constructed from materials that are known to be quite stable. Thus, the amounts of corrosion that are likely to occur are relatively small. There are three areas of concern

© Woodhead Publishing Limited, 2013

about medical device corrosion. The first is the threat to the integrity and function of the device. For example, it would be bad if the enclosure of a pacemaker was able to corrode completely through and expose the interior of the device to the body (and vice versa). A typical pacemaker case is about 250 μm (0.010 in.) thick. It must last for at least 10 years, and perhaps twice that. Thus, if the rate of any form of corrosion is greater than 12.5 μm/year, the device case may be breached. Notice that such a requirement does not depend on whether we are concerned with uniform or non-uniform corrosion. A breach is a breach.

It is also important to realize that even the corrosion of internal components within a medical device can be very detrimental. For example, the case of the battery inside a pacemaker or other medical device might corrode through and thus compromise both the functioning of the battery as well as the electronics and other components in the vicinity of the battery. A complete breach is not all we need to be concerned about. Corrosion may also decrease the mechanical strength or electrical conductivity of some vital component and thus indirectly cause a failure. A third concern is that the corrosion products may expose the body to a threat from toxicity.

So far everything that has been said applies equally to all metal parts of a medical device. However, the focus of this chapter is on welds. Why are they special? The simple answer is that welds are special and deserve more attention because they are complicated alloys, usually much more so than the rest of the device, and thus more susceptible to problems.

What is not obvious is that two very corrosion-resistant metals can be welded together and the result is a weld that is not very corrosion resistant. For example, consider the welding of two pieces of stainless steel, which are by themselves quite resistant to corrosion. To understand why their weld might not be corrosion resistant we need to consider why the stainless steel is corrosion resistant in the first place. Stainless steel would readily corrode if it were not for the nanometers thick layer of chromium oxide that forms on the outer surface. If the welding process (which may be done in an inert atmosphere) does not re-form this protective oxide, the weld will not be corrosion resistant. Many metal systems behave similarly. In addition to that, very complex intermetallic compounds can form in weld zones. These are often not completely understood and depend on details of the welding process like temperature, amount of energy, and time. Furthermore, for dissimilar metal welds, the possible intermetallic compounds formed are often surprisingly reactive, even if their parent alloys are stable. Phase diagrams are very useful to help predict the intermetallic compounds that form during welding.

Because the details of welds are less predictable than normal metallurgy, it is very important to be suspicious of weld corrosion and thus do a thorough

© Woodhead Publishing Limited, 2013

assessment before marketing any implantable medical device. This is not so different from special military and space applications where high reliability is expected, the time frames of use may be long, and the devices themselves are not very accessible for repair or inspection.

7.1.3 The goals of a corrosion assessment

It is obvious that predicting adequate device integrity is a goal of corrosion assessment. Actually, corrosion is one of many assessments that must be made to ensure an implantable medical device will perform its intended function over the expected longevity. It is difficult to make exact, detailed predictions about corrosion over a long time period of a decade or more. This is especially true when one considers non-uniform corrosion that may happen quickly once it starts. Hence, a major goal of a corrosion assessment is to determine whether a given system shows any propensity for localized corrosion.

Another goal is to show that tiny amounts of innate general corrosion that occur in all systems will have no practical effect on the implanted device. This may amount to demonstrating that there is no practical loss of material during the implant duration, and is equivalent to proving a large safety factor so that even if the corrosion estimate is off by a significant amount, it will cause no problem. Such a strategy is wise since corrosion has shown itself to be very sensitive to small changes in environment and the presence of contaminants. This is one reason why a very controlled manufacturing process is a critical part of any corrosion mitigation strategy. It is vastly important that sources of possible contaminants, like chloride and less corrosion-resistant metals, be controlled and minimized as well as having manufacturing processes, like welding, be very consistent once a suitable process has been identified.

7.2 Measurements of corrosion

The goals of corrosion measurements are to determine the mode (uniform or localized) and rate of corrosion (material penetration rate in distance per time and elemental corrosion product release rate in mass per time). Measurements of corrosion are made by testing a weld sample in the actual (i.e. *in vivo*) or simulated (i.e. *in vitro*) implant environments to assess the impact of corrosion on device performance. Since human clinical and animal tests involve both ethical and cost constraints, routine corrosion tests are normally carried out in simulated implant environments. The preparation and design of the sample are also important test considerations (see Sections 7.4 and 7.5).

© Woodhead Publishing Limited, 2013

Table 7.1 Common immersion tests

Immersion test	Corrosion rate or risk	Standard
Mass change, galvanic, open circuit potential	Rate	ASTM G31, ASTM G71, ASTM G5
Active device	Rate	None
Water exposure (humidity, liquid soak, and boiling)	Risk	ASTM A967, practice A and B; ASTM F1089
Salt spray	Risk	ASTM A967, practice C; ASTM B117
Pitting and crevice	Risk	ASTM G48
Intergranular, sensitization	Risk	ASTM A262 practice B; ASTM A763, practices X, Y, and Z

Notes: Test results for corrosion rate are analysed by mass change, solution analysis, corrosion potential versus time trend, and microscopic inspection. Test results for corrosion risk are analysed by microscopic inspection only.

In vitro corrosion tests are either immersion tests or direct measurements of the electrical current produced by corrosion. Immersion testing consists of exposing the sample to simulated implant conditions and inspecting the sample and environment some time later for evidence of corrosion. Table 7.1 lists common immersion tests along with some aspects of their use (Cramer and Covino, 2003; Jones, 1996; Korb and Olson, 1987). Direct corrosion current measurements use electrical test equipment (such as potentiostats and frequency response analysers) to control the energy applied to the sample and measure the corrosion current using various established test methods (see Section 7.3). Measurements of corrosion current are useful as corrosion current can be directly converted to corrosion rate using Equation [7.1].

The active device test is an interesting example of an immersion test where a weld is subjected to the therapy waveform under simulated implant conditions. For multiple samples, testing in separate containers allows for solution analysis to determine the sample corrosion rate via the corrosion products produced. The use of electrical test equipment allows for periodic queries of the potential vs time trend and surface changes of the sample via capacitance. It is also useful to devise functional tests of the weld (electrical or mechanical) to assess its performance before and after test.

Simulation of the implant environment is crucial to performing a valid corrosion measurement. The challenge for the corrosion engineer is to replicate the most important factors. Fortunately, the implant environment is fairly stable and well studied (see Table 7.2). If necessary, it is possible to characterize the implant environment by consulting tabulated data (Duck, 1990; Lentner, 1980, 1985, 1990) or by performing a limited number of animal experiments.

© Woodhead Publishing Limited, 2013

Table 7.2 Environmental variables affecting weld corrosion risk and implant conditions for each.

Variable	Description	Effect of increasing value or composition change	Human *in vivo* condition
Time	Calendar exposure time	Increases corrosion risk	Expected implant time
Temperature	Temperature at the implant site	Depends on corrosion rate limiting reaction; normally increases corrosion risk	37°C
Pressure	Atmospheric pressure	Increases gas solubility in the electrolyte	1 atm
Gas composition	Mole fraction composition of the gas phase	Controls the dissolved gas composition in the electrolyte	Implant site and tissue specific
Electrolyte composition	Mole fraction composition of the liquid phase	Controls the corrosion rate through the pH, reactant and product concentrations, and corrosion accelerating species (such as Cl^-)	Implant site and tissue specific; normal pH 7.4
Potential/ current	Imposed electrical signals due to galvanic cells or active device waveforms	Increases corrosion risk	Material specific for passive devices; also waveform and design-specific for active devices
Mass transport	Mode and rate of reactant and product transport to/ from the weld surface	Depends on corrosion rate limiting reaction and implant environment	Implant time, site, and tissue specific; normally limited for a tissue-encapsulated device

The environmental variables which affect weld corrosion are all parameters which change the conditions at the weld–electrolyte interface. Normally the implant environment can be adequately simulated using 0.9 wt% saline (i.e. NaCl) or pH 7.4 phosphate buffered saline at 37°C and 1 atm. The presence of chloride ions is important as it is well known that halogen ions increase corrosion risk by decreasing the stability of passive oxide films (such as on stainless steel, titanium, and aluminium). Other important

© Woodhead Publishing Limited, 2013

considerations include dissolved oxygen and carbon dioxide as well as the presence of protein.

The presence of oxygen can increase corrosion (due to increased reduction rates for an oxygen reduction rate controlled process) or decrease corrosion (due to enhanced passive oxide film stability). As the oxygen concentration in the body is less than the fully aerated test condition (3.0 mL/L vs 5.5 mL/L, respectively), it is necessary to understand the effect of oxygen on the particular corrosion situation under study prior to testing (Letner, 1990; Weast, 1983). Protein adsorption is one of the first events that occurs at the site of a device implant as part of the foreign body response (Ratner *et al.*, 2004); however, the use of protein in testing can normally be neglected.

As device implant times are long, compressing test time through the use of accelerated testing is often necessary. The goal of accelerated testing is to maximize the test acceleration factor such that acceptable performance for the full implant time of the device may be demonstrated within the product development timeline. The acceleration factor for the test is determined by a ratio of the test variables or of the corrosion rates for accelerated and non-accelerated tests. Accelerated test results are only valid when the mode of corrosion and the mechanism of corrosion rate control can be shown to be the same as for the non-accelerated *in vivo* situation. The variables which can be used to accelerate corrosion are compressed use cycles, temperature, and reactant concentration.

Acceleration by compressed use cycles is performed by increasing the frequency of known elements of the use condition (i.e. the electrical waveform or mechanical stresses). Further acceleration may be obtained by reducing or eliminating rest periods (i.e. increasing duty cycle). Temperature is a common accelerant applied to corrosion; however, the actual effect of temperature depends upon the rate limiting reaction. Commonly, temperature is expected to accelerate corrosion by increasing the value of I_{corr} (see Equation [7.2]). The value of I_{corr} is also dependent upon the reactant concentrations adjacent to the surface of the weld. Common reactants which can affect the corrosion rate are oxygen, chlorine, protons (i.e. hydronium ions from acid), and metal ions. Knowledge of the implant environment is essential for the acceleration of corrosion as it is difficult to justify the use of an accelerated condition which cannot be related to the actual implant environment.

The desired output of a corrosion assessment is evidence of the weld's resistance to corrosion. This evidence may be as simple as a weld free of corrosion after a period of immersion or a measurement of I_{corr}; however, other metrics are available by closer inspection of the sample and sample environment. Sample inspection can determine the corrosion mode (uniform or localized) from the presence of corrosion product and the appearance (or not) of localized corrosion features such as pits and crevices.

© Woodhead Publishing Limited, 2013

Mass change, sample volume change (from measured dimensions), and pit or crevice volume can all be translated into corrosion rate using Faraday's law and assumptions regarding the corrosion reactions and material density. Metallographic methods may be used to mount and cross-section samples for a more detailed microscopic view of corrosion damage and interior device spaces (Vander Voort, 1984, 2004). The extent of localized corrosion (pit or crevice depth) can be revealed in well-prepared cross-sections, but the calculation of the volume removed is difficult without making assumptions regarding the pit or crevice depth and shape. White light interferometry is a superior technique to directly measure the volume of the material removed (Holme and Lunder, 2007). In this way, a penetration rate for a survey of features may be calculated. As it is often impractical to image an entire sample, microscopy results can be used to estimate the overall corrosion rate if assumptions are made for the distribution of corrosion damage across the sample surface. ASTM G46 provides a guide and methods for surveying corrosion damage.

ASTM G102 instructs the corrosion engineer regarding the use of Faraday's law to calculate corrosion rates in the form of penetration rates (distance per time). The penetration rates calculated from Faraday's law using the entire sample volume and area presume uniform corrosion. Assumptions regarding the distribution and shape of localized corrosion features can be used to calculate the localized corrosion penetration rate in a similar way. Time-varying corrosion rates may also be handled using an integral of the rate over the desired time (this requires multiple sampling time points). Years is the typical unit of time as the corrosion rates of medical devices and materials are normally quite low.

Solution analysis for dissolved metallic elements can also be used to determine corrosion rate. There are two main methods for solution analysis – inductively coupled plasma–atomic emission spectroscopy (ICP–AES) or mass spectroscopy (ICP–MS). The two methods differ in terms of cost (AES < MS) and detection limit (MS < AES). Typical detection limits for AES and MS vary by lab and analyte but are typically in the range of 10 and 0.1 ppb, respectively (Harris, 2003). Each medical device weld and design has a different acceptable maximum amount of corrosion; such a threshold should be considered when selecting the test duration and solution analysis method as the combination determines the minimum detectable corrosion rate. The requested solution analysis should include measurements for all major alloying elements (wt% > 1) or dissolved elements (as determined from literature or prior experience). The elemental concentration data must be re-combined computationally to yield a metallic dissolution rate. For both the use of Faraday's law and solution analysis for calculations of the corrosion rate, the methodology used for the calculations should be recorded to support the results.

© Woodhead Publishing Limited, 2013

7.3 Direct measurements of corrosion current

Direct measurements of corrosion current are possible using suitable sample and test cell designs and electrical test equipment. Corrosion currents are clearly observable for both uniform and localized corrosion, but uniform corrosion current is much easier to translate into a corrosion penetration rate. Area normalized corrosion current only makes sense for uniform corrosion. As for immersion tests, sample and sample environment inspection after test are required to gain the maximum amount of information from the effort. The methods which are useful for measuring corrosion current include polarization, galvanic, and electrochemical impedance spectroscopy (EIS) tests.

Polarization tests can be used both for direct measurement of uniform corrosion rate (I_{corr}) and for the comparative assessment of localized corrosion risk. The method described here is based on voltage control of the corrosion rate and the Tafel equation (Equation [7.4]). There are many standardized methods for performing polarization measurements (ASTM G5, G59, G61, G100, F746, and F2129).

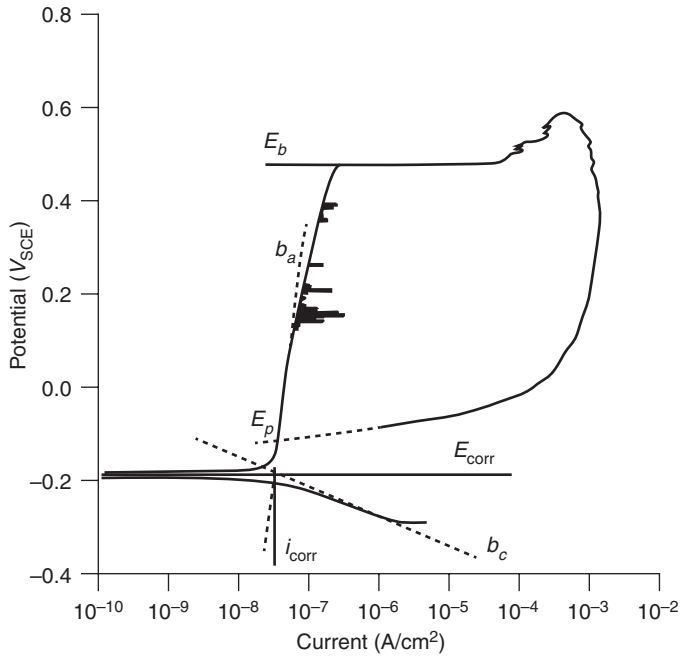
$$\eta = b_a \log(I) - b_a \log(I_{corr}) \qquad [7.4]$$

Polarization scans are made by scanning the electrode potential at a constant rate and measuring the current response; other methods also exist such as measuring current over a series of fixed potential values. Polarization scans to determine the corrosion rate are typically performed at a slow scan rate to minimize the effects of non-steady state reaction rates and the current error due to capacitive charging. Care must be used in designing the test sample and in setting up the test cell to yield useable results. Possible sources of error include non-corrosion oxidation reactions and non-voltage (i.e. reactant mass transport) rate control (Scully and Kelly, 2003).

There are two regions of the polarization plot which are of interest – small and large overpotentials. Different information regarding the corrosion performance of the weld can be derived from each overpotential region. Figure 7.2 shows a polarization scan from a typical corrosion experiment. Polarization scans at high overpotentials ($\eta > 30$ mV) are likely to introduce sample damage due to the forced corrosion. Evidence of corrosion damage can be seen in Figure 7.2 by the spikes indicating pitting on the forward scan and by the elevated current on the reverse scan. Corroded test samples cannot be re-used unless all corrosion damage can be removed (such as by re-polishing the sample surface).

At small values of overpotential ($\eta < 30$ mV) near E_{corr}, a linear plot of potential versus current can be obtained (see Fig. 7.3). The linear region typically consists of ±5–30 mV adjacent to E_{corr}. The slope of the plot in Fig. 7.3 is

© Woodhead Publishing Limited, 2013



7.2 Polarization scan for a 304SST sample performed in N_2 de-aerated, pH 7.4 phosphate buffered saline from –0.2 V vs open circuit potential (OCP) to 1 mA/cm^2 at 0.167 mV/s = 0.6 V/h, with the reverse scan also shown. The dashed lines, b_a and b_c, are the anodic and cathodic Tafel slopes which intersect at E_{corr} and I_{corr} (indicated by the solid horizontal and vertical lines, respectively). E_b and E_p are the breakdown and passivation potentials.

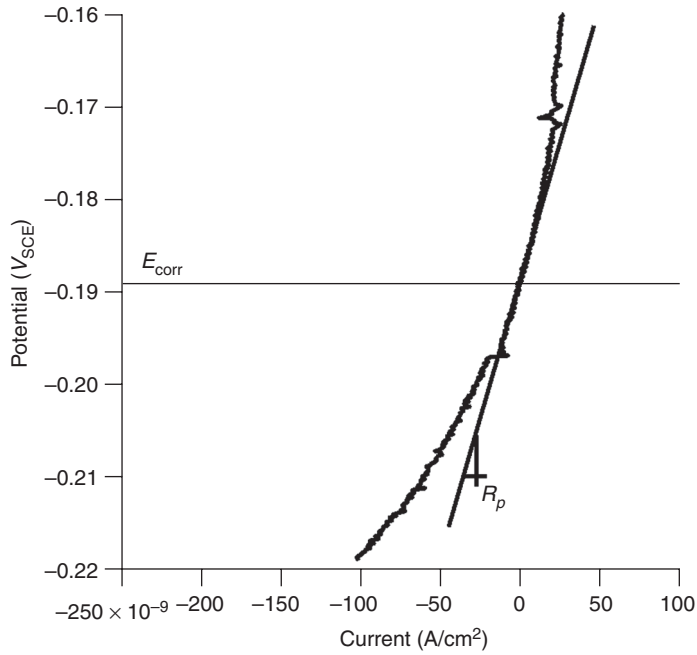
the polarization resistance (R_p) which may be used to calculate the corrosion current if the Tafel slopes (b_a and b_c) are known (see Equations [7.5] and [7.6] and ASTM G59); here B is the Stern–Geary coefficient. The Tafel slopes may be determined from regions of the Tafel plot at large overpotential.

$$R_p = \frac{B}{I_{\text{corr}}} \qquad [7.5]$$

$$B = \frac{b_a b_c}{\left[2.303\left(b_a + b_c\right)\right]} \qquad [7.6]$$

Figure 7.4 shows a typical Tafel plot. The linear portions of the E vs log(I) plot nearest to E_{corr} yield the Tafel slopes – b_a positive of E_{corr} and b_c negative of E_{corr}. From the Tafel equation (Equation [7.4]) we know that the intersection of the lines with slopes b_a and b_c on the polarization plot occurs at E_{corr}

© Woodhead Publishing Limited, 2013



7.3 Polarization resistance plot showing potential versus current for ±30 mV around E_{corr}. Polarization data from Fig. 7.2.

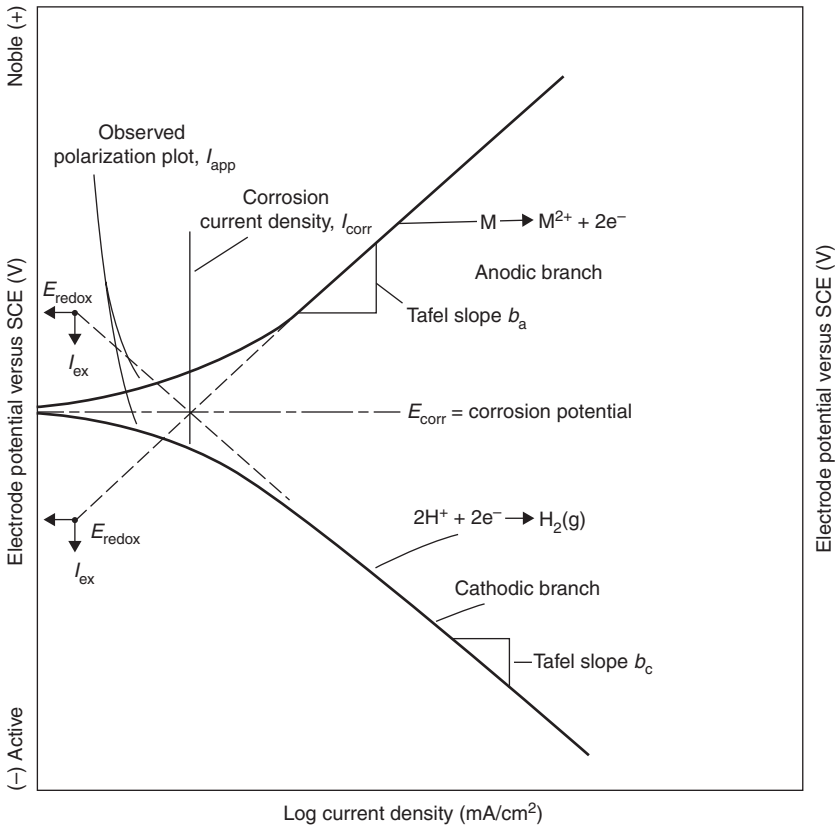
and the corrosion current (log (I_{corr})). This is a second means of determining I_{corr} called the Tafel extrapolation method – there is no standardized method for this technique.

So far we have used the data from the polarization scan to determine the rate of uniform weld corrosion. Polarization data may also be used to determine the susceptibility of a weld or material to localized corrosion (pitting or crevice) or to compare the stability of materials. Figure 7.2 shows points labeled E_b and E_p – the breakdown and re-passivation potentials, respectively. These points are taken at very large overpotential and yield comparative data about the stability of the metallic passivation layer and about the corrosion behavior.

Welds and materials whose corrosion rate is limited by a passivating oxide film may exhibit a breakdown potential (E_b) at which the slope of the potential vs corrosion current curve abruptly increases. The greater the value of E_b, the greater is the stability of the passivation mechanism and weld. The breakdown potential is typically defined as the initiation point of an increase of log(I) by at least two powers of ten (ASTM F2129).

After observing E_b, a polarization scan is typically reversed back to its starting potential. The behavior of the potential vs log(I) data over this reverse scan indicates the sample tendency to undergo pitting or crevice

© Woodhead Publishing Limited, 2013



7.4 Tafel plot showing Tafel slopes and extrapolation to graphically determine the values of E_{corr} and I_{corr}. The Tafel current is located at the intercept of the Tafel slopes, b_a and b_c. E_{corr} and I_{corr} are determined from this intercept. Saturated calomel electrode (SCE). (Taken from Wagner and Traud, 1938.)

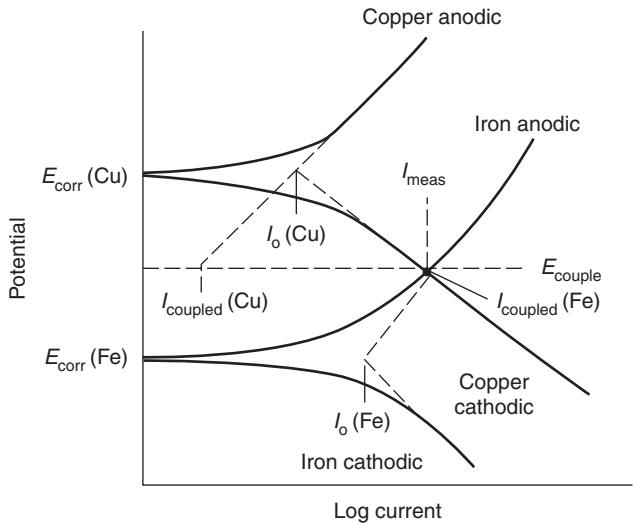
corrosion. If the reverse scan re-traces its forward path or falls below it, the risk of localized corrosion is low. If the current on the reverse scan remains elevated, it is likely that localized corrosion is present. Transient current spikes on the forward scan are another indicator of localized corrosion – these are localized corrosion events (pits or crevices) that spontaneously re-passivate. On the reverse scan, E_p is the protection potential where the reverse scan crosses the forward scan (ASTM F2129). The higher the value of E_p or the smaller the magnitude of $(E_b - E_p)$, the more resistant is the weld or material to localized corrosion.

Galvanic corrosion is caused by the electrochemical interaction of different metals or alloys (or by differing environmental conditions on the same material). One material or area serves as the counter-electrode to another corroding material or area; the materials and areas must be in both electrical

© Woodhead Publishing Limited, 2013

Table 7.3 Key variables and effects of galvanic corrosion

Variable	Effect of increase on corrosion rate
Ionic resistance	Decrease
Ohmic resistance	Decrease
Area ratio ($A_{reduction}/A_{oxidation}$)	Increase
Environmental uniformity	Decrease

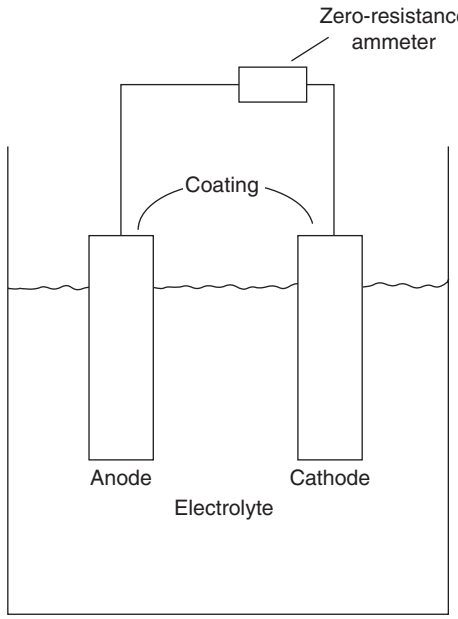


7.5 Use of polarization scans to predict the risk and rate of galvanic corrosion. (Taken from Hack and Taylor, 1987.)

and ionic contact. The main variables involved in galvanic corrosion are summarized in Table 7.3 along with their effects.

The risk and rate of galvanic corrosion may be predicted if polarization scans for the two materials of interest are available. Figure 7.5 shows polarization scans for two hypothetical materials (Cu and Fe) displayed on the same plot. It can be seen in Fig. 7.5 that galvanic corrosion is possible with copper serving as the counter-electrode to the corroding iron. The use of current (not area normalized current) is significant as the current density (current per area) of each material's polarization scan must be converted to current to reflect the surface area ratio present. The intersection of the polarization scans occurs at E_{corr} and I_{corr} for the galvanic couple. The predictive power of this technique depends on the accuracy of the polarization scans. If a risk of galvanic corrosion is indicated, it is recommended to complete a test for galvanic corrosion.

© Woodhead Publishing Limited, 2013



7.6 Galvanic corrosion test cell configuration for direct measurement of galvanic current. (Taken from Hack and Taylor, 1987.)

ASTM G71 provides a guide for performing galvanic corrosion testing. In its simplest form, a galvanic corrosion test is an immersion test with the entire galvanic couple contained on a single sample and immersed in electrolyte. The corrosion rate is then determined by mass loss, solution analysis, sample inspection, or a combination of the three. It is more advantageous to obtain a direct measurement of the corrosion rate by current measurement if possible. For a direct measurement, knowledge of the corroding system is used to separate the sample areas where reduction and oxidation occur and each portion is prepared as a separate test sample. Electrical connection is made external to the test cell where both samples are immersed under implant conditions. In this configuration, a zero-resistance ammeter can be used to monitor the galvanic current between the samples (see Fig. 7.6). Considerable time may be required for a stable galvanic current to be established (days to months); thus, maintenance of the test environment is critical. The expected trend for the current is to decrease and asymptotically approach a stable value over time.

For representative results it is important to approximate the area ratio, electrical resistance, and relative position present in the actual device. For the galvanic testing of welds, direct galvanic current measurement requires

© Woodhead Publishing Limited, 2013

the weld to be sectioned from the base material; in this case it may be more realistic to immersion test the entire device with the weld.

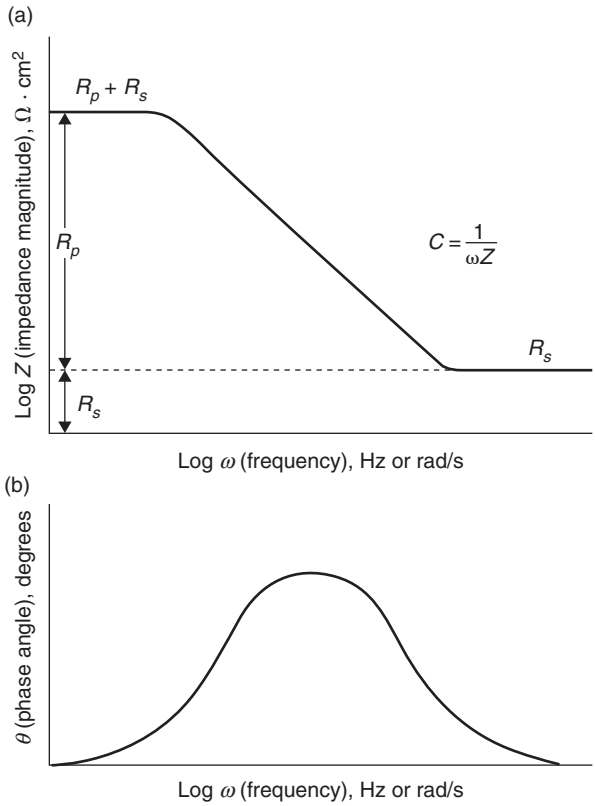
EIS is a measurement technique whereby a small sinusoidal input signal is applied to an electrical test sample (typically in a three-electrode test cell) and the sinusoidal response is measured for amplitude and phase-lag (Orazem, 2008). The input and output signals are paired voltage and current data. Through Ohm's law, the data pair may be converted into impedance. The introduction of the frequency time domain coverts resistance to impedance – impedance is resistance on a complex plane (real ~ in-phase, and imaginary ~ out-of-phase) measured in Ohms.

For corrosion measurements, EIS experiments are typically performed using a ±10 mV potential input signal to stimulate a current output signal over a frequency range from 10^5 Hz down to frequencies as low as 10^{-3} Hz. The potential signal is normally applied about E_{corr}, but the measurements can be performed at any desired potential. As the current signals are small and sensitive to noise, it is important to perform EIS experiments using a Faraday cage. A description of the symbols and basic equations used to describe impedance can be found in Orazem (2008) and Bard and Faulkner (2001).

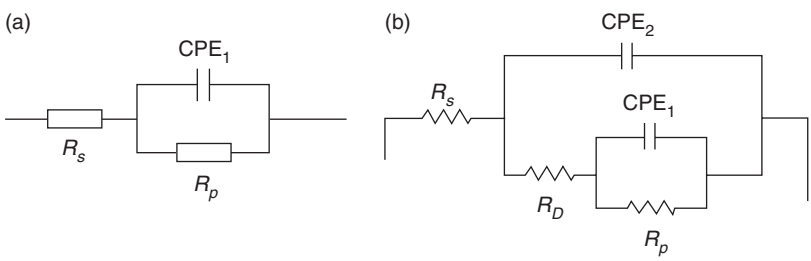
Figure 7.7 shows a typical graphical presentation of impedance data from a corrosion experiment. The value of using EIS to measure the corrosion rate is obtained by fitting an equivalent circuit to the impedance data. Software routines available with EIS measurement systems perform both EIS measurements and equivalent circuit fitting. EIS experiments performed near E_{corr} (as opposed to large overpotential polarization experiments) are non-destructive due to the small induced current. Thus, EIS may be used to monitor the corrosion rate of a sample over time provided that the test environment can be stably maintained. Figure 7.8 shows two common equivalent circuits which may be used to model impedance data. Note that constant phase elements (CPEs) are used in place of simple capacitors. CPEs can be thought of as non-ideal capacitors and are used to account for the effects of large electrochemical surface area and many parallel RC time constants. Circuit (b) may be used to model corrosion under paint or a defective passive film.

EIS data can be used to calculate corrosion rate through the determination of the polarization resistance (R_p) and prior knowledge of the Tafel slopes (b_a and b_c) using Equation [7.5] and [7.6]. It should be stressed that the use of this method requires knowledge of the corrosion area such that R_p can be area normalized. This requirement limits the use of this technique to uniform corrosion. In instances where the corroding area is unknown (such as localized corrosion using circuit (b)), while R_p may still be quantified, it cannot be assigned to a specific area. Thus, EIS for localized corrosion can be used to rank welds in terms of corrosion risk but not to measure the rate.

© Woodhead Publishing Limited, 2013



7.7 Example impedance data from a corrosion experiment; Bode plots of (a) total impedance and (b) phase angle vs log(frequency). (Taken from Scully and Kelly, 2003.)



7.8 EIS equivalent circuits for modeling EIS data from a corrosion experiment, (a) Randle's circuit and (b) two parallel resistor-capacitor (RC) time constants (τ = RC). R_s is the solution resistance, R_p is the polarization resistance, CPE_1 is the double-layer capacitance, R_D is the defect resistance, and CPE_2 is the passive film capacitance. (Taken from Mansfeld, 2003 and Mansfeld *et al.*, 1993.)

© Woodhead Publishing Limited, 2013

The use of EIS to monitor long-term corrosion is possible by following the trend of R_p (as R_p decreases, the rate of corrosion increases).

EIS is also useful for determining electrochemical surface area and for following surface area changes over time (such as may be due to corrosion). Both of the circuits in Fig. 7.8 measure double-layer capacitance using a CPE circuit element. The modeled equivalent circuit parameter values may be converted to an effective double-layer capacitance value as described in Hirschorn *et al*. (2010). Whether modeled as a simple capacitor or CPE, double-layer capacitance may be converted to microscopic surface area if an area-specific capacitance value for the corroding electrode is known (Murray *et al*., 1988). As such values have not been compiled for all electrode materials in all situations, it may not be possible to make a quantitative conversion; however, changes in double-layer capacitance are directly proportional to changes in surface area.

7.4 Considerations when gathering corrosion data

A critical decision that must be made in performing corrosion measurements is whether to test coupons or actual parts. Coupons are purpose-build weld samples for testing, while actual parts can be complete devices or subassemblies. Coupons can be more convenient but may require a separate manufacturing process and material supply from the device. If a coupon is chosen, care must be taken to ensure that the coupon is representative of the finished device with respect to materials, processes, and design. If a device is chosen for testing, size and fixturing concerns determine its utility. If a device is too large or small, it may be difficult to find a suitable test cell or equipment to accurately measure its corrosion rate. If too large, a good strategy is to fashion a test coupon from the device. If too small, several devices can be tested in parallel. Standardized test methods are a good source for possible test sample designs (ASTM F746, F2129, G5, G61, and G71).

The corrosion performance of a weld may be tested as part of a larger device or in isolation from adjacent device areas. While testing in an assembly may be more realistic, the test results will be less specific to the properties of the weld and more a function of the overall corrosion performance of the entre assembly. Testing the weld alone involves selecting a method for isolating the weld – by creating a welded test coupon, by mechanically sectioning the weld out of the larger device, by masking device areas outside the weld, or by miniaturizing the test cell such that only the weld is exposed (Garcia *et al*., 2008; Policastro *et al*., 2012; Suter and Bohni, 1997). Such decisions must be made in advance of testing based upon the desired goals of the test plan and the utility and economy of testing.

© Woodhead Publishing Limited, 2013

Table 7.4 Test specimen considerations

Source of variation	Corrosion test considerations
Man	Handling, contamination, operator variability
Materials	Supplier change, design change, composition variation, mechanical dimension variation, lot-to-lot variation
Methods	Process change, process variation, final process including sterilization and packaging, implant procedure
Machines	Process change, process variation, fixturing, set-up variation, contamination
Measurements	Precision, accuracy, test method, gauge study
Environment	Implant conditions (mechanical, electrical, chemical), test conditions, process environment, condition variations

The sources of variation inherent in the materials and methods used to produce the actual device must be considered when selecting and preparing a test specimen – failure to do so can generate invalid test results. In evaluations of medical device welds it may be necessary to consider applying conditioning steps prior to testing in order that the condition of the sample more closely matches its implanted state. Relevant considerations to ensure a representative corrosion test sample are summarized in Table 7.4. The reader should note the similarities between Table 7.4 and an Ishikawa or fishbone diagram for sources of process variation. The sample variables which affect the corrosion susceptibility of a weld are those that affect the surface of the sample. Table 7.5 summarizes the surface-condition variables which determine the corrosion risk of a weld sample.

One of the main factors controlling corrosion risk is the choice of the metal exposed to the electrolyte; the engineering of a stable weld–electrolyte interface decreases the corrosion risk. The surface roughness factor of a sample increases corrosion risk due to the probabilistic nature of corrosion – more area equals more risk. Additionally, surface roughness caused by pit or crevice-like features increases corrosion risk due to the formation of isolated environments which may accelerate corrosion. For active devices, additional surface area may decrease corrosion risk by decreasing current density. Geometry affects corrosion risk through crevice forming features which create isolated environments and through outside corners which concentrate current density. Inclusions of foreign materials or minor alloying elements on the sample surface increase corrosion risk due to possible galvanic interactions with the base material and through the additional surface area and pits which are formed after dissolution of the inclusions. Contamination on the weld surface can increase corrosion risk as the contaminants may contain chemical species which accelerate corrosion.

© Woodhead Publishing Limited, 2013

Table 7.5 Surface-condition sample variables affecting weld corrosion risk

Variable	Description	Effect
Material	Inherent stability of base-material weld alloy, or passivating surface oxide	Increasing stability decreases corrosion risk; galvanic cells increase corrosion risk
Surface roughness factor	Ratio of electrochemical surface area (wettable area including micro-scale features) to geometric surface area	Increasing value increases the corrosion risk for passive devices but may decrease the risk for active devices
Geometry	Sample shape including outside corners and pit or crevice-forming features	Outside corners increase corrosion risk for imposed current and voltage; pit or crevice-forming features increase corrosion risk
Inclusions	Minority metal or alloy impurities which form small particles upon solidification	Inclusions on the sample surface increase corrosion risk
Contamination	Embedded particles and machining lubricants on the weld surface	Increase corrosion risk

The number of samples to test is another important consideration. The number of samples required is determined by the precision and reliability required for the corrosion assessment. Good questions to consider are: What is the standard deviation of typical corrosion-rate measurements? What is the impact of corrosion to device function? What is the allowable patient or supplier risk of a corrosion failure? If a predicate design exists, is equivalence sufficient? How much improvement is required for a new design?

If at all possible, answer these questions before embarking on a test plan, and reference existing data sources whenever possible. It is advisable to use statistical methods to determine a sample size (ASTM G16 and Roberge, 2003). If no previous data exists with which to estimate the typical variation of the results for a corrosion test, consult the open literature, standardized test methods (especially round-robin test results), or corrosion handbooks (Cramer and Covino, 2003; Korb and Olson, 1987) for results from a similar material and test method.

7.5 Test sample preparation

Once a sample design has been selected, the sample must be prepared for test. There are two general types of corrosion tests – immersion and direct corrosion current measurements. Immersion tests require a minimum of

© Woodhead Publishing Limited, 2013

sample preparation, including cleaning and possibly a means for suspending the test articles in solution. Care must be taken in designing a specimen holding mechanism as contact between the specimen and the walls of the test vessel, other specimens, or a rack can create crevice-like isolated environments which may unrealistically accelerate corrosion. Immersion tests can be conducted in fully immersed, partially immersed, or gaseous exposure variations where the immersion medium is a liquid electrolyte. While full immersion is the most likely experienced test condition for medical device welds, the other variations should also be considered with knowledge of the use conditions. The preparation for any test which requires electrical measurements is more involved.

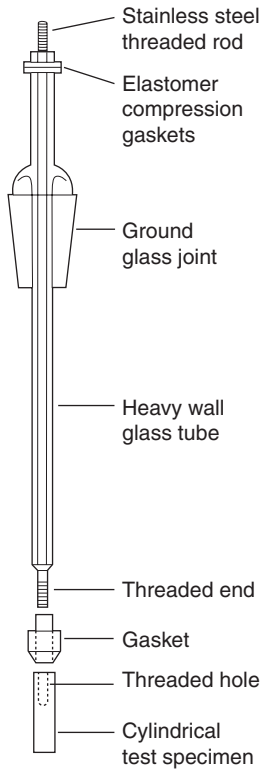
Most published corrosion studies involve grinding, polishing, and cleaning steps as part of preparing specimens for test; however, this practice may not be useful for testing medical device welds. If a simple comparative test of materials or devices is desired, standard sample preparation steps may be acceptable (ASTM G1). However, if a corrosion assessment for a finished device or weld is the goal, the test plan should be conducted using specimens in their as-manufactured state with a minimum of additional preparation steps.

Many standardized electrical test methods for corrosion assume a specific sample form factor (ASTM G5, G61, and F746); however, for medical device or weld corrosion testing, sample form factor flexibility is important (ASTM F2129). Reference to a standardized sample form and assembly will be used here to illustrate the important aspects of electrical sample construction (see Fig. 7.9).

The important aspects of electrical sample creation are electrical contact, sealing, and masking. A means of electrical contact to the sample is commonly created using a lead wire in electrical contact with the test sample. Electrical contact can be created by welding or by the use of conductive adhesive (such as silver-filled epoxy) – there are disadvantages to both methods. The creation of a welded connection requires fixtures for the weld and compatibility of the two materials being welded. Further, a weld creates heat-affected zones (in addition to the weld under test) that can affect the test results and should be masked. The use of conductive adhesive adds a foreign material to the test environment whose exposure will impact test results.

Materials that are used for masking must not react with the sample surface or release leachants which are electrochemically active or which contaminate the test surface. Masking materials that have been used with success include epoxy, silicone medical adhesive, lacquers (such as those used for metal plating – see Tolber Microstop), and photoresist. Good adhesion of the masking material is critical for valid test results. Loss of masking material adhesion leads to the formation of crevice-like microenvironments which accelerate corrosion and skew results.

© Woodhead Publishing Limited, 2013



7.9 Standardized test electrode and holder. (Taken from Mansfeld, 2003.)

Even if the electrical lead wire is of the same material as the test sample, it still must be isolated from the test environment so that it does not contribute to the current being measured. A good strategy for accomplishing this is to encase the lead wire in silicone or polyurethane tubing and backfill the lumen of the tubing where it contacts the device with silicone medical adhesive or another masking material.

Once a sample has been prepared for testing, it should be cleaned prior to placement in the test cell to remove the residues from sample preparation and handling. Cleaning should be completed as close to the start of testing as possible. Three cleaning steps are recommended: detergent washing to remove dirt and ionic contamination, organic solvent washing to remove grease and organic contamination, and water rinsing. Water rinsing is normally used after both detergent and organic cleaning steps and immediately prior to testing. Drying the sample between cleaning steps (using ambient drying, oven drying, or pressurized inert gas or air drying) is also important to prevent contamination of the next cleaning step. Care should be used to

© Woodhead Publishing Limited, 2013

ensure that the drying process does not introduce additional contamination (e.g., from compressor oil, particulates, or handling). If samples must be stored, they should be kept in a low-humidity environment such as a desiccator or glove box in a clean glass container. The use of glass containers is important to prevent contamination of the sample surface by plasticizers (such as from the surface of plastic containers and bags).

7.6 Instrumentation and equipment

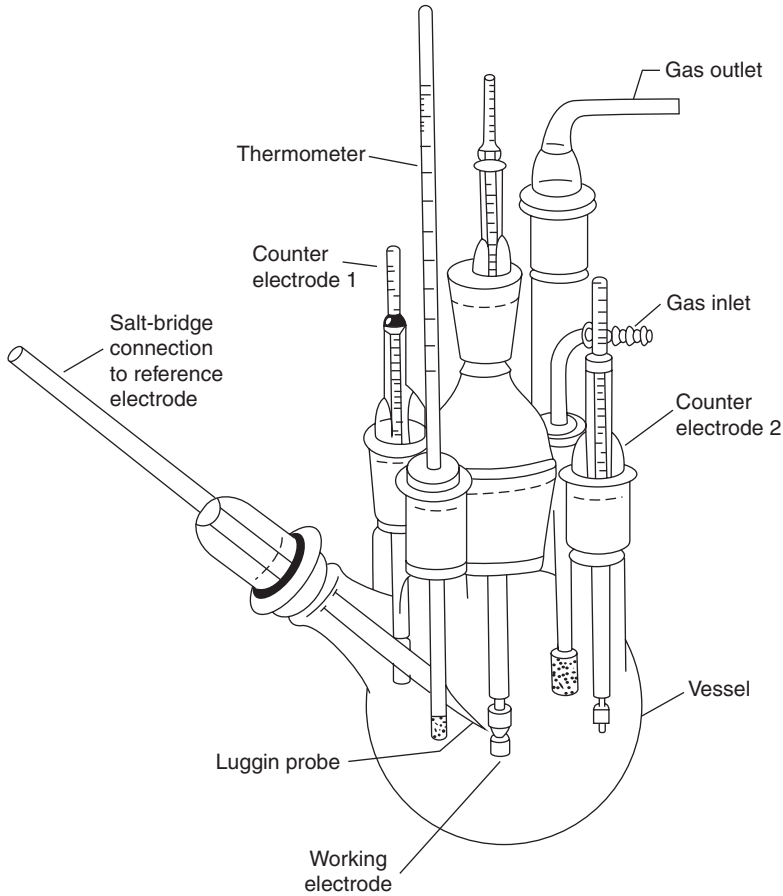
To conduct corrosion measurements, the basic instrumentation and equipment consists of a potentiostat and a test cell. For immersion corrosion tests, only a test cell is required. Modern potentiostats are computer controlled and some are even multi-channel and allow for the parallel testing of multiple samples. The instrument control software packages offer a variety of pre-programmed test methods and data analysis routines. Many potentiostats now include a built-in frequency response analyser function which may be used for EIS measurements. Good reviews of the types, uses, and configuration of electrochemical test equipment exist and should be consulted for further information (Mansfeld, 2003).

Test cell refers to the container in which a corrosion test is conducted. In general, the test cell design should be only as complex as necessary to simulate the implant conditions. For an immersion corrosion test, the test cell is normally a simple test rack, beaker, or sealable jar. For immersion tests in sealed containers, cell storage in an oven may provide a convenient means of temperature control. While less complex, the immersion test cell shares many of the same requirements with the more complicated electrical test cell used for direct measurements of corrosion current. Figure 7.10 shows the design of a three-electrode electrical test cell, and Table 7.6 lists the cell components from Fig. 7.10 along with their function and requirements.

The strategy to be considered when selecting a test cell is to ensure that no aspect of the cell design or materials will affect the results observed on the test sample. Gas-tight refers to the ability of the test cell to maintain a positive pressure of the gas being sparged relative to ambient conditions. It is common to use a water-filled air lock upstream of the test vessel to verify cell sealing and gas flow. For long-term tests, evaporation of the electrolyte due to gas sparging is an issue which may be addressed by periodic additions of the electrolyte solvent to restore the original volume or by pre-saturating the sparge gas with water using a bubbler. Liquid-tight, in regards to the working electrode holder, refers to the necessity of preventing electrolyte contact with the means of electrical connection. Inert refers to the requirement that none of the cell components react with or emit leachants which affect the test result.

The counter-electrode surface area requirement is necessary to ensure that the corrosion current on the working electrode is not limited by the

© Woodhead Publishing Limited, 2013



7.10 Electrical three-electrode corrosion test cell. (Taken from Scully, 1987.)

area of the counter-electrode or by a non-uniform electric field. The vessel volume requirement ensures that there are both sufficient electrolyte and reactants to prevent artificial mass-transport limitations on the working electrode corrosion rate (typical test cells contain 10–100 mL/cm^2 of working electrode). If possible, any temperature-control heating elements and stirring mechanisms should be physically remote from the test cell as these are common sources of electrical noise. For this reason, the test cell is often located within a Faraday cage to further reduce interference from electrical noise. Because the implant environment for a tissue-encapsulated device contains minimal mass transport, stirring of the test cell is likely unnecessary. During testing, the outlet of the gas sparge is often moved above the electrolyte surface to minimize stirring.

© Woodhead Publishing Limited, 2013

Table 7.6 Electrical test cell components, functions, and requirements

Component	Function(s)	Requirement(s)	Common materials/types
Salt bridge with Luggin probe	Ionic connection between test cell and RE; contains electrolyte; minimizes R_s	Positionable near WE; low leak rate of electrolyte; non-conductive; durable, gas-tight connection with vessel; inert	Glass tube with 1–3 mm diameter porous tip (typically Vycor glass)
Reference electrode (RE)	Quantifies potential of WE on a RE scale	Stable; accurate potential; resists contamination; durable	Most common are Ag/AgCl and Hg/Hg_2Cl_2
Counter electrodes	Balances current on WE	Surface area at least 10× greater than the WE; inert; uniform electric field w.r.t. WE; gas-tight connection with vessel and CE	Graphite or Pt
Working electrode (WE)	Test sample	Clean; representative; relevant	Disc, cylinder, coupon, or device/subassembly
Working electrode holder	Provides electrical connection to WE	Gas-tight connection with vessel; liquid- and gas-tight connection with WE; low resistance; inert	Wire or threaded rod inside a sealed, insulating sleeve or tube (glass or polymer)
Vessel	Contains electrolyte, gas, and cell components	Liquid-tight; gas-tight; inert; durable	Glass or inert plastic (PTFE or HDPE) of 250–1000 mL volume
Gas control	Allows for the sparging of various gasses and gas mixtures into the test cell and electrolyte	Gas-tight connection with vessel; maximize gas–liquid contact area; inert; positionable; adjustable flow-rate	Glass or plastic tube (PTFE, HDPE, or silicone) with a porous glass frit; 50–150 mL/min flow rate
Temperature control	Allows for the control of the temperature of the vessel, cell components, and electrolyte	Responsive; accurate; precise; low electrical noise	Jacket on cell with circulating water bath, immersion water bath, or oven; operating range 25–90°C
Stirring control	Allows for the mixing of the electrolyte	Allows for adjustable mixing; low electrical noise	Magnetic stir plate or provided by the convective action of gas sparging
Electrolyte	Provides ionic connection between cell components	Simulates the implant condition; stable	Typical simulated body fluids are 9 g/L NaCl and pH 7.4 phosphate buffered saline (PBS)

© Woodhead Publishing Limited, 2013

7.7 Interpretation of data

Every medical device weld has a point of greatest vulnerability (PGV) to corrosion damage as created by combined dimensional, mechanical, and electrical requirements. Additional requirements on the maximum corrosion rate are created by consideration of the impact of dissolved elements on patient toxicity. After the corrosion mode and rate have been characterized it is the responsibility of the corrosion engineer to assess the risk of corrosion to device function and patient safety.

The use of the corrosion rate for a corrosion prediction depends on the type of corrosion: uniform or localized. A uniform corrosion rate is applied as measured at the PGV. Conversely, a localized corrosion rate should be applied in a worst-case scenario given its inherent variability; the use of worst-case may entail assuming that all corrosion occurs in one location with a single pit or a representative distribution of localized corrosion features. Other methods of corrosion rate application can certainly be conceived, but a requirement for all of them is that the rationale is well considered and documented.

Mechanical requirements interact with corrosion due to the material removal and consequent reduction in dimensions. Further, localized corrosion creates pits or cracks which can act as stress concentrators that can greatly reduce the mechanical performance of a weld, material, or design. In assessing the risk of corrosion to mechanical weld performance, it is critical to understand the impact of dimension changes and flaws on device function. Such an assessment requires the corrosion engineer to work closely with the device design team. It is possible that additional mechanical testing of corrosion samples or normal welds with induced flaws or dimension reductions will be useful for assessing the risk of corrosion.

As above, the interaction of corrosion damage with weld or device electrical requirements necessitates a similar assessment of uniform or localized corrosion damage on device function. Again, it is necessary for the corrosion engineer to work closely with the device team. Further, any risk due to the accumulation of corrosion product should be considered (especially in the instance where corrosion may affect a mechanical electrical contact).

Even if considerations of corrosion damage with respect to mechanical and electrical requirements proves of little risk to device function, the rate of corrosion must still be considered in terms of patient toxicity. For toxicity analysis, Equation [7.1] is used to convert the corrosion current into a mass release rate for the elements in the weld. If solution analysis has been performed, such data may be used directly for this purpose. Databases exist (e.g. IRIS, Integrated Risk Information System) which list toxicity information for various elements; further, references for the elemental composition of various tissues and elemental excretion rates and routes should be

© Woodhead Publishing Limited, 2013

consulted when considering the toxicological risk of corrosion (Duck, 1990; Lentner, 1980, 1985, 1990). In the case of toxicity, the mode of corrosion is not important – only the elemental corrosion product release rate. Toxicity assessments require the corrosion engineer to collaborate with toxicologists and other biological response experts in order to develop a prediction of the risk of corrosion to patient safety. For a majority of medical device materials and devices, toxicity is usually not a concern because release rates are low.

7.8 Mitigations for weld corrosion

If corrosion is found to be an issue for the medical device weld under test, there are a number of different mitigation strategies which may be explored, as shown in Table 7.7.

Finding mitigations for a weld corrosion issue involves thinking broadly and creatively about all aspects of the material, sample preparation, and testing. First and foremost, the test method should be scrutinized to ensure that any observation of corrosion is valid. Only after the corrosion result has been verified should the other questions be considered. The types of solutions that are possible will depend on the stage of the product development

Table 7.7 Weld corrosion prevention strategies and considerations

Strategy	Questions
Test method	Was testing performed per procedure? Is the observed corrosion a test artifact? Were the samples properly prepared?
Device design	Is weld needed or can it be removed? Does the design of the weld accelerate corrosion? Can the weld be isolated from electrolyte contact? Is the device performing as intended?
Material selection	Is a galvanic couple present? Can more corrosion resistant metals be used? Do the metals meet specification? Did the supplier change? Did the supplier process change? Is the weld alloy less corrosion resistant than the parent materials?
Active device issue	Is the waveform correct? Can the waveform be changed?
Pre-weld preparation	Were the materials passivated? Were the materials cleaned?
Weld process	Does the weld process make the materials more likely to corrode? Can the weld process be changed? Is poor fixturing an issue? Was a cover gas used? Did the process change? Is process variability a concern?
Post-weld preparation	Was the weld passivated? Was the weld cleaned? Was the weld annealed? Could the weld be sensitized?
Protective coating	Can a protective coating be applied? Will the coating adhere and remain pin-hole and defect free?

© Woodhead Publishing Limited, 2013

project; in general, the availability of convenient solutions decreases with project time. Certainly, many solutions are possible given unlimited time and resources, but the corrosion engineer must be practical and seek an optimal solution given the inherent time and resource constraints. A good approach to maximizing the available solutions is to identify high corrosion-risk welds and test them as early in the project as possible. The corrosion engineer must be especially sensitive to material and process changes over time – welds that are not initially a concern for corrosion can become so if material specifications, material suppliers, or processes change.

7.9 Future trends

While corrosion and its causes have been studied extensively, advances in medical device design, materials, science, and computing power require the medical device corrosion engineer to continually refine the test methods for and understanding of corrosion.

The present state of corrosion assessment and testing is adequate for use by the medical device industry to market safe and reliable devices. What is needed is additional research with the goal of refining the understanding of the specific factors of the implant environment which impact the corrosion performance of medical device materials. These details may prove important as the trends of smaller device size and decreased cost combine to require the use of novel materials and decreased material dimensions.

One criticism of using *in vitro* test data to predict the implanted corrosion performance of a medical device weld is that the *in vitro* test environment does not exactly mimic the implant environment. Implanted welds are subject to all the complexities of the host immune response (Ratner *et al*., 2004), and it is difficult to ensure a test method captures all of the important aspects. For example, published literature contains conflicting reports regarding the effect of adsorbed proteins on metallic corrosion (Clark and Williams, 1982; Karimi *et al*., 2011). The specific effect of protein on corrosion (accelerating or protecting) seems to depend on the material and device being tested. The fact that these devices are put into diseased patients adds another degree of uncertainty. For example, many diseases are associated with infections which are oxidative in nature and may affect corrosion behavior.

Most corrosion-test methods account for ionic content, dissolved gas, temperature, and major protein species. Even so, it is possible for test data to differ somewhat from implant results (Witte *et al*., 2006). It would be useful for improved test methods to be developed via a refined understanding of the corrosion-relevant aspects of the implant environment (i.e. most test methods do not account for the direct action of living cells). It is conceivable that future test methods may use living cells and cell culture conditions (Tang *et al*., 2006).

© Woodhead Publishing Limited, 2013

Related to improvements in corrosion-test methods is the concept of designed experiments with the goal of establishing a direct correlation between *in vitro* and implant corrosion results. Due to the lack of full confidence in bench test data, animal experiments are routinely used to verify and validate bench results for many aspects of medical device development. However, animal experiments are costly in terms of time, resources, and animal life. If a correlation were developed between bench test and implant corrosion results (especially accelerated test results), time, expense, and animals could be spared. This type of correlation may need to be developed for each device type or tissue environment. Collaboration of the corrosion engineer with medical, veterinary, and biological experts is the key to the success of any such effort.

Computing power and speed continue to rapidly advance, and one of the fields to benefit is computer modeling. The medical device community is increasingly interested in the use of computer modeling to predict implanted device performance. Results from such efforts could be used to quickly test design and material options via computer models with the aim of improving device reliability. A key to accurate modeling efforts is a detailed understanding of use conditions, as these are inputs to any computer-based simulation. Another key is selection of the necessary variables to be included in the model. Computer simulations depend on detailed knowledge of the microstructure and properties of the materials being used. As the understanding of the impact of use conditions and material properties on corrosion performance is advancing, it would be useful to incorporate this knowledge into a predictive computer-based model. It is preferred for such a model to start from first principles to predict corrosion rates and device performance for a variety of materials and designs. Companies such as Vextec (www.vextec.com) are presently working in this direction with the aim of predicting the overall reliability of a device population by taking into account design, material microstructure, and process variability.

7.10 Sources of further information

Additional sources of information regarding corrosion (including books, journals, standards committees, and academic and industrial organizations) have been tabulated by Cramer *et al*. (2003, p. 999) and Bard and Faulkner (2001, p. 39).

7.11 References

ASTM International (2010), A262–10: Standard practices for detecting susceptibility to intergranular attack in austenitic stainless steels, Conshohocken, PA, USA, ASTM International.

© Woodhead Publishing Limited, 2013

ASTM International (2009), A763–93: Standard practices for detecting susceptibility to intergranular attack in ferritic stainless steels, Conshohocken, PA, USA, ASTM International.
ASTM International (2005), A967–05: Standard specification for chemical passivation treatments for stainless steel parts, Conshohocken, PA, USA, ASTM International.
ASTM International (2009), B117–09: Standard practice for operating salt spray (fog) apparatus, Conshohocken, PA, USA, ASTM International.
ASTM International (2009), F746–04: Standard test method for pitting or crevice corrosion of metallic surgical implant materials, Conshohocken, PA, USA, ASTM International.
ASTM International (2010), F1089–10: Standard test method for corrosion of surgical instruments, Conshohocken, PA, USA, ASTM International.
ASTM International (2008), F2129–08: Standard test method for conducting cyclic potentiodynamic polarization measurements to determine the corrosion susceptibility of small implant devices, Conshohocken, PA, USA, ASTM International.
ASTM International (2003), G1–03: Standard practice for preparing, cleaning, and evaluating corrosion test specimens, Conshohocken, PA, USA, ASTM International.
ASTM International (2004), G5–94: Standard reference test method for making potentiostatic and potentiodynamic anodic polarization measurements, Conshohocken, PA, USA, ASTM International.
ASTM International (2010), G16–95: Standard guide for applying statistics to analysis of corrosion data, Conshohocken, PA, USA, ASTM International.
ASTM International (2004), G31–72: Standard practice for laboratory immersion corrosion testing of metals, Conshohocken, PA, USA, ASTM International.
ASTM International (2005), G46–94: Standard guide for examination and evaluation of pitting corrosion, Conshohocken, PA, USA, ASTM International.
ASTM International (2009), G48–03: Standard test methods for pitting and crevice corrosion resistance of stainless steels and related alloys by use of ferric chloride solution, Conshohocken, PA, USA, ASTM International.
ASTM International (2009), G59–07: Standard test method for conducting potentiodynamic polarization resistance measurements, Conshohocken, PA, USA, ASTM International.
ASTM International (2009), G61–86: Standard test method for conducting cyclic potentiodynamic polarization measurements for localized corrosion susceptibility of iron-, nickel-, or cobalt-based alloys, Conshohocken, PA, USA, ASTM International.
ASTM International (2009), G71–81: Standard guide for conducting and evaluating galvanic corrosion tests in electrolytes, Conshohocken, PA, USA, ASTM International.
ASTM International (2010), G102–89: Standard practice for calculation of corrosion rates and related information from electrochemical measurements, Conshohocken, PA, USA, ASTM International.
Bard, A. J. and Faulkner, L. R. (2001), *Electrochemical Methods: Fundamentals and Applications*, Hoboken, NJ, USA, John Wiley & Sons.
Clark, G. C. F. and Williams, D. F. (1982), 'The effects of proteins on metallic corrosion', *J. Biomed. Mat. Res.*, **16**, 125–134.

© Woodhead Publishing Limited, 2013

Cramer, S. D. and Covino, B. S. (2003), *ASM Handbook: Volume 13A Corrosion: Fundamentals, Testing, and Protection*, Materials Park, OH, USA, ASM International.

Cramer, S. D., Covino, B. S., Holcomb, G. R., and Ziomek-Moroz, M. (2003), 'Information sources and databases for the corrosionist', in S. D. Cramer and B. S. Covino, eds, *ASM Handbook: Volume 13A Corrosion: Fundamentals, Testing, and Protection*, USA, ASM International, 999–1001.

Duck, F. A. (1990), *Physical Properties of Tissue: A Comprehensive Reference Book*, San Diego, CA, USA, Academic Press.

Garcia, C., Martin, F., de Tiedra, P., Blanco, Y., and Lopez, M. (2008), 'Pitting corrosion of welded joints of austenitic stainless steels studied by using an electrochemical minicell', *Corr. Sci.*, **50**, 1184–1194.

Hack, H. P. and Taylor, D. (1987), 'Evaluation of galvanic corrosion', L. J. in Korb and D. L. Olson, eds. *ASM Handbook: Volume 13 Corrosion*, USA, ASM International, 234–238.

Harris, D. C. (2003), *Quantitative Chemical Analysis*, New York, NY, USA, W. H. Freeman & Co.

Hirschorn, B., Orazem, M. E., Tribollet, B., Vivier, V., Frateur, I., and Musiani, M (2010), 'Determination of effective capacitance and film thickness from constant-phase-element parameters', *Echim. Acta.*, **55**, 6218–6227.

Holme, B. and Lunder, O. (2007), 'Characterisation of pitting corrosion by white light interferometry', *Corr. Sci.*, **49**, 391–401.

Jones, D. A. (1996), *Principles and Prevention of Corrosion*, Upper Saddle River, NJ, USA, Prentice Hall.

Karimi, A., Nickchi, T., and Alfantazi, A. (2011), 'Effects of bovine serum albumin on the corrosion behavior of AISI 316L, Co-28Cr-6Mo, and Ti-6Al-4V alloys in phosphate buffered saline solutions', *Corr. Sci.*, **53**, 3262–3272.

Korb, L. J. and Olson, D. L. (1987), *ASM Handbook: Volume 13 Corrosion*, USA, ASM International.

Lentner, C. (1980), *Geigy Scientific Tables, Vol. 1: Units of Measurement, Body Fluids, Composition of Body, Nutrition*, West Caldwell, NJ, USA, Ciba-Geigy Corporation.

Lentner, C. (1985), *Geigy Scientific Tables, Vol. 3: Physical Chemistry, Composition of Blood, Hematology, Somatometric Data*, West Caldwell, NJ, USA, Ciba-Geigy Corporation.

Lentner, C. (1990), *Geigy Scientific Tables, Vol. 5: Heart and Circulation*, West Caldwell, NJ, USA, Ciba-Geigy Corporation.

Mansfeld, F. (2003), 'Electrochemical methods of corrosion testing', in S. D. Cramer and B. S. Covino, eds, *ASM Handbook: Volume 13A Corrosion: Fundamentals, Testing, and Protection*, USA, ASM International, 446–462.

Mansfeld, F., Shih, H., Greene, H., and Tsai, C. H. (1993), 'Analysis of EIS data for common corrosion processes', in J. R. Scully, D. C. Silverman, and M. W. Kendig, eds, *STP 1188: Electrochemical Impedance: Analysis and Interpretation*, USA, ASTM International, 37.

Murray, J. N., Moran, P. J., and Gileadi, E. (1988), 'Utilization of the specific pseudocapacitance for determination of the area of corroding steel surfaces', *Corrosion*, **44**, 533–538.

Orazem, M. E. and Tribollet, B. (2008), *Electrochemical Impedance Spectroscopy*, Hoboken, NJ, USA, John Wiley & Sons.

© Woodhead Publishing Limited, 2013

Policastro, S. A., Auyeung, R. C. Y., Martin, F. J., Rayne, R. J., Pique, A., Lewis, A., Geltmacher, A., and Natishan, P. M. (2012), 'An approach for determining microscale electrochemical behavior', *J. Electrochem. Soc.*, **159**, C15–C24.

Ratner, B. D., Hoffman, A. S., Schoen, F. J., and Lemons, J. E. (2004), *Biomaterials Science (2nd edn): An Introduction to Materials in Medicine*, London, UK, Elsevier Academic Press.

Roberge, P. R. (2003), 'Statistical interpretation of corrosion test results', in S. D. Cramer and B. S. Covino, eds, *ASM Handbook: Volume 13A Corrosion: Fundamentals, Testing, and Protection*, USA, ASM International, 425–429.

Scully, J. R. (1987) 'Electrochemical methods of corrosion testing', in L. J. Korb and D. L. Olson, eds, *ASM Handbook: Volume 13 Corrosion*, USA, ASM International, 212–220.

Scully, J. and Kelly, R. G. (2003), 'Methods for determining aqueous corrosion reaction rates', in S. D. Cramer and B. S. Covino, eds, *ASM Handbook: Volume 13A Corrosion: Fundamentals, Testing, and Protection*, USA, ASM International, 68–86.

Suter, T. and Bohni, H. (1997), 'A new microelectrode method to study pit initiation on stainless steels', *Echim. Acta.*, **42**, 3275–3280.

Tang, Y.-C., Katsuma, S., Fujimoto, S., and Hiromoto, S. (2006), 'Electrochemical study of type 304 and 316L stainless steels in simulated body fluids and cell cultures', *Acta. Biomat.*, **2**, 709–705.

Vander Voort, G. F. (1984), *Metallography: Principles and Practice*, New York, NY, USA, McGraw-Hill Book Company.

Vander Voort, G. F. (2004), *ASM Handbook: Volume 8 Metallography and Microstructures*, USA, ASM International.

Wagner, C. and Traud, W. (1938), 'Über die deutung von korrosionsvorgängen durch überlagerung von elektrochemischen teilvorgängen und über die potentialbildung an mischelektroden', *Z Elektrochem.*, **44**, 391–402.

Weast, R. C. (1983), *CRC Handbook of Chemistry and Physics*, Boca Raton, FL, USA, CRC Press, Inc.

Witte, F., Fischer, J., Nellesen, J., Crostack, H.-A., Kaese, V., Pisch, A., Beckmann, F., and Windhagen, H. (2006), 'In vitro and in vivo corrosion measurements of magnesium alloys', *Biomaterials*, **27**, 1013–1018.

© Woodhead Publishing Limited, 2013

8

Laser hermetic welding of implantable medical devices

J. XIE, Advanced Bionics, USA

DOI: 10.1533/9780857096425.2.211

Abstract: Hermeticity is required for implantable medical devices to protect the microelectronic circuits inside the device from moisture-related failures when the device is implanted in the human body. Pulsed Nd:YAG laser welding is the most often used hermetic sealing technique in the medical-device industry due to the reliability and consistency of seam welds. To better understand and use laser hermetic welding for implantable medical devices, this chapter discusses the theory of laser conduction welding including absorption of laser energy and the laser melting process, fundamentals of laser beams and optics, critical process parameters, typical weld defects and their root causes. Additionally, testing methods for the hermeticity of welded implantable medical devices, such as helium mass spectrometry and residual gas analysis, are briefly described.

Key words: hermeticity, hermetic welding, laser welding, Nd:YAG pulsed laser, focused laser beam, laser absorption, laser melting, weld defect, implantable medical device, implant, titanium, reliability, leak test.

8.1 Introduction

Implantable medical electronic devices, such as pacemakers, implantable cardioverter defibrillators and neurostimulators (spinal-cord stimulators, deep-brain stimulators and cochlear implants, etc.), manage and treat physiological conditions within the human body, for example cardiac arrhythmia, chronic pain, Parkinson's disease and profound deafness. The patient's demands for improved life quality drive the implantable medical electronic devices to grow fast in a rate of double-digitals over last decade. These implantable electronic devices typically consist of microelectronic circuits hermetically sealed in a metal or ceramic package. To protect the microelectronic circuits in the sealed package, the package is required to be hermetically sealed for implantation in human body. The moisture from body fluid can directly cause the failure of microelectronic circuits in case of hermeticity loss. The implantable medical electronic devices are generally considered as the most reliable assemblies and the reliability is the top priority for

© Woodhead Publishing Limited, 2013

commercially distributed devices over performance, size and cost. Among all failures of the implantable medical electronic devices, hermeticity loss is one of the top failure modes (Liu *et al.*, 2007).

Laser welding is the most often used hermetically sealing technique in the manufacturing of implantable medical devices. Specially, pulsed Nd:YAG lasers are typically used to hermetically weld a metallic case to seal the microelectronic circuits inside. Laser welding is performed in a controlled inert gas environment and the inert gases are sealed into the device. In this chapter, the theory of laser absorption by the metals and laser melting process are described to better understand the laser welding process, the requirements to achieve consistent hermetic weld and the factors affecting the weld quality are discussed. In addition, the testing methods of hermeticity, including helium mass spectrometer and residual gas analysis, are briefly explained.

8.2 Hermetic-sealing techniques

There are a number of welding and joining techniques that can potentially provide a hermetically sealed joint for implantable medical devices. However, many of them have limitations to use for the application of implantable medical devices:

- *Micro-TIG or micro-plasma welding*: Although the micro-scale arc/plasma welding techniques have lower heat input than most arc fusion welding processes, the heat input is still too high to microelectronic components in the device and it is possible thermally damage the components during welding.
- *Electron beam (EB) welding*: EB welding is a low heat input process which does not thermally damage the electronic circuits but the requirement of vacuum for electron beams limits the efficiency in manufacturing.
- *Circular projection welding*: This technique might be used for a certain round joint design but the process is sensitive to the surface conditions and the long-term hermeticity in volume production is a concern.
- *Solid-state welding techniques such as friction welding, ultrasonic welding and resistance seam welding*: These processes have a physical contact to the components of the device and the geometry of the device constrains the applications to medical devices. Some of the techniques could be used for dissimilar metal joints in component level, but it is rarely used for final hermetic welding of a device due to long-term reliability.
- *Brazing*: This is a high-temperature process in an oven and typically used for the manufacturing in component-level assembly.
- *Metal to glass sealing*: The process is typically used for component level and the process temperature is lower than brazing.

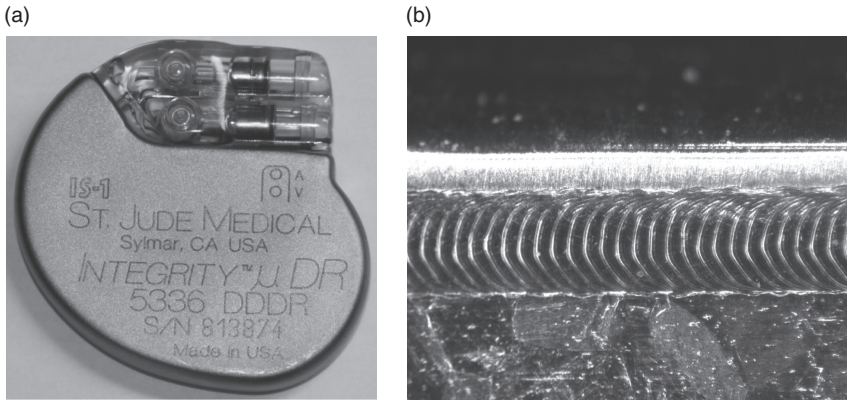
© Woodhead Publishing Limited, 2013

Laser welding is the most commonly used technique to hermetically seal the device in the medical-device industry. Laser welding offers a number of benefits over other welding and joining processes:

- *Reliability*: Laser hermetic seam weld is one of the most reliable hermetic-sealing joints. The seam-weld metal has almost the same mechanical and physical properties as the base metals.
- *Low heat input*: Laser heat input is significantly less than other welding processes. Pulsed laser welding is often used over CW (continuous wave) laser welding for further reduction in heat input. The average laser power used for implantable medical device is about 10–30 Watts.
- *Localized heating*: The temperature in the weld area is high but it decreases dramatically along the distance. This feature minimizes the chance of thermal damage to microelectronic components during welding.
- *Minimal weld distortion due to the low heat input*: Implantable medical devices typically use thin-wall metallic cases which potentially lead to distortion after welding due to the residual stress around the seam weld.
- *Consistency of weld quality*: The stable output of laser pulses makes consistent and repeatable hermetic welds. This is a guarantee for long-term hermeticity in volume manufacturing.
- *Autogenous welding*: No filler material is needed but a good fit-up between two parts is required.
- *Precision process*: The tiny laser spot of a focused laser beam makes it possible to weld the small devices.
- *Non-contact process*: Laser welding can be performed in a limited space if the access of the laser beam is available. The non-contact process feature provides the flexibility in join design as well.
- *Ease of automation*: A laser system is typically integrated with an automatic motion system to achieve uniform overlap rate of pulsed spot welds for irregular-shape medical devices.

There are a number of industrial lasers potentially available for hermetic welding of implantable medical devices (such as sealed CO_2 lasers, diode-pumped or lamp-pumped Nd:YAG lasers, fibre lasers, near-infrared wavelength or green lasers, continuous wave or pulsed lasers). However, pulsed Nd:YAG lasers with the fundamental wavelength (1060 nm) are currently most often used in the volume manufacturing in the medical-device industry due to the factors of laser pulse output, laser energy stability, equipment reliability and maintenance and capital and operational cost. All discussion in the chapter is based on pulsed Nd:YAG laser welding, unless otherwise specified. An implantable pacemaker hermetically

© Woodhead Publishing Limited, 2013



8.1 Hermetically welded pacemaker (Xie and Safarevich, 2003).

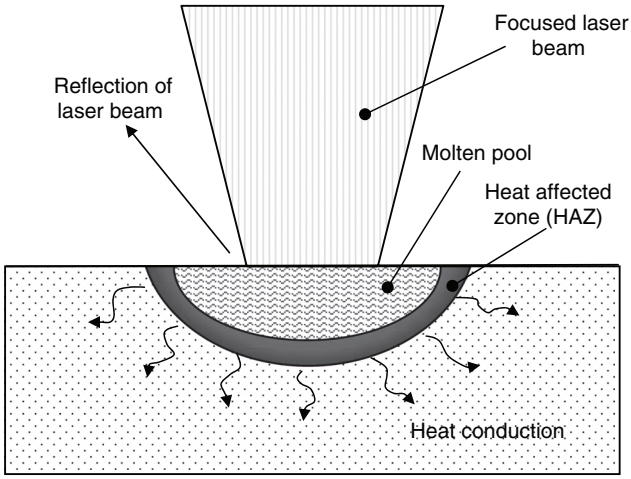
welded by a pulsed Nd:YAG laser (Xie and Safarevich, 2003) is shown in Fig. 8.1.

8.3 Laser conduction welding

Implantable medical devices are designed to be miniature and lightweight so that a thin metallic case is used for hermetic sealing. As a result, laser conduction welding mode instead of keyhole welding mode is more appropriate to achieve the shallow weld of the thin cases. Laser conduction welding mode is a process whereby a focused laser beam impinges upon the surface of the metallic substrate and the laser beam is partially absorbed by the metallic surface to melt the substrate by heat conduction and the rest the laser beam is reflected away by the surface (Fig. 8.2). A portion of absorbed laser energy is conducted away in the substrate as heat loss and a heat affected zone (HAZ) is formed adjacent to the molten pool. As a result, the weld depth is smaller than weld width in the conduction welding mode (Fig. 8.3a). The weld surface is smooth with no or little spattering after welding.

Keyhole welding mode is a process in which the laser beam has a power density high enough to vaporize a substantial amount of material to create a 'keyhole' in the substrate (Xie, 1999, 2002). Nearly 100% laser beam is 'absorbed' or trapped by the keyhole due to multiple reflections along the side wall of the keyhole. In the keyhole welding mode, the weld depth is typically equal or greater than the weld width as shown in Fig. 8.3b. Spattering is often observed in the keyhole welding due to the violent movement of liquid in the keyhole and vaporizing of liquid metals (Xie, 1999). Keyhole welding mode is rarely used for implantable medical devices due to the

© Woodhead Publishing Limited, 2013



8.2 A focused laser beam impinges on a metallic surface.

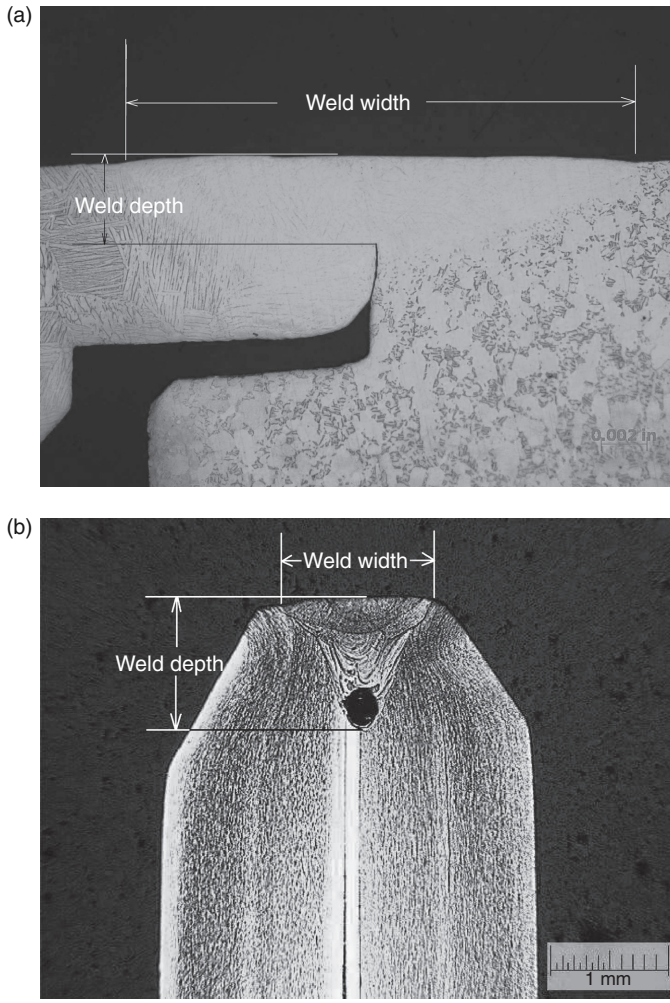
possible collapse of the keyhole to cause a void at the bottom of the weld. The hermeticity of implantable medical devices is not guaranteed when a void is present in the laser weld (Fig. 8.3b). For a non-hermetic weld such as mechanical connection joints, both keyhole and conduction welding modes can be used depending on a specific joint design and joint requirements.

In laser conduction welding, the power density of Nd:YAG laser beams is typically in the order of 10^9 W/m^2 or higher depending on materials to be welded. For the materials with high absorptivity and low thermal conductivity, such as titanium or stainless steel, it is relatively easy to achieve a keyhole welding mode at a certain power density than the materials with a low absorptivity (gold, platinum, etc.). Experimental analysis shows that the weld depth increases slowly with the power density in conduction welding mode but it sharply increases with power density once a keyhole is created.

8.3.1 Laser energy absorption

The absorption of laser energy by a specific material, or absorptivity, is an important parameter affecting the material melting in laser conduction welding. Only a portion of the incident laser energy is absorbed for welding and the rest of laser energy is reflected away by the substrate surface. The absorption is basically a process of laser–materials interactions and the process is usually called Fresnel Absorption (Xie *et al.*, 1997). According to the classical theory of electrodynamics, the components of the electric field of lasers interact with the electric dipole moments of the metal atoms. The infrared absorption of metals mainly depends on conductive absorption

© Woodhead Publishing Limited, 2013



8.3 Cross-sections of laser welds by conduction and keyhole welding: (a) conduction weld; (b) keyhole weld.

by free electrons. The energy of these energetic electrons is transferred to the vibrating lattice by collisions which heat up the material. Therefore, the absorption of laser energy by metals largely depends on conductive absorption by free electrons and the absorptivity is a function of the electrical resistivity of the substrate (Xie *et al.*, 1997).

The Hagen–Ruben relation, which defines the reflectivity of a solid surface in terms of the frequency of radiation of the conductivity of the solid, is used to determine the absorptivity (Xie *et al.,* 1997).

© Woodhead Publishing Limited, 2013

$$A = 365.15\sqrt{\frac{\rho_{DC}}{\lambda}} \quad [8.1]$$

where ρ_{DC} is the DC resistivity of metals in units of Ω-m and λ is the wavelength of laser beams in unit of μm. For Nd:YAG lasers with a wavelength of 1.06 μm, the absorptivity becomes:

$$A_{Nd:YAG} = 354.67\sqrt{\rho_{DC}} \quad [8.2]$$

In the case of CO_2 lasers with a wavelength of 10.6 μm, the absorptivity is

$$A_{CO_2} = 112.2\sqrt{\rho_{DC}} \quad [8.3]$$

Equation [8.3] is the equation same as that obtained by other researchers based on Fresnel absorption of CO_2 lasers (Arata and Miyamota, 1972). It can be seen from Equations [8.2] and [8.3] that the absorptivity of Nd:YAG lasers is 3.16 times higher than that of CO_2 lasers.

The absorptivity can be estimated for some metals using the above equations and given electric resistivity from the references (Touloukian *et al.*, 1970; Iida and Guthrie 1988). The absorptivity for both CO_2 and Nd:YAG lasers is calculated in Table 8.1. Note that the theoretical absorptivity is based on the assumption of pure polished metallic surface and no vapour plums above the substrate surface.

Titanium and its alloys are often used for implantable medical devices due to the features of biocompatibility, corrosion resistance, light weight, mechanical properties and manufacturability (formability and weldability).

Table 8.1 Absorptivity (%) of laser beam at room and melting temperature

	Room temperature		Melting temperature (liquid state)	
	CO_2 laser	Nd:YAG laser	CO_2 laser	Nd:YAG laser
Aluminum	1.86	5.88	6.4	20.2
Copper	1.55	4.89	5.1	16.1
Iron	3.07	9.71	13.0	41.1
Nickel	4.70	14.88	10.3	32.6
Titanium	8.13	25.70	13.7	43.3
Carbon steel	2.75	8.69	12.1	38.2
Stainless steel	9.72	30.72	14.0	44.2

Source: Xie *et al.* (1997).

© Woodhead Publishing Limited, 2013

Compared with other metals, titanium has a higher absorptivity and is easy for laser welding at low laser energy. In laser conduction welding, it is expected that the absorptivity of titanium substrate is higher than the value in liquid state in Table 8.1 due to the high temperature of molten pool but the vapour or plasma plume above the titanium substrate may affect the absorption of the Nd:YAG laser beam as well. In general, titanium and its alloys have excellent laser weldability and good welds can be achieved without significantly technical hurdles for medical devices.

A surface oxide of metals can significantly increase the absorptivity of laser beams. An experiment showed that the absorptivity of cold rolled steel was almost doubled after exposed to an air furnace at 1000°C for 40 s (Xie and Kar, 1999). Titanium is an active element and can be oxidized quickly when exposed to a temperature above 500°C in air and the surface turns to be discoloured (blue, straw or purple). When titanium is exposed to air at the room temperature, a thin and shine oxide film is formed on the surface to protect the bulk titanium from further oxidizing. The thin oxide film formed at room temperature has no impact on the laser welding process.

It is noted from the Table 8.1 that copper has the lowest absorptivity and majority of laser energy is reflected away. This explains that copper is very difficult for Nd:YAG lasers to weld at the wavelength of 1.06 μm, but copper is a suitable material for laser welding fixture as the laser beam will not damage the fixture in case of misfiring and copper is also an excellent heat sink to protect the device from overheating.

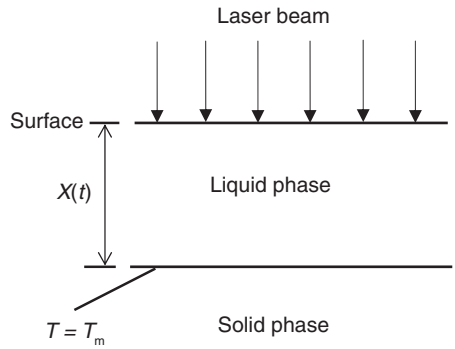
8.3.2 Laser melting process

Once the laser beam irradiates on the surface of a substrate and is absorbed by the substrate, the surface temperature increases until melting to form a weld pool. The boundary of liquid and solid phases $X(t)$ – melt depth during welding or weld depth after welding – keeps moving down until the laser is turned off. The laser melting process can be simplified as a one-dimensional heat conduction problem with the assumption that the diameter of the laser beam is large enough compared with the regions of interest as described in Fig. 8.4.

There are a number of mathematical models to predict the weld depth at various conditions and assumptions. The simplest expression of melt depth with an assumption of same thermal and physical properties in the solid and liquid phases is given by (Cohen and Epperson, 1968)

$$X(t) = \frac{0.16AI}{\rho L}(t - t_m) \qquad [8.4]$$

© Woodhead Publishing Limited, 2013



8.4 A semi-infinite substrate under laser irradiation.

where $X(t)$ is the melt depth, A is the absorptivity, I is the power density of laser beam, ρ is the density, L is the latent heat, t is the time from the start of the laser irradiation and t_m is the time to start melting at the substrate surface. The melting time t_m is given by (Cohen and Epperson, 1968)

$$t_m = \frac{\pi k_s^2 T_m^2}{4\alpha_s (AI)^2} \qquad [8.5]$$

Here α and k are thermal diffusivity and thermal conductivity while the subscript s and l represent solid and liquid phases, respectively. T_m is the melting temperature of substrate.

A more precise model was developed to consider the difference of thermal and physical properties in solid and liquid phases and the Stefan condition of latent heat transfer at the solid–liquid boundary (Xie and Kar, 1997) is considered. The governing equations and the boundary conditions in the model are given below

$$\frac{\partial^2 T_l(x,t)}{\partial x^2} - \frac{1}{\alpha_l}\frac{\partial T_l(x,t)}{\partial t} = 0 \qquad 0 \le x \le X(t) \qquad [8.6]$$

$$\frac{\partial^2 T_s(x,t)}{\partial x^2} - \frac{1}{\alpha_s}\frac{\partial T_s(x,t)}{\partial t} = 0 \qquad X(t) \le x \le \infty \qquad [8.7]$$

$$T_l(x,t) = T_s(x,t) = T_m \qquad x = X(t) \qquad [8.8]$$

$$k_l \frac{\partial T_l(x,t)}{\partial x} = k_s \frac{\partial T_s(x,t)}{\partial x} - \rho L \frac{\mathrm{d}X(t)}{\mathrm{d}t} \qquad x = X(t) \qquad [8.9]$$

© Woodhead Publishing Limited, 2013

$$-k_l \frac{\partial T_l(x,t)}{\partial x} = AI \qquad x = 0 \qquad [8.10]$$

$$T_s(x,t) = T_0 \qquad x \to \infty \qquad [8.11]$$

$$T_s(x,t) = T_0 \qquad t = 0 \qquad [8.12]$$

$$X(t) = 0 \qquad t = 0 \qquad [8.13]$$

Here T_i, α_i and k_i are temperature, thermal diffusivity and thermal conductivity of the i-th phase respectively, where $i = l$ and $i = s$ represent the liquid and solid phase respectively. x is the distance from the surface of the workpiece, t is the irradiation time, T_m is the melting point, ρ is the density, L is the latent heat of fusion, T_0 is the initial temperature.

The above-mentioned equations are a set of non-linear partial differential equations due to the non-linearity of the Stefan condition at the solid–liquid interface and an approximate solution was obtained for the one-dimensional phase-change heat conduction problem with time-dependent surface temperature involving laser irradiation (Xie and Kar, 1997). The approximate solution for the melt depth and melting velocity is found to be

Melt depth:

$$X(t) = \left[-\frac{b_1}{2} + \left(\frac{b_1^2}{4} + \frac{a_1^3}{27} \right)^{1/2} \right]^{1/3} + \left[-\frac{b_1}{2} - \left(\frac{b_1^2}{4} + \frac{a_1^3}{27} \right)^{1/2} \right]^{1/3} - \frac{\alpha_l m_s}{16AI} \qquad [8.14]$$

Melting velocity:

$$\frac{\mathrm{d}X(t)}{\mathrm{d}t} = \frac{2AI}{\left[k_s \left(T_m - T_0 \right)/\alpha_s + \rho L \right] \left\{ 1 + \sqrt{1 + \left(AIX(t)/\alpha_l \left[k_s \left(T_m - T_0 \right)/\alpha_s + \rho L \right] \right)} \right\}} \qquad [8.15]$$

where

$$a_1 = \frac{3\alpha_l^2 m_s^2}{16(AI)^2} \left(\frac{48(AI)^2 t}{\alpha_l m_s^2} + 31 \right) \qquad [8.16]$$

$$b_1 = -\frac{\alpha_l}{AI} \left[\frac{\alpha_l^2 m_s^3}{32(AI)^2} \left(\frac{72A^2 I^2 t}{\alpha_l m_s^2} + 47 \right) + \frac{3t(3A^2 I^2 t + 2\alpha_l m_s^2)}{m_s} \right] \qquad [8.17]$$

© Woodhead Publishing Limited, 2013

$$m_s = \rho[c_p(T_m - T_0) + L] \quad [8.18]$$

The solutions for melt depth and melting velocity are quite complicated and difficult to use for a practical problem. It is found that the melt depth and average melting velocity can be further simplified when the power density of laser beams is greater than 10^9 W/m^2:

$$X(t) = 1.31\left(\frac{\alpha_l A I t^2}{\rho[c_P(T_m - T_0) + L]}\right)^{1/3} \quad [8.19]$$

$$\bar{v} = 2\left\{\frac{\alpha_l A I}{\rho[c_P(T_m - T_0) + L]X(t)}\right\}^{1/2} \quad [8.20]$$

Equation [8.19] describes the dynamics of the melting process under laser irradiation and provides a relationship among the melt depth $X(t)$, power density I and irradiation time t for various materials in laser conduction welding. At the beginning of laser irradiation, the melt depth increases rapidly with time and then increases slowly. It was reported that the theoretical results had a good agreement with experimental data for 304 stainless steel and copper alloy (Xie and Kar, 1997). The average melting velocity in Equation [8.20] increases as the power density increases and decreases as the melt depth increases, and such a trend has been observed in experimental studies as well.

It is also interesting to estimate the time to reach the melting and vaporizing temperature for various materials. Based on the mathematical model of laser melting described above (Xie and Kar, 1997), the melting and vaporizing time are obtained as follows:

Melting time:

$$t_m = \frac{\pi k_s^2 (T_m - T_i)^2}{4\alpha_s (AI)^2} \quad [8.21]$$

Vaporizing time:

$$t_v = t_m + \frac{k_l(T_v - T_m)\rho}{2(AI)^2}[c_P(T_m - T_0) + L] + \frac{\alpha_l \rho}{3(AI)^2}[c_P(T_m - T_0) + L] \times \left\{\left[1 + \frac{k_l(T_v - T_m)}{\alpha_l \rho[c_P(T_m - T_0) + L]}\right]^{3/2} - 1\right\} \quad [8.22]$$

© Woodhead Publishing Limited, 2013

Table 8.2 Times to melt and vaporize under Nd:YAG laser irradiation

	Power density = 10^9 W/m^2		Power density = 10^{10} W/m^2	
	Melting time t_m (s)	Vaporization time t_v (s)	Melting time t_m (s)	Vaporization time t_v (s)
Aluminum	4.4×10^{-3}	1.6×10^{-2}	4.4×10^{-5}	1.6×10^{-4}
Copper	4.6×10^{-2}	1.0×10^{-1}	4.6×10^{-4}	1.0×10^{-3}
Iron	3.0×10^{-3}	2.2×10^{-2}	3.0×10^{-5}	2.2×10^{-4}
Titanium	5.8×10^{-4}	2.0×10^{-3}	5.8×10^{-6}	2.0×10^{-5}
Stainless steel	5.6×10^{-4}	2.9×10^{-3}	5.6×10^{-6}	2.9×10^{-5}

Source: Xie and Kar (1997).

The melting and vaporizing time for Nd:YAG laser beams at two power densities are given in Table 8.2.

From Table 8.2, it can be seen that the times to reach melting and boiling temperatures at the substrate surface are found to be very short (about a few microseconds or less) at high-power densities. When reaching the boiling temperature, a vapour/plasma above the substrate may partially block the laser beam from reaching the substrate. Generally, the vapour or plasma in conduction welding is not as significant as keyhole welding, and the wavelength of Nd:YAG lasers is less sensitive to the blockage by the vapour/plasma plume than CO_2 lasers which has a long wavelength of 10.6 μm.

8.4 Focused laser beams

A laser beam is usually focused on the surface of a part to achieve the highest power density at the part. The power density of a focused laser beam or intensity, I, is defined as

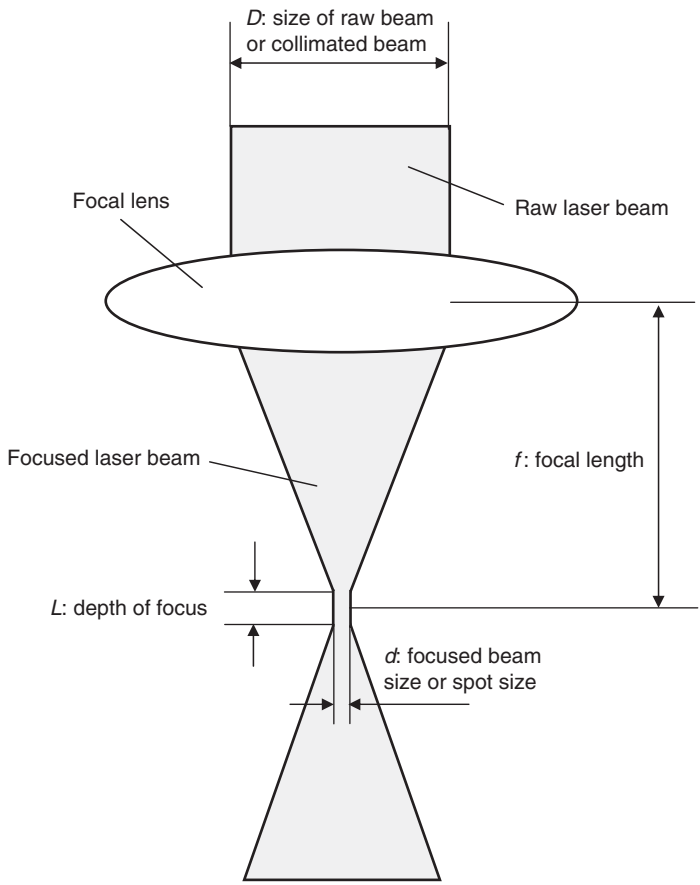
$$I = \frac{P}{A_1} \qquad [8.23]$$

where P is the peak power and A_1 is the area of the focused laser beam $\left(A_1 = \pi d^2/4\right)$. The size of the focused beam or spot size, d, is given by

$$d = \frac{1.27\lambda f M^2}{D} \qquad [8.24]$$

where λ is the wavelength, f is the focal length, D is the size of raw beam as shown in Fig. 8.5. M^2 is a measure of beam quality that shows the power density distribution of a laser beam. A low value of M^2 indicates good beam quality and ability to be focused to a small spot. When M^2 is equal to 1, the power density distribution is in the form of perfect Gaussian distribution

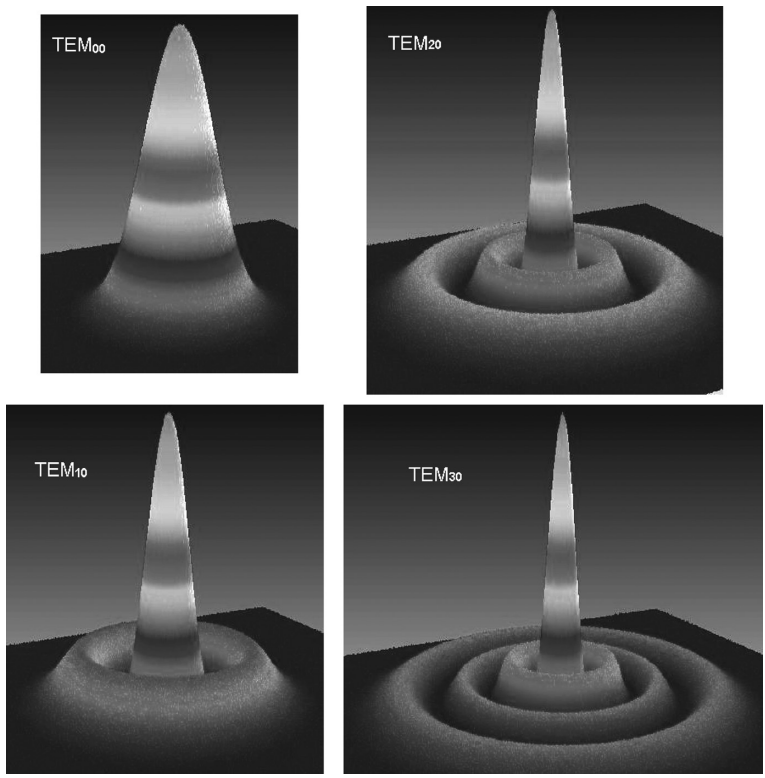
© Woodhead Publishing Limited, 2013



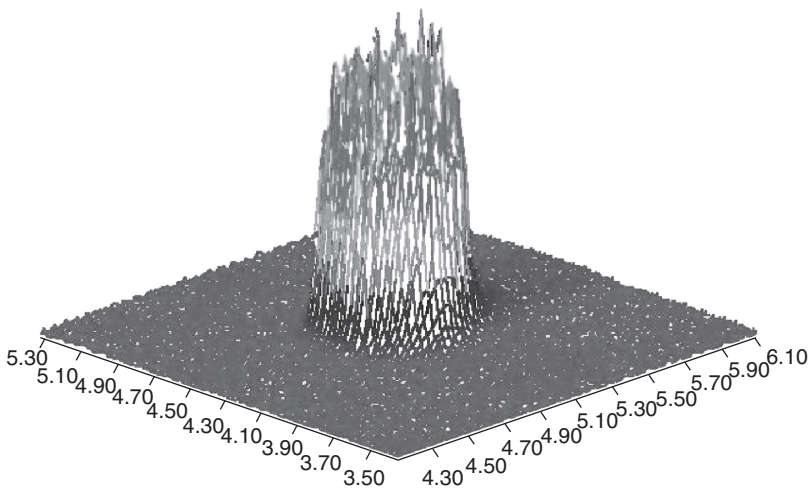
8.5 Focused laser beam.

and it is described as TEM_{00} (TEM – transverse electromagnetic mode) as shown in Fig. 8.6. For circular laser beams with a TEM_{pq} mode, the beam quality is $M^2 = (2p + q + 1)^{1/2}$. For example, the value of M^2 is 2 for TEM_{11} and M^2 =1.73 for TEM_{10}. According to Equation [8.24], the better the beam quality or lower value of M^2, the smaller the spot size or the better in focusability. For flash-lamp-pumped Nd:YAG lasers, the value of M^2 is large in a typical range of 20–200 depending on a number of factors including the laser emitting methods, laser power and optical systems. It has recently been reported that the beam quality (M^2) of fibre Nd:YAG lasers is about 1.1, close to the Gaussian distribution ($M^2 = 1$). A power-density distribution of a 4000-W Nd:YAG laser is shown in Fig. 8.7. It can be seen that the beam quality of the Nd:YAG laser is not Gaussian distributed and the power-density distribution is flat at top. However, the spot size is about 0.5 mm, which is still small enough for precise laser welding.

© Woodhead Publishing Limited, 2013



8.6 Transverse electromagnetic mode of laser beam, TEM_{pq} (courtesy of Spiricon software).



8.7 Power density distribution of a high power Nd:YAG laser at 150-mm focal length.

© Woodhead Publishing Limited, 2013

The question that needs to be answered is what impact does the beam quality have on the laser welding process, specifically on the hermetic welding of implantable medical devices. In general, a flat distribution of power density with a large value of M^2 is preferred for conduction welding mode if the laser beam can be focused to a spot small enough. A low value of beam quality (M^2) indicates a high-power density at the centre that might be easier to lead to keyhole welding mode at high energy. As mentioned in the previous section, keyhole welding mode is prone to weld voids due to instability of the keyhole and spattering during welding. For implantable medical devices, the large value of M^2 or poor beam quality is acceptable, and actually a slightly larger spot size is helpful in covering the entire seam joint in case of offsetting the laser beam to the seam joint.

However, a large value of depth of focus is preferred. While the depth of focus does not affect the laser welding process, it does have an impact on the process robustness. In laser welding, a laser beam is typically focused on the part surface to achieve the maximum power density and the part surface must be kept within the range of depth of focus to keep consistent power density during welding. As a result, a large depth of focus is preferred in laser welding for improved process robustness. The depth of focus, L, is given by:

$$L = \left(\frac{8\lambda}{\pi}\right)\left(\frac{f}{D}\right)^2 \qquad [8.25]$$

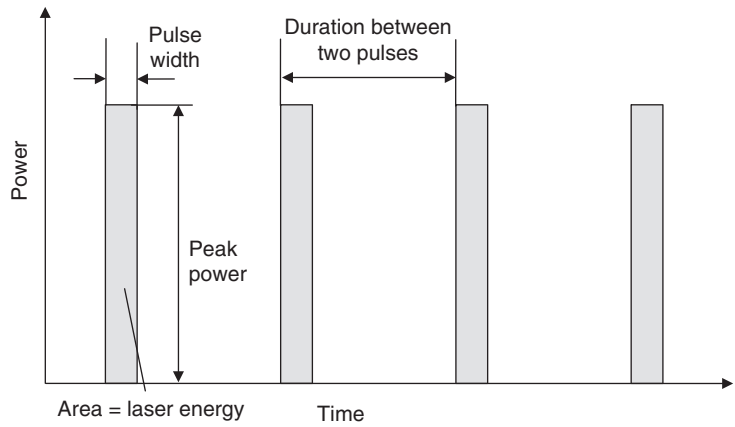
8.5 Laser welding parameters

As discussed before, a pulsed Nd:YAG laser system is typically used to weld implantable medical devices to minimize the heat input during laser welding, instead of continuous wave (CW) lasers whose power output is constant over time. For example, if a pulsed laser welding process of a titanium part has welding parameters of pulse energy 2.0 Joules/pulse, pulse width 2 ms and pulse repetition 10 Hz, the average power of the laser welding process is equal to a lamp bulb at 20 Watts (2.0 J/pulse × 10 pulses/s = 20 Watts). In case of CW laser welding, the required laser power is in the order of one hundred watts to melt the titanium forming a weld. The low average power in pulsed laser welding is able to melt metallic parts due to the high peak power of 1 kW (2.0 J ÷ 2.0 ms = 1 kW).

The pulsed laser welding parameters to be developed for each application include:

- Laser energy, which determines the weld depth in laser conduction welding, is typically between 1 and 4 Joules for the hermetic welding of titanium/titanium alloy case.

© Woodhead Publishing Limited, 2013



8.8 Laser pulses.

- Pulse width (or pulse duration), which governs the power density at a certain energy, is typically within 1–8 ms for this kind of application.
- Pulse repetition (or pulse frequency) controls the overlap rate of two adjacent spot welds. The high pulse frequency achieves a high overlap rate.
- Travel speed controls the overlap rate as well. The low travel speed results in a high overlap rate.

The definition of laser pulses are shown in Fig. 8.8 and the relations among the parameters are described in Equations [8.26] to [8.28].

$$\text{Laser energy} = \text{Pulse width} \times \text{Peak power} \quad [8.26]$$

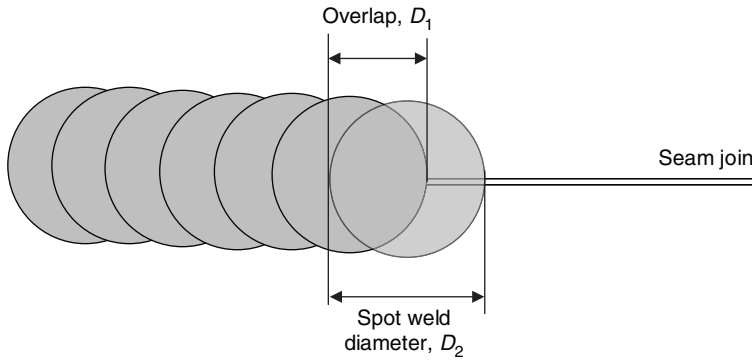
$$\textit{Mean} \text{ laser power} = \text{Pulse energy} \times \text{Pulse frequency} \quad [8.27]$$

$$\text{Pulse frequency} = \frac{1}{\text{Duration between two pulses}} \quad [8.28]$$

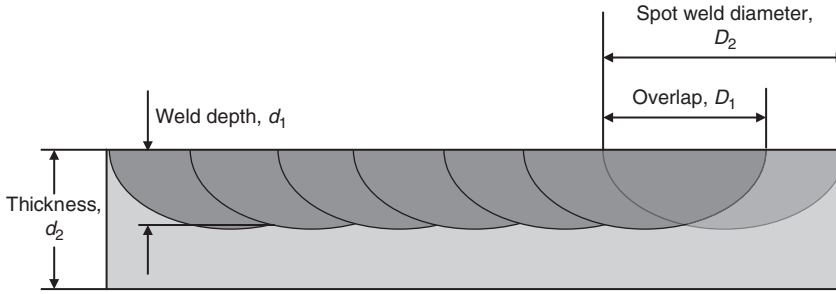
A pulsed laser seam weld is shown in Fig. 8.9. The overlap rate of adjacent spot welds is an important parameter to guarantee the hermeticity of a welded device. The overlap rate is typically greater than 70% for the purpose of hermetic welding. In many cases, the overlap rate is about 80% or higher. The overlap rate is defined as follows:

$$\text{Overlap rate} = \frac{\text{Overlap}, D_1}{\text{Spot weld diameter}, D_2} \quad [8.29]$$

© Woodhead Publishing Limited, 2013



8.9 Overlap of pulsed laser seam weld.



8.10 Cross-section along the seam weld joint.

When laser seam welding is performed on a two-dimensional plane, it is relatively easy to achieve the consistent overlap rate over the entire seam weld by moving the device mounted on an X–Y table while the laser beam is kept stationary. In case of an irregular three-dimensional shape of an implantable medical device, special CAM (computer-aided manufacturing) software may be needed for the welding motion program in order to achieve the consistent overlap rate over the entire seam weld. The CAM software is able to create the coordinates of X, Y, Z and rotary axes and travel speed for each pulse weld based on the irregular three-dimensional shape of the device to guarantee the same overlap rate everywhere.

A full penetration weld is usually required for structural seam welds under a high mechanical stress and fatigue in service. However, implantable medical devices are not subject to a high mechanical stress so a partial penetration weld is acceptable as shown in Fig. 8.3a. The partial penetration of a seam weld is defined as

$$\text{Penetration} = \frac{\text{Weld depth, } d_1}{\text{Thickness, } d_2} \qquad [8.30]$$

© Woodhead Publishing Limited, 2013

In Fig. 8.3a, the penetration is about 40%. The overlap rate can be estimated from the cross-section of seam weld in Fig. 8.10 as well.

8.6 Requirements for laser hermetic welds

Other than the requirement of weld depth and overlap rate, a ductile seam weld must be achieved for the implantable medical devices with titanium cases. Titanium and its alloys are the materials most often used for the case to hermitically seal the implantable medical device. However, titanium is an active element especially in the liquid state during welding. Titanium in liquid state can react with oxygen, nitrogen and hydrogen to cause a significant increase in brittleness and reduction in the ductility so inert gas such as argon and helium are used as shielding gas to protect the molten weld pool during welding. The source of oxygen and nitrogen are mainly from the air when improper shielding occurs during welding. A study showed that the hardness of commercial pure (CP) grade-2 titanium weld was increased from 242 to 373 Hv when 10% oxygen was added into the argon shielding gas (Li *et al.*, 2005). In addition, the inert shielding gas is sealed inside the device for improved device reliability. As a result, a controlled environment with inert gases is typically used for laser hermetic welding while moisture, oxygen or nitrogen are controlled at a low level.

There is a microstructure change in titanium material after laser welding. It was reported that for CP grade-2 titanium the microstructure changed from an equiaxed alpha of relatively uniformed grain size (about 10–15 μm) to a mixed coarse-grained serrated alphas and a smaller amount of fine-grained acicular alpha, and the hardness changed from 191 to 242 Hv (Li *et al.*, 2005). The change in microstructure is mainly due to the rapid heating and cooling in laser welding. The impact of the microstructure changes on reliability and performance of implantable medical devices is insignificant.

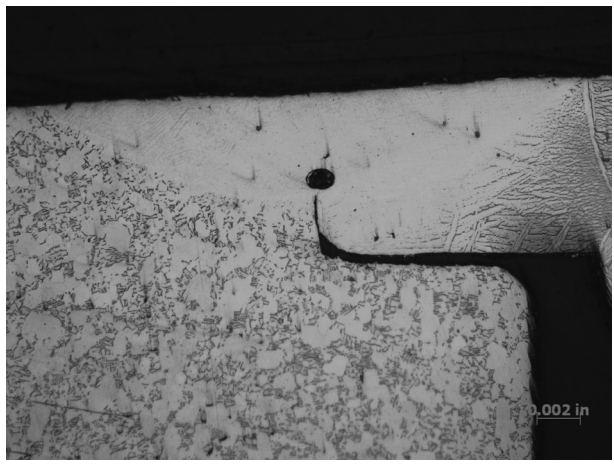
Although the titanium and its alloys have excellent weldability and good seam welds can be achieved in a controlled environment, there are a number of possible weld defects to affect the device hermeticity and reliability. The typical weld defects in the laser hermetic welding of implantable medical devices including the following:

- *Blow hole*. A typical blow hole at the seam weld is shown in Fig. 8.11. This defect is caused by a bulk polymeric material sandwiched in the weld joint which is vaporized at the high temperature during welding. The gas venting from the bulk polymer causes a path in the liquid weld pool and the venting path becomes a blow hole on the seam weld after the solidification of the weld pool. The device with a blow hole will fail in the subsequent helium leak test to identify the hermeticity loss.
- *Void in weld*. When a tiny bulk polymer material is vaporized in the weld pool, the evaporation gas bubbles might be trapped in the weld pool

© Woodhead Publishing Limited, 2013



8.11 Blow hole at seam weld.



8.12 Voids observed in cross-sections of welds.

forming a void (Fig. 8.12). The trapped voids are not visible from the weld surface and do not affect the hermeticity of the device, but the total weld depth is affected. The true weld depth should be the weld depth minus the diameter of the void if the void is right at the seam joint.

- *Pinhole*. The gas bubbles evaporated from the tiny bulk polymer might be just floating to the weld surface at the time of weld solidification. The surface voids are called pinholes as shown in Fig. 8.13. The pinholes do not affect the hermeticity in most cases but it might be a cosmetic issue.
- *Cracking*. The cracking on the seam weld mostly results from the metallurgical problems to make the titanium weld brittle (Fig. 8.14). Substantial

© Woodhead Publishing Limited, 2013



8.13 Pinholes on weld surfaces.



8.14 Cracking on welds.

foreign material or contamination are decomposed during welding and enter into the liquid weld pool to alter the metallurgy of titanium. The metallurgical alternation significantly increases the hardness and brittleness and potentially results in cracking to lose the hermeticity.

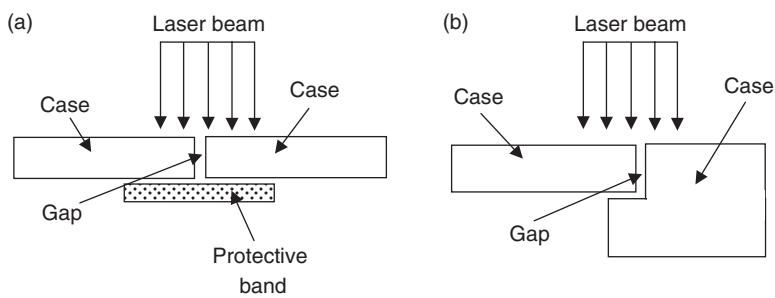
- *Weld discolouration*. The titanium seam weld is shiny silver if proper shielding is used. In case of discolouration on welds, such as yellow, purple or blue colours, it is an indication of oxide or nitride due to the contamination in shielding environment or poor shielding. The discoloured weld might be brittle with a high hardness and potentially

© Woodhead Publishing Limited, 2013

lead to cracking on the seam weld. A slight discolouration might have a limited impact on the mechanical properties of weld metal (Li *et al.*, 2005) and technically the weld might be acceptable for the implantation, but the non-conforming issue needs to address to meet GMP (Good Manufacturing Practice) requirements. Contamination in the weld joint may cause local weld discolouration as well.

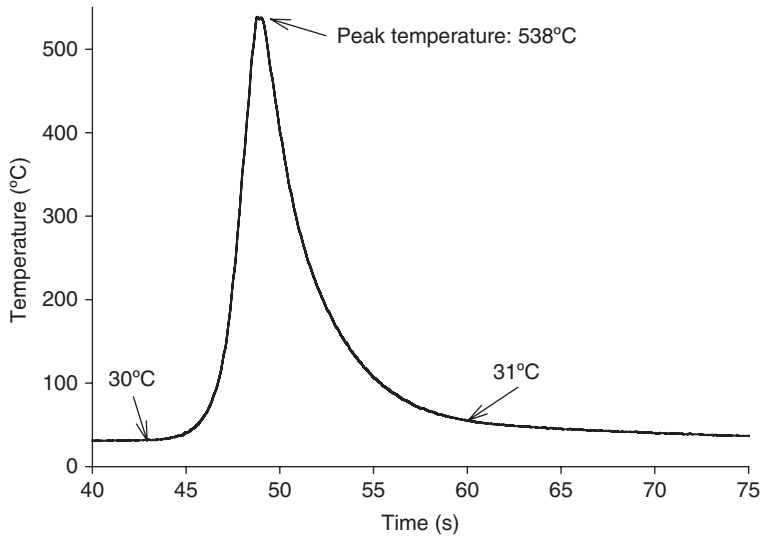
A butt joint is typically used for laser hermetic welding of implantable medical devices. There are two issues that need to address in the joint design:

1. Potential damage of internal components by laser-beam irradiation from the gap between the case halves. A gap is always found between two case halves and it is possible for the laser beam to go through the gap to directly hit the internal components. As a result, a protective band underneath is needed (Fig. 8.15a) or the butt joint has a step to block the laser beam irradiation (Fig. 8.15b). The protective band can be spot welded to one side of the case half to align with another half when mating.
2. Thermal damage by heat conduction during laser welding. Laser welding is a high-temperature process to melt the metal cases and there is a potential to thermally damage the internal components or reflow the adjacent soldering or brazing joints by heat conduction. The thermal damage by heat conduction is minimal with a proper joint design as laser welding is a localized heating process and the temperature dramatically decreases along the distance. The temperature at the bottom of the protective band was measured in laser welding of a thin titanium case and the temperature rising and cooling cycle is shown in Fig. 8.16. It can be seen that the peak temperature is about 538°C and the duration at the high temperature is short. For example, the duration above 500°C and 400°C are 0.75 and 1.9 s, respectively. Therefore, the thermal damage from laser welding to the internal components is limited due to localized



8.15 Butt joint design to protect internal components from laser damage: (a) butt joint with a protective band; (b) butt joint with a step.

© Woodhead Publishing Limited, 2013



8.16 Temperature cycle under protective band during laser welding.

heating and small amount of heat input. If necessary, a protective layer around the internal components may be used.

8.6.1 Leak test of welded devices

All laser welded implantable medical devices must be subject to leak test in manufacturing to ensure the hermeticity. Military standard MIL-STD-883 Method 1014 (Seal) specifies the fine and gross leak-testing methods, and the most commonly used fine leak-testing method is the helium mass spectrometer. Helium gas is chosen for mass spectrometer leak testing due to the unique features of helium:

- Helium is present in trace amounts in the atmosphere (5 ppm).
- Helium has a high diffusivity due to the small size of molecules.
- Helium ions are easily separated from other ion species due to the significantly different mass-to-charge ratio.
- Helium is an inert, non-toxic and non-flammable gas.

Helium mass spectrometers are a well-established instrument with very high detection sensitivity and analytical capability. Gas molecules are vacuum pulled into the leak detector for ionizing by a hot filament and then separated into ion beams according to their mass-to-charge ratio. The helium ion beam is tuned so that only the helium ion beam is allowed to strike the

© Woodhead Publishing Limited, 2013

ion collector to produce an ion current. Then the ion current is amplified to display as a helium leak rate.

Residual gas analysis (RGA) is often used to verify the hermeticity of implantable medical devices, especially after implantation in human body for a certain period of time. RGA is a quantitative method to analyse the internal gas compositions of a hermetically sealed device. The RGA results can be used to compare to the original gases sealed in the device to understand the hermeticity loss.

RGA is performed by piercing the sealed device to release the internal gases from the device to a mass spectrometer. MIL-STD-883 Method 1018 (Internal Gas Analysis) specifies the calibration requirement, sample preparation and testing procedures. All of gases greater than 0.01% by volume shall be reported and typically the gases to be reported include N_2, Ar, He, O_2, CO_2, CH_4, NH_3, H_2 and water (H_2O). In addition to the moisture content we concern most other gas compositions such as oxygen or nitrogen, if any, from RGA testing may provide additional information on hermetic-sealing process issues.

In laser hermetic welding of implantable medical devices, a controlled inert gas environment to prevent liquid metal from oxidizing during welding is used and then the inert gases are simultaneously sealed in the device. The inert gases can be argon, helium or mixture of argon/helium, but helium should be used for the subsequent helium leak test. A mixture of argon and helium is often used for economic reasons since helium is more expensive than argon. In case of RGA results to show the significant change in gas compositions when compared to original gases sealed in manufacturing, it suggests that this device may loss the hermeticity or issues to seal wrong gases during manufacturing.

8.7 Conclusion and future trends

Pulsed Nd:YAG laser welding is a hermetic-sealing technique often used for implantable medical devices to protect the microelectronic circuits inside. Pulsed Nd:YAG laser welding is a stable, precision and non-contact process offering a number of benefits such as reliably hermetic sealing, low heat input, localized heating, minimum weld distortion and ease of automation, and has been successfully used for high-volume manufacturing of implantable medical devices. A high yield in manufacturing depends on a number of factors such as proper joint designs, materials selection, development of process parameters and process control. In this chapter, the theory of laser conduction welding, including absorption of laser energy and laser melting process, fundamentals of laser beams and optics, critical process parameters, typical weld defects and root causes, has been discussed to help better understand the laser welding process for implantable medical devices. It is

© Woodhead Publishing Limited, 2013

hoped that that the contents of this chapter can help the medical-device industry develop a proper laser welding process to achieve the highest quality of implantable medical devices.

There is a strong desire from patients to use smaller implantable medical devices so that thinner and small metallic cases have to be used to hermetically seal the device. In the application of implantable sensors, a thin metal diaphragm (equal or less than 25 μm) is needed to hermetically weld to a device with no distortion, no weld defects, good fatigue strength and good yield. These are the challenges to the laser hermetic welding technique and a number of issues need to be addressed to achieve a high-quality and highly reliable seam joint, for example,

- The joint design is critical to weld the parts together with a significant difference in thickness. The successful joint design needs to consider the heat balance during welding, release of weld residual stress, weldability of materials combination, laser–material interaction and visual detectability of weld defects.
- Proper tack weld techniques (laser welding, projection welding or solid-state welding, etc.) to minimize the distortion or the welding sequence to minimize the residual stress.
- Proper process parameters for a robust process in volume production and minimum distortion such as low heat input and small laser beam.
- Good inert gas shielding to the weld pool in a controlled environment.
- Precision fixture or seam-tracking techniques.

The development of laser techniques in recent years might be helpful in overcoming the challenges. There are a number of new lasers that can potentially be used for welding applications, including short wavelength lasers (green laser at the wavelength of 532 nm or UV lasers at 355 nm), while the fundamental Nd:YAG lasers have a wavelength of 1064 nm, high-power diode lasers, disk lasers and fibre lasers. The short wavelength lasers are able to improve laser absorptivity and are good for some high reflective materials (gold, platinum, copper, etc.). Fibre lasers have great potential for use in hermetic welding of implantable medical devices. The fibre laser beam has a high beam quality close to Gaussian distribution (TEM_{00}) due to the length of fibre cavity to eliminate thermal distortion of optical path and therefore the fibre laser beam can be focused to a very small spot. It has been reported that the spot size of the focused laser beam could be as small as 15 μm and can be used for small device welding coupled with a precision fixture. Other than the small beam size, the fibre lasers offer excellent beam stability, short pulse and minimized heat affected zone (HAZ). In addition, unlike a conventional laser in which the laser cavity is constructed from components such as mirrors, rods and lenses, the laser cavity in fibre lasers is constructed

© Woodhead Publishing Limited, 2013

monolithically by the doped active fibre with several meter-long and fibre Bragg gratings replacing conventional dielectric mirrors to provide optical feedback. An immediate advantage of this is that there is no need for alignment, adjustment or subsequent cleaning of optical surfaces once the laser has been built, which means little or no maintenance requirement.

8.8 References

Arata, Y. and Miyamota, I. (1972), 'Some fundamental properties of high power laser beam as a heat source (Report 2): CO_2 laser absorption characteristics of metal', *Trans. Japan Weld. Soc.*, **3**, 152–162.

Cohen, M. E. and Epperson, J. P. (1968), 'Electron beam and laser beam technology', *Adv. Electron.*, **4**, 139–186.

Iida, T. and Guthrie, R. I. (1988), *The Physical Properties of Liquid Metals*, Oxford, Clarendon.

Li, X., Xie, J. and Zhou, Y. (2005), 'Effects of oxygen contamination in the argon shielding gas in laser welding of commercially pure titanium thin sheets', *J. Mater. Sci.*, **40**, 3437–3443.

Liu, X., Demosthenous, A. and Donaldson, N. (2007), 'Implantable stimulator failures: Causes, outcomes, and solutions', *Proceedings of the 29th Annual International Conference of the IEEE EMBS*, Lyon, France, 5786–5789.

Touloukian, Y. S., Powell, R. W., Ho, C. Y. and Klemens, P. G. (1970), *Thermophysical Properties of High Temperature Solid Materials*, Vols 1, 3 and 10, New York, Macmillan.

Xie, J. (1999), 'Plasma fluctuation and keyhole instability in laser welding', International Conference on Applications of Laser and Electro-Optics (ICALEO '99), Laser Institute of America, D11–D20.

Xie, J. (2002), 'Dual beam laser welding', *Weld. J.*, **81**, 223s–230s.

Xie, J. and Kar, A. (1997), 'Mathematical modeling of melting during laser materials processing', *J. Appl. Phys.*, **81**, 3015–3022.

Xie, J. and Kar, A. (1999), 'Laser welding of thin steel sheet with surface oxidation', *Weld. J.*, **78**, 343s–348s.

Xie, J., Kar, A., Rothenflue, J. and Latham, W. (1997), 'Temperature-dependent absorptivity and cutting capability of CO_2, Nd:YAG and chemical oxygen-iodine lasers', *J. Laser Appl.*, **9**, 77–85.

Xie, J. and Safarevich, S. (2003), 'Laser materials processing for medical devices', *Proceedings of ASM Materials & Processes for Medical Devices*, Anaheim, California, USA, 25–30.

© Woodhead Publishing Limited, 2013

9

Validating hermeticity in welded metallic implantable medical devices

K. J. ELY, GlaxoSmithKline Corporation, USA

DOI: 10.1533/9780857096425.2.236

Abstract: The term hermetic seal has various meanings to many in the medical industry. All enclosures will leak, just at different rates. The process and design goal is to manage this leak rate to ensure the package remains safe and effective for the patient or users throughout its design life. The word hermetic is taken from the name of the Ancient Greek alchemist Hermes Trismegistus who is claimed to have invented a magic seal to make vessels airtight. This chapter will highlight several aspects of hermetic seals, and will present the first principles of this process, to enable all practitioners to discover Hermes' 'magic' seal.

Key words: hermetic, leak rates, molecular flow, viscous flow, moisture ingress.

9.1 Introduction

Hermetic sealing is a key step in maintaining long-term performance of many medical devices. While electrical and mechanical designs can work safely and effectively in the laboratory or manufacturing environment, devices can and will fail when implanted if not properly sealed to prevent ingress of biological material or to prevent loss of internal gases. Failure can also occur prior to implant during shipping and handling, and exposure to harsh environmental conditions prior to the final-use conditions.

Early electronic enclosures were hermetically sealed to prevent ingress of moisture. This moisture content could excite and promote localized corrosion cells, which degrade metallic circuits and eventually cause total circuit failure.[1,2] Current devices such as implantable defibrillators generate very high voltages, and require specialized gases within the enclosure to maintain arc suppression. Loss of these critical gases will allow arcing and also lead to damage of critical circuits.[3]

While a good hermetic seal is vital to the overall performance of the device, cleanliness of the components plays a major role. This is especially true for devices that are low-voltage impedance matched, or microwave

© Woodhead Publishing Limited, 2013

units that require low losses. High ionic contaminants in these assemblies can lead to corrosion, dendritic growth or whiskers, leading to short circuits or poor electrical performance.[4]

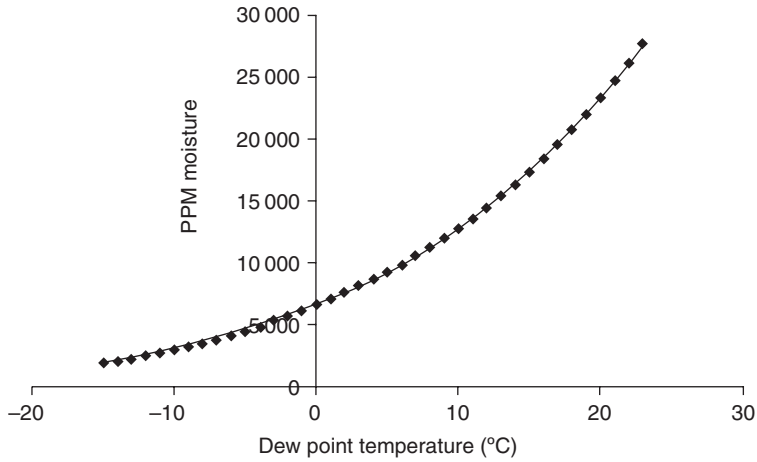
The term hermetic seal has various meanings to many in the medical industry. All enclosures will leak, just at different rates. The process and design goal is to manage this leak rate to ensure the package remains safe and effective for the patient or users throughout its design life. Webster's dictionary cites the definition of 'hermetic' as: 'Completely sealed; especially, sealed against the escape or entry of air'. The word hermetic is taken from the Ancient Greek alchemist Hermes Trismegistus who is claimed to have invented a magic seal to make vessels airtight. The following sections of this chapter will highlight several aspects of hermetic seals, and will present the first principles of this process, to allow all practitioners to discover Hermes' 'magic' seal.

9.2 The physics of leak rates

The initial need for hermeticity was to ensure the electronics or mechanical assembly remained in an effective moisture environment. Ingress of moisture from the body or from outside air can lead to corrosion cells on the circuitry.

Ingress of moisture to an enclosure raises the internal moisture content to the point that condensation can occur. While this is not a key issue for human implantable devices, which will assume a stable body temperature, the transit, storage and shipping of devices can often expose the units to condensation temperatures. The electronics industry has focused on keeping moisture contents below 5000 ppm for most hermetic devices. This requirement is driven by simple atmospheric physics as shown in the moisture vs dew point temperature plot of Fig. 9.1. In this plot it can be determined that for moisture levels of 6000 ppm, the dew point temperature is the freezing point of water, 0°C (32F). This means that, at 6000 ppm internal moisture, condensation as water droplets will form on the internal circuits at low temperatures. If ionic contaminates are present, the condensed moisture can solvate and activate these contaminants forming ionic compounds that under applied voltages and current act as a plating cell. The resulting oxidation-reduction reactions form corrosion products that degrade the metallic conductors. This degradation will eventually lead to open or short circuits and limit the device lifetime. Often the device electrical performance fails specification long before catastrophic conductor damage occurs.[5,6] For these reasons, early electronic systems for military applications were designed to a limit of 5000 ppm moisture so that the dew point was below freezing.[7]

© Woodhead Publishing Limited, 2013



9.1 Plot of internal moisture content vs dew point temperature. This graph should be used to ensure the full range of environmental temperature exposure does not allow liquid droplets (condensate) to form on internal surfaces.

Current devices often use other techniques to maintain proper moisture content. These techniques incorporate moisture 'getters' in the form of silica gel packets, coatings, or hydrophilic plastic inserts to preferentially absorb moisture and prevent high levels of moisture even if a seal is compromised. Some commonly used desiccants for electronic devices are shown in Table 9.1.[8,9]

The second key requirement for hermetic seals is to maintain the designed gas environment within the sealed system. This requirement typically pertains to the need for electrical arc suppression within devices that are designed for high voltages (>250 V) or high currents (>50 mA). Common gases for these types of circuits include nitrogen, argon, helium and sulfur hexafluoride. The arc-suppression capability of these gases is shown in Table 9.2 for a range of gaps. The gap width is critical in maintaining or extinguishing an electrical arc. Along with the gap, is the shape of the conductor carrying the voltage also has a strong effect on maintaining or promoting arcs. Much work has been done to study these arc processes, generally using a spark-gap system where a fixed pointed electrode is offset from a flat plate. The environmental gases are imposed at the gap and voltage is applied until an arc jumps the gap. The ability of the arc to jump the gap is a strong function of the gap distance, the 'sharpness' of the electrode point, the applied voltage and ionization characteristics of the gases in the gap. Ingress of moisture and oxygen will poison the gas mix and degrade the ability of the system to maintain arc suppression.[10]

© Woodhead Publishing Limited, 2013

Table 9.1 Commonly used desiccants and getters for internal moisture controls

Material test condition	Molecular sieve (synthetic zeolite)	Silica gel	Montmorillonite clay
Overview	Synthetically produced zeolites characterized by pores and crystalline cavities of extremely uniform dimensions Higher in cost Manufacturing environment in which these materials are used must be well controlled	Most widely known and versatile of all desiccant products Non-corrosive Non-toxic	Repeated regeneration possible Clay granules have up to 30% greater density than silica gel or molecular sieves – thus can occupy less space Variability in performance due to its source because it is a naturally occurring material
Adsorptive capacity for H_2O at 25°C, 60% RH	Medium (~22% wt)	High (~30% wt)	Medium (~22% wt)
Adsorptive capacity for H_2O at 25°C, 40% RH	High (~20% wt)	High (~20% wt)	Medium (~17% wt)
Adsorptive capacity at low RH levels, at 25°C, 10% RH	Excellent (~15% wt)	Poor (~5% wt)	Fair (~7% wt)
Adsorptive capacity at high temperatures, at 85°C	Excellent	Poor	Poor
Adsorption rate	Excellent	Good	Good

Source: Courtesy of Guidant – Boston Scientific.

Table 9.2 Arc-suppression capability of various gases

Gas	Dielectric strength	V/V_{air}	kV/cm	kV/cm (calc from DS)	kV/0.005 inches (calc from DS)
He	0.15			5.175	0.657
Ar	0.18			6.21	0.789
CO_2	0.88			30.36	3.856
O_2	0.92	0.85		31.74	4.031
Air	0.97	1	30	33.465	4.250
N_2	1	1.15	34.5	34.5	4.382
SF_6	2.5	3	90	86.25	10.954

© Woodhead Publishing Limited, 2013

9.2.1 Leak paths

When testing devices for leak rate, the final measurement is the sum of all leaking paths. Sometimes these are easy to detect and are 'gross' defects, and others are extremely difficult to detect and may in fact change over time. Regardless of the rate of leak, some general physical principles apply to all leaks:

- Diffusion and flow of gases will occur to normalize concentrations.
- Diffusion and flow of gases will occur from the high concentration into the lower concentration.
- Leaks will follow the pressure differential from high to low.
- Measured leak rates are the sum of all active leak paths.
- Many leak paths will become blocked or sealed by contaminants, oils, corrosion products, or liquids.
- Gases and vapours will leak faster than liquids.
- Gases and vapours will leak through smaller features than liquids.
- Leak rates generally show logarithmic decay, but over short time spans can be modelled with linear equations.
- Straight leak paths will have higher leak rates than tortuous leak paths of equal length.

Leak paths allow gases or vapour to escape from an enclosure.[11] While the internal gases escape, external gases are allowed in and contaminate the environment. To understand the flow rate through these small orifices and cracks, we must understand the flow properties of gases under various conditions.

From vacuum technology we know that gases flow under conditions of molecular or viscous flow.[12] Molecular flow is typical of vacuum conditions below 4 mT, and is driven by the collision of molecules with the walls of the tube or crack through which it flows. Since most medical devices are sealed at room pressure or slightly positive pressure, the gas concentration within the device is very high (relative to vacuum) and the molecules mean-free-path distances are very short. This means the molecules interact and collide with each other far more frequently than the walls of the tube or crack they are flowing through. Therefore, the characteristic gas viscosity best describes the gas-flow properties within a device and for leaks above 10^{-5} He atm/cc.

Many leak testers impose a vacuum differential on the device under test. In this manner the pressure outside the device is lowered to enhance the flow of gas out of the device and into the test unit. In these cases, the flow of gas from the device can be molecular flow. In molecular flow, there are so few gas molecules that the mean-free path between molecules is large in

© Woodhead Publishing Limited, 2013

Table 9.3 Dimensionless Reynolds and Knudsen numbers

Flow type	Typical Reynolds numbers	Typical Knudsen numbers
Turbulent	>2300	–
Viscous	<1200	<0.01
Molecular flow	–	>1.00

comparison with the crack or tube they are flowing through. In this case the gas has a higher probability of interacting with the walls of the crack or tube than with a fellow gas molecule. This type of flow cannot be characterized by viscosity, as there are no longer any shear forces acting on the gas molecules as they flow past each other. This gas flow situation occurs at low pressures (<10 mTorr) and low leak rates, typically 10^{-7} He atm/cc or better.

These flow regimes are described in vacuum technology as turbulent flow (high Reynolds number), viscous flow (medium Reynolds number) and molecular flow (low Knudsen number). The transition between flow regimes is best estimated by use of the Reynolds and Knudsen numbers.[13] Table 9.3 lists the approximate range of the Reynolds and Knudsen numbers that describe the transitions between flow regimes. The relative numbers are derived in the next section.

Reynolds number is defined as:

$$R = \frac{apU}{n} \qquad [9.1]$$

where:

a = tube or crack radius
p = gas density
U = flow velocity
n = viscosity

Similarly, the Knudsen number is defined as the ratio of the molecular mean-free path L to the radius of the crack or tube:

$$K = \frac{L}{a} \qquad [9.2]$$

And the mean free path is defined as:

$$L = \frac{0.707}{\pi d^2 N} \qquad [9.3]$$

© Woodhead Publishing Limited, 2013

where:

d = molecular diameter
N = number of molecules per unit volume

The rate of flow of gas through a crack or small diameter tube is given by:

$$Q = P\frac{\mathrm{d}v}{\mathrm{d}t} \quad [9.4]$$

where:

Q = throughput of gas
P = pressure at measurement point
$\mathrm{d}v/\mathrm{d}t$ = volume flow rate

The overall throughput Q is dependent on the overall resistance to flow across the length of the tube or crack. For most leaks, there is a strong pressure differential from the inside or beginning of the crack or tube, to the end of the crack or tube and the outside environment. The throughput Q can then be written as a function of:

$$Q = \frac{P_{\mathrm{ex}} - P_{\mathrm{ent}}}{Z} \quad [9.5]$$

or as:

$$Q = C\left(P_{\mathrm{ex}} - P_{\mathrm{ent}}\right) \quad [9.6]$$

where:

P_{ex} = the pressure at the exit point of the leak
P_{ent} = the pressure at the entrance point of the leak
Z = resistance to flow
C = conductance of flow

It is worth noting that Equations [9.5] and [9.6] are analogous to Ohm's Law, which relates the flow of electrical current (I) through a resistance (R) under the influence of a potential difference (Volts).

$$I = \frac{V}{R} \quad [9.7]$$

© Woodhead Publishing Limited, 2013

So in a similar manner to electrical circuits, the resistance to gas flow is found to be the sum of the resistances in the system, given as:

$$Z_{\text{total}} = Z_1 + Z_2 + Z_3 + \cdots + Z_n \qquad [9.8]$$

where Z_{total} is the total resistance to gas flow and the contributing factors include the resistances of changes in direction (tortuosity), diameter, coatings, contaminants, partial blockages and the like.

These basic elements of gaseous flow form the key background to work completed by French scientist Poiseuille. In his work on gases, he derived the following equation that describes the viscous flow of gases through a straight tube of small cross section. This equation generally holds for pressures above 10^{-3} torr, where gas viscosity is still a dominant feature of the flow. Below this pressure, viscosity no longer describes the molecular motion.

The Poiseuille equation is given as:

$$Q = \frac{3.1416\, d^4}{128\, nl} \times P_{\text{ave}} \left(P_{\text{ex}} - P_{\text{ent}} \right) \qquad [9.9]$$

where:

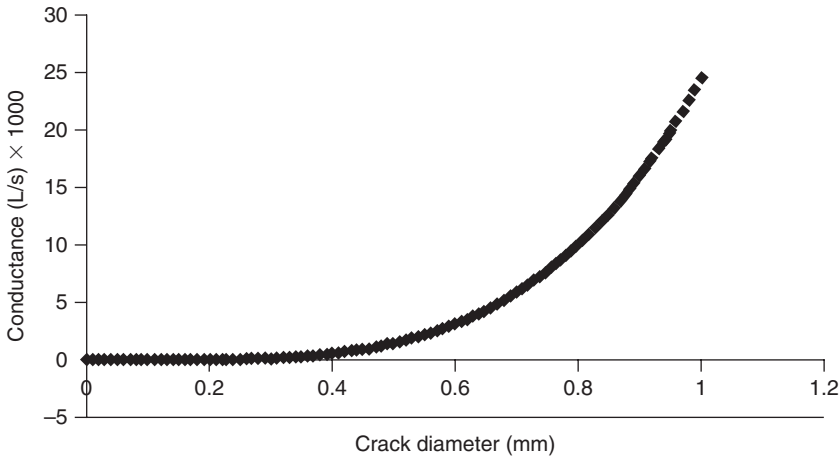
Q = flow
d = tube diameter
l = tube length
n = gas viscosity
P_{ave} = average of P_{ex} and P_{ent}
P_{ex} = pressure at exit point
P_{ent} = pressure at entrance point

Combining this equation with the conductance Equation [9.3] we yield the most used form of the Poiseuille equation:

$$C = \frac{3.1416\, d^4}{128 nl} \times P_{\text{ave}} \qquad [9.10]$$

From Equation [9.10] we see that the conductance (typical units L/s) is a strong function of the tube diameter. Therefore, as the effective crack diameter or cross-section decreases, the ability to maintain a leak path of significant flow diminishes rapidly. A plot of conductance versus crack/tube diameter is given in Fig. 9.2.

© Woodhead Publishing Limited, 2013



9.2 Plot of air conductance (L/s) vs tube diameter '*d*' and a fixed crack length of 1 mm and viscosity of 1 poise at 1 atm differential.

Other key insights from Equation [9.10] relate to the gas property of viscosity and the overall crack length. As the gas viscosity increases and or the crack-length path increases, the leak-flow rate decreases.

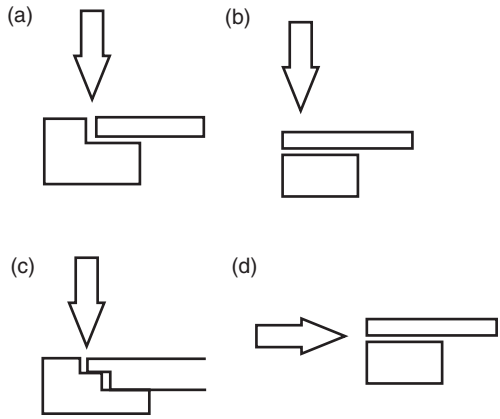
The Poiseuelle equation can be used to optimize the seal design. The best design will not allow for a straight-through crack but instead will change direction. Seam or joint designs that meet this requirement will be discussed later in this section. Further, any potential leak path should be made very long relative to the crack diameter. Finally, the choice of sealing gas, while not always a process choice, should be as high a viscosity as possible and of highest molecular weight possible to reduce the potential for flow.

9.2.2 Joint designs for hermetic sealing of electronic enclosures

Previous chapters of this book will have discussed material selections for medical devices and reviewed the welding and joining requirements for those materials. This section will review some selected joint or seam designs in current medical devices that yield hermetic seals with very low leak rates.[14]

Figure 9.3 shows several typical joint designs. A simple overlap seam weld with a full or partial penetration weld or braze is sufficient to form an excellent hermetic seam. Penetration into the parent materials across the seam is required, but full penetration of the parent materials is not. The important feature of a hermetic seam is the area joined at the interface of the two

© Woodhead Publishing Limited, 2013



9.3 Typical joint designs for hermetic seals in medical devices. (a) Lap seam weld; (b) through thickness lap weld; (c) stepped lap seam weld; (d) off axis lap weld.

mating surfaces, not the penetration in the second or most inner material. In fact, it can be shown that over-penetration leads to severe defects, increased stresses and a higher potential for cracks.

Two key aspects must be maintained for high process yields for hermeticity. These requirements include:

- tight fit-up of the joint;
- good fixturing that controls the fit-up during the welding and joining process;
- proper penetration or wetting of the seal area;
- proper or optimized overlap of pulsed weld zones;
- cleanliness;
- proper material choice to avoid cracking or delamination in the seal area.

A key similarity in many medical devices is the need for a small thin-walled can or container to hold the necessary electronics, power supply, batteries, capacitors and other circuit functions. This package must be hermetic to at least moisture ingress, but is typically gas tight to even low volumes of helium. Typical housings in medical are MP35N, 316L, or the most common, commercially pure titanium. Hermeticity is required to ensure moisture attack cannot cause corrosion and eventual shorts or opens of the circuits. Note that many hermetic enclosures in use today also incorporate getters for oxygen and moisture, to improve long-term reliability and quality. Regardless of the sealing technique, a minimum of 50% spot-to-spot overlap is recommended, with 75–80% overlap common practice. Also, note that the important aspect is to achieve overlap of the weld zones at the interface of the joint. Over-penetration of individual spots is detrimental and penetration

© Woodhead Publishing Limited, 2013



9.4 Schematic diagram of overlap pulse requirement and penetration in an overlap weld design. Note it is the weld area at the interface that drives hermeticity, not penetration into the innermost layer.

does not correlate to hermeticity; it is the continuity of the seal at the interface. This is shown schematically in Fig. 9.4.

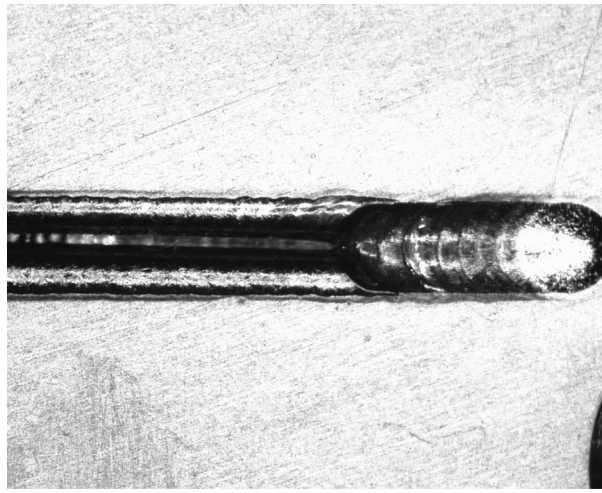
Three processes have been widely used to hermetically seal thin-walled medical cans:

- resistance-seam welding;
- plasma-seam welding;
- laser-seam welding.

Resistance welding is an excellent choice when the can materials are resistive as in the case of MP35N or 316L stainless steel. Opposed electrodes are clamped against a flange of the housing and slowly rotated to traverse the length of the package. Current and voltage is applied to form overlapping resistance weld spots. After the first pass along two parallel sides, the electrodes retract, the part rotates 90° and the process is repeated along the two remaining sides. Circular packages can also be sealed with this technique. Disadvantages of the process are the requirements for a flanged cover, which is often nickel and gold plated. In this manner the resistance weld is actually a resistance braze, forming a eutectic alloy of gold–nickel at the interface. This allows the process to run somewhat faster and use less heat input than full fusion welding of the higher melting point MP35N or 316l stainless steel.

Plasma welding has hermetically sealed more medical pressure bellows than any other process. Pressure bellows are formed from a stack of preformed thin metal discs, sealed along their periphery. In a manner similar to arc processes for sealing wire tips, the arc is drawn to the sharp edge of the disc, melting and sealing the disc edge. The process produces a weld seam very similar to pulsed laser welding, but with slightly increased heat input. It is an excellent process for sealing flanged enclosures as well. Its disadvantage is the heat input for deeper penetration welds, as well as the close proximity of the torch face to the weld zone itself.

© Woodhead Publishing Limited, 2013



9.5 Example of a poor hermetic seam due to poor joint fit-up. At the start of the weld the gap was too large and pull-back occurred. As the gap decreased, the weld melt was able to bridge the gap and begin to form a seam. When the gap exceeds approximately 10% of the thinner material, the surface tension forms a ball on the edge of the joint, negating flow across the joint. (Photo courtesy of Edison Welding Institute.)

Laser welding is today the most popular and easy to implement for hermetic sealing. Advantages are the ease of 'point-and-shoot' line-of-sight welding capability, and the ease with which automation can track odd package shapes and configurations. Deeper penetration welds can be developed without overheating critical glass or ceramic feed-throughs, and weld cycle time is the shortest for laser welding. Disadvantages are often the initial start-up capital cost, training and laser-safety requirements, and the need for excellent part fit-up. A general rule of good laser welds is the joint fit-up must have a maximum joint gap of 10% of the thinner material. Excessive gaps cause the laser to punch through one layer causing a hole, or the edges of the seam pull back due to the molten material surface tension. An example of a seam weld with too much gap is shown in Fig. 9.5. Note the smooth-balled edges on each side of the seam. An example of a well-formed hermetic seam weld is shown for a pacemaker pulse generator in Fig. 9.6.

A key item to note is that fixturing of the device and the material cleanliness will define the process yield. The fixturing and the welding process must control and optimize the heat input so that warping or expansion of the joint gap does not occur. When the fixturing is insufficient or the thermal inputs too high, the weld seam pushes ahead a bow-wave of thermal

© Woodhead Publishing Limited, 2013



9.6 Example of a well-formed and polished hermetic seam in the titanium shell of a heart pacemaker. (Photo courtesy of Guidant Corporation.)

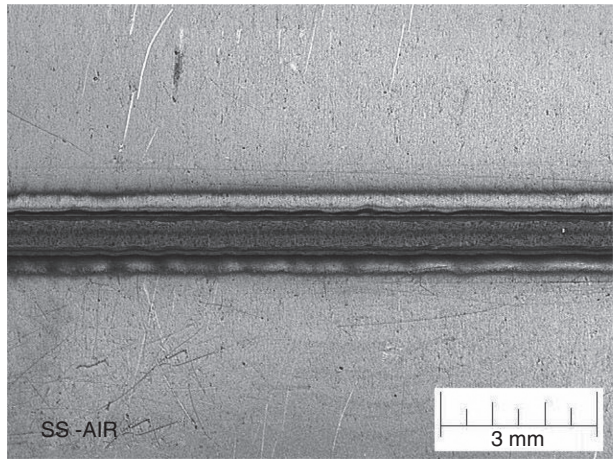
energy. This excess heat causes expansion of the weld joint that can lead to defects in the weld seam. This is typically seen to occur at some mid-point in the weld seam, where the process starts properly but then loses the weld seam thereafter.

Another key defect is due to poor cleanliness. Most welding processes have a very high-energy density, which can cause vaporization of most organic contaminants. These contaminants will boil rapidly and flash off, leaving cracks, craters and other defects that lead to high leak rates.

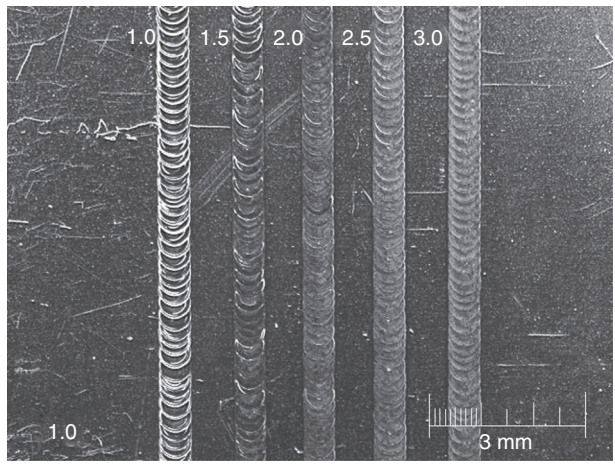
Cleanliness of the weld zone is also a strong function of the gases used during the sealing process. Argon, nitrogen, helium, and hydrogen are often used in combination to promote a smooth shiny weld zone that does not entrap gases or contaminates, or cause sooting. A laminar flow of low-pressure gas is recommended over the weld zone to control ingress of oxygen and to promote good thermal control of the weld pool. The effects of cover gas can be seen in Figs 9.7 and 9.8. In these examples, the stainless-steel plates were conduction welded with a low-power laser to yield a partial penetration weld seam. The degree of spatter, surface cleanliness, and overall penetration are affected by the choice and presentation of cover gas.

A second element of the gas choice during sealing is to use one of the gases for leak detection post-welding. Most medical-device manufacturers use a mix of argon–helium during the welding process. This choice allows a helium-leak-check system to be used post-welding to determine the leak rate of helium gas exiting the device through any cracks, crevices, or other defects in the enclosure.[15,16]

© Woodhead Publishing Limited, 2013



9.7 304 SS plate with partial penetration welds without cover gas. Note the surface oxidation and spread of the heat affected zone. (Photo courtesy of Edison Welding Institute.)



9.8 304 SS plate with partial penetration welds with helium–argon cover gas. Note the reduced surface oxidation and minimal spread of the heat affected zone. The numbers are the laser pulse width at constant power for all welds shown. (Photo courtesy of Edison Welding Institute.)

9.3 Measurement of leak rates – testing and verification

There are a wide variety of methods and techniques to determine the quality of a hermetic seal. Each technique has limitations on the level of defect that can be reliably detected. Helium mass spectrometry is an excellent

© Woodhead Publishing Limited, 2013

method on which to compare the various techniques. Where possible the approximate helium-leak rate for each method is given. The key techniques in use today include the following:

- Bubble test (10^{-4}–10^{-5} He atm/cc),
- Weight loss (10^{-1}–10^{-3} He atm/cc),
- Radioactive tracer gas (10^{-7}–10^{-9} He atm/cc),
- Helium mass spectrometer (10^{-5}–10^{-9} He atm/cc),
- Flow rate detection (10^{-1}–10^{-9} He atm/cc),
- Enclosure stress state (10^{-4}–10^{-5} He atm/cc).

Each of these will be described in further detail below.

9.3.1 Bubble test

Leak testing by detection of bubbles is likely the easiest and most common method. The typical approach is to fully submerge the sealed device in a small tank of fluid, and simple visual inspection or magnifying glass is used to inspect for a stream of bubbles emanating from the seal. The tank of fluid is often water, but low viscosity silicone oil, fluorinert, or solvents such as hexane or alcohol are also used. The tank of fluid is often heated to some degree, which serves to expand the gases enclosed in the device and provide an adequate pressure differential to drive the leak out of the package. A magnifying glass is very helpful, as is a vibration-free location, as the bubble stream can be very small. The advantage of this approach is its very low cost of implementation and its detection of the exact leak location. Once located, some defects can be re-sealed or re-welded to repair the leaking zone. A disadvantage is the limit of the leak-detection capability. The bubble test will typically correlate to helium-leak rates near 10^{-4} or 10^{-5} He atm/s.

9.3.2 Weight loss

A simple weight loss can also be used for some devices. Liquid-filled devices or devices filled with heavy gases such as tetrafluoroethane (134a refrigerant gas) can easily detect some leaks by simple weight loss. In this technique a laboratory analytical scale is used to weigh the device. A typical process is to equilibrate the sample for 24 h at room temperature and then record the initial weight to an accuracy of 0.1 mg. The device is then left in the equilibration chamber for 72 h and the second weight is then recorded. The weight loss is then calculated and scaled to a loss rate in units of mg/day or mg/year. The longer the time delay between measurements the more accurate the test. This test, like bubble testing, is easy to implement and very low

© Woodhead Publishing Limited, 2013

cost. However, the method is not very specific, does not delineate the location of the leak, and lacks sensitivity. It is also an off-line test and not easily amenable to full-scale production.

9.3.3 Radioactive tracer gas

Radioactive tracer gas is an early method used in many OEM electronic packages developed for defence and space applications. The technique imposes a mixture of krypton-85 and dry nitrogen gas onto a package. A 'bomb' is used for this purpose, which is a simple closed system similar to a pressurized paint can. The sealed devices are bombed with the gas mixture at a slight overpressure to force the gas mixture into the device via any cracks or pores. The devices are then removed, passed through an air knife to remove residual gases adhered to the exterior surfaces, and then placed into a Geiger counter (scintillation detector). The Geiger counter detects the number of Kr-85 particles forced into the device. A calculation is then made based on a fixed equation that uses the concentration of the Kr-85 gas, the mix ratio of nitrogen, the bomb pressure and the exposure time. This technique is included here for completeness, but has fallen from common use due to the radioactive tracer gas. Current laws have curtailed the availability and ease of use of the Kr-85 gas, and significant safety and environmental controls are now necessary to incorporate its use.

9.3.4 Helium mass spectrometer

The helium mass spectrometer has been the most used method in the medical-device industry. The systems, while complex in theory and somewhat expensive, are safe, reliable, and capable of detecting the smallest leaks. Current units are fast, simple to calibrate, and are used in off-line, at-line and in-line techniques to support full production testing.

In this method helium gas is detected as it flows out of the sealed device. The device is expected to have some volume or concentration of helium gas. The device is placed in a controlled volume chamber and pumped down to hard vacuum. The pressure differential causes helium atoms to flow out of cracks, crevices, and pores and is detected by the tuned mass spectrometer. The technique is very sensitive as it counts the actual molecules of helium and calculates the leak rate. Typical leak rates for well sealed medical devices such as pacemakers and defibrillators are 1×10^{-8} He atm/s.

As indicated above a concentration of helium is required in the package. Early techniques of leak detection 'bombed' the package to force helium gas inside the enclosure. Helium has the advantage of the next-to-smallest atomic size (only hydrogen is smaller), is inert, and is a favored cover gas for

© Woodhead Publishing Limited, 2013

laser and arc welding. Early practices often sealed the device in open air or nitrogen, so that little helium volume or concentration was inside the package during sealing. Helium was then forced into the package by bombing for minutes to hours in a pressurized can with pure helium. Current practice completes the welding and joining operation in a controlled atmosphere including a controlled volume of helium, 1–10% by volume is typical. By welding in the helium concentration, direct measurement of the helium by mass spectrometry can occur.

9.4 Determining leak rate based on helium content

The concept of leak detection by helium mass spectrometry grew out of the defence electronics era via the methods described in MIL-STD-883, test method 1014 for seal integrity. The approach was studied and developed at the Rome Air Development Center (RADC) in the 1960s.[4,7] The concepts and methods of this standard are still used today as the baseline approach for bubble, radioactive tracer, optical stress, dye penetrant and helium test conditions.

As stated in an earlier section, the key reason for hermetic sealing is to avoid ingress of moisture and subsequent corrosion and failure of the electronic circuits. To keep the internal moisture content below that needed for condensation, the moisture content must be maintained below 5000 ppm. In work completed to meet this requirement, researches at RADC determined air-leak rates for various size packages to maintain this moisture content over the device lifetime. The baseline criteria for air-leak rates by volume are given in Table 9.4.

The limit provided for electronic devices is an air-leak rate of 1×10^{-6} atm. cc/s air for internal free space volumes greater than 0.4 cc. Most implantable medical devices will use this baseline specification for an air-leak rate to maintain proper seal integrity and to scale the different measurement techniques.

The table of air-leak rates forms the basis on which to scale the measurements of the helium-leak test. The method uses the well-known Howell–Mann equation that relates the air-leak-rate specification for the given

Table 9.4 Package volumes and specification air leak rates to maintain 5000 ppm moisture limit

Volume	Allowed air leak rate
0.1 cm^3 or less	5×10^{-8} atm cm^3/s
0.1–0.4 cm^3	1×10^{-7} atm cm^3/s
0.4 cm^3 or greater	1×10^{-6} atm cm^3/s

© Woodhead Publishing Limited, 2013

volume to the required helium-leak rate measured by mass spectrometry. This scaling equation is necessary for two reasons. First, helium has a far different diffusion rate and atomic size. Helium is therefore able to leak at a far higher rate than air through the same crack or pore. Second, the leak rate is not linear and has an expected exponential decay. This exponential rate affects two processes in the leak-rate method, getting the helium into the sealed package by bomb pressurization, and extracting the helium out of the sealed package by vacuum pressure differential. The Howell–Mann equation was built around the concept of pressure bombing the part to be tested. The bomb was a sealed pressure vessel where the sealed device was over pressured with 40 psi helium for minutes to hours, to force some volume of helium inside the package. The volume or concentration of helium in the package will affect the leak-rate measurement and must be accounted for in the equation. The concentration of helium in the package is an important variable. In the extreme case of a gross leaker where all the helium has leaked out prior to mass spectrometer testing, the test system will pump down and yield a very low leak rate, but obviously a false test. The variables used in the Howell–Mann equation are given below.

9.4.1 Variable definitions

R_1 = helium-leak rate – scaled leak rate of helium using L

Decay = decay in leak rate – exponential decay in leak rate based on hold time T_2

$L = 1 \times 10^{-6}$ atm.cc/s air – standard leak rate related to package volume

$M_a = 28.7$ – molecular weight of air

$M_{He} = 4$ – molecular weight of helium

Content = 0.95/100 – percent helium in device at time 0 (example = 0.95%)

$P_e = 760 \times$ content torr – partial pressure of He in device

$P_0 = 760$ torr – standard atmospheric pressure

$T_2 = 2 \times 3600$ s – maximum 2 h exposure in ambient air prior to leak test

$V = 1.5$ cc – minimum internal free space volume (example 1.5 cm^3)

$$R1 = \frac{LP_e}{P_0}\left(\frac{M_a}{M_{He}}\right)^{0.5} \cdot \left[1 - e^{-\frac{LT_1}{VP_0}\left(\frac{M_a}{M_{He}}\right)^{0.5}}\right] \cdot e^{-\frac{LT_2}{VP_0}\left(\frac{M_a}{M_{He}}\right)^{0.5}} \quad [9.11]$$

© Woodhead Publishing Limited, 2013

9.4.2 Using the Howell–Mann rate calculations

It is generally desirable to split the equation into two parts. In the initial use of the equation the typical operation used a pressure bomb to force the leak test gas into the already sealed device. The second part of the equation measured the amount of the gas that leaked out during the hold period. In most current instances, there is already an imposed volume of tracer gas captured in the device during welding and sealing.

In the case of many implantable defibrillators and pacemakers, the volume of tracer gas is near 1%.

The typical two-part equation is split by R_1, and the decay portions of the calculation given as:

$$R_1 = L \times \left(\frac{P_e}{P_0}\right) \times \left(\frac{M_a}{M_{He}}\right)^{1/2} \times e^{-\left(L \times (T_2/V) \times P_0\right) \times \left(M_a/M_{He}\right)^{1/2}} \quad [9.12]$$

$$\text{Decay} = e^{-\left[\left(L \times (T_1/V) \times P_0\right) \times \left(M_a/M_{He}\right)^{1/2}\right]} \quad [9.13]$$

Therefore decay ~ 1, as T_2 must be > 100 h to achieve a decay of 0.999 with internal volume of 1.5 cc.

Therefore R_1 for most situations can be simplified to (example for 0.95% He):

$$R_1 = L_0 \times \left(\frac{P_e}{P_0}\right) \times \left(\frac{M_a}{M_{He}}\right)^{1/2} 1 \times 10^{-6} \times \left(760 \times \frac{0.0095}{760}\right) \times \left(\frac{28.7}{4}\right)^{1/2}$$

$= 2.56 \times 10^{-8}$ atm.cc/s He – leak rate spec based on 0.95% helium.

Allowing for a 10% equipment error on leak testers, this value equates to a minimum leak rate of 2.3×10^{-8} atm.cc/s He.

Using the formula above, leak rates are calculated for percentage helium content in a typical medical device and listed in Table 9.5. The change in helium-leak rate based on the concentration of helium in the package is plotted in Fig. 9.9.

The data from Table 9.5 can also be used to calculate the minimum detectable helium content in a hermetic device. It is often desirable to set a baseline specification for a whole family of medical devices of similar size. An example is to determine the minimum helium content within a package if we establish a baseline leak rate of 9×10^{-9} atc.cc/s Helium. This can be determined as follows:

© Woodhead Publishing Limited, 2013

Table 9.5 Calculation of helium-leak rate based on air-leak rate of 1.0×10^{-6} and the effect of helium concentration within the package with standard calibration error on the mass spectrometer

% He	Leak rate spec (atm.cc/s He)	Leak rate spec – equipment error at 10% (atm.cc/s He)
100	2.70×10^{-6}	2.43×10^{-6}
5	1.35×10^{-7}	1.21×10^{-7}
4	1.08×10^{-7}	9.72×10^{-8}
3	8.10×10^{-8}	7.29×10^{-8}
2	5.40×10^{-8}	4.86×10^{-8}
1.90	5.13×10^{-8}	4.62×10^{-8}
1.80	4.86×10^{-8}	4.37×10^{-8}
1.70	4.59×10^{-8}	4.13×10^{-8}
1.60	4.32×10^{-8}	3.88×10^{-8}
1.50	4.05×10^{-8}	3.64×10^{-8}
1.40	3.78×10^{-8}	3.40×10^{-8}
1.30	3.51×10^{-8}	3.16×10^{-8}
1.20	3.24×10^{-8}	2.92×10^{-8}
1.10	2.97×10^{-8}	2.67×10^{-8}
1	2.70×10^{-8}	2.43×10^{-8}
0.95	2.56×10^{-8}	2.30×10^{-8}
0.90	2.43×10^{-8}	2.19×10^{-8}
0.85	2.29×10^{-8}	2.06×10^{-8}
0.80	2.16×10^{-8}	1.94×10^{-8}
0.75	2.02×10^{-8}	1.82×10^{-8}
0.70	1.89×10^{-8}	1.70×10^{-8}
0.65	1.75×10^{-8}	1.58×10^{-8}
0.60	1.62×10^{-8}	1.46×10^{-8}
0.55	1.48×10^{-8}	1.33×10^{-8}
0.50	1.35×10^{-8}	1.22×10^{-8}
0.45	1.21×10^{-8}	1.09×10^{-8}
0.40	1.08×10^{-8}	9.72×10^{-8}
0.35	9.45×10^{-9}	8.51×10^{-9}
0.30	8.10×10^{-9}	7.29×10^{-9}
0.25	6.75×10^{-9}	6.08×10^{-9}

The leak rate spec of 2.43×10^{-8} atm.cc/s equates to 1% helium per Table 9.4.

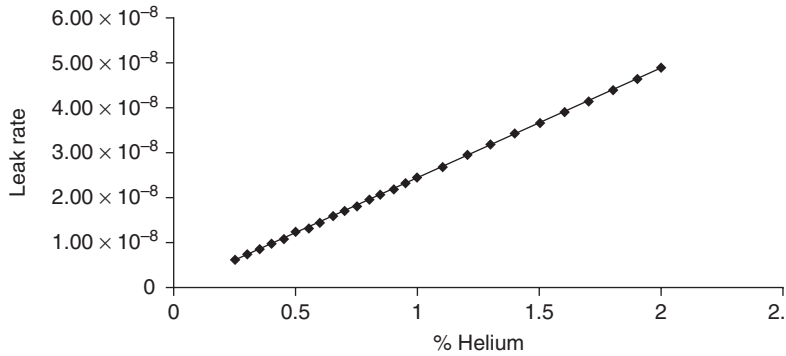
Desired Leak Rate spec 9×10^{-9} atm.cc/s equates to X% helium.

Therefore $X = (9 \times 10^{-9}$ atm.cc/s)/$(2.43 \times 10^{-8}$ atm.cc/s) = 0.37% helium.

This type of calculation helps the process engineers set the sealing process to guarantee there is enough helium inventory in the sealed device to meet the requirements of the leak test.

Note that this helium limit could be further reduced if calibrated controls were available below 9×10^{-9} (and they are). Provided that calibration

© Woodhead Publishing Limited, 2013



9.9 Plot of the change in scaled helium-leak rate vs helium content sealed or bombed into the package.

sources and controls are met, the detectable limit of helium and therefore the helium-gas content during the test can be extremely low. Note also that in a returned medical device many years old, the device could be quite hermetic and yet have no detectable helium tracer gas. It is therefore recommended that leak-rate testing include both a gross- and fine-leak-detection method.

9.4.3 Flow-rate detection

Several test systems are now available that use a technique to measure the actual flow rate of gas out of a sealed package. In this method, a sealed device is placed into a chamber of known fixed volume. A vacuum is imposed on the volume, and all residual gas is removed. As most devices are sealed at or near 1 atmosphere pressure, the vacuum imposes a pressure differential across the hermetic seal. The inner gases of the sealed device leak out, and the overall flow of gas is detected. Detection methods can use a variety of methods including flame ionization, heated filament/element, or calibration against a fixed and calibrated orifice plate. The heated filament and orifice plate are the most common. In the heated filament systems, the thermal conductivity of the escaping gases change the resistivity in the heated wire. This shift is proportional to the concentration and flow rate of the gases. Similarly, a calibrated orifice plate of fixed leak path length and diameter can be used. In this system, the detection gas is calibrated for flow through a know leak path (orifice). This is compared with the gases drawn out of the enclosure during test. The advantage of these systems is their increased sensitivity and detection limit. The test time can very rapid and many of these systems are used at-line and in-line for leak detection during production.

© Woodhead Publishing Limited, 2013

Disadvantages are higher cost, inability to precisely locate a leak, and some difficulty in calibration. These systems must be carefully set up and tuned to the gases used.

A third method of flow-rate detection is pump down transients. This is especially effective with large-volume packages. The technique is fairly simple in that again the package is placed in a known-volume chamber and exposed to vacuum. As explained earlier the vacuum causes a pressure differential and the enclosed gases flow across the pressure gradient. If the package is leaking, the vacuum system must work much harder to exhaust the extra gases. The time and effort to pump down is a direct correlation of the leak rate. The easiest way to correlate the pump down transients is to confirm various leak rates of packages and then plot the vacuum pressure in torr vs time. Leaking packages will have a far higher time constant to reach low torr values than sealed units. The method is accurate, easy to implement, and yields a simple go no-go method amenable to at-line testing.

9.4.4 Enclosure stress state

An emerging method now finding acceptance is a novel technique that measures the stress state of the enclosure. The method begins in a similar manner to those suggested above where the package is exposed to a pressure differential. The pressure differential will cause the enclosure walls to bulge inward or outward depending on whether the outside environment is pressurized or de-pressurized. A laser beam is then used to reflect off the surface and measure the deflection. If the package is leaking, the degree of deflection is reduced as the package can quickly equilibrate to the pressure differential. Further, a set of calibration curves can be developed on leaking and non-leaking devices such that the degree of deflection versus pressure differential can be plotted. The rate of the deflection change with time can also be used to correlate to leak rate. This method has the advantage of speed, good low-leak-rate-detection limit, and is applicable to high-rate production. Disadvantages include the need for good uniformity of the surface condition, good control of the enclosure material properties, and the requirement for some level of laser safety.

9.5 References

1. Viswanadham, P. and Singh, P., *Failure Modes and Mechanisms in Electronic Packages*. 1998: Chapman & Hall.
2. Ohring, M., *Reliability and Failure of Electronic Materials and Devices*. 1998: Academic Press.
3. Thompson, J.J., *Conduction of Electricity through Gases*. 2005: Wexford College Press.

© Woodhead Publishing Limited, 2013

4. Thomas, R.W., Moisture myths and microcircuits, 1972: RADC.
5. Pecht, M.G., Ardebili, H., Shukla, A.A., Hagge, J.K., Jennings, D., Moisture ingress into organic laminates. *IEEE Trans. on Components and Packaging Technology*, 1999. **22**(1): 104–110.
6. Wong, E.H. and Rajoo, R., Moisture absorption and diffusion characterization of packaging materials-advanced treatment. *Microelectronics Reliability*, 2003. **43**: 2087–2096.
7. Mil Std 883, mil-c-38510 method 1014.11.
8. Amkor Technology, *MQFP Moisture Absorption/Desorption Data*. 2004. www.quicklogic.com/images/military_mqfp_moisture.pdf.
9. Sorbent Systems, *Desiccant Chart Comparisons*. 2004. www.sorbentsystems.com/desiccants_charts.html.
10. *CRC Handbook of Chemistry and Physics*, 84th edn, 1982: CRC Press, Inc., pp. 15–34.
11. Keller, S.W., Determination of the leak size critical to package sterility maintenance, PhD dissertation, VPI&SU, Aug. 1998, Blacksburg, VA.
12. O'Hanlon, J.F., *A User's Guide to Vacuum Technology*, 2003: John Wiley & Sons Inc.
13. Rack, P.D., Class notes on vacuum technology II, University of Tennyson, Department of Materials Science and Engineering.
14. Ely, K.J. and Zhou Y., Microjoining in medical components and devices, Chapter 23 in *Microjoining and Nanojoining* (Ed. Zhou, Y.), 2008: Woodhead Publishing Limited.
15. Axelson, L. and Calvin S., Aseptic integrity and microhole determination of packages by gas leakage detection, *Packaging Technology and Science*, 1991. **4**: 9–20.
16. Greenhouse, H., Lowry, R. and Romenesko, B., *Hermeticity of Electronic Packages*, 2nd edn, 2011: Elsevier Press.

© Woodhead Publishing Limited, 2013

10

Overview of welding methods for medical plastics

H. J. YEH, Amgen Inc., USA

DOI: 10.1533/9780857096425.3.261

Abstract: This chapter presents a technical review of the welding technologies for medical plastics. It covers both the fundamentals of the plastic-welding process and an overview of the major welding technologies used in medical plastics. Plastic-welding processes can be divided into three different groups based on the mechanism of heat generation: external heating methods, where the thermal energy is applied externally onto the surface of the part such as hot plate, extrusion, hot gas, laser, and infrared (IR) welding; internal heating methods, where the heating is generated mechanically, electrically, or electromagnetically by internal molecular vibration or friction at the joint interface such as ultrasonic, vibration, spin, dielectric, and microwave welding; and implant heating methods, where heating is initially produced in a susceptor placed at the joint interface and then conducted to the parent material such as resistive implant, induction implant, microwave implant, and IR/laser implant welding.

Key words: weldability, solvent bonding, through-transmission radiation welding, radiation welding of fluoro-polymers, joining of catheters.

10.1 Introduction

With advances in raw polymer materials and their manufacturing processes, many plastics are able to offer flexibility, consistency and cost effectiveness in design and manufacturing processes while at the same time meeting the stringent requirements of the well-regulated medical-device industry. As a result, the usage of plastics in the medical-device industry has been increasing steadily since the discovery of synthetic polymers. More and more, plastic devices are being developed and commercialized to replace existing metal devices. Medical plastics have been used in different applications in the FDA's device classifications (Class I, II, III), ranging from a simple tool such as a tongue depressor, to a complex balloon/stent catheter system that goes inside a human body during surgery with the stent being implanted inside a patient's artery.

© Woodhead Publishing Limited, 2013

Joining plastic components becomes necessary when molding complex products (or other primary processes) is difficult and/or cost prohibitive. In other applications, joining is also needed between parts that come from different primary processes, such as between extruded sheet/tubing and molded parts. Unlike metal welding, the joining/welding of plastics has frequently been overlooked by the mainstream plastic industry. It has been regarded as a secondary operation in the plastic manufacturing processes. In many real-world examples that I have dealt with during my consulting career, welding consideration is frequently treated as an 'afterthought' in a typical plastic-product development cycle. In reality, however, the performance of the final product depends equally on both primary and secondary operations. Any component can be molded precisely but if assembled/welded improperly, it is still considered a reject.

Typical joining methods for plastics include adhesive bonding, mechanical fastening, and welding.

10.1.1 Adhesive bonding

Different adhesives with specific bonding processes (such as dispensing and curing) can be used to bond dissimilar plastics and thermoset plastics, as well as different types of materials such as metals and plastics.

10.1.2 Mechanical fastening

Mechanical fastening does not provide bonding between the two surfaces of the parts to be joined. The joint strength is provided by mechanically joining two parts together through pre-designed fitting (such as snap fit or press fit) or by the addition parts such as a bolt or rivet.

10.1.3 Welding

As its title implies, this chapter will focus on the welding of medical plastics and provide an overview of the main welding processes used in the medical-device industry. As the awareness of recycling and other environmental issues increase, welding is becoming a natural choice with regards to the joining of thermoplastics. The welding process itself has some attractive features:

- strong joint (comparable to parent material);
- short process time (for most medical-device applications);
- no new material (such as adhesives) is required except the implant welding processes;
- it can be automated and integrated into manufacturing processes.

© Woodhead Publishing Limited, 2013

An array of welding techniques is available for different applications. Choosing an appropriate welding method can directly affect the product integrity and the manufacturing cost. Many criteria can be used to select an appropriate joining method but the decision is usually based on the following variables: application of the joint, cost, process time, reliability of the joint, material issues, additional manufacturing processes required, operating conditions, loading, geometry, weight, and size. This chapter is intended to provide a brief overview of different welding techniques for medical plastics. It will also compare the benefits and limitations of the welding techniques in relation to other medical-device manufacturing processes.

10.2 Fundamental processes of plastics welding

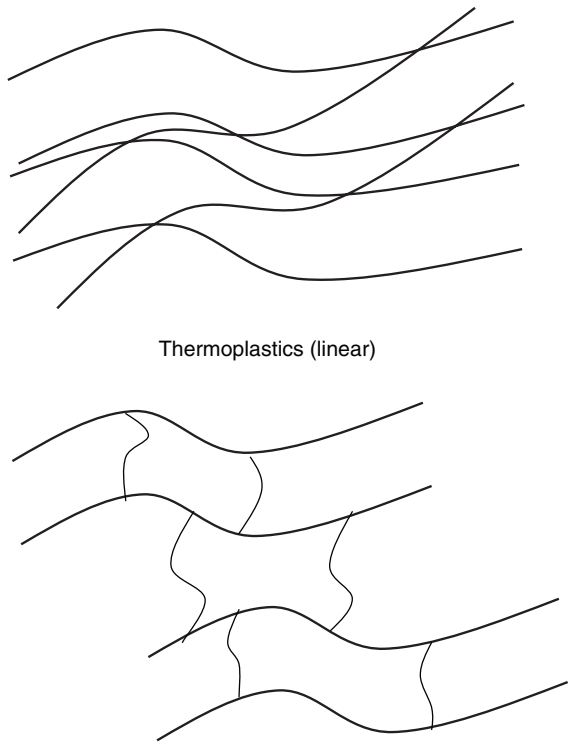
Plastics can be categorized into thermoplastics and thermosets. Thermoplastics can be softened and melted upon heating. Thermosets, on the other hand, cannot be softened or melted once they are made due to their cross-linked structure (see Fig. 10.1). Because fusion is required for the welding process, only thermoplastics can utilize welding as a joining process.

There are four fundamental steps in a welding process – heating the joint surface, application of pressure, intermolecular diffusion and cooling.[1]

Heating of the joint surface is the most important step. Different welding methods differ in the heating method that is used. The heating can be divided into three types (see Fig. 10.2):

1. *External heating*: heat is externally applied onto the surface of the part. Typical processes are:
   - conduction: hot plate, extrusion;
   - convection: hot gas;
   - radiation: laser, infrared.
2. *Internal heating*: heat is generated by internal molecular vibration or friction at the joint interface. The energy sources can be mechanical or electric/electromagnetic. Typical processes include ultrasonic, vibration, spin, and RF/dielectric.
3. *Implant heating*: thermal energy is produced by heating a susceptor (energy absorber) at the joint interface where the energy sources can be converted from different types of energy such as electrical or electromagnetic energy. Typical processes are induction implant, resistive implant, microwave implant, and infrared/laser implant. Two key characteristics of the susceptors are the ability to absorb the energy from the particular energy source and the ability to provide compatibility (weldability) between the two pieces of the parts to be joined.

© Woodhead Publishing Limited, 2013

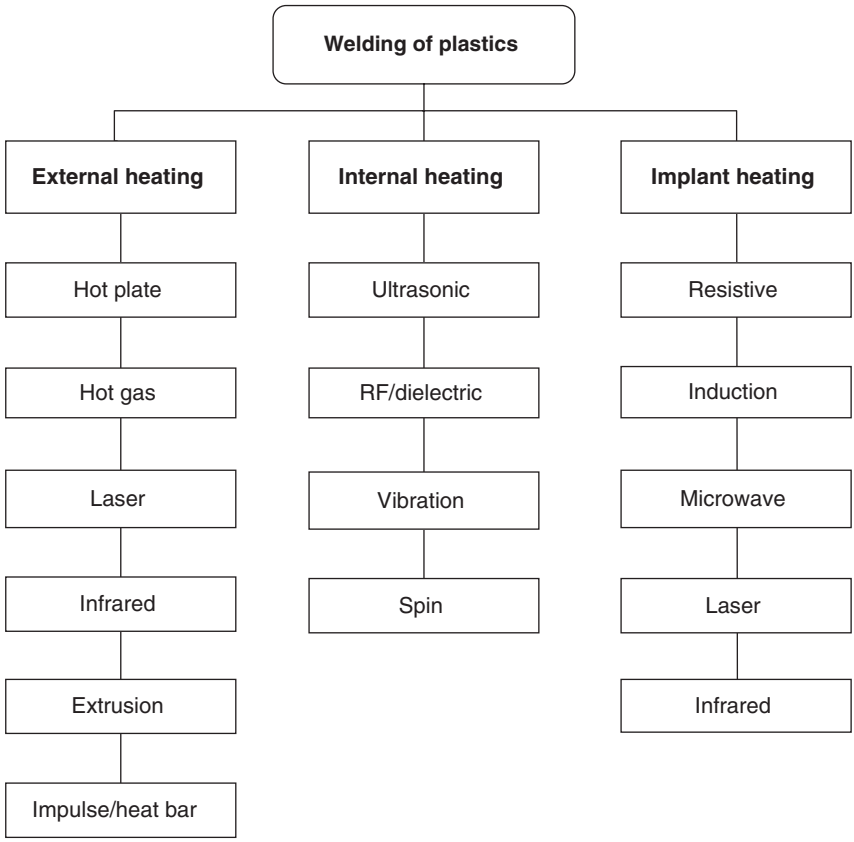


10.1 Thermoplastics vs thermosets.

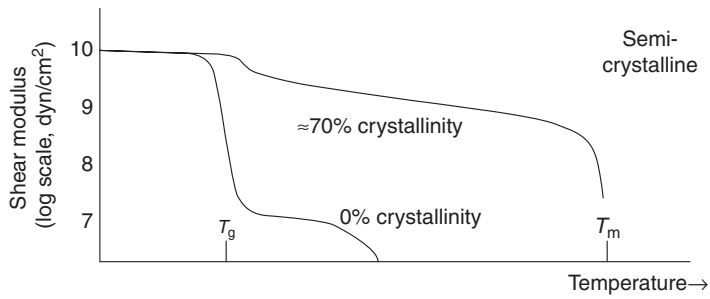
Different materials require different levels of heating. As a rule of thumb, semicrystalline thermoplastics require a heating temperature higher than the melting temperature. And amorphous thermoplastics require heating temperatures higher than glass transition temperature (see Fig. 10.3). The corresponding process parameters for the heating process are heating time and temperature. Controlling heating time as a process parameter ensure that a sufficient molten layer is created during the heating process such that the uniform diffusion process at the joint interface can occur under the preset pressure, ensuring that a strong joint strength can be achieved.

Application of pressure presses two melted parts together to have an intimate contact at the joint interface. Some heating (welding) methods require higher pressure because the heating is generated by relative mechanical motion between two parts such as ultrasonic, vibration, and spin-welding processes. The corresponding process parameters for this particular process are weld force/pressure and hold time. An analytical force/pressure

© Woodhead Publishing Limited, 2013

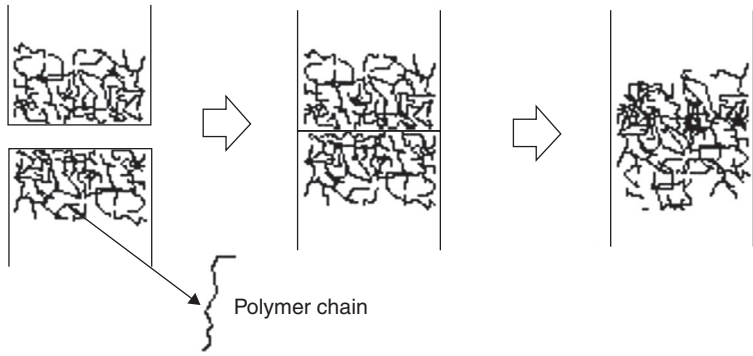


10.2 Welding of plastics based on heating techniques.



10.3 Modulus vs temperature for amorphous (0% crystallinity) and semicrystalline polymers.

© Woodhead Publishing Limited, 2013



10.4 Diffusion process (chain entanglement).

application process can be described as a squeeze-flow process that is commonly observed in polymer processing. Plate II (see Plate II in color section between pages 300 and 301) shows a flow pattern of the joint interface of a hot-plate welded-plastic sample. It is important to note that the final material left in the joint interface is the material that comes from the central portion of the molten layer. The original top surface of the molten layer is squeezed out and forms weld beads at the side.

Intermolecular diffusion is similar to the healing of the polymer–polymer interface. The main purpose is to let the chain molecules move across the interface to create chain entanglement (see Fig. 10.4). The important aspect of this is the time required for the complete healing. Many studies have shown that the time required for healing is much less than the time required for flow and wetting.

Cooling is the process when the melted polymer is resolidified to provide structural strength. The cooling rate may have some effect on the microstructure of the semicrystalline thermoplastics. This becomes more pronounced when a large molten layer is created in a welding process such as hot-plate welding. But in many cases, short cooling times are more desirable for cost reductions.

10.2.1 Key welding process parameters

Based on these welding steps, there are some common process parameters:

1. Energy input:
   (a) temperature of the heating element;
   (b) amplitude of vibration;
   (c) power/energy related terms (current level, watts, etc.).

© Woodhead Publishing Limited, 2013

2. Weld time:
   (a) How long is the weld interface being heated?
3. Weld pressure:
   (a) Depending on the welding processes, a preset pressure is applied during or after the heating/welding process.
4. Distance/collapse control:
   (a) A specific collapse or travel distance during welding could be used to control the completion of the welding process.
5. Cooling time:
   (a) Cooling time is part of the cycle time required for the welding process. Welding process with a larger heat-affected zone will require more cooling time and results in a longer process/cycle time.
6. Good fixturing to ensure a uniform energy and pressure is applied over the joint interface.

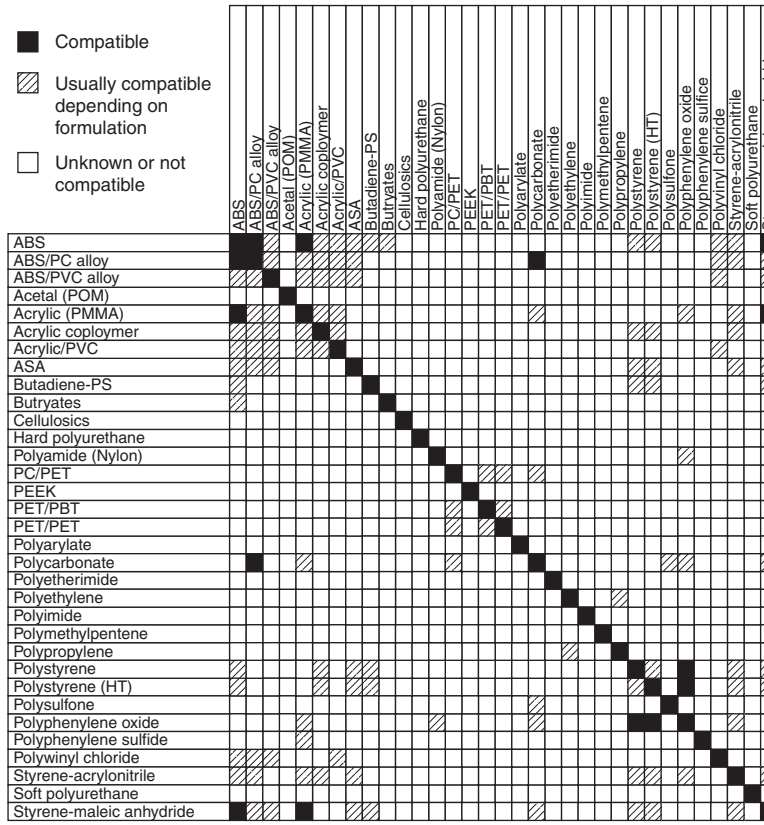
10.3 Medical plastics and weldability

Depending on the application there are different requirements for medical-device development. Typical key requirements in the medical-device development are biocompatibility, plastic material performance, and manufacturing processability. If welding is one of the manufacturing processes required, the weldability must be considered in addition to other requirements when choosing the plastic materials. Ideally, one should always try to use the same or similar plastic for the two parts to be welded if possible. However, in the real world there are limitations on material selection depending on the applications and designs. Figure 10.5 shows a weldability table that lists the compatibility of different polymers that can be used as a reference to aid selection of appropriate plastics for general welding considerations. This table should be used as a starting point just for compatibility considerations. There are other welding-related factors affecting the selection of the plastic materials for medical devices, which will be discussed when different welding processes are covered in later sections of this chapter.

10.3.1 Alloys and copolymers

Two key subsets of polymer materials are alloys and copolymers. They offer unique properties for specific applications. Their weldability is more difficult to estimate but as a rule of thumb welding between similar materials should produce acceptable weld strength for specific applications. Based on the alloy combination, one can also expect that welding strength between two plastics that could form an alloy is generally acceptable. For example,

© Woodhead Publishing Limited, 2013



10.5 Weldability table for thermoplastics.

welding between these plastics might be able to produce weld strength well above the particular application that you are looking for:

- acrylonitrile butadiene styrene (ABS) and polyvinyl chloride (PVC)
- polycarbonate (PC) and ABS;
- acrylic and PVC;
- ABS/PVC alloy and acrylic copolymer;
- PC/ABS alloy and acrylic;
- PC/ABS alloy and acrylic/PVC alloy.

10.3.2 Plastic with fillers or regrind

In general any increase of fillers or regrind in the plastics means less virgin polymer available for welding purpose. The weld strength will be reduced as the content of filler or regrind increases.

© Woodhead Publishing Limited, 2013

10.3.3 Moisture

Some polymers are hygroscopic, such as polycarbonate, nylon, polysulfone, and PET; if the materials are not dried or exposed in a high-humidity environment before welding takes place, foamy structure (air bubbles) could occur at the joint area. Larger heating area will make the condition worse. As a result, joint quality will suffer. In general, it is desirable to do welding right after the molding process with minimal exposure to the high-humidity condition. If this is not possible, an additional drying process will be necessary before the welding process takes place.

10.3.4 Special additives and colorants

Additives are considers as impurity or foreign material to the base polymer. These usually reduce the weldability. Colorants do not usually interfere with welding, but titanium dioxide used as a white pigment has some noticeable impact on the weldability.

10.3.5 Testing of weldability

There is an easy and straight forward way of manually testing the weldability between two unknown plastics:

1. Prepare a hot metal plate that is capable of producing a temperature for up to 400°F. Use a sheet of fiber-reinforced Teflon cloth as a non-stick coating by clipping it on the metal plate surface.
2. Prepare two test bars (similar to a regular tensile test specimen) out of the plastic on which you want to do the weldability test.
3. Hold the test bars against the hot plate (the temperature should be higher than Tg or Tm of the plastic) with a small pressure until a small molten layer form on each bar (usually takes around 5 s).
4. Quickly remove the bars from the plate and carefully align and push the two molten layers against each other and maintain the pressure for another 10 s to let it solidify and cool down.
5. If these two plastics are compatible/weldable, the joint should be able to hold up when you try to pull them apart.

10.4 Part and joint design

Joint-design considerations for welding processes should be treated as part of DFM/DFA (design for manufacturing and assembly) process. In

© Woodhead Publishing Limited, 2013

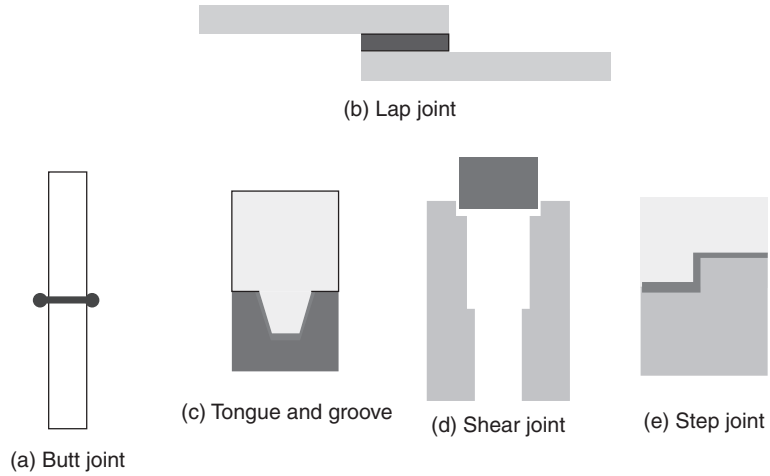
my past experience as a consultant, joint design for welding processes is frequently treated as an afterthought. Many parts are designed and prototyped without having an appropriate joint design based on an appropriate joining/welding process. As a result they fail to meet the final functional requirements and are forced to be modified in the last-minute scrambling.

A good joint design is a critical step in achieving final joint results. Depending on the welding processes selected, there are different joint designs available. As a rule of thumb, welding processes that use mechanical movement/vibration (such as ultrasonic, vibration, spin-welding processes) as a heating mechanism have a critical and sensitive joint design to the final joint strength because the efficiency of the heat generation is dependent on the design.

One key concept about the joint design is to integrate it into the overall part design. Here are some factors that need to be considered during the joint- and part-design stage:

1. To simplify difficult molding or manufacturing processes: When a complicated part geometry prevents a molding tool design or a molding process from producing the whole part, it can be molded into two or multiple parts and then joined together by a welding process. In this case, how and where to separate the complex part into two or more parts could be limited by the molding process, additional manufacturing process required, or the available welding process to join the parts together and provide sufficient joint strength. For example, some of the smaller medical-use filters are put together by welding two top and bottom molded halves with a membrane in between.
2. Functional or strength requirement for the joint (geometry of the joint): Is there a specific functional or strength requirement for the joint? In some cases, a hermetic seal is required to create an enclosure when joining two halves together. In other cases, depending on the joint-strength requirement, joint design could be all around the joint interface or it could be just at some intermittent spots (designed to be breakable or detachable).
3. What welding process can be used? Different plastic materials and welding processes usually require different joint designs. Even with the same welding process, depending on the functional requirements, the joint design could be different too. Welding-related aspects of the joint design will be discussed separately in the later sections of the welding processes.

© Woodhead Publishing Limited, 2013



10.6 Typical joint designs for plastic welding.

The typical joint designs are described below (see also Fig. 10.6):

(a) Butt joint: this is the most straightforward joint design for welding process. The joint interface is perpendicular to the direction of the force application.
(b) Lap joint: two joining surfaces are joined by overlapping onto each other.
(c) Tongue and groove joint: joint interface is a matching male (T shape) to female (U shape) joint design. This joint design provides self-aligning and is more suitable for hermetic-seal applications. However, there is a requirement on the minimal wall thickness especially for the ultrasonic welding process.
(d) Shear joint: this is a special joint design for ultrasonic welding where an interference between two matching parts is required. This is also a good joint design for hermetic-seal applications.
(e) Step joint: this joint design has a step where it provides more joint area and a mean of alignment.

10.5 Processes with external heating

This is when heat is applied externally onto the part surfaces to be joined. The heat source can be a hot plate, hot gas, or infrared heater. After the surfaces are melted, the heat source is removed and the two melted interfaces are pressed together. Unless the parts to be welded have thin enough material

© Woodhead Publishing Limited, 2013

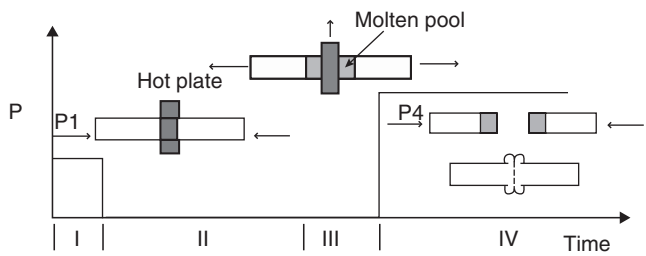
that heat can be transferred from the heating surface (such as thin film) to the joint interface quickly, these two parts have to be heated separately and then brought together under a preset pressure – that is, a change-over time will need to be included in the overall process cycle time.

10.5.1 Hot-plate welding

Hot-plate welding uses a contact-type heating process (see Fig. 10.7). Heat is carried out by thermal conduction from the hot plate to the parts. Hot-plate welding is not a popular welding method used in medical-device industry because it is more suitable for large parts and requires a longer process time. However, it offers simple process control and very consistent results. The size of the part can be as big as the hot platen. It can be an irregular shape as long as the temperature on the platen is uniform. Good control of the heating temperature and heating time is required to ensure uniform melting at the joint interface. It is possible to weld dissimilar but compatible thermoplastics using the hot-plate process. Two hot platens with different temperature setting are required to compensate for different melting temperatures of the compatible plastics. Butt joint is the most common joint design used for hot-plate welding. Also, the hot-plate-welding process will create a weld bead where the molten material is squeezed out during the welding process.

10.5.2 Heat sealing/welding (impulse sealer)

The heated bar or impulse heat sealer is commonly used to seal thermoplastic thin films and laminates. The process is very similar to hot-plate welding process. The heating energy is provided by a two heated bars (maintained at the heating temperature) or two resistive thin metal stripes (heat generated only when the current passing through the stripes is turned on). PTFE



10.7 Hot-plate welding (P is the pressure, P1 is the heat pressure, P4 is the weld pressure). I, heating with pressure; II, heating without pressure; III, change-over; IV, welding/forging.

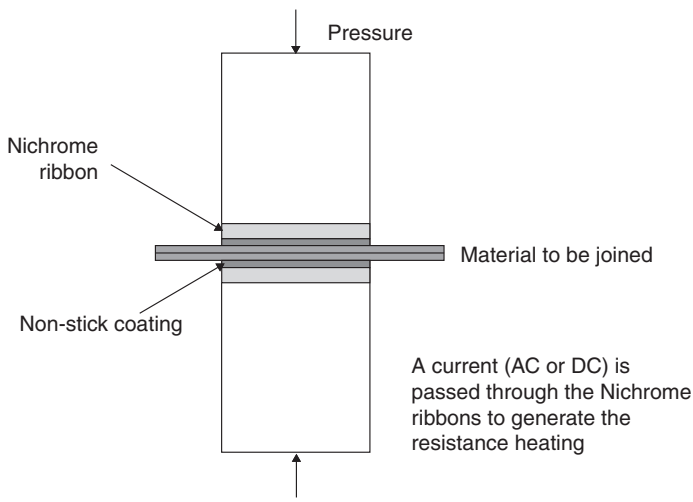
© Woodhead Publishing Limited, 2013

or Kapton film is usually used in between the heating element and the films to be welded as a non-stick layer. During the welding process, pressure is applied onto the films in between the heating elements. In some cases, if the film is thin enough for heat to be conducted through the film quickly, one-sided heating element can be sufficient. For the heated-bar sealing process, sometimes a cooling tool with a shape similar to the heated bar can be used to cool down the joint interface right after the heating process to help re-solidify the joint area and prevent the reopening of the joint. The key welding parameters are bar temperature, welding time, and weld pressure. The main application for this welding technique is to seal of packaging materials such as blister pack and tray. The heated-bar sealing process can also be used to seal a small membrane onto a plastic substrate.

Impulse welding is the process by which electricity is used to create heat through a high-resistance wire (see Fig. 10.8). The wire is typically nickel–chromium encapsulated in a non-stick coating. A current will cause the wire to heat rapidly then transfer to the materials. Traditional impulse welding processes have limited controls over the heating and cooling cycles. This results in a continuous heat build-up in the machine cycles, negatively affecting the repeatability of subsequent welds.

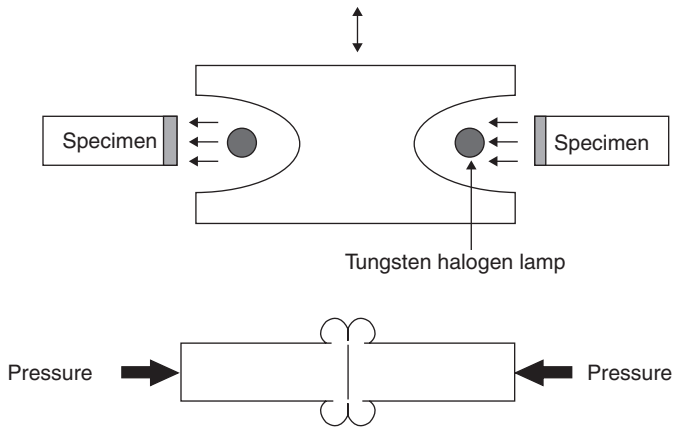
10.5.3 Infrared welding

Infrared welding uses a non-contact type heating process (see Fig. 10.9). Heating is carried out by thermal radiation from the infrared lamp. The

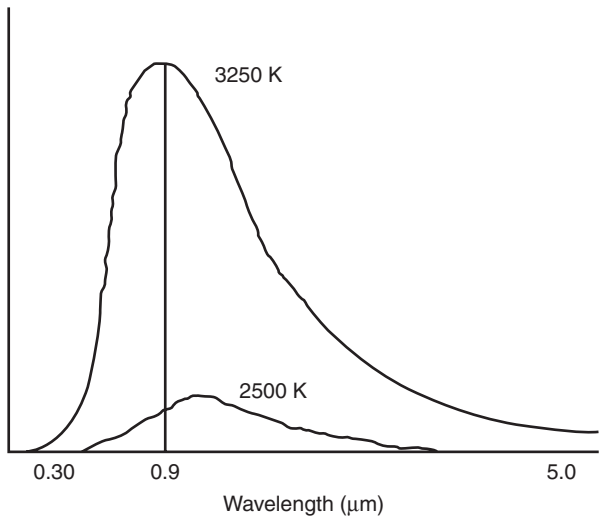


10.8 Impulse heat-sealing process.

© Woodhead Publishing Limited, 2013



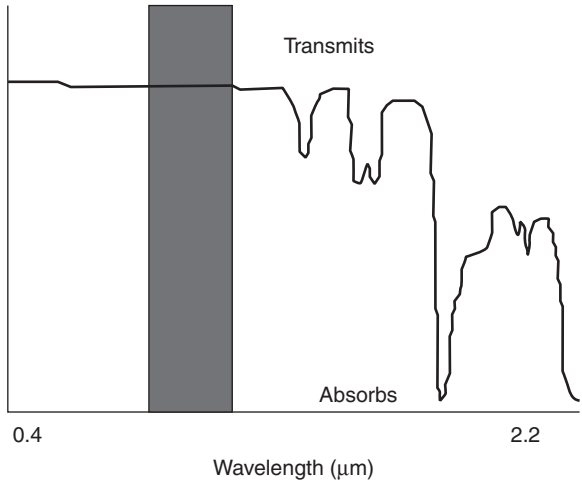
10.9 Non-contact infrared welding.



10.10 Typical wavelength distribution for a quartz halogen IR lamp.

radiation wavelength is dependent on the temperature of the heating element following Wien's law (see equation below). Figure 10.10 shows the wavelength distribution of a typical quartz halogen IR lamp at different temperatures. At the peak temperature, the corresponding wavelength is around 0.9 μm. Figure 10.11 shows a relatively low absorption of a typical natural-color plastic material around the near IR wavelength. This wavelength range is suitable for through-transmission welding applications.

© Woodhead Publishing Limited, 2013



10.11 IR lamp near infrared wavelength transmission for most of the transparent (or natural-color) polymers.

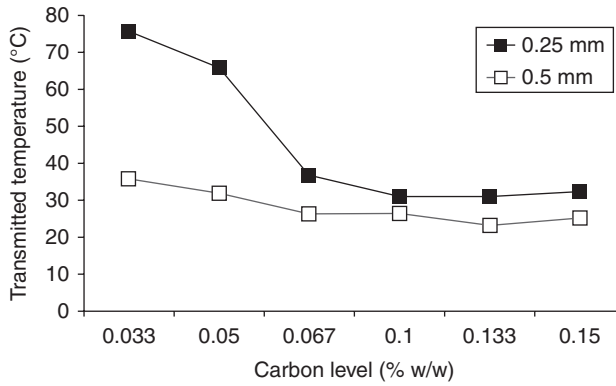
Wien's law:

$$\lambda_{max} T = 0.2898 \text{ cm deg K}$$

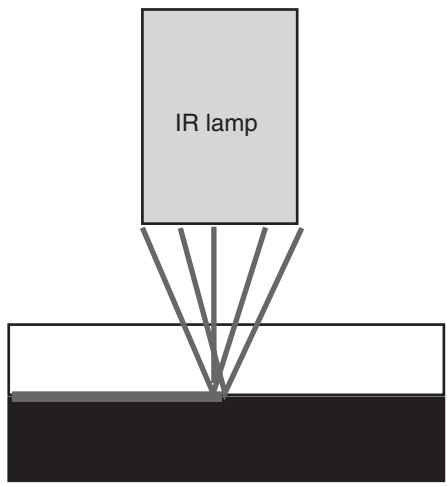
Different thermoplastics and thermoplastics with different pigmentation absorb infrared energy differently. Black thermoplastics absorb more infrared energy than other color materials. Natural and transparent thermoplastics usually have the least absorption. Studies have been done in this area on characterization of IR heating absorption.[2] Figure 10.12 shows how the carbon black content in polyethylene could impact the heat absorption efficiency for IR welding. For a typical quartz halogen IR lamp, you begin to see the impact of the heat absorption when the carbon black content level in a polyethylene thin sheet is greater than 0.06%. Therefore, selective heating (through transmission) is possible for infrared welding (lap joint with transparent layer on top or an absorbing layer between two transparent parts to be joined, see Fig. 10.13). Through-transmission, welding can be operated in step-wise or continuous mode where either the heat source or the work piece can move or rotate at a constant speed.

For direct-heating butt-joint operation (non-contact, external heating), the infrared process is very similar to hot-plate welding. Heating time and heating distance are the variables that control the amount of heat input. One key advantage of the direct IR over hot-plate welding is that the heat source only needs to be turned on during the heating cycle. No preheating is required as in the hot-plate welding process. However, this type of operation works better with darker-color plastic parts because transparent or

© Woodhead Publishing Limited, 2013



10.12 IR heating absorption efficiency (measured by temperature) of polyethylene with different carbon black levels.



10.13 Through transmission infrared welding of plastics.

light-color parts will have much less energy absorption with a high-intensity quartz halogen IR lamp, and, as a result, very inefficient heating. Some other lower-intensity radiant heaters with lower peak temperatures than the quartz halogen lamp can actually have higher heating efficiency even with natural-color plastic parts because of their longer wavelengths and higher energy absorption.

Limitations of infrared welding include a shorter lamp life and the availability of different size/shape of the lamps. Currently, only line and spot heating elements are available for high-intensity lamps, but some heating patterns can be achieved by combining spot heaters together. Furthermore

© Woodhead Publishing Limited, 2013

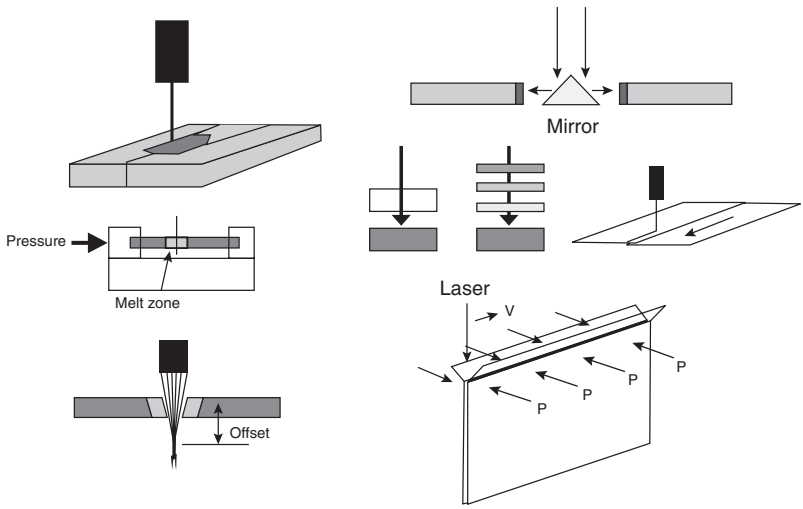
some translucent parts could actually absorb IR radiation energy (melting at the top surface) during through-transmission welding. However, studies have shown that as long as appropriate filters are applied, a good-quality weld can be obtained.

Due to the limitations and suitability for specific applications, infrared welding has not been used widely. However, it has great potential because of its unique characteristics of radiant heating. Many research studies have been conducted on how to combine, enhance, and transport the IR energy to the joint area efficiently. Different approaches have been evaluated in utilizing light pipes (quartz rods), fiber-optic bundles based on single and modified multiple focusable IR spot lamps. Plate III (see Plate III in color section between pages 300 and 301) shows some examples of the welded parts using these techniques. In my opinion, through-transmission IR welding is underutilized because it is not readily available commercially. Most of the commercial IR welding machines are targeted to replace traditional hot-plate welding machines. More development work is needed to further advance the through-transmission IR welding for specific commercial applications.

10.5.4 Laser welding

Laser welding has a much greater heat density than infrared welding. Unlike infrared, laser has a single-wavelength radiation. Nd-YAG, CO_2 and diode lasers are the most frequently used lasers for joining thermoplastics. One unique characteristic of laser is the high-energy concentration and the precision of the heating area. The wavelength of a laser determines the material interaction between the laser and the plastic materials. Most thermoplastics are considered opaque with the wavelength of CO_2 laser. On the other hand, YAG and diode lasers have much shorter wavelengths and can penetrate through some transparent and natural-color plastics with minimal absorption. Similar to the infrared processes, different materials and pigmentation may affect the absorption efficiency of the laser radiation. These effects can be suitable for selective heating (through-transmission welding or implant-laser welding) for YAG and diode lasers. For example, if you have an application where you need to melt the transparent tubing from external surface, the CO_2 laser will be a better choice than the YAG or diode lasers. However, if you have an application where a transparent tubing overlaps a dark tubing inside, then YAG and diode lasers can be used to create bonding at the interface of these two tubings. YAG and diode lasers are also suitable for fiber -transmission beam delivery, which makes the laser-welding process much simpler and more flexible. Figure 10.14 shows different laser-welding-process configurations. Laser welding is not the most commonly used welding process because of its high-capital and maintenance costs. However, with the unique heating characteristics and price reduction of the laser systems as

© Woodhead Publishing Limited, 2013



10.14 Different laser-welding process configurations (where V is speed and P is applied pressure).

laser technology advances more and more applications of laser welding are expected in the future.

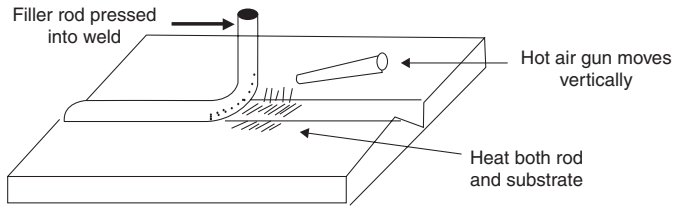
10.5.5 Hot-gas welding

Hot-gas welding is not a common welding technique used in the medical-device industry. In traditional hot-gas welding, heating is done by directing hot gas or air at the joint area to melt the surfaces (see Fig. 10.15). A filler rod is used for some joint designs. It usually has the same composition as the substrate. Both the filler rod and substrate surfaces are melted and then welded. In most of the cases, compressed air is a popular choice. In some cases, non-oxidizing gases such as nitrogen are used for oxidation-sensitive materials. Unlike the traditional hot-gas welding process, for medical-device applications hot gas can be used as a non-contact heating source for preheating, fusion, and welding applications. In the welding case, no additional filler rod is used. One thing to keep in mind is that hot-gas heating is not very uniform or precise. If non-contact hearing is required, I would suggest looking into IR heating rather than hot-gas heating.

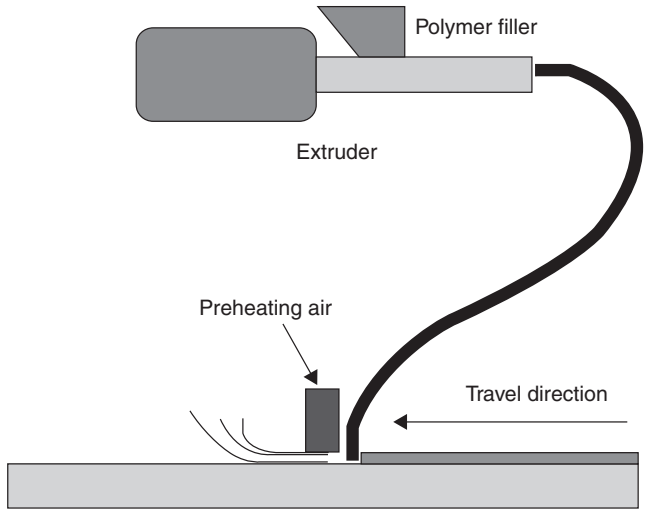
10.5.6 Extrusion welding

Extrusion welding is similar to a combination of hot-melt adhesive and hot-plate or hot-gas welding (see Fig. 10.16). It is not commonly used in the

© Woodhead Publishing Limited, 2013



10.15 Hot-gas welding.



10.16 Extrusion welding.

medical-device industry. The melted polymer is injected into the weld zone with the hot gas or a heated shoe preheating the substrates to be joined. The injected polymer should be the same material as the substrate. The heated shoe is usually coated with PTFE and can come in different shapes to suit different part geometries. The application of extrusion welding is similar to that of hot-gas welding. A skilled operator is needed when manual welding is used.

10.6 Processes with internal heating

One unique aspect of this internal-heating welding process is that the heating and application of the pressure occurs at the same time throughout the welding process. This eliminates the change-over time and offers faster overall process time.

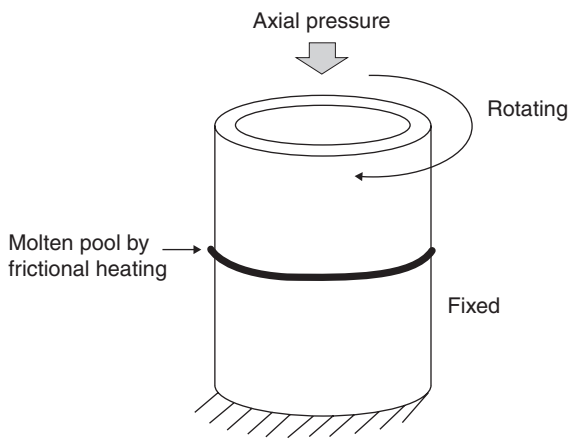
© Woodhead Publishing Limited, 2013

10.6.1 Spin welding

Frictional heating is generated by rotating one part against another under pressure (see Fig. 10.17). One part is fixed while the other is rotated with a controlled angular velocity. Spin-welding machines are equipped with either a flywheel which allows presetting of the energy level, or a servo motor which can control the speed and orientation precisely. Spin welding can produce high-quality welds with a short process time and good reproducibility, but it is only suitable for circular parts (or parts with circular bondlines). It can produce good strong weld but it generates weld flash during the welding process. Typical butt, shear, tongue, and groove joint designs can be used for spin welding. A joint design with a flash trap should be considered if flash generation is a concern for the product. It is possible to make welds under liquid environments but higher-energy input will be required because of the energy dissipation into the liquid.

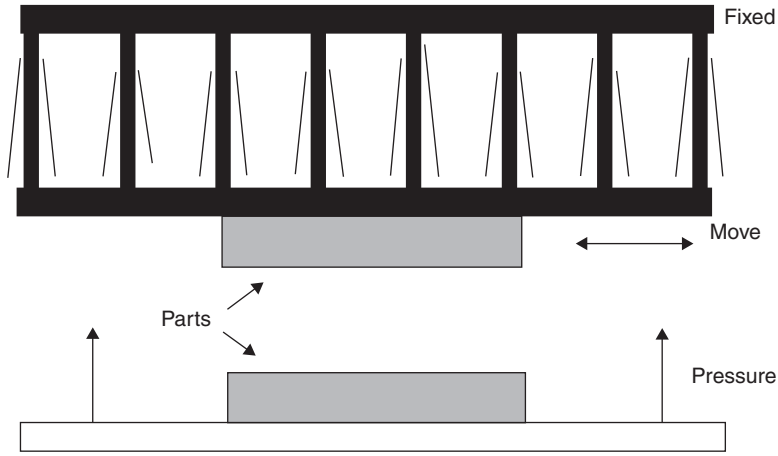
10.6.2 Vibration welding

In vibration welding, heating is generated by rubbing two bars linearly under pressure and at a preset frequency and amplitude (see Fig. 10.18). Usually the process works best when the joints are planar, but parts with angles of less than 10° are weldable. Short process times and narrow weld zones make the process more tolerant of moisture in the polymer. Typical joint designs are butt joint and tongue and groove with a flash trap. Typical amplitudes range from 0.5 to several millimeters and frequencies range from 100 to 500 hertz. A typical vibration-welding machine is quite big and expensive compared with other welding processes. It is more frequently used for



10.17 Spin welding.

© Woodhead Publishing Limited, 2013



10.18 Vibration welding.

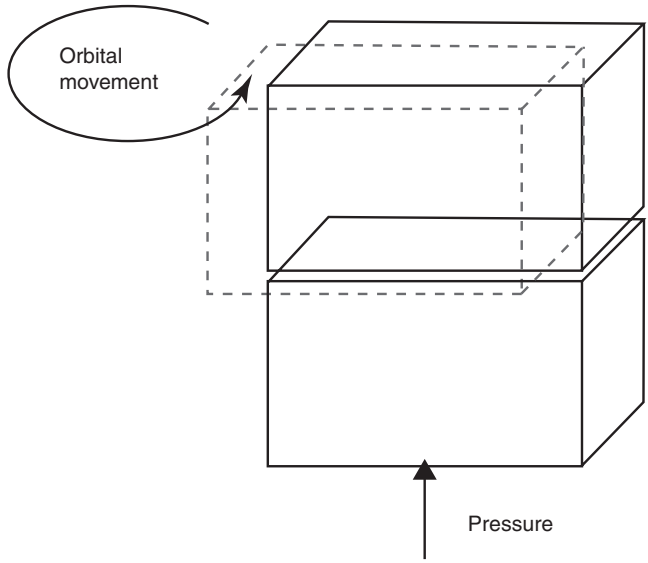
unique applications that are challenging for other welding processes such as large-part and/or difficult to weld high-temperature semicrystalline plastics. It is commonly used in the automotive industry rather than in the medical-device industry.

Orbital-vibration welding (see Fig. 10.19) is a newer approach. The main advantage with orbital welding is that it can be used to weld large structures with much more uniform joint strengths than the traditional linear-vibration-welding process.

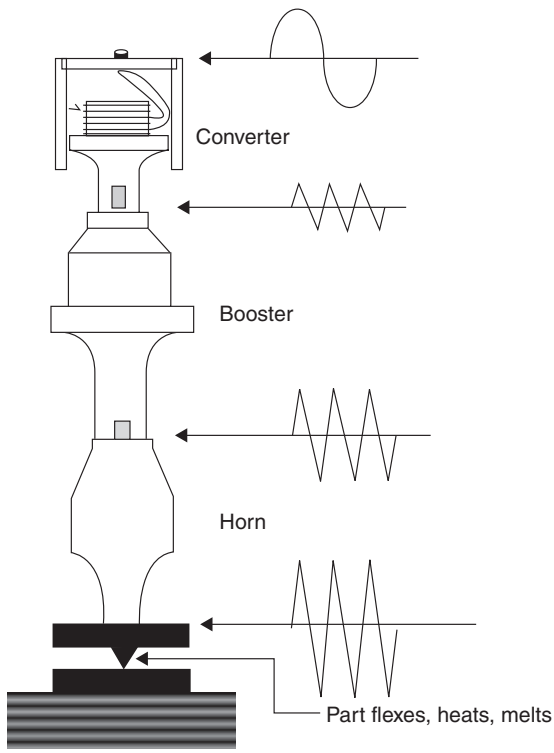
10.6.3 Ultrasonic welding

High-frequency (15–70 kHz) vibrational energy is transmitted vertically to the joint surface by a horn assembly during ultrasonic welding (see Fig. 10.20). The asperity on the joint surface dissipates into heat and leads to the melting of the joint surface. Important process parameters include the amplitude of vibration, welding time, collapse distance, welding energy, and welding pressure. The higher the operating frequency, the smaller the horn required. For a joint area smaller than the size of a dime, 40 kHz or higher is preferred. Ultrasonic welding is the best choice for amorphous thermoplastics because they are more rigid and have a more definitive transition temperature. Some semicrystalline thermoplastics can be ultrasonically welded at distances from the horn up to about 6 mm (near field welding). For far-field welding (distances longer than 6 mm), amorphous thermoplastics have a better chance of being successfully welded. Joint design is important in ultrasonic welding. Typical joint designs include the energy director and shear type. An energy director is an artificial asperity which is molded

© Woodhead Publishing Limited, 2013



10.19 Orbital-vibration welding.



10.20 Ultrasonic welding.

© Woodhead Publishing Limited, 2013

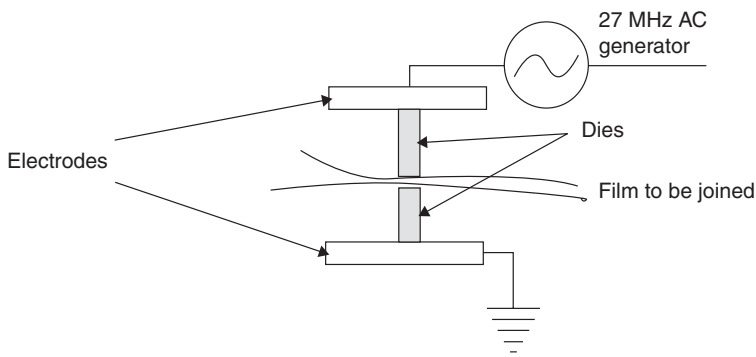
in the bondline for initial melting to occur. A shear-type joint design is like an interference between two parts. This type of joint design is more suitable for semicrystalline thermoplastics. Ultrasonic plunge (step-wise) welding is usually limited to small parts, but scan (continuous) welding (parts are moved at a constant speed) can be used for thin long parts. Ultrasonic welding is the most commonly used welding process for plastic joining and is used in all sorts of industry sectors including the medical industry. 40 kHz ultrasonic welding machines are particularly useful for many small medical components. Chapter 11 discusses ultrasonic welding in more detail.

10.6.4 Dielectric (RF) welding

Dielectric heating operates at a high frequencies at in multiples of 13 MHz, typically at 27.12 MHz. The alternating electric field delivered by electrodes forces the dipoles in polar molecules to rotate and generate heat (see Fig. 10.21). This method is good for thin and polar materials such as PVC, polyurethanes, and polyamides. Design of dies (connected to electrodes) is important for RF welding because the final joint shape and quality depends mainly on the dies. It can be designed to have decorative edges or to precut the surplus material for manual peeling. This method is commonly used in medical/health care applications such as for bags or pouches. Chapter 12 discusses dielectric welding in more detail.

10.7 Processes with implant welding

Implant welding requires an additional susceptor (energy absorber) at the joint interface to provide the localized heating. Two key characteristics of the susceptors are the abilities to absorb the energy from the particular energy source and to provide compatibility (weldability) between the two pieces of the parts to be joined. One critical aspect of this type of welding is



10.21 Dielectric (RF) welding.

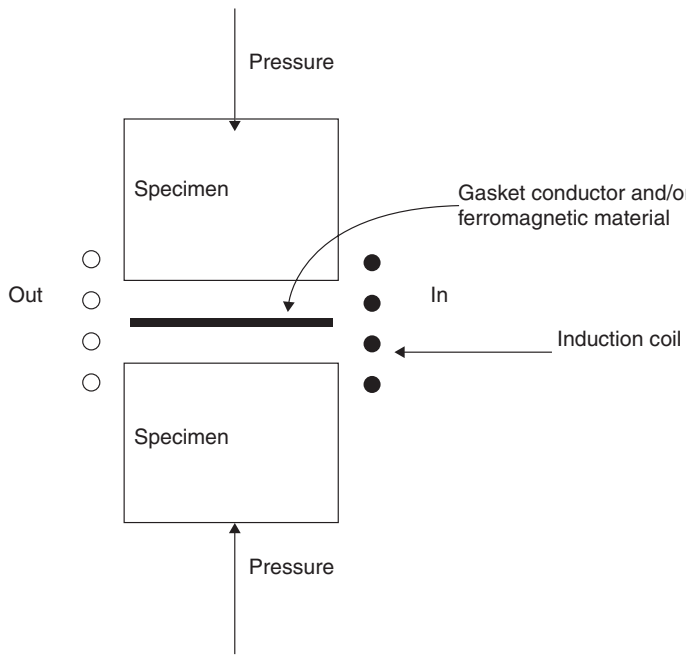
© Woodhead Publishing Limited, 2013

that the selection of the susceptor material must meet the biocompatibility requirement of the particular medical device's intended use.

10.7.1 Induction-implant welding

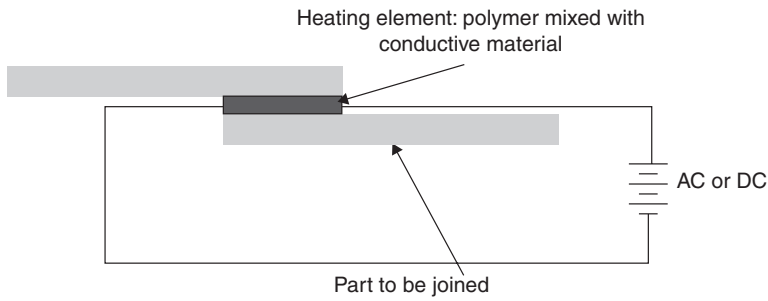
When an eddy current is induced inside the conducting material such as graphite fiber, metal, carbon powders or metal foils, resistance heating occurs (see Fig. 10.22). Usually, the electrically conductive powders or fibers are mixed or braided with thermoplastic powders or fibers that are used as heating susceptors. The susceptors are implanted in the bondline and will remain in the bondline after welding. It is a non-contact heating process. The electromagnetic field is applied to the work pieces by a coil, which is connected to a power generator. Coil design and fixturing are critical to achieving efficient and uniform heating. The fixturing should be made of electrical non-conductive material that can provide pressure during the welding process to ensure intimate contact at the joint interface. An induction generator converts 60 Hz electrical power to kilohertz (kHz) or even megahertz (MHz) range high-frequency power.

One main advantage of this method is that the joint can be three dimensional as long as the coil design can provide a uniform heating. One popular



10.22 Induction-implant welding.

© Woodhead Publishing Limited, 2013



10.23 Resistive-implant welding.

application for both medical and food packaging is the sealing of metal/foil packaging material such as foil laminate used in a pouch or bottle-cap seal.

10.7.2 Resistive-implant welding

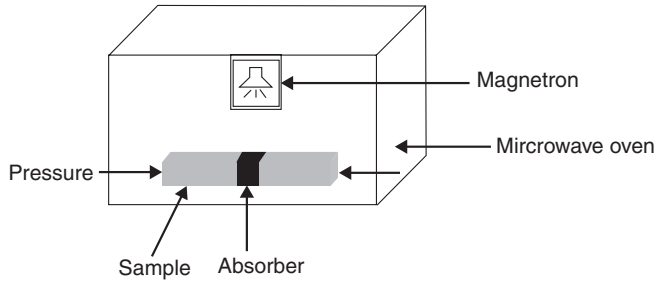
This process is similar to induction-implant welding except that the heating is generated by directly passing a current to the heating susceptors (see Fig. 10.23). A three-dimensional and large/long joint can be achieved by this method. Due to the complexity of the process and the need for an additional compatible susceptor, resistive-implant welding is only used in very unique applications.

10.7.3 Microwave-implant welding

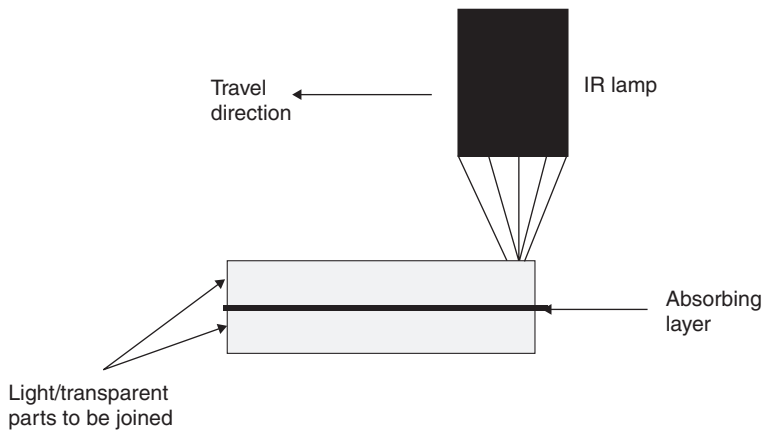
Typical microwave welding operates at 2.45 GHz (see Fig. 10.24). Different materials can be heated by microwaves with different mechanisms. Ionic current can be generated in polymers with a high carbon black content. Dielectric losses (heating) are generated when dipoles try to reorient themselves under the field. Sensitizing materials such as carbon black or highly polar organic materials can be blended with polymers to make sensitizers heating susceptors. In microwave heating, the dimensions of most parts are smaller than, or of the same order as, the wavelength. The basic concepts of low-frequency electrical principles have to be replaced by the concept of 'electromagnetic waves': energy is generated with magnetrons, transmitted via wave guides, and emitted from resonating spaces or cavities.

Microwave heating can be operated in either single-mode or multi-mode. For the single-mode operation, a wave guide is needed. The cavity can be tuned to have high-efficiency heating. For the multi-mode operation (domestic microwave oven), a metal fan is employed to stir the field and make it more uniform. Microwave welding is a relatively new welding process. Theoretically,

© Woodhead Publishing Limited, 2013



10.24 Microwave-implant welding.



10.25 Laser and IR implant welding.

it is possible to design a microwave-heating system that will generate a uniform heating for a complex joint geometry (three dimensional).

10.7.4 IR/laser-implant welding

Because the ability to absorb IR/laser radiation energy is different from different plastics and different pigmentation, it is possible to do implant welding by placing an absorbing layer, such as black polymer, in between two IR/laser transparent plastic parts to initiate the heating (see Fig. 10.25). The susceptor can be made of the same polymer as the part to be joined with the addition of carbon black pigmentation.

10.8 Potential impacts from other manufacturing processes

There are different primary manufacturing processes for medical plastics, such as molding and extrusion. These are the processes that convert the raw

© Woodhead Publishing Limited, 2013

polymer materials to components. Welding and assembly processes are considered secondary manufacturing processes and usually take place after the primary manufacturing processes. The other important process that could happen before or after the welding process for medical devices is the sterilization process. Usually, sterilization processes have a minimal impact on the welding process. Here are some factors that should be taken into consideration in the overall manufacturing processes and weld quality control:

1. *Gamma and E-beam radiation sterilization:*
   (a) Radiation sterilization can potentially cause cross-linking in some polymers. This could potentially reduce the weldability of the polymers.
   (b) Process temperature for E-beam sterilization is much higher than gamma radiation. More stress relaxation could happen in E-beam process.
2. *Steam sterilization (autoclaving):* steam sterilization could potentially distort parts because of the high process temperature (120°C heating) and exposure cycle. Typically, autoclave uses terminal sterilization where the sterilization process is done with the final product. This means that the sterilization process is done after all assembly processes are completed, including the welding process. Therefore, the weldline must withstand the sterilization thermal cycle and maintain its functional requirements, such as seal integrity.
3. *Ethylene oxide (EtO) sterilization:* one critical aspect for EtO sterilization is that the residual EtO should be removed completely. Therefore, one consideration is that the weld joint design should make sure that there will be no chance of EtO entrapment after a weld is made.
4. *Welding of two components made from different primary processes:* in a situation where welding of similar polymers takes place but one part is made from molding and the other is made from extrusion process. One needs to anticipate that plastic parts coming from the same polymer-grade raw material might behave differently during heating because different primary processes were used. For example, extrusion parts will have a highly oriented molecular structure. During welding when (heating takes place), the extruded parts could distort more than the molded parts because highly oriented residual stresses inherently exist in the extruded parts. For this type of welding application, it is desirable to select a welding process with more localized heating area.

10.9 Special applications for welding of medical plastics

In this section we extend our discussions to the welding of medical plastics for certain specific applications in the medical device industry.

© Woodhead Publishing Limited, 2013

10.9.1 Radiation welding of fluoropolymers

Some polymers have molecular weights that are too high for conventional processing

Teflon (PTFE) and UHMWPE are polymers that share similar characteristics. Teflon has a high melting temperature of 327°C and when it melts it forms a gel that cracks when force is applied. However, because of its unique properties and characteristics, Teflon is widely used in medical-device applications. In a conventional process, PTFE particles are sintered into shapes or bulk forms. Welding of PTFE to PTFE directly is very difficult because of the unique characteristics of the PTFE. However, a different form of fluoro polymer, Teflon PFA, which is very similar to PTFE due to its chemical structure, can be processed conventionally. PFA is clearer than PTFE with a lower melting temperature of 310°C. Because of the processability of the PFA, it can act as a hot-melt glue for PTFE.

Welding of Teflon can be done with traditional welding techniques using Teflon PFA as a hot-melt glue as long as the high melting temperature can be achieved. However, for a clean and good-quality weld, through-transmission radiation welding will produce the best results. The radiation energy source can be from infrared lamps or YAG or diode lasers.

In through-transmission radiation welding, radiation light passes through a transmitting PTFE polymer onto an absorbing PFA polymer that is in contact. Natural PTFE looks white but it is very transparent to both IR and lasers in 1 micron wavelength range. The key is to add pigment (such as carbon black, low percentage is fine) to the PFA to turn it into an absorbing material for IR and laser in that wavelength range. During the welding process, heat will be generated at the PFA absorbing layer and melt both PFA and PTFE to create a good joint interface. A good welding result can be obtained through good control of heating temperature of around 340°C with a longer weld time combined with uniform pressure during welding. Plate IV (see Plate IV in the color section between pages 300 and 301) shows welded PTFE samples using the through-transmission IR principle with black PFA at the joint interface.

Safety note

Welding areas should be well ventilated when welding fluoropolymers because toxic polymer fumes can be generated during the welding process.

10.9.2 Joining of catheters using laser and infrared bonding (welding) technology

One special application in the medical device is the laser welding of the catheters. I was involved in the early development of the laser welding of

© Woodhead Publishing Limited, 2013

catheters in the late 1990s. Since then, laser-welding applications of the catheter system have taken off. It has been used in percutaneous transluminal coronary angioplasty (PTCA) catheters where the welding of the balloon to the catheter is applied. Both butt and lap joint designs can be used to laser weld catheters in different applications. There are many custom-built laser-welding machines available for catheter applications in the medical-device industry.

There are two types of joining techniques in the assembly of plastic catheter products. The first type is adhesive bonding. The other type is welding or thermal fusion bonding. The only advantage of adhesive bonding is that it can be used for bonding thermoset plastics or bonding between two different plastics. However, because of the small dimension for the catheters, the bonding process (dispensing of adhesive, fixturing, and curing) requires very precise process control. As a result, getting a consistent joint quality could be a challenging task.

Welding, on the other hand, does not introduce additional chemicals during the process. Some type of energy source is needed for fusion bonding to occur. For the traditional catheter joining process, two types of welding techniques are used: hot air and RF welding. For both techniques, heat is applied to the surface of the tubular part and then conducted to the joint interfaces. The main challenge for the traditional welding is the efficiency and precision of the heating. Hot air is intrinsically an imprecise heating process due to the uncontrollable air flow. RF welding is actually an indirect heating process where heat is generated in a heated tool by RF energy and then conducted from the tool to the surface before finally being transferred to the joint interfaces through thermal conduction in the plastic. Because of the large heating area and poor thermal conduction, these traditional welding methods cannot control the heating at the joint interfaces precisely and consistently. Also, for balloon catheter bonding applications, it could be even more challenging due to the thin balloon wall that could be damaged easily by imprecise heating. A large heating area also means the mechanical property of the joint area of the catheter could change and compromise the functional performance of the catheter.

Unlike traditional welding methods, laser welding offers a precise and localized heating – a key advantage over traditional welding. Other than precise heating, one unique process characteristic is the ability to do either direct heating or through-transmission heating by selecting an appropriate laser to match up with the right material. These characteristics have made laser bonding very attractive to the catheter assembly process. For example, the CO_2 laser has a longer wavelength of 10 600 nm, where all the plastics are opaque to the laser and will absorb the laser energy directly. On the other hand, for Diode or YAG lasers, due to their shorter wavelengths (from 800 to 1064 nm), the laser energy can pass through the natural or transparent plastics and facilitate through-transmission welding (please refer to Section 10.7.4).

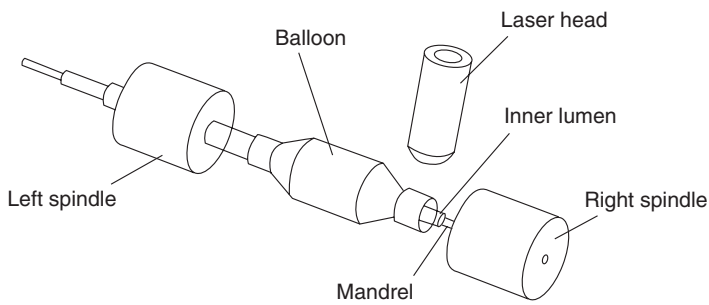
© Woodhead Publishing Limited, 2013

One of the biggest advantages for Diode and YAG lasers is that they are suitable for fiber-optic transmission which simplifies beam delivery and makes it easier for high-speed applications. However, pure through-transmission welding cannot provide a good surface heating to smooth out the transition area around the tubing edge as in with the CO_2 laser. Especially for joining balloon to catheter (PTCA application), the CO_2 laser can heat and melt the thin outer layer efficiently and bond the outer layer to the catheter uniformly and consistently with low energy consumption.

Another welding technology similar to laser that can be used for catheter joining is infrared (IR) welding. The typical IR lamp energy intensity is not as high as the typical laser and it cannot be focused down to as tiny a spot as in a laser. However, because it is not monochromatic like a typical laser and its wavelength is distributed around 1 μm, it can offer the benefits of both direct and through-transmission welding (combination effects of YAG/diode and CO_2 lasers). Two critical areas that could help IR welding become more suitable for catheter application are an increased heating intensity with more focus area and a better control of selective (through-transmission vs direct) heating. Many studies have been done with IR welding of plastic parts in recent years, and I am confident that once more R&D effort is put into the IR welding for catheter application its great potential will be realized.

Similar to other welding processes, catheter bonding/welding requires precise process control and fixturing. Figure 10.26 shows a typical balloon and catheter laser-bonding process where a rotating mandrel and spindle welding set-up is used to maintain a uniform heating and pressure. The main focus is always on how to apply the heat and pressure uniformly during the welding process. The laser heat source can move along the spindle axis to control the bond length and multiple bonds.

Different approaches are utilized to control the application force and final shape of the joint areas of a catheter and balloon parts. Utilizing fixtures with high temperature shrink tubes (such as FEP, fluorinated ethylene propylene) or glass molds under a heat source such as a hot-air station is the



10.26 Laser-welding application for balloon and catheter bonding.

© Woodhead Publishing Limited, 2013

traditional way to form or fusion bond catheter and balloon applications. Without doubt, laser or IR as a heat source can offer more flexibility in the fixtures and produce products of more consistent quality.

10.9.3 Solvent bonding/welding

Solvent bonding/welding is not the most environmental friendly method to join plastics but it does provide a unique and efficient joining method for some medical plastics (mainly amorphous) including PVC, ABS, PC, Acrylic, and PS. For medical-device applications, solvent bonding is widely used in bonding tubings and ports for blood or IV solution bags, mainly because of the circular joint interface with a pre-designed interference provides a perfect way to maintain an intimate contact between two parts without any additional fixturing.

The processes of solvent bonding/welding is similar to a typical welding processes (see Section 10.2) except the heating energy is replaced by the solvent and the cooling is replace by the evaporation/drying:

1. application of solvent at the joint interface;
2. application of pressure;
3. intermolecular diffusion;
4. evaporation/drying of the solvent.

The key principle for solvent bonding is to use solvent to dissolve surfaces to be joined and allow movement of the polymer chains in between the joint interface. In other words, the two polymers to be joined need to be compatible to each other in order to create intermolecular chain movement across the joint interface.

Examples of compatibility of polymers for solvent bonding:

1. Same polymer:
   (a) bonding PVC tubing to PVC tubing or port using cyclohexane.
2. Similar polymers that can form an alloy or mixture (have common solvent):
   (a) bonding acrylic to ABS using MEK (methyl ethyl ketone);
   (b) bonding acrylic to PVC using 75% cyclohexane and 25% MEK.
3. Different polymers that are not compatible and do not have a common solvent but have a mutually compatible polymer:
   (a) bonding of PC to flexible PVC tubing using 10% plexiglass with 50/50 cyclohexanone and MEK;
   (b) bonding of HIPS to PVC tubing using 10% plexiglass with 50/50 cyclohexanone and MEK.

© Woodhead Publishing Limited, 2013

One important note to keep in mind is that many amorphous polymers that can be solvent bonded are also vulnerable to environmental stress cracking. Therefore, the selected solvent should not act as a stress crack promoter for either one of the plastic materials to be joined.

A successful solvent bonding/welding operation has five key elements:

1. Selection of the right solvent that is able to dissolve the plastics (see Table 10.1).
2. Selection of the right polymers with compatible physical properties and right solvents to form a joint (see Table 10.2).
3. Application of the right and uniform amount of solvent to the joint area using different techniques:
   (a) bonding between round tubings:
      i. Dip-dab: dip the part to be joined into a tray filled with solvent (the depth of the solvent level is constantly controlled), dab the

Table 10.1 Selection of the solvents for the bonding amorphous polymers

	Solvents (boiling point °C)
ABS	Methyl ethyl ketone – MEK (40) Methyl isobutyl ketone (40) Methylene chloride (40)
Acrylic	Ethylene dichloride (84) Methylene chloride (40) Vinyl trichloride (87) Methyl ethyl ketone (40)
PC Polycarbonate	Ethylene dichloride (41) Methylene chloride (40) Methyl ethyl ketone
PS Polystyrene	Ethylene dichloride (84) Methyl ethyl ketone (80) Methylene chloride (40) Toluene (110) Acetone (57) Xylene (138)
PVC	Acetone (57) Cyclohexane (80) Methyl ethyl ketone (80) Tetrahydrofuran (65)
Polyester	Cyclohexanone – Cyclo (155)
Polybutadiene	Cyclohexane Toluene (110) Hexane (68) Benzene (80)
Polysulfone	Methylene chloride (40)

© Woodhead Publishing Limited, 2013

Table 10.2 Compatible polymers with solvents for bonding

	PVC	ABS	PC	Polybutadiene
Acrylic	Cyclo	MEK	10% plexiglass in 20% cyclo, 70% MEK	
	75% cyclo, 25% MEK		10% plexiglass in 75% cyclo, 25% EA	
	75% cyclo, 25% ethyl acetate (EA)			
ABS	75% cyclo, 25% MEK			
	75% cyclo, 25% EA			
PC	10% plexiglass in 50% cyclo, 50% methylene chloride			
	10% plexiglass in 50% cyclo, 50% MEK or 50% EA			
HIPS	10% plexiglass in 50% cyclo, 50% methylene chloride			
Polyetheramide	10% plexiglass in 50% cyclo, 50% methylene chloride			
Polyester				100% cyclo + 5% urethane

dipped part with a screen mesh or a form pad to get rid of the excess solvent.

ii. Solvent dispenser: use a dispenser to control the amount of solvent dispensed each time.

(b) Bonding between rigid surfaces:

i. Brush-on: the solvent can be brushed on the surfaces to be joined but an additional fixture is usually needed to maintain the pressure between the two parts before the handling strength is developed.

ii. Capillary: this is a method typically used for joining acrylic parts with a consistent gap between two parts where the solvent is applied with a hypodermic needle right into the gap.

4. Joint-design configuration:

(a) Maintain intimate contact before the initial handling strength is established: this could be done through joint part geometries, interference fit or external force by fixturing. Obviously, the simplest way to do this is by interference fit. A popular example is bonding

© Woodhead Publishing Limited, 2013

flexible tubing to another flexible tubing or a rigid port. A range of acceptable interference and length of overlap of the joint can be derived empirically based on the joint-strength requirements.
   (b) If bonding between a flexible tubing and a rigid tubing is needed, it is better to insert the rigid tubing into the flexible tubing to take advantage of the elastic tension of the flexible tubing to maintain intimate contact.
   (c) It is desirable to have clearance at the lead in angle/area and interference at the inside fit.
   (d) Joining between two rigid cylindrical parts will require a matching set of locking tapers.
5. Good overall process control:
   (a) Good process control for all the sub-processes involved in the solvent bonding is the key to a consistent bond quality.

10.9.4 Testing of joints

Once a weld is made it becomes a part of the medical device. Testing is usually required after a welding process in order to confirm that the weld quality is good enough for the intended functions and the overall performance of a device to meet the original design requirements.

During the welding-process development, testing should be focused on understanding the impact of the welding parameters to the weld quality. Three approaches that are very useful in understanding the welding parameters during the welding-process development are listed below:

1. Joint cross-section examination: The most straightforward way of evaluating the weld quality is to cut cross-section areas along the weld line to visually evaluate the joint interface. The joint interface of different cross-section areas should show uniformity.
2. Tensile test of samples from the joint area: Another way of evaluating the joint is to cut samples from the joint area and conduct tensile test to confirm the uniformity of the weld strength along the weld line.
3. Conduct a design of experiment to optimize the welding-process parameters based on the intended acceptance criteria such as joint strength or other quality attributes.

Testing approach selection depends on many factors, including:

1. Sensitivity/accuracy of the test: If the sensitivity/accuracy requirement is very high, a special precision instrument is required along with specified

© Woodhead Publishing Limited, 2013

testing environment. Some special sample preparation might be needed before the test.
2. Non-destructive vs destructive: Non-destructive testing or inspection can be used for in-line testing and can be used for 100% testing. Destructive testing can only be used for final testing with sampling.
3. In-line testing: This type of test should be simple, quick, and non-destructive. It can be used in the component level or the subassembly level. It can be used for 100% testing.
4. Final testing: This type of test is usually conducted after the final assembly is done. This could be a functional test of an overall performance test. It can be destructive with a sampling plan to meet lot release requirements.

When a hermetic seal/weld is required for the welding process, different testing approaches can be used depending on the testing requirements. For example:

(a) Leak test: there are different leak tests with different sensitivity level available.
(b) Burst test: burst the constrained sample with air or hydraulic pressure.
(c) Pressure: pressure decay, or pressure difference, etc.

10.10 References

1. Benatar, A. and Gutowski, T. G., 'Methods for fusion bonding thermoplastic composites', *SAMPLE quarterly*, Vol. **18**, No. 1, Oct. 1986, 34–41.
2. Yeh, H. J. and Grimm R. A., 'Infrared welding of thermoplastics: Colored pigments and carbon black levels on transmission of infrared radiation', Proceedings of the 1998 ANTEC, Society of Plastics Engineers, May 1998.

© Woodhead Publishing Limited, 2013

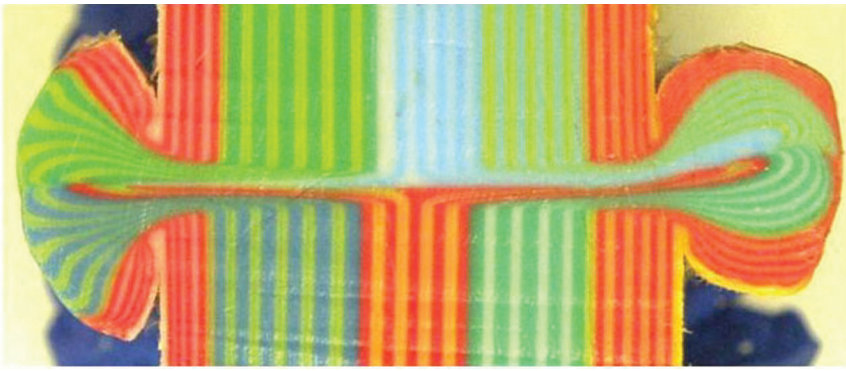


Plate II (Chapter 10) Squeeze flow model shown at the joint interface.

© Woodhead Publishing Limited, 2013

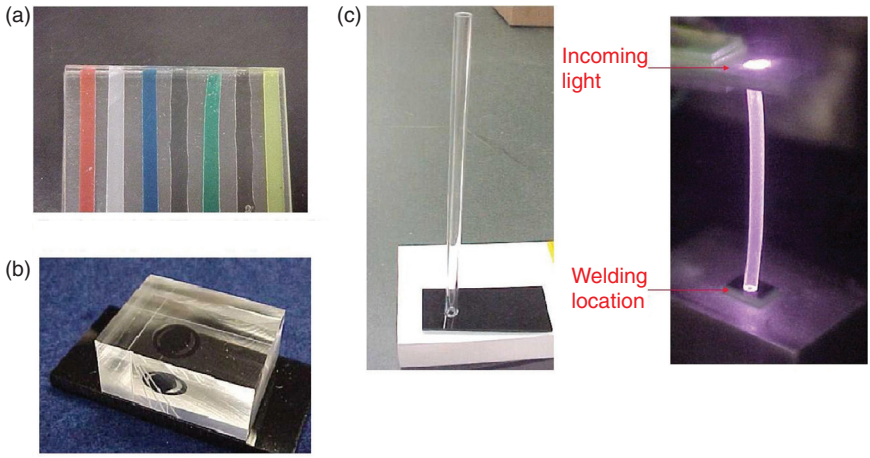


Plate III (Chapter 10) Through-transmission infrared welding: (a) of acrylic with strips of different color at the interface; (b) through ½ inch transparent block; (c) using the light pipe principle.

© Woodhead Publishing Limited, 2013

(a)



(b)

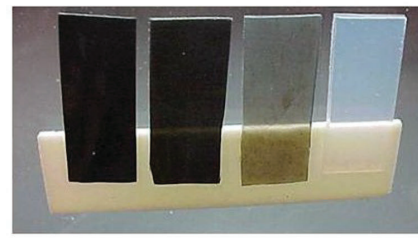


Plate IV (Chapter 10) Examples of infrared welding of PTFE.
(a) Hermetic seal of PTFE with black PFA as an absorbing layer using IR welding. (b) IR welding of PFA with different levels of carbon black content to PTFE.

© Woodhead Publishing Limited, 2013

11

Ultrasonic welding of medical plastics

H. J. YEH, Amgen Inc., USA

DOI: 10.1533/9780857096425.3.296

Abstract: A technical review of ultrasonic welding for medical plastics is presented in this chapter. The fundamentals of the ultrasonic-heating mechanism are explained followed by a description of the ultrasonic-welding process and process parameters. Key factors affecting the welding process and weld quality are discussed based on practical industrial applications. Selection of medical plastics and impacts of material structure for ultrasonic-welding applications are covered under the weldability discussion. Principles for joint designs and horn designs for ultrasonic-welding applications are explained. The chapter also discusses some approaches for the ultrasonic-welding process optimization and troubleshooting. Finally, the overall advantages and limitations of the ultrasonic-welding process are discussed, and the chapter concludes with an overview.

Key words: welding, ultrasonic, medical, plastics, devices, horn design, weldability, joint design.

11.1 Introduction

From low-power ultrasound imaging of prenatal babies to particle dispersion, ultrasound technology has been used in a wide variety of industrial applications for decades. Ultrasonic energy is a form of vibratory energy with a frequency range from 20 kHz to hundreds MHz. One of the key applications of high-power ultrasonic energy is ultrasonic welding. Ultrasonic energy has been used to join both metal and plastic parts in the industry with different heating/joining mechanisms. It has been used in many different industries such as the automotive, medical/healthcare, electronic, packaging, and other consumer-product industries. Since the early sixties when the first ultrasonic joining was used on joining plastics, it has become the most popular joining method for joining plastic parts for different industries including the medical-devices industry.

During an ultrasonic-welding process, intense ultrasonic vibrations, applied to the top part through a horn (sonotrode), are used to locally heat and melt the joint interface of the two parts that have been brought into contact under static pressure. When the vibrations stop shortly, the molten

© Woodhead Publishing Limited, 2013

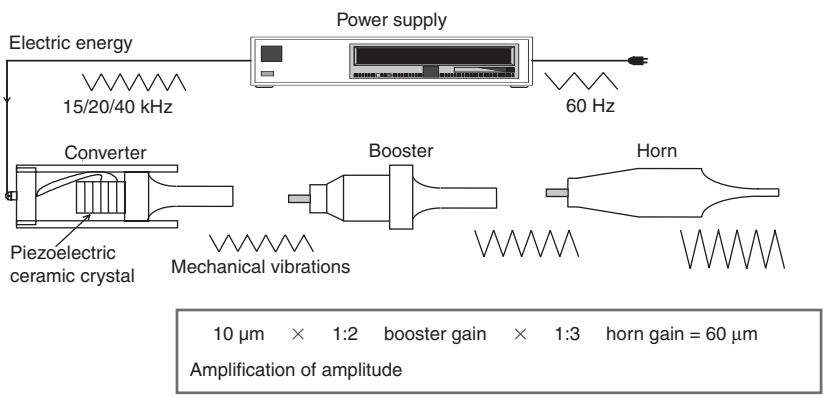
plastic solidifies and the parts are welded. The advancements in modern electronic systems and precision-motion control have made ultrasonic equipment more efficient. With all the accumulation of the technical knowledge in horn and part/joint design, the applications of ultrasonic welding have been widened and joint quality made more reliable.

Examples of medical devices that use ultrasonic welding are especially abundant in disposable parts, such as a variety of filters and connectors, IV catheters, dialysis tubes, cardiometry reservoirs, hospital gowns, face masks, and sterile garments.

This chapter is intended to provide broad and useful information on ultrasonic welding of medical plastics. It covers the fundamental and practical aspects of the ultrasonic welding of plastics and its other joining applications.

11.2 Ultrasonic-welding processes fundamentals

Figure 11.1 shows the essential components for an ultrasonic-welding system. The power supply is designed to generate high-frequency (15, 20 or 40 kHz) electrical energy from standard electrical power (50/60 Hz). The electrical energy is converted into vertical, low-amplitude mechanical vibrations by a piezoelectric transducer. The vibration produced by the piezoelectric transducer is transmitted to the horn through a booster. The booster can be used to amplify or reduce the amplitude of vibration. Booster ratios from 0.6 to 2.5 are usually available for different applications and they are identified by color. The horns used for ultrasonic assembly are generally custom made to suit the application. The purpose of the horn is to properly transmit the ultrasonic vibratory energy to the designated workpiece area so that heating is localized to the joint area. The shape of a horn may be designed to provide additional amplification of the amplitude. The horn is designed to

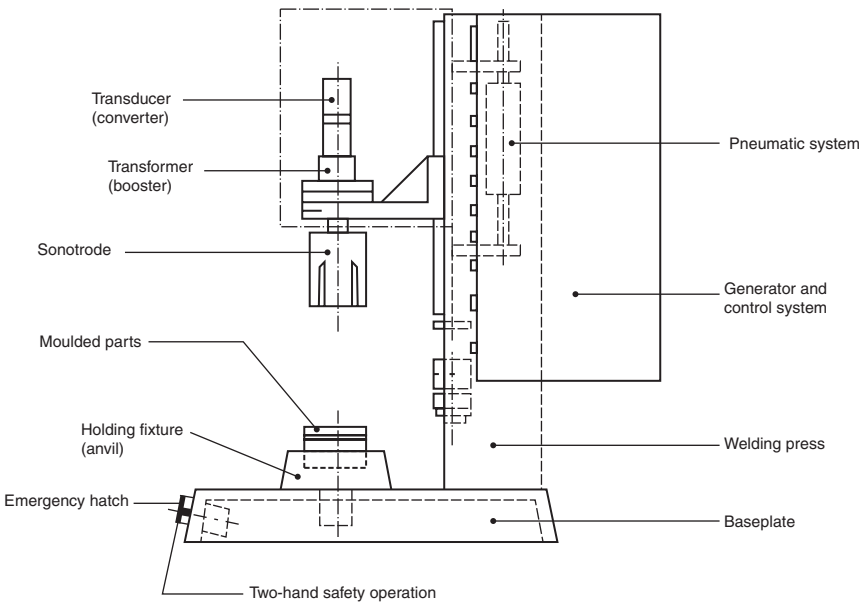


11.1 Main components for an ultrasonic-welding system.

© Woodhead Publishing Limited, 2013



11.2 Typical bench-top ultrasonic-welding equipment from various venders. (Courtesy of Dukane, Branson, Sonics and Materials.)



11.3 Key components of an ultrasonic-welding machine.

deliver the vibratory energy to the workpiece uniformly with minimal stress concentration on itself.

Figure 11.2 shows typical bench-top ultrasonic-welding equipments from different venders. The assembly stand/press holds the stack (converter–booster–horn assembly; see Figs 11.3, 11.4, and 11.5) that has to be perpendicular to the anvil. The anvil is a base to provide support for the fixture that holds the part during welding. The fixture provides support for both bottom and top parts to be welded. The bottom part should be fixed and the top part should be aligned with the bottom part yet free to move up and down when

© Woodhead Publishing Limited, 2013



11.4 Converter booster and horn assembly (the stack) for 20 kHz ultrasonic machine.



11.5 Boosters and horns for 40 kHz ultrasonic machine.

© Woodhead Publishing Limited, 2013

Table 11.1 Summary of ultrasonic-welding machine characteristics based on operation frequencies and their applications

Frequency	10 kHz	20 kHz	40 kHz	70 kHz
Power rating	4+ kW	4 kW	1 kW	100 W
Amplitude	100+ μm	50+ μm	25+ μm	12 μm
Advantage	Powerful, large part	Good balance	Small parts, no noise	Very small parts, no noise
Limitation	Cost, noise	Some noise	Part size	Part size

the horn makes contact with the top surface. A static pressure is applied on the workpieces by the horn through a press system to make sure the ultrasonic energy is transmitted to the workpiece efficiently.

The higher the frequency (shorter wavelength) used in the power supply, the lower the amplitude of vibration and power can be generated. Table 11.1 shows the typical machine characteristics and applications for different frequencies.

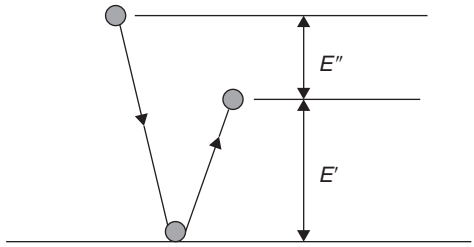
Similar to other plastic-welding processes, there are four fundamental steps in the ultrasonic-welding process – heating of the joint surface, application of pressure, intermolecular diffusion, and cooling (see Chapter 10):

1. *Heating of the joint surface* is the most critical step during the welding process. Ultrasonic welding has a very complicated heating process. Traditional materials are generally considered as either elastic solids or viscous fluids. Thermoplastic polymers are viscoelastic materials that differ from elastic solids and viscous fluids. When a viscoelastic material is subjected to a sinusoidal (cyclic) strain, the corresponding stress will lag behind the strain by a phase angle. This out-of-phase relationship is referred to as the loss modulus and it is where the energy dissipation/loss (heating when subjected to ultrasonic vibrations) comes from. In simple energy terms, this can be explained as energy balance in potential energy. For example, when a viscoelastic ball is released to the ground, it bounces back lower than the original height. The bounce-back height is considered as recovered energy that stored in the system (E', storage modulus) while the difference between the heights is considered as energy loss (E'', loss modulus) (see Fig. 11.6).

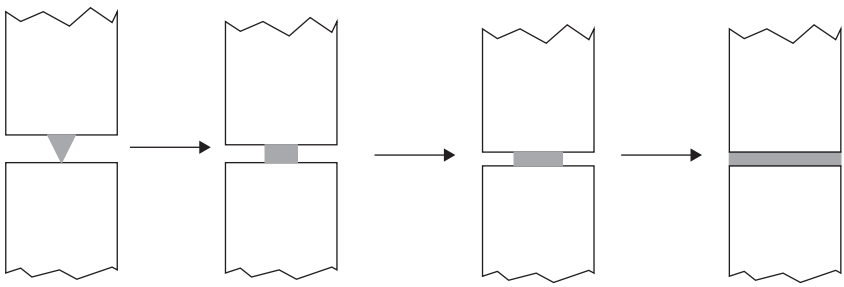
   The relationship between the E'' and E', can be described by the loss tangent where the δ is the phase angle between the stress and strain. The loss tangent for typical polymer is from 0.001 to 0.5. The higher the loss tangent, the more the energy dissipation during the ultrasonic vibration:

$$\tan\delta = \frac{E''}{E'}$$

© Woodhead Publishing Limited, 2013



11.6 Storage modulus vs loss modulus.



11.7 Heating and welding through ultrasonic energy with an energy director at the joint interface.

This loss energy is converted into heat that raises the temperature of the system.

The average energy dissipation per unit time or the heat generation rate can be computed using the following equation:[1]

$$Q = \pi f \varepsilon^2 E''$$

where

f = frequency
ε = strain amplitude
E'' = loss modulus – material property

This describes the localized heating at the joint interface in the near-field welding situation. Note that the strain (amplitude of vibration) is in squired. This shows that the amplitude of vibration is the most dominant variable in determining the heating rate. Once the melting is generated in the initial contact area, heat is transferred to the surrounding cooler material. Meanwhile the molten material will start to flow and spread over the interface (see Fig. 11.7).

© Woodhead Publishing Limited, 2013

2. *Application of pressure* is to apply a static pressure onto the top part using a horn to press two parts together to make an intimate contact at the joint interface during welding. Because the viscosity of the molten plastics is high, this step is required for flow and wetting to take place. The molten-plastic flow can be described by the squeeze flow of polymer processing. Ultrasonic-welding process requires a relatively high static pressure during vibration because the heating is generated by relative mechanical motion between two parts.
3. *Intermolecular diffusion* is similar to the healing of a molten polymer to polymer interface. The key aspect for this step is to let the chain molecules diffuse across the interface to create chain entanglement. Studies have shown that time required for healing is much shorter than the time required for flow and wetting.[2]
4. *Cooling* is the step when melted polymer is re-solidified to provide the joint strength. The cooling rate may have some effects on the microstructure of the semi-crystalline thermoplastics. However, for ultrasonic welding, because of the localized heating, only a very short cooling time is needed and a very smaller area is affected.

11.3 Ultrasonic-welding process parameters and control

This section discusses key ultrasonic welding processes and their process parameters. Depending on the different ultrasonic machine vendors, the process control options could vary slightly.

11.3.1 Power requirement

The power requirement is mainly dependent on the size (total area) of the weld and the part material. Also a different frequency of operation offers different amplitude of vibration and power input. As shown in Table 11.1, from 10 to 70 kHz, different frequency ultrasonic-welding equipments offer different-power input and sizes of the part can be welded. Also, semi-crystalline plastics with high melting temperature usually need a higher energy input rate offered by a higher-power machine. Typical welding machines can offer up to 3–4 kW power output for each single transducer. But efforts have been made into combining multiple transducers/power supplies together to offer more power to weld much bigger size of welds. Specialized digital power generators are required to provide the convertors with the identical acoustical signal. It could potentially offer much higher power output for larger parts.[3]

© Woodhead Publishing Limited, 2013

11.3.2 Process control

A typical ultrasonic-welding machine offers different control modes of operation. One typical process control is to preset a process parameter value. And when the value is reached, the energy input will stop.

Weld time

The welding process (ultrasonic energy is activated) will stop when the weld time is reached at the preset level. This is an open-loop control because it is based on the assumption that weld time is proportional to the weld energy. But in reality this relationship only holds when other factors of the welding process are under precise control.

Weld energy

In a normal ultrasonic-welding process, weld-energy control is a good way to start up and understand a new welding application. The welding process will stop when the weld energy value is reached at the preset level. This is a closed-loop control because the energy level is a good representation of melting, and thus, joint strength.

Collapse distance

When using collapse-distance control, welding process will stop when a preset collapse distance of the parts is reached. This is also a closed-loop control because the collapse distance of the parts is directly related to the joint quality. This is a good way to control the welding process when the final length of the joined part is critical. For some specific applications, such as insertion or secondary welding operation (two welds on one part), it is necessary to control the collapse distance.

In general, weld-energy or collapse control is recommended. But good dimension control of the parts is important for collapse control. More advanced machines allow the user to monitor the above mentioned parameters. The best approach is to preset one control parameter (energy or collapse) and monitor the other two parameters. The other two parameters should consistently be within a limited range. If the other two parameters are far out of range, this usually indicates that problems occurred during the welding process.

11.3.3 Other process parameters

Amplitude of vibration

As mentioned in Section 11.2, this is the most dominant parameter to control the heat generation rate. A higher booster ratio increases the amplitude of

© Woodhead Publishing Limited, 2013

vibration, leading to a higher heat-input rate. As a result, the same amount of energy can be reached with less weld time. But on the other hand, the part is more vulnerable to vibratory damage. Some advanced machines allow the user to control the amplitude of vibration during the welding process to control the heating rate to deal with specific challenging semi-crystalline polymers. A higher amplitude of vibration is recommended for semi-crystalline polymers because they require a higher heating rate.

Weld pressure/force

During the welding process a preset static pressure is applied by the horn/booster assembly to the top part to maintain an intimate contact at the joint interface. The weld pressure is critical and has to be optimized. If the pressure is too low, heat generation may be erratic and result in a non-uniform weld strength along the weldline. If the pressure is too high, most of the molten polymer may squeeze out from the weld zone or parts may simply jammed together without welding, especially in an interference joint design.

Most ultrasonic-welding machines use pneumatic pressure control. New advanced machines use servo motors to control the force and collapse distance more precisely. Some servo-controlled machines are equipped with dual pressure control which allows the presetting of two pressure levels during the welding process. This provides a higher heating rate at the first high-pressure level to initiate melting followed by a second low-pressure level to maintain the melting condition and also keep the molten polymer in the weldline.

Trigger force

This controls when the ultrasonic energy is activated. When weld force reaches a preset level (trigger force), it triggers the ultrasonic vibration and starts the weld process. Pretriggering is very useful for specific ultrasonic application such as the insertion process. This means the ultrasonic energy becomes active before the horn contacts the parts. If the trigger force is too high, it can ram the parts together and energy may be transmitted through the weld zone down to the bottom part which will result in less melting.

Down speed

A faster down speed reduces the cycle time, but it needs to be optimized with the weld pressure to make sure the top part is not jammed into the bottom part when an interference joint design is used.

© Woodhead Publishing Limited, 2013

11.3.4 Types of welding process operation

Plunge or continuous welding

The most common ultrasonic-welding process is plunge welding. The welding process is completed by moving the horn up and down within a small duration time when the actual welding takes place. The parts to be welded can be fed into and removed from the fixture manually or automatically after each welding cycle is completed. Many medical devices, such as filters and connectors, are made in this manner.

For continuous-welding processes, the horn is activated continuously and the parts are fed in between the horn and fixture continuously. The most common application is the welding of fabric or film where the weld seam is long and continuous. There are special horn and anvil designs for these specific applications. One or both of them can be rotary shaped. A combination of technical and empirical horn and fixture design processes to achieve the uniform amplitude of vibration and maintain uniform stress level throughout the expected life of the horn and fixture during the production is required to this type of operation. Another special application is the simultaneous sealing and cutting by using a special horn design with a sharp edge.

Rotary-table or continuous-conveyer process

An automatic-welding production line can be achieved by indexing through multiple stations by either a rotary process or a linear continuous process. A rotary-table process can be designed into several stations such as a parts feeding station, a checking alignment station, a main welding station (or multiple welding stations), and an inspection and reject stations. One key aspect for this design is to maintain the precise alignment of the rotary table during the welding process. If there is an issue with the alignment of the rotary table and the welding station, the weld quality will be impacted.

Using a linear continuous process, the process design can be suitable for either conveyor-type operations where the parts (or a continuous web) are fed into the conveyer and the welding stations and inspection stations are in sequence. The main difference is that the parts are carried by a moving fixture on a conveyer in between stations. During the welding process, each part is sitting on an individual fixture that matches the base of the welding station. Therefore, the alignment during the welding is relying on matching each fixture to the base of the welding station. If there are multiple fixtures, it is important to make sure their alignment is consistent in order to produce consistent joint quality.

© Woodhead Publishing Limited, 2013

11.4 Weldability

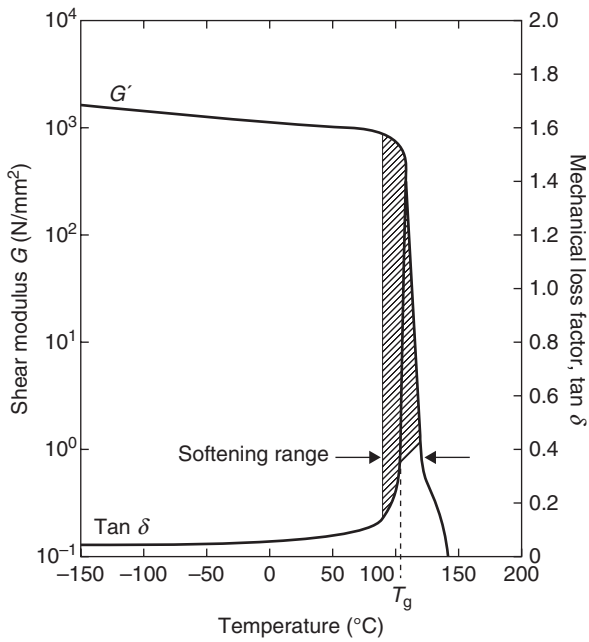
For general guidelines on the weldability of thermoplastics polymers, please refer to Fig. 10.5 in Chapter 10. Please note that the weldability of ultrasonic welding is more sensitive to other factors like polymer type and joint design.

11.4.1 Material structure and properties

Amorphous vs semi-crystalline

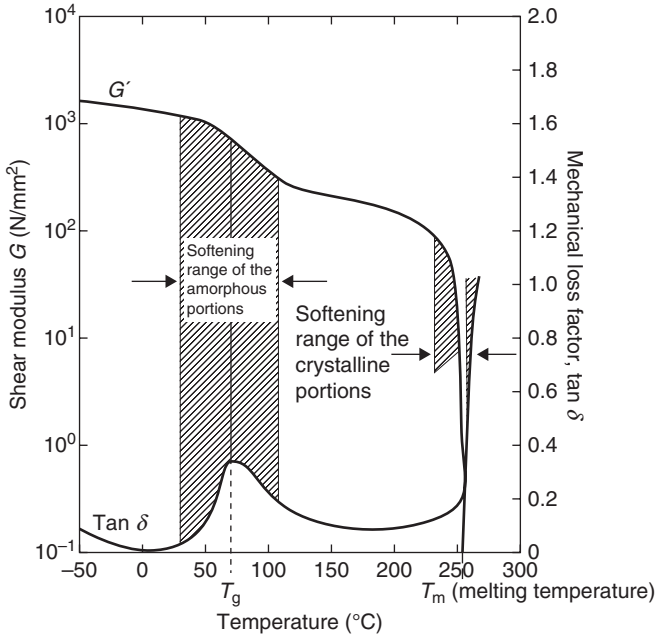
Figure 11.8 shows the shear modulus and loss tangent of amorphous polymers over a range of temperatures. Amorphous polymer can maintain a high modulus of elasticity before it reaches the thermoelastic range (around glass transition temperature). This means more ultrasonic energy can be passed to the joint interface rather than being lost inside the polymer. Typical amorphous polymers includes ABS, PS, PMMA, and PC.

Figure 11.9 shows the shear modulus and loss tangent (dissipation factor) of semi-crystalline polymers over a range of temperatures. Semi-crystalline polymer usually has a higher loss tangent at a low temperature range where the ultrasonic energy is used to heat the amorphous region of



11.8 Shear modulus and loss tangent of amorphous polymer.

© Woodhead Publishing Limited, 2013



11.9 Shear modulus and loss tangent of semi-crystalline polymer.

the semi-crystalline polymer. This means the ultrasonic energy is attenuated inside the polymer rather than transmitted to the joint interface. Figure 11.10 also shows a semi-crystalline polymer that has a distinct melting temperature. It requires a much higher heating rate to get the polymer to melt and to prevent the molten polymer from resolidifying. With a combination of both amorphous portions and crystalline portions coexists in semi-crystalline polymers, it makes ultrasonic welding of semicrystalline polymers rather challenging comparing to amorphous polymers. This further explains why semi-crystalline polymers are not recommended for far-field ultrasonic welding applications. Typical semi-crystalline polymers include acetal, nylon, polyester, polypropylene, and polyethylene.

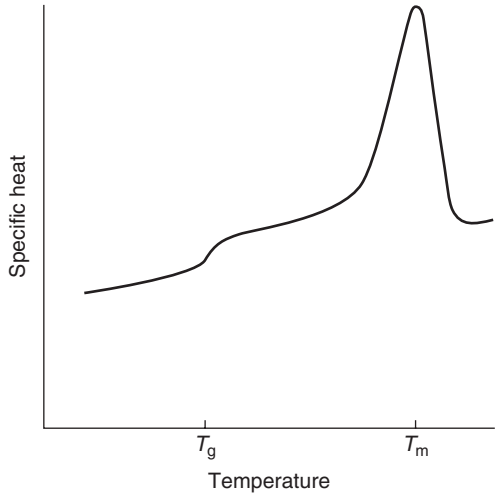
Additives

Additives, such as transferable mold release agents, plasticizers, lubricants, flame retardants, or impact modifiers usually reduce the weldability of the polymers.

Colorants

Most colorants do not interfere with ultrasonic welding, but white colorant (titanium dioxide) has a noticeable negative effect on weldability.

© Woodhead Publishing Limited, 2013



11.10 Glass transition temperature (T_g) and melting temperature (T_m) for a typical semi-crystalline polymer.

Filler materials

Minerals, metallic powders, and chopped glass fibers are used to enhance or alter physical properties for the resin. Usually, when the filler content of the resin is less than 10%, it is possible to improve the weldability by increasing its stiffness. But as the content of the filler material increases, the base resin material available for welding is also decreasing. Filler content exceeding 35% may encounter a substantial decrease in weldability. One unique phenomenon that could happen due to the squeeze flow of the molten layer is the unfavorable orientation of the filler material at the joint interface. This could significantly reduce the joint strength in comparison to that of the base material.

Moisture

Some hygroscopic polymers, such as nylon, polycarbonate, polyester, and polysulfone, if allowed to absorb moisture before welding, may bubble (foamy condition) at the joint area once the water-boiling temperature is reached. This could result in a lower weld strength, a non-hermetic seal, or a poor appearance (porosities). In general, ultrasonic welding produces very localized heating and the impact due to moisture is not as significant compared to that of a large heating area such as hot-plate welding. As a rule of thumb, it is desirable to dry these hygroscopic polymers before welding or to perform the welding as close to the molding process as possible to prevent the parts from absorbing moisture from the environment.

© Woodhead Publishing Limited, 2013

Grade/alloy/blend

Different grades of similar polymers may have different melt index and results in flow and wetting problems during the welding process. Alloys and blend polymers may have different melt index and melting temperature which will reduce the weldability between them.

Regrind

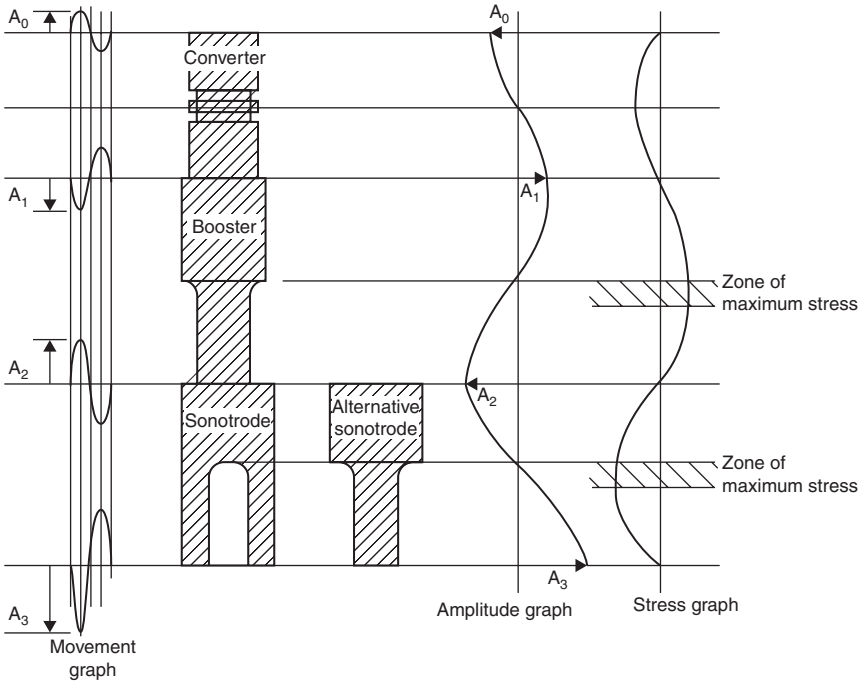
Regrind plastic can be added to the original resin to save material cost. In general, less than 10% of regrind content is permissible. Higher regrind content will reduce the weldability and make the weld strength inconsistent.

11.5 Horn design

Horn design is a complicated process that requires technical knowledge in wave propagation, material properties and accumulation of empirical experience. But with the technological advances in finite element method (FEM) and the availability of huge data bases, horn design has become much easier from a long iterative process.

Before getting into the specifics of the horn design, we need to understand the wave propagation on the overall system – from converter to horn. Figure 11.11 shows how the amplitude of vibration changes from converter, booster to horn (vibration system) at a resonant frequency (such as 20 kHz) where the maximum amplitude occurs at the top and bottom surfaces of each component. The length of the components should be at half wavelength of the longitudinal wave to make the vibration system resonant at 20 kHz. The main wave concerned is the longitudinal-wave propagation (up and down vibration in the vertical axis) since it is the direction of the vibration against the parts to be welded. Note that for each component, its total length represents half the wavelength of the wave that propagates in the specific material of each component because the wave propagates differently in different materials. If the length of the horn is not right or the design of the horn is not optimized such that the resonant condition around 20 kHz is not obtained, the whole vibration system may not be in tune (resonant). As a result, the whole system will not be operable because it will overload the electrical system due to the low efficiency. As a result, the horn will need to be rebuilt or modified. The nodal point of each component, where the amplitude is zero, is located close to the longitudinal center of the components but the exact location (shifting up or down from center) depends on the geometry of the specific component. Because of the zero movement (vibration), the nodal point of the converter and booster is usually the place where the ultrasonic machine holds these two components.

© Woodhead Publishing Limited, 2013

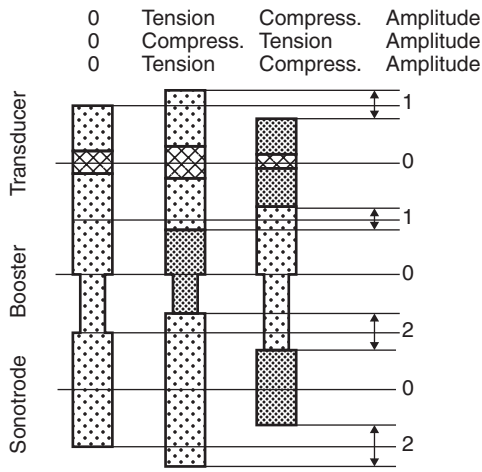


11.11 Amplitude of vibration changes along the stack. (A_0, amplitude of vibration entering the converter, A_1, amplitude of vibration entering the booster, A_2, amplitude of vibration entering the horn, A_3, amplitude of vibration at the interface of horn/part)

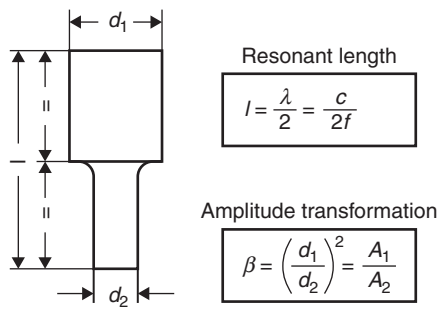
The booster is usually the component to further increase or reduce the amplitude of the vibration. But the horn itself also can do the job if designed correctly. Figures 11.12 and 11.13 show the rough relationship between the amplitude ratio (gain or reduction) and the top and bottom areas of the horn. This type of estimation is only good for simple geometry. There is a more complicated mathematical relationship that can describe the ratio between the mass of the top and bottom halves and the amplitude of the top and bottom surfaces. When the horn geometry becomes complicated, the amplitude prediction at the bottom of the horn could become a small FEM (finite element method) project. Plate V (see Plate V in the color section between pages 300 and 301) shows the mode of vibration (exaggerated) for a larger horn. In order to make the amplitude of vibration at the bottom more uniform across the whole bottom surface, slots are introduced. Using FEM can precisely predict the size and location of the slots in order to get an even distribution of the vibration at the bottom surface of the horn.

It is desirable to have the top surface area of the horn the same or greater than the bottom surface of the booster to obtain a high coupling efficiency.

© Woodhead Publishing Limited, 2013



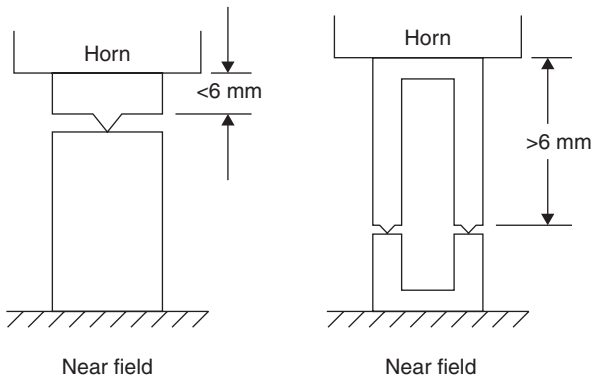
11.12 Vibration mechanism of an ultrasonic-welding system (0, nodal points at transducer, booster, horn where the amplitude of vibration is minimal; 1, maximal amplitude of vibration at both ends of the transducer; 2, maximal amplitude of vibration at both ends of the horn).



11.13 Resonant length and amplitude relationship (amplitude gain). λ, wavelength; *c*, velocity of sound; *f*, resonant frequency; A_1, area of face 1; A_2, area of face 2.

On the other hand, the bottom half of the horn design is usually determined by the final shape of the joint area or the part geometry. This could become very tricky if only a small portion of the total bottom surface is needed. Sometimes, a hollow horn is used to accommodate a ring shape joint area. When high area/mass reduction of the bottom half of the horn is needed, it is desirable to use a 1:1 ratio or amplitude-reduction booster to avoid an un-tunable situation of the system. FEM is a good simulation tool to make sure the horn design for challenging conditions such as un-tunable situations, uneven amplitude distribution, and high-stress areas can be resolved.

© Woodhead Publishing Limited, 2013



11.14 Near-field and far-field ultrasonic welding.



11.15 Thin-wall welding application.

The length of the horn depends on the material of the horn and the frequency of the vibration (wave propagation). Aluminum and titanium are the most popular material for horn construction. For a 20 kHz ultrasonic system, the length of a simple geometry horn for both aluminum and titanium is around 5 inches long. This is close to the half wavelength of the speed of the wave propagation on the particular material of the horn at 20 kHz. By the same token, the horn length for the same material for a 40 kHz is around 2.5 inches. Figures 11.4 and 11.5 show the stack of the converter–booster–horn system with 20 and 40 kHz. We can also understand that the amplitude of vibration of 40 kHz is about half of the 20 kHz. Based on this, we can also understand why 40 kHz is more suitable for smaller parts. On the other hand, a 15 kHz welding machine is capable of handling much

© Woodhead Publishing Limited, 2013

larger parts and offers a higher amplitude of vibration–higher heat generation rate.

11.6 Part and joint design

Part and joint design is critical to the final device product quality. This should be part of the device and process development. It should be considered as a part of the Design for Manufacturing and Assembly processes (DFM/DFA).

11.6.1 Part design

Different welding process requires different considerations during the part-design stage. It is important to design the part with an ultrasonic-welding process in mind rather than try to change the part design after encountering welding problems.

Near field vs far field

The distance between the location of the joint and the location where the horn contacts the top surface of the part is critical in many applications. If the distance is shorter than 6 mm (1/4″), it is considered near field welding. Otherwise, it is considered to be far-field welding (Fig. 11.14). Near-field welding is always more desirable than far-field welding especially for semi-crystalline polymers. In far-field ultrasonic welding, ultrasonic energy needs to travel longer through the polymer where wave propagation and attenuation could both happen. For a semi-crystalline polymer, more ultrasonic energy is attenuated in the far-field situation. As a result, initial heating could happen at the horn and part interface and make it almost impossible to create a joint at the part to part interface.

Parallel and uniform contact

It is desirable to have a planar joint interface and have it parallel to the horn contact plane. The top surface of the part should have a uniform contact with the horn surface. The joint area should be right underneath the horn's bottom surface.

Stress risers

Part design should avoid any potential stress risers. Sharp transitions in geometry, holes/voids, or appendages (tabs, metal attachments, etc.) could concentrate the vibratory energy and create local melting or cosmetic damages to the part.

© Woodhead Publishing Limited, 2013

Table 11.2 General guidelines on dimensions and tolerance for joint design

Part dimension	Interference per side	Dimension tolerance
<0.75″ (18 mm)	8–12 mils 0.2–0.3 mm	(±) 1 mil (0.025 mm)
0.75″–1.5″ 18–35 mm	12–16 mils 0.3–0.4 mm	(±) 2 mils (0.05 mm)
>1.5″ (35 mm)	16–20 mils 0.4–0.5 mm	(±) 3 mils (0.075 mm)

Resonance effects (diaphragmming, hot spots/damages, non-uniform melting)

When welding a thin-walled structure, the whole part could undergo a resonant vibration. Depending on the part geometry and the frequency, the amplitude of the vibration varies along the walls. As a result, some undesirable melting spots could occur along the walls in addition to the joint area (see Fig. 11.15). In some cases, changes of frequency, amplitude, or horn design can eliminate the problem. But sometimes changes of geometry, such as gate location, wall thickness, or the incorporate ribs and stiffeners, may be needed.

11.6.2 Joint design

Joint design is a very critical step in part design. It should be considered in the part-design stage and incorporated into the molding (or other primary) processes. Typical joint design includes the energy director and the shear-joint designs. The initial contact area between the two mating surfaces should be small to initiate the melting. The contact between the two mating surfaces should be uniform along the whole weld line. Table 11.2 shows some general guidelines for typical joint-design dimensions and tolerances.

Considerations

In order to select an appropriate joint design, there are some important factors that need to be considered. The following is just a general guideline:

1. *Type of plastics*: amorphous – energy-director joint; semi-crystalline—shear joint.
2. *Weld requirement*: hermetic seal – shear joint; appearance—flash trap, tongue and groove joint; high strength requirement—larger joint area; location of the joint – where the ultrasonic energy can efficiently transmit to the joint from horn.

© Woodhead Publishing Limited, 2013

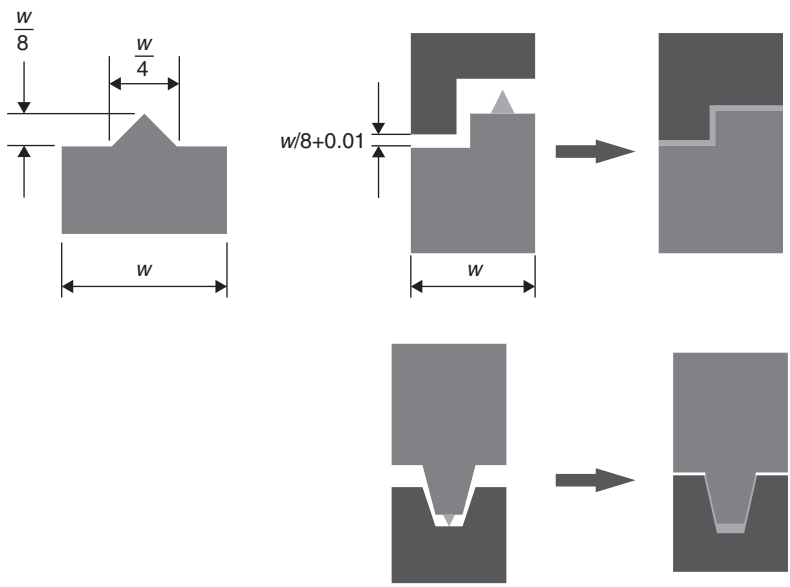
3. *Self-alignment*: shear joint or tongue and groove joint, or energy-director joint with additional part design (pins, sockets, etc.).
4. *Loose-fitting joint*: two parts should be free to move vertically with each other.

Energy director

- butt joint;
- step joint;
- tongue and groove.

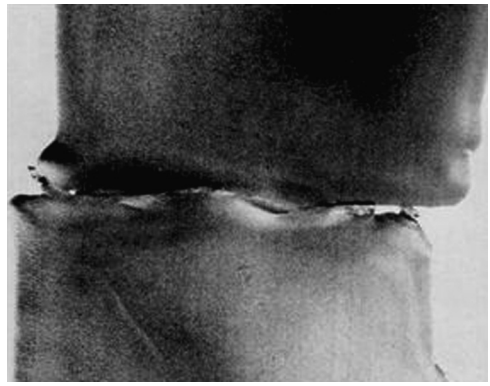
The energy director is an artificial asperity (triangular-shaped) which is pre-molded at the bondline for initial melting to occur. This is the joint design that is recommended for amorphous polymers.

The angle (apex) that contacts the mating surface can be either a 60° or a 90° angle. A 90° angle is usually good for amorphous polymers, but for high-melt temperature polymers, like polysulfone and polycarbonate, and semi-crystalline polymers a 60° angle is a better choice. Energy-director design could be incorporated with different part designs. Figure 11.16 shows the butt, step and tongue, and groove-energy-director joint designs. Intermittent energy-director joint designs can be used when less joint strength



11.16 Typical energy director and tongue and groove joint designs.

© Woodhead Publishing Limited, 2013



11.17 A cross-section of a joint interface from an energy-director joint design.

and non-hermetic joints are needed. Figure 11.17 shows a cross-section of a melted joint interface of a typical energy-director joint design.

Shear (interference)

Shear type joint designs require an interference between two parts. Therefore, good dimension and tolerance control is critical to the shear joint design in order to produce a consistent joint strength. The welding process will melt the interference continuously (from the lead-in area down along the vertical walls) to prevent resolidification of the molten polymer. Therefore, the shear-joint design is more suitable for semi-crystalline thermoplastics. It is usually self-aligning and is more suitable for hermetic and strong joint requirements. A sufficient wall thickness to provide a rigid sidewall support is critical to prevent the part from deflection during welding. Shear-joint design can be incorporated with different part designs. Figure 11.18 shows some of the different shear-joint designs. One important note for shear-joint design is to avoid a "press-fit" situation from happening during welding. When designing the shear joint, one needs to make sure the wall is rigid enough to maintain the interference rather than yielding to the pressing force and the top part is press fitted into the bottom part and mechanically connected together by press fitting rather than welded together. Figure 11.19 shows a cross-section of a melted joint interface of a typical shear-joint design.

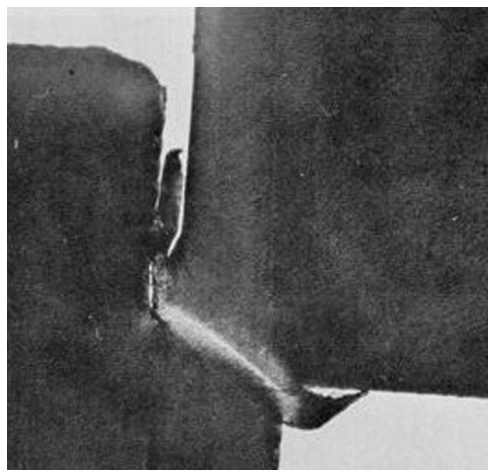
Textured surface

The textured surface joint design is to have small surface projections molded into the joint surfaces. This is the most effective when used against

© Woodhead Publishing Limited, 2013



11.18 Typical shear joint designs.



11.19 A cross-section of a joint interface from a shear joint design.

an energy-director joint design on the other side of part. It enhances friction and promotes a more uniform melting along the joint interface.

11.7 Process optimization

When a new application is determined to be put into production, welding-process optimization is required to set up the right welding conditions. The optimization process should be conducted on the actual

© Woodhead Publishing Limited, 2013

production environment (machine, horn, fixturing, material, etc.). If there is a change in the production environment, a new optimization process should be performed. The following are typical steps for the optimization process:

1. Approximate condition: Conduct preliminary trials to get the approximate welding conditions.
2. Designed experiments: Select a set of critical welding parameters and responses to run the designed experiments. Typical parameters are:
   - weld energy (weld time, collapse distance);
   - amplitude of vibration;
   - weld pressure;
   - trigger force;
   - down speed.

   Typical responses are:
   - weld strength;
   - leakage;
   - other requirements.
3. Regression analysis: Set up a process model which relates the responses (requirements) to the welding parameters. Once the model is established, graphs showing the optimized welding conditions and relationship between the parameters and the requirement can be generated.

11.8 Other specific applications

Ultrasonic energy can be used for a variety of different applications for joining plastic parts in addition to the regular the welding process. The following are the typical applications.

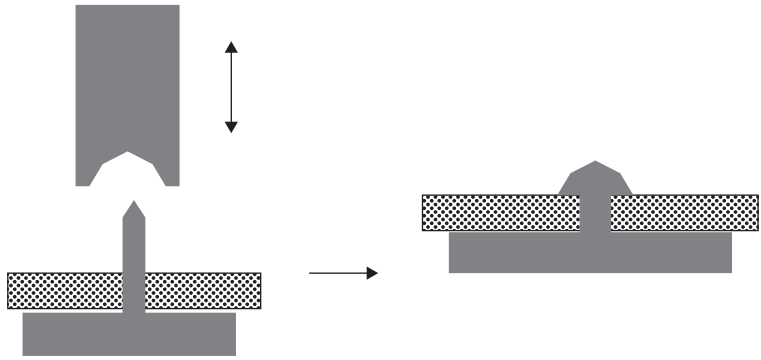
11.8.1 Staking

The staking process is similar to riveting. Protruding studs which are made on the thermoplastic parts during the injection-molding process are formed into heads using ultrasonic energy. It can be used to join metals to plastics or to join dissimilar plastics. Figure 11.20 shows some typical stake designs.

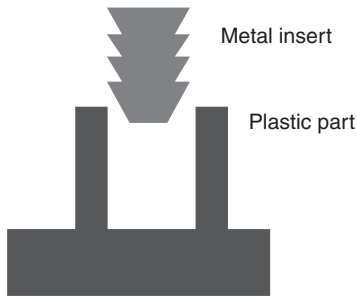
11.8.2 Insertion

Ultrasonic insertion is a very efficient way to install metal inserts to thermoplastic parts. The bottom surface of the horn should be hardened. Replaceable tips are recommended. The depth of the insertion needs to be controlled (collapse distance control is a good option). The pretriggering of

© Woodhead Publishing Limited, 2013



11.20 Other ultrasonic-welding applications: staking.



11.21 Other ultrasonic-welding applications: insertion.

the ultrasonic energy with a slow down speed, a low amplitude and a low to moderate thruster pressure is recommended. Figure 11.21 shows a typical ultrasonic-insertion operation.

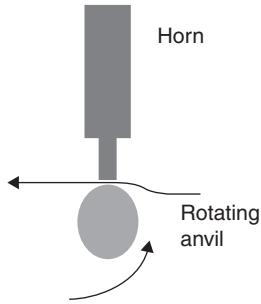
11.8.3 Spot welding

This is very useful when constructing a complex or large structure (with hard-to-reach areas) with sheets of material. Depending on the materials, the thickness of the top layer can be up to about 6 mm or (1/4″) thick. The welding is normally conducted with a hand-held welding unit.

11.8.4 Stud welding

Stud welding is used when moderate weld strength or a non-gas-tight application is needed. A typical stud welding uses the shear joint design. It is also very useful to tack a dissimilar layer in place with a molded rivet.

© Woodhead Publishing Limited, 2013



11.22 Other ultrasonic-welding applications: sewing; sealing.

11.8.5 Swaging

Swaging uses ultrasonic energy to melt and reform a ridge (side wall or projection) of plastic to swage it onto a different material. Pretriggering and a high thruster pressure is recommended for this process.

11.8.6 Scan welding: sewing, slitting, sealing

Ultrasonic welding can be conducted in a continuous operation. Scan welding of rigid thermoplastics is possible with self-aligning part/joint designs. Other applications for scan welding are for textile and film bonding, such as sewing, slitting and sealing. These thin thermoplastic materials can be sealed with patterns or edge-sealed (slitting) with two or more layers (woven and/or non-woven materials). A typical sewing (or continuous sealing) welding operation is shown in Fig. 11.22. Either one or both of the horn and anvil can be in rotary shape. But as mentioned in the welding operation section, designing a rotary horn for a production line is very complicated and will require heavy R&D investment just for the ultrasonic-welding process.

11.8.7 Degating

Ultrasonic degating melts the polymer at the location of sharp profile change. This technique can be used in separation injection molded parts from their runner systems.

11.9 Troubleshooting

Troubleshooting for the ultrasonic-welding process can be difficult because it is a complicated process. The following are the most commonly encountered problems.

© Woodhead Publishing Limited, 2013

11.9.1 Alignment

Good alignment is needed to make sure that the contact between the horn and part and the two part mating surfaces is uniform. Non-uniform contact means non-uniform strength.

11.9.2 Material issues

Polymer grade should be the same in order to insure a good joint quality. If welding is conducted on two parts from different suppliers, one needs to make sure that the resins are the same. Unfavorable additives, fillers or wet polymer situations could reduce joint strength.

11.9.3 Process parameters

Are the parameters optimized? Are there any changes in welding environment (equipment, horn, fixture, etc.) after process optimization?

11.9.4 Part-dimension consistency

Part-dimension consistency is similar to alignment. Inconsistent part dimension could cause inconsistent joint quality. Parts from multi-cavity molding are subjected to dimension inconsistency.

11.9.5 Part/joint design

Is part/joint design fundamentally sound? General considerations for part and joint designs should be followed.

11.10 Advantages and limitations

Table 11.1 shows the typical machine characteristics and applications for welding machines with different frequencies. For the medical-device industry, 20 and 40 kHz are the most popular welding machines. It is the most commonly used welding process for medical-device industry. It provides some unique applications where no other welding process can provide with some limitations.

Compared with other welding processes, the advantages and limitations are as follows:

- strong joint (comparable to parent material);
- short process time (usually less than 1 s);

© Woodhead Publishing Limited, 2013

- no new material is required;
- tolerance of contaminated surfaces;
- easy for automation;
- self-cleaning at the joint interface;
- suitable for different joining application such as staking, insertion, etc.

However, on the other hand, there are also limitations and shortcomings:

- it is a complicated process (troubleshooting may be difficult);
- limitations on size and geometry: thin wall, curved surfaces;
- limitations on complicated parts where metal components or any loose components are present;
- some thermoplastics are difficult to weld (especially in the far-field situation).

11.11 References

1. Tolunay, M.N., Dawson P.R. and Wang K.K., "Heating and bonding mechanisms in ultrasonic welding of thermoplastics," *Polymer Engineering and Science*, Vol. **23**, No. 13, Sept. 1983, pp. 726–733.
2. Wool, R.D. and O'Connor K.M. "A theory of crack healing in polymers," *Journal of Applied Physics*, Vol. **52,** No. 10, Oct. 1981.
3. Herrmann, T. "Ultrasonic twin converter technology for welding large plastic parts or packages," *ANTEC*, 2003, pp. 1140–1146.

© Woodhead Publishing Limited, 2013

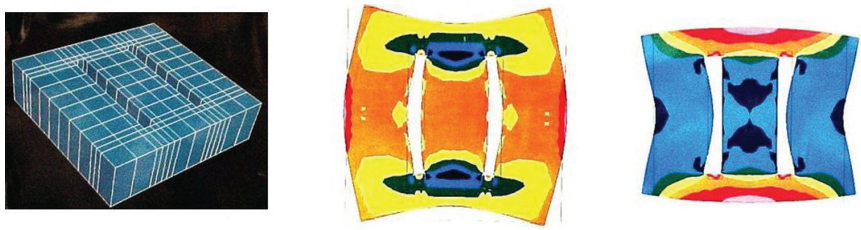


Plate V (Chapter 11) Simulated mode of vibration of a vibrating horn at 20 kHz.

© Woodhead Publishing Limited, 2013

12

Radio frequency (RF)/dielectric welding of medical plastics

H. J. YEH, Amgen Inc., USA

DOI: 10.1533/9780857096425.3.323

Abstract: A technical review of radio frequency (RF)/dielectric welding/sealing for medical plastics is presented in this chapter. The fundamentals of the dielectric heating mechanism are explained followed by a description of the dielectric sealing process and process parameters. Key factors affecting the sealing process and seal quality are discussed based on practical industrial applications. Selection of medical plastics for RF sealing applications is covered under the weldability discussion. The chapter also discusses some unique testing approaches for the RF sealing process. Finally, the overall advantages and limitations of the RF sealing process are discussed, and the chapter concludes with an overview.

Key words: radio frequency (RF), dielectric, high frequency, dielectric heating mechanisms, heating, welding, sealing, medical, plastics, devices, RF die design, tear seal design, arcing, buffers, RF weldability, seal and pouch testing.

12.1 Introduction

Dielectric welding/sealing can also be called high-frequency or radio frequency (RF) welding/sealing. The term 'RF' is used because the welding frequencies fall in the MHz range. Dielectric heating technology has been used in plastic sealing for decades. It uses high-frequency electromagnetic energy to generate heat at the joint interface for plastic materials with high lossy dielectric properties. Because the electric field intensity decreases with distance for the electrodes, there is a thickness limitation (typically is less than 2.0 mm, depending on the polymer material properties) in order to maintain an efficient and uniform heat generation. The main reason it is called sealing is that the most common application of RF welding is for sealing different types of films or sheet materials such as vinyl, polyurethane, ABS, polycarbonate, PET, EVA, or nylon. Similar applications have been used in different industries, such as in the production of binders, raincoats, shower curtains, and blister packs. Because of its good and consistent seal quality, RF sealing has been used for sealing bags, pouches, and other applications where a hermetic seal (air or liquid tight) is required. For the

© Woodhead Publishing Limited, 2013

medical-device industry, RF sealing of PVC sheets has been expanded to a unique technology for making products from small medical bags/pouches to large inflatable patient beds. The RF technology in medical-device applications advances rapidly. More complicated RF sealing processes to accommodate the connections between the bag and soft- and hard-tubing materials were developed and eventually integrated into the overall RF sealing processes. A typical RF sealing machine for medical solution and blood-bag manufacturing consists of complicated electrode configurations where different types of sealing and cutting can be performed simultaneously or sequentially. The machine takes in raw materials such as PVC sheeting and tubing, and at the end of the sealing processes shoots out bags that are ready for filling and further processing. The most common dielectric sealing of medical-device applications can be seen in the disposable sets (bags/pouches) for blood transfusion and IV fluids.

12.2 Dielectric heating fundamentals

This section explains how the dielectric heating is generated and why only certain polymeric films can be RF welded.

12.2.1 Heating mechanisms

Dielectric heat sealing uses electricity to generate heat volumetrically within a material, instead of forcing heat conductively into the material from its surface. The main heating mechanism of the dielectric welding process can be best explained by the polarization from an alternating electric field. There are different types of polarization under the influence of a high-frequency electric field:

- Electronic/electric polarization: the electrons in atoms are oriented relative to the nucleus when aligning to the changing electric field.
- Ionic polarization: cations and anions (charged particles) in an ionic crystal are moving with respect to each other according to the electric field.
- Dipole/orientation polarization: permanent dipoles (molecules) are aligned to the alternating electric field. The phase shift causes the molecules to collide and create internal friction.
- Maxwell–Wagner polarization (interfacial, or space charge): charge build-up in interface in heterogeneous systems.

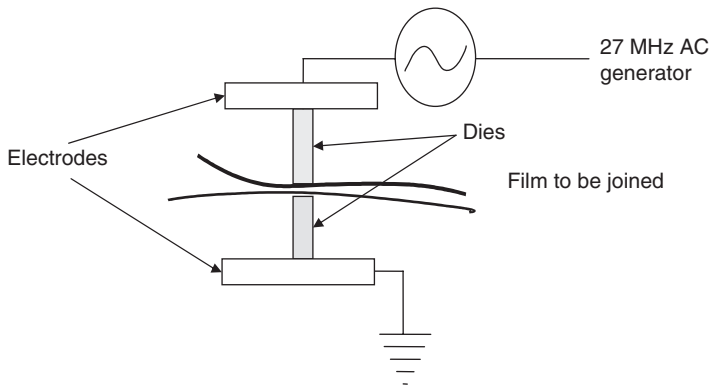
However, when we consider the frequency range (27.12 MHz), the power range of a typical dielectric RF heating, and the electrical and physical properties (dielectric constant, polar molecular structure, viscosity) of the polymers, the

© Woodhead Publishing Limited, 2013

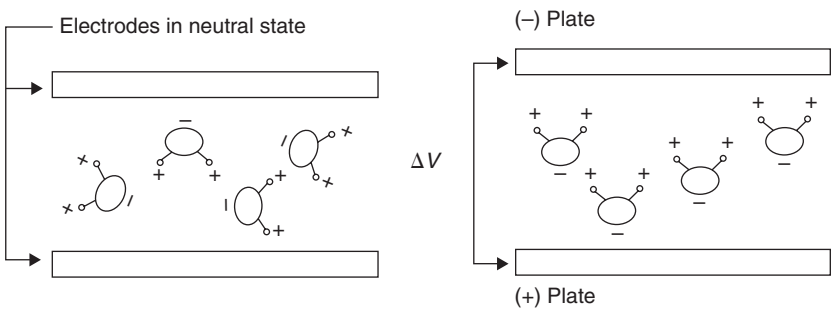
most dominant heating (loss) mechanism is dipole/orientation polarization. This is the heating mechanism we that will be focused on in this chapter.

Dipole polarization

Dipole dielectric heating is accomplished by applying a high-frequency alternating electric field to a lossy dielectric polymer. The electric field is created between two electrodes with dies connected to them (Fig. 12.1). Polar polymers have polar molecular structure such that when the molecules are exposed to the alternating electric field, they tend to align in the field direction so that the positive end of the dipole will align with the negative charges according to the electric field (see Fig. 12.2). However, because of the unique high lossy dielectric properties in some polymers, when the dipoles reorient according to the high-frequency alternating electric field, their orientation becomes out-of-phase (or phase shift, movement of the molecules lagging alternating electric field) where the misalignment between the dipoles happens and as a result creates internal molecular frictional heating.



12.1 Overall schematic of the RF sealing process.



12.2 Polarization of the molecules when they are exposed to the alternating electric field.

© Woodhead Publishing Limited, 2013

The power dissipated during dielectric or RF heating is governed by the following formula:

$$P = \omega \varepsilon_0 \varepsilon''_{\text{eff}} E^2_{\text{rms}}$$

or

$$P = 5.56 \times 10^{-11^*} f * \varepsilon''_{\text{eff}} E^2_{\text{rms}}$$

or

$$P = 5.56 \times 10^{-11^*} f * \varepsilon' * \tan(\delta) * E^2_{\text{rms}}$$

where

P = power dissipated (W/m^3)
ε_0 = permittivity of vacuum (8.84 * 10^{-12} F/m)
E_{rms} = electric field strength (V/m)
$\omega = 2\pi f$ = angular frequency (f in Hz)
$\varepsilon''_{\text{eff}}$ = effective dielectric loss factor of the polymer
$\varepsilon'' = \varepsilon' * \tan(\delta)$ (dielectric loss factor of the polymer) (efficiency of the electromagnetic energy conversion into heat)
$\tan(\delta) = \varepsilon''/\varepsilon'$ (loss tangent or dissipation factor) (material's capability of absorbing electromagnetic energy)
δ = the loss angle or the phase shift between the electric field and the molecules orientation

$$\varepsilon' = \frac{\varepsilon}{\varepsilon_0}$$

where ε' = dielectric constant (or relative permittivity of the polymer – ratio of the permittivity of the polymer ε to the permittivity of vacuum, all ε' values of polymers are >1). This value directly reflect the extent to which the polymer can be polarized.

The amount of the electromagnetic energy that will convert into heat is dependent on the atomic and molecular structure of the polymer, the frequency of the electric field and the field strength. In an electric term, we refer it to dielectric loss factor. The dielectric constant is a material property. It determines the extent of dipole polarization. The dielectric loss factor is the one that determines the conversion of electric energy into heat. This also explains why dielectric heating only works on dipolar polymers with high dielectric loss, such as PVC.

© Woodhead Publishing Limited, 2013

Table 12.1 Dielectric properties of some materials at different temperatures and 30 MHz frequency

Material	Temperature (°C)	ε' dielectric constant	ε'' dielectric loss factor
Water	25	78	0.4
PVC	20	2.86	0.029
Nylon 66	25	3.2	0.072
Polyethylene	25	2.25	<0.0004
PTFE		2.1	
Polystyrene		2.4	

Effects of frequency and temperature

Two key material related factors that could determine the heat generation are the dielectric constant and the dielectric loss factor (or loss tangent, loss factor is defined by the product of loss tangent and dielectric constant). Table 12.1 shows the values of the dielectric constant and dielectric loss factor of some material at room temperature under 30 MHz frequency.[1] One critical aspect of the dielectric constant is that both the dielectric constant and the loss factor increase when temperature increases. For dipole polarization, there is a relaxation time t defined as the time required for preferentially oriented molecules to relax back to 36.8% of the original condition upon sudden removal of the exposure from the electric field. For a given material there is a maximum value for the dielectric loss factor at a specific relaxation frequency ($f_c = 1/2\pi t$). In an ideal case, you want to operate the heating in a frequency range where the dielectric loss factor is at its maximum value. The other critical factor is the temperature change (increase) during the dielectric heating. When a polymer's dielectric loss factor increases significantly with temperature during dielectric heating, a thermal runaway condition could occur and lead to thermal degradation (hot spot) of the polymer (i.e., the high temperature causes the dielectric loss to rise which causes internal heating in the polymer, leading to higher temperature and further increase in loss).

12.3 Dielectric welding/sealing process description and process parameters

Similar to other welding process, four fundamental steps of welding also apply to dielectric welding (see Chapter 10 overview of the welding of medical plastics).

© Woodhead Publishing Limited, 2013

Dielectric sealing is achieved by sending a high-frequency electric-field current through two or more thin layers of thermoplastic material placed between two electrodes through specific dies. The two matching dies are shaped in the image of the required seal. The dies are usually mounted on two platens that are attached to a pneumatic or hydraulic press to provide pressure during the sealing process. The high-frequency energy produces localized heating through the heating mechanism described in the previous section. Once the joint interface melts and allows their molecules to intermingle, fusion bonding between two sheets is created. The power input is then turned off, and the molten polymer is allowed to solidify during a holding period. The resulting seal strength can be comparable to the original sheeting materials.

A typical dielectric welding/sealing machine consists of these basic elements:

1. High-voltage power generator with frequency of 27.12 MHz where the system can be tuned and the total power output controlled through the electrodes and dies.
2. A pneumatic or hydraulic press where two electrodes are attached to two aluminum platens so that their movement (distance) and pressure can be controlled precisely.
3. A pair of dies made from brass are attached to the electrodes (aluminum platens) to serve as the heating elements where the final shape of the seal can be formed. The movement and pressure of the dies are controlled by the press.
4. A nest or fixture that can hold and provide support for the sheets other than the seal area during sealing process.

12.3.1 Key process requirements and parameters

Power requirement

In order to identify the right machine to use, a user must figure out the power necessary to perform a successful seal. This is mainly dependent on the total seal area for each sealing cycle. A tear seal only counts a fraction of a flat seal area. A larger area requires higher power. As a rule of thumb, 1 kW per 1000–2000 mm^2 can be used to estimate the power requirement. Please consult with the sealing machine manufacturer for a recommendation. Sheet-material thickness can complicate the power requirement if it gets so thin (less than 0.01″ or 0.25 mm thick) that the dies become a dominant heat sink that prevents sufficient heating and melting of the

© Woodhead Publishing Limited, 2013

material in between the dies. In this case, buffer material can be used as a heat insulator. The buffer material will be discussed in more detail in a later section.

Interdependency of process parameters

To some limited extent, these process parameters are interrelated. For example, higher power input can increase the heating rate of the sealing process and reduce the seal time. The pre-seal pressure can affect the seal time too because it can change the effective material thickness during sealing. Die temperature control can also impact the power input and seal time because it changes the dielectric loss and the heat loss through the dies. It is critical to identify a process window where a stable sealing process can be established with an acceptable seal quality.

Power input

Higher power input can reduce the seal time required. However, the voltage increase can lead to a more sensitive sealing process where any imperfection in alignment, material impurities, could lead to arcing and inconsistent seal quality. Most dielectric sealing machines in the market are equipped with an arc suppressor. Whenever an arc suppressor is triggered without any obvious reasons, it means the power-input level for that particular seal geometry is reaching its maximum level. To achieve a stable process is more important than to have a shorter seal time because any short circuit caused by high-power input/short seal time could damage the machine and dies where significant machine down time could incur.

Weld/seal time

The seal time is the time required for the power to stay turned on until the target (higher than melting or transition) temperature at the joint interface is reached. This is one of the key parameters to determine the amount of the melting and as a result the final seal thickness and the size of the weld beads.

Weld pressure or collapse distance

Having pressure control before and after power input is desirable. Application of pre-seal pressure is important because it will determine the effective material thickness before sealing begins. It is also beneficial to have both pressure and final collapse control, because pressure is critical to create a consistent seal and collapse control can avoid over thinning of the material at the seal interface right after melting occurs and prevent arcing.

© Woodhead Publishing Limited, 2013

Hold time

After the power input is turned off, the dies are held together with a preset pressure for a preset hold time. This is to make sure the molten material at the joint interface is solidified and a seal strength is established before releasing the die pressure.

Die temperature

Section 12.2.1 discussed the temperature dependence of the dielectric loss. It is desirable to control the temperature of the dies to maintain a consistent sealing process. This can be achieved by running cooling water through the metal base platens where the dies are attached to. Dies can be regarded as a heat sink during the sealing process to provide fast re-solidification of the molten layer. However, as the sealing process runs for a typical production line, thousands of seals are generated and it does not take long for the dies to become hot. If the die cooling system is not functioning properly, it is very easy for the dies to get hot. Once the dies become hot, the die heat sink effect is significantly reduced and results in higher temperature in the polymeric film which could lead to higher dielectric loss and increase in heat generation. As a result, thermal runaway could happen and lead to arcing and inconsistent seal quality. Some plastics that do not have the best dielectric properties will require pre-heating of the electrode to improve their weldability. For example, polyamide (nylon) typically requires pre-heating the electrode to about 50°C in order to have a good seal quality.

Single-versus double-cycle process, simultaneous versus sequential

It is always desirable to complete a sealing process with one single sealing cycle. But when different seals with different power distributions are required, a single-cycle die design can be very challenging. For example, an application that requires a flat/planar seal and a circular/non-planar seal (around a rigid port) to be completed in the same sealing process can become complicated. In this case, a double-cycle sealing process can produce a much better seal quality with a simpler die design. However, it also requires a longer processing time. Different approaches on the sealing steps can also be an important factor to consider when designing the machine configuration. One good example is the sealing of medical bags where the port seals and the bag peripheral seal are needed to complete the sealing process. This can be achieved by either sealing the port seal first then the peripheral seal with sequential steps or with a double-cycle sealing process

© Woodhead Publishing Limited, 2013

where a port seal is introduced by an additional mandrel die in between the top and bottom dies first. Then, a peripheral seal is done between the top and bottom dies with the second sealing cycle while the pressure between the top and bottom dies are maintained throughout both cycles. One main advantage of using a double-cycle sealing process over two separate sealing steps is that it is easier to maintain the seal alignment for both seals because the same fixture and sealing pressure are maintained, while the top and bottom platens are remain closed.

12.3.2 Sealing process automation

There are many different ways to automate the dielectric sealing process, depending on the throughput and how complicated the seals are. The following lists the three most common configurations are used in the industry:

1. Semi-automatic manual loading machine: this type of machine requires the operator to manually feed the sheeting materials onto the bottom die and fixture area. The bottom platen and die can shuttle in and out horizontally and the top platen with the top die can move down vertically to match up the bottom die and generate the seal. This is the most suitable for low throughput requirements with a low capital investment (see Fig. 12.3).
2. Turntables with indexing: this is used mainly to accommodate more complicated sealing requirements. Multiple stations are utilized to provide different sealing and other assembly processes. This can be configured with an operator feeding at different stations or an automatic feeding system at the different stations. Each station can be single- or double-cycle sealing process (see Fig. 12.4).
3. Linear continuous conveyer automatic machine with 2-up or more—high throughput machine: when a high throughput is needed, a much bigger machine with a linear continuous conveyer, where the film (web in roll) is fed into the machine continuously, can be used. Multiple stations can be integrated into the line where single- or double-cycle sealing process can be used for each station. Also, depending on the throughout requirement, it can be a 2-up or more for the conveyer line. Different feeding systems can be integrated into the stations depending on the part geometry and material types. As a typical high throughput medical-bag production-line machine, one can envision that two rolls of web (as top and bottom sheets) being fed into the line continuously where the web is precut and multiple stations perform the peripheral seal, tear seal, insertion of tubing as ports, and port seals, etc.,

© Woodhead Publishing Limited, 2013

(a)



(b)

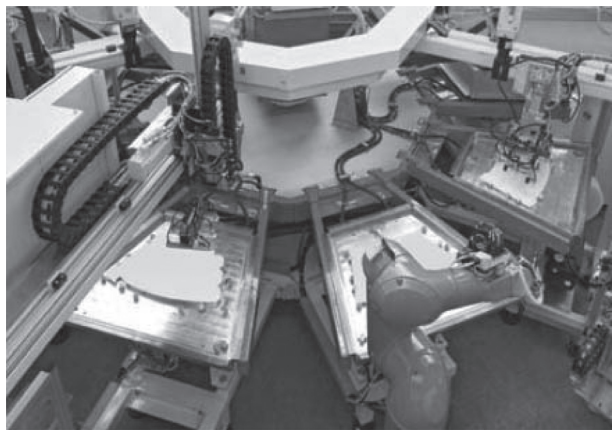


12.3 Semi-automatic shuttle loading RF machine. (Courtesy of Keifel (b) and Alloyd (a).)

depending on the applications. As a good quality-control measure, inspection and testing can be integrated into the production line at appropriate stations to ensure only a good quality product is produced. One of the key things regarding the machine configuration is the flexibility of the power-generator arrangement. This type of machine can require multiple stations with a high power requirement. Careful consideration for the extra power supply and extra space is always a good strategy. Figure 12.5 shows typical linear continuous RF welding system for blood-bag applications.

© Woodhead Publishing Limited, 2013

(a)



(b)



12.4 Turntable with indexing RF welding systems. (Courtesy of Keifel (a) and Alloyd (b).)

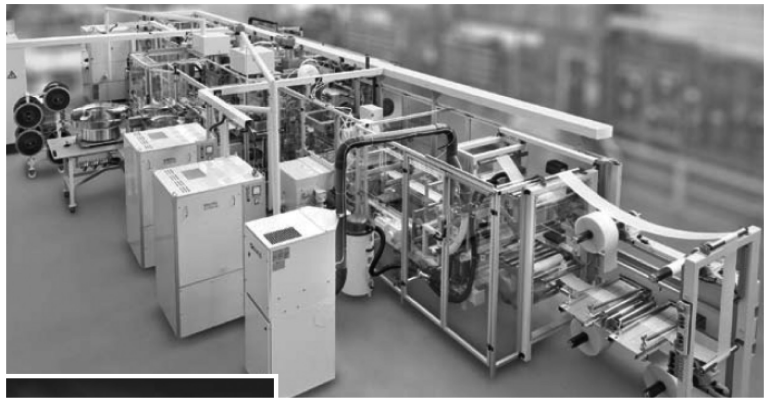
12.4 Key factors affecting the sealing process and seal quality

This section discusses key factors that could affect sealing process control and final seal quality. It provides important background information that will help engineers to understand some practical RF sealing process applications.

12.4.1 Die design

A good die design is a prerequisite for achieving a quality seal. Two key aspects determine the final shape of the seal. Firstly, if the dies are not

© Woodhead Publishing Limited, 2013



12.5 Keifel high throughput linear continuous automatic RF welding system for blood-bag applications. (Courtesy of Keifel.)

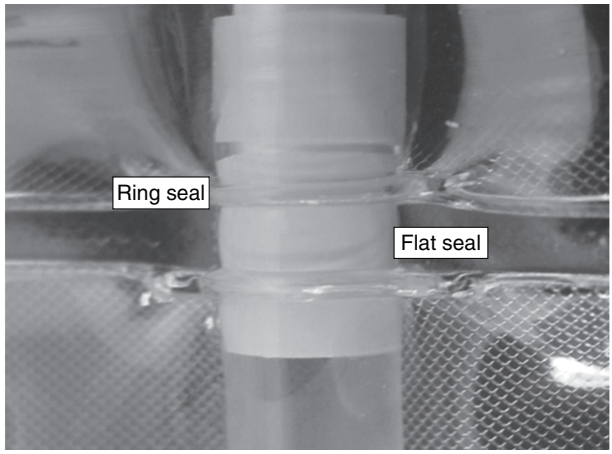
matched perfectly, the final seal will show the mismatch and could become the weakest link of the overall seal. The other aspect is that the efficiency of the dielectric heating process is dependent on the die design.

Complex die design – non-planar and three dimensional

Traditional dielectric sealing die design is all vertical circuit flow direction from top to bottom dies. With a double-cycle sealing application, die design could become complicated because of the potential multiple circuit flow directions. This brings an additional degree of freedom to the die design where heating patterns could be more complicated and three dimensional rather than just in vertical direction.

In some complicated applications, heating has to happen on a non-planar (non-linear) surface where the dies has to be designed to follow the contour but at the same time ensuring the whole electrical system is tunable and generating a uniform electric field (heating) during the sealing process. Non-planar die design can be very tricky and any misstep may lead to non-uniform heating and result in bad-quality seal or unstable sealing process where arcing could happen. A double-cycle sealing process can simplify the die design for a multiple seals application where both a planar and a non-planar seals are required. A die design for double-cycle application usually involves multiple dies (more than two sets of die) and switching circuits during different cycles. Plate VI (see Plate VI between pages 300 and 301) shows one die set design with two potential switching circuits. Panel (a) in Plate VI shows a single-cycle welding process with a combined electrodes configuration where the electric field flows vertically. Panel (b) shows a double-cycle welding process where the electric field flows vertically for a flat seal in the first welding cycle and

© Woodhead Publishing Limited, 2013



12.6 Seal sample contains both flat seal and ring seal.

then flows horizontally in the ring seal in the second welding cycle. Figure 12.6 shows a seal sample that is sealed from sheet material onto a rigid port through a flat/ring seal die design using a RF sealing process.

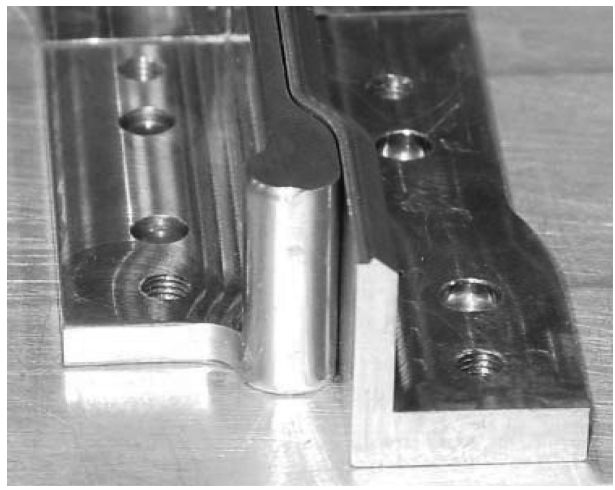
When multiple dies are in close proximity, the maintenance of the precise gaps between dies and insulation between dies are critical to the consistency of the sealing process and the quality of the seal. One way to achieve this is to incorporate insulate material such as UHMWPE with matching geometry in between the dies. Also for double-cycle die design, one must consider the distribution of the overall capacitance of the circuit due to the three-dimensional die design. One rule of thumb for this is to avoid too much overlapping areas when two active dies are in close proximity.

Tear seal die design

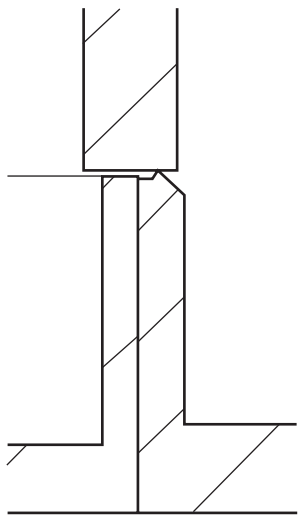
Tear seal is utilized to cut the unwanted portion of the sheeting material after the sealing process. The die design for tear seal is different than a typical seal. Figure 12.7 shows a typical tear seal die design where a regular flat seal is right next to it. These dies are actually on the bottom side. The matching top dies are just flat dies (see Fig. 12.8 for cross-section view). The tear seal is always located on the outside edge right next to a regular seal.

Also die design should be an iterative process. For each iteration, you evaluate the seal and modify the dies accordingly as necessary. For any complicated die design, one must consider the structure integrity of the dies design because the dies have to go through hundred of thousands of cycles under pressure. Brass is a good candidate for the die material because it has electrical and material properties. One thing to keep in mind is that all die design must avoid sharp edges.

© Woodhead Publishing Limited, 2013



12.7 Bottom flat seal and tear seal (outside edge) die design; die is attached to an aluminum base plate.



12.8 Set of dies with flat and tear seal.

12.4.2 Uniformity is key

Uniformity plays a key role in the dielectric sealing process. Good die design is essential to ensure that the electric field created between the dies is uniform. A good dielectric sealing machine must provide precise uniform

© Woodhead Publishing Limited, 2013

pressure application and movement control. Uniform dielectric heating is key to uniform seal quality and it depends on the uniform distance between the dies where the electric field is created. To insure a stable sealing process and consistent seal quality, dies, press platens and nest/fixture for the sheet material must provide uniform pressure (maintaining parallel) and precise movement during the sealing process.

12.4.3 Arcing

Arcing could happen when unexpected thinning of the sheet material during the sealing process. When the power input/seal time is excessive, coupled with high seal pressure, too much material squeeze-out (large weld bead) could happen and lead to thinning of the material in between the dies. When it is thin enough to reducing the material's ability to electrically insulate the upper and lower dies, current flow between the dies and as a result arcing happens. An uncontrolled arc can damage (burn) the sheet material, the die, and even the circuit of the machine. More importantly the significant down time will incur where repair can be performed.

Arcing could also happen with inappropriate die design where the thickness of the seal or the electric-field distribution is not uniform. Sharp corners and edges on dies may also cause arcing. The die edges should always be rounded and smooth. Arcing may also occur because of dirt or foreign matter on the material or dies. To avoid this, care must be taken to keep the material and the machine clean. When arcing occurs, the dies must be re-evaluated to understand the root cause of the arcing. Modification of the dies might be necessary. Also dies must be smoothed out and cleaned thoroughly.

Arc suppression

Most sealing machine is supplied with arc-suppression devices. It enables the machine to sense the possibility of an arc and turn off the power before an arc can occur. A sensing control which can be set by the machine on different sealing areas to prevent arcing during production runs.

12.4.4 Buffers

A thin layer of polymer (or laminate) materials with high dielectric properties and (insulator/barrier material), such as Teflon, Phenolic, and Mylar, can be used for some specific dielectric sealing applications to get better process stability and consistent seal quality.

© Woodhead Publishing Limited, 2013

The buffers are usually placed in between the sheet material and the dies. They do not increase the heating efficiency of the sealing process. However, they can add benefits in the following ways:

1. add an extra insulating layer to provide more stable dielectric heating (prevent arcing) especially when the sheeting material is thinner than 0.01 inch;
2. serve as a thermal insulator between the sheet material and dies;
3. provide extra cushion for non-uniformity of the electric field or pressure;
4. some buffers can reduce adhesion of the seal to the dies.

But one thing to keep in mind is that when dealing with a complicated, double-cycle and continuous sealing process, it is difficult to incorporate any buffers in the sealing process.

12.5 Weldability

Like other welding process, weldability of the plastics for dielectric sealing process is a dominant factor during the initial welding-process selection. Two main material/electrical properties discussed earlier in the heating-mechanism section are the dominant factors for weldability:

1. high dielectric constant;
2. high dielectric loss.

Typical materials suitable for dielectric sealing applications are polar thermoplastic polymers such as PVC (vinyl), nylons, PET, EVA, PVDC, ABS, and urethanec. Table 12.2 shows the weldability of all thermoplastic polymers. PVC has been used in the medical bags/pouches application for decades mainly because of the excellent dielectric sealing properties. Because of the environmental concerns, non-PVC materials have been under development to replace the existing PVC bags/pouches and tubing.

12.6 Testing approaches for seals and the dielectric sealing process

Testing can have different objectives during different stages of medical-device product commercialization. During the sealing-process development phase, testing is conducted to understand the process parameters and eventually optimize the sealing process. This can be done through a design of experiment process with testing of seal strength or other quality characteristics/

© Woodhead Publishing Limited, 2013

Table 12.2 RF welding weldability for different plastics

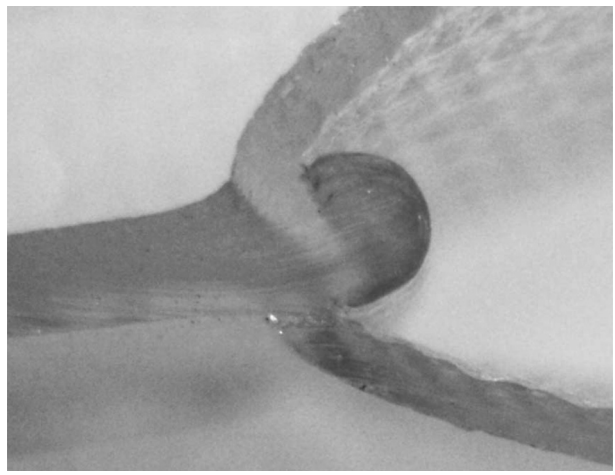
Material	Excellent	Good	Fair	Poor	None
ABS polymers		x			
Acetal (Delrin)				x	
Acetal copolymer				x	
Acrylics			x		
Aclar			x		
APET (amorphous PET)		x			
Barex 210	x				
Barex 218	x				
Butyrate		x			
Cellophane					x
Cellulose acetate (clear)		x			
Cellulose acetate (color)		x			
Cellulose acetate butyrate		x			
Cellulose nitrate			x		
Cellulose triacetate			x		
CPET (crystalline PET)					x
Diallyl phthalate polymer, glass-filled				x	
Epoxy resins			x		
Ethyl cellulose					x
EVA (ethyl vinyl acetate)		x			
EVOH (ethyl vinyl alcohol)			x		
Melamine-formaldehyde resin		x			
Methylacrylate			x		
Nylon (polyamide)			x		
Pelathane		x			
PET (polyethylene terephthalate)		x			
PETG (polyethylene terephthalate glycol)	x				
Phenol-formaldehyde resin		x			
Pliofilm (rubber hydrochloride)	x				
Polyamide			x		
Polycarbonate				x	
Polychlorotrifluoroethylene				x	
Polyester				x	
Polyethylene (all)					x
Polymide				x	
Polymethyl (methacrylate)			x		
Polypropylene					x
Polystyrene					x
Polytetrafluoroethylene (Teflon)					x
Polyurethane			x		
Polyurethane foam				x	
Polyurethane-vinyl film		x			
Polyvinyl acetate		x			
Polyvinyl chloride (PVC) (flexible, clear)	x				
Polyvinyl chloride (PVC) (color)	x				

(*Continued*)

© Woodhead Publishing Limited, 2013

Table 12.2 Continued

Material	Excellent	Good	Fair	Poor	None
Polyvinyl chloride (PVC) (opaque)		x			
Polyvinyl chloride (PVC) (semi-rigid)		x			
Polyvinyl chloride (PVC) (rigid)			x		
Polyvinyl chloride (PVC) (flexible, glass-bonded)	x				
Polyvinyl chloride (PVC) (coated cloth and paper)	x				
Polyvinyl chloride (PVC) (adhesive emulsions)	x				
Rubber					x
Rubber, compounded			x		
Rubber, Hevea				x	
Saran (polyvinylidene chloride)	x				
Silicones					x
Teflon (tetrafluoroethylene)					x
Urea-formaldehyde resin		x			



12.9 PVC RF sealing seal cross-section with weld bead.

attributes as criteria for evaluation. Two measureable test results listed below are good ways to evaluate the quality of a seal:

1. weld bead size (final thickness) and symmetry (see Fig. 12.9);
2. peel strength of the seal.

© Woodhead Publishing Limited, 2013

During the production process, testing is carried out to make sure that the products produced are within the specifications with the specified confidence level before releasing to end user. For a typical dielectric sealing process, there are some key characteristics that we should either monitor or test to make sure the seal quality is meeting our expectation. Some of the tests are destructive tests which have to be conducted after the product is produced. Some non-destructive tests can be done at different stages before or during the production process to reduce the rejection rate. For example:

- Raw material level:
  - Check thickness uniformity of sheet material before sealing process – this can be done in-line right before sealing process
- Sub-assembly level:
  - Sealed container (pouch or bag) can be leak tested non-destructively in-line right after the sealing process.
- Final assembly level:
  - Sealed pouches are connected together by tubing as an assembled disposable kit. These final assembled pouches can be leak tested destructively by a special constraint/fixture with a pressure source.

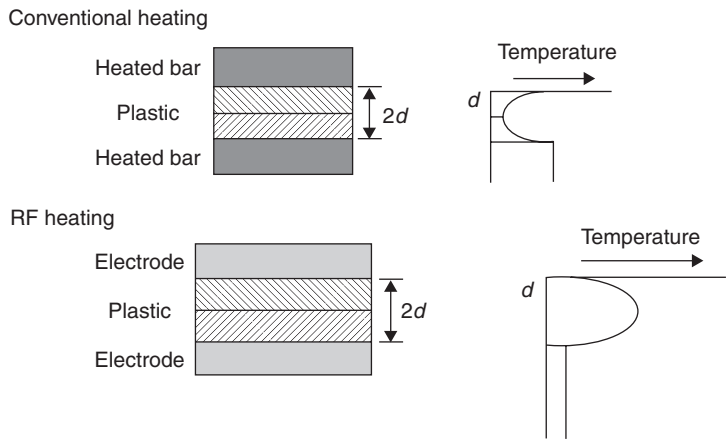
12.7 RF welding process advantages, limitations and future trends

12.7.1 RF welding process advantages and limitations

Compared to other sealing processes, RF sealing provides some unique advantages that other welding processes can not offer:

1. Precise, efficient, and localized heating occurs from the joint interface. Figure 12.10 shows a temperature profile comparison for traditional heat sealing and RF sealing. The die temperature can be controlled to compensate for the thickness of the sheet material. Also, sticking to the die/tool is not an issue for RF sealing.
2. Some unique and complicated RF seals can be created for tubing and bag applications. Tear seals and regular seals can be integrated into the overall sealing process to streamline the process.
3. Hermetic seals can be achieved.
4. The seal is considered flash free.
5. Automation is easy.

© Woodhead Publishing Limited, 2013



12.10 Temperature profiles for RF sealing vs conventional heat sealing.

On the other hand, there are some limitations:

1. It is only applicable to some thermoplastics;
2. PVC is the most suitable material for RF welding for medical-device applications but it exhibits hazardous waste issues;
3. Safety shielding is required;
4. Limits on joint thickness.

12.7.2 Future trends in RF welding

One of the major R&D areas in RF welding that medical-device companies are working on is the RF welding/sealing of medical pouch/bag system (with ports) using non-PVC and/or non-DEHP PVC materials. PVC material has been known for containing harmful components such as vinyl chloride monomer (VCM) and ethylene dichloride (EDC) which can release dioxin when incinerated. Also, a plasticizer DEHP (bis(2-ethylhexyl) phthalate) that has been commonly used to soften the rigid PVC for use in medical-device applications has many potential health concerns when used improperly. Many efforts from the medical-device industry are focused on identifying materials to replace PVC and yet being able to continue utilizing the similar RF welding processes. Proprietary material (including multi-layer material structures) development for bags, pouches, and ports for medical applications for RF welding is still a very active research and development area as many medical-device companies are trying to provide non-PVC and non-DEHP PVC disposable sets for applications in IV, dialysis, blood transfusion areas.

© Woodhead Publishing Limited, 2013

Another area of research efforts is the continuing improvement of the current RF sealing system, in particular how to simplify the integration of peripheral sealing (such as port sealing) into the main sheeting-material sealing by a combination of new die designs and new material/component configurations.

12.8 Reference

1. E. Riande and R. Diaz-Calleja, *Electrical Properties of Polymers*, New York, Marcel Dekker, 2004.

© Woodhead Publishing Limited, 2013

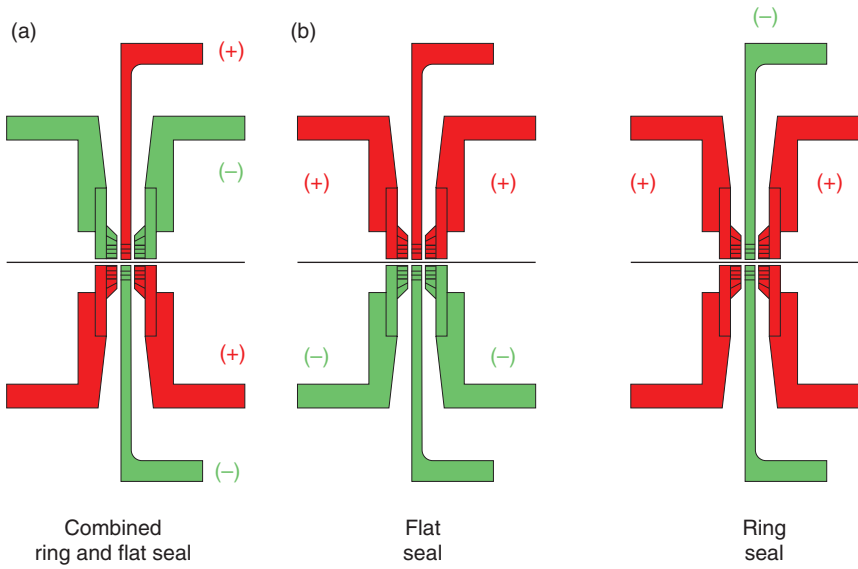


Plate VI (Chapter 12) (a) Polarity of the dies during flat seal and ring seal – single-cycle welding process (red, positive electrode (+); green, negative electrode (–)). (b) Polarity of the dies during flat seal and ring seal – two-cycle welding process (red, positive electrode (+); green, negative electrode (–)).

© Woodhead Publishing Limited, 2013

13

Transmission laser welding strategies for medical plastics

I. JONES, TWI Ltd, UK

DOI: 10.1533/9780857096425.3.344

Abstract: This chapter describes the various methods of using lasers to weld plastics. Particular attention is paid to the most commonly used method – transmission laser welding. The different types of equipment available are discussed, including the laser types, beam delivery and clamping equipment. The user is assisted in application of laser welding by the inclusion of successful joint designs, suggested monitoring methods and information on the effects of the main welding process parameters.

Key words: medical, plastics, polymers, welding, laser, moulded, packaging, textiles, tubing, microfluidic, monitoring, quality control.

13.1 Introduction

Laser welding is suitable for joining sheet, film and moulded thermoplastics and textiles. Lasers can deliver well-controlled amounts of energy to a precise location due to the ease of controlling the beam size, and the range of methods for precise positioning and movement of the beam. Complex forms can be welded using high-resolution positioning and welds from less than 100 μm wide. This makes them suitable in a wide variety of applications including catheters, microfluidic devices, tubing, packaging, electronic cases and textiles by using different material-handling equipment.

13.2 Advantages and limitations of laser welding

The main advantages of using laser welding over other welding processes are:

- short weld times and high-speed processing (typically less than 1 s);
- highly adaptable process – through the use of optical scanning of the beam it is possible to change between designs easily;
- automated technique – straightforward to put into production;
- consistent performance (once weld parameters are optimised) – a reliable process with good monitoring and control procedures;

© Woodhead Publishing Limited, 2013

- clean non-contact process – can be used in a clean-room environment;
- minimal thermal damage to product: heating location is precisely defined and the weld cycle is short allowing little time for conduction to areas surrounding the welds;
- joint designs are typically simple flat to flat surfaces;
- low energy consumption;
- hermetic seals possible;
- no vibration or movement of the parts required during welding – the parts are located and clamped before welding begins;
- no particulates or large melt bead is produced – no requirement for joint designs to trap the melt flash;
- weld sizes can be defined from 1 μm up to 10 mm wide allowing application to small complex parts and larger parts as required;
- no surface damage – in transmission laser welding all the heating takes place at the joint line;
- multiple layers can be welded simultaneously by transmitting the beam through the upper material layers;
- thin, flexible substrates and elastomers can be readily welded, and rigid materials can be welded to flexible materials;
- suitable for high-melting-point polymers and those with low-melt viscosities such as polyamides;
- can be used to join dissimilar materials by using a compatible film interlayer.

The main disadvantages of laser welding are:

- the upper part must transmit at least 10% of the laser-beam energy to the joint line (for transmission laser welding but not direct laser welding);
- there are part thickness limitations in semi-crystalline materials with high crystallinity, such as PEEK;
- laser-absorbing material must be added to one of the plastics or as a coating or film interlayer at the joint surface – though for direct laser welding the laser wavelength can be selected to absorb into most plastics;
- joint surfaces must be in intimate contact for welding to be successful – good-quality surfaces and suitable clamp designs are required;
- eye and skin protection must be considered when using laser equipment.

These advantages and disadvantages are summarised in Table 13.1.

13.3 Process description

Two general forms of laser welding exist: direct laser welding and transmission laser welding.

© Woodhead Publishing Limited, 2013

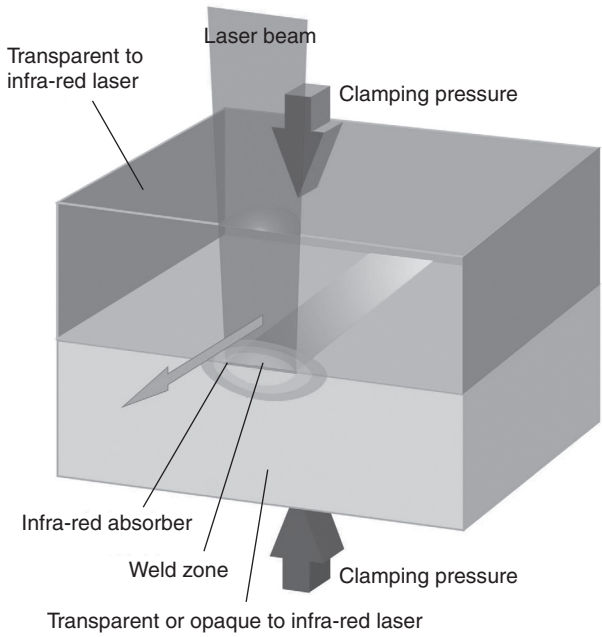
Table 13.1 Advantages and disadvantages of transmission laser welding

Advantages	Disadvantages
Automated process.	The top part must transmit the laser radiation.
Good monitoring and quality-control procedures.	Laser-absorbing material must be added to one of the plastics or at the joint surface.
Joint designs are simple flat to flat surfaces in general.	Equipment can be expensive.
Hermetic seals possible.	Joint surfaces must be of good quality.
Fast (<1 s) weld possible depending on size.	Part clamping must be designed carefully to ensure contact during welding.
No contact with heated tools.	Health and safety issues relating to the use of lasers.
No vibration.	Part thickness limitations, especially for highly crystalline materials, such as PEEK.
No particulate generation.	
Precise placement of welds (50 μm or less).	
No surface damage.	
Low residual stresses.	
Complex shapes possible.	
Localised heating – no thermal damage close to weld.	
Multiple layers can be welded simultaneously.	
Thin, flexible substrates or elastomers can be welded.	
Suitable for high-melting-point polymers and those with low-melt viscosities, such as polyamides.	
Can join dissimilar materials by using a compatible IR-absorbing interlayer.	
Little or no flash.	

In direct laser welding the materials are heated from the outer surface possibly to a depth of a few millimetres. Normally, no specific radiation absorber is added to the plastics. Laser sources from 2.0 to 10.6 μm wavelength are typically used. At 10.6 μm (CO_2 laser), radiation is strongly absorbed by plastic surfaces, allowing high-speed joints to be made in thin films. Developments have also been made using a CO_2 laser transmissive cover sheet as a clamp and heat sink to make welds in thicker plastics without material loss at the surface. At 2.0 μm wavelength where the absorption is less strong, a fibre or Holmium:YAG laser can be used to make welds in sheet a few millimetres thick. Direct laser welding is not widely applied for joining plastics but has potential for wider use.[1–3]

Transmission laser welding is now widely used for joining thermoplastics in industry, using laser sources with wavelengths from 0.8 to 1.1 μm, such as diode, Nd:YAG and fibre lasers. The radiation at these wavelengths is less readily absorbed by natural plastics. Laser-absorbing additives are therefore put into the lower part or applied as a thin surface coating at the joint. The parts are positioned together before welding and the laser beam passes through the upper part to heat the joint at the absorbing surface of the lower

© Woodhead Publishing Limited, 2013



13.1 Diagram of transmission laser welding showing the movement of a beam over a workpiece. The lower part can be arranged to be an infrared absorber or the absorber may be placed at the joint surface.

part (Fig. 13.1). The absorber in or on the lower plastic is typically carbon or an infrared absorber with minimal visible colour (Clearweld), which allows a wide range of part colours and appearances to be welded. Transmission laser welding is capable of welding thicker parts than direct welding, and since the heat-affected zone is confined to the joint region no marking of the outer surfaces occurs.[4]

The maximum thickness of the upper part is determined by the transmission properties of the material; transmission laser welding is only possible if over 10% of the energy is transmitted to the joint interface.

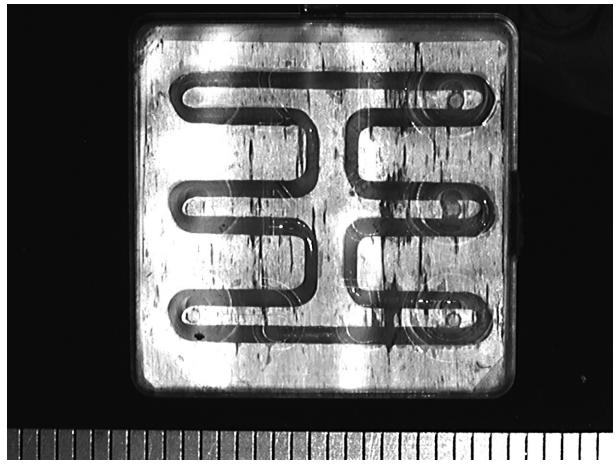
Transmission laser welding can also be used to weld film and sheet materials. The laser source is scanned over the two parts just in advance of clamping using a roll-processing method.

An example of a transmission laser welded part is shown in Fig. 13.2.

13.3.1 Modelling

Thermal modelling of polymer welding is applied most easily when the process is predominantly one of diffusion at the surfaces and has minimal melt flow. Transmission laser welding is one such process. Models may be based on

© Woodhead Publishing Limited, 2013



13.2 Transmission laser welded polystyrene microfluidic component. Welded using beam manipulation with scanning optics.

classical heat-flow equations for a specified joint design or using finite element methods. The models typically use details of the materials' radiation absorption coefficient, thickness, reflectivity, melting point, density, heat capacity and thermal conductivity, whilst also taking into account the laser-beam profile, laser power and welding speed. Through analysis of the heat flow it is possible to generate the thermal history for all points in joint during the welding cycle. Thus it can provide the weld dimensions, the peak temperature and, with details of the materials' mechanical properties, the residual stress remaining after welding can be estimated. Plate VII (see Plate VII between pages 300 and 301) shows a typical output from a finite element thermal model.[5–8]

13.3.2 Colour independence

As already described, the absorber used in transmission laser welding is often carbon black, which obviously affects the colour of the lower part being joined. Alternative absorbers are now available which have very little visible colour (Clearweld materials). They can be applied by liquid coating onto the joint surface or as an additive within the resin of the lower material. The additives are based on infrared absorbing dyes which have been tested for biocompatibility. They absorb the laser sources strongly and yet have very little absorption in visible ranges.

By using the Clearweld materials, completely transparent products can be laser welded, which is of particular importance in the medical industry where an initial indication of cleanliness and lack of contamination is important. An example of a laser-welded transparent medical device is shown in Fig. 13.3.[9]

© Woodhead Publishing Limited, 2013



13.3 Laser-welded transparent medical devices.

13.4 Main welding parameters and effects

As with all plastics-welding processes, the three critical process parameters are temperature, time and pressure. In laser welding these are controlled by laser power, laser spot size, irradiation time (either fixed or moving systems), the presence of laser-absorber materials and clamping load.

The energy density used during welding combines the process parameters of temperature and time. It is determined by the laser power, the spot size at the joint, and the irradiation time (for fixed processes) or welding speed (for processes in which the part moves with respect to the laser):

$$\text{Energy density} = \frac{\text{Power} \times \text{Time}}{\text{Spot size}}$$

or

$$\text{Energy density} = \frac{\text{Power}}{\text{Spot width} \times \text{Speed}}$$

If the energy density is too low then insufficient heating takes place and the material at the joint is not held at a high enough temperature for a sufficiently long time to form a strong weld. If the energy density is too high, then excess heating can degrade the polymer at the joint, resulting in porosity, or,

© Woodhead Publishing Limited, 2013

in extreme cases, burning or charring of the polymer. Either case results in a weld of lower strength than the optimum. In practice, a relatively wide processing window can usually be found within which satisfactory welds can be produced. Typically laser-welding applications use an energy density within the range 0.1–2 J/mm^2, although this will vary depending on the depth of melt required to ensure a satisfactory joint. Although the energy density can be used to characterise the welding process, it should be treated with caution. The conduction of heat away from the joint during welding means that using the same energy density will not necessarily result in the same quality of weld. For example, with a constant spot width, doubling the power will usually allow the speed to be more than doubled, whilst retaining the same performance from the weld.

The other factor affecting the amount of energy made available to the weld is the density and absorbance of the absorber present at the joint interface. A higher density of absorber will allow the weld to be made faster or with a lower-power laser.

The pressure applied is controlled using the clamping system. If the workpieces are not clamped together during welding, or if the pressure at the joint is insufficient, then the joint faces will not be in intimate contact. This will result in poor conduction of heat to the upper workpiece and limited interdiffusion of polymer chains across the joint interface.

Both effects result in a weld of lower strength than the optimum. Care is needed to ensure that a clamping load actually provides pressure at the joint. Typically, clamping pressure in the range 0.1–1 N/mm^2 is used. If the workpieces bend under the clamping load in such a way that the joint is distorted then a poor weld can result. For this reason, it is often useful to have some compliance, for example an elastomeric element, in the clamping system.

13.5 Forms of equipment

A laser-welding system will typically consist of a laser source, a beam-delivery system and workpiece clamping or manipulation.

13.5.1 Laser types

The main types of laser used for transmission laser welding are diode, Nd:YAG and fibre lasers in the wavelength range 0.8–1.1 μm. At longer IR wavelengths, CO_2 and other lasers with a wavelength in the region of 2.0 μm, may be used for direct welding (Table 13.2).

© Woodhead Publishing Limited, 2013

Table 13.2 Laser types used for welding plastics

	Nd:YAG	Diode	Fibre	CO_2	Ho:YAG or Tm:YAG
Wavelength (nm)	1064	780–980	1000–2100	10 600	~2000
Efficiency[a]	3	30	20	10	3
Approximate cost for 100 W system (€k)	60	15	40	15	150+
Beam quality[b]	High	Low	High	High	High

[a] Efficiency is the percentage of the electrical power consumed by the laser that is emitted in the beam.
[b] Beam quality is the ability to focus the beam to a small spot size with a high-energy density.

Nd:YAG

Nd:YAG lasers are widely used in industry for materials processing. High-power systems are bulky, but lower-power systems are relatively compact. Water cooling is usually required. The beam is transferred from the laser to the workpiece via an optical fibre. It is feasible to combine the beam from more than one laser to produce higher powers if required. The high-beam quality allows relatively small spot sizes to be produced.

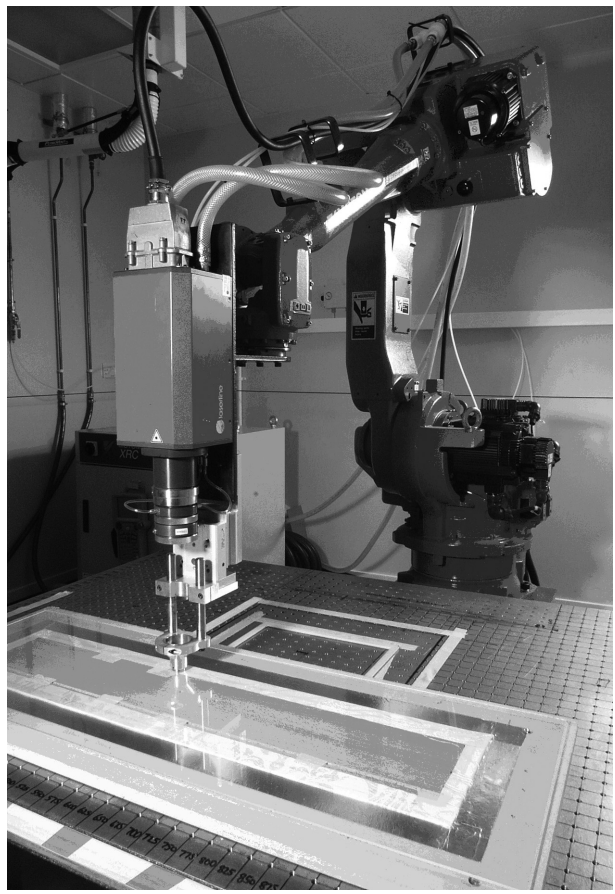
Diode

Diode lasers produce radiation at a wavelength of 780–980 nm. Water cooling is usually required. Their relatively low-beam quality means that they cannot be used to produce a spot size as small as Nd:YAG or fibre lasers. However, this is rarely a problem for plastics laser welding, where the relatively low purchase and running costs have attracted a great deal of interest. The beam may be delivered by an optical fibre, but the diode is sufficiently small and light that it is often feasible to use a direct system, in which the diode is included with a lens system in a single unit, typically ~150 × 150 × 300 mm. This unit can readily be mounted on a gantry system or robot arm to manipulate the beam (Fig. 13.4).

Fibre

Rare-earth doped fibre lasers typically supply a wavelength in the range 1000–2100 nm. In the field of materials processing, much interest has focused on wavelengths around 1100 nm to provide a direct replacement for Nd:YAG lasers, with equivalent beam quality, but greater efficiency. Systems are relatively compact and can be air cooled. In the field of plastics welding

© Woodhead Publishing Limited, 2013



13.4 Diode laser mounted on a robot arm.

the use of fibre lasers has been demonstrated for a range of applications, including precision welding, films, textiles and larger moulded parts.

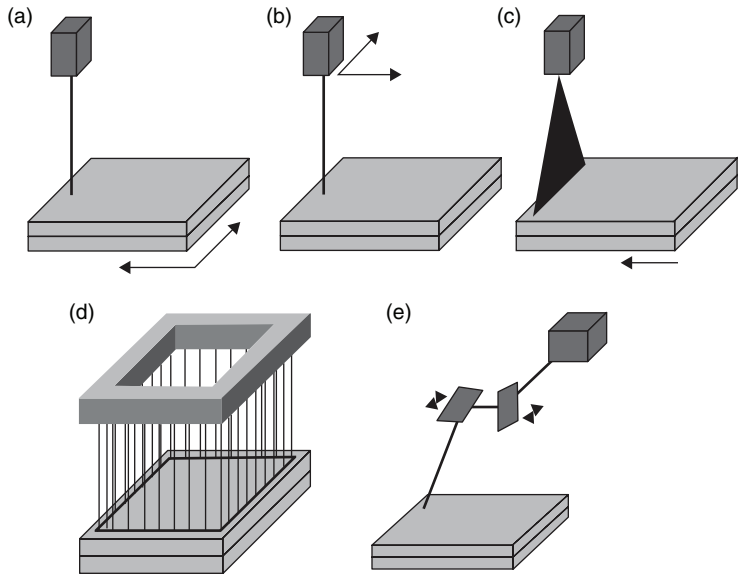
CO_2 laser

CO_2 lasers are widely use in industry for cutting plastics. High-power systems are bulky with gas-flow systems incorporated, but lower-power systems are relatively compact. The beam is transferred from the laser to the workpiece via mirrors. Focused spot sizes of less than 200 μm are available.

2.0 μm wavelength lasers

There are YAG and fibre lasers available emitting at a wavelength in the region of 2.0 μm. They are less commonly used than the other sources and

© Woodhead Publishing Limited, 2013



13.5 Laser beam and workpiece manipulation. (a) Moving workpiece. (b) Moving laser. (c) Curtain laser. (d) Simultaneous welding. (e) Scanning laser. (From Reference 10.)

more expensive. The beam can be delivered down a fibre optic, usually has good beam quality and can provide small focused spot sizes.

13.5.2 Beam delivery

The beam or workpiece manipulation equipment for laser welding will typically take one of the forms illustrated in Fig. 13.5, or a combination of one or more of these.

Moving workpiece

With the laser fixed, the part can be manipulated to form a continuous weld. This can be achieved, for example, with rollers, or a single- or two-axis moving table. This type of system is relatively simple to set-up and programme, but would not normally be used if three-dimensional welds are required.

Moving laser

The optical system for a fibre delivered laser, or the laser head for a direct diode laser can be mounted on a variety of robotic systems. These range from simple two-axis gantry systems to multiple-axis robotic arms. The laser

© Woodhead Publishing Limited, 2013

is manipulated around the part to be welded, potentially allowing complex, three-dimensional welds to be produced. To facilitate automatic production, it is feasible to combine a moving laser with a moving part, for example by using a rotating table to present different faces of a component to a laser mounted on a robot arm.

Curtain laser

The laser energy is spread into a line and then passed over the component, either by moving the laser or by moving the part. A mask is typically used to ensure that only the relevant areas of the component are exposed to the radiation. This is particularly suited to small components with a complex weld geometry. The process would usually be used only to produce two-dimensional welds. The welds may be completed very quickly with a single sweep of a line source.

Simultaneous welding

If a large number of identical welds is required then an array of diode lasers can be assembled in the shape of the weld to be produced. This is then used to irradiate the whole joint simultaneously, with a typical cycle time of 1–3 s. This approach is well suited to automated assembly. The equipment used is frequently based on ultrasonic welding equipment and this process is typically used in place of ultrasonic welding where a good cosmetic appearance is required or for components that are sensitive to vibration. Two- and three-dimensional welds can be produced. Since the entire joint is welded at the same time, this allows more collapse of the polymer at the joint, and therefore wider part tolerances.

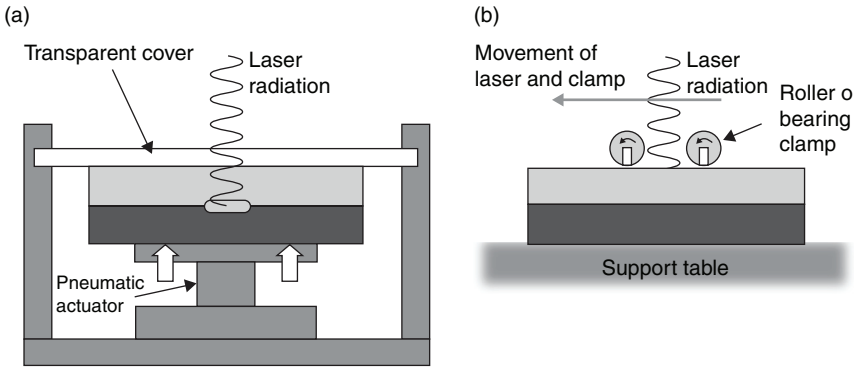
The methods for simultaneous welding include development of light guides, fed by fibre-optic bundles, which are shaped to the item being welded. The light guide therefore provides both heating and clamping to the whole part at the same time.[11]

Scanning laser

The laser radiation is manipulated by a pair of orthogonal rotating mirrors over an area that may range from 50 mm × 50 mm up to approximately 1000 mm × 1000 mm. In general, a larger working area implies a longer working distance and a larger spot size. It is possible to co-ordinate a number of scanning systems to give a larger working area. In general, only two-dimensional welds can be produced.

Repeatedly scanning the laser at high speed over the same path can be used to give quasi-simultaneous welding. As for simultaneous welding, this

© Woodhead Publishing Limited, 2013



13.6 Clamping systems for through-transmission laser welding (a) Fixed clamp. (b) Moving clamp. (From Reference 10.)

heats the entire joint area at the same time, allowing more collapse of the material in the joint and potentially allowing wider tolerances.

An alternative approach is to direct a scanning beam onto a mirror surrounding the weld line. This has been carried out using a cone-shaped mirror surrounding a cylindrical part, allowing tube tips or small round components to be welded simultaneously.[12]

13.5.3 Clamping

A wide variety of clamping systems have been used for transmission laser welding. They are mostly variants of the two systems illustrated in Fig. 13.6.

Variants of the fixed clamp include systems using mechanical fastenings, rather than an actuator, to apply a load. In the simplest variant, if the part design allows it, a bolt can be passed through the workpiece to apply the load. The transparent cover must be rigid enough to provide the clamping pressure. Thick acrylic or plain plate glass can be used. Borosilicate glass is less vulnerable to thermal shocks during welding, but more expensive. For welding of high-temperature polymers, quartz glass may be used. In all cases it is important to ensure that suitable safety precautions are taken to avoid the risk of injury if the transparent cover breaks while it is under load.

The moving clamp can use bearings, rollers or a simple sliding shoe to apply a clamping load. Because the load is applied only at the point where the joint is irradiated, clamping loads may be much lower when a moving clamp is used. There is therefore less risk of distorting the workpiece, and equipment can be less bulky. This is particularly advantageous for large components, where application of a suitable clamping pressure to a large area can require large loads.

© Woodhead Publishing Limited, 2013

Welding in a nip between two rollers is typically used to weld two flexible materials together or a flexible film to a rigid base. The laser beam is directed towards the nip between the rollers and positioned to heat both internal surfaces of the joint just before they are pressed together. Very high-speed processing (over 500 m/min) has been demonstrated using this technique.

Another method of applying force at the point of heating, a variation of the moving clamp, is to transmit the laser beam through a ball-shaped transmissive clamp. The ball rolls in an air bearing socket. The air flow also helps to keep it clean and maintain a consistent transmission of energy. Such a clamp has been used successfully with 3-D robotic-welding equipment for complex-shaped parts.[12]

13.6 Weldable materials

This section describes the range of plastics and textiles that can be welded using the laser process, and the material characteristics that are important. Dissimilar material combinations are also considered.

13.6.1 Weldable plastics

A wide range of plastics can be welded using laser-welding procedures. The process is tolerant of a wide range to melting temperatures, a wide range of melt viscosities and of materials that readily oxidise in air. This is because the temperature at the joint can be readily controlled, the melt zone is of minimal volume, and is generally trapped at the joint line by surrounding solid material. Material in a variety of forms can also be readily processed, including film and sheet, moulded parts, elastomers, fabrics and dissimilar combinations of those types.

The main limitation in materials selection is the presence of dark colours and opaque additives. It must be remembered that for *transmission* laser welding, at least one of the parts must transmit a proportion of the laser energy. This therefore limits the use of carbon-black pigments and other opaque pigments such as titanium dioxide to the side of the joint away from the laser. This is not the case in *direct* laser welding.

13.6.2 Transmission properties

The transmission properties of plastics vary with the type of polymer, the crystallinity and the additive or pigment content. It has already been stated that for transmission laser welding it is preferable for the part closest to the laser to be more than 10% transmissive. Transmission measurement is

© Woodhead Publishing Limited, 2013

carried out using a calorimeter to measure a laser pulse energy directly and then with the test material between the sensor and the laser source. The pulse energy measured in these two cases is compared. A more detailed measurement includes the reflection of energy at the surface, which can be significant for some materials and will also limit the energy available to the weld.

The spherulites in semi-crystalline plastics and any particulate or fibre additives lead to scattering of the laser beam. This leads to a reduction in beam intensity at the weld interface. Measurements can be used to indicate the size of such effects to allow the beam shape and process parameters to be controlled accordingly.

Typically amorphous plastics (e.g. polycarbonate, polymethylmethacrylate, polystyrene) with minimal additive content can be welded in thicknesses up to at least 100 mm. Semi-crystalline plastics (e.g. polyethylene, nylon) are suitable for laser welding up to a thickness of 10 mm. Some materials, such as polyetheretherketone (PEEK), can only be welded when the thickness is less than 1 mm using transmission laser welding. Glass-fibre additives tend to increase the beam scattering, but do not prevent laser transmission. Other additives such as carbon-black or titanium-dioxide pigments will block or reflect the beam, and prevent welding.

13.6.3 Compatible combinations

In general, only similar plastics can be welded together. However there are some combinations of different plastics that are compatible with each other. Compatible combinations are shown in Table 13.3.

Table 13.3 Weld compatibility between different plastics

Plastic	Good compatibility	Some compatibility
ABS (acrylobutylstyrene)	Acrylic	Polystyrene SAN (styreneacrylonitrile)
Acrylic	ABS Polycarbonate	SAN
Polycarbonate	Acrylic	Polyphenylene oxide
Polystyrene	Polyphenylene oxide	ABS SAN
SAN		ABS Acrylic Polyphenylene oxide Polystyrene
Polyphenylene oxide	Polystyrene	Polycarbonate SAN

© Woodhead Publishing Limited, 2013



13.7 Protective clothing with seams welded and hence sealed using laser welding.

13.6.4 Textiles

Fabrics are most commonly joined by stitching, a highly labour-intensive process that renders production cost-prohibitive in many parts of the world. It also makes holes in the fabric, which impairs the strength of the resulting seam and limits the performance of seams that need to be sealed.

The principal advantages of laser welding for joining textiles include high production rates; sealed seams; no melting of external fabric texture; single-sided access so welds can be produced beneath other layers of fabric; seam flexibility; and robotic manipulation for automated joining.

Applications such as inflatable product construction, sealed mattress assembly, medical furniture and protective clothing (Fig. 13.7) have been studied, with successful demonstration of representative seams that meet the performance requirements of the applications.[13] Laser welding of flexible

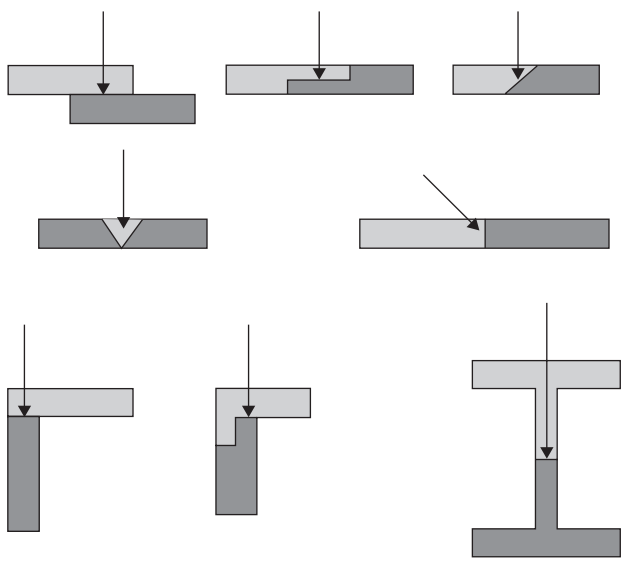
© Woodhead Publishing Limited, 2013

implantable products has also been developed. This is for the construction of vascular grafts, where polyester fabric can be joined to support stents using a cost-effective, automated process.[14]

The laser-welding procedure used for textiles is generally based on the Clearweld method of transmission laser welding, but direct welding using either diode or CO_2 laser sources is also feasible.

13.7 Joint designs

A selection of successful joint designs suitable for transmission laser welding is shown in Fig. 13.8. In general, it must be ensured that the energy reaching the joint interface is sufficient for melting the interface material without overheating the material on the outer surface and, as far as possible, evenly distributed at the interface. Extra care may be required to ensure even distribution of energy for interfaces angled to the beam direction or for complex-shaped parts that have different thicknesses along the joint line. Parts must be well fitting. A surface roughness less than 50 μm may be used as a general rule of thumb. Joints are often designed to be self-aligning, may incorporate a snap-fit to hold parts in place for welding or can be sized to allow self-clamping. As an example, tubes may be arranged to have an interference fit to allow self-clamping.[15]



13.8 Joint designs suitable for transmission laser welding.

© Woodhead Publishing Limited, 2013

13.8 Monitoring and quality control

Laser welding is unique in the precision with which the location and amount of energy applied can be controlled. To take advantage of this potential, a rapid and accurate monitoring method is required.

Monitoring may be applied for a number of reasons, to confirm that various stages of the process have occurred, as well as to assess the quality of the weld:

- confirmation that the infrared absorber is applied correctly to parts before welding;
- indication that the parts are in contact during process;
- indication that weld heating is being carried out and control of temperature;
- indication that the parts are in contact after completion;
- indication that the weld has been achieved after completion;
- indication that the weld quality and strength are satisfactory.

Monitoring methods can give information for most of these points with varying degrees of confidence; however, it must be noted that complete quality and weld strength assurance can only be achieved with destructive testing.

Monitoring of other polymer-joining methods is generally carried out by monitoring process parameters, such as energy utilised and displacement. These can also be applied with laser welding, but the process is also well suited to the use of optical methods, such as infrared thermography. This, and other optical methods, are summarised in Table 13.4.[16]

13.9 Applications

Typical medical applications that have been considered or put into production are summarised below.

13.9.1 Microfluidic devices and microelectromechnical systems (MEMS)

Laser welding procedures for microfluidic devices have been developed and described in detail.[17,18] Smaller-scale biological analysis or chemical micro-reactors (e.g. 50 × 25 mm platforms) are being developed in plastics so that smaller samples can be used or sample processing can be carried out more cheaply. Typically these have been made of glass with small fluid channels (~100 μm wide), and sealed with adhesives. In many applications there is a drive to mass produce the units and hence a need for lower-cost

© Woodhead Publishing Limited, 2013

Table 13.4 Summary of the features of the optical monitoring methods

Monitoring method	Suitable for	Advantages	Limitations	Availability
Visible light imaging	Viewing the weld during and after the welding process. For both absorber resin and coating methods with IR and carbon-black absorbers.	Easy to set-up and use. Indicates weld region where the two joint surfaces have merged.	Only suitable for transparent and translucent upper materials.	Off-the-shelf components.
Infrared thermography	Temperature measurement and heating control during the welding process. For IR and carbon-black resin based systems. Care needed in use with IR absorber coatings.	Provides rapid temperature reading of use in control of the laser power in real time.	Difficult to use with low-emissivity materials and where upper material transmission is poor.	Available at relatively low cost.
Infrared imaging	Verifying location of absorber coating before and after welding, showing where heating has occurred. Also gives image of heated zones just after welding.	Proven laboratory technique suitable for checking coatings on parts before welding and the extent of the weld afterwards.	Interference from the laser wavelength if used at the time of welding. Not useful for weld checking of absorber filled resins after welding.	Might also be used at the time of welding with further development.
Spectrometry	Measuring the coating absorption before and after the weld, and potentially during the weld. Verification of an intimate surface connection.	Checks position and concentration of the coating before welding and that remaining after welding.	Difficult method to use at the time of welding. Not useful for weld checking of absorber filled resins after welding.	Might also be used at the time of welding with further development.

© Woodhead Publishing Limited, 2013

materials and manufacturing procedures. Use of plastics is being considered widely and joining methods are needed to provide the precision, reproducibility and speed for mass production. Laser welding is well suited to meet these challenges and can be used to seal round the channels or round electronic connections or devices. Different processing options have been suggested for the manufacture of micro devices. These include using line beam as a curtain of energy over the whole part either with or without a mask, or by scanning a small spot source around individual channels. Both can provide rapid manufacture with high quality and reliability of sealing and in particular without damage to the channels in the units as a result of the welding process. The two methods of processing can be applied to different application areas or product designs.

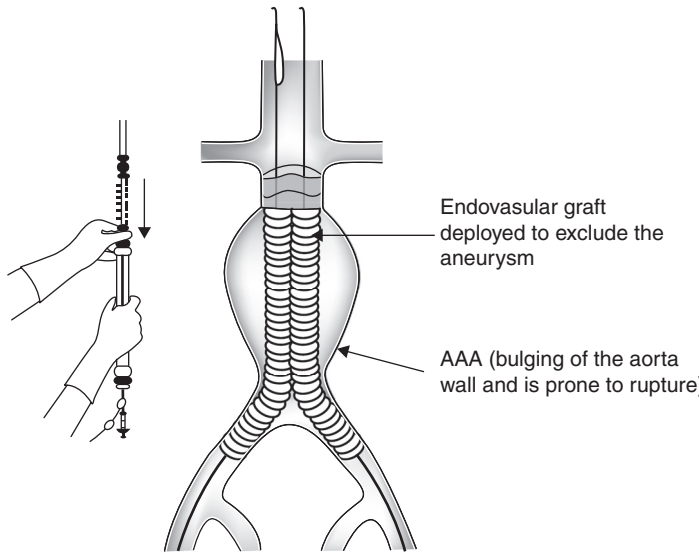
13.9.2 Catheters and small-diameter tubing

Butt joints between tube ends, lap joints between tubes of different diameters, for tip attachments and for balloon sealing and longitudinal tube welding have all been demonstrated using laser welding on a range of small-diameter tubes.[19] A balloon catheter is composed of a polymer balloon that is attached to a polymer shaft at two points called the distal and proximal bonds. The bonds have been conventionally made using cyanoacrylate or UV curing adhesive; however, with performance requirements of bond strength, flexibility, profile and manufacturing costs these bonds are increasingly being made by welding using laser, RF and Hot Jaw methods. Laser welding has typically been carried out using a CO_2 laser to provide direct heating in combination with shrink polymer tubing to support the materials. The position and volume of melting can be controlled using rotating supports, optical scanning of the laser, and control of the temperature and time of heating. It is possible to shape the tip and balloon overlap regions using this processing. More recently, alternative techniques using selective laser absorbers and shorter wavelength diode and fibre lasers have been developed and applied to catheters and tubing. An example of a longitudinal seam weld is shown in Plate VIII (see Plate VIII between pages 300 and 301). In this case an infrared absorbent coating was applied along the edge surfaces to be joined, and a laser beam much larger than the joint region was directed over the whole joint region, providing selective heating only where the laser and the absorber coincided at the joint.

13.9.3 Textiles – vascular graft

As already discussed, laser processing can be used to join textiles. This procedure has been applied in the joining of vascular grafts, where nitinol stent

© Woodhead Publishing Limited, 2013



13.9 Schematic illustration of the AAA along with the Anaconda endovascular device manufactured by Vascutek Ltd. (Picture courtesy of Vascutek Ltd.)

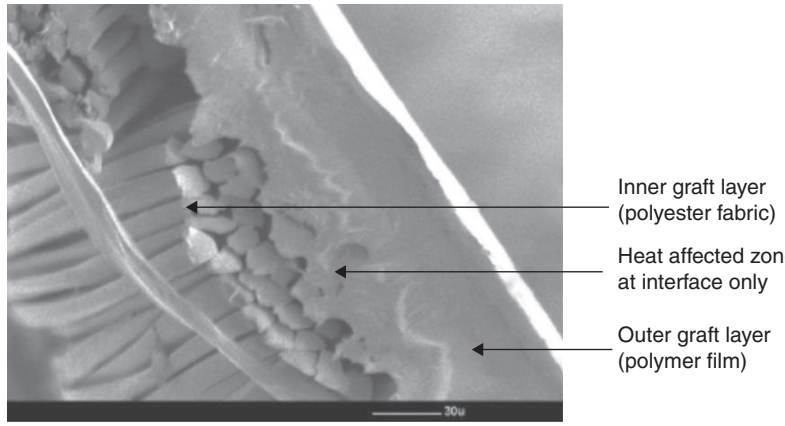
wire rings must be attached to a polyester fabric tube to hold the tube open. An abdominal aortic aneurysm (AAA) is a type of cardiovascular disease, a life-threatening condition that occurs when a section of the abdominal aorta, the body's main circulatory vessel, weakens and bulges outwards, as shown in Fig. 13.9, to form a fragile, balloon-like swelling which is prone to rupture.

Currently, weaving is used to produce the textile graft material, and hand-sewing is used to add the Nitinol ring-stents to the graft, which is very complex and highly labour intensive with quality dependent on the operator. Some of the joining techniques that have been considered in place of manual stitching are listed below:

- automated sewing machines;
- adhesive bonding;
- laser welding (Clearweld process);
- ultrasonic welding;
- hot-air welding.

After a series of preliminary feasibility trials, laser welding showed potential as a novel, alternative manufacturing technique to assemble the stent-grafts.

© Woodhead Publishing Limited, 2013



13.10 Cross-sectional view of a laser weld between polyester fabric and polyester film.

The laser-welding process consists mainly of three stages:

(i) application of Clearweld laser absorber dye at the interface of the two materials being welded;
(ii) assembly of the seam and application of clamping pressure;
(iii) irradiation of the seam with a near infrared laser (940 nm) to melt the material where the absorber has been applied and create a permanent weld at the interface between the two materials being joined.

The main purpose of sewing the Nitinol ring-stents to the graft fabric is to hold it securely in place to keep the graft fabric tube open at all times. Using the laser-welding technique, this is achieved by introducing an outer film layer and welding it to the inner polyester graft fabric thereby sandwiching the rings in between the two layers and securely holding it in place. The heat-affected zone generated during the laser-welding process is localised and restricted to the interface between the two layers (see Fig. 13.10) and hence the Nitinol ring-stents are not affected by the heat generated. A very thin layer of polymer is melted in each graft layer and the application of clamping pressure brings the melted fibres in contact. The clamping pressure is maintained as the melted fibres cool and solidifies to produce a permanent weld.

Laser welding using polyester fabric on polymer film configuration proved to be ideal to provide some fibres melt into the film but not through the full thickness. During tensile tests, most of the samples failed in the parent material rather than at weld location or along edge of the weld, indicating

© Woodhead Publishing Limited, 2013

a strong weld. Furthermore, this material combination resulted in minimal bulk (thickness) at the joint location and hence was suitable for use in the final-product configuration.

It is clear as a result of extensive feasibility studies that laser welding (using the Clearweld process) could potentially replace hand-sewing as it offers many functional advantages over conventional joining techniques, thereby reducing production times, costs and improving the quality and durability of the products.[20]

Laser welding has also been considered for other medical-textiles applications such as seam sealing of gowns, manufacture of dressings and for making sealed seams in hospital furniture reducing the chance of transferred infection by enabling greater cleanliness around the seams.

13.9.4 Sealed bags and inflatable devices

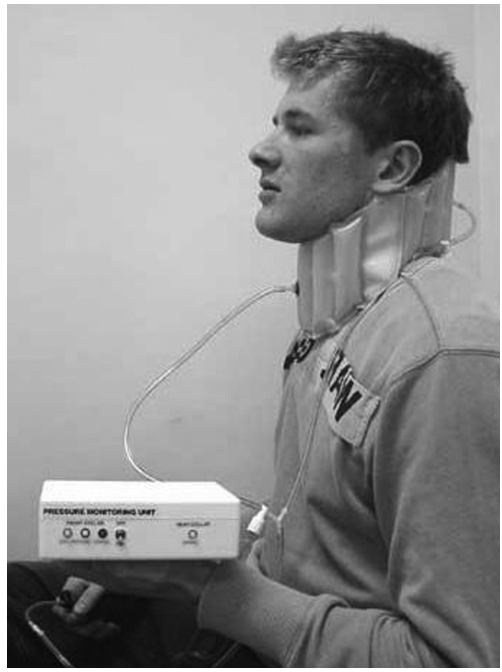
Continuous seam sealing using laser welding has been applied to thin films to create products that can be inflated or used as containers. Examples include an inflatable neck brace and ostomy bags. More detail about the neck-brace application is provided below[10] and serves to demonstrate application to inflatable devices.

The Royal National Hospital for Rheumatic Disease (RNHRD) in Bath, UK, has developed the concept of an inflatable brace for the immobilisation of neck injuries. This can be inflated to a high pressure when a high level of support is required, for example when the patient is travelling. The pressure can be reduced when greater mobility is required, for example while eating. The material selected for the brace was Hytrel®, a thermoplastic polyester elastomer from DuPont™. For simplicity, two sheets were welded together, forming a number of interconnected inflatable chambers. The brace could be customised for each patient. This steered the choice of welding process towards laser welding, using equipment that could be rapidly programmed to produce different sizes tailored to individual patient measurements. A moulded lug for inflation was welded directly to the Hytrel® sheet. The processing used a diode-laser system mounted above a two-axis CNC manipulating table. The profile of the welds to be made were defined by the CNC table, and could easily be adjusted. Prototype parts have been successfully tested, and one is shown in Fig. 13.11.

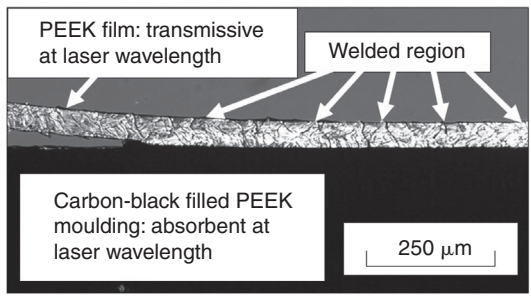
13.9.5 Polyetheretherketone (PEEK) film and implants

Polyetheretherketone is an engineering polymer with high strength and stability in harsh chemical and high-temperature environments. It also has a high wear resistance, and low coefficient of friction. It has a high melting

© Woodhead Publishing Limited, 2013



13.11 Prototype neck brace undergoing testing. (Courtesy of RNHRD.)

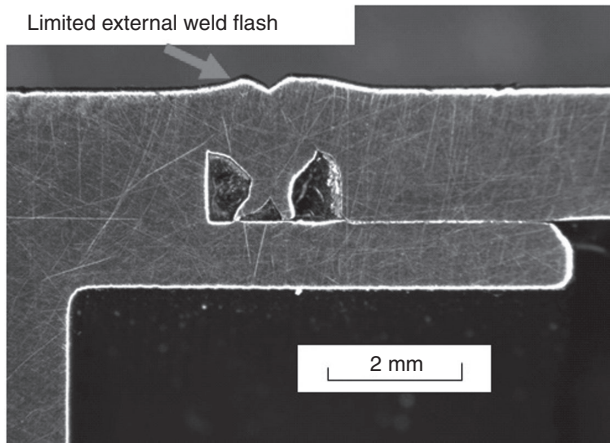


13.12 Transmission laser welding of natural PEEK film to carbon pigmented moulded material.

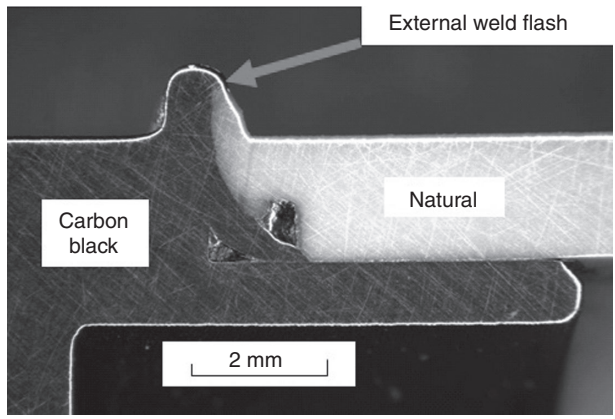
point of 343°C and typically a highly crystalline structure that limits laser transmission to approximately 1 mm in thickness. PEEK-OPTIMA®, supplied by Invibio®, is a medical grade for use in long-term implanted medical devices, with potential for packaging of electronic components. When assembling such components it is necessary to prepare hermetic joints.

There is therefore considerable interest in the use of welding processes for part assembly. Laser processes are suited to welding PEEK in film

© Woodhead Publishing Limited, 2013



13.13 Cross-section of direct laser weld between two carbon-black filled parts.



13.14 Cross-section of laser weld between carbon-black filled and natural parts.

and thin moulded forms (< 1 mm) using transmission laser welding (Fig. 13.12). For thicker PEEK products, direct laser welding can be used that does not rely on transmission of the laser through the highly crystalline polymer.

Direct laser welding has been demonstrated for sealing of cylindrical test cylinders, 24 mm in diameter, 16 mm tall, and with a wall thickness of 3 mm. Equipment was designed to spin the part underneath a diode laser to provide simultaneous heating of the circumference of the joint. A WeldControl system was used to monitor the weld temperature and provide feedback to

© Woodhead Publishing Limited, 2013

adjust the laser power and maintain the weld temperature at the required level just above the melting point of the plastic. Excellent welds were produced in black to black and black to natural samples. The weld time in each case was approximately 10 s. Figures 13.13 and 13.14 show micrographs of cross-sections through the welds. A bubble test showed good hermeticity in the welds.

13.10 References

1. Jones, I. A. and Taylor, N. S. High speed welding of plastics using lasers. ANTEC 1994, conference proceedings – Society of Plastics Engineers, San Francisco, May 1994.
2. Kurusaki, Y., Matayoshi, T. and Sato, K. Overlap welding of thermoplastic parts without causing surface damage by using a CO_2 laser. ANTEC 2003, conference proceedings – Society of Plastics Engineers, Nashville, May 2003.
3. Herfurth, H., Ehlers, B., Heinemann, S. and Haensch, D. New approaches in plastic welding with diode lasers. Laser Materials Processing. ICALEO '99, conference proceedings, San Diego, November 1999.
4. Jones, I. A., Taylor, N. S., Sallavanti, R. and Griffiths, J. Use of infrared dyes for transmission laser welding of plastics. ANTEC 2000, conference proceedings – Society of Plastics Engineers, Orlando, May 2000.
5. Kennish, Y. C., Shercliffe, H. R. and McGrath, G. C. Heat flow model for laser welding of polymers. ANTEC 2002, conference proceedings – Society of Plastics Engineers, San Francisco, May 2002.
6. Grewell, D. and Benatar, A. Modelling heat flow for a moving heat source to describe scan micro-laser welding. ANTEC 2003, conference proceedings – Society of Plastics Engineers, Nashville, May 2003.
7. Abed, S., Knapp, W. Ghorbel, E., Agrebi, K. and Laurens, P. Thermal modelling of the laser welding of polypropylene. Lasers in Manufacturing 2003, proceedings of 2nd International WLT Conference, Munich, June 2003.
8. Jones, I. A. and Olden, E. A thermal model for transmission laser welding of thermoplastic polymer, TWI Members report 708/2000, July 2000.
9. Klein, R. and McGrath, G. Creating transparent laser weldings on thermoplastic components. Joining Plastics 2006, conference proceedings, London, April 2006.
10. Warwick, C. M. and Gordon, M. Application studies using through-transmission laser welding of polymers. Proc. Joining Plastics 2006, 25–26 April 2006, NPL, London.
11. Caldwell, S. and Rooney, P. Design flexibility in waveguides and lightpipes for TTIr plastics welding. ANTEC 2004, conference proceedings – Society of Plastics Engineers, Chicago, May 2004.
12. www.leister.com.
13. Jones, I. A. Improving productivity and quality with laser seaming of fabrics. *Technical Textiles International*, p. 35, May 2005.
14. Patil, A., Jones, I., Ashton, T. and Tavakoli, M. Investigation into novel joining techniques for rapid and automated manufacturing of a new generation

© Woodhead Publishing Limited, 2013

of endovascular grafts. Proceedings of Health Technologies KTN/University of Brighton Annual Conference, 3 April 2008.
15. Kirkland, T. R. Practical joint designs for laser welding of thermoplastics. ANTEC 2004, conference proceedings – Society of Plastics Engineers, Chicago, May 2004.
16. Jones, I. A. and Rudlin, J. Process monitoring methods in laser welding of plastics. Joining Plastics 2006, conference proceedings, London, April 2006.
17. Jones, I. A. and Loyo-Maldonado, V. Comparison of laser welding methods for microfluidic devices, Joining Plastics 2010 – 2nd DVS/WJS Conference, Dusseldorf, 2 November 2010.
18. Chen, J.-W. and Zykbo, J. M. Diode laser bonding of planar microfluidic devices, MOEMS, bioMEMS, diagnostic chips and microarrays. Proc. SPIE 5718, pp. 92–98, 2005.
19. Flanagan, A. J. Laser welding of balloon catheters, Proc. SPIE 4876, p. 517, 2003.
20. Patil, A., Jones, I. and Ashton, T. New manufacturing methods for vascular grafts using laser welding and laser cutting techniques, Joining Plastics 2010 – 2nd DVS/WJS Conference, Dusseldorf, November 2010.

© Woodhead Publishing Limited, 2013

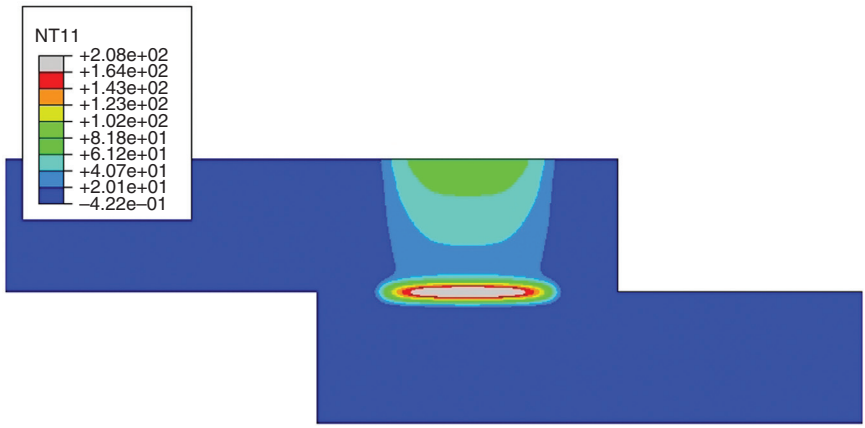


Plate VII (Chapter 13) Output from a finite element thermal model for transmission laser welding of plastics. The heating zone is highly localised to the joint interface.

© Woodhead Publishing Limited, 2013

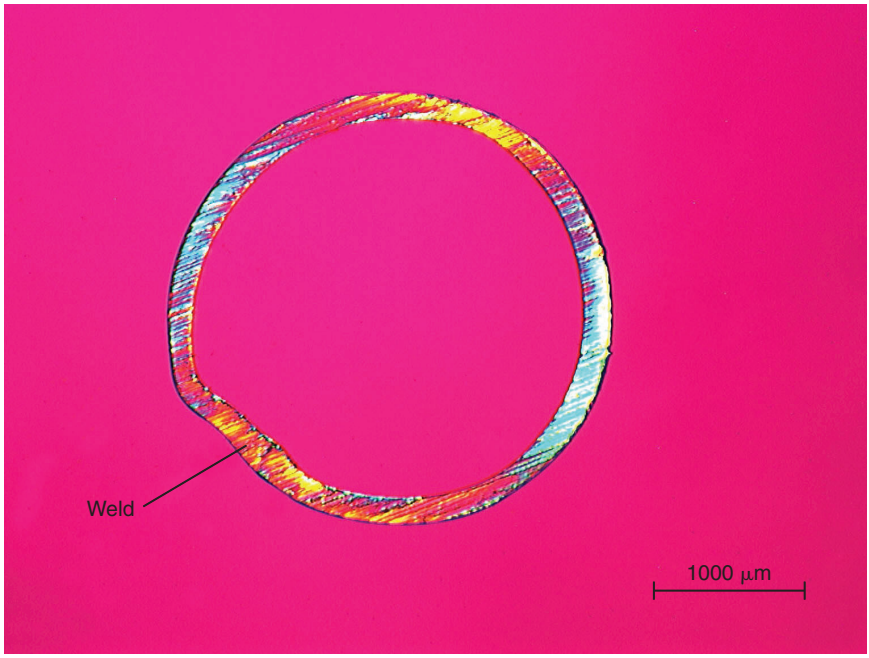


Plate VIII (Chapter 13) Longitudinal seam welding using diode laser in 2 mm diameter tubing.

© Woodhead Publishing Limited, 2013

14

Bonding strategies and adhesives for joining medical device components

K. CHAFFIN, C. TAYLOR and
T. GRAILER, Medtronic, Inc., USA

DOI: 10.1533/9780857096425.3.370

Abstract: Implanted medical devices rely on many different and complex joints between dissimilar materials. Adhesives provide one solution for creating such joints. While long-term implants have the advantage of being in a constant-temperature environment, these adhesive joints need to meet the additional challenges of complex loading conditions and ever increasing device-lifetime requirements. The principles of joint design, namely avoiding peel and cleavage-loading conditions, must be scaled down to meet the ever decreasing device sizes. Because the long-term reliability of an adhesive joint under wet fatigue loading conditions generally scales with the adhesion strength between the adhesive and the substrate, surface modification strategies are often employed to improve joint strengths. Any primers or adhesives must meet the biocompatibility requirements which in large part address leachable toxicity. As a result, the use of many fast- or light-cure adhesives is very limited in long-term implant applications. As such, the industry is constrained to relatively few adhesive chemistry options. In this chapter, we review joint design strategies, present methods to test the adhesive strength, discuss methods for improving adhesion strength and provide lessons learned from examples of joints.

Key words: Adhesion, bonding mechanisms, surface treatments, joint design, adhesion testing, adhesives.

14.1 Introduction

In many respects joining polymers in medical devices is similar to bonding in other applications such as automotive, aerospace, and construction industries. Obvious considerations are made for regulatory-agency requirements, body-contacting applications, and necessary durability testing. Generally,

© Woodhead Publishing Limited, 2013

dissimilar materials can be joined through many different methods. Joints can be mechanical, riveted, screwed and clamped; they can be welded with temperature and pressure; they can be formed by applying an adhesive to the interface, or they can be solvent bonded. In each case, joint design is the single most important factor in determining the overall strength of the joint. When using an adhesive, wettability and intimate contact are required to harness both mechanical and van der Waals interactions that maximize the bond strength. Surface treatments, such as gas-plasma modifications and primer coatings, are used to engineer the surface energetics of the substrates and to, potentially, create covalent bonds at the adhesive interface. Solvent-bonding techniques require thermodynamic compatibility between the two substrates and the selected solvent. Testing the strength of the adhesive bond and predicting durability over the life of a medical device is critical to assessing the performance of both the adhesive and the substrate surface treatment.

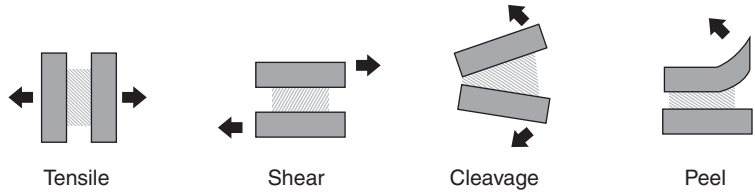
Adhesives have many advantages over other methods of bonding. They offer a more uniform stress distribution across the joint and improve fatigue performance. Adhesives are also compatible with complex geometries and joint designs. In many cases, adhesives are used because of their ease of assembly, particularly pressure sensitive adhesives (PSAs). Furthermore, adhesives are used because they can electrically insulate, dampen, seal and enable the bonding of heat-sensitive materials. Joints designed with an adhesive bond can be stiffer than those made with other joining technologies. The integrity of an adhesive joint is critically dependent on the surface preparation. Further cautions for designing with adhesives include possible toxicity of adhesive components and partially cured adhesive (particularly UV initiators in fast-cure chemistries), slow processing time, a lack of non-destructive quality control, difficulty reworking a joint, and a tendency for adhesive joints to fail with excessive thermal cycling.

In this chapter we will discuss how to design an adhesive joint, how to engineer the adhesive–substrate interface for maximizing bond strength and durability, and how to test an adhesive joint to predict its reliability for use in a medical device. Furthermore, the adhesive classes available for use in the medical-device industry will be reviewed.

14.2 Designing a joint with adhesive

The key design rule for an adhesive joint is to eliminate peel or cleavage forces. Adhesives perform poorly under peel and cleavage-loading conditions. To prove this to yourself, take a piece of tape and adhere it to a flat surface, with one end sticking off the edge of the surface. Pull the end back towards the end that is adhered to the surface. By doing this, you are putting the adhesive in peel or, more precisely, a 180° peel geometry. It is easy

© Woodhead Publishing Limited, 2013



14.1 Loading conditions for an adhesive joint. The substrate is shown as solid, the adhesive is represented by the patterned area, and the loads are shown with the arrows.

to remove from the surface. Adhesive joints perform best in shear-loading conditions. To demonstrate, re-adhere the tape, or start with a new piece. Pull the free end straight back toward you, keeping the force parallel to the surface. Now you are putting a shear load on the adhesive bond. You can likely apply a force large enough to break the substrate (tape backing). This is a simple demonstration that is intended to reinforce the point that joint design is the single most important factor in determining the joint strength.

There are four basic types of loading conditions for a joint.[1] These are shown in Fig. 14.1. Because use conditions vary, most joints experience multiple loading conditions and environments. Therefore, it is critical to understand the most severe loads and design the joint to minimize peel and cleavage forces.

Tensile loading occurs when the plane of the adhesive is oriented perpendicular to opposing forces. Failure typically occurs when a crack or defect at the highly stressed outside edge propagates. In practice, designing joints to be in pure tensile is challenging. First, rarely are loading conditions known to be perfectly parallel. Any asymmetry in the loading conditions puts the joint into cleavage mode, resulting in lower than anticipated failure strengths as compared with joints tested in tensile-mode conditions. Second, it is difficult to control the bondline thickness. Any variability in the bondline thickness will put the joint into cleavage, reducing the failure strength of the bond. The tensile strength is measured as ultimate failure strength per bonded area (load/area).

Shear loading occurs when the loading forces are acting parallel to the plane of the adhesive. Joints are generally strongest when in shear because the forces are distributed across the entire plane of adhesive. Failure occurs when a crack or defect at the highly stressed leading or trailing edge propagates. The stress on the edges can be reduced, thus increasing the efficiency of the bond by tapering the thickness of the substrate and the leading and trailing edges.[2] The strength of the adhesive bond scales with the bonded area. The shear strength is measured as ultimate failure strength per bonded area (load/area). There is an optimum bondline thickness that should be

© Woodhead Publishing Limited, 2013

evaluated with the adhesive and substrate combination being considered.[3] Too little adhesive and the bondline can become adhesive 'starved' and the result can be low joint strength. Too thick of a bondline is described as 'adhesive rich'. A thick bondline can be subject to plane strain conditions and any cohesive weakness of the adhesive layer can dominate the overall joint strength. The optimum bondline thickness will be somewhere between the adhesive starved and the adhesive rich regimes and will maximize joint strength. The bondline thickness is typically controlled through the use of molded-in standoffs in the joint. For test-level specimens, glass beads or fibers are often used to control the bondline thickness.

Peel and cleavages forces are always undesirable.[4] This loading situation occurs when the applied load acts to pry the adherends apart. The peel condition occurs when one or both of the substrates or adherends is flexible. Cleavage occurs when the substrates or adherends are rigid. Joints loaded in peel/cleavage offer considerably lower strengths than joints loaded in shear. This is because in peel/cleavage the load is concentrated on the small leading edge of the joint. The units used for recording the strength of this type of bond are indicative of this concentrated load. Rather than reporting the joint strength in load per bonded area as is done for tensile or shear conditions (load/area), these joints have strength reported as load per width of bond (load/width).

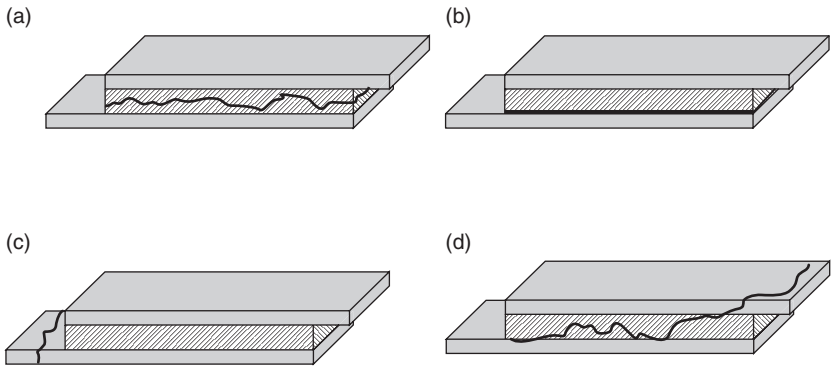
Joint design is the single most important factor in determining the overall bond strength. Guidelines for joint design include:

- Design the joint such that operating loads stress the adhesive in shear.
- Avoid peel and cleavage-loading conditions.
- Distribute loads uniformly over the bonded area.

14.2.1 Assessing how adhesive joints fail

It is important to understand how the joint has failed during service before deciding a course for corrective action. The mode of failure will reveal the weakest link in the system and dictate the course of action for an effective redesign. Adhesive joints can fail in four main ways as shown in Fig. 14.2. Joints can fail cohesively within the adhesive. This failure mode occurs when the crack propagates through the bulk of the adhesive. Joints can fail adhesively. This failure mode occurs when a crack propagates along the adhesive bond interface, between the adhesive and the substrate. Joints can fail cohesively within the substrate or the adherend. Finally, joints can fail in a mixed mode, where the crack wanders, propagating through all three areas, the adhesive, the interface and the substrate. A mixed-mode failure is most

© Woodhead Publishing Limited, 2013



14.2 When the crack propagates through the adhesive layer (a), the failure mode is cohesive. When the crack propagates at the interface between the adhesive and the substrate (b), the failure mode is adhesive. When the crack propagates through the substrate or adherend (c), the failure is cohesive within the substrate. When the crack is not well controlled (d), mixed mode failure occurs. Mixed mode failures often result from complex loading conditions.

often a result of complex loading conditions. Generally a substrate or adherent failure mode is considered desirable, as this indicates that the adhesive joint is stronger than anything else in the system and joint design can be considered successful. Be careful making such assumptions. The strength of an adhesive bond is extremely rate sensitive. Bond strengths must be tested in a manner that simulates both the load distribution and the failure mode of the actual use situation. For example, if a joint in a medical device is subjected to *in vivo* wet cyclic loading conditions, producing adhesive failure at the interface between the adhesive and the substrate, then testing that same joint, wet or dry, in a manner that produces cohesive failure (failure within the adhesive layer) teaches nothing about the joint strength in the use condition. That is, in the use situation the failure is between the adhesive and the substrate, while the simulated test conditions result in a crack propagating through the adhesive itself. The different path of crack propagation makes it impossible to compare the *in vivo* situation with the *in vitro* test situation.

In the medical-device world, the choices for substrates and adhesives are relatively limited. When selecting an adhesive–substrate combination, it is desirable to create model test systems that isolate the loads to a single condition (see ASTM standards). These simplified joints allow one to apply uniform loading conditions across the joint and to assess the weakest link in the system. In these model systems it is quick and easy to assess the available combinations of substrates and adherents against the primary loading conditions to select the optimal joint materials.

© Woodhead Publishing Limited, 2013

14.2.2 Measuring the work of adhesion (G_0)

Adhesive forces are the forces that hold two materials together at their surfaces. Cohesive forces are the forces that hold two adjacent molecules of a single material together. The work of adhesion is defined as the energy required to move two surfaces out of contact. If this is measured as force verses displacement, the work of adhesion is the integrated area under the curve. However, if not performed carefully, these force verses displacement curves are more representative of the practical adhesion than the true work of adhesion.[5] Practical adhesion refers to the total amount of energy measured when the joint is destroyed. Why does the work of adhesion differ from the practical adhesion? Because when a joint is pulled, often many other deformation forces are measured in addition to the interfacial deformation force. Equation [14.1] describes the relationship between the practical adhesion, the work of adhesion, and those additional deformation forces.[6]

$$\text{Practical adhesion } (G) = \text{work of adhesion } (G_0) + \text{work of other deformations} \quad [14.1]$$

Because most adhesives are polymers that have a strain-rate dependence due to their viscoelastic nature, the rate of testing must be considered when trying to isolate the work of adhesion. Therefore Equation [14.1] can be re-written as follows:

$$G = G_0\left(1 + f\left(\frac{1}{\text{temperature}}, \text{rate}\right)\right) \quad [14.2]$$

The first term in the equation represents the work of adhesion and the second term represents the work of mechanical deformation and/or damage. The work of adhesion will be isolated when the rate of testing approaches zero. Likewise, increasing the temperature will minimize the contribution of forces of deformation for a polymeric substrate. A thought experiment to demonstrate this point is to pull a rubber band between your fingers. The deformation of the rubber band results in a measurable force. Now imagine the rubber band is bonded to your table top. Pull up on the loop and the rubber band deforms as the bond to the table top releases. When measuring the total energy required to delaminate the rubber band, what portion of the total energy is due to stretching the rubber band, and what portion is the energy required to delaminate the bond? Which force is dominating the measurement? By minimizing

© Woodhead Publishing Limited, 2013



14.3 An acetoxy cured silicone medical adhesive is used to seal the interface between the titanium device and the polyurethane connector module. The arrow indicates the adhesive joint that is filled with medical adhesive.

the energy that the rubber band contributes to the total energy measures, one can isolate the energy required to pull the bond from the table; that is the work of adhesion (G_0).

One of the most common adhesives in the long-term implanted medical devices is silicone medical adhesive. Two common substrates for these long-term implants are both polyurethane and titanium. Many pacemakers, defibrillators and neurological stimulators are designed using medical adhesive to seal the joint between the polyurethane connector module and the titanium can as shown in Fig. 14.3. The silicone medical adhesive must maintain bonding to both polyurethane and titanium for the life of the device, which can be as long as 15–20 years for systems with rechargeable batteries. Insulated electrical leads that carry the energy from the device to the heart/spine can place cleavage-loading conditions on the joint. For this reason, 'pin and strap' technology is used to secure the connector module mechanically to the can. 'Pin and strap' is a mechanical fixation strategy. The adhesive is supplemental, providing a seal, and is not load bearing due to the poor performance of adhesive joints in cleavage, a poor loading condition for adhesive alone.

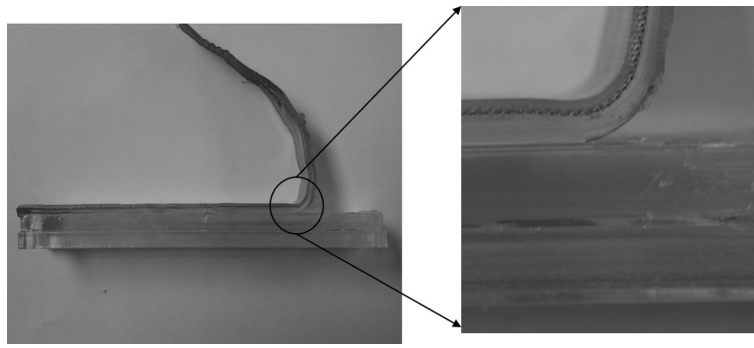
© Woodhead Publishing Limited, 2013

Due to the extreme *in vivo* conditions (cyclic fatigue at 1 Hz) and the expanding implant times, improvements in the strength of this bond are always desired. To test the strength of the medical adhesive bond to each of the substrates, the silicone medical adhesive is applied to the surface of the polyurethane or the titanium in separate experiments. Because this bond is most susceptible to an adhesive failure mode, one way to improve the bond strength is to apply a primer to the interface between the silicone medical adhesive and the substrate (polyurethane or titanium). To evaluate a series of possible primers, it is important to measure the work on adhesion—the energy required to separate the two interfaces in contact. To measure the work of adhesion, the bond must be pulled in a manner that allows the crack to run along the interface. We can use the poor performance of joints in the peel-loading condition to our advantage in such evaluation tests were we to want to understand the interfacial energy of adhesion (i.e., the adhesion force between the substrate and the adhesive).

Here is a thought experiment. Suppose you want to evaluate three different primer systems against a control joint having no primer to understand if there is room to improve the interfacial bond strength. You place the device shown in Fig. 14.3 in the clamps of an Instron and measure the force as a function of grip displacement, loading the interface in tensile. The control joint failed at a lower energy than the primer joints, but there was no difference in measured failure energy for the three primer systems. You examine the failure modes. The control failed adhesively – at the interface. For all three primer systems, there is adhesive on both sides of the interface and you conclude that the joint failed cohesively within the thickness of the adhesive. Because the cohesive strength of the adhesive was not variable in the primer experiment, the result was no measured difference in the energy of bond failure for the three primer samples. How does one evaluate which primer is most effective? To evaluate the primer the crack must propagate through the interface where the primer was applied. Putting the joint in peel gives the best chance of creating an adhesive failure mode. Think back to the tape adhered to the table experiment. The joint is weakest in peel; therefore, it is desirable to put an adhesive in peel when trying to evaluate the strength of the interface. Furthermore, to measure G_0; all deformation forces must be minimized.

Figure 14.4 shows the sample configuration for measuring the work of adhesion between the flexible silicone medical adhesive and a rigid substrate like polyurethane, 75D durometer. The flexible wire mesh imbedded within the silicone medical adhesive minimizes the forces generated by stretching the bulk of the adhesive. The crack can be initiated and the energy required to propagate a peel crack in the medical adhesive at the polyurethane interface can be measured.

© Woodhead Publishing Limited, 2013



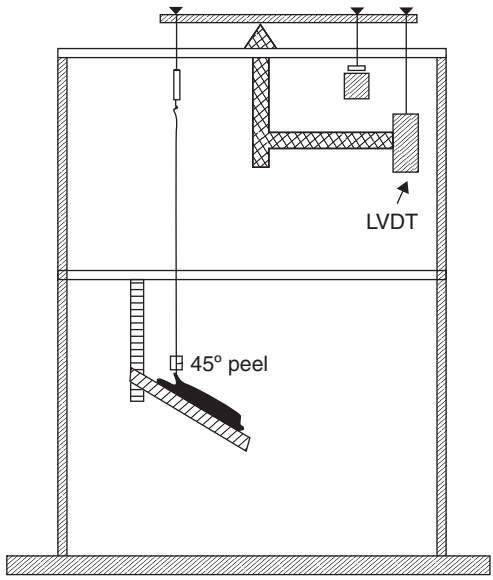
14.4 Sample configuration for measuring G_0 for a flexible silicone medical adhesive bonded to a rigid substrate.

This bond can be loaded into an Adhesion Durability Tester (ADT)[7] to test the bond in peel, under creep (low-strain rate – to minimize extraneous deformation forces), and in water at body temperature. Such conditions give a good correlation to low-strain cyclic loading *in vivo*. That is, bonds that perform well in this test tend to have long *in vivo* durability. The ADT was designed to produce adhesive failures, mimicking the most common failure mode observed *in vivo*. Figure 14.5 shows a schematic of the ADT, where a linear voltage displacement transducer measuring the rate that the crack propagates under the applied load. The adhesive bond is pulled at a 45° peel angle. If the crack propagates along the interface at a slow rate, the work of adhesion is high. If the crack propagates along the interface at a fast rate, the work of adhesion is low.

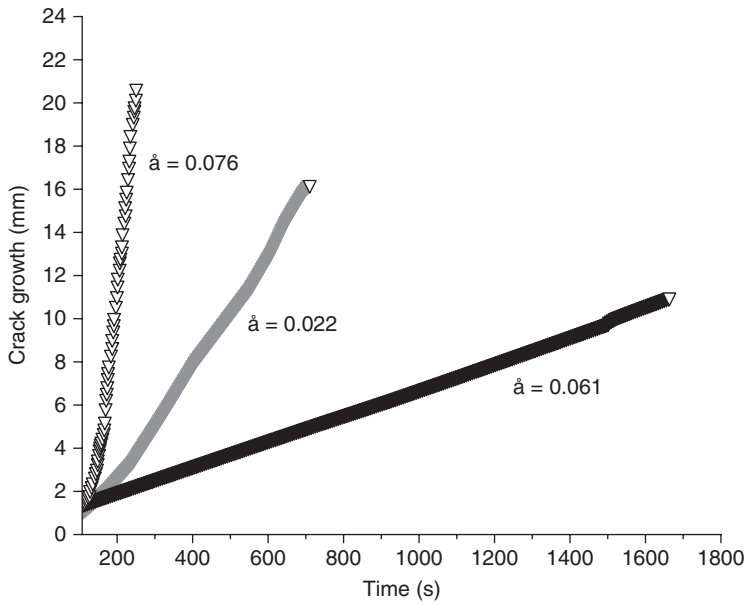
Back to the thought experiment where the three different primers for a medical adhesive interface were evaluated against the control joint that contained no primer. In tensile, all primed bonds failed cohesively while the control joint failed adhesively. Such a test clearly establishes the control joint as inferior to the primed joints, but which of the other primers have the highest work of adhesion, the one that you want to use on your device joint? Loading bonds prepared with each of the primers into the ADT produces the results shown in Fig. 14.6.

The slow rate of testing as well as the weak configuration of peel loading allows the primer systems to be ranked. In this case, the primer system represented by the black line propagates at a lower rate than either of the other primer systems tested under the same conditions. Therefore, the primer system represented in black produced the strongest bond. In all three cases, the bonds had adhesive failure, but they differ by orders of magnitude. This is in contrast to the cohesive failure mode of a traditional stress–strain test, where the cohesive failure mode masked this very large, and potentially critical, difference in the primer systems.

© Woodhead Publishing Limited, 2013



14.5 The schematic of the ADT shows the adhesive bond loaded at a 45° peel load. The sample sits in a water bath that is maintained at 37°C.

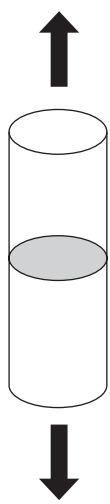


14.6 The ADT apparatus measures the crack growth rate, å, over time. Cracks at low energy interfaces propagate quickly, while cracks at high energy interfaces propagate slowly. This test method allows for differentiation of three primer systems that showed equivalency in a traditional tensile test due to a cohesive failure mode.

© Woodhead Publishing Limited, 2013

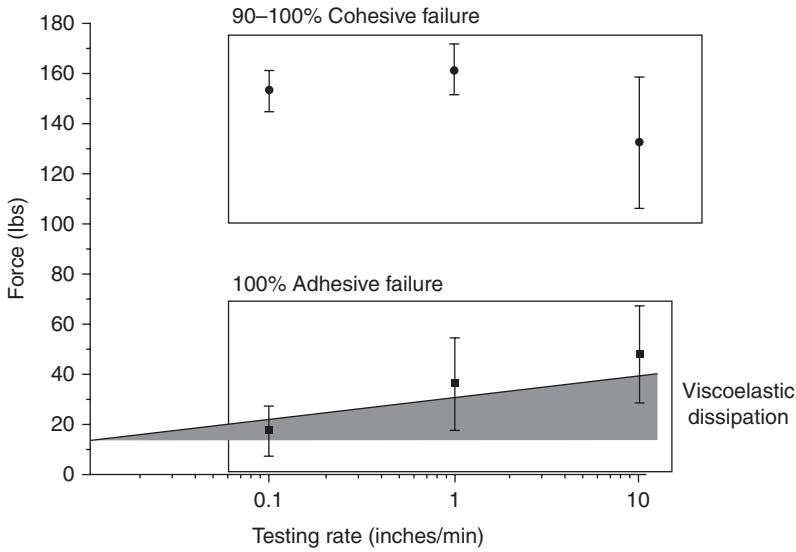
It can be difficult to evaluate different adhesive systems when the cohesive properties of the adhesive are changing. The real challenge is to find common testing conditions that will result in an adhesive failure mode for all the adhesives considered. In the case study below, two space-filling epoxy adhesives were being evaluated for their adhesive strength for a bond with titanium. Because the adhesive is a not flexible at the service conditions, the peel bond configuration could not be used. A tensile loading condition was chosen for the evaluation. Because it is important to measure the adhesive strength against substrates that represent the same mechanical finish as will be used in the device, titanium discs were punched from actual titanium devices. These discs were screened for flatness and cleaned as intended in the manufacturing process. The samples were built as shown in Fig. 14.7, where the adhesive was injected in a disposable cylindrical tube, the titanium disc was placed using an alignment tool to assure a perpendicular alignment, and then more adhesive was injected. The system was cured and the disposable cylindrical form was carefully removed from the test sample, where the test sample comprised the adhesive containing the titanium disc in the center. Finally, any adhesive was removed from the edge of the titanium disc before testing.

Testing was performed on the two epoxy systems as a function of strain rate. The test results are shown in Fig. 14.8. At all strain rates tested, one adhesive always failed cohesively – within the bulk of the adhesive. The



14.7 The tensile specimen used to test the adhesive bond between a stiff epoxy adhesive and a titanium disc. Such a joint design allowed for the epoxy to be evaluated against the actual titanium surface used in the medical devices.

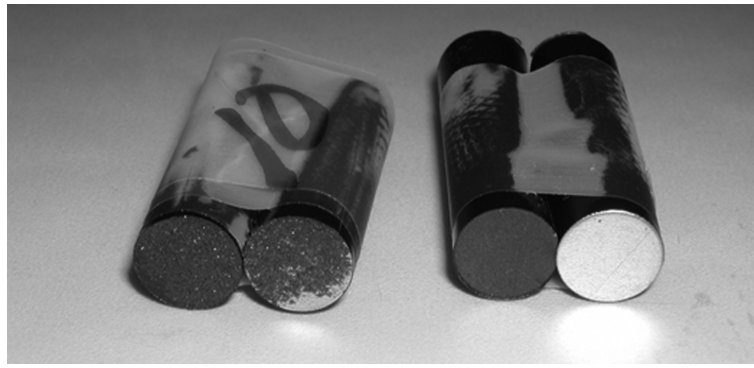
© Woodhead Publishing Limited, 2013



14.8 The force of failure is plotted as a function of testing rate for two epoxy systems bonded to titanium and subjected to tensile loading. One epoxy system failed cohesively and shows very little rate dependence (represented by the circles). The second epoxy, represented by the squares, failed adhesively. The failure load decreased with decreasing test rate. Extrapolation to a testing rate of zero gives G_0 for the bond. The difference between G_0 and the failure load is accounted for by the loads due to viscoelastic dissipation.

other epoxy always failed adhesively, at the titanium interface. The failure modes of the two epoxy systems are shown in Fig. 14.9. Because the failure modes were different, the epoxy systems could not be evaluated comparatively. As described in Equation [14.2], the work of adhesion can be measured when the testing rate goes to zero. Extrapolating to zero rate for the epoxy system that failed adhesively gives a G_0 = 16 lbs. The higher failure forces for the higher rate tests include the forces of the viscoelastic dissipation. The contribution of viscoelastic dissipation is represented by the shaded area in Fig. 14.8. The G_0 was not measured for the system that failed cohesively because the crack did not propagate at the adhesive interface, but within the epoxy itself. New test conditions must be selected to evaluate G_0 for this epoxy system. Slower test rates are required. The invariant load response of this system indicated that the cohesive properties were relatively unchanged within the testing rates explored. That is, the epoxy must be either on the rubbery plateau (above the glass-transition temperature (T_g) for the crosslinked system) or in the glassy regime (below T_g—see Section 14.2.3), as in both of these

© Woodhead Publishing Limited, 2013



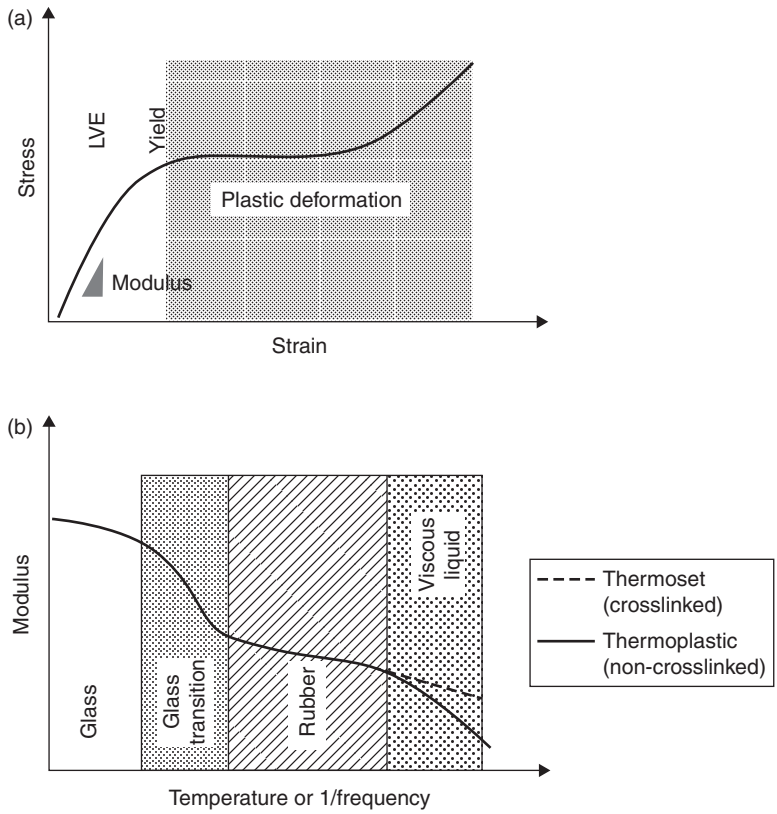
14.9 The sample on the left shows cohesive failure, where epoxy remains on the titanium surface after failure. The sample on the right shows adhesive failure, where the adhesive is cleanly removed from the titanium surface.

regimes the rate dependence is minimized. It is important to understand the viscoelastic properties of the adhesives in the joint being tested, as the rate of the joint test may change the load response of the joint considerably.

14.2.3 Viscoelasticity of polymers and adhesives

Polymers are viscoelastic because they have long chains that are highly entangled with each other.[8] As a consequence, these long chains are not free to move without coordinating their motion with neighboring chains. The result is a time and temperature-dependent response to deformation. This response occurs both in the linear portion and the non-linear portion of the stress–strain curve. This rate effect is nicely demonstrated with Silly Putty®. If you pull Silly Putty® slowly, the chains have time to respond to the applied strain and they will flow by one another, failing cohesively at a relatively low force. At fast deformations, the chains remain entangled with their neighbors, and the applied load results in chain breakage. The failure mode is still cohesive but the failure force is higher than in the low-frequency test. Temperature can be a surrogate for frequency.[9] At high temperatures, the chains have more mobility. Therefore, if strain is kept constant, and the temperature is high, the higher mobility of the chains will allow those chains to undergo coordinated motion and slide by one another, resulting in a low-force response. At cold temperatures, molecular motion is reduced and the mechanical response to the applied strain results in a higher force.

© Woodhead Publishing Limited, 2013



14.10 A typical stress–strain curve for a polymeric adhesive is shown in (a), where, like all polymeric materials, there is a linear portion, the slope of which is the Young's modulus, a yield region, and a plastic deformation region. Because polymeric materials comprise long molecules that require coordinated motion, their response to an applied load is both temperature and frequency dependent. The temperature–frequency relationship of the linear region (LVE) can be characterized by DMA as shown in (b). Polymeric materials can either be a glass, if the temperature of service is below the glass-transition region, or they can be rubbery, if the temperature of service is above the glass-transition temperature.

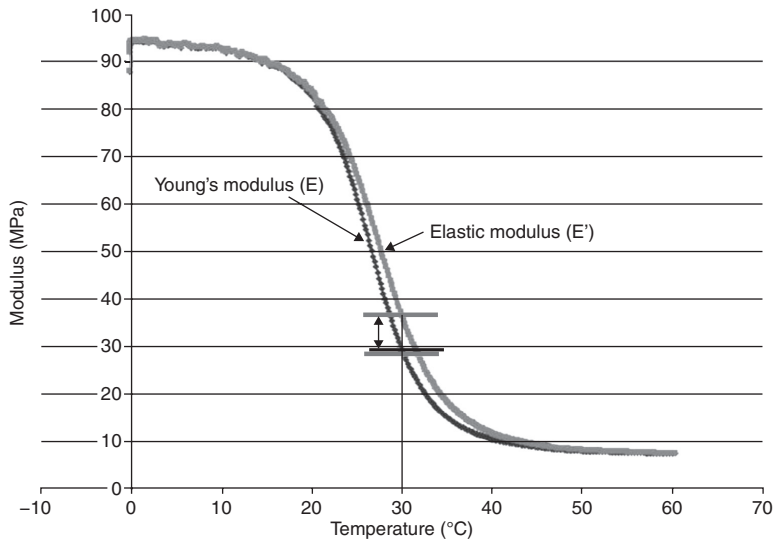
The time- and temperature-dependent response in the linear region of the stress–strain curve (at elongations below the yield point) is referred to as the linear viscoelasticity (LVE) of the polymeric material. A characteristic polymeric stress–strain curve is shown in Fig. 14.10a. The linear regime is highlighted at low strains. This regime is often characterized with dynamic mechanical analysis (DMA) to show how the response changes with either temperature or frequency. The resulting data, shown in Fig. 14.10b, is called

© Woodhead Publishing Limited, 2013

the thermo-mechanical spectrum of the polymer or adhesive. The polymer or adhesive has a glassy region, the glass-transition temperature region, the rubber plateau and for non-crosslinked systems, a terminal flow region. Crosslinked adhesives have a rubber plateau that extends infinitely or until a temperature that results in thermal instability or degradation. This is because the chains are chemically bonded together in crosslinked systems, preventing flow. In other words, there are no temperatures or frequencies that will allow the chains to flow by one another.

Note: for those familiar with DMA, recall that DMA measures the elastic modulus rather than the Young's modulus. For the purpose of this chapter these moduli are used interchangeably. The reason being, that the Young's modulus and the elastic modulus only differ slightly in the transition region. The two moduli are compared in Fig. 14.11.

An understanding of the service conditions with respect to the thermo-mechanical response of the adhesive is critically important to predicting the properties of the adhesive joint. If the service conditions result in the adhesive being in the glassy region, the slope of modulus with respect to either frequency or temperature is shallow. A similar shallow slope exists for adhesives in operating in their rubbery zone. In these regions, the cohesive failure loads will have only slight dependence on temperature or frequency.

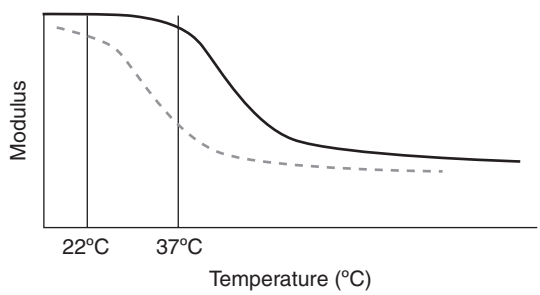


14.11 For practical assessments, the Young's modulus and the elastic modulus can be used interchangeably. The two values differ slightly in the glass transition region.

© Woodhead Publishing Limited, 2013

However, if service conditions put the adhesive in its glass-transition zone, the properties of the joint can change dramatically with changes in testing frequency or temperature. This can make accelerated testing designs problematic.

A crosslinked epoxy is used to adhere the electronic module assembly and the battery to the inside of the titanium shields of an implantable pacemaker. The electronic module assembly and the battery communicate through a series of wires. Flexing of the titanium shields puts fatigue forces on the wire, which can result in fatigue failure of the wire if the load or the number of cycles becomes high. The epoxy has two purposes: to provide stiffness and to provide high adhesion strength. Two different adhesives were considered for the application. Let us do the following thought experiment: We tested the bond stiffness and adhesion strength of the two epoxy systems at room temperature (22°C). The performance of these epoxies was indistinguishable. The thermo-mechanical spectra of these epoxies is shown in Fig. 14.12. Which epoxy will perform the stiffness function at the service conditions of body temperature (37°C)? The epoxy represented by the black line in Fig. 14.12 will be considerably stiffer than the epoxy represented by the dashed line at body temperature. This is the reason that it is important to understand the thermo-mechanical spectrum of the adhesive being considered. Furthermore, testing the adhesive at body temperature becomes critically important when designing a system with a glass transition temperature near the service temperature. Matching the exact temperature or frequency conditions of service becomes less critical when the adhesive system is being used at conditions away from the transition region as the modulus/temperature/frequency relationships are weaker in these regions.



14.12 The thermo-mechanical spectra of two crosslinked epoxy systems evaluated for the attachment of the electronic module assembly and the battery to the titanium pacemaker.

© Woodhead Publishing Limited, 2013

14.2.4 Accelerated testing of adhesive joints

Before designing an accelerated test strategy, one must evaluate how the joint will fail in service.[10] Remember, it is important to match the failure mode of the joint test to that anticipated in service to learn anything about that joint performance in service. *In vivo*, adhesive joints can fail due to excessive loads, in cyclic flex or fatigue loading, due to swelling of the adhesive or substrate, due to thermal shock, or fail through chemical degradation. For the purpose of this chapter, let us assume that we have chosen a biostable adhesive that does not chemically degrade during the timeframe of use. In which case, we have the possibility of mechanical failure at the interface (adhesive) or within the adhesive itself (cohesive) due to overload, fatigue, swelling, or thermal shock. There is also an additional failure possibility, chemical failure at the interface. However, you will learn in the next section that the creation of a chemical bond at the interface is a special case that must be engineered explicitly. Due to the limited material choices for medical devices, there is rarely the material flexibility to engineer chemical interfacial bonds. As a consequence, most bonds are mechanical in nature, not chemical.

Often in the medical-device industry, we refer to ASTM F1980–02, *Standard Guide for Accelerated Aging of Sterile Medical Device Packages*, to design our accelerated tests. This test references the Arrhenius equation, where van 't Hoff's observation is applied, as shown in Equation [14.3]. This principle was established by observing that the reaction rate of rate of gas molecules roughly doubles for every 10°C increase in reaction temperature. This method teaches that a material held at a temperature higher than the service temperature will age via chemical reaction faster than it will at the service temperature. A shorter time at a high temperature will simulate a longer time at the service temperature. Therefore, if a material passes a simulated lifetime age according to the Arrhenius equations and results in a favorable outcome, the polymeric system should survive its anticipated service life.

$$\frac{\text{Time}_{\text{Room temp}}}{\text{Time}_{\text{Accelerated}}} = Q_{10}^{[(T_{\text{acc}} - T_{\text{RT}})/10]} \qquad [14.3]$$

where $\text{Time}_{\text{Accelerated}}$ = time the sample is exposed to achieve a desired shelf time; $\text{Time}_{\text{Room temp}}$ = desired shelf time; Q_{10} = 2, aging factor for a 10°C increase or decrease in temperature (van't Hoff's observation: the rate of chemical reactions double with every 10°C increase in temperature); T_{acc} = accelerated aging temperature (°C); T_{RT} = room/ambient temperature for storage (°C).

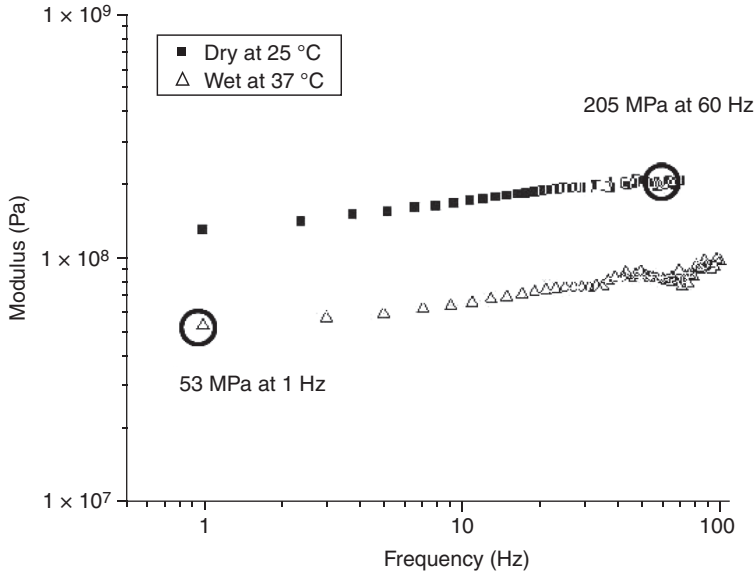
© Woodhead Publishing Limited, 2013

Not so fast for adhesive bonds! The Arrhenius equation is an empirical relationship that was established for the prediction of chemical reactions. Chemical bonds are rarely responsible for the forces holding an interface together. The most common cause of adhesive failure is a stress discontinuity at the interface that results in the propagation of a crack at that interface. The stress discontinuity can result from (i) a modulus discontinuity between the substrate and the adhesive where an applied load (or repeated cyclic load) results in an interfacial stress riser; (ii) preferential swelling of the adhesive or substrate by body fluids that result in expansion of the adhesive or substrate, imparting a stress riser at the interface; and (iii) thermal cycling or shock of a joint comprising materials with different coefficients of thermal expansion.

With this in mind factors that accelerate the decay of an adhesive bond include temperature cycling, constant loading (creep), cyclic loading and humidity/environment. Often the combination of more than one of these factors is substantially more severe than any of the factors alone.[11] When designing an accelerated test strategy for the joint in question, apply the combination of factors that best simulate the anticipated service conditions of the joint. For example, in the automotive industry, joints are accelerated aged by applying a constant load (creep), cycling the joints through a salt solution daily, and storing in a humidity cabinet at elevated temperature and humidity. Time to failure is recorded and the results are compared with real-time testing to establish an acceleration factor. It is clear that this accelerated test was designed with all of the possible environmental assaults incorporated in addition to extreme temperature, humidity and loading conditions to produce an accelerated failure model.

A solvent bond in a polyurethane lead body (long polymeric tubes containing the metallic conductors that carry the energy from the pacemaker to the heart) was tested at accelerated flex fatigue conditions. The joint was testing at extreme curvature and at a fast frequency (60 Hz) to the total number of life cycles anticipated in the actual application. This test was run dry and at room temperature. The actual application would have a flex frequency of about 1 Hz (the rate of a beating heart), would be saturated with blood, and would be at 37°C body temperature. Understanding the thermo-mechanical spectrum of the joint in the two different test conditions gives an appreciation of the extreme nature of the accelerated test. The thermo-mechanical spectrum is shown in Fig. 14.13. The load generated at the solvent bond in the polyurethane lead body was four times greater in the accelerated test (60 Hz, dry, room temperature) than the load expected *in vivo* (1 Hz, wet, body temperature). The higher loads generated at the accelerated conditions will accelerate failure. The acceleration factor must be established with real-time/condition testing to failure.

© Woodhead Publishing Limited, 2013



14.13 The load generated for the joint testing at the accelerated conditions, 60 Hz, dry, at 25°C is four times greater than the load expected *in vivo* (wet, 37°C, 1 Hz). The acceleration factor must be established with real-time/condition data.

14.3 Mechanisms of adhesion

This section will discuss basic mechanisms of adhesion, specifically forces that act across the interface between medical-device components to be bonded or between the adhesive and the substrates. Because these forces act at a molecular or atomic scale across the interface, intimate contact between the adhesive and the substrate is needed in order to benefit from these mechanisms. Practically, these forces can be loosely grouped into several categories: mechanical, intermolecular (van der Waals), and primary (covalent) forces.[12–14] An adhesive bond may rely on more than one mechanism to achieve full bond strength.

Mechanical forces: The mechanical mechanism relies on the adhesive to fill crevices and voids of substrate surfaces to create an interlocking structure. This composite structure ideally has the mechanical strength of the weakest component of the system, therefore, the bulk strength of the substrate or adhesive. Because of this, bonds that rely on mechanical interlocking can be quite strong. This mechanism is the most common and the easiest to implement. Roughening a smooth surface with sandpaper before painting is an example of using mechanical interlocking to improve adhesion.

© Woodhead Publishing Limited, 2013

Two conditions need to be met in order to maximize mechanical interlocking: the substrate surface should be rough and the adhesive must flow into this microscopic topography and 'wet out' the surface. Without intimate contact, voids will form in the adhesive/substrate interphase and the joint strength will be reduced. The concept of wetting of the adhesive on the substrate will be discussed in a later section. In addition to creating texture for mechanical interlocking, roughening the surface also increases the substrate surface area on a microscopic scale. If the adhesive is in intimate contact with the substrate, this allows for more opportunities for primary or intermolecular forces to act across the interface; the joint surface has more area for chemical bonding. Practically, since adhesion is measured as the force required to pull a joint apart per bonded area, increasing surface area on a microscopic scale increases the apparent adhesion.

Intermolecular forces: Intermolecular forces, or van der Waals forces, act between molecules and do not involve the formation of covalent bonds. Electrons are not permanently shared in this type of bond. Therefore, intermolecular forces are relatively weak compared with covalent bonding. Van der Waals forces arise from several different types of interactions of localized areas of charge on molecules (dipoles):

- Electrostatic interactions between permanent dipoles: These dipole–dipole interactions involve the transient attractive forces of two oppositely charged dipoles. Hydrogen bonding within water is a very common example of this. The electronegative oxygen of one H_2O molecule is attracted to the electropositive hydrogen of another H_2O molecule. In hydrogen bonding the dipoles, or the electronegative or positive nature of parts of the water molecule, are permanent, but the intermolecular interactions between these dipoles are not.
- Induced dipole–permanent dipole interactions: In this case one of the dipoles is induced by its environment and interacts with a permanent dipole. The induced dipole is a localization of molecules electron cloud and transient in nature.
- London dispersion forces: These are weak interactions between multiple-induced dipole forces.

Although van der Waals forces are weak compared with covalent bonds, they are very common and contribute to the bond strength of many adhesive joints. These bonds are prevalent because they do not require a specific chemistry to form, simply oppositely charged dipoles. However, because van der Waals forces act on a molecular and atomic scale, intimate contact between molecules of the adhesive and of the substrates is essential for this type of bonding to occur. Hydrogen bonding between electropositive

© Woodhead Publishing Limited, 2013

areas of polymers chains or adhesive molecules and electronegative metal oxides on the surface of many metals is a common example of intermolecular forces used in adhesive joints.

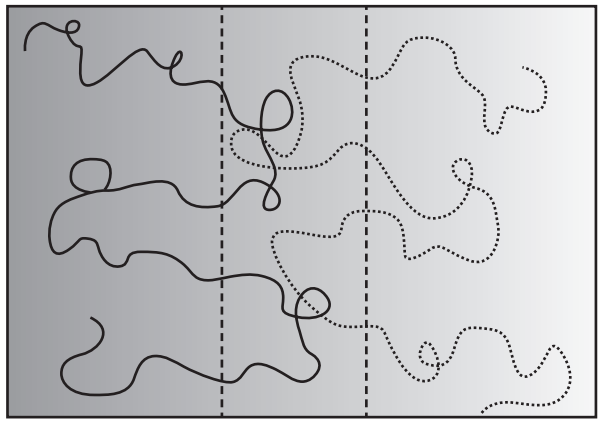
Primary forces: In this mechanism covalent bonds are formed across the interface; electrons are shared between atoms and permanent chemical bonds are created. Covalent bonds are very strong and, when achieved in an adhesive joint, result in strongly bonded components or coatings. Since these primary forces act on an atomic scale intimate contact between the adhesive and the substrate is necessary; the adhesive must wet and spread on the substrate. Additionally, reactive species in the adhesive must come within Angstroms of the corresponding reactants on the joint surface. The adhesive itself is composed of many components, only some of which are responsible for bonding to the substrate. Therefore, mobility of chemical species within the adhesive is an important consideration in creating covalent bonds across the interface of an adhesive joint. This mechanism is the least prevalent bonding mechanism and is the most difficult to achieve.

Entanglements: The utilization of entanglement across the interface is considered a special case adhesion mechanism. That is, this mechanism of adhesion does not occur by accident, but must be engineered into the system. To create a bond that takes advantage of interfacial entanglements requires three things: (1) the thermodynamic compatibility of the materials being joined such that an interphase can be created; (2) enough chain mobility (through the application of heat or the introduction of a solvent) that allows the chains to entangle within the interphase; (3) the chains that entangle must be long enough to form mechanically sufficient entanglements—otherwise the entangled chains have no strength and act as interfacial contaminates that impede bond strength.[15] The interfacial entanglement mechanism is drawn pictorially in Fig. 14.14. A well-designed adhesive bond takes advantage of multiple mechanisms of adhesion.

14.3.1 Wettability and surface energy

Wettability of the adhesive on the substrates of an adhesive joint is an important consideration in designing component bonds in medical devices.[16] In order to take advantage of the mechanisms discussed in the previous section, the adhesive must completely cover the substrate, fill microscopic crevices and not bead up. The adhesive should be in intimate contact or wet the substrate. Wettability is driven by the surface energy (γ) of the liquid adhesive with respect to the substrate. For good wetting the surface energy of the substrate should be greater than the surface energy (or surface tension) of the adhesive. For poor wetting the surface energy of the substrate is less than the surface energy of the adhesive. The thermodynamic

© Woodhead Publishing Limited, 2013



14.14 Diagram showing interfacial entanglements that can occur when the two materials in close contact have the thermodynamic compatibility that creates an interphase that allows for the incorporation of entanglements. These entanglements only will produce an interface capable of withstanding mechanical loading if the interfacial entangled chains are well anchored into the bulk structure.

tendency to decrease the energy of the system is the driving force for wetting. In general terms, a low energy adhesive readily will wet and cover a high-energy substrate surface because the overall energy of the system is reduced. Conversely, a liquid adhesive will bead up on a substrate with a lower surface energy. For example, most liquids will bead up on a low energy fluorocarbon surface, such as the Teflon surface of a sauté pan. No thermodynamic advantage is gained by the higher energy liquid spreading on the lower energy Teflon pan.

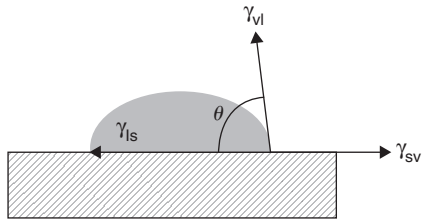
Surface energies or surface tension can be measured by examining contact angles. The contact angle is defined by solid surface and a line drawn tangent to the curve of a drop of liquid where the liquid touches the solid. This is shown below in Fig. 14.15.

Equation [14.4], the Young Equation, describes the system of a drop of a liquid sitting on a surface with the solid–vapor, solid–liquid and vapor–liquid interfaces in equilibrium.[17] Contact angle goniometers and dynamic contact angle analyzers use these principles to routinely measure contact angles. Additionally, specially prepared pens and dyes can be placed on a surface for a comparative assessment of surface energy.

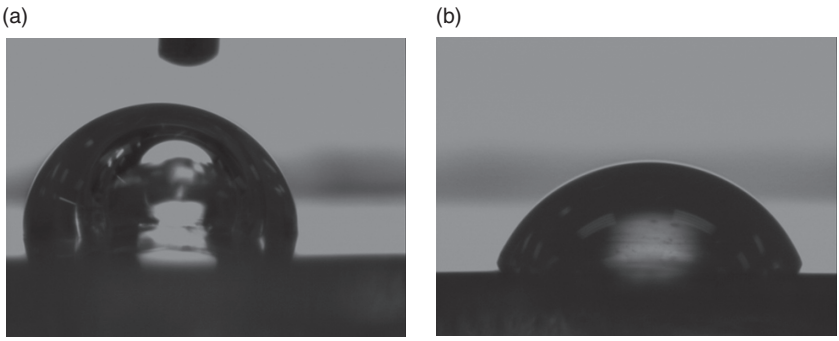
$$\gamma_{sv} = \gamma_{sl} + \gamma_{vl} \cos \theta \qquad [14.4]$$

where θ is the contact angle; γ_{sv} = solid–vapor; γ_{sl} = solid–liquid; γ_{vl} = vapor–liquid.

© Woodhead Publishing Limited, 2013



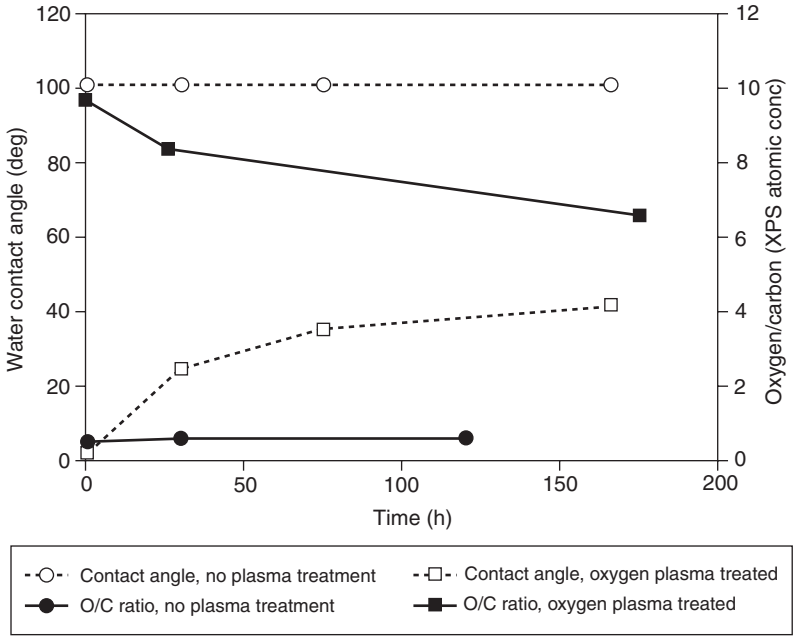
14.15 Diagram illustrating the contact angle (θ) formed by a drop of liquid on a solid surface.



14.16 Photographs of water droplets on an uncleaned molded polyurethane connector module (a) (contact angle is 103°) and a cleaned connector module (b) (contact angle is 70°).

In adhesion discussions, water contact angles are often used to describe the surface state of solid materials. Surfaces which are completely wet by water are called hydrophilic. Surfaces on which water beads up are called hydrophobic. In very general terms, it is difficult to bond to hydrophobic surfaces. The hydrophobic nature of the surface impedes spreading of most adhesive chemistries and may also indicate that the surface is contaminated with waxes, grease, processing aids, silicone oils, etc. These contaminants have low surface tensions and readily spread on many solids. A contamination layer will result in poor adhesion unless removed. Water contact angles can be used to assess the cleanliness of surfaces to be bonded. For example, the surfaces of polyurethane components are often contaminated with waxy processing aids. This polyurethane material is shown on the top of the device picture in Fig. 14.3. Changes in the water contact angle can indicate the effectiveness of cleaning. This is illustrated in Fig. 14.16. The contact angle of a drop of water on the surface of an uncleaned polyurethane connector module is 103°, whereas the contact angle on an effectively cleaned connector module is 70°.

© Woodhead Publishing Limited, 2013



14.17 Graph depicting water contact angles (left axis) and oxygen/carbon (O/C) ratios measured by XPS (right axis) for siloxane primer films with and without an oxygen plasma post-treatment.

14.3.2 Hydrophobic recovery

Contact angle measurements are able to detect contaminants and changes in surface chemistry that are generally only visible with sophisticated surface analysis techniques such as *x*-ray photoelectron spectroscopy (XPS) and time of flight secondary ion mass spectrometry (ToF SIMS).[18] This information is important because even very low levels of contamination or small changes in the surface chemistry can impact adhesive bond strength. These changes can take place during storage after a device has been cleaned, but before bonding.

The thermodynamic forces that govern wetting behavior also drive adsorption of volatile contaminants or the diffusion of mobile additives in a polymeric resin. Volatile hydrocarbon or silicone contamination from the manufacturing or laboratory atmosphere can readily adsorb onto high surface energy substrates. Mobile components (processing aids, unreacted monomer, waxes, etc.) of polymers can diffuse to surfaces and form weak boundary layers. Additionally, the orientation of hydrophobic sections of a polymer chain can reorient to the polymer surface and reduce surface

© Woodhead Publishing Limited, 2013

energy. This phenomenon is called hydrophobic recovery.[19–23] The example described below and shown in Fig. 14.17 illustrates the reversion of a hydrophilic surface to a more hydrophobic surface.[24]

Siloxane coatings deposited from reactive gas plasmas are hydrophobic with water contact angles measured at approximately 100° (open circles in Fig. 14.17). During storage in a petri dish in a laboratory environment, the surface is stable over 150 hours with little change in the water contact angle or oxygen to carbon ratio measured by XPS (filled circles). Treating this siloxane surface with an oxygen gas plasma changes the surface chemistry and energy. Immediately after treatment the surface is completely wettable and the water contact angle is zero (open squares). However, over the course of 2 days the surface recovers some of its hydrophobic nature. The water contact angle increases to approximately 40° and the oxygen to carbon ratio drops from approximately 9.7 to 6.6 (filled squares).[24] This example illustrates the need to bond an adhesive joint as soon as possible after substrate cleaning or pre-treatment.

The concepts of wettability and surface energy can be applied practically when choosing materials for an adhesive joint. An adhesive/substrate combination should be chosen in which the adhesive will readily wet the substrate surface enabling mechanical interlocking, van der Waals bonding or covalent bonding. That is, an adhesive should be chosen with a surface tension equal to or less than the surface energy of the substrate in order to achieve this wetting and intimate contact. Additionally, water contact angles can be used to test the cleanliness of medical device components and the effectiveness of surface pretreatments that modify surface chemistry.

14.3.3 Weak boundary layers

Weak boundary layers, which can impede adhesion, are found at the interface between the adhesive and the substrate.[25] Many different materials can function as a weak boundary layer. As discussed in the previous section, contaminants, processing oils, waxes, detergent residue, brittle or water soluble oxide layers and adsorbed water can all act as weak boundary layers. These materials displace the adhesive from the substrate surface, intercept potential bonding sites, and, in the case of adsorbed liquids can plasticize the adhesive making it soft. This softening may create a stress discontinuity at the interface and weaken the joint. Weak boundary layers on joint components should be removed before bonding. It is imperative to understand the timeframe in which weak boundary layers can reform. If possible, it is ideal to perform the bonding process immediately following substrate pre-treatment.

© Woodhead Publishing Limited, 2013

14.4 Adhesion promotion

In addition to optimizing joint design and choosing an appropriate adhesive, the strength and durability of an adhesive joint can be improved by cleaning and modifying the substrate surfaces.[26] The goals of surface treatments are to remove weak boundary layers, promote intimate contact, increase wettability of the adhesive on the substrates and provide a surface chemistry that can react with both components of the joint – the substrate and the adhesive. A variety of mechanical, wet chemical and vacuum processes can be used to achieve these goals. Surface treatments often have multiple effects on the morphology and chemistry of the substrate surface. It is important to be aware of unintended consequences and, as discussed in a previous section, bond the adhesive joint as soon after cleaning or surface treatment as possible.

Roughening the surface: Roughening the surface of substrates creates surface features that can be filled with adhesive, thus promoting mechanical interlocking. Additionally, roughening increases surface area and potential sites for intermolecular and covalent bonding. Removing material from the surface can also aid in cleaning by removing contamination, however, care should be taken to remove all debris which could serve to create a weak boundary layer.

Metal and polymer surfaces can be roughened mechanically with abrasives such as sand paper, by grit or bead blasting, water jet profiling, etc. These processes can alter surface morphology on the microscopic to visible scale. Substrates surfaces can also be roughened by chemical means. Acid and basic solutions can be used to etch and create texture on metal, and in some cases, polymer surfaces. For example, aqua regia solutions of nitric and hydrochloric acid can be used to etch platinum/iridium alloys used in medical devices. The disposal of spent etching solutions often makes the use of this technique unattractive. It is also possible to use vacuum or atmospheric plasma processes to roughen substrate surfaces on a microscopic scale. These can be physical processes, such as argon sputtering, or chemical processes involving reactive gas plasmas. It should be noted that these wet and vacuum chemical processes leave behind etch residues that can be detrimental to adhesion. It is necessary to understand the potential of creating etch residues and develop procedures to remove or neutralize them.

Cleaning: Numerous procedures and materials have been developed to remove contaminants from surfaces. It is useful to understand the contaminants in the component manufacturing process in order to choose the best cleaning procedures. Detergent solutions (e.g., Micro 90, LiquiNox, etc.) target multiple types of contaminants such as oil, grease, flux, particulates, hard water stains and biological debris. Solvents have long been used to remove waxes, mold release agents and oils present on component polymer surfaces,

© Woodhead Publishing Limited, 2013

however, new green manufacturing processes continue to be implemented. Super critical CO_2 processes have been implemented successfully for solvent free cleaning of medical device components. Additionally, many of the processes discussed in the previous section (wet chemical etching, plasma and vacuum processes) will remove contamination, in addition to roughening the surface.

Cleaning can often be facilitated by the addition of energy to the cleaning bath. Heat increases solubility of contaminants in the cleaning solution. Stirring and the use of an ultrasonic bath will also improve cleaning effectiveness by moving contaminants away from the components. Adequate rinsing is a critical part of cleaning that is often overlooked. In a cleaning bath contaminants are removed from the component, but can redeposit onto the surface. Rinsing helps to manage this re-deposition. Understanding the contaminant load of the cleaning bath and changing the solutions accordingly can reduce the re-deposition of contaminants. Additionally, cleaning should not negatively affect the bulk properties of the component. For example, acetone used as a cleaning solvent can induce crazing in polysulfone that has been molded with high residual stress.

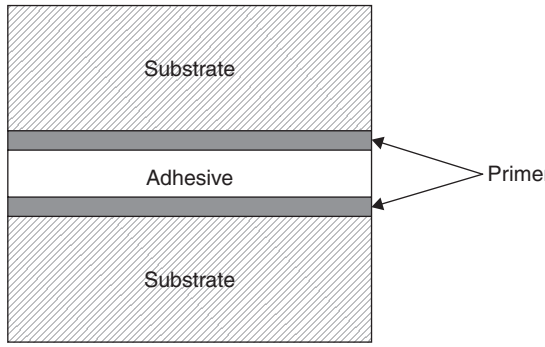
In choosing a cleaning process it is important to consider the potential contaminants, the effectiveness of the cleaning method, the level of cleanliness needed for adhesion and the effect on the bulk properties or functionality of the component.

Primers: Primer films or coupling agents (shown in Fig. 14.18) are used as a bridging layer between the substrate and the adhesive.[27] It is important for a primer to be well adhered to both the substrate and the adhesive or it becomes a weak boundary layer. Primers, when chosen wisely, can promote intimate contact, improve wetting of the adhesive on the surface and alter the chemistry of the substrate surface to suit the adhesive and promote chemical bonding or an entangled interphase.

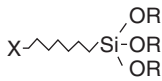
Primers can be grouped into different categories: reactive and entanglement primers. Silane coupling agents are a very common reactive primers used to promote adhesion between metal or glass and polymeric adhesives,[28] shown in Fig. 14.19. These primers consist of alkoxy groups that hydrolyze to Si-OH and then bond to the substrate and an organic tail containing a functional group (X) that is compatible with the adhesive. Amine, epoxy and vinyl functional silane primers are common. These primers are usually applied as dilute solutions in water or alcohol. Care must be taken as excess primer on the adherend surface acts as a weak boundary layer. This is often observable as a fine white residue.

Entanglement primers are used to promote wetting and the entanglements of polymer chains from the adhesive. They may simply be adhesive dissolved in a solvent. The low viscosity of these primers allows them to

© Woodhead Publishing Limited, 2013



14.18 Diagram of an adhesive joint incorporating a primer film.



14.19 Chemical diagram of silane coupling agent.

spread more readily over the substrate surface. Because they are chemically similar to the adhesive, chain entanglement is favored.

Primer films can be deposited using a variety of application methods such as dip coating, spin coating, electrostatic spray coating, vacuum or plasma deposition, or with a brush. Plasma deposition merits special consideration because the excited, high-energy state of a plasma can readily promote adhesion of the depositing primer to the substrate without having to follow typical chemistry rules. The best application method will depend on the primer itself and on the part geometry.

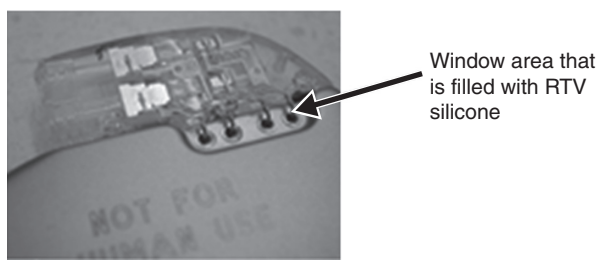
14.5 Types of adhesives used in medical devices

There are different requirements for adhesives used in short-term, disposable devices that have little to no blood contact, compared with those used in long-term implantable devices that are tissue and blood contacting. In the latter case, stringent criteria for leachables, stability and toxicity restrict adhesive options. In contrast, short-term use materials do not require the long-term stability in the harsh environment of the human body. Adhesive degradation such as hydrolysis and oxidation are typically not considered in disposable medical-device products. Also, some adhesives produce extractable or leachable products, whether through degradation or from additives and synthesis residuals, that are harmful to surrounding tissue. These materials should not be used in long-term implantable devices, but often are found in medical devices that are short-term, non-implanted use.

© Woodhead Publishing Limited, 2013

Adhesives can be space-filling or non-space-filling. In space-filling applications, the adhesive itself needs to have both cohesive strength and adhesive strength to support the design loading conditions. In a non-space-filling application, the adhesive can be a thin coating that is applied to the joint to facilitate either a thermal-bonding process or a solvent-bonding process. Adhesives can be one-part or two-part systems. In a one-part system, the resin and the cure agent/crosslinker/catalyst are supplied in a single cartridge. The chemistry of the adhesive system is designed such that the cure agent cannot undergo reaction at the cartridge storage conditions prior to use. The reaction of these systems is initiated by some outside condition such as moisture, heat, or acid. Exposure to the conditions required for curing initiates the cure agent and the reaction proceeds. In two-part adhesive systems, the resin and catalyst are supplied in two separate cartridges. Mixing occurs at the time of use and cure proceeds upon contact if the two components are properly blended. Working times for the two-part systems are reduced for fast-curing systems.

The main adhesive chemistries used for long-term implantable medical devices are polyurethanes, silicones and epoxies. Polyurethanes and silicones are also used as medical-device materials, as they are known to be stable when implanted in the body. Silicones adhesives (sealants) are space filling and can be one-part RTV (room temperature vulcanized) or two-part systems. The RTVs are a moisture-activated system that upon curing evolves acetic acid, methanol, or oxime, depending on the chemistry. Because the RTV systems are moisture cured (water must diffuse into the structure and acetic acid must be liberated), the use of these adhesives is restricted to shallow bondlines that tend to have large surface areas. An example of such an application is shown in Fig. 14.20, where the feedthrough wires on the pacemaker are covered with the RTV to protect the metal components from the body salts that could result in corrosion. In this case, the RTV must form a durable and reliable bond with a number of different substrates that include



14.20 RTV silicone is dispensed onto device and prevents fluid ingress into electrical components. Joints designed with RTVs must be shallow and have a large surface area to facilitate the water and acetic acid diffusion that is required for cure.

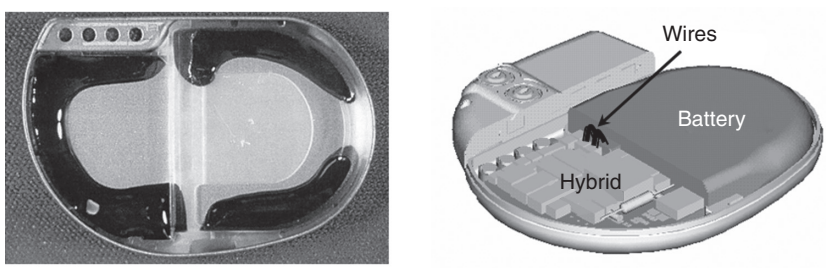
© Woodhead Publishing Limited, 2013

polyurethane, epoxy, titanium, stainless steel and MP35N alloy. The cure of RTVs is accelerated by increasing the humidity. A common mistake is to try to accelerate the cure of these materials by placing the joint assembly into an oven. Because hot air has reduced water capacity, the cure rate for these moisture-cured systems may be reduced.

Two-part silicones are typically mixed in equal parts and use a platinum catalyst to facilitate the crosslinking reaction. These materials will cure at room temperature, but can be accelerated with increasing temperature. Caution should be used as changing the cure path of an adhesive may alter the adhesion strength or the cohesive properties of the adhesive. Unlike RTVs, these adhesive can be used in enclosed joints of undetermined thickness, because the cure mechanism relies on heat, not on the diffusional transport of water and acetic acid.

Epoxy adhesives are space filling and can be either one- or two-part. Because one-part systems generally require a high temperature or other external factors to initiate the cure, two-part systems are often used for joints that are hidden and/or cannot withstand large temperature excursions. For example, medical devices that contain electronics and batteries cannot withstand large thermal excursions. Therefore, pacemakers that contain such electronics and batteries generally utilize two-part systems. One such two-part system is used to adhere the battery and the electronic module assembly to the titanium can of the pacemaker, as shown in Fig. 14.21. This is the same adhesive system that was used in the example depicted in Fig. 14.12. In the pacemaker application, a second titanium shield is welded to the first after bonding of the internal components. The result is a hermetically sealed device that does not come into contact with the biological environment; therefore this adhesive system is non-body contacting.

Solvent welding/bonding is often used to seamlessly bond similar materials to each other. This type of bonding strategy is used for non-space filling applications, between two materials that are thermodynamically compatible



14.21 Epoxy dispensing pattern on the inside of pacemaker titanium shield. The battery and the hybrid/electronic modulus assembly are placed on the adhesive and the assembly cures at room temperature.

© Woodhead Publishing Limited, 2013

and in intimate contact. For example, two different polyurethanes, having different durometers such as 55D and 80A, are often joined along a catheter, resulting in a device that has variable stiffness along the length. The solvent is introduced at the interface that is in intimate contact. The solvent lowers the glass-transition temperature of the polymer upon contact. The affected chains become mobile. The increased mobility of polymer chains on both sides of the interface result in interfacial entanglements *if*, and *only if*, the polymers sitting at the interface are miscible or thermodynamically compatible *and* the two materials sitting at the interface are in contact. A strong bond forms if the chains form adequate interfacial entanglements (driven by the solvent compatibility and solvent volume applied) and when the solvent is completely removed from the bond after the entanglement occurs. Interfacial contaminates (weak boundary layers) such as additives in the polymer that aid in extrusion (wax) can impede adequate bond formation if not removed from the surface before bonding.

Pressure sensitive adhesives (PSAs) are an assembly aid in the construction of medical devices. PSAs are generally considered to be non-space filling and most are non-reactive. These materials are usually supplied as tapes of varying thickness. For a PSA to work, the adhesive must flow into the rough surface features of the substrate. This takes time and pressure, parameters specified by the manufacturer in the technical data sheet. Because the PSA must be a flowable system to create bond, the PSA has the ability to flow *after* the bond is created, when the device is in service. This necessitates that the PSA attached components be secured by an additional mechanism. Mechanical stops have been utilized in combination with PSAs to prevent movement of components. Alternately, a supplemental addition of a curable, space filling adhesive system might be used to secure the components in the final assembly step.

The main adhesives used for short-term non-implantable medical devices are materials that are inexpensive and cure fast. These include cyanoacrylates and light curable materials. Cyanoacrylates, a.k.a. SuperGlue™, are widely available in different chemistries for multiple substrates, and can be offered in low- to high-viscosity formulations. These are one component adhesive systems that are limited to thin bond lines or non-space filling applications. Cyanoacrylate formulations have an acidic stabilizer that prevents the adhesive molecules from reacting in the tube. When applied, low levels of moisture on the substrate surface neutralize the acid stabilizer, initiating anionic polymerization of linear polymer chains, from the surface into the bulk. The interpenetrating nature of the acrylate polymer created is responsible for the joint strength. Cyanoacrylates are not used for long-term body-contacting medical-device applications because this chemistry is not hydrolytically stable and will eventually bio-resorb. However, this attribute makes cyanoacrylate chemistry perfect for wound-closure applications.

© Woodhead Publishing Limited, 2013

Light curable adhesives are the fastest curing adhesives, sometimes curing in a matter of seconds. These adhesives contain a photo initiator that when exposed to light, most often UV light, initiate a free radical or cationic reaction. When the light source is removed, the free radical cure schemes stop, while formulations with cationic chemistry continue to react. While widely used in non-implanted medical devices, these are not used in body-contacting long-term implants due to the toxicity of the photo initiators currently available. To use a light curable adhesive, the entire joint must be accessible by the light source. Adhesive, buried in joints that cannot be exposed to the light beam, will not cure, a phenomenon known as 'shadowing'. This limits the joints to clear materials with good UV transmission, or simple joint designs. To combat this issue dual cure formulations have been developed that offer the quick curing using light sources, and then offer a secondary cure mechanism for the shadowed areas, either by moisture or heat.

14.6 Conclusion

Joint design is the single most important factor in determining the overall joint strength. Joint designs must be created to minimize peel- or cleavage-loading conditions. When joints fail, they can fail adhesively, along the interface, cohesively, within the bulk of the adhesive, within the substrate, or in a complex manner that can result in a wandering crack. If the failure strength of the joint is not adequate for the application, then joint re-design should be the first consideration. At the small lengths scales required in medical devices, often joint re-design is a difficult option to consider. In those cases, one might be able to improve joint strength by understanding the failure mode of the joint and implementing improvements to that part of the system. Of critical importance is to assure that the failure mode observed in the *in vitro* evaluation of the joint matches that anticipated or observed *in vivo*. If the failure mode is cohesive, within the adhesive material, strategies to improve the biostability and/or the bulk strength of the adhesive must be employed. More often than not, the *in vivo* environment produces an adhesive failure mode. The interfacial interactions can be improved to increase the adhesion strength of the joint. These interfacial interactions include modifying the mechanical roughness features of the substrate, improving substrate–adhesive wettability, implementing primers to harness covalent interfacial interactions, eliminating weak boundary layers through better cleaning methods, and enhancing interfacial entanglements in systems compatible with this approach.

There are a limited number of adhesive chemistries available for use in medical devices because of performance in the body and toxicity considerations. The adhesive options are even further restricted for use in long-term

© Woodhead Publishing Limited, 2013

tissue and blood-contacting applications. Long-term implant adhesive options tend to focus on silicones and epoxies. In addition, PSAs (isolated from body tissue) are sometimes employed in combination with other stabilizing strategies due to the flow properties of the non-reactive PSA systems. Disposable medical devices tend to use fast-cure systems such as cyanoacrylate and UV curable systems. The adhesive selection process must take into account the substrate chemistry, the bulk strength requirements for the adhesive, the adhesive strength requirements of the interface, the environmental conditions during device usage, any manufacturing constraints like cycle times, and any thermal excursion constraints of the device or component containing the joint. One component adhesive systems require some external condition to initiate cure such as heat. These systems have the advantage of long working times for adhesive application. Two component systems begin to cure upon mixing, where the degree of mixing and the metering of each component is critical to the final adhesive properties. These materials have short working times, as the viscosity begins increasing at the point of mixing. However, these systems offer the advantage of a room-temperature cure, often a critical criteria for medical devices that have temperature excursion limitations due to the incorporation of batteries.

14.7 Sources of further information and advice

Fundamentals of Adhesion, edited by Lieng-Huang Lee, Plenum Press (1991).

Adhesive Bonding, edited by Lieng-Huang Lee, Plenum Press (1991).

Adhesion and Adhesive Technology: An Introduction, A. V. Pocius, Hanser Gardner Publications (1997).

Handbook of Adhesives and Sealants, Edward M. Petrie, McGraw-Hill Professional (1999).

Adhesion and Adhesives: Science and Technology, A. J. Kinloch, Chapman & Hall, (1987).

14.8 References

1. Petrie, E. M., *Handbook of Adhesives and Sealants*, New York: McGraw Hill, 2000.
2. Kline, R. A., ed. Mittal, K. L., 'Stress analysis of adhesively bonded joints,' *Adhesive Joints: Formation, Characteristics, and Testing*, New York: Plenum Press, 1984, pp. 587–610.
3. Kinloch, A. J. and Moore, D. R., 'The influence of adhesive bond line thickness on the toughness of adhesive joints', *The Application of Fracture Mechanics to Polymers, Adhesives and Composites*, ed. Moore, D. R., Kidlington, Oxford, GB: Elsevier, 2004, pp. 149–155.

© Woodhead Publishing Limited, 2013

4. Chastian, C. E., 'Designing adhesive joints', *Appliance Engineer*, vol. **8**. no. 4, 1974, pp. 22–25.
5. Ahagon, A. and Gent, A. N., 'Effect of interfacial bonding on the strength of adhesion', *Journal of Polymer Science, Polymer Physics*, vol. **13**, 1975, pp. 1285–1300.
6. Chun, H. and Gent, A. N., 'Effect of length and number of interlinking molecules on the strength of adhesion', *Journal of Polymer Science, Part B: Polymer Physics*, vol. **34**, no. 13, pp. 2222–2229.
7. Shepard, N. E. and Wightman, J. P., 'A simple device for measuring adhesive failure in sealant joints', *Science and Technology of Building Seals, Sealants, and Weatherproofing: Seventh Volume ASTM STP 1334*, ed. Klosowski, Jerome M., West Conshohocken, PA: American Society for Testing and Materials, 1998.
8. Young, R. J. and Lovell, P. A., *Introduction of Polymers: Second Edition*, New York: Chapman & Hall, 1991.
9. Macosko, C. W., *Rheology Principles, Measurements, and Applications*, New York: VCH Publishers, 1994.
10. Nelson, W., *Accelerated Testing*, New York: Wiley, 1990.
11. Dickie, R. A., Debolt, M. A., and Ward, S. M., *Stress Durability Testing of Adhesively Bonded Steel*, SAE 950128 Society of Automotive Engineers, Inc., Warrendale, PA, 1995.
12. Pocius, A. V., *Adhesion and Adhesives Technology: An Introduction*, 2nd edn, Hanser Gardner Publications, 2002, pp. 78–86.
13. Comyn, J., 'What are adhesives and sealants and how do they work', in *Adhesive Bonding Science, Technology and Applications*, ed. Adams, R. D., Cambridge: Woodhead Publishing, 2000, pp. 41–51.
14. Baier, R. E. Shafrin, E. G. and Zisman, W. A. 'Adhesion: mechanisms that assist or impede it', *Science*, vol **162**, 1968, pp. 1360–1368.
15. Chaffin, K. A., Knutsen, J. S., Brant, P., Bates, F. S., 'High-strength welds in metallocene polypropylene/polyethylene laminates', *Science*, vol. **288**, 2000, pp. 2187–2190.
16. Kinloch, A. J., *Adhesion and Adhesives: Science and Technology*, London: Chapman & Hall, 1987, pp. 18–55.
17. Schrader, M. E., 'High and medium energy surfaces: ultrahigh vacuum approach', in *Modern Approaches to Wettability Theory and Applications*, ed. Schrader, M. E. and Loeb, G. I., New York: Plenum Press, 1992, p. 54.
18. Watts, J. F., 'Surfaces: how to assess', in *Adhesive Bonding Science, Technology and Applications*, ed. Adams, R. D., Cambridge: Woodhead Publishing, 2000, pp. 52–74.
19. Fritz, J. L. and Owen, M. J., 'Hydrophobic recovery of plasma-treated polydimethylsiloxane', *Journal of Adhesion*, vol. **54**, 1995, pp. 33–45.
20. Everaert, E. P., VanderMei, H. C., Devries, H. J., and Busscher, H. J., 'Hydrophobic recovery of repeatedly plasma-treated silicone rubber 1. Storage in air', *Journal of Adhesion Science and Technology*, vol. **9**, 1995, pp. 1263–1278.
21. Everaert, E. P., VanderMei, H. C., and Busscher, H. J., 'Hydrophobic recovery of repeatedly plasma-treated silicone rubber 2: a comparison of hydrophobic recovery in air, water, or liquid nitrogen', *Journal of Adhesion Science and Technology*, vol. **10**, 1996, pp. 351–359.

© Woodhead Publishing Limited, 2013

22. Owen, M. J. and Smith, P. J., 'Plasma treatment of polydimethylsiloxane', *Journal of Adhesion Science and Technology*, vol. **8**, 1994, pp. 1063–1075.
23. Morra, M., Occhiello, E., Marola, R., Garbassi, F., Humphrey, P., and Johnson, D., 'On the aging of oxygen plasma-treated polydimethylsiloxane surfaces', *Journal of Colloid and Interface Science*, vol. **137**, 1990, pp. 11–24.
24. Taylor, C. E., 'Plasma treatment of aluminum for adhesive bonding', MS thesis, University of Cincinnati, Cincinnati, OH, 1996.
25. Pocius, *Adhesion and Adhesives Technology*, pp. 159–160.
26. Brewis, D., 'Surfaces: how to treat', in *Adhesive Bonding Science, Technology and Applications*, ed. Adams, R. D., Cambridge: Woodhead Publishing, 2000, pp. 75–88.
27. Pocius, *Adhesion and Adhesives Technology,* pp. 151–155.
28. Plueddemann, E. P., *Silane Coupling Agents*, New York: Plenum Press, 1982.

© Woodhead Publishing Limited, 2013

15

Advanced metal–ceramic joining techniques for orthopaedic applications

G. SALA, Aerospace Engineering Department, Italy

DOI: 10.1533/9780857096425.4.407

Abstract: The types of metals and ceramics to be joined, their application, features and characteristics are preliminarily summarized. The main challenges are pointed out and discussed, possible solutions envisaged. As a consequence, general methods for joining metals to ceramics are presented. Their strong and weak points and possible outcomes are presented. The so-called direct bonding methods are discussed, in particular solid-phase, non-fusion welding. Strengths and weaknesses of techniques and materials are considered, as well as further concerns such as biocompatibility, thermal/chemical performances and long-term degradation. Indirect bonding methods are described, such as liquid-phase and solid-phase bonding, as well as active brazing techniques. Joining procedures, brazing agents, possible features and drawbacks, experimental testing issues and feasible applications are considered. Finally, expected future developments and their likely applications are presented together with sources of further information.

Key words: metals–bioceramics joining techniques, solid-phase welding, liquid-phase bonding, active brazing, brazing agents.

15.1 Introduction

Orthopaedic biomaterials dominate the market of biomaterials, thanks to their capability of restoring mobility and quality of life through fixation devices and joint replacements. The best-performing load-bearing joint-replacement prostheses should have a hybrid structure, made of metallic components, where strength, stiffness, fracture toughness and fatigue endurance are required, and ceramic components, where corrosion resistance, bio compatibility, friction coefficient and wear rate are of primary concern. This is why it is more and more desirable to combine the properties of ceramics and metals in medical devices (implantable prostheses or instrumentary tools). The challenge is to join metallic and ceramic components in such a way as to make the assembly able to sustain life-long cyclic loading, reliably and safely, even if their different chemistry, structures and properties can make their joining difficult or impossible (Pask, 1987). By the

© Woodhead Publishing Limited, 2013

way, ceramic-to-metal joining represents a major issue in case of implantable neuromodulation medical devices as well, which require a hermetic sealing between ceramic housing and metallic flanges. As a matter of fact, neuromodulation is currently a hot research area in the implantable medical device industry (Koch, 2007; Daulton, 2010; Fowler *et al*., 2010; Haller *et al*., 2010; He and Colvin, 2010; Tziviskos, 2010; Blischak, 2011; Chiao and Chiao, 2011).

Theoretically, the components of hybrid metal–ceramic medical devices can be joined by means of three techniques: mechanical joining through integral attachment features (e.g. Morse taper); direct joining by means of solid- or liquid-phase bonding; indirect bonding by means of brazing or soldering agents (Carim *et al*., 1993). For realizing a reliable direct/indirect joint, an intimate contact between the adherents is needed, to be converted into an atomically bonded interface; besides, this interface must be able to accommodate residual stresses due to CTEs mismatch and generated by temperature variations during service (Loehman and Tomsia, 1988).

An innovative technique called active brazing, which uses special braze agents containing active metals (e.g. Ti or Zr) able to react with ceramics, can presently be considered the most promising process for joining metallic and ceramic parts of medical devices. Although brittle microstructures containing intermetallic compounds may be created at the interface, limiting its capability to accommodate CTEs mismatch, the prostheses assembled by active brazing have demonstrated being able to withstand not only large forces occurring during machining and polishing, but also simulated long-lasting physiological loads.

Besides active brazing technique, some other innovative processes are likely to be successfully adopted to join metals and bio-ceramics, in the field of both solid- and liquid-phase bonding. Solid-phase welds already demonstrated to be suited for joining metals and ceramic through different friction-welding processes, like ultrasonic welding and ultrasonic brazing. Very much promising are the 'functional graded material (FGM) joints', which are able to join even strongly misfitting adherents through several interlayers of gradually varying metal–ceramic compositions. Combustion synthesis (CS) and self-propagating high-temperature synthesis (SHS) represent the more efficient techniques to produce graded layers.

Although ceramics melt at a very high temperature, inducing phase transformation and cracking inside the heat-affected zone, liquid-phase techniques, especially those based on a high-energy density process, like EBW and LBW, are becoming more and more popular, thanks to their capability to produce deep weld beads and narrow heat-affected zones. Electron beam brazing and laser brazing may be used as well: here electrons or photons beams locally heat a joint, where the filler metal is pre-placed in some form.

© Woodhead Publishing Limited, 2013

The main advantages of these processes consist in very rapid heating, very small thermally affected zone and accurate dimensional control.

15.2 The challenges of joining metals to ceramics

The worldwide market of biomaterials is dominated by orthopaedic biomaterials, which are enormously successful in restoring mobility and quality of life to millions of individuals each year, thanks to reconstructive implants (joint replacements) and fracture management products (fixation devices). Orthopedic biomaterials should be chosen among those materials which are able to withstand, over the years, high fatigue loading, being in the meantime bio compatible, corrosion-resistant and mechanically efficient (Pope and Fleming, 1991). Notwithstanding hundreds of different orthopaedic applications exist in the field of fixation and total joint arthroplasty (TJA), only a few orthopaedic polymers, metals and ceramics dominate, listed in Table 15.1 together with their primary uses (Hallab *et al.*, 2004).

The principal function of long bones is to bear loads; therefore the most suited materials to replace their joints (hip, knee, shoulder and elbow) are metals. They provide appropriate characteristics in terms of strength, stiffness, toughness, hardness, durability, corrosion endurance and bio compatibility, even if their strength and stiffness considerably exceed those of bone, often leading to stress-shielding effects. The mechanical properties of main bio-metals are reported in Table 15.2, compared with bio-polymers and bio-ceramics. Among the three most popular families of orthopaedic metal alloys (titanium-based, cobalt-based, stainless steel), many different types are available, each of them particularly suited for specific applications. However, their widespread adoption as load-bearing implant materials is mainly due to high corrosion resistance; on the other

Table 15.1 Most common orthopaedic biomaterials with their primary uses

Material	Primary use(s)
Titanium alloy (Ti6Al4V)	Plates, screws, TJA components (non-bearing surfaces)
Co–Cr–Mo alloy	TJA components
Stainless steel	TJA components, screws, plates, cabling
Poly-methyl-methacrylate (PMMA)	Bone cement
Ultra-high-molecular-weight-poly-ethylene (UHMWPE)	Low-friction inserts for bearing surfaces in TJA
Alumina (Al_2O_3)	Bearing-surfaces TJA components
Zirconia (ZrO_2)	Bearing-surfaces TJA components

Adapted from Hallab *et al.*, 2004, p. 528.

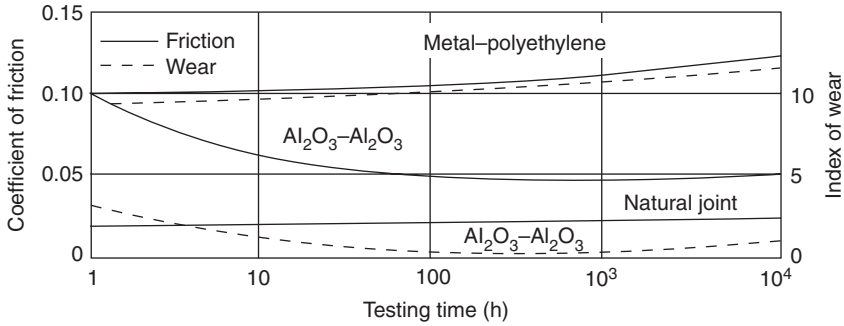
© Woodhead Publishing Limited, 2013

Table 15.2 Mechanical properties of the most popular orthopaedic biomaterials

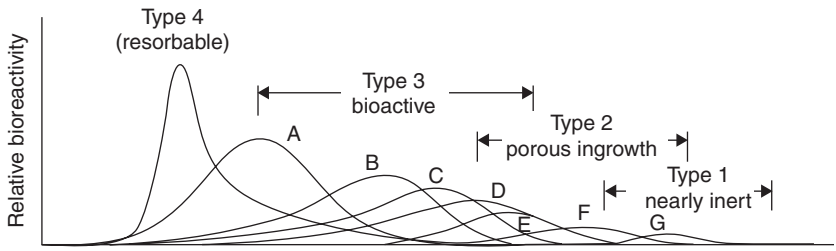
Orthopaedic biomaterials	ASTM designation	Stiffness (GPa)	Yield strength (MPa)	Ultimate strength (MPa)*	Fatigue endurance (MPa)*	Hardness HVN †	Ultimate strain (%)
Cortical bone							
Low strain	–	15.2	114t	150c–90t	30–45	–	–
High strain	–	40.8	–	400c–270t	–	–	–
Polymers							
UHMWPE	ASTM F648	0.5–1.3	20–30	30–40t	13–20	60–90 (MPa)	130–500
PMMA	ASTM F451	1.8–3.3	35–70	38–80t	19–39	100–200 (MPa)	2.5–6.0
Ceramics							
Al_2O_3	ASTM F603	366	–	3790c–310t	–	20–30 (GPa)	–
ZrO_2	ASTM F1873	201	–	7500c–420t	–	12 (GPa)	–
Metals							
Stainless steel	ASTM F138	190	792	930t	241–820	130–180 (GPa)	43–45
Co–Cr alloys	ASTM F90	210	448–1606	1896t	586–1220	300–400 (GPa)	10–22
Pure titanium	ASTM F67	110	485	760t	300	120–200 (GPa)	14–18
Ti 6Al 4V	ASTM F136	116	897–1034	965–1103t	620–689	310 (GPa)	8

Adapted from Hallab *et al.*, 2004, p. 535.
* c, compression; t, tension.
† HVN, Vickers Hardness Number, kg/mm.

© Woodhead Publishing Limited, 2013



15.1 Friction and wear of Al_2O_3–Al_2O_3 hip joint compared to a metal–polyethylene prosthesis and a natural joint in *in-vitro* tests. (Source: Reprinted from Hench and Best, 2004, p. 158.)

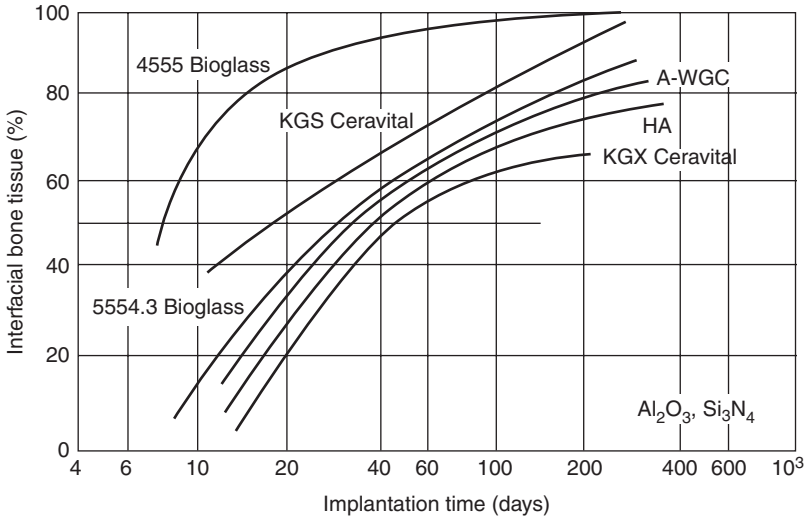


15.2 Relative rates of bioreactivity for ceramic implants materials. A, 4555 Bioglass; B, KGS Ceravital; C, 55S4.3 Bioglass; D, A/W glass–ceramic; E, hydroxyapatite; F, KGX Ceravital; G, Al_2O_3, Si_3N_4. (Source: Reprinted from Hench and Best, 2004, p. 154.)

hand, they are generally affected by high density, elevated friction coefficient and low wear resistance (Barbosa, 1992). These drawbacks have given to ceramics the opportunity to become a viable solution for certain specific applications (Hench, 1991).

Among different kinds of ceramics, only dense, non-porous, nearly inactive ones are suited for bearing surfaces of TJA components, where their excellent biocompatibility, elevated compressive ultimate strength, low coefficient of friction and high wear resistance (Fig. 15.1) can be exploited thanks to their low rate of bio-reactivity (Fig. 15.2) and absence of formation of interfacial bone tissue (Fig. 15.3) (Hench and Best, 2004). Although adopted in Europe for over 40 years, it is only relatively recently that the FDA (3 Feb. 2003) has approved non-cemented ceramics cups press-fitted into the hip acetabulum. The mating femoral ball is made of ceramics as well, connected through a Morse taper to the metallic stem (Fig. 15.4). Prostheses for TJA of elbow, shoulder and knee, provided with ceramics parts (heads,

© Woodhead Publishing Limited, 2013



15.3 Time dependence of formation of bone bonding for the materials shown in Fig. 15.2. (Source: Reprinted from Hench and Best, 2004, p. 154.)



15.4 Ceramic cup and femoral ball.

© Woodhead Publishing Limited, 2013

condyles) have been implanted for many years as well and are likely to be FDA approved in the near future.

If their grains are very small (<5 μm) and have a very narrow size distribution, the ceramics get excellent tribologic properties (friction and wear), since very low surface roughness values (R_a < 0.02 mm) are obtained. This leads to wear of ceramics-on-ceramics sliding surfaces being nearly ten times lower than corresponding metal–polymer coupling (Cooper *et al*., 1991). In general, long-term outcomes are excellent, although stress-shielding effects due to high elastic modulus of ceramics could result in bone atrophy and acetabular cup loosening, mainly in the case of old patients and osteoporotic bone. Concerns about alumina (Al_2O_3) brittleness and poor tensile strength are addressed by reducing grain size and porosity, increasing degree of purity and improving processing routes (i.e. adopting hot isostatic pressing, HIP). Zirconia (ZrO_2) was introduced 25 years ago as an alternative to Al_2O_3 in consideration of its superior strength (100% higher) and modulus (80% lower) over competitors; such properties make ZrO_2 possibly more resistant and mechanically compatible with surrounding bone material (Hench *et al*., 1991).

In synthesis: the best load-bearing joint-replacement prosthesis (hip, knee, shoulder, elbow) should have a hybrid structure, and be made of metallic components (stem) where strength, stiffness, fracture toughness and fatigue endurance are required, and ceramic components (ball-and-socket, condyles articulating surfaces) where corrosion resistance, bio compatibility, friction coefficient and wear rate have to be considered. These are the reasons why it is frequently desirable to combine the properties of ceramics and metals in medical devices (implantable prosthesis or instrumentary tool as well): joining these basically dissimilar materials has now become necessary, not simply interesting. The challenge is to join metallic and ceramic components in such a way to make the assembly able to sustain life-long cyclic loading, reliably and safely.

Compared to metals, ceramics are stronger (mainly in compression), more capable of retaining stiffness, strength, hardness and wear endurance at high temperature, more resistant to corrosion and oxidation (even at high temperature), less thermally and electrically conductive and less sensitive to thermal expansion/contraction. Some of these differences are shown in Table 15.3. Such different properties are due to basic differences in atomic microstructure. The micro-structure of ceramics is made of ionic, covalent or mixed ionic-covalent bonds, while the micro-structure of metals consists of typical metallic bonds, where a lattice of positive ions is permeated by a cloud of electrons, free of moving under the action of electric or thermal stimuli. Such different kinds of bonds lead to different values of melting point, strength and stiffness. In particular, all these are higher for ceramics than for metals, thanks to their ionic and covalent bonds, which are intrinsically

© Woodhead Publishing Limited, 2013

Table 15.3 Properties of bioceramics and some metals for comparison

Material	Melting point (°C)	Stiffness (GPa)	Hardness HVN (GPa)	Toughness K_{Ic} (MPa $m^{1/2}$)	CTE (10^{-6}/°C)	Resistivity (Ω-m)	Thermal conductivity (J/s-m °K)	
							100 °C	1000 °C
Alumina	2050	360–380	20–30	3–5	8.0	10^{8}–10^{10}	3.0	6.3
Zirconia	2690	150–200	12	9	6.5	10^{10}	2.0	2.3
Steel	1536	200	(*)	60–140	12.1	10×10^{-8}	75	–
Cobalt	1495	185	(*)	300	12.3	5.0×10^{-8}	69	–
Nickel	1453	180	(*)	350	13.3	3.5×10^{-8}	61	–
Titanium	1668	117	(*)	55–115	8.4	5.6×10^{-7}	17	–

Adapted from Messler, 2004, p. 586.
HVN, Vickers Hardness Number, kg/mm.
(*) Dependent on alloying.

stronger (Hench and Wilson, 1991). Another basic difference between ceramics and metals resides in brittleness of the former vs the ductility of the latter (due to the ability of metals to slip without disrupting atomic-level periodicity, thanks to the movement of dislocations). Furthermore, differences in electrical, thermal, optical and magnetic properties are owed to differences in electron distribution and spins. On the other hand, at micro-structural level, ceramics contain flaws, cracks and pores, which limit tensile strength and tension-tension or alternate fatigue endurance, because such load conditions open and extend flaws, unstably propagating cracks up to sudden, brittle failure (Hench and Wilson, 1993). Welding, brazing and soldering of ceramics give rise to larger and more complex dislocations that (with the exception of nano-structured ceramics) may prevent ductile deformations and induce low toughness and poor energy absorbing capability. For all that, each of the two materials is able to fulfil different requirements, even if their different chemistry, structures and properties can make their joining difficult or impossible (Messler, 2004).

Theoretically, the components of hybrid metal–ceramic medical devices can be joined by means of one of these three techniques: (i) mechanical joining by interlocking, fastening or through integral design attachment features (e.g. Morse taper); (ii) direct joining by means of non-fusion (solid-phase) or fusion (liquid-phase) bonding; (iii) indirect bonding by means of polymeric adhesives, glasses, brazing or soldering agents. With the exception of mechanical joining, to realize a stable and reliable joint, different conditions should be met: (a) an intimate (atomic level) contact between the adherents has to be achieved; (b) the contacting surfaces should be converted into an atomically bonded interface; (c) the interface must be able to accommodate the residual stresses due to adherents CTE mismatch and generated during

© Woodhead Publishing Limited, 2013

cooling down after fabrication or temperature variation during service (e.g. autoclave sterilization cycles) (Tomsia *et al*., 1991).

15.3 Mechanical joining techniques

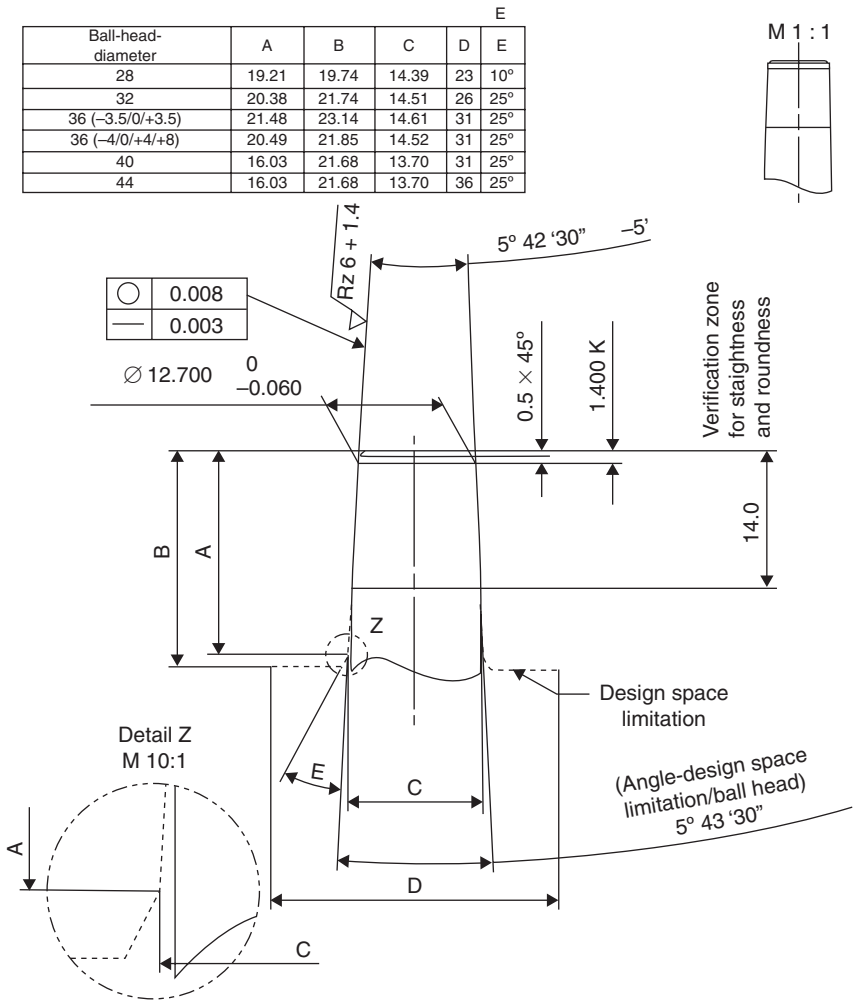
Mechanical joining between metals and ceramics can be performed through several methods, like interlocking, press-fitting, clamping, fastening and integral threading. In case of fastening, possible damages due to inherent ceramics brittleness could arise. Such damages may derive from bearing and clamping loads and have to be limited by adopting large contact areas (bolt heads, nuts and washers), as well as compliant interlayers (metal liners, sleeves and inserts). Besides, holes for studs, pins and fasteners are difficult to be machined in ceramics, owing to cutting-tool wear and possible ceramics chipping and cracking; preferably, they should be integrally moulded and fired-in; in any case, generous fillets have to be provided. Moreover, since compressive stresses are better tolerated by ceramics than tensile ones, design should avoid complex states-of-stress (e.g. bending and deviated compression) leading to dangerous situations. Finally, large differences between CTEs of metals and ceramics should be accurately considered to reduce the effects of thermal loading due to autoclave sterilization process. Having this in mind, suitable types of ceramics and metals should be chosen for minimizing such a mismatch; deformable metallic fasteners should allow a certain degree of mutual displacement (slippage) between adherents; ductile intermediate components should be provided, able to plasticize and flow (Messler, 2004).

The main advantages of mechanical vs brazed joints are: good mechanical strength under moderate loads (even at high temperature), capability to accommodate strain mismatches due to thermo-elastic differences and, above all, possibility of intentional disassembling to repair, upgrade and modify instrumentary tools and ancillary equipments. Besides, such a characteristic lends modularity to families of implantable devices and allows to customize (in the surgical room) implantable systems made of different components. To integrally connect metallic and ceramic parts through mating geometric features, these should be built into the devices at the initial design stage, like in the case of Morse taper coupling between head and stem of hybrid metal–ceramic hip and shoulder prostheses.

In a Morse taper coupling, the conical female cavity (bore) is characterized by an angle slightly unlike the angle of the stem male cone (trunnion). So doing, if the two mating parts are coupled, they are not in contact on a surface but along a circumference; for this reason, when the trunnion compresses the wall of the bore and tends to expand it, the stresses that arise create a built-in constraint between the two parts. A modular system based on Morse taper coupling offers the capability to combine every trunnion supplied by a producer with every bore made by another producer, provided

© Woodhead Publishing Limited, 2013

Ball-head-diameter	A	B	C	D	E
28	19.21	19.74	14.39	23	10°
32	20.38	21.74	14.51	26	25°
36 (–3.5/0/+3.5)	21.48	23.14	14.61	31	25°
36 (–4/0/+4/+8)	20.49	21.85	14.52	31	25°
40	16.03	21.68	13.70	31	25°
44	16.03	21.68	13.70	36	25°

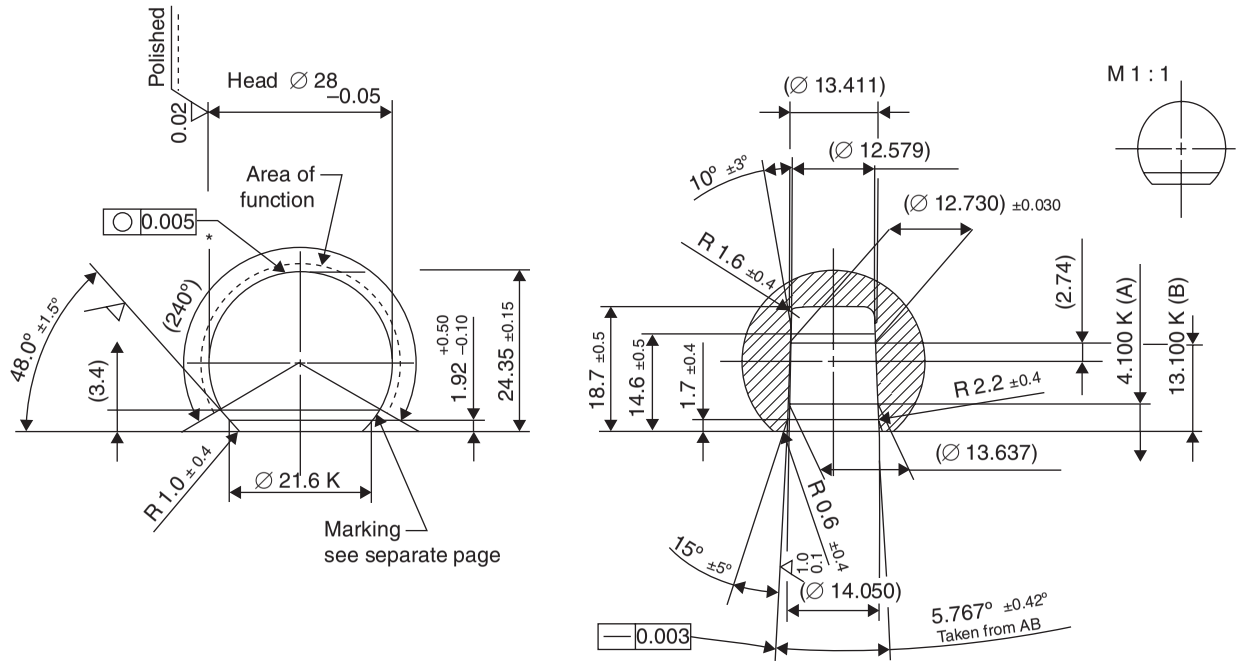


15.5 Conical male cone (trunnion).

they have the same degree of tapering. On the other hand, remarkable concerns of fretting and wear afflict such kind of mechanical connection.

An international standard does not exists to define dimensions and tapering of male and female cones, but main producers of ceramic heads for hip prostheses have imposed their standard to which the dimensions of metallic stems cones have to comply (Figs 15.5 and 15.6). Besides, in order to allow complete inter-changeability between ceramic and metallic heads, the dimensions of metallic heads should conform to such standard as well. As a consequence, the so-called 'Euro-cone 12–14' has almost imposed itself among the totality of hip prostheses producers.

© Woodhead Publishing Limited, 2013



15.6 Conical female cavity (bore).

© Woodhead Publishing Limited, 2013

15.4 Direct and indirect bonded joining techniques

A direct joining process leads to the connection between two materials thanks to the formation of primary bondings similar to those found in the original adherents; intermediate materials are not required.

An indirect joining process uses an intermediate material, which allows to overcome the incompatibilities (chemical, physical, thermal) of the two adherents.

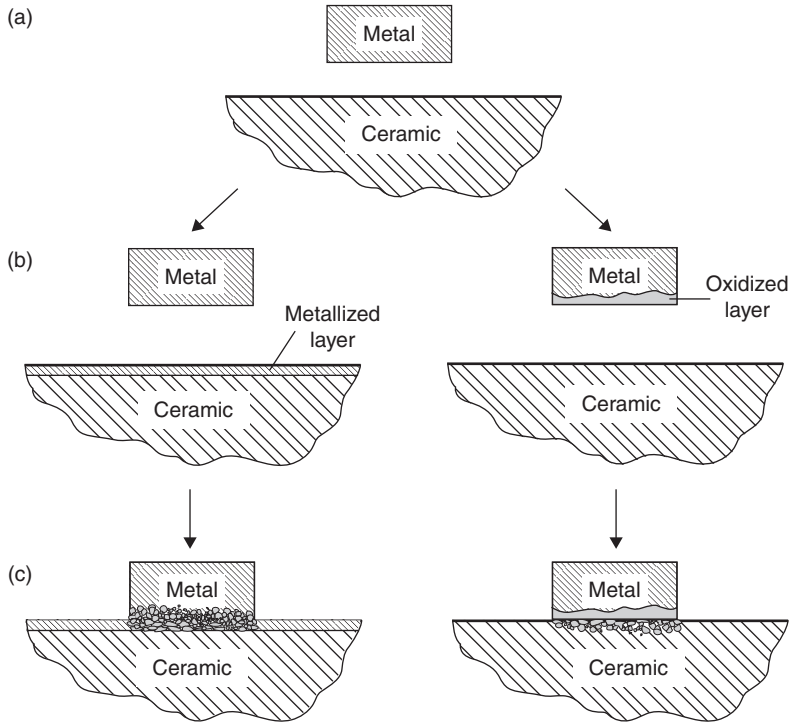
15.4.1 Direct bonding techniques

A process of direct joining leads to the indissoluble connection between two materials thanks to the formation of primary bondings equal or similar to those found in the adherent materials: no intermediate materials are required. Metals and ceramics may be directly joined preferably through solid-phase non-fusion processes (diffusion welding) or (seldom) fusion techniques. These latter techniques are rarely adopted since intermixing of ceramic and metal liquid phases can hardly occur at atomic level due to basic differences between materials. Viceversa, non-fusion techniques like diffusion bonding, friction welding, chemical vapour deposition (CVD) and physical vapour deposition (PVD) are widely used, even if CVD and PVD are often not considered true welding processes because materials are joined atom-by-atom and not in-bulk.

Solid-phase diffusion welding has become very popular and is widely used thanks to its capability to achieve an atomic-level interface contact. To this purpose, very smooth and perfectly fitting surfaces have to be matched, in order to guarantee an intimate contact between a very large number of microscopic asperities, through which diffusion occurs. At the beginning, plastic deformation of metallic adherent happens, followed by creep, grains growth and diffusion in both metal and ceramic (Fig. 15.7). Similar melting points of adherents is not needed and successful welding of noble (Pt, Au, Ag, Pd) and transition (Fe, Ni, Co) metals to oxide-bioceramics (Al_2O_3) are reported. Their resistance to chemical and electrochemical corrosion, long-term stability and good reliability during service are well documented in literature (Kamachimudali *et al.*, 2003; Jiang *et al.*, 2005; Xiaochun *et al.*, 2008; Atabaki, 2010). Diffusion bonding usually takes several minutes or a few hours (Messler, 2004).

Solid-state bonding process depends on the combination of surface and bulk chemical reactions. In general the adherents should be heated up to temperatures close to metal melting point while pressed together at pressures of 1–10 MPa, respectively suited for noble and transition metals. Shear ultimate can reach 80–100 MPa. The strength of the joint is also strongly dependent on the coefficient of thermal expansion (CTE) of the metallic

© Woodhead Publishing Limited, 2013



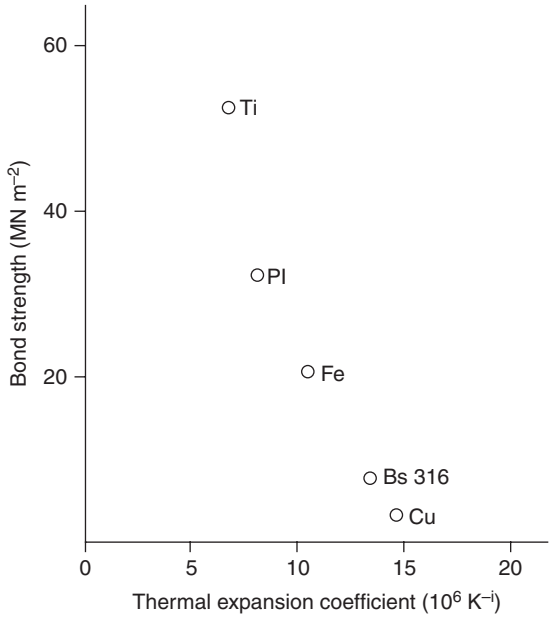
15.7 Schematic illustration of the stages of solid-phase bonding of metals to ceramic. (Source: Reprinted from Messler, 2004, p. 709.)

adherent, as shown in Fig. 15.8. Mechanical performances of the joint descend not only from the nature and the compatibility of the adherents, but also from the proper choice of technological parameters, like process temperature, pressure and duration, as well as surfaces roughness, cleanliness and possible pre-conditioning. Adherents contours should be free from contaminants, and a certain degree of metal roughness and ceramic smoothness are beneficial. It is convenient to increase process duration, bonding pressure and, above all, temperature, owing to the dependency of diffusion rate D on the absolute temperature T given by the Arrhenius relationship:

$$D = e^{-Q/RT} \qquad [15.1]$$

where Q is the activation energy needed to start diffusion and R is the gas constant. However, too long process duration or too high temperature levels can induce chemical reactions at the interface, leading to ceramic discolouration, degradation, mismatch strains and residual stresses due to the misfitting of specific volumes of reaction products. In general, vacuum

© Woodhead Publishing Limited, 2013



15.8 A plot of diffusion bond strength versus CTE for various metal–alumina combinations. (Source: Reprinted from Messler, 1993, p. 516.)

or inert environment should be preferred, even if, in particular cases, an oxygen-rich atmosphere may improve the bonding between noble metals and oxide-bioceramics (Al_2O_3, ZrO_2).

Diffusion in ceramics is more difficult to induce than in metals since diffusion of two or more elements should maintain charge neutrality in ionically bonded materials. This is difficult to obtain, since diffusion is a stochastic process and non-metallic species are usually much larger than metallic ones. Besides, diffusion is a process largely relying on temperature: since diffusion rates speed-up at values approaching 60–70% of metal melting temperatures and ceramics are inherently refractory (i.e. have very high melting points) materials, satisfactory diffusion rates inside ceramics can hardly be obtained in case of low-melting metallic adherents (Messler, 2004).

Other solid-state non-fusion techniques are: electrostatic bonding, where a voltage applied across the adherents improve ionic conduction and induce electrostatic attractive forces, friction welding and ultrasonic welding, although these two latter processes are made difficult by ceramics inherent low plasticity. In any case, once the bonding between a metal and a ceramic is obtained, its stability and reliability should be preserved during the entire service life of the assembly. The main issue concerns its ability to accommodate non-mechanical strains and residual stresses due to CTE mismatch.

© Woodhead Publishing Limited, 2013

They arise at metal–ceramic interface during cooling down after joint fabrication or are due to temperature excursion during autoclave sterilization of the implantable prosthesis or instrumentary tool. To this regards, a proper design of the device is of crucial importance, even though diffusion-bonded joints can hardly accommodate such kind of mismatches, owing to the high values of pressure which have had to be applied to cause bonding.

15.4.2 Indirect bonding techniques

The most widely used method for obtaining strong and reliable joints between metals and ceramics consists in using intermediate materials, which allows the chemical, physical, thermal and mechanical incompatibilities of these classes of materials to be overcome. These materials may be polymeric adhesives, glasses, glass–ceramics, oxide-mixtures or (more often) metals or metallic alloys. The intermediates may be in solid- or liquid-state, but, in any case, give rise to the so-called indirect bonding techniques.

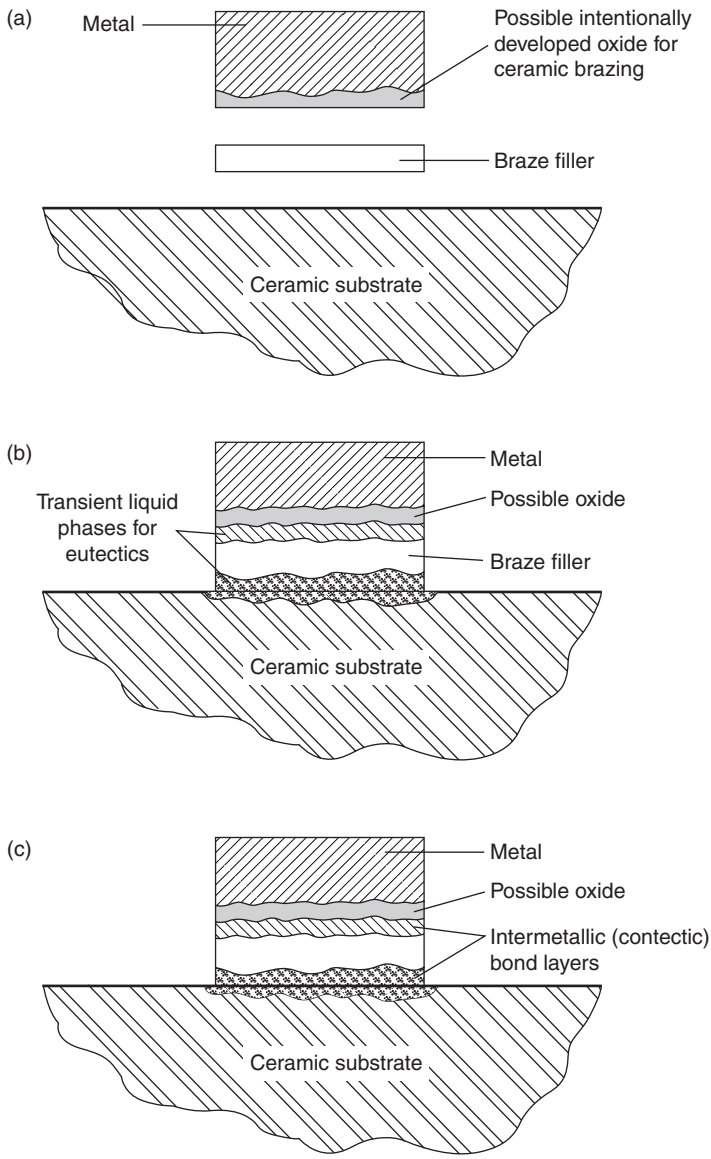
In general, solid-phase indirect bonding techniques performed through hot-pressed metallic interlayers are characterized by two advantages if compared with liquid-phase processes: (i) since bonding agent remains in the solid-state, no concerns about metal–ceramic wettability arises; (ii) intrinsic ductility of metallic interlayer is particularly efficient in accommodating CTE mismatches. This particularly holds when low-melting-point metals are adopted and low process temperatures can be kept; besides, the danger of thermal degradation is minimized. The best choice for solid-phase indirect bonding interlayers is aluminum (for joining Al_2O_3 to titanium alloys or stainless steel in instrumentary tools), to be replaced by silver when parts of implantable devices (which must comply with biocompatibility requirements) have to be joined.

In liquid-phase indirect bonding, glasses or (more often) molten metals fill the meatus between the faying surface of metal and ceramic (Fig. 15.9). The bonding occurs if both materials are satisfactorily wetted by filler and if adhesion resists to post-fabrication cooling down. Depending on the filler melting temperature, the process is called either brazing ($T_m > 450°C$) or soldering ($T_m < 450°C$). In general, glasses wet oxide-ceramics better than metals do, but these latter are more capable to accommodate the effects due to CTEs mismatch.

Usually, ceramics poor wettability descends from their localized ionic or covalent bonding, which reduces very much electrons movement capability. This particularly holds for oxide-ceramics, while borides, nitrides and – mainly – carbides can often be wetted well.

To promote wetting, inherently different materials should be made similar. The problem is to join two dissimilar un-compatible surfaces, one

© Woodhead Publishing Limited, 2013



15.9 Schematic illustration of the stages of liquid-phase bonding of metals to ceramic. (Source: Reprinted from Messler, 2004, p. 708.)

ceramic, the other metallic. To make them compatible, two approaches can be adopted: (a) to oxidize the metallic surface; in this way, the ceramic being an oxide as well, we can join an oxide to an oxide; and (b) to cover the ceramic surface with a metallic layer; in so doing, we can join a metal to

© Woodhead Publishing Limited, 2013

a metal. Metallizing can be accomplished through sintered metal powder technique, titanium hydride powder activation or refractory-metal salt process. Other methods for ceramic metallization may consist in metal–glass surface powder sintering, CVD, PVD, sublimation (vacuum metallizing), sputtering, ion plating and plasma spraying.

Another approach, called active brazing, consists in using a filler (brazing agent) containing an active metal (e.g. Ti or Zr) which reacts with the ceramic (Nicholas, 1986). Although brittle micro-structures containing intermetallic compounds may be created at the interface, limiting its capability to accommodate CTEs mismatch, active brazing can presently be considered one of the most promising techniques for structurally joining metallic and ceramic parts of medical devices (Nicholas and Crispin, 1989).

15.5 Active brazing joining techniques

Molten metals do not directly wet ceramics owing to different atomic structures. The same happens in case of indirect joining using passive filler metals (brazes). Vice versa, active brazes, doped with reactive alloying elements, induce chemical interactions with ceramics and allow more stable joints.

15.5.1 Metallurgy of active brazing

Active brazing is particularly suited to produce ceramic–metal joints. Generally molten metals do not wet ceramic materials due to the fundamentally different atomic structures. In order to wet the ceramic material, active brazes are doped with extremely reactive alloying elements like Ti or Zr (Paiva and Barbosa, 1997). The metallurgical effect of those active filler metals is to induce a chemical interaction between the filler metal and the ceramic during the brazing process. Due to a mismatch in thermal expansion coefficients of ceramics and metals, residual stresses are induced into the ceramic that can cause its failure, provided the misfit is large enough and no stress relaxation measures are undertaken. Hence, the development of ductile filler metals, in order to limit thermally induced stresses in the ceramic, is crucial. Moreover, the ceramic–metal joint has to fulfil the mechanical requirements.

For biocompatibility reasons, the metallurgical realm for the filler metals has to be restricted to alloys predominantly based on precious metals like the elements Ag, Au and Pd. To join bio-ceramics and Ti6Al4V, which is the typical alloy for the production of orthopaedic endoprosthes, these alloys must be doped with either Ti or Zr. The maximum brazing temperature has to be limited to 950°C due to possible micro-structural transformations of Ti6Al4V and with that also the liquidus temperature of the active

© Woodhead Publishing Limited, 2013

braze is limited. The liquidus temperature of Ag (961°C), Au (1064°C) and Pd (1552°C) is too high to fulfil such a requirement. Hence, non-reactive and non-toxic alloying elements, able to lower the liquidus temperature of the precious metals, are demanded. Phase diagram and biocompatibility literature show that promising elements are In, Al, Ga, Cu, Sn and Si, elements which allow reducing the liquidus temperatures for either Ag and Au. The liquidus temperature of Pd is too high to be employed as matrix metal. Therefore Pd has to be excluded as matrix metal and more Au- and Ag-based alloys should be examined. Table 15.4 lists 72 viable filler metals produced by arc-melting; chemical composition is reported, starting with the base metal and giving the percentage weight content of alloying elements; melting and wetting behaviour and hardness are indicated as well (Sicking, 2000). Noble metals Au, Ag and Pd are fully biocompatible, Al and Sn are surely non-biocompatible, while the bio compatibility of In and Ga is still questionable, even if considered satisfactory in most literature (Kimura, 1988; Iijima, 1989; Chandler *et al*. 1994; Wataha *et al*., 1994).

Due to the overwhelming importance of the wetting behaviour, wetting tests should be performed for all filler metals containing active elements and typical bio-ceramics alumina (Al_2O_3) and zirconia (ZrO_2) in a vacuum furnace (950°C/10 min heating/cooling rate). Most of the Ag-based alloys show an acceptable ($\alpha < 90°C$) or good ($\alpha < 30°C$) wetting behaviour and thick reaction layer on both substrates. An increase in the Au content leads to an enhanced wetting angle and reduced reaction layer thickness. For this reason only four Au-containing alloys (numbers 39, 58, 59, 72) may be considered as promising. An interesting aspect is the change in colour of the zirconia substrate due to the chemical reaction in the interface. This change is a hint referring to the extent of the occurring interface reaction. The colour change is caused by an oxygen diffusion from the former stochiometric ZrO_2 to the reaction layer which is formed at the ceramic–metal interface. A detailed evaluation and assessment of melting ranges (T_{sol}/T_{liq}), hardness and micro-structure shows the suitability of 38 filler metals among the original 72. The additional consideration of wetting behaviour and filler metal spreading on oxide ceramics substrates, as well as the discolouration of ZrO_2 lead to the selection of 11 most promising active brazes (numbers 5, 9, 11, 18, 27, 38, 39, 45, 58, 59, 72).

Brazing experiments should be performed in a vacuum furnace with a vacuum quality of 5×10^{-5} to 1×10^{-4} mbar to further investigate the suitability of such active brazes. The ceramic samples to be employed have a surface roughness of $R_a < 0.4$ μm since wetting experiments show that a higher surface quality does not induce a significant improvement in the wetting behaviour. A maximum brazing temperature of 950°C and a dwell time of 10 min are employed to evaluate the suitability of the filler metals for joining Ti6Al4V to oxide ceramics. These parameters guarantee a sufficient

© Woodhead Publishing Limited, 2013

Table 15.4 Chemical composition, melting and wetting behaviour and hardness of 72 viable filler metals, fabricated by arc melting

Braze number	Composition	Temperature			Wetting angle α (°)		Hardness HV 0.2
		T_{sol} (°C)	T_{liq} (°C)	ΔT (°C)	Al_2O_3	ZrO_2	
1	AgIn5Ti1	925	960	35	34	36	58.3
2	AgIn10Ti1	877	940	63	30	30	61.7
3	AgIn15Ti1	813	898	85	33	54	74.4
4	AgIn5Ti3	923	951	28	28	29	71.1
5	AgIn10Ti3	883	922	39	25	29	74.5
6	AgIn15Ti3	825	914	89	30	33	85.0
7	AgIn5Zr1	915	951	36	43	24	64.5
8	AgIn10Zr1	876	921	45	24	34	73.1
9	AgIn15Zr1	815	887	72	29	28	85.4
10	AgIn5Zr3	915	950	35	34	41	79.6
11	AgIn10Zr3	885	920	35	25	29	102.5
12	AgIn15Zr3	819	900	81	30	40	93.4
13	AgAl1Ti1	920	957	37	41	38	71.4
14	AgAl3Ti1	858	906	48	37	34	75.1
15	AgAl5Ti1	799	857	58	90	90	77.6
16	AgAl1Ti3	937	969	32	22	48	61.5
17	AgAl3Ti3	876	919	43	21	52	80.2
18	AgAl5Ti3	826	882	56	24	20	86.6
19	AgAl1Zr1	934	963	29	26	30	69.0
20	AgAl3Zr1	861	908	47	43	38	52.7
21	AgAl5Zr1	796	854	58	40	>90	72.8
22	AgAl1Zr3	950	974	24	35	23	85.5
23	AgAl3Zr3	889	931	42	33	24	65.5
24	AgAl5Zr3	822	876	54	28	38	72.9
25	AgGa3Ti1	890	954	64	32	17	50.1
26	AgGa5Ti1	841	925	84	46	42	52.0
27	AgGa7Ti1	795	900	105	21	29	67.5
28	AgGa3Ti3	919	979	60	21	33	50.7
29	AgGa5Ti3	831	946	115	35	27	44.7
30	AgGa7Ti3	818	916	98	37	34	50.2
31	AgGa3Zr1	890	955	65	45	33	55.4
32	AgGa5Zr1	839	927	88	57	46	57.6
33	AgGa7Zr1	818	899	81	28	28	60.1
34	AgGa3Zr1	910	975	65	40	20	63.4
35	AgGa5Zr1	890	944	54	20	90	62.6
36	AgGa7Zr1	831	926	95	42	22	64.9
37	AgPd5Al15	782	852	70	–	–	98.5
38	AgPd5Al5Ti3	828	877	49	40	33	65.4
39	AgAu10Al5Ti3	780	864	84	29	25	93.7
40	AgAu30Al5Ti3	741	853	112	–	–	200.2
41	AgAu50Al5Ti3	752	774	22	–	–	358.5
42	AuAl4Ti3	579	607	28	–	135	283.5
43	AuAl2Ti3	527	571	44	–	151	288.5
44	AgPd5In10	889	934	45	–	–	59.1
45	AgPd5In10Ti3	882	928	46	–	20	58.1
46	AgPd5In10Zr3	880	925	45	24	42	77.7
47	AgPd5In10Zr2,1	880	926	46	62	69	94.8
48	AgPd10In10	881	932	51	–	–	63.8

(*Continued*)

© Woodhead Publishing Limited, 2013

Table 15.4 Continued

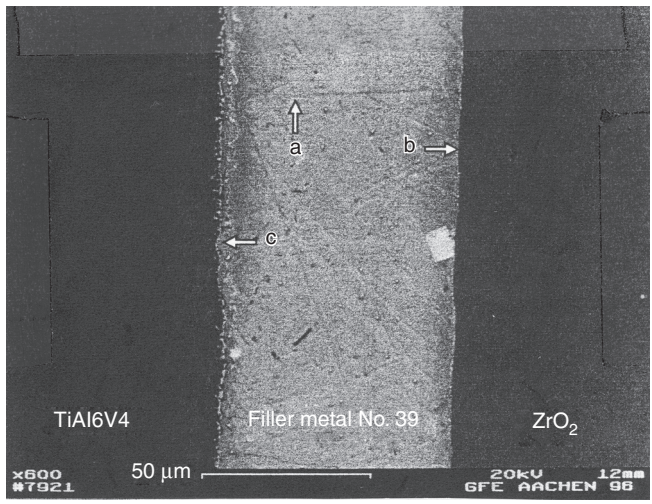
Braze number	Composition	Temperature			Wetting angle α (°)		Hardness HV 0.2
		T_{sol} (°C)	T_{liq} (°C)	ΔT (°C)	Al_2O_3	ZrO_2	
49	AgPd15In15	829	898	69	–	–	86.0
50	AuAg45In10Ti3	884	>1000	-	–	–	113.1
51	AuAg45In10Zr3	849	892	43	–	–	85.0
52	AuAg45In10Pd3	829	953	124	–	–	73.7
53	AuAg15In10Ti3	611	808	197	–	–	167.1
54	AuIn23Ti3	467	512	45	–	–	281.2
55	AuIn23Zr3	470	483	13	–	–	302.5
56	AuIn23Pd3	478	601	123	–	–	374.2
57	AuIn7Ti3	642	1059	417	–	75	217.1
58	AuSn19Ti3	273	354	81	60	95	169.4
59	AuSn19Zr3	286	339	53	110	3	180.3
60	AuSn19Pd3	306	358	52	–	–	193.1
61	AuAg16Pd3Sn10	537	549	12	–	–	147.8
62	AuSi3,05Ti3	377	841	464	140	116	350.2
63	AuAg23,5Si9,3Ti3	486	946	460	52	128	174.5
64	AuAg13,8Si2,44Ti3	417	768	351	71	78	221.6
65	AgAu16In7Al1Ti3	508	812	304	–	–	201.1
66	AuIn4.5Al1	817	840	23	–	–	131.9
67	AuIn4.5Al1Ti3	537	591	54	–	–	230.0
68	AuIn4.5Al1.5Ti5	481	507	26	–	90	262.0
69	AuIn6Ga1	870	892	22	–	–	112.7
70	AuIn4.5Al0.25Ga0.8	894	917	23	–	–	94.8
71	AuAl10.5Ga2	934	949	15	–	–	112.1
72	AuCu20Ti3	924	943	19	–	69	200.0

energy input to trigger the chemical reaction at interface and to avoid harmful micro-structural transformations of Ti6Al4V. Brazing experiments point out how difficult is to actively braze Al_2O_3 and Ti6Al4V: as a matter of fact, with the exception of filler metal number 38, all joints crack due to CTEs mismatch. Viceversa, brazing experiments employing ZrO_2 and Ti6Al4V show encouraging results. Metallographic evaluation and discolouration of ZrO_2 lead to the selection of the best seven active brazes (numbers 5, 9, 11, 18, 38, 39, 45) among the original 11. Further analysis of interfacial reaction products allows to select three filler metals: numbers 38 and 39 may be selected due to their excellent mechanical behaviour, number 9 in consideration of preliminary biocompatibility tests. Table 15.5 summarizes the results of four-point-bending mechanical tests performed on samples actively brazed with these three filler metals and different brazing parameters. However, a set of optimized parameters has to be defined for filler metals according to two criteria: maximization of mechanical strength and minimization of energy input.

© Woodhead Publishing Limited, 2013

Table 15.5 Four-point-bending strength of coupons actively brazed with filler metals number 39, 38 and 9

Filler metal		Number 39		Number 38		Number 9		
Dwell time		10 min	5 min	10 min	5 min	10 min	5 min	0 min
Brazing temp.	950°C	377.2	304.7	254.0	223.3	102.0	–	–
	900°C	391.1	245.7	139.0	190.0	–	89.6	103.2
	850°C	–	–	–	–	–	–	24.8



15.10 SEM image of an actively brazed Ti6Al4V–ZrO_2 joint with filler metal number 39. (a) Filler, (b) filler–ceramic interface and (c) metal–filler interface.

Figure 15.10 shows a SEM image of an actively brazed Ti6AlV4–ZrO_2 joint employing the optimized set of parameters for braze number 39. The corresponding line-scan shows that the filler metals micro-structure is almost homogeneous and contains mainly silver with little aluminium in solid solution. The grid content is next to zero. Table 15.6 shows quantitative analysis of a representative peak within the filler metal (spot a in Fig. 15.10). The filler metal thickness is around 65 µm. The white-coloured hard phase is made of Au, Al, Ti and Zr. The reaction layer at the interface between filler metal and ZrO_2 is hardly visible but is thinner than 1 µm (spot b in Fig. 15.10). A grey-coloured band of thickness 3–5 µm appears between filler metal and Ti6Al4V (spot c in Fig. 15.10). The line-scan shows an enrichment of Au, Al and Ti for this zone. A quantitative analysis of a representative peak gives the chemical composition reported in Table 15.7. Figure 15.11 shows a SEM image of Ti6Al4V–ZrO_2 joint brazed with the optimized set of parameters for

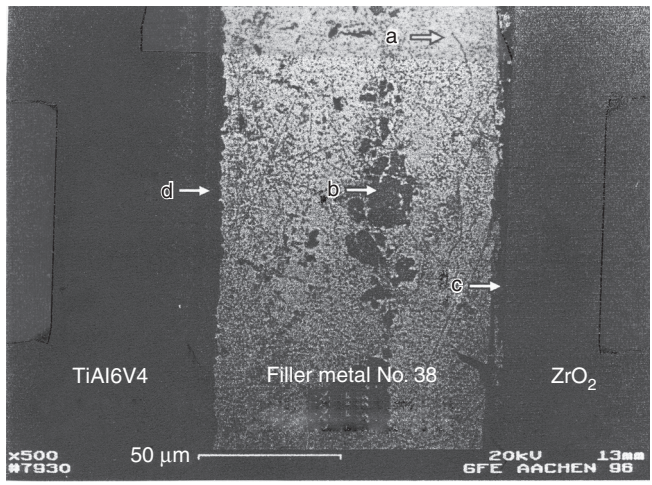
© Woodhead Publishing Limited, 2013

Table 15.6 Quantitative SEM analysis of filler metal number 39 (spot a in Fig. 15.10)

Element	Weight %	Atomic %
Silver (Ag)	94.97	86.94
Gold (Au)	1.61	0.81
Aluminum (Al)	3.25	11.90
Titanium (Ti)	0.17	0.35

Table 15.7 Quantitative SEM analysis at Ti6Al4V – filler–metal interface (spot c in Fig. 15.10)

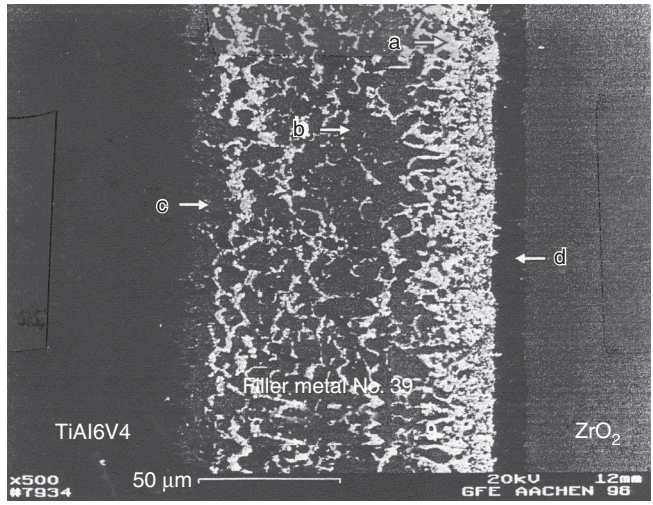
Element	Weight %	Atomic %
Silver (Ag)	1.89	1.10
Gold (Au)	44.47	14.18
Aluminum (Al)	14.16	32.96
Titanium (Ti)	39.48	51.76



15.11 SEM image of an actively brazed Ti6Al4V–ZrO_2 joint with filler metal number 38. (a) Filler, (b) inclusion, (c) filler–ceramic interface and (d) metal–filler interface.

braze number 38. Figure 15.12 shows a typical SEM image of Ti6Al4V–ZrO_2 joint brazed with filler metal number 9. A quantitative SEM analysis shows that the higher thickness of the reaction layer and the Ti-containing hard phase at mid-seam lead to lower mechanical performances. When filler metal number 9 is adopted, Ti coming from Ti6Al4V has no barrier which avoids erosion into the seam: as a consequence the lowest strength is achieved.

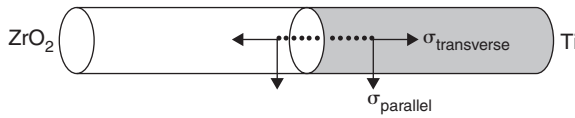
© Woodhead Publishing Limited, 2013



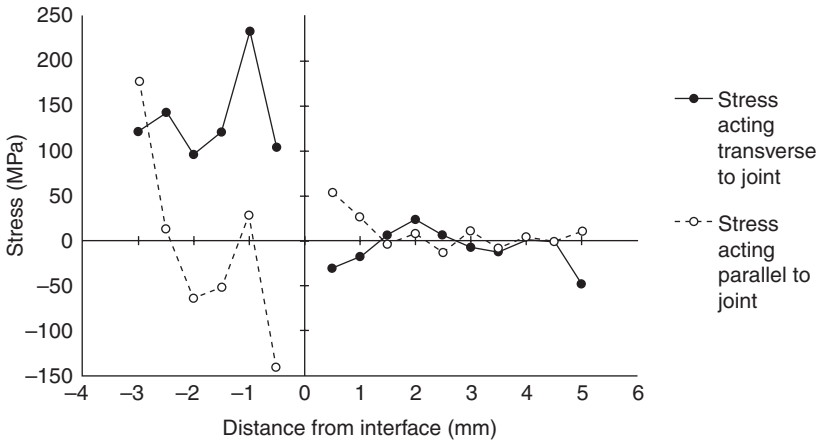
15.12 SEM image of an actively brazed Ti6Al4V–ZrO_2 joint with filler metal number 9. (a) Filler, (b) inclusion, (c) metal–filler interface and (d) filler–ceramic interface.

Joining of metals to ceramics leads to development of residual stresses due to the CTEs mismatch between the two materials. The magnitude and the nature (compressive or tensile) of such stresses depend on the extent of such mismatch, the component dimensions and the brazing temperatures. These stresses are usually the highest in magnitude at and near the joint region. High tensile stresses reduce the strength of joints and lead to cracking. A knowledge of such stresses, along with the results of mechanical tests are necessary to optimize the choice of brazing alloy and brazing parameters. To measure residual stresses, cylindrical metal/ceramic coupons 50 + 50 mm long, 10 mm in diameter may be used, whose geometrical details are summarized in Fig. 15.13. The measurement must be carried out across the joint interface at different locations and intervals of 0.5 mm along two directions viz. transverse and parallel to the joints. An X-rays stress analyser should be used to perform the measurement. Reflection may conveniently be analysed along 222 crystallographic plane with filtered Cr radiation (Ti6Al4V) and 133 crystallographic plane with filtered Co radiation (ZrO_2). The irradiated area should be small enough (typically 0.5 mm × 4 mm). The beam-length direction must always be parallel to the joint interface in order to have a linear distance resolution of 0.5 mm. The measurements is usually performed according to the $\sin^2\Psi$ method. For each stress computation, strain acting along eight different Ψ-directions are measured from X-ray diffraction line-shift analyses. It is convenient to use a least-square linear fitting procedure for computing stresses (elastic moduli taken from literature may be

© Woodhead Publishing Limited, 2013



15.13 Specimens for four-point-bending testing.



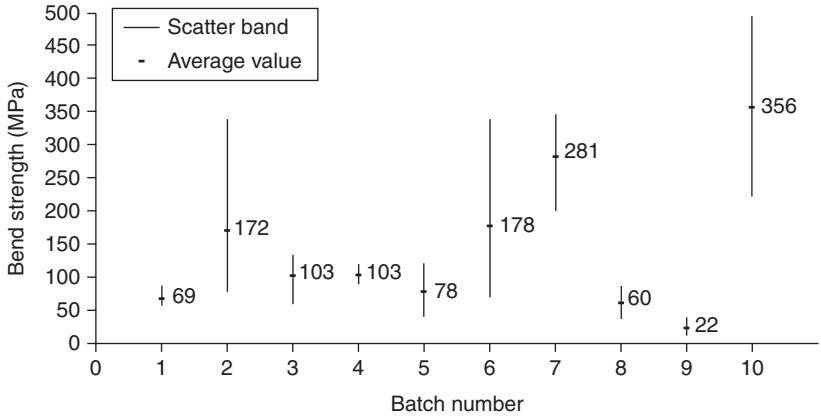
15.14 Residual stress measurement across Ti6Al4V (left) and ZrO_2 (right) joint.

used to obtain stresses from measured strain data). A typical result is shown in Fig. 15.14. The measures at ZrO_2 side of the joints show negligible scatter: stresses are mostly compressive and low in magnitude, except at regions very close to the joint interface where increase significantly. At Ti6Al4V side of the joints, tensile stresses are present at most locations. Close to the interface, most cases indicate low tensile or compressive stresses. This has to be expected, since CTEs mismatch is mostly felt in these areas. In case of Ti6Al4V–Al_2O_3 joints, measurements at Al_2O_3 side point out steep compressive stresses up to 1.5 mm from the interface, in both longitudinal and transverse directions.

15.5.2 Mechanical characterization

The mechanical characterization of actively brazed joints is generally performed through four-point-bending tests, using cylindrical specimens 10 mm in diameter, with 40 mm outer span and 20 mm inner span. The specimens are made of two halves, one metallic (Ti6Al4V) and one ceramic (Al_2O_3 or ZrO_2) brazed together. Since ceramic represents the critical part of the specimen, testing should be carried out in compliance with standards for

© Woodhead Publishing Limited, 2013



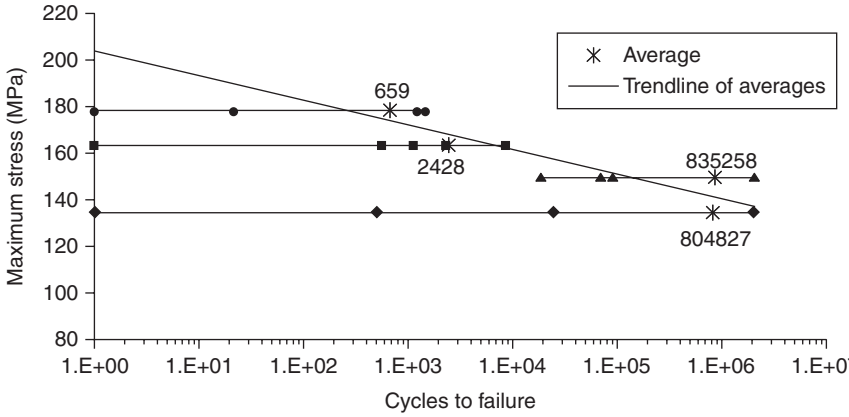
15.15 Four-point-bending static strength of brazed specimens (see Table 15.8).

Table 15.8 Correspondence between test batches and filler metals

Test batch number	Filler metal number	Composition	Metal adherent	Ceramic adherent
1	CB1	AgCu19,5In5Ti3	Ti6Al4V	ZrO_2
2	VH 780	AgCu28	Ti6Al4V	ZrO_2
3	5	AgIn10Ti3	Ti6Al4V	ZrO_2
4	9	AgIn15Zr1	Ti6Al4V	ZrO_2
5	11	AgIn10Zr3	Ti6Al4V	ZrO_2
6	18	AgAl5Ti3	Ti6Al4V	ZrO_2
7	38	AgPd5Al5Ti3	Ti6Al4V	ZrO_2
8	45	AgPd5In10Ti3	Ti6Al4V	ZrO_2
9	38	AgPd5Al5Ti3	Ti6Al4V	Al_2O_3
10	39	AgAu10Al5Ti3	Ti6Al4V	ZrO_2

bending tests of technical ceramics (e.g. AFNOR B41–104). Testing has to be performed in servo-hydraulic testing machines under position control and slow cross head displacement rate (0.1–0.5 mm min^{-1}). Fatigue tests should be performed in servo-hydraulic machines as well, using the same loading set-up and frequencies not higher than 10 Hz in tension-tension ($R = 0.1$). Figure 15.15 presents the results of static tests performed on specimens brazed with the filler metals summarized in Table 15.8. These tests show poor mechanical performances of most Ti6Al4V–Al_2O_3 specimens, to the exception of those brazed with filler metals 9, 38, 39. Testing on Ti6Al4V–ZrO_2 specimens should be performed with both 'white' and 'black' zirconia. The dark layer appearing in white zirconia near the brazed interface, due to diffusion phenomema, is detrimental because of aesthetic reasons, but does not affect mechanical performances.

© Woodhead Publishing Limited, 2013



15.16 Four-point-bending fatigue strength of brazed specimens.

Fatigue tests should be performed under the same four-point-bending condition, at a maximum stress level slightly lower than the ultimate static bending strength and run-out at 2×10^6 cycles. Tests results are summarized in Fig. 15.16. Notwithstanding high scatter in results, mainly affecting the first-quarter cycle (loading to start point), a qualitative trend-line can be established. SEM fracture surface analysis does not reveal any crack propagation. In most cases, fractures close to the point of maximum stress suggest mixed-mode failures, with cracks running from the ceramic-filler–metal interface to the metal-filler–metal one.

15.5.3 *In-vitro* testing

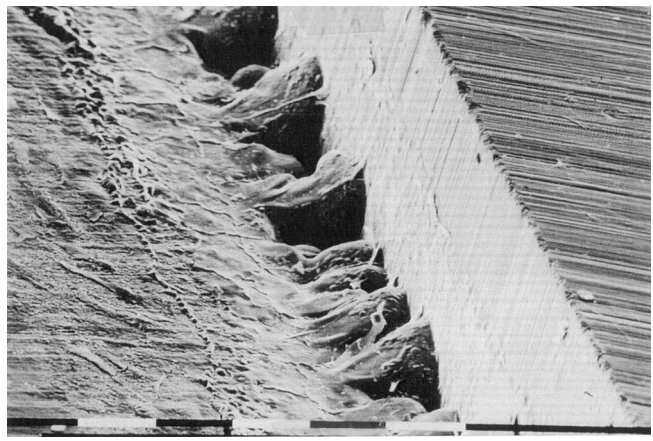
To *in-vitro* evaluate biocompatibility characteristics of metal–ceramic brazed joints and to assess the most suited filler metals, three crucial aspects should be analysed: (i) cell growth in presence of the material to be tested; (ii) cell adhesion and spreading; (iii) cell differentiation analysis. Human osteoblasts are employed as *in-vitro* cells assay. Osteoblasts are seeded in triplicate onto the Ti6Al4V-Al_2O_3 brazed samples and onto the negative control (polystirene dishes), using multiwell plates, at a density of 4000 cells/mL, in DMEM – 10% FCS. The incubation times are 24 h, 4, 7, 14, 21, 28 days. At the end of each incubation period, cells are detached from the substrate by tripsinization and incubation in trypan blue. The number of living cells is measured by using both haemocytometer and MTT colorimetric assay. The number of floating cells, the number of cells adhering to substrate and the ratio adhering/floating cells are assessed in each brazed sample. As far as cell differentiation analysis is concerned, osteoblasts cultures are stained

© Woodhead Publishing Limited, 2013

with a modified von Kossa procedure for detection of Ca++ deposition. The presence of alkaline phosphatase (ALP) activity is determined through the Gomori's method. The production of alkaline phosphatase is measured in cell lysates obtained after sonication of the cell pellet, by means of spectrophotometric analysis. Immuno-histochemistry uses the following antibodies: anti-type I, type II and type III collagen, anti-osteonectin, anti-vimentin and anti–fibronectin. Each slide is observed by light-microscopy and analysed by an image-analysis system. Samples for cell-adhesion analysis are prepared and observed using SEM.

Osteoblast count shows that filler metals numbers 5, 9 and 11 do not significantly inhibit osteoblasts proliferation as compared with control cultures. Cell survival is about 50% for filler metals numbers 39, 45 and 38, while commercial brazes CB1 – AgCu19,5In5Ti3 and VH 780 – AgCu28 show a high degree of citotoxicity. The number of floating cells is high for filler metals numbers 5, 9 and 11, owing to the persistence of a de-differentiated condition of the cultured cells. The number of adhering cells, which is related to the differentiation process of cultured cells, is high for filler metals numbers 39, 9, 11 and 45, while cell attachment is not detectable for filler metal number 18, CB1 and VH 780. If one consider the ratio between adhering and floating osteoblasts, or the ratio between the adhering and the total cell count, filler metals numbers 39 and 45 exhibit the highest values, followed by numbers 9, 38 and 11. As far as cell differentiation is concerned, filler metals numbers 11, 45 and 9 show the highest values of ALP production in the culture medium all along the culture period, followed by numbers 18 and 39. Moreover, if the ratio between ALP production and total number of cultured cells or the number of adhering cells is considered, filler metals numbers 45, 11, 18, 39 and 9 perform better. Such results suggest that only filler metals numbers 45, 11, 18, 39 and 9 are able to induce osteoblasts differentiation, while all the other ones seem to inhibit this process, as confirmed by histochemical analysis. Calcium deposition, as revealed by the von Kossa staining method, is found on filler metals numbers 39, 45 and 11. Immuno-histochemistry with anti-type I collagen antibodies is highly positive in samples numbers 39, 45 and 9. Anti-type III collagen immune reaction show to be positive in filler metals numbers 39, 45 and 9. Anti-osteocalcin is positive in filler metals numbers 39, 11 and 9. Finally, anti-vimentin is positive in filler metals numbers 45, 39, 11 and 9. As far as the morphology of adhering osteoblasts is concerned, cells show to be polygonal or elongated in shape, with the maximum diameters ranging between 15 and 20 μm, bearing villi, phyllopodia and lamellopodia. For CB1 filler metal, the number of adhering osteoblasts is low, above all on the brazed surface. They are flattened- and spindle-shaped, indicating the condition of metabolic resting. Osteoblasts adhesion in VH 780 filler metal is mild on the brazed surface as well. Most of them are flattened, but some are swollen and metabolic active.

© Woodhead Publishing Limited, 2013



15.17 Adhering cells on sample brazed with filler metal number 39.

The number of adhering cells per unit area is high in number 5 filler metal, but flattened, polygonal and not showing typical features of cells differentiation. Osteoblasts are less numerous in numbers 9, 11 filler metals, where the brazed surface shows both spindle-shaped and swollen cells, while osteoblasts are much more numerous on the metallic (Ti6Al4V) surface. On the contrary, filler metal number 18 shows a higher number of adhering cells on the ZrO_2 surface, but are located far from the brazed surface. Subtile osteoblast cytoplasmic elongations bridging the two opposite surfaces can be found in filler metal number 38, where the number of cells per unit area is high on the brazed surface as well. Filler metal number 45 shows a high percentage of adhering osteoblasts. Cells are well differentiated and metabolically active. Filler metal number 39 shows the most effective features: osteoblasts number per unit area is about 4–5 times higher than for other filler metals. Cells are firmly attached to both ZrO_2/Ti6Al4V surfaces and to the brazed area. They are swollen, exhibiting a ruffled surface and are actively sintetizing collagen and bone matrix (see Fig. 15.17). To quantitatively assess the *in-vitro* biological response of each filler metal, a scoring scale can be used. A score ranging from 1 to 9 is assigned to each filler metal per each test (cell growth, cell adhesion, ALP production, cell differentiation and cell adhesion on the brazed surface), depending on their better or worse behaviour. The results are reported in Table 15.9: filler metal number 39 gets the highest score, followed by samples numbers 45, 9, 11 and 5. The analysis of the results allows one to divide filler metals into four groups:

1. Filler metals numbers 9 and 11 promote osteoblasts growth and stimulate bony phenotype expression, but inhibit cells adhesion;

© Woodhead Publishing Limited, 2013

Table 15.9 Ranking of filler metals according to cell growth, cell adhesion, ALP production, cell differentiation and cell adhesion on brazed surface

Filler metal	Cell growth	Cell adhesion	ALP production	Cell differentiation	Cell adhesion brazed surface	Total
CB1	2	2	4	2	3	13
VH 780	1	1	1	1	1	5
5	7	4	2	7	7	27
9	8	7	5	6	5	31
11	9	6	8	5	2	30
18	3	3	7	4	6	23
38	4	5	3	3	4	19
45	5	8	9	8	8	38
39	6	9	6	9	9	39

2. Filler metals CB1 and VH 780 inhibit cell growth, attachment and osteoblast differentiation;
3. Filler metals numbers 18 and 38 show a slight growth curve, very bad adhesiveness and do not inhibit differentiation;
4. Filler metals numbers 39 and 45 enhance cell proliferation, attachment and differentiation.

15.5.4 Industrial processing

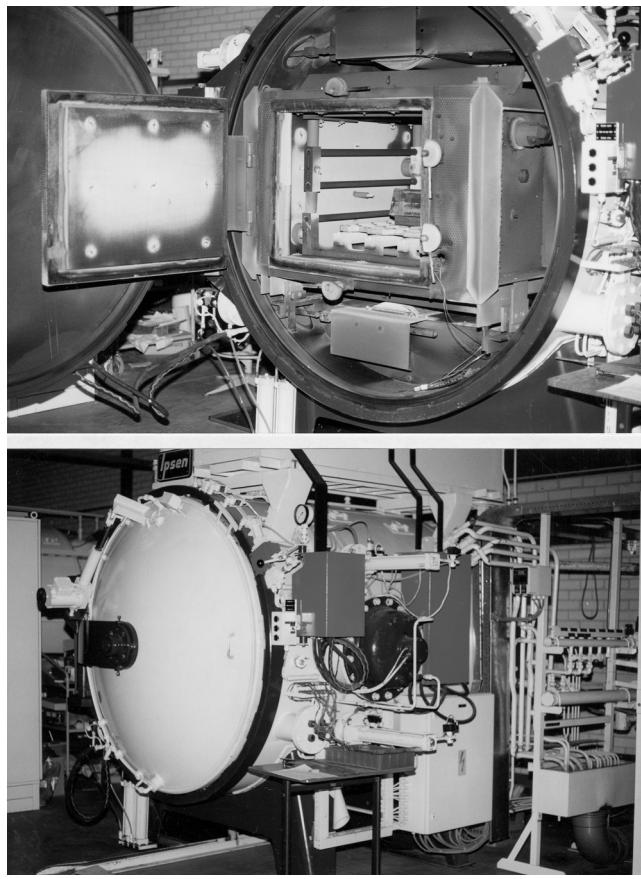
Typical active brazing conditions for joining Al_2O_3 or ZrO_2 ceramics to Ti6Al4V alloy are given in Table 15.10.

The type of brazing furnace should be chosen once components dimensions and optimum brazing conditions are identified. Different kinds exist, equipped with graphite or molybdenum heating elements; the main choice criteria should take into account: (a) maximum temperature capability (compliant with brazing temperature); (b) temperature uniformity; (c) chamber dimensions (compliant with the dimensions of the parts to be brazed and brazing fixtures); (d) cooling rate capability (<5°C/min); (e) degree of vacuum ($<2 \times 10^{-6}$ mbar). Figures 15.18 and 15.19, respectively, show furnace and metal/ceramic cylindrical coupons aligned within the fixture, with numbers 9, 38 and 39 braze foils placed at samples interface contacts. Titanium parts should be placed upon ceramic parts to guarantee uniform self-weight loading during brazing. The fixture keeps the samples inclined at 10° from the vertical and is provided with a front cover to enable uniform heating/cooling conditions. Figure 15.20 reports the theoretical brazing cycle for

© Woodhead Publishing Limited, 2013

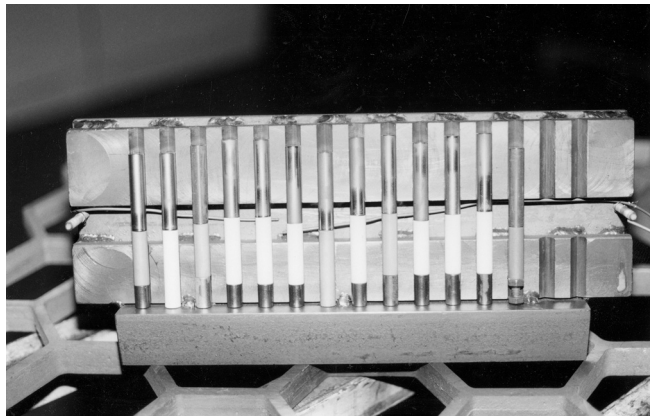
Table 15.10 Typical active brazing conditions for joining Al_2O_3 or ZrO_2 ceramics to Ti6Al4V alloy

Atmosphere:	5×10^{-5} to 1×10^{-4} mbar (vacuum)		
Heating cycle:	1. heating rate:	20°C/min	(20–700°C)
	1. dwell time:	10 min	
	2. heating rate:	10°C/min	(700°C – T_{braze})
	Brazing temperature:	T_{braze}	(according to filler-metal specifications)
	2. dwell time:	t_{dwell}	(according to filler-metal specifications)
	1. cooling rate:	20°C/min	(T_{braze} – 500°C)
	2. cooling rate:	<5°C/min	(500°C–20°C)

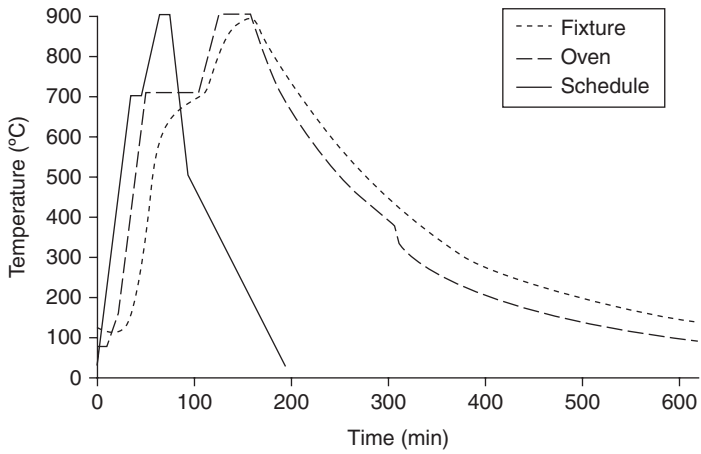


15.18 Graphite-heating-elements vacuum brazing furnace.

© Woodhead Publishing Limited, 2013



15.19 Arrangement of cylindrical samples within the fixture before brazing.

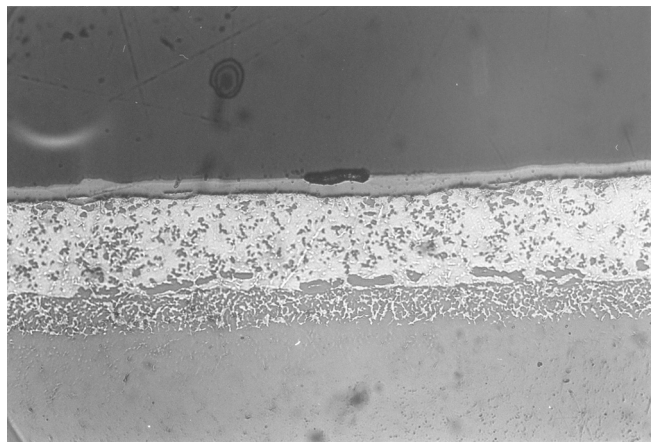


15.20 Temperature brazing cycle for filler metal number 39.

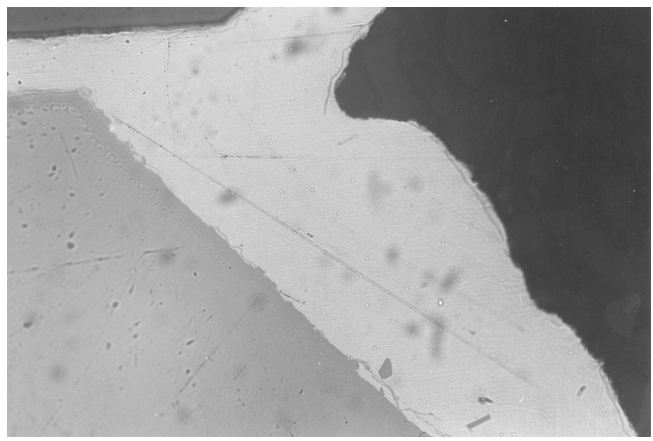
filler metal number 39, along with actual temperature profiles measured by means of thermo-couples inside furnace and fixture.

Once brazing process is completed, SEM analysis should be performed, considering both as-brazed surfaces and cross-sections made through the joints. Figures 15.21 and 15.22, respectively, show the typical micro-structure of numbers 38 and 39 alloys brazed joints. Figure 15.23 reports the compositional (energy dispersive X-ray spectroscopy – EDX) dot mapping for Ag, Al, Ti, Au and Zr (from top left to bottom right, respectively), showing the elemental partitioning between different micro-structural features. Selected area EDX analyses may be carried out at different locations and

© Woodhead Publishing Limited, 2013



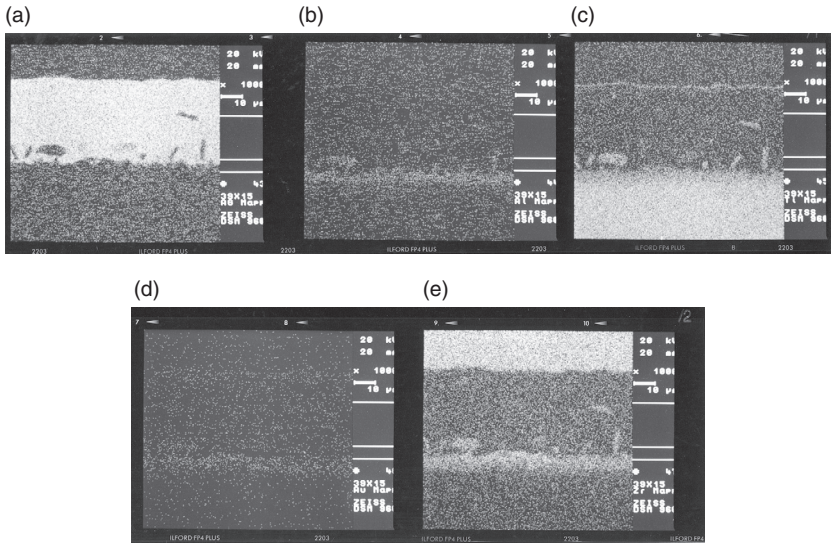
15.21 Centre of the joint brazed with filler metal number 38. Wide zirconia discolouration, reaction between brazing agent and titanium alloy and voids should be noted. Magnification × 2000.



15.22 Edge of the joint brazed with filler metal number 39. Absence of zirconia discolouration and limited reaction between brazing agent and titanium alloy should be noted. Magnification × 2000.

interesting micro-structural features, to semi-quantitatively determine their compositions. The energy dispersion spectra obtained from number 39 brazed joints are shown in Fig. 15.24. From the strength, micro-structure and joint integrity points of view, filler metal number 39 can be considered the best choice for industrial production of brazed-metal/ceramic orthopaedic prostheses. However, the wettability on ceramic could be improved through pre-metallization for obtaining more uniform braze interface.

© Woodhead Publishing Limited, 2013



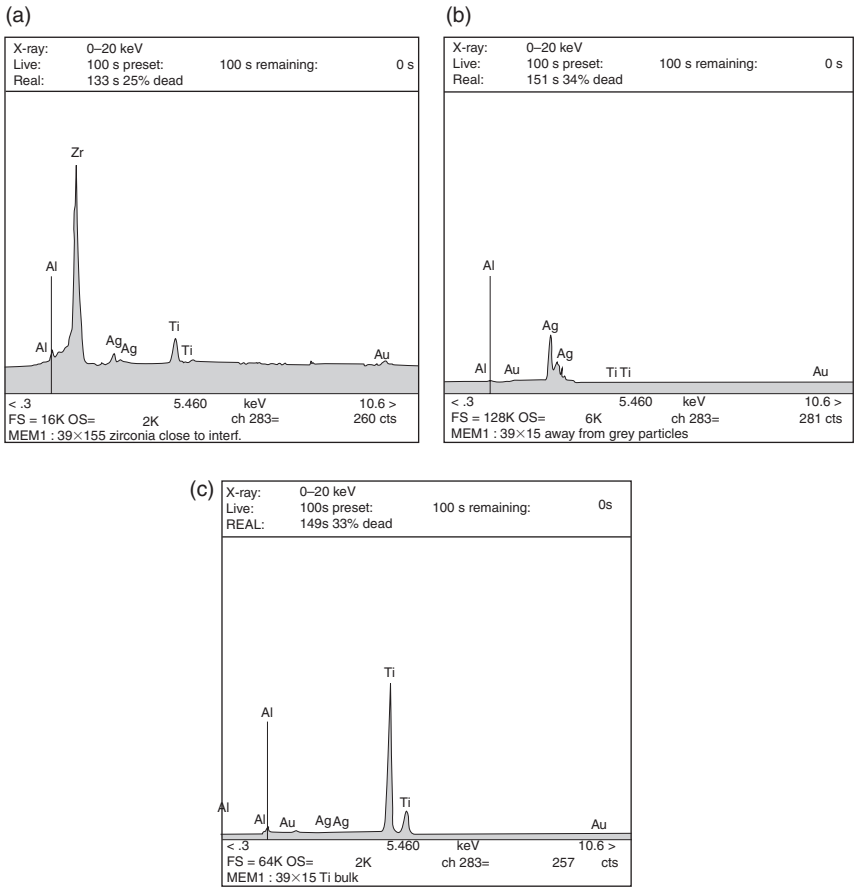
15.23 Compositional EDX dot mapping of the joint brazed with filler metal number 39. (a) Ag, (b) Al, (c) Ti, (d) Au, (e) Zr.

The nominal chemical composition of the filler metal is decisive to get optimal brazing results. However, it has to be remembered that the production route (laboratory scale vs industrial scale) may influence the properties of the final active braze foils. Quantitative EDX analysis on a fixed area should be used to determine the chemical composition of un-brazed foils, even if, owing to the hard-phase formation and different homogeneity of braze foils, an exact quantitative comparison is seldom possible. Moreover, the EDX analysis is not suitable to analyse the accurate titanium content. Besides measurement point, chemical composition often depends on measurement method (SEM, EDX-area, chemical wet analysis) as well. For this reason, one of these has to be chosen as the preliminary reference method.

15.5.5 Example: knee prosthesis

The ceramic condyles and the metallic body of a hybrid knee prosthesis are brazed together by means number 39 filler metal. Foils 75–80 μm in thickness are used, previously heated in vacuum at 500°C for 5 min to reduce hardness and increase ductility. The post-production examination points out some cavities at titanium/ceramic interfaces due to excessive machining clearance. As a consequence, a general rule must established, according to which clearance should not be larger than brazing foils thickness (80 μm). Non-destructive X-rays analysis shows that the brazed joint is quite uniform at the bottom horizontal contact surface, while at the 90° bend region,

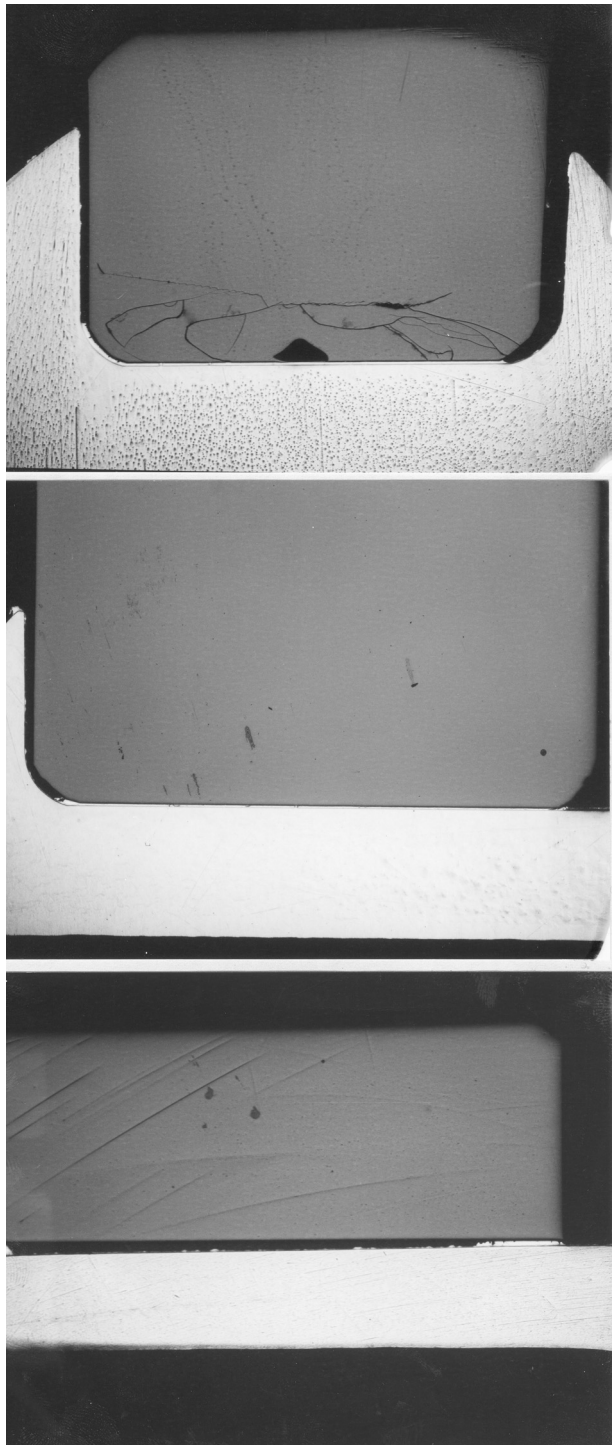
© Woodhead Publishing Limited, 2013



15.24 Energy dispersion spectra at various locations of the joint brazed with filler metal number 39: (a) 3 μm from interface, inside ZrO_2; (b) inside homogeneous brazed area; (c) 150 μm from interface, inside T16Al4V.

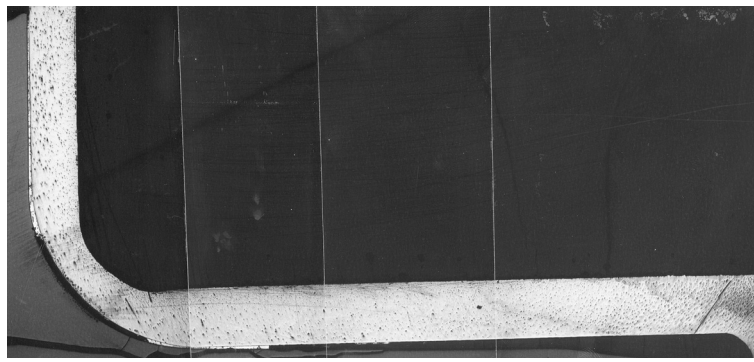
some non-brazed areas appear, due to misfitting between the parts in the as-machined conditions. To verify the homogeneity of the brazed joint, longitudinal and transverse cross-sections have to be cut, polished and analysed through optical microscopy. Metallographic investigation indicates the absence of voids, porosities and cracks. However, the onset of cracks due to intrinsic brittleness of brazing joints is one of the major concerns in industrial applications and is well documented in literature (Cannon *et al.*, 1991; Howe, 1993; Soon-Bok *et al.*, 1995; Waddell *et al.*, 2007). Figures 15.25 and 15.26 point out the features of transverse and longitudinal sections respectively, and show that locations with large clearance are not sufficiently brazed. Composition and micro-structural homogeneity of brazing foils are

© Woodhead Publishing Limited, 2013



15.25 Appearance of the transverse section cut across the brazed joint.

© Woodhead Publishing Limited, 2013

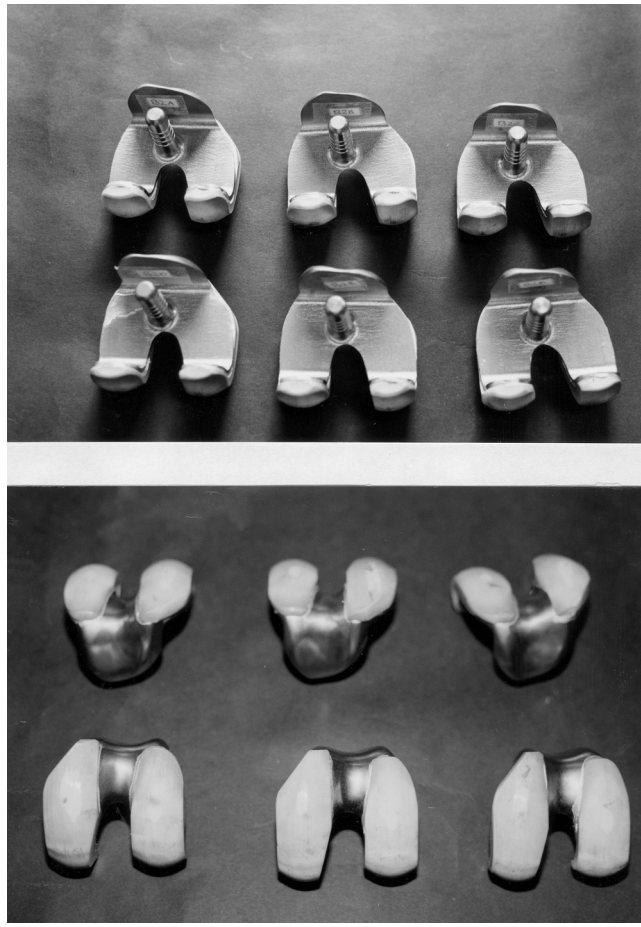


15.26 Appearance of the longitudinal section cut across the brazed joint.

analysed by means of an EDX Analyser in a Scanning Electron Microscope: large amounts of second-phase particles can be found, consisting of Au, Al and Ti, while the matrix is rich with Ag. However, since the areas considered are few square microns wide (owing to small size of electron beam), the analysis is not reliable in providing information about the bulk composition of the braze foil: to this purpose, wet chemical analysis method should be preferred. On the basis of these post-production analyses, the prostheses design should be optimized, enabling a better fitting between metallic and ceramic parts, to improve the integrity of the brazed joint. Besides, where clearances lie within the range 200–300 μm, a double layer of brazing foils should be used. Finally, special fixtures should be provided to hold metallic and ceramic components tightly together during brazing. On the basis of these experiences, some general rules can be established to obtain a good-quality brazed-metal/ceramic prosthesis (Murray *et al*., 1999):

- Tolerances in excess of about 100 μm should be avoided. Use of double layer of brazing foils helps, but not with large cavities. This has to do with the low flow properties of the braze, which reduce the capability of filling the cavities by capillary action;
- Misfits between metallic and ceramic parts are due to clearance and/or possible movements within the holding jigs at high brazing temperature. Special jigs have to designed to avoid/minimize this drawback;
- If brazing conditions are optimized, the metallic parts are shiny and the ceramic ones are free from any vapour condensation (see Fig. 15.27). In this case, the joint strength is satisfactory and the prostheses are able to withstand not only large forces occurring during machining and polishing of finished prostheses, but also simulated physiological loads (12 000 N ultimate load, 2000 N fatigue load up to 5 millions cycles – with 4.86 mg/million cycle weight loss).

© Woodhead Publishing Limited, 2013



15.27 Semi-finished metal–ceramic knee prostheses before final grinding and polishing.

15.6 Future trends

Besides active brazing technique, some other innovative processes are likely to be successfully adopted to join metals and bio-ceramics, in the field of both solid- and liquid-phase welding.

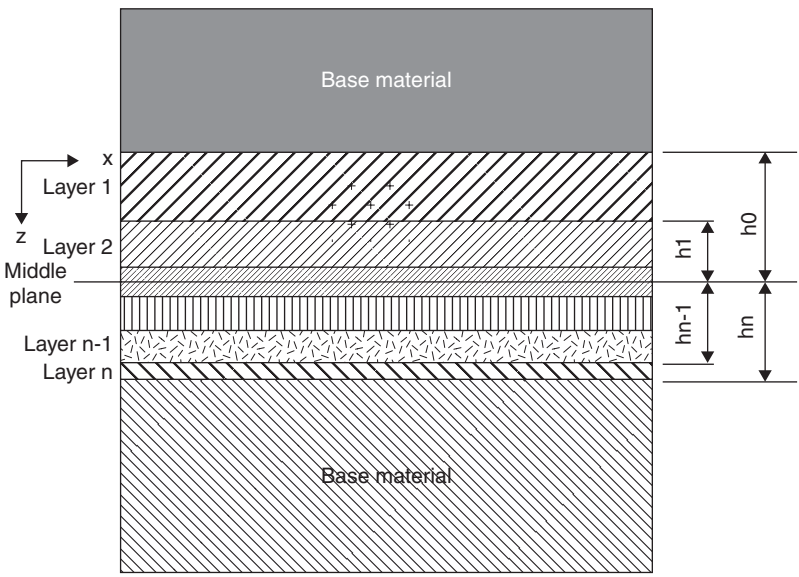
Solid-phase welds already demonstrated to be suited for joining metals and ceramic through different friction-welding processes, like ultrasonic welding and ultrasonic brazing. In ultrasonic welding, reciprocal micro-motion between the adherents is provided by ultrasonically induced vibrations. Notwithstanding ceramics have inherently poor ductility, a certain degree of plastic deformation is necessary to accomplish friction welding. Ultrasonic brazing is just an ultrasonically-assisted conventional technique, where

© Woodhead Publishing Limited, 2013

vibrations allow to remove air bubbles from the molten filler to improve wetting and filling.

Very promising are the 'functional graded material (FGM) joints', which are able to join even strongly misfitting adherents through several interlayers of gradually varying metal–ceramic compositions. Combustion synthesis (CS) and self-propagating high-temperature synthesis (SHS) represent the more efficient techniques to produce graded layers. They both are exothermic brazing processes, but in SHS a progressive reaction happens, whose front sweeps through the volume of reactants, while in CS a sudden reaction occurs. The reactants consist in powders of elemental metal and oxide, placed between the adherents. The heat generation is high enough to cause substrate surface melting and to create liquid-phase products. The reactants are packed between the solid adherents (Fig. 15.28); this sandwich is then unidirectionally compressed while the reaction is ignited: as a consequence, problems may arise if non-flat, contoured surfaces have to be joined.

Although ceramics melt at very high temperature and induce phase transformation and cracking inside the heat-affected zone, liquid-phase techniques, especially the ones based on high-energy density process, are destined to increase their popularity. Electron-beam welding (EBW) and laser-beam welding (LBW) were already used in some cases to weld corrosion-resistant metals to oxide ceramics. Both EBW and LBW use a



15.28 Schematic illustration of a functionally graded material (FGM) joint between a metal and a ceramic. (Source: Reprinted from Messler, 2004, p. 710.)

© Woodhead Publishing Limited, 2013

very high-intensity beam to produce heating and induce welding, being the energy highly concentrated by electro-magnetic or optical lens, respectively. The energy density in these processes can reach 10^{10}–10^{13} Wm^{-2}, compared with 5×10^{8} Wm^{-2} typical of conventional processes. The kinetic energy of electrons (EBW) and photons (LBW) is converted into heat as soon as the particles hit the adherents and cause melting and vaporization in a very localized area. Both processes are able to produce deep and narrow weld beads, as well as narrow heat-affected zones. In general, the EBW process is performed autogenously; in this case, matching between adherents surfaces should be perfect. However, when thick sections have to be welded, filler metal is needed, preferably in the form of *in situ* shims, since getting wire down into a deep weld is difficult. LBW is usually performed autogenously as well, but using wires as filler metal. Shielding of EBW process is guaranteed by a certain degree of vacuum (typically 10^{-3}–10^{-5} bar), which is needed for allowing the electron beam to flow towards the adherents without collisions in the air. Alternatively, shielding of LBW process is accomplished by means of inert gases, which are supplied to create a non-oxidizing atmosphere in the vicinity of weld pool.

Finally, electron-beam brazing and laser-brazing processes can be used as well: the beams of electrons or photons locally heat a joint, where the filler metal is pre-placed in some form (layers, shims, rings). The main advantages of these processes consist in very rapid heating, very small thermally affected zone and accurate dimensional control. Like EBW and LBW, both laser-brazing and electron-beam-brazing processes should be shielded as well, respectively using inert atmosphere and vacuum (Messler, 2004).

15.7 Sources of further information and advice

Further information on these and related subjects can be found in the books, journals, scientific societies and technical agencies listed below:

Books

Black, J. (1992), *Biological Performance of Materials: Fundamentals of Biocompatibility*, New York, Marcel Dekker.

Boretos, J. W. and Eden, M. (1984), *Contemporary Biomaterials: Materials and Host Response, Clinical Application, New Technologies and Legal Aspects*, Park Ridge, NJ, Noyes Publications.

Messler, R. W., Jr. (1999), *Principles of Welding: Processes, Physics, Chemistry and Metallurgy*, New York, John Wiley & Sons.

Park, J. B. (1979), *Biomaterials: An Introduction*, New York, Plenum.

Park, J. B. (1984), *Biomaterials Science and Engineering*, New York, Plenum.

Schwartz, M. M. (1990), *Ceramic Joining*, Materials Park, OH, ASM International.

© Woodhead Publishing Limited, 2013

Journals

Advanced Materials and Processes (ASM)
American Ceramic Society Bulletin (American Ceramic Society)
Biomaterials (including Clinical Materials) (Elsevier)
Biomaterials Forum (Society for Biomaterials)
Biomaterials: Processing, Testing and Manufacturing Technology (Butterworth)
Biomedical Materials (Elsevier)
Biomedical Materials in Engineering (Pergamon Press)
British Ceramics Transactions and Journal (Institute for Ceramics)
Ceramic Forum International (Deutsche Deramische Geselleschaft)
Ceramics Abstract (American Ceramic Society)
Journal of the American Ceramic Society (American Ceramic Society)
Journal of Biomaterials Applications (Technomics)
Journal of Biomedical Materials Research (Wiley)
Journal of Biomedical Materials Research: Applied Biomaterials (Wiley)
Journal of Engineering in Medicine (Institution of Mechanical Engineers)
Journal of Material Science (Springer)
Materials in Medicine (Chapman & Hall)
Materials Science and Engineering (Elsevier)
Medical Device Research Report (Association for the Advancement of Medical Instrumentation)
Medical Device Technology (Astor Publishing Corporation)
Welding Journal (American Welding society)

Scientific societies and technical agencies

American Ceramic Society (ACS)
American Welding Society (AWS)
Biomedical Engineering Society
European Society for Biomaterials
Metals and Ceramic Information Center (MCIC)
National Institute of Ceramic Engineers (NICE)
Society for Biomaterials

15.8 References

Atabaki, M. M. (2010), 'Recent progress in joining of ceramic powder metallurgy products to metals', *Metalurgija*, **16**(4), 255–268.

Barbosa, M. A. (1992), *Biomaterials: Hard Tissue Repair and Replacement*, London, Elsevier-Science North-Holland.

Blischak, B. R. (2011), 'System and method for making an implantable pump thinner', United States Patent No. US 7,896,866 B1.

Cannon, R. M., Dalgleish, B. J., Dauskardt, R. H., Oh, T. S. and Ritchie, R. O. (1991), 'Cyclic fatigue-crack propagation along ceramic/metal interfaces', *Acta Metallurgica et Materialia*, **39**(9), 2145–2156.

Carim, A. H., Schwartz, D. S. and Silberglitt, R. S. (1993), *Joining and Adhesion of Advanced Inorganic Materials*, Warrendale, PA, Materials Research Society.

© Woodhead Publishing Limited, 2013

Chandler, J. E., Messer, H. H. and Ellender, G. (1994), 'Cytotoxicity of gallium and indium ions compared with mercuric ion', *Journal of Dental Research*, **73**(9), 1554–1559.

Chiao, M. and Chiao, J. C. (ed.) (2011), *Biomaterials for MEMS*, Singapore, Pan Stanford Publishing Pte Ltd.

Cooper, J. R., Caravia, L., Dowson, D. and Fisher, J. (1991), 'Ceramic bearing surfaces in total artificial joints', *Journal of Medical Engineering Technology*, **15**, 63–67.

Daulton, J. (2010), 'Self-centering braze assembly methods', United States Patent No. US 7,766,216 B2.

Fowler, B. C., Miazga, J. and Bielstein, M. L. (2010), 'Implantable medical devices and associated systems and methods', United States Patent No. US 2010/0185268 A1.

Hallab, N. J., Jacobs, J. J. and Katz, J. L. (2004), 'Orthopedic application', in Ratner, B. D., Hoffman, A. S., Schoen, F. J. and Lemons, J. E. (eds), *Biomaterials Science*, London, Elsevier Academic Press, 527–556.

Haller, M. I., He, T. X. and Daulton, J. (2010), 'Assembly for a microstimulator', United States Patent No. US 7,781,683 B2.

He, T. X. and Colvin, M. S. (2010), 'Hermetically bonding ceramic and titanium with a Ti-Pd braze interface', United States Patent No. US 7,771,838 B1.

Hench, L. L. (1991), 'Bioceramics: from concept to clinic', *Journal of the American Ceramic Society*, **74**, 1487–1510.

Hench, L. L. and Best, S (2004), 'Ceramics, glasses and glass-ceramics', in Ratner, B. D., Hoffman, A. S., Schoen, F. J. and Lemons, J. E. (eds), *Biomaterials Science*, London, Elsevier Academic Press, 153–170.

Hench, L. L., Ferber, M. K. and Tennery, V. J. (1991), 'Structural applications for technical, engineering and advanced ceramics: medical and scientific products', in Schneider, S. J. (ed.), *Engineered Materials Handbook: Ceramics and Glasses*, Materials Park, OH, ASM International, 1007–1014.

Hench, L. L. and Wilson, J. (1991), 'Bioceramics', *MRS Bulletin*, **16**, 62–74.

Hench, L. L. and Wilson, J. (1993), *An Introduction to Bioceramics*, Singapore, World Scientific Publishing.

Howe, J. M. (1993), 'Bonding, structure and properties of metal/ceramic interfaces: Part 2 Interface fracture behaviour and property measurement', *International Materials Reviews*, **38**(5), 257–271.

Iijima, S. (1989), 'Histopathological study of the effect of pure metals to the periodontal tissues', *Nihon Shishubyo Gakkai Kaishi*, **31**(4), 997–1020.

Jiang, G., Mishler, D., Davis, R., Mobley, J. P. and Schulman, J. H. (2005), 'Zirconia to Ti-6Al-4Va braze joint for implantable biomedical device', *Journal of Biomedical Materials Research Part B: Applied Biomaterials*, **72B**, 316–321.

Kamachimudali, U., Sridhar, T. M. and Baldev, R. (2003), 'Corrosion of bio implants', *Sadhana (Indian Academy Proceedings in Engineering Sciences)*, **28**(3–4), 601–637.

Kimura, Y. (1988), 'Effects of indium and tin addition to Ag-Cu alloys on the biocompatibility', *Gifu Shika Gakkai Zasshi*, **15**(2), 366–391.

Koch, K. P. (2007), 'Neural prostheses and biomedical microsystems in neurological rehabilitation', *Acta Neurochir. Suppl.*, **97**(1), 427–434.

Loehman, R. E. and Tomsia, A. P. (1988), 'Joining of ceramics', *Ceramic Bulletin*, **67**, 375–384.

© Woodhead Publishing Limited, 2013

Messler, R. W. Jr. (1993), *Joining of Advanced Materials*, Burlington, MA, Elsevier/Butterworth-Heinemann.

Messler, R. W. (2004), *Joining of Materials and Structures*, Oxford, Elsevier/Butterworth-Heinemann.

Murray, M. G. S., Facchini, A., Sicking, R., Specchia, N., Pathiraj, B., Gomez, A. and Sala, G. (1999), 'Development of an advanced ceramic/titanium alloy knee joint', Procs. Bioceramics 12, Nara, Japan, 1114–1122.

Nicholas, M. G. (1986), 'Active metal brazing', *Br. Cram. Trans. J.*, **85**, 144–155.

Nicholas, M. G. and Crispin, R. M. (1989), 'Brazing ceramics with alloys containing titanium', *Ceram. Eng. Sci. Proc.*, **10**, 1602–1610.

Paiva, O. C. and Barbosa, M. A. (1997), 'Production, bonding strength and electrochemical behaviour of commercially pure Ti/Al2O3 brazed joints', *Journal of Materials Science*, **32**, 653–659.

Pask, J. A. (1987), 'From technology to the science of glass/metal and ceramic/metal sealing', *Ceramic Bulletin*, **66**, 1587–1593.

Pope, M. H. and Fleming, B. C. (1991), 'Knee biomechanics and materials', in Laskin, R. S. (ed.), *Total Knee Replacement*, London, Springer Verlag, 25–38.

Sicking, R. (2000), *Beitrag zur entwicklung eines biokompatiblen aktivlotes zum fugen von oxidkeramik an TiAl6V4*, Aachen, Shaker Verlag.

Soon-Bok, L., Kobayashi, H. and Huh, J. W. (1995), 'Fatigue strength and fracture mechanism of ceramic-metal joints under cyclic bending', *International Journal of Fatigue*, **17**(6), 427–435.

Tomsia, A. P., Pask, J. A. and Loehman, R. E. (1991), 'Joining', in Schneider, S. J. (ed.), *Engineered Materials Handbook: Ceramics and Glasses*, Materials Park, OH, ASM International, 477–546.

Tziviskos, G. (2010), 'Hermetic seal', United States Patent N° US 7,837,085 B1.

Waddell, J. N., Ichim, I., Lee, H., Fangtao, L., Payna, A. G. T. and Swain, M. V. (2007), 'Fatigue failures of bar-attachment brazed joints for implant-supported overdentures', *Engineering Fracture Mechanics*, **74**(7), 1148–1159.

Wataha, J. C., Nakajima, H., Hanks, C. T. and Okabe, T. (1994), 'Correlation of cytotoxicity with elemental release from mercury- and gallium-based dental alloys *in vitro*', *Dental Materials*, **10**(5), 298–303.

Xiaochun, L., Xugang, Z., Werschmoeller, D., Hongseok, C. and Xudong, C. (2008), 'Embedded micro/nano sensors for harsh engineering environments', *Sensors – 2008 IEEE*, 1273–1276.

© Woodhead Publishing Limited, 2013

16

Tissue adhesives and sealants for surgical applications

P. JARRETT, Ocular Therapeutix, USA and
A. COURY, Coury Consulting Services, USA

DOI: 10.1533/9780857096425.4.449

Abstract: This chapter reviews tissue sealants and adhesives used in surgery, which can be categorized as bioresorbable or biostable and synthetic or bio-derived. The fastest growing of these categories commercially is synthetic bioresorbable sealants, which form into solid gel *in situ*. Key characteristics of mechanical properties, application to tissue, mechanisms of bonding and biocompatibility are discussed. Finally, descriptions of the major commercial surgical sealants and adhesives in each category are described.

Key words: adhesive, sealant, bioresorbable, biostable, synthetic, bio-derived.

16.1 Introduction

This chapter will cover topical and implantable tissue adhesives and sealants. These materials differ from pressure-sensitive bandages and electrode adhesives, and each present distinctly different problems of bonding mechanisms and biocompatibility. They are also fundamentally different than hemostats, which are solely intended to coagulate autologous blood. Internal tissue adhesives and sealants depend on the formation of a bond at the interface with the substrate tissue. To establish a good bond, these agents are usually applied to the tissue as a low-viscosity liquid that then solidifies *in situ*, providing intimate tissue contact and a mechanically interlocking interface with secondary bonding interactions coming into play. Other methods of bond formation such as covalent bonding have been used with some success (Smith, 2004; Park and Lakes, 2007). The chemical nature of this bond is important to its strength and to the impact on the health of the tissue being sealed. The mechanism and chemistry of *in situ* bond formation will be discussed as will key considerations of efficacy and biocompatibility.

Sealants and adhesives have long been sought for surgical use (Cooper and Falb, 1968). Today they are used in many surgical arenas (Wheat and

© Woodhead Publishing Limited, 2013

Wolf, 2009), notably in vascular, gastrointestinal, ocular, neural, spine and lung. Difficult to seal tissues such as liver (Berrevoet and de Hemptinne, 2007) have long been an area of investigation for fibrin adhesives. In vascular surgery (Schenk *et al*., 2003) sealants have been used to minimize bleeding and the use of sealants for femoral artery closure following angiography and angioplasty procedures has grown recently, with several products on the market. The use of adhesives in ocular tissues has long been a clinical interest (Singh *et al*., 2010; Wathier and Grinstaff, 2010). The use of fibrin glue and cyanoacrylate adhesives for corneal perforation repair (Lagoutte *et al*., 1989; Sharma *et al*., 2003) has been an 'off label' practice for decades. Sealants and adhesives have been used for prevention of epithelial in-growth after laser refractive surgery (Anderson and Hardten, 2003; Narváez *et al*., 2006). Corneal incision sealing has also been a growth area since the advent of 'sutureless incisions' in cataract surgery (Kalayci *et al*., 2003; Grinstaff, 2007). Sealing air leaks after lung surgery (Bayfield and Spotnitz, 1996; Wain *et al*., 2001; Reul and Walsh, 2005; Rathinam *et al*., 2009). Adhesives have also been used extensively in ENT procedures (Schneider, 2009). Fibrin glue has been used in sealing cerebrospinal fluid leaks (Shaffrey *et al*., 1990; Patel *et al*., 1996), but now new synthetic bioresorbable adhesives are indicated for this application (Cosgrove *et al*., 2007).

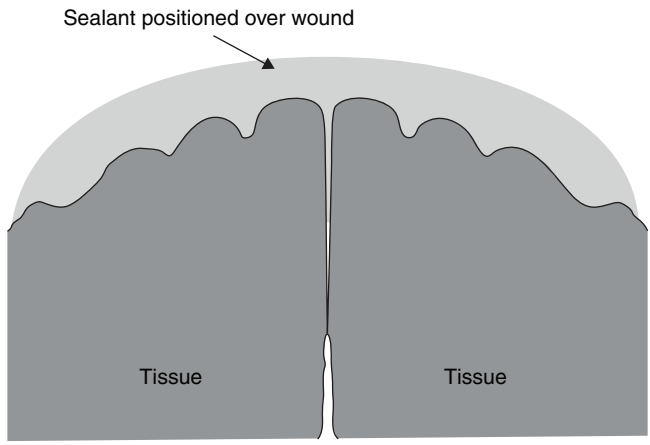
An important synthetic biostable material, commonly known as 'bone cement', is composed of a prepolymer of polymethylmethacrylate (PMMA) that polymerizes *in situ* to provide a rigid mechanical fixation of, for example, a hip prosthesis. These and related cement materials are not strictly adhesives or sealants, but rather grouts or potting compounds, so they will not be treated in this review.

16.2 Principles of tissue adhesives and sealants

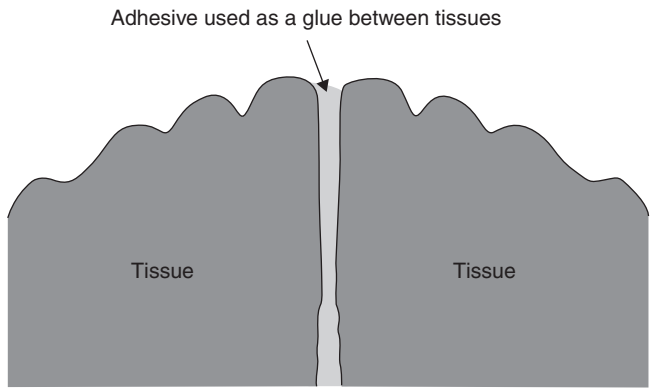
The purpose of a tissue sealant is to form an adherent barrier over an opening in tissue that can prevent fluid or particulate ingress or egress through the tissue opening (Fig. 16.1). The sealant must be capable of adhering to the tissue substrate sufficiently to remain in place under the forces acting upon it for a duration sufficient to allow healing to take place. Typically, sealants rely on transformation from a low-viscosity liquid to a flexible or semi-rigid solid during which chemical bonds (covalent, ionic or other secondary bonds) are formed, leading to a molecular network formation.

Tissue adhesives are materials that can be used as a 'glue' to hold tissue surfaces together. The adhesive can be placed between tissues to be held in apposition until healing occurs (Fig. 16.2). However, unless the adhesive provides a means to support tissue in-growth and penetration, the placement of adhesive between tissues can impede the healing process. Alternatively,

© Woodhead Publishing Limited, 2013



16.1 A surgical sealant or adhesive is placed over the incision to provide apposition and to prevent fluid ingress or egress. This application method allows healing by primary intention.



16.2 A resorbable tissue adhesive may be placed between tissues. This approach relies on healing by secondary intention.

an adhesive is placed across the outer surface of tissues on either side of a wound as in Fig. 16.1 to hold the tissue in apposition.

The properties of the ideal tissue adhesive or sealant are listed below:

- safe;
- effective;
- bioresorbable;
- easy to use;
- inexpensive.

© Woodhead Publishing Limited, 2013

Safe: The product or metabolites must not present toxicological or mechanical risks that could impair healing or damage tissue.

Effective: The material must be able to establish and hold a bond with the intended substrate tissue. The material itself must have strength and flexibility sufficient to avoid failure under the forces acting upon it in the intended use.

Bioresorbable: Once the adhesive has done its job it should exit the area as soon as possible, and in a benign fashion.

Easy to use: The product must be quick and easy to prepare for use. Ancillary equipment or energy sources should be minimized since they take time to prepare for use and they require maintenance and storage. Storage of the material should require minimal special conditions, such as refrigeration or freezing, since these storage places limit its availability at short notice.

Inexpensive: Wound closure and leak prevention have predominantly been accomplished until now using fastening devices such as sutures, staples, clips and meshes. To achieve wide acceptance, the adhesive must not add a large additional cost to primary procedures.

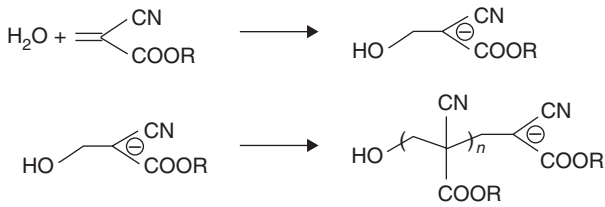
The types of tissue adhesives and sealants can be categorized as follows:

- synthetic bioresorbable;
- synthetic biostable;
- bio-derived bioresorbable;
- bio-derived biostable.

Each type of tissue adhesive or sealant has its place under different medical circumstances. Synthetic biostable adhesives such as cyanoacrylates ('crazy glues') are most often used topically to close simple skin wounds (Spotnitz and Burks, 2010). Cyanoacrylate adhesives are also used 'off label' in situations where other solutions are unavailable, such as battlefield injuries and certain ophthalmic surgical procedures. Cyanoacrylates have the advantages of ease of application and rapid solidification times. The disadvantages of synthetic biostable sealants such as cyanoacrylates include significant heat generation and local toxicity. Heat is liberated from the exothermic polymerization reaction (Fig. 16.3), which can cause local tissue damage. Local toxicity results from any residual monomer present and the formation of degradation products such as formaldehyde in the case of the monomers with lower molecular weight side chains (Webster and West, 2002). Typically they form fairly rigid solids with excellent adhesion. If placed between apposing tissues, cyanoacrylates can act as a biological barrier and interfere with the healing process.

Synthetic bioresorbable sealants are generally hydrogels designed to incorporate hydrolyzable linkages into the molecular structure such

© Woodhead Publishing Limited, 2013



16.3 Polymerization of cyanoacrylate transforms the liquid monomer to a solid adhesive.

that hydrolysis causes the deconstruction of the molecular network into water-soluble degradation products. Chemically these hydrolyzable linkages (usually esters) are similar to chemistries used in other synthetic bioresorbable devices such as degradable sutures (e.g. Vicryl®). Sealant materials developed in this category have been primarily hydrogels, due to their tissue-like compliance and to the very mild inflammatory tissue responses hydrogels elicit. These materials can be designed to degrade over a period of days to weeks, depending on the specific need for long-term wound reinforcement.

Bio-derived sealants fall into two major categories, biostable and bioresorbable. In many cases the bio-derived sealants utilize synthetic components in their formulation.

Bio-derived biostable materials have been developed, such as the early material known as GRF (gelatin resorcinol formaldehyde) adhesive used to treat aortic dissections (Chao and Torchiana, 2003). BioGlue® is an albumin–glutaraldehyde adhesive in commercial use today for sealing aortic dissections and vascular prosthesis–tissue junctions among other applications.

Bio-derived bioresorbable adhesives include mainly 'fibrin glues' which have been in use for over 100 years (Spotnitz, 1996), indicating a longstanding need for surgical sealants and adhesives. Tisseel® is generally considered a fibrin adhesive, but is actually indicated as an adjunct to standard surgical techniques (such as suture and ligature) to prevent fluid leakage, for example, from colonic anastomoses following the reversal of temporary colostomies (Baxter Healthcare Corp, 2009b).

Hybrid adhesives or sealants are based on synthetic protein-based materials. Such materials include adhesives based on mussel glue (Brubaker *et al.*, 2010; Lee *et al.*, 2011) and a silk-elastin protein polymer (Capello, 1997; Rabotyagova *et al.*, 2011). These technologies have long appeared promising as adhesives and sealants, although none have yet emerged from the laboratory to commercialization. Several other novel hydrogel materials are in various stages of research or development currently (Mai-ngam *et al.*, 2005; McCrea *et al.*, 2011; McKerracher, 2011; Murakami *et al.*, 2009; Wang *et al.*, 2010).

© Woodhead Publishing Limited, 2013

16.3 Definitions and general considerations

- Adhesive: agent that bonds with a surface or between two surfaces, for example tissue to tissue, or tissue to biomaterial.
- Sealant: agent that bonds to tissue surrounding an opening, such as a wound or incision, to halt the ingress or egress of liquid or gas.
- Adherend/substrate: material containing a surface to be bonded.
- Bond: area of contact between two surfaces that requires a force to separate.
- Bond strength (adherence): force to separate two surfaces at the bond.
- Adhesion: force required to separate two materials based on chemical interactions.
- Mechanical interlock: contribution to bond strength based on interdigitation of adhesive and adherend surfaces. (Cohesive failure of one or the other material determines force of mechanical interlock.)
- Cohesive failure: failure within the structure of the adherend or adhesive.
- Adhesive failure: failure at the interface of the adherend and adhesive.

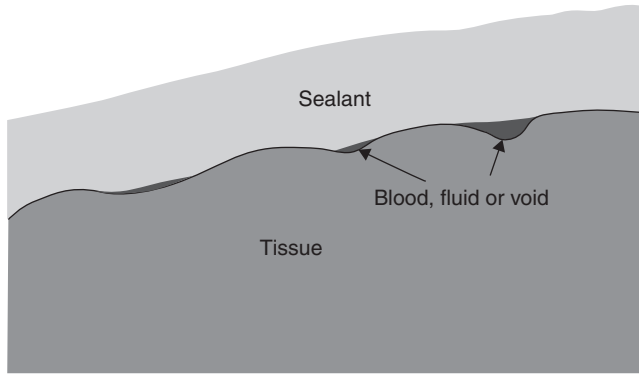
16.4 Mechanisms of bonding

The strength of bonding between the adhesive or sealant and the tissue is determined by the mechanism of bonding. Several mechanisms of bonding for adhesives to adherend have been found to occur under various circumstances. Bond forces can be derived from several physical or chemical interactions and are most often a combination of mechanisms as listed below:

- mechanical interlock;
- interdiffusion;
- covalent chemical bonds;
- ionic bonds;
- secondary chemical bonds:
  - hydrogen bonding;
  - dipole–dipole interactions;
  - ion–dipole interactions;
  - dispersion forces;
- combinations of mechanisms.

Mechanical interlock is the classical adhesion mechanism employed in general adhesives, and it is the most prevalent mechanism of adhesion for surgical adhesives and sealants. Mechanical interlock, depicted in Fig. 16.4, relies

© Woodhead Publishing Limited, 2013



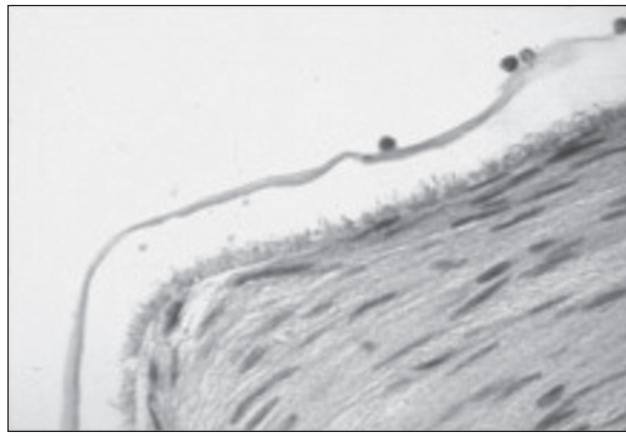
16.4 Tissue surface should be clean and dry to avoid weak boundary layers formed by collections of fluid, foreign matter, air voids, etc.

on the irregularities of the tissue-surface topography. When good intimate tissue content is achieved, the interdigitation of the tissue surface with the *in situ* solidified adhesive provides the mechanical interlock. Surface contaminants such as blood or other fluids can cause a weak boundary layer, effectively blocking access of the sealant to the tissue surface (Browdie and Cox, 2007). Contaminants can collect in depressions of the tissue surface as depicted in Fig. 16.4. This type of bond can be extremely strong, with bond separation tests usually exhibiting cohesive failure, where the tissue–material bond strength exceeds the strength of the adhesive material itself. The strength of this type of adhesion varies with the tissue type being bonded. In general, tissue having more irregular topography provides a stronger bond to the adhesive. Injured tissue where sub-epithelial tissue is exposed has been found to provide the best adherend (Reul and Walsh, 2005). This de-epithelialized tissue is typically found adjacent to incisions and wounds, or in areas of dissection, etc. Incisions or tissue injuries of different types, for example scalpel blade or electro-cautery, provide a wide variation in de-epithelialized surface area.

In addition to promoting mechanical interlock, the increased surface area of contact of irregular or roughened surfaces provides enhanced opportunity for other bonding forces to act in concert with mechanical interlock at the interface. In all cases surface preparation and application procedure are key components to achieving good bond strength. Figure 16.5 is a histological section showing a hydrogel sealant (FocalSeal S, a Dural Sealant developed by Focal, Inc.) (Alleyne *et al.*, 1998) that has established a good mechanical interlock bond with the tissue surface.

Some surgical procedures result in broad areas of exposed tissue, such as areas of dissection, which provide excellent areas for bonding if clear of

© Woodhead Publishing Limited, 2013



16.5 Stained tissue section showing FocalSeal S sealant on the luminal surface of an endothelium denuded artery. The irregularities of the sealant–tissue interface illustrate mechanical interlock bonding.

blood or other contaminating fluids. Care must be taken in these tissues, however, to avoid interference with the healing process.

Most adhesives and sealants are not designed to promote rapid tissue in-growth and may interfere with healing. Bioresorbable sealants and adhesives are designed to gradually lose strength and mass over time. The strength and mass loss rate of the sealant must be considered in developing a surgical procedure that incorporates sealants applied to broad areas.

16.5 Application methods

The method used to apply a tissue adhesive or sealant is an important component to achieving a good bond. Applicators provide a method for conveying the material to the site as well as to prepare the site. Some agitation of sealant or adhesive on the surface improves the ability to achieve good intimate contact with the tissue by displacing or incorporating any fluid or foreign matter on the tissue surface. Brushing and spraying are the most commonly used methods to provide agitation at the interface.

Considerations for tissue surface preparation:

- *Clean surface*: The surface should be clear of any blood clots and other loose material.
- *Fluid presence*: The presence of fluid at the tissue site can interfere with the adhesive either by dilution at the interface – for water-based or water-soluble adhesives – or by creating a boundary layer trapped between the adherend and adhesive (Fig. 16.4). Any fluid at or near the

© Woodhead Publishing Limited, 2013

site of application should be removed before the adhesive is applied. Alternatively, the sealant or adhesive formulation can be designed to function with some dilution by liquid without excessive loss of properties.

- *Fluid flow*: Bleeding or fluid infiltration can dilute water-based or water-soluble adhesives and can severely inhibit contact bonding of hydrophobic polymers. Flowing fluid can also dislocate or wash away the adhesive before solidification can occur. Scrupulous efforts to halt fluid flow should be made prior to application of the adhesive. In some cases it is possible to temporarily stop or reduce flow long enough for a fast-setting sealant to obtain sufficient adhesion to contain further fluid egress.
- *Injured tissue*: Adherence to intact epithelium is often difficult to achieve due to smooth surfaces that do not promote mechanical interlocking. Procedures such as dissection or electro-cautery result in roughened, dry surfaces at the wound margins that promote mechanical interlocking. Adherence to the injured tissue at the wound edges, therefore, is often stronger than adjacent uninjured tissue. In preparing a wound, efforts should be made to clean injured tissue and ensure good intimate contact with the adhesive or sealant to achieve the strongest possible bond. The injured layer of tissue is usually stable during the healing process and healing proceeds normally in the healthy tissue below and adjacent to the injury. Of course, the presence of necrotic tissue elicits an inflammatory response. Inflammation may cause significant local concentrations of oxygen-derived free radical species that can degrade biomaterials (Coury, 2004).

16.6 Synthetic bioresorbable sealants

The synthetic bioresorbable materials have been the fastest growing segment of surgical tissue sealant and adhesive technologies with several new sealants entering the market in the US and Europe in the last few years. This is primarily due to their biocompatibility, cost effectiveness, reproducibility and ease of manufacturing. In addition, synthetic materials can be tailored to achieve properties best suited to the surgical application for which they are designed.

First among the synthetic bioresorbable sealants are the polyethylene glycol-based sealants. The polyethylene glycol (PEG) based sealants are specialized to achieve properties best suited to the intended surgical procedure. Typical properties that are manipulated are:

- Gel time – the time required for gelation to occur. The gel time can vary from nearly instantaneous to minutes. The choice of gel time is usually a

© Woodhead Publishing Limited, 2013

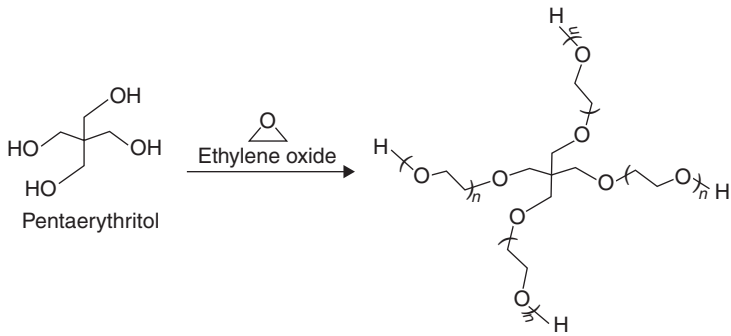
function of how it will be applied by the surgeon. A spray system is best suited to a fast gel time, whereas slower gel times are required for more meticulous application requirements such as ocular surgery or minimally invasive dural sealing. Viscosity control is mandatory to achieve optimal application properties for the various techniques.

- Swelling – the degree the gel swells once it is fully cured, usually over a specified period of time while soaking, for example in phosphate buffered saline (PBS) solution at 37°C. In situations where the sealant is applied in confined spaces, such as in spinal surgery, low swelling is required to avoid unnecessary pressure on local tissues that may be injured such as nervous tissue. Clinical cases have occurred in which high-swelling materials used in the spine have resulted in patient injury (Mulder *et al.*, 2009; Epstein, 2010; Thavarajah *et al.*, 2010). High swelling can also cause injury by desiccating attached tissue.
- Modulus – the stiffness of the gel is inversely proportional to its compliance. Matching compliance to the tissue adherend is important for maintaining good bonding. In addition, compliance mismatch can cause local stresses on tissue, which may be injurious or may cause undesirable tissue remodelling responses.
- Strength – The strength of the gel determines its ability to avoid cohesive failure. This is a greater concern during the period shortly following surgery when the sealant must bear the full responsibility for leak prevention. As healing occurs under the sealant, the fibrin clot and developing tissue matrix add their strength, which offsets the loss of strength of bioresorbable sealants over time.
- Degradation rate – The degradation rate of the adhesive or sealant should be sufficient to provide time for adequate healing to occur, but prolonged material persistence should be minimized. Persistence of the material at the site can be problematic if a prolonged inflammatory response occurs.

The primary method for manipulation of properties such as swelling and modulus is via the structure of the crosslinked network. Several strategies have been employed in network design; specific strategies include PEG functionality (number of reactive end groups per molecule), crosslinker functionality, segmented PEG with hydrophobic and hydrophilic segments.

PEG is synthesized by the living polymerization of ethylene oxide, which provides the ability to precisely control molecular weight. In addition, these PEGs have very narrow molecular weight distributions, virtually monodisperse, which provides good control over the molecular network of the gel formed from PEG macromonomer. The structure of the macromonomer can be controlled to have a defined number of terminal ends.

© Woodhead Publishing Limited, 2013



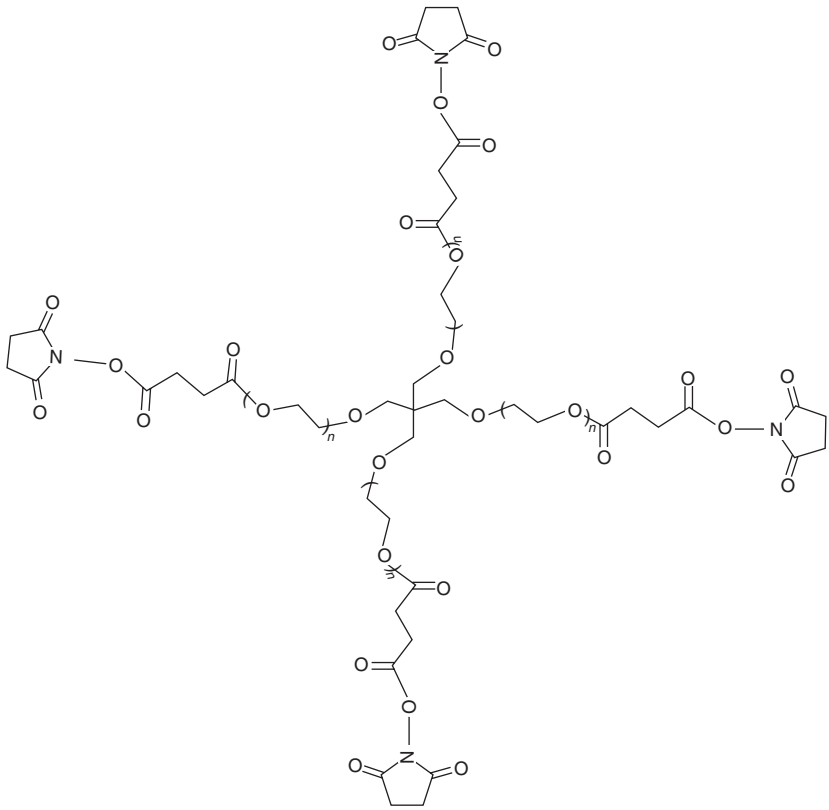
16.6 Four-armed PEG synthesis.

Multi-armed or branched PEG molecules can be made with two to several terminal ends that can be modified to provide reactive end groups. In these structures the ethylene oxide polymerization is initiated with a multifunctional molecule to form multiple arms of equal length; the number of arms is determined by the functionality of the initiator, for example pentaerythritol (four arms) (Fig. 16.6) or hexaglycerol (eight arms) (Harris and Zalipski, 1997).

Reactive end groups are affixed to the PEG termini (Fig. 16.7). The reactive end groups are then used to crosslink the PEG molecules to form a molecular network. The branches or 'arms' of the PEG, combined with the molecular weight between crosslinks (Mc), determine the architecture and the crosslink density of gel. The moieties between crosslinks contain hydrolyzable linkages such as ester or carbonate groups for controlled degradability. Figure 16.7 depicts a PEG molecule bearing succinimidyl esters as hydrolyzable sites. Crosslink density is a controlling factor for properties such as modulus, swelling and degradation rate (Coury, 2004).

Dendritic molecular architectures (Grinstaff, 2007) employ a similar strategy to the multi-armed PEG structures, but accomplish it in a slightly different way – using multi-functional amines crosslinked with di-functional PEG. Dendritic structures progressively branch as the molecule grows from a central initiator by adding multifunctional segments to form a multiple of molecular termini with each successive 'generation' of branches. Once the desired number of termini is reached the ends are modified to enable crosslinking to form a gel. Dendritic amines crosslinked with difunctional reactive PEG molecules have been employed commercially (Wathier *et al.*, 2005). Also, polyamines such as branched polyethyleneimines (PEI) have been used to form multifunctional reactants in a similar fashion (Carnahan and Butlin, 2010).

© Woodhead Publishing Limited, 2013

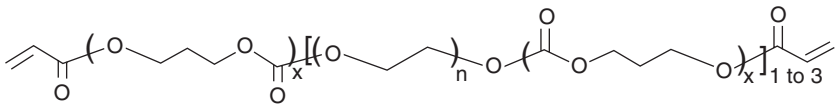


16.7 Four-armed PEG functionalized with N-hydroxy-succinimidylsuccinate.

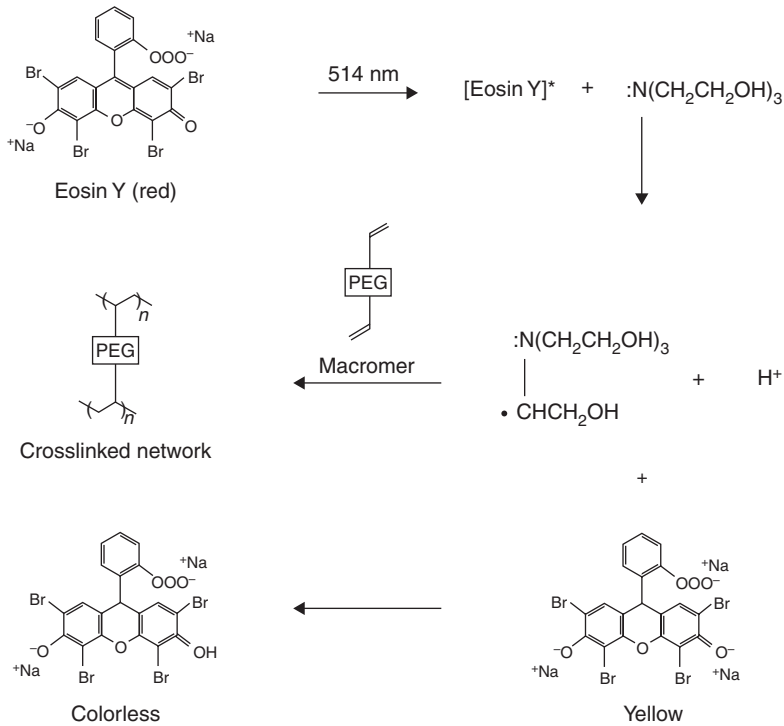
Segmented PEG architectures have been made which bear hydrophilic PEG segments and hydrophobic segments in a linear or branched arrangement (Sawhney *et al.*, 2001). The hydrophobic segments provide a way to use secondary associative forces to achieve control over properties such as swelling and modulus. The hydrophobic segments can also contain hydrolyzable linkages to provide a mechanism for resorbability of the sealant.

The crosslinking mechanism for these PEG architectures can be any high-efficiency reaction that does not produce toxic side (reaction) products. End groups such as acrylates or methacrylates provide double bonds, which act as sites for addition reactions. Figure 16.8 is a diagram of the macromonomer used in FocalSeal L (Genzyme), an FDA approved lung sealant (Focal Inc., 2000). Free radical polymerization is used to crosslink these groups (Sawhney *et al.*, 1994). The free radical polymerization method can be accomplished by different chemical initiation schemes such as Fenton's reaction (ferrous plus hydroperoxide form radical initiators) or by use of an energy source (e.g. UV

© Woodhead Publishing Limited, 2013



16.8 Structure of the FocalSeal L macromonomer.

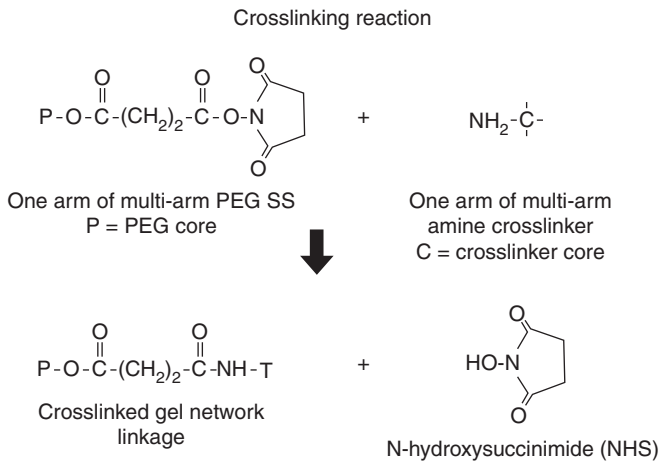


16.9 Light activated polymerization of FocalSeal L lung sealant.

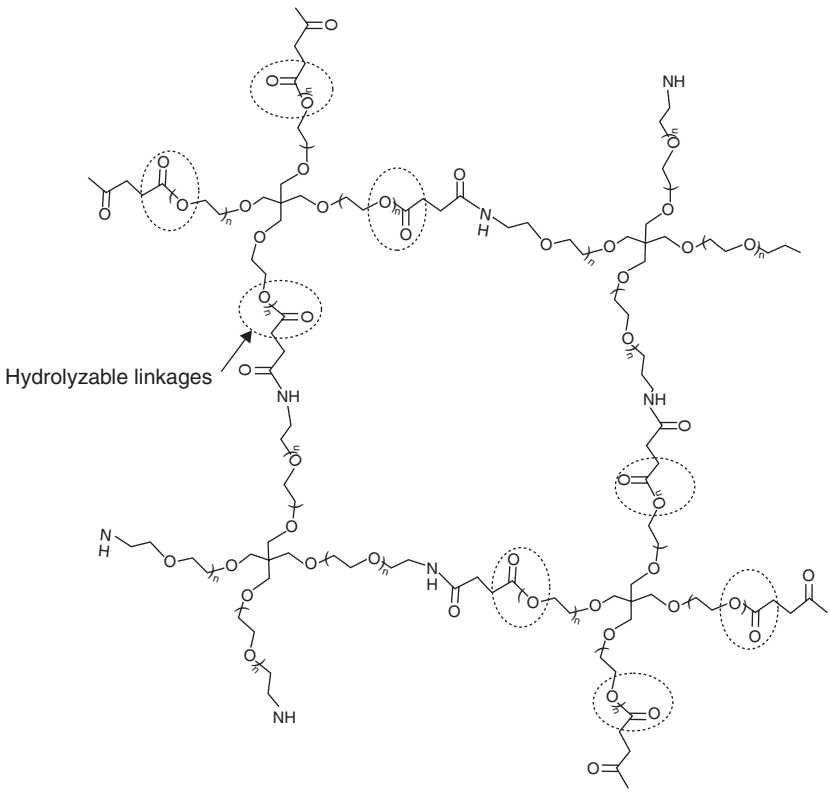
light or heat) to activate a free radical initiator. Light activated polymerization of FocalSeal L is accomplished by a reaction scheme (Fig. 16.9) that utilizes visible light-sensitive dye to initiate the polymerization reaction.

Another crosslinking method that has been employed is the reaction of electrophilic and nucleophilic groups (Bennett *et al.*, 2003). Electrophilic groups such as N-hydroxysuccinimidyl (NHS) esters have been paired with nucleophilic groups such as primary amines or thiols to enable nucleophilic substitution reaction crosslinking. Figure 16.10 shows the crosslinking reaction between a multi-armed PEG terminated with N-hydroxysuccinimidysuccinate end groups when reacted with a multi-armed amine. In this case each crosslink results in the liberation of one NHS molecule, a water-soluble and non-toxic by-product. Double

© Woodhead Publishing Limited, 2013



16.10 Cross linking reaction of PEG SS end groups with primary amines.



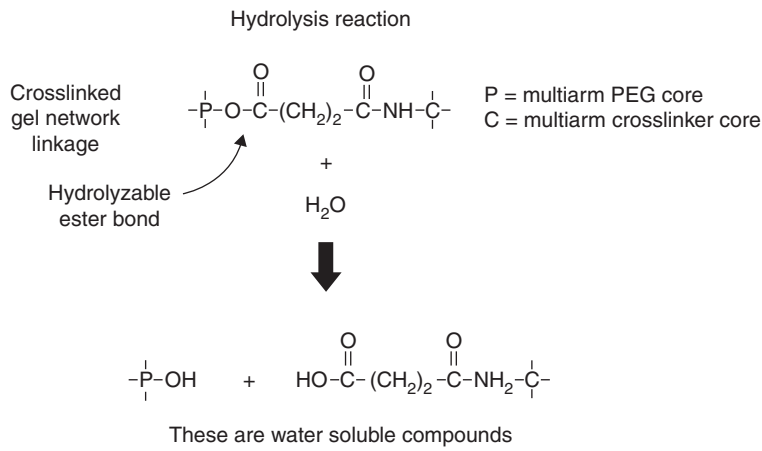
16.11 Schematic of a PEG hydrogel structure.

© Woodhead Publishing Limited, 2013

bonds have also been used as sites for crosslinking via Michael addition of nucleophiles such as thiols (Metters and Hubbell, 2004). A schematic structure of a crosslinked hydrogel formed from a four-armed PEG-NHS and a four-armed PEG amine is depicted in Fig. 16.11.

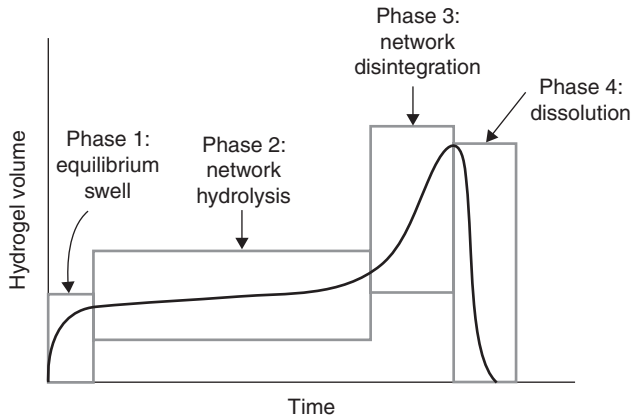
16.6.1 Bioresorption of synthetic hydrogel sealants

Degradation of synthetic bioresorbable hydrogel sealants or adhesives is accomplished by incorporation of a cleavable linkage (see Fig. 16.11). The linkages used with nearly all commercial synthetic resorbable materials are hydrolyzable esters. Esters are used because the rate of hydrolysis can be well controlled by the structure of the ester linkage or segments of ester linkages selected. Figure 16.12 shows a schematic of the hydrolytic degradation mechanism of a hydrogel having strategically placed ester linkages. The molecular network forms the structural members of the hydrogel, and incorporation of hydrolyzable linkages provides a means for disintegration of the molecular network. As these linkages are cleaved the gel weakens evenly throughout its bulk. This type of degradation is often termed 'bulk degradation' and is characterized by four phases. The first phase involves swelling to equilibrium accompanied by a proportionate loss of modulus. The second phase involves the gradual cleavage of hydrolytically labile bonds with a corresponding growth in volume and additional loss of modulus and strength. The third phase, actually a continuation of the second phase, shows an acceleration of swelling as the gel's molecular network approaches disintegration. The final phase involves mass and volume loss until complete



16.12 Hydrolysis reaction of PEG succinate linkages.

© Woodhead Publishing Limited, 2013



16.13 Phases of synthetic hydrogel degradation by hydrolysis. Hydrogel sealants swell, soften and weaken after implantation. This process generally follows a sequence of four phases. The surgeon should consider the volumetric changes as well as the material property loss progression during the sealant residence time.

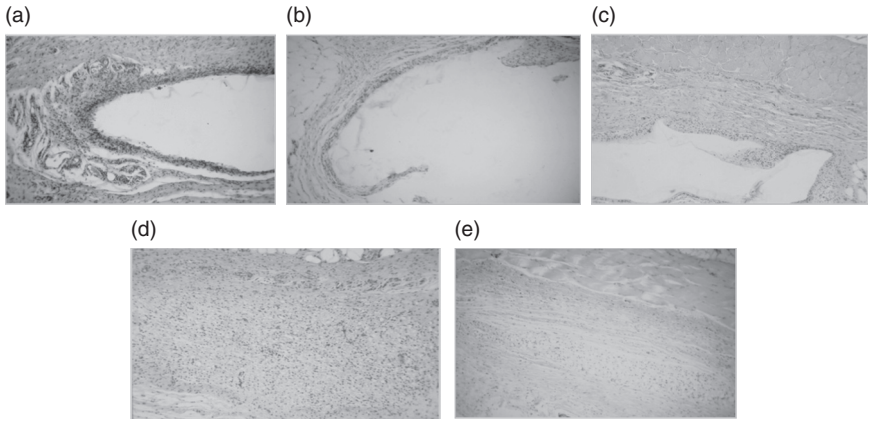
dissolution occurs (Fig. 16.13). Where compression of sensitive tissues in confined spaces is a concern, such as in spinal dura sealing (Mulder *et al*., 2009; Epstein, 2010; Thavarajah *et al*., 2010), the surgeon must consider the volumetric changes as well as the material property loss progression during the sealant residence time.

Some biomaterials are designed for 'surface erosion', in which the material shrinks like a lozenge. Polymers exhibiting this type of behaviour are hydrophobic and generally contain freely hydrolyzable groups such as anhydrides so that degradation occurs at a rate faster than water permeation (Dang *et al*., 1996). The series of photomicrographs in Fig. 16.14 track the resorption of FocalSeal-S, a sealant developed for cranial dural incisions, over 60 days after subcutaneous implantation in rats. As the implant undergoes bulk degradation with solubilization of the degradation products, the implant shrinks, with tissue growth advancing as the material surface retreats. A mild inflammatory response to the degradation products is evidenced by macrophages present around the gel borders.

16.7 Commercial resorbable synthetic sealants and adhesives

The availability of commercial sealants and adhesives has grown significantly in recent years. An impressive list of materials for use in various

© Woodhead Publishing Limited, 2013



16.14 Resorption of FocalSeal S rat subcutaneous implants: (a) 3 days, (b) 14 days, (c) 28 days, (d) 35 days, (e) 60 days.

surgical applications is shown in Table 16.1. A brief description of each product is given below.

16.7.1 DuraSeal Dural Sealant System (Covidien)

The DuraSeal Dural Sealant System consists of components for preparation of a synthetic absorbable sealant, and an applicator for delivery of the sealant to the target site (Fig. 16.15). The sealant is composed of two solutions, a high molecular weight polyethylene glycol (PEG) ester solution and a low molecular weight trilysine amine solution (referred to as the 'blue' and 'clear' precursors, respectively). When mixed together, the precursors crosslink to form the hydrogel sealant. The mixing of the precursors is accomplished as the materials exit the tip of the spray applicator. The hydrogel implant is absorbed in approximately four–eight weeks, sufficient time to allow for dural healing. The DuraSeal Dural Sealant System is indicated for use as an adjunct to sutured dural repair during cranial surgery to provide watertight closure (Cosgrove *et al*., 2007). Clinical testing was conducted in Europe (Boogaarts *et al*., 2005) in 46 patients (in cranial and spinal dural incisions) and in the United States (Cosgrove *et al*., 2007) in 111 patients (cranial) with demonstrated CSF leaks. In both studies 100% of patients were without leaks after sealing.

The DuraSeal material has also been adapted to spinal-cord sealing (DuraSeal Spine, Fig. 16.16) with the aid of a gas-assisted spray-delivery system (Wright *et al*., 2009). Clinical-sealing results for the US DuraSeal Spine study were significant: 100% watertight in the sealant group (102/102) vs 64% (36/56) in the standard of care group.

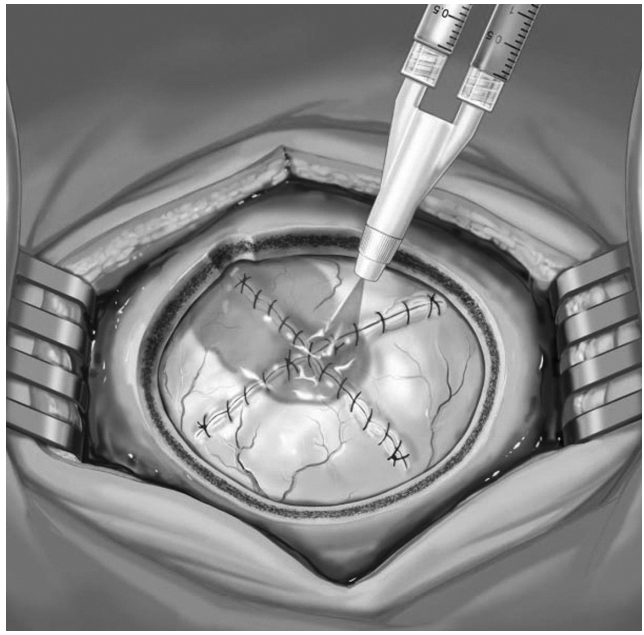
© Woodhead Publishing Limited, 2013

Table 16.1 Commercial bioresorbable synthetic tissue adhesives and sealants

Brand name	Surgical application	Composition	Manufacturer	Available
Adherus™ Dural Sealant	Dura	PEG–NHS, PEI	HyperBranch	EU
Adherus™ Spinal Sealant	Dura	PEG–NHS, PEI	HyperBranch	EU
Adherus™ Vascular Sealant	Vascular	PEG–NHS, PEI	HyperBranch	EU
AngioSeal	Femoral artery plug	Collagen	St. Jude Medical	EU, USA
CoSeal	Arterial and vascular	PEG–NHS, PEG thiol	Baxter Health Care	EU, USA
DuraSeal Cranial	Dura	PEG–NHS, trilysine	Covidien	EU, USA
DuraSeal Spine	Dura	PEG-NHS, trilysine	Covidien	EU, USA
DuraSeal Xact	Dura	PEG–NHS, trilysine	Covidien	EU, USA
Exoseal	Femoral artery plug	Collagen	Cordis (J&J)	EU, USA
FocalSeal L	Lung	PEG, light cure	Genzyme	EU, USA (discontinued)
FocalSeal S	Cranial and spinal dura	PEG, light cure	Genzyme	EU (discontinued)
Mynx vascular closure system (VCS)	Femoral artery plug	Preformed PEG xerogel	Access Closure	EU, USA
OcuSeal	Ocular	PEG–NHS, dendrimer amine	B&D	EU
ReSure Ocular Sealant	Ocular	PEG–NHS, trilysine	Ocular Therapeutix	EU
TissuePatch	Lung, dura, general	PLGA, P(AA/NHS)	Tissuemed	EU
VascuSeal	Vascular	PEG–NHS, trilysine	Covidien	EU
VasoSeal	Femoral artery plug	Collagen	Datascope	EU, USA

P(AA/NHS) refers to NHS modified poly(acrylic acid) and PLGA refers to a lactide-glycolide copolymer.

© Woodhead Publishing Limited, 2013



16.15 Application of DuraSeal to an incision.

16.7.2 FocalSeal L (Genzyme)

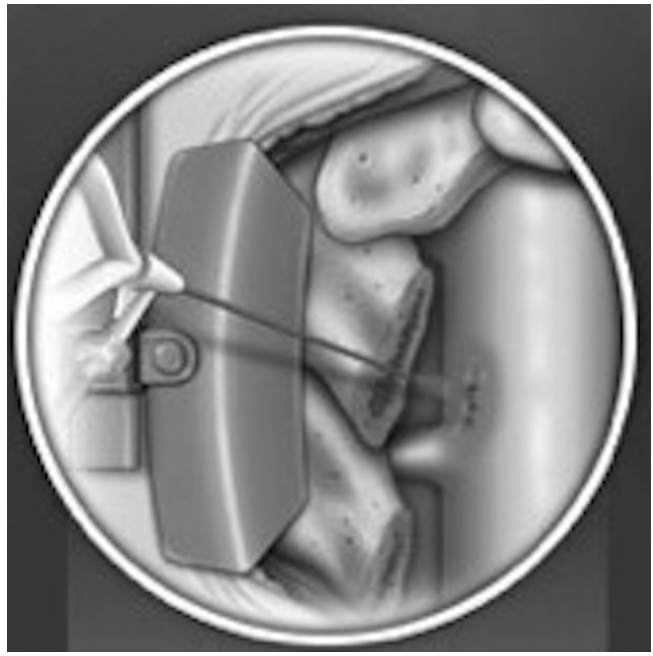
FocalSeal L was approved as a lung sealant in the US in 2000 (Wain *et al.*, 2001). The FocalSeal L product is shown in Fig. 16.17. It consisted of:

- a primer – a lyophilized powder, a diluent solution and a flow-through brush applicator;
- a sealant – a frozen solution in a syringe and a flow-through brush applicator;
- a xenon light source and a sterilizable fiber optic light wand.

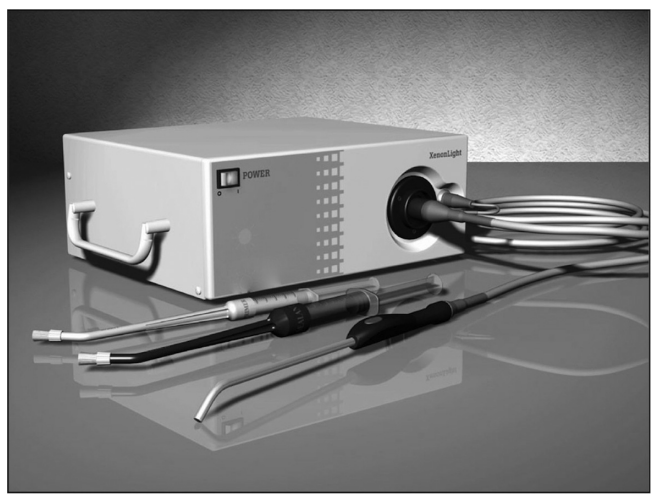
Although the product performed well for its intended use, it was withdrawn from the market in 2003 due to a combination of factors including high manufacturing cost, slow adoption and a change in company business direction.

In this system a multiblock copolymer macromonomer (Fig. 16.7) composed of PEG and trimethylene carbonate formed a sealant *in situ* upon exposure to a high-intensity blue light (480–520 nm). Eosin Y and triethanolamine act together as a photoinitiator for the macromonomer polymerization reaction. The reaction scheme is shown in Fig. 16.8. A xenon light

© Woodhead Publishing Limited, 2013



16.16 Illustration of DuraSeal Spine in use.



16.17 FocalSeal prepared for use.

© Woodhead Publishing Limited, 2013

source was used to direct light through a sterile reusable fibre-optic wand to the wound site. Gelation occurred in a few seconds, although full strength was achieved by continuing illumination for approximately 40 s.

The molecular structure of the macromonomer provided excellent elasticity and strength, allowing the material to function as a lung sealant where continuous expansion and contraction occur. To enhance bonding to lung tissue, a primer was included in FocalSeal L. The primer was a lower molecular weight PEG macromonomer with a lower viscosity and a higher concentration. The higher concentration allowed the primer to accommodate dilution from surface moisture and lower viscosity allowed improved penetration into tissue micro-topological features. The primer was designed to be applied in a thin layer just prior to application of the sealant layer. Before the light initiated polymerization reaction, a Fenton initiation reaction was employed to form a thin layer of gel at the tissue interface upon mixing the primer with the sealant on the tissue. Intermingling of the primer and sealant on a molecular level prior to gelation provided covalent coupling to sealant macromonomer. Application of additional sealant was followed by illumination to drive the photopolymerization reaction.

16.7.3 FocalSeal S (Genzyme)

FocalSeal S was approved as a dural sealant in the EU (Alleyne *et al.*, 1998). The FocalSeal S product was similar to FocalSeal L, but was designed specifically for minimal swelling in the cranial and spinal area.

16.7.4 OcuSeal Liquid Ocular Bandage (B&D)

OcuSeal™ Liquid Ocular Bandage (Fig. 16.18) is intended for direct application on the surface of the eye to form an ocular bandage, thereby covering an opening in the eye and providing an immediate protective barrier (Johnson *et al.*, 2009). This material uses a multi-armed polyamine that is crosslinked with a difunctional PEG N-hydroxysuccinimidylsuccinate. The material is provided in a multicomponent applicator that is assembled prior to use. The contents of two compartments in the applicator are mixed together to initiate the gelation reaction. The elongated gel time allows passage of mixed material through a flow-through brush, which aids corneal application. Gelation occurs on the tissue surface.

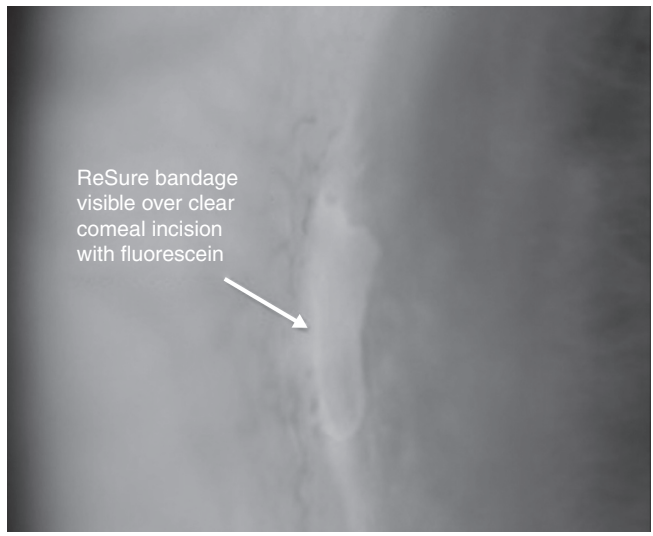
16.7.5 ReSure Ocular Bandage (Ocular Therapeutix)

ReSure Ocular Bandage (Fig. 16.19) is intended for covering ocular incisions and wounds on the surface of the eye. It is available in Europe, but

© Woodhead Publishing Limited, 2013

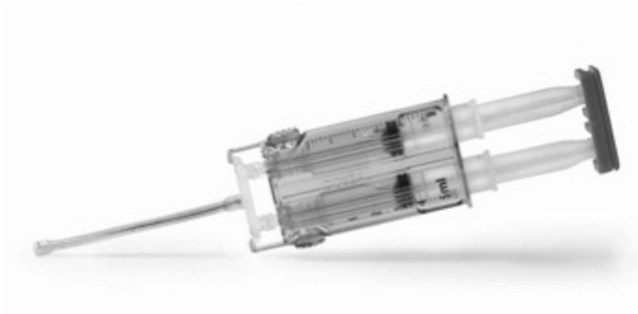


16.18 The OcuSeal applicator after assembly and ready to apply. OcuSeal is intended for application to the eye surface over wounds and incisions.



16.19 ReSure Ocular Bandage covering a corneal incision one day after cataract surgery.

© Woodhead Publishing Limited, 2013



16.20 CoSeal prepared for use.

is not currently available in the United States. The technology is similar to the DuraSeal Sealant described above. The system consists of components for preparation of the synthetic absorbable bandage, and an applicator for delivery of the sealant to the target site. The sealant is composed of two solutions, a multifunctionalized PEG ester solution and a tetrafunctional trilysine amine solution (referred to as the 'blue' and 'clear' precursors, respectively). When mixed together, the precursors crosslink to form the hydrogel sealant. A drop of each component is mixed together with the applicator just prior to use.

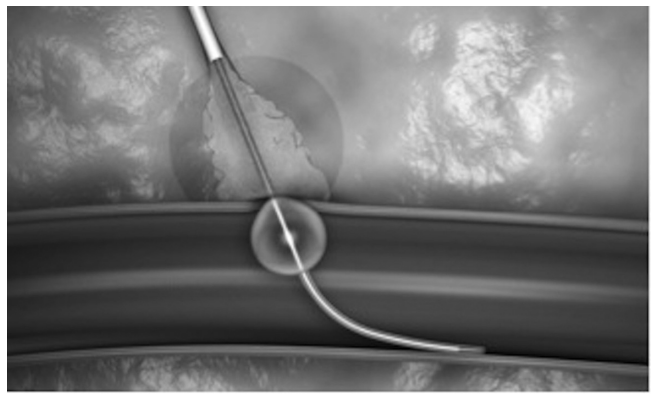
16.7.6 CoSeal Surgical Sealant (Baxter Health Care)

CoSeal Surgical Sealant (Glickman *et al*., 2002), for peripheral vascular reconstruction, is composed of two synthetic polyethylene glycols (PEGs), a dilute hydrogen chloride solution and a sodium phosphate/sodium carbonate solution (Fig. 16.20). These components come in a kit that includes an applicator(s). CoSeal is composed of (Hill *et al*., 2001) a four-arm PEG have been functionalized with N-hydroxysuccinimdylglutarate and a four-armed PEG thiol. Each has a molecular weight of approximately 10 000 Da. Before use the polymers are dissolved separately in their respective phosphate/carbonate buffer or hydrogen-chloride solutions. Each solution is then drawn into a syringe and assembled into a delivery device. At the time of administration, the mixed PEG solutions form a hydrogel that adheres to tissue and synthetic graft materials (Baxter Healthcare Corp, 2003).

16.7.7 Mynx vascular closure system (VCS) (Access Closure, Inc.)

Mynx is indicated for use to seal femoral arterial access sites (Access-Closure, Inc., 2010), reducing times to hemostasis and ambulation in

© Woodhead Publishing Limited, 2013



16.21 The Mynx sealant being deployed on the arteriotomy.

patients who have undergone diagnostic or interventional endovascular procedures (Scheinert *et al*., 2007). The sealant is based on a freeze-dried polyethylene glycol (PEG) 'xerogel' that instantly expands in the tissue tract upon contacting blood and tissue fluids, forming a hydrogel clot (see Fig. 16.21). The sealant then dissolves within 30 days, leaving a healed artery.

16.7.8 AngioSeal

(St. Jude Medical) The Angio-Seal™ vascular closure device consists of an intravascular bioresorbable anchor and an extravascular bovine collagen sponge, which are connected by an absorbable synthetic suture. Figure 16.22 is an illustration of the deployment of the device (Abando *et al*., 2004).

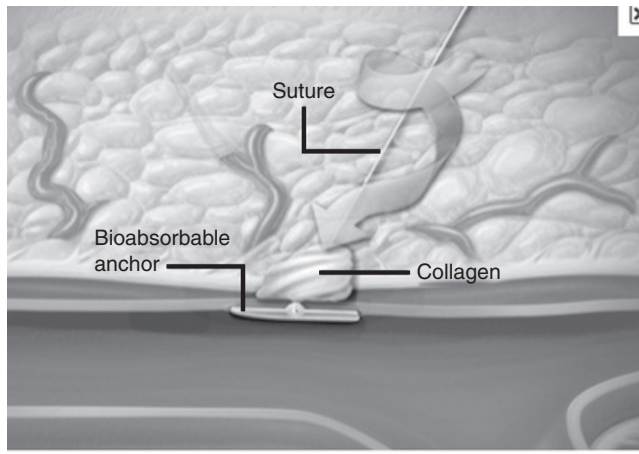
16.7.9 Exoseal (Cordis, J&J)

The Exoseal vascular closure device (Wong *et al*., 2009) is a wound fibrous plug composed of poly(glycolic acid) (PGA) fibre. PGA is a bioresorbable material commonly used in bioresorbable sutures such as Dexon (Covidien). This device relies on blood clotting in the fibrous plug to form a seal. Figure 16.23 is an illustration of the device after implantation.

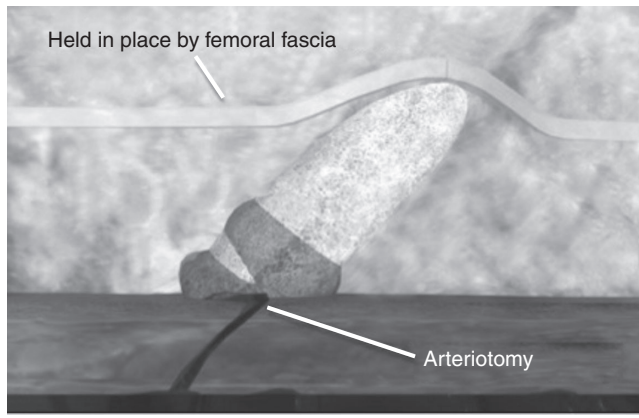
16.7.10 Adherus™ (HyperBranch)

HyperBranch has introduced a series of sealant products into Europe and has a clinical trial under way in the US (HyperBranch, 2010). The hydrogel is formed by reaction of a branched polyethyleneimine bearing

© Woodhead Publishing Limited, 2013



16.22 Illustration of AngioSeal after implantation.



16.23 Exoseal PGA plug for vascular closure.

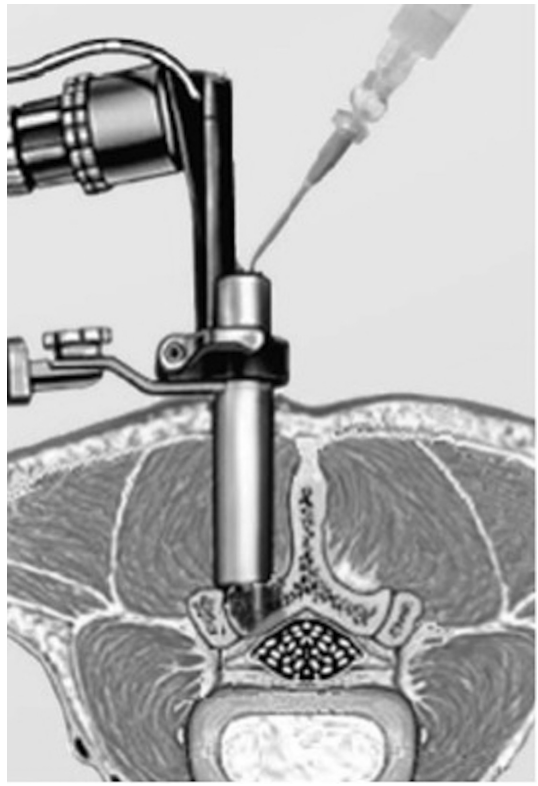
multiple primary amines with an NHS-activated PEG. The resulting sealant is resorbed over approximately 90 days (Carnahan and Butlin, 2010).

The Adherus Dural Sealant is used (in the EU) as an aid in dural repair in cranial surgeries such as the treatment of intracranial aneurysms, tumours and spinal-disc disease.

The Adherus Spinal Sealant is used (in the EU) as an aid in dural repair in minimally invasive spinal surgeries. This product is additionally claimed to act as an adhesion barrier. It is delivered by an applicator that is designed for endoscopic spinal procedures (Fig. 16.24).

HyperBranch's Adherus Vascular Sealant mechanically seals the sutured anastomosis sites of blood vessels and artificial grafts to prevent blood leakage. It is applied from a ready to use delivery system.

© Woodhead Publishing Limited, 2013



16.24 Adherus Spine in use.

TissuePatch (Tissuemed, Leeds UK) is a surgical sealant film with EU approval for general surgery, lung and dural applications (Puppa *et al*., 2010; Ferroli *et al*., 2011). The technology is based on a bioresorbable poly(lactide-co-glycolide) (PLGA) film laminated with a film of poly(acrylic acid-co-N-vinylpyrrolidone) partially substituted with N-hydroxysuccinimide (NHS). The NHS groups provide reactive groups that form covalent linkages with nucleophilic species on the tissue surface, specifically targeting proteins bearing primary amines.

Three variants of TissuePatch have been developed: TissuePatch3, TissuePatchDural and TissuePactchThoracic. TissuePatch3 is indicated for general and thoracic sealing. TissuePatchDural and TisuePatchThoracic are designed specifically for dural and thoracic sealing respectively. The patch is applied by pressing the reactive side of the laminate against the tissue for at least 30 s. The stated mode of action (Tissuemed, 2012) is the formation of ionic and covalent interactions with the tissue. The material gradually degrades and resorbs over about 50 days.

© Woodhead Publishing Limited, 2013

16.8 Commercial resorbable bio-derived sealants and adhesives

This group of materials consists of two principal types: fibrin glue and albumin crosslinked with functionalized PEG (see Table 16.2).

16.8.1 Fibrin sealants

Fibrin sealants are composed of several components that are combined as two solutions to form the two-part adhesive preparation. The main components, fibrinogen and thrombin, are produced from pooled human blood. In many formulations Factor XIII, a crosslinking agent also from human origin, is included. The leading product in this sector is Tisseel (Baxter Healthcare Corp, CA), which is sold in different formats. The most advanced and easy to use format is the Tisseel Duo product with frozen pre-filled syringes (Fig. 16.25).

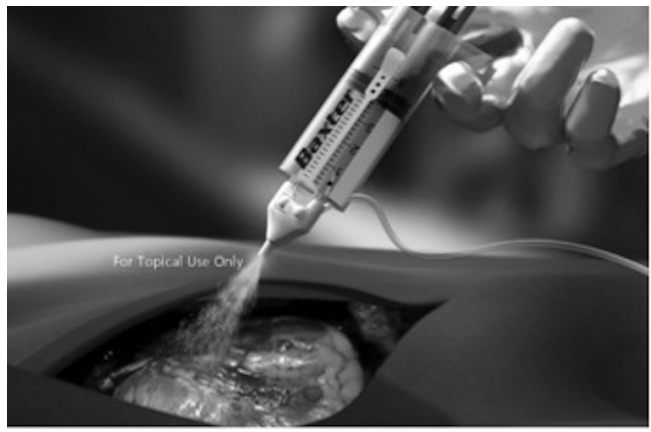
The Tisseel pre-filled syringe (frozen) with DUO Set contains a sealer protein solution and a thrombin solution with compositions as follows (Baxter Healthcare Corp, 2009b):

- *Sealer protein solution*:
  Total protein: 96–125 mg/mL
  Fibrinogen (human): 67–106 mg/mL
  Aprotinin fibrinolysis inhibitor (synthetic): 2250–3750 KIU/mL
  Other ingredients include: human albumin, tri-sodium citrate, histidine, niacinamide, polysorbate 80 and water for injection (WFI).

Table 16.2 Commercial boiresorbable bio-derived tissue adhesives and sealants

Brand name	Surgical application	Composition	Manufacturer	Available
Tisseel	Cardiovascular and general surgery	Fibrin	Baxter Health Care	EU, USA
Evicel	Cardiovascular and general surgery	Fibrin	Johnson & Johnson	EU, USA
Vitagel	Cardiovascular and general surgery	Fibrin	Orthovita	EU, USA
CryoSeal	Cardiovascular and general surgery	Fibrin	Thermogenesis Corporation	EU, USA
ProGel	Lung	Albumin–PEG	NeoMend	EU, USA

© Woodhead Publishing Limited, 2013



16.25 Fibrin sealant in use.

- *Thrombin solution*:
  Thrombin (human): 400–625 units/mL
  Calcium chloride: 36–44 μmol/mL
  Other ingredients include: human albumin, sodium chloride and WFI

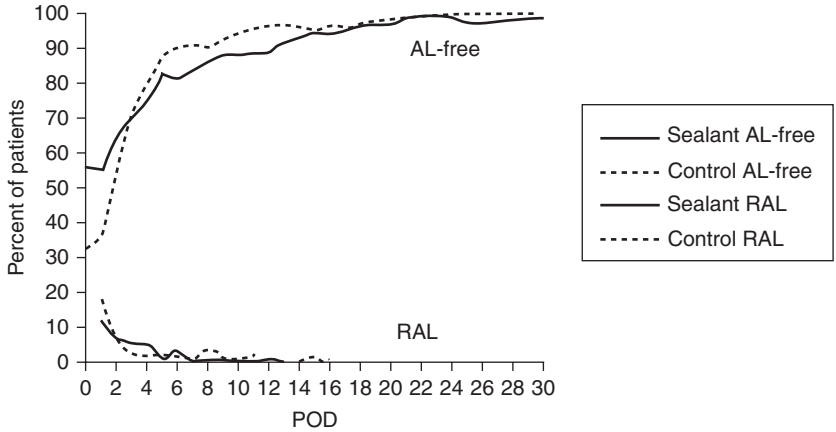
Mixing the sealer and thrombin solutions in equal proportions initiates the clotting cascade. A two-syringe sprayer can also be used to mix and spray, which is preferred when applying a thin layer over a large area.

Fibrin sealants are useful for their hemostatic properties. The resorption is a result of natural fibrinolysis, which can be controlled by formulation. The bond strength to internal tissues is limited when compared with synthetic sealants and adhesives.

16.8.2 PEG/albumin – NeoMend

NeoMend Inc. 'ProGEL™ Surgical Sealant' is intended as an adjunct to standard tissue-closure techniques for sealing or reducing air leaks incurred during pulmonary surgery (Neomend Inc., 2010). ProGEL is a two component hydrogel sealant, consisting of a human serum albumin solution and difunctional PEG N-hydroxysuccinimidylsuccinate, a dried powder reconstituted with sterile water. Mixed at the time of application, the liquid components quickly cure *in situ* to form a flexible patch for sealing and/or reducing air leaks in the lung (NeoMend Inc., 2012). After application, the body resorbs the patch material within 28 days. This material was tested clinically (Fig. 16.26), showing a marginal benefit in leak rates.

© Woodhead Publishing Limited, 2013



16.26 NeoMend's ProGel Surgical Sealant clinical study of sealant applied over sutures showed early post-operative day (POD) benefit in air leak (AL) rates compared with suture alone and similar recurrent air leak (RAL) rates.

16.9 Commercial biostable bio-derived sealants and adhesives

This class of materials uses at least one component that is biologically derived, such as albumin or gelatin. Although these products contain natural components, the extensive reactions used to effect gelation render them biostable. BioGlue, for example, uses bovine serum albumin, but then crosslinks it by reaction with glutaraldehyde (Chao and Torchiana, 2003), creating a new chemical species that is unrecognizable by proteolytic enzymes. Depending on the degree of crosslinking, biodegradation or biodeterioration of such materials by enzymes is therefore minimal, that is, the material is biostable. There are two commercial products currently available in this class of adhesives/sealants as shown in Table 16.3.

16.9.1 Biological surgical G.R.F (MicroVal)

Gelatin-resorcinol-formaldehyde-glutaraldehyde (GRFG) is a contemporary version of an early bio-derived adhesive that uses gelatin and resorcinol crosslinked by formaldehyde. In this system, gelatin and resorcinol are dissolved in water and a second solution containing dissolved formaldehyde and glutaraldehyde initiates crosslinking when added. The mechanism of curing has not been fully described, but it is likely the gelatin and resorcinol do not intercrosslink, rather forming an interpenetrating network (IPN), each separately reacting with aldehyde.

© Woodhead Publishing Limited, 2013

Table 16.3 Commercial biostable bio-derived tissue adhesives and sealants

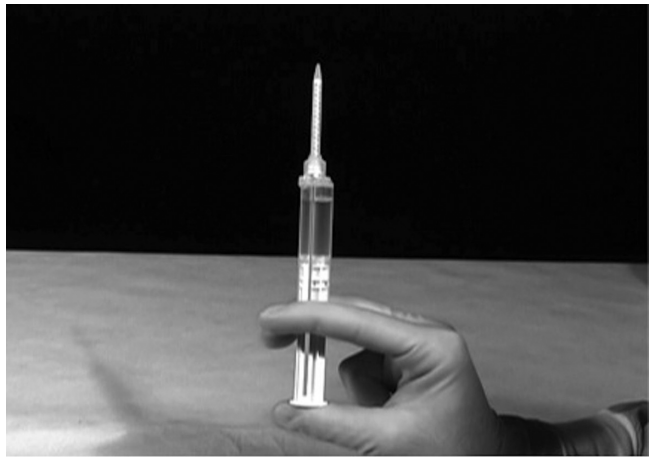
Brand name	Surgical application	Composition	Manufacturer	Available
Biological surgical G.R.F	Vascular	GRFG	MicroVal	EU
BioGlue	Albumin–glutaraldehyde	Albumin–glutaraldehyde	CryoLife	EU, USA

The degree of crosslinking to achieve gel formation is low, so although aldehyde is largely consumed by crosslinking, presence of a small amount of residual aldehyde is likely. Formaldehyde, in particular, has known negative toxicity and carcinogenicity profiles, so partial or complete replacement of formaldehyde with less toxic aldehydes such as glutaraldehyde and glyoxal have been explored. The GRF adhesives have been surpassed by more advanced and less toxic materials. These alternative aldehydes are still quite toxic to nervous and ocular tissue and can cause local tissue necrosis and inflammation. Gluetiss® (Berlin Heart), which uses both glutaradehyde and glyoxal, was originally indicated for treating aortic dissections and remains commercially available in some countries.

16.9.2 BioGlue (CryoLife)

A tissue adhesive in current use with some similarities to GRF is the commercially available BioGlue® Surgical Adhesive (Fig. 16.27) (Chao and Torchiana, 2003; Friedman and Schalch, 2008; Rathinam *et al.*, 2009; Chauvet *et al.*, 2011). It is a two-component formulation composed of solutions of purified bovine serum albumin (BSA) and glutaraldehyde that mixes as it is extruded through a static mixer. The material reaches adequate strength in 2 min (Cryolife Inc., 2010). Originally approved for aortic dissections by the FDA under the Humanitarian Device Exemption (HDE) in 1999, BioGlue was later approved for vascular anastomosis sealing (CryoLife, Inc., 2001). The glutaraldehyde is claimed to react with tissue proteins in addition to the BSA, forming covalent adhesive-tissue bonds. Company literature (CryoLife, 2012) explains that BioGlue degrades via proteolysis and that it can be slow to resorb dependent on the quantity of adhesive applied. No reference could be found, however, demonstrating the material is actually resorbable so it is classified herein as biostable. As in the case of GRF, the toxicity of BioGlue is a serious concern as glutaraldehyde is toxic to ocular and nervous tissue.

© Woodhead Publishing Limited, 2013



16.27 BioGlue prepared for use.

16.10 Commercial biostable synthetic sealants and adhesives

Synthetic biostable adhesives function by undergoing a physical change from liquid to solid on the tissue surface, thereby engaging a physical bond with the underlying tissue surface irregularities. In the case of cyanoacrylate, this transformation is a moisture induced polymerization of the cyanoacrylate monomer. Biostability refers to the irreversibility of the transformation. Biostable materials are characterized by the lack of degradable molecular linkages that can be exploited to reduce crosslinking or molecular weight. The use of such materials should be limited to topical areas where the material eventually falls or wears off.

16.10.1 Cyanoacrylates

Cyanoacrylates are indicated for topical skin-closure applications, but have been used as adhesives in other areas where unusual circumstances or emergency situations presented, such as battlefield injuries and some ophthalmology procedures (Chan and Boisjoly, 2004). Cyanoacrylates present toxicity concerns due to three factors: local heat generation due to the highly exothermic polymerization reaction, residual monomer and hydrolytic degradation products. Internal use of cyanoacrylates can result in inflammatory response, delayed healing and necrosis. While low molecular weight side chain cyanoacrylates such as ethyl-2-cyanoacrylate degrade via

© Woodhead Publishing Limited, 2013

Table 16.4 Commercial biostable synthetic tissue adhesives and sealants

Brand name	Surgical application	Composition	Manufacturer	Available
Dermabond	Topical	n-Octyl-2-cyanoacrylate	Johnson & Johnson	EU, USA
Histoacryl	Topical	n-Butyl-2-cyanoacrylate	B. Braun	EU
Indermyl	Topical	n-Butyl-2-cyanoacrylate	Covidien	EU, USA
Liquiband	Topical	n-Butyl-2-cyanoacrylate	Medlogic	EU, USA

hydrolysis, toxic degradation products such as formaldehyde are liberated, potentially causing local tissue toxicity (Webster and West, 2002). Higher molecular weigh side chains, such as n-butyl and n-octyl, are employed in commercial topical sealants due to their hydrolytic stability, higher viscosity and reduced exotherm from polymerization. These higher molecular weight variants overcome much of the toxicity concerns, but at the cost of becoming biostable, making them unsuited to internal use. The commercial cyanoacrylate adhesives are listed in Table 16.4.

16.11 Conclusion

The difference between adhesives and sealants is fundamental to the material-design considerations for the device. Adhesives can either join tissues together at the top edges or by being interposed between the separated tissue surfaces. In the latter case, the treatment must be evaluated for its potential to delay healing. Sealants, which cover a leaking wound, but do not penetrate the wound, must be evaluated for their ability to withstand pressure from these fluids, both along the sealant/tissue interface and through the sealant bulk. The chemistry of the *in situ* solidification reaction must be evaluated for local chemical or thermal effects on the tissue. Recent advances in synthetic bioresorbable materials, especially hydrogels, offer surgeons new opportunities to speed surgery and improve outcomes.

16.12 Sources of further information and advice

Anderson, J. 2004, 'Inflammation, wound healing and the foreign-body response', in B. Ratner, A. Hoffman and J. Lemons (eds), *Biomaterials Science: An Introduction to Materials in Medicine*, 2nd edn, Elsevier Academic Press, Amsterdam; Boston.

Anger, W.H. 2010, 'Surgical sealant for preventing air leaks after pulmonary resections in patients with lung cancer', *AORN*, vol. **92**, no. 3, pp. 351–352.

Avalos-González, J., Portilla-deBuen, E., Leal-Cortés, C.A, Orozco-Mosqueda, A., del Carmen Estrada-Aguilar, M., Velázquez-Ramírez, G.A., Ambriz-González,

© Woodhead Publishing Limited, 2013

G., Fuentes-Orozco, C., Guzmán-Gurrola, A.E. and González-Ojeda, A. 2010, 'Reduction of the closure time of postoperative enterocutaneous fistulas with fibrin sealant', *World Journal of Gastroenterology: WJG*, vol. **16**, no. 22, p. 2793.

Bachet, J., Goudot, B., Dreyfus, G.D., Brodaty, D., Dubois, C., Delentdecker, P. and Guilmet, D. 1999, 'Surgery for acute type A aortic dissection: the Hôpital Foch experience (1977–1998)', *Annals of Thoracic Surgery*, vol. **67**, no. 6, pp. 2006–2009.

Berdahl, J.P., Johnson, C.S., Proia, A.D., Grinstaff, M.W. and Kim, T. 2009, 'Comparison of sutures and dendritic polymer adhesives for corneal laceration repair in an in vivo chicken model', *Archives of Ophthalmology*, vol. **127**, no. 4, pp. 442–447.

Bhatia, S.K. and Arthur, S.D. 2008, 'Poly(vinyl alcohol) acetoacetate-based tissue adhesives are non-cytotoxic and non-inflammatory', *Biotechnology Letters*, vol. **30**, no. 8, pp. 1339–1345.

Birth, M., Figueras, J., Bernardini, S., Troen, T., Günther, K., Mirza, D., Mortensen, F.V. and others 2009, 'Collagen fleece-bound fibrin sealant is not associated with an increased risk of thromboembolic events or major bleeding after its use for haemostasis in surgery: a prospective multicentre surveillance study', *Patient Safety in Surgery*, vol. **3**, no. 1, p. 13.

Bitton, R. and Bianco-Peled, H. 2008, 'Novel biomimetic adhesives based on algae glue', *Macromolecular Bioscience*, vol. **8**, no. 5, pp. 393–400.

Black, J. 2006, *Biological Performance of Materials Fundamentals of Biocompatibility*, Taylor & Francis, Boca Raton, FL.

Box, G.N., Lee, H.J., Abraham, J.B.A., Deane, L.A., Santos, R.J.S., Elchico, E.R., Khosravi, A., Abdelshehid, C.A., Alipanah, R., Li, K., Moskowitz, R.M., Philips, J.M., Edwards, R.A., Borin, J.F., McDougall, E.M. and Clayman, R.V. 2009, 'Evaluation of the outcomes of electrosurgical induced bowel injury treated with tissue glue/sealant versus sutured repair in a rabbit model', *Journal of Endourology*, vol. **23**, no. 3, pp. 535–540.

Buskens, E., Meijboom, M.J., Kooijman, H. and Van Hout, B.A. 2006, 'The use of a surgical sealant (CoSeal) in cardiac and vascular reconstructive surgery: an economic analysis', *Journal of Cardiovascular Surgery*, vol. **47**, no. 2, pp. 161–170.

Cabral, J. and Moratti, S.C. 2011, 'Hydrogels for biomedical applications', *Future Medicinal Chemistry*, vol. **3**, no. 15, pp. 1877–1888.

Chenault, H.K. 2010, 'Protein-based polymer tissue adhesives for medical use', US 7837986.

Chenault, H.K. and Figuly, G.D., 2008, 'Tissue adhesives with modified elasticity', US 2008/0004421 A1.

Chew, A.C.Y., Tan, D.T.H., Poh, R., Htoon, H. M., Beuerman, R.W. and Mehta, J.S. 2010, 'Effect of intracameral injection of fibrin tissue sealant on the rabbit anterior segment', *Molecular Vision*, vol. **16**, p. 1087.

Confluent Surgical 2005, *DuraSeal Dural Sealant Instructions for Use*, Confluent Surgical.

Confluent Surgical 2009, 'SSED – DuraSeal Spine Sealant System – P080013'.

Cordis Corp 2011, *EXOSEAL Brochure*, Cordis Corp.

Degoricija, L., Johnson, C.S., Wathier, M., Kim, T. and Grinstaff, M.W. 2007, 'Photo cross-linkable biodendrimers as ophthalmic adhesives for central lacerations and penetrating keratoplasties', *Investigative Ophthalmology & Visual Science*, vol. **48**, no. 5, pp. 2037–2042.

© Woodhead Publishing Limited, 2013

Duarte, A.P., Coelho, J.F., Bordado, J.C., Cidade, M.T. and Gil, M.H. n.d., 'Surgical adhesives: Systematic review of the main types and development forecast', *Progress in Polymer Science*, Available online 14 December 2011, viewed 26 March 2012, www.sciencedirect.com/science/article/pii/S0079670011001365.

Elvin, C.M., Brownlee, A.G., Huson, M.G., Tebb, T.A., Kim, M., Lyons, R.E., Vuocolo, T., Liyou, N.E., Hughes, T.C., Ramshaw, J.A.M. and Werkmeister, J.A. 2009, 'The development of photochemically crosslinked native fibrinogen as a rapidly formed and mechanically strong surgical tissue sealant', *Biomaterials*, vol. **30**, no. 11, pp. 2059–2065.

Elvin, C.M., Danon, S.J., Brownlee, A.G., White, J.F., Hickey, M., Liyou, N.E., Edwards, G.A., Ramshaw, J.A.M. and Werkmeister, J.A. 2010, 'Evaluation of photo-crosslinked fibrinogen as a rapid and strong tissue adhesive', *Journal of Biomedical Materials Research Part A*, vol. **93A**, no. 2, pp. 687–695.

Elvin, C.M., Vuocolo, T., Brownlee, A.G., Sando, L., Huson, M.G., Liyou, N.E., Stockwell, P.R., Lyons, R.E., Kim, M., Edwards, G.A., Johnson, G., McFarland, G.A., Ramshaw, J.A.M and Werkmeister, J.A 2010, 'A highly elastic tissue sealant based on photopolymerised gelatin', *Biomaterials*, vol. **31**, no. 32, pp. 8323–8331.

Ethicon, Inc. 2009, EVICEL Fibrin Sealant (Human) package insert, Ethicon, Inc.

Figueras, J., Llado, L., Miro, M., Ramos, E., Torras, J., Fabregat, J. and Serrano, T. 2007, 'Application of fibrin glue sealant after hepatectomy does not seem justified', *Annals of Surgery*, vol. **245**, no. 4, pp. 536–542.

Floris, R., Salvatore, C., Fraioli, B., Pastore, F.S., Vagnozzi, R. and Simonetti, G. 1998, 'Trans-sphenoidal treatment of postsurgical cerebrospinal fluid fistula: CT-guided closure', *Neuroradiology*, vol. **40**, no. 10, pp. 690–694.

Fortune, D.H., Kettlewell, G., Mandley, D.J., Morris, D. and Thompson, I. 2009, 'Tissue-adhesive materials', US 2009/0044895 A1.

Fortune, D.H., Kettlewell, G., Mandley, D.J., Thompson, I. and Cook., D 2010, 'Tissue-adhesive formulations', US 7727547.

Fransen, P. 2010, 'Reduction of postoperative pain after lumbar microdiscectomy with DuraSeal Xact Adhesion Barrier and Sealant System', *The Spine Journal: Official Journal of the North American Spine Society*, vol. **10**, no. 9, pp. 751–761.

Fukuchi, T., Sueda, J., Usumoto, N., Okuno, T., Kalayci, D., Sawhney, A. and Hirose, T. 2003, 'Hydrogel tissue adhesive: feasiblity study for intraocular use ERG and histology', *Investigative Ophthalmology & Visual Science*, vol. **44**, no. 5, p. 3015.

Geister Medizintechnik GmbH 2012, GLUETISS Product Brochure, www.geister.com.

Gong, G., Wartchow, C. and Schlosser, A. 2010, 'Tissue adhesive compositions and methods thereof', US 2010/0297218 A1.

Guilmet, D., Bachet, J., Goudot, B., Laurian, C., Gigou, F., Bical, O. and Barbagelatta, M. 1979, 'Use of biological glue in acute aortic dissection: preliminary clinical results with a new surgical technique', *Journal of Thoracic and Cardiovascular Surgery*, vol. **77**, no. 4, pp. 516–521.

Hadba, A.R. and Stopek, J.B. 2010, 'Tissue adhesives and sealants and method for their use', US 7858079.

Hammerslag, J.G. and Quinn, J. 2009, 'Controlled viscosity tissue adhesive', US 2009/0036921 A1.

© Woodhead Publishing Limited, 2013

Hidas, G., Kastin, A., Mullerad, M., Shental, J., Moskovitz, B. and Nativ, O. 2006, 'Sutureless nephron-sparing surgery: use of albumin glutaraldehyde tissue adhesive (BioGlue)', *Urology*, vol. **67**, no. 4, pp. 697–700.

Jackson, M.R. 2001, 'Fibrin sealants in surgical practice: an overview', *American Journal of Surgery*, vol. **182**, no. 2, pp. S1–S7.

Jankowitz, B., Atteberry, D., Gerszten, P., Karausky, P., Cheng, B., Faught, R. and Welch, W. 2009, 'Effect of fibrin glue on the prevention of persistent cerebral spinal fluid leakage after incidental durotomy during lumbar spinal surgery', *European Spine Journal*, vol. **18**, no. 8, pp. 1169–1174.

Kim, K.D. and Wright, N.M. 2011, 'Polyethylene glycol hydrogel spinal sealant (DuraSeal Spinal Sealant) as an adjunct to sutured dural repair in the spine: results of a prospective, multicenter, randomized controlled study', *Spine*, vol. **36**, no. 23, pp. 1906–1912.

Koranyi, G. 2004, 'Cut and paste: a no suture, small incision approach to pterygium surgery', *British Journal of Ophthalmology*, vol. **88**, no. 7, pp. 911–914.

Küçükaksu, D.S., Akgül, A., Çağli, K. and Taşdemir, O. 2000, 'Beneficial effect of BioGlue® surgical adhesive in repair of iatrogenic aortic dissection', *Texas Heart Institute Journal*, vol. **27**, no. 3, pp. 307–308.

Lim, K. and Tan., L 2009, 'Interaction force measurements for the design of tissue adhesives', *Acta Biomaterialia*, vol. **5**, no. 1, pp. 84–92.

Lowinger, J., Lowinger, B., DeLustro, F., Cox, D. and Browdie, D.A. 2009, 'Tissue adhesive sealant', US 2009/0287313 A1.

Lu, H.S.M. 2010, 'Dextran-based polymer tissue adhesive for medical use', US 2010/0255101 A1.

Lundblad, R.L. 2009, *Application of Solution Protein Chemistry to Biotechnology*, CRC Press/Taylor & Francis, Boca Raton, FL.

Lutolf, M.P. and Hubbell, J.A. 2005, 'Synthetic biomaterials as instructive extracellular microenvironments for morphogenesis in tissue engineering', *Nature Biotechnology*, vol. **23**, no. 1, pp. 47–55.

Mahdavi, A., Ferreira, L., Sundback, C., Nichol, J.W., Chan, E.P., Carter, D.J.D., Bettinger, C.J., Patanavanich, S., Chignozha, L., Ben-Joseph, E. and others 2008, 'A biodegradable and biocompatible gecko-inspired tissue adhesive', *Proceedings of the National Academy of Sciences*, vol. **105**, no. 7, p. 2307.

Malapert, G., Hanna, H.A., Pages, P.B. and Bernard, A. 2010, 'Surgical sealant for the prevention of prolonged air leak after lung resection: meta-analysis', *The Annals of Thoracic Surgery*, vol. **90**, no. 6, pp. 1779–1785.

Miller, S.H, Price, G., Buck, D., Neeley, J., Kennedy, T.J., Graham, W.P., 3rd and Davis, T.S. 1979, 'Effects of tourniquet ischemia and postischemic edema on muscle metabolism', *The Journal of Hand Surgery*, vol. **4**, no. 6, pp. 547–555.

Mo, X., Iwata, H. and Ikada, Y. 2010, 'A tissue adhesives evaluated in vitro and in vivo analysis', *Journal of Biomedical Materials Research Part A*, vol. **94A**, no. 1, pp. 326–332.

Mortenson, M.M., Xing, Y., Weaver, S., Lee, J.E., Gershenwald, J.E., Lucci, A., Mansfield, P.F., Ross, M.I., Cormier, J.N. and others 2008, 'Fibrin sealant does not decrease seroma output or time to drain removal following inguino-femoral lymph node dissection in melanoma patients: a randomized controlled trial (NCT00506311)', *World Journal of Surgical Oncology*, vol. **6**, p. 63.

© Woodhead Publishing Limited, 2013

Oelker, A.M., Berlin, J.A., Wathier, M. and Grinstaff, M.W 2011, 'Synthesis and characterization of dendron cross-linked PEG hydrogels as corneal adhesives', *Biomacromolecules*, vol. **12**, no. 5, pp. 1658–1665.

Osbun, J.W., Ellenbogen, R.G., Chesnut, R.M., Chin, L.S., Connolly, P.J., Cosgrove, G.R., Delashaw Jr., J.B., Golfinos, J.G., Greenlee, J.D.W., Haines, S.J., Jallo, J., Muizelaar, J.P, Nanda, A., Shaffrey, M., Shah, M.V., Tew Jr., J.M., van Loveren, H.R., Weinand, M.E., White, J.A. and Wilberger, J.E. n.d., 'A multicenter, single-blind, prospective randomized trial to evaluate the safety of a polyethylene glycol hydrogel (duraseal dural sealant system) as a dural sealant in cranial surgery', *World Neurosurgery*, published online 10 December 2011, viewed 25 March 2012, www.sciencedirect.com/science/article/pii/S1878875011014872.

Panda, A., Kumar, S., Kumar, A., Bansal, R. and Bhartiya, S. 2009, 'Fibrin glue in ophthalmology', *Indian Journal of Ophthalmology*, vol. **57**, no. 5, p. 371.

Pathak, C.P., Barman, S.P., Philbrook, C.M., Sawhney, A.S., Coury, A.J., Avila, L.Z. and Kieras, M.T. 2001, 'Multiblock biodegradable hydrogels for drug delivery and tissue treatment', US 6201065.

Peng, H.T. and Shek, P.N. 2010, 'Novel wound sealants: biomaterials and applications', *Expert Review of Medical Devices*, vol. **7**, no. 5, pp. 639–659.

Preul, M.C., Campbell, P.K., Bennett, S. L and Muench, T.R. 2006, 'A unique dual-function device – a dural sealant with adhesion-prevention properties', *European Musculoskeletal Review*, 2006, pp. 41–44.

Redl, H., Khakpour, Z., Ariagno, S.R., Kellner, A. and Zakarija, L.G. 2009, 'Hand triggered tissue sealant spray apparatus and system', US 7537174.

Redl, H., Schlag, G. and Eibl, J. 2011, 'Fibrinogen-based tissue adhesive containing an elastase inhibitor', US 7892802.

Rehor, A. and Cerritelli, S. n.d., 'Polymeric tissue sealant', US 2008/0253987 A1.

Reynolds, M.W., Clark, J., Crean, S., Samudrala, S. and others. 2008, 'Risk of bleeding in surgical patients treated with topical bovine thrombin sealants: a review of the literature', *Patient Safety in Surgery*, vol. **2**, no. 1, p. 5.

Sawhney, A.S., Lyman, M.D., Jarrett, .PK. and Rudowsky, R.S 1999, 'Compliant tissue sealants', US 6177095.

Schwabbauer, M.L. 1975, 'Use of the latent image technique to develop and evaluate problem-solving skills', *American Journal of Medical Technology*, vol. **41**, no. 12, pp. 457–462.

Sehl, L.C., Trollsas, O.M., Wallace, D.G., Toman, D., DeLustro, F.A., Schroeder, J.A. and Chu, G.H n.d., 'Adhesive tissue repair patch and collagen sheets', US 2010/0233246 A1.

Serra-Mitjans, M, Belda-Sanchis, J and Rami-Porta, R 2005, 'Surgical sealant for preventing air leaks after pulmonary resections in patients with lung cancer', *Cochrane Database of Systematic Reviews (Online)*, no. 3, p. CD003051.

Shalaby, S.W. and Vaughn, M.A. 2008, 'Polyester/cyanoacrylate tissue adhesive compositions', US 7351426.

Shalaby, S.W., Vaughn, M.A., Lindsey, J.M. and III n.d., 'Cyanoacrylate tissue adhesive formulations with multipurpose rheology modifiers', US 2009/0264555 A1.

Shammas, N.W., Rajendran, V.R., Alldredge, S.G., Witcik, W.J., Robken, J.A., Lewis, J.R., McKinney, D., Hansen, C.A., Kabel, M.E., Harris, M., Jerin, M.J., Bontu, P.R., Dippel, E.J. and Labroo, A. 2002, 'Randomized comparison of vasoseal and angioseal closure devices in patients undergoing coronary angiography

© Woodhead Publishing Limited, 2013

and angioplasty', *Catheterization and Cardiovascular Interventions*, vol. **55**, no. 4, pp. 421–425.

Shinya, N., Oka, S., Miyabashira, S., Kaetsu, H., Uchida, T., Sueyoshi, M., Takase, K., Akuzawa, M., Miyamoto, A. and Shigaki, T. 2009, 'Improvement of the tissue-adhesive and sealing effect of fibrin sealant using polyglycolic acid felt', *Journal of Investigative Surgery*, vol. **22**, no. 5, pp. 383–389.

Silverman, H.G. and Roberto, F.F. 2007, 'Understanding marine mussel adhesion', *Marine Biotechnology*, vol. **9**, no. 6, pp. 661–681.

Spotnitz, W.D. and Burks, S. 2008, 'Hemostats, sealants, and adhesives: components of the surgical toolbox', *Transfusion*, vol. **48**, no. 7, pp. 1502–1516.

Spotnitz, W.D., Burks, S.G. and Prabhu, R. 2005, 'Fibrin-based adhesives and hemostatic agents', In Quinn, J. V. (ed.), *Tissue Adhesives in Clinical Medicine.* BC Decker, Hamilton, Ontario, pp. 77–112.

Sternberg, K., Rohm, H.W., Lurtz, C., Wegmann, J., Odermatt, E.K., Behrend, D., Michalik, D. and Schmitz, K.-P. 2010, 'Development of a biodegradable tissue adhesive based on functionalized 1,2-ethylene glycol bis(dilactic acid). I.', *Journal of Biomedical Materials Research Part B: Applied Biomaterials*, **94b**(2), August 2010.

Suzuki, Y., Ujiie, H., Takahashi, N. and Iwaki, M. 2010, 'Biological repair material compatible with biological tissue adhesive', US 7722934.

Tredree, R., Beierlein, W., Debrix, I., Eisert, A., Goffredo, F., Gómez de Salazar, E, Rambourg, P., Saint-Remy, J.M., Sturm, C. and Watson, N. 2006, 'Evaluating the differences between fibrin sealants: recommendations from an international advisory panel of hospital pharmacists', *European Journal of Hospital Pharmacy Science*, vol. **12**, no. 1, pp. 3–9.

Vera, L., Benzerroug, M., Gueudry, J., Varin, R., Haghighat, S., Gérard, G and Muraine, M. 2009, 'Mise au point sur l'utilisation des colles tissulaires en ophtalmologie', *Journal Français d'Ophtalmologie*, vol. **32**, no. 4, pp. 290–305.

Vollenweider, L., Murphy, J.L., Xu, F., Brodie, M., Lew, W.L., Dalsin, J.L. and Lee, B.P. 2010, *Biomimetic Adhesive Coatings for Soft Tissue Repair*, Nerites Corp., 15th International Coating Science and Technology Symposium, September 13–15, 20.

von der Brelie, C, Soehle, M Burkett, C.J., Patel, S., Tabor, M.H., Padhya, T. and Vale, F.L. 2011, 'Polyethylene glycol (PEG) hydrogel dural sealant and collagen dural graft matrix in transsphenoidal pituitary surgery for prevention of postoperative cerebrospinal fluid leaks', *Journal of Clinical Neuroscience*, vol. **18**, no. 11, pp. 1513–1517.

Wagman, M.E., Qi, K., Kunitsky, K. and Yim, H.W. 2009, 'Hydrogel tissue adhesive having increased degradation time', US 2010/0160960 A1.

Weinstein, J.S., Liu, K.C., Delashaw, J.B., Burchiel, K.J., van Loveren, H.R., Vale, F.L., Agazzi, S., Greenberg, M.S., Smith, D.A. and Tew, J. 2010, 'The safety and effectiveness of a dural sealant system for use with nonautologous duraplasty materials', *Journal of Neurosurgery*, vol. **112**, no. 2, pp. 428–433.

Weisel, J. and Cederholm-Williams, S. 1997, 'Fibrinogen and fibrin: characterization, processing and medical applications', in A.J. Domb, J. Kost and D.M. Wiseman (eds), *Handbook of Biodegradable Polymers*, Harwood Academic Publishers, Australia; United States, pp. 347–366.

Xie, H. 2009, 'Tissue sealant made from whole blood', US 2009/0011043 A1.

© Woodhead Publishing Limited, 2013

Zawaneh, P.N., Singh, S.P., Padera, R.F., Henderson, P.W., Spector, J.A. and Putnam, D. 2010, 'Design of an injectable synthetic and biodegradable surgical biomaterial', *Proceedings of the National Academy of Sciences*, vol. **107**, no. 24, p. 11014.

Zhang, S. and Ruiz, R. n.d., 'Stable and sterile tissue adhesive composition with a controlled high viscosity', US 2009/0318583 A1.

Zhang, S., Ruiz, R. and Sr. n.d., 'Cyanoacrylate tissue adhesives with desirable permeability and tensile strength', US 2011/0117047 A1.

16.13 References

Abando, A., Hood, D., Weaver, F. and Katz, S. 2004, 'The use of the Angioseal device for femoral artery closure', *Journal of Vascular Surgery*, vol. **40**, no. 2, pp. 287–290.

AccessClosure, Inc. 2010, *Mynx Cadence Instructions for Use*, AccessClosure, Inc.

Alleyne, C.H., Cawley, C.M., Barrow, D.L., Poff, B.C., Powell, M.D., Sawhney, A.S. and Dillehay, D.L. 1998, 'Efficacy and biocompatibility of a photopolymerized, synthetic, absorbable hydrogel as a dural sealant in a canine craniotomy model', *Journal of Neurosurgery*, vol. **88**, no. 2, pp. 308–313.

Anderson, N.J. and Hardten, D.R. 2003, 'Fibrin glue for the prevention of epithelial ingrowth after laser in situ keratomileusis', *Journal of Cataract and Refractive Surgery*, vol. **29**, no. 7, pp. 1425–1429.

Baxter Healthcare Corp. 2003, 'SSED – CoSeal™ Surgical Sealant – P030039'.

Baxter Healthcare Corp. 2009a, *CoSeal Surgical Sealant Instructions for Use*, Baxter Healthcare Corp.

Baxter Healthcare Corp. 2009b, *TISSEEL [Fibrin Sealant] Instructions for Use*, Baxter Healthcare Corporation.

Bayfield, M.S. and Spotnitz, W.D. 1996, 'Fibrin sealant in thoracic surgery: pulmonary applications, including management of bronchopleural fistula', *Chest Surgery Clinics of North America*, vol. **6**, 576–583.

Bennett, S.L., Melanson, D.A., Torchiana, D.F., Wiseman, D.M. and Sawhney, A.S. 2003, 'Next-generation hydrogel films as tissue sealants and adhesion barriers', *Journal of Cardiac Surgery*, vol. **18**, no. 6, pp. 494–499.

Berrevoet, F. and de Hemptinne, B. 2007, 'Clinical application of topical sealants in liver surgery: does it work?', *Acta chirurgica Belgica*, vol. **107**, no. 5, p. 504.

Boogaarts, J.D., Grotenhuis, J.A., Bartels, R.H.M.A. and Beems, T. 2005, 'Use of a novel absorbable hydrogel for augmentation of dural repair: Results of a preliminary clinical study', *Neurosurgery*, vol. **57**, no. 1 Suppl., pp. 146–151.

Browdie, D.A. and Cox, D. 2007, 'Tests of experimental tissue adhesive sealants: analysis of strength effects in relation to tissue adhesive sealant standards', *Texas Heart Institute Journal*, vol. **34**, no. 3, p. 313.

Brubaker, C.E., Kissler, H., Wang, L.J., Kaufman, D.B. and Messersmith, P.B. 2010, 'Biological performance of mussel-inspired adhesive in extrahepatic islet transplantation', *Biomaterials*, vol. **31**, no. 3, pp. 420–427.

Capello, J. 1997, 'Genetically engineered protein polymers', in A.J. Domb, J. Kost and D.M. Wiseman (eds), *Handbook of Biodegradable Polymers*, Harwood Academic Publishers, Australia; United States, pp. 387–416.

Carnahan, M.A. and Butlin, J.D.G. 2011, 'Crosslinked polyalkyleneimine hydrogels with tunable degradation rates', US 2011/0044932 A1.

© Woodhead Publishing Limited, 2013

Chan, S.M. and Boisjoly, H. 2004, 'Advances in the use of adhesives in ophthalmology', *Current Opinion in Ophthalmology*, vol. **15**, no. 4, pp. 305–310.

Chao, H.-H. and Torchiana, D.F 2003, 'BioGlue: albumin/glutaraldehyde sealant in cardiac surgery', *Journal of Cardiac Surgery*, vol. **18**, no. 6, pp. 500–503.

Chauvet, D., Tran, V., Mutlu, G., George, B. and Allain, J.-M. 2011, 'Study of dural suture watertightness: an in vitro comparison of different sealants', *Acta Neurochirurgica*, vol. **153**, no. 12, pp. 2465–2472.

Cooper, C.W. and Falb, R.D. 1968, 'Surgical adhesives', *Annals of the New York Academy of Sciences*, vol. **146**, no. 1, pp. 214–224.

Cosgrove, G.R., Delashaw, J.B., Grotenhuis, J.A., Tew, J.M., Van Loveren, H., Spetzler, R.F., Payner, T., Rosseau, G., Shaffrey, M.E., Hopkins, L.N. and others. 2007, 'Safety and efficacy of a novel polyethylene glycol hydrogel sealant for watertight dural repair', *Journal of Neurosurgery*, vol. **106**, no. 1, pp. 52–58.

Coury, A. 2004, 'Chemical and biochemical degradation of polymers', in B. Ratner, F. Schoen, A. Hoffman and J. Lemons (eds), *Biomaterials Science: An Introduction to Materials in Medicine*, 2nd edn, Elsevier Academic Press, Amsterdam; Boston, pp. 696–706.

CryoLife, Inc. 2001, 'SSED – CryoLife BioGlue Surgical Adhesive – P010003'.

CryoLife, Inc. 2010, *BioGlue Surgical Adhesive Instructions for Use*, CryoLife, Inc.

CryoLife, Inc. 2012, 'CryoLife: BioGlue® Surgical Adhesive', viewed online 26 March 2012, www.cryolife.com/international/products/bioglue-surgical-adhesive.

Dang, W., Daviau, T. and Brem, H. 1996, 'Morphological characterization of polyanhydride biodegradable implant Gliadel® during in vitro and in vivo erosion using scanning electron microscopy', *Pharmaceutical Research*, vol. **13**, no. 5, pp. 683–691.

Epstein, N.E. 2010, 'Dural repair with four spinal sealants: focused review of the manufacturers' inserts and the current literature', *The Spine Journal*, vol. **10**, no. 12, pp. 1065–1068.

Ferroli, P., Acerbi, F., Broggi, M., Schiariti, M., Albanese, E., Tringali, G., Franzini, A. and Broggi, G. 2011, 'A novel impermeable adhesive membrane to reinforce dural closure: a preliminary retrospective study on 119 consecutive high-risk patients', *World Neurosurgery*, Available online 1 November 2011, viewed 26 March 2012, http://linkinghub.elsevier.com/retrieve/pii/S1878875011011016.

Focal Inc. 2000, 'SSED – FocalSeal-Synthetic Absorbable Sealant P990028'.

Friedman, M. and Schalch, P. 2008, 'Middle turbinate medialization with bovine serum albumin tissue adhesive (bioglue)', *The Laryngoscope*, vol. **118**, no. 2, pp. 335–338.

Glickman, M., Gheissari, A., Money, S., Martin, J., Ballard, J.L. and others. 2002, 'A polymeric sealant inhibits anastomotic suture hole bleeding more rapidly than gelfoam/thrombin: results of a randomized controlled trial', *Archives of Surgery*, vol. **137**, no. 3, p. 326.

Grinstaff, M.W. 2007, 'Designing hydrogel adhesives for corneal wound repair', *Biomaterials*, vol. **28**, no. 35, pp. 5205–5214.

Harris, J.M. and Zalipski, S. 1997, *Poly(ethylene Glycol): Chemistry and Biological Applications*, American Chemical Society, Washington, DC.

Hill, A., Estridge, T.D., Maroney, M., Monnet, E., Egbert, B., Cruise, G. and Coker, G.T. 2001, 'Treatment of suture line bleeding with a novel synthetic surgical sealant in a canine iliac PTFE graft model', *Journal of Biomedical Materials Research*, vol. **58**, no. 3, pp. 308–312.

© Woodhead Publishing Limited, 2013

Hyperbranch. 2010, *Safety and Effectiveness of the Adherus Dural Sealant System When Used as a Dural Sealant in Cranial Procedures,* ClinicalTrials.gov identifier NCT01158378, HyperBranch Medical Technology, Inc.

Johnson, C.S., Wathier, M., Grinstaff, M. and Kim, T. 2009, 'In vitro sealing of clear corneal cataract incisions with a novel biodendrimer adhesive', *Archives of Ophthalmology*, vol. **127**, no. 4, pp. 430–434.

Kalayci, D., Fukuchi, T., Edelman, P.G., Sawhney, A.S., Mehta, M.C. and Hirose, T. 2003, 'Hydrogel tissue adhesive for sealing corneal incisions', *Ophthalmic Research*, vol. **35**, no. 3, pp. 173–176.

Lagoutte, F., Gauthier, L. and Comte, P. 1989, 'A fibrin sealant for perforated and preperforated corneal ulcers', *British Journal of Ophthalmology*, vol. **73**, no. 9, pp. 757–761.

Lee, B.P., Messersmith, P.B., Israelachvili, J.N. and Waite, J.H. 2011, 'Mussel-inspired adhesives and coatings', *Annual Review of Materials Research*, vol. **41**, no. 1, pp. 99–132.

Mai-ngam, K., Prahsarn, C., Seetapan, N. and Chumningan, P. 2005, 'Thermo-responsive chitosan-g-poly-N-isopropylacrylamide for tissue adhesives', *Proceedings of the 8th Polymers for Advanced Technologies International Symposium*, Budapest, Hungary.

McCrea, K.R., Ward, R.S. and Tian, Y. 2011, 'Silicone hydrogels for tissue adhesives and tissue dressing applications', US 2011/0086077 A1.

McKerracher, L. 2011, 'Methods for making and delivering Rho-antagonist tissue adhesive', US 2011/0086077 A1.

Metters, A. and Hubbell, J. 2004, 'Network formation and degradation behavior of hydrogels formed by Michael-type addition reactions', *Biomacromolecules*, vol. **6**, no. 1, pp. 290–301.

Mulder, M., Crosier, J. and Dunn, R. 2009, 'Cauda equina compression by hydrogel dural sealant after a laminotomy and discectomy: case report', *Spine*, vol. **34**, no. 4, pp. E144–E148.

Murakami, Y., Yokoyama, M., Nishida, H., Tomizawa, Y. and Kurosawa, H. 2009, 'In vivo and in vitro evaluation of gelation and hemostatic properties of a novel tissue-adhesive hydrogel containing a cross-linkable polymeric micelle', *Journal of Biomedical Materials Research Part B: Applied Biomaterials*, vol. **91B**, no. 1, pp. 102–108.

Narváez, J., Chakrabarty, A. and Chang, K. 2006, 'Treatment of epithelial ingrowth after LASIK enhancement with a combined technique of mechanical debridement, flap suturing, and fibrin glue application', *Cornea*, vol. **25**, no. 9, pp. 1115–1117.

Neomend Inc. 2010, 'SSED – ProGEL™ Pleural Air Leak Sealant – P010047'.

NeoMend Inc. 2012, *ProGELTM Surgical Sealant Instructions for Use*.

Park, J.B. and Lakes, R.S. 2007, *Biomaterials*, Springer Science + Business Media, LLC, New York.

Patel, M.R., Louie, W. and Rachlin, J. 1996, 'Postoperative cerebrospinal fluid leaks of the lumbosacral spine: management with percutaneous fibrin glue', *American Journal of Neuroradiology*, vol. **17**, no. 3, pp. 495–500.

Puppa, A.D., Rossetto, M. and Scienza, R. 2010, 'Use of a new absorbable sealing film for preventing postoperative cerebrospinal fluid leaks: remarks on a new approach', *British Journal of Neurosurgery*, vol. **24**, no. 5, pp. 609–611.

© Woodhead Publishing Limited, 2013

Rabotyagova, O.S., Cebe, P. and Kaplan, D.L. 2011, 'Protein-based block copolymers', *Biomacromolecules*, vol. **12**(2), pp. 269–289

Rathinam, S., Naidu, B.V., Nanjaiah, P., Loubani, M., Kalkat, M.S., Rajesh, P.B. and others. 2009, 'BioGlue and Peri-strips in lung volume reduction surgery: pilot randomised controlled trial', *Journal of Cardiothoracic Surgery*, vol. **4**, p. 37.

Reul, R. and Walsh, G. 2005, 'Tissue adhesives in thoracic and cardiovascular surgery', in K.L. Franco and J.B. Putnam (eds), *Advanced Therapy in Thoracic Surgery*, B.C. Decker, Hamilton, Ont.; Lewiston, NY, pp. 47–60.

Sawhney, A.S., Jarrett, P.K., Coury, A.J., Rudowsky, R.S., Powell, M.D., Avila, L.Z., Enscore, D.J., Goodrich, S.D., Nason, W.C. Yao, F., Weaver, D. and Barman, S.P. 2001, 'Polymerizable biodegradable polymers including carbonate or dioxanone linkages', US 5900245.

Sawhney, A.S., Pathak, C.P., van Rensburg, J.J., Dunn, R.C. and Hubbell, J.A. 1994, 'Optimization of photopolymerized bioerodible hydrogel properties for adhesion prevention', *Journal of Biomedical Materials Research*, vol. **28**, no. 7, pp. 831–838.

Scheinert, D., Sievert, H., Turco, M.A., Schmidt, A., Hauptmann, K.E., Mueller, R., Dadourian, D., Krankenberg, H. and Grube, E. 2007, 'The safety and efficacy of an extravascular, water-soluble sealant for vascular closure: initial clinical results for MynxTM', *Catheterization and Cardiovascular Interventions*, vol. **70**, no. 5, pp. 627–633.

Schenk, W.G., Burks, S.G., Gagne, P.J., Kagan, S.A., Lawson, J.H. and Spotnitz, W.D. 2003, 'Fibrin sealant improves hemostasis in peripheral vascular surgery: a randomized prospective trial', *Annals of Surgery*, vol. **237**, no. 6, pp. 871–876.

Schneider, G. 2009, 'Tissue adhesives in otorhinolaryngology', *GMS Current Topics in Otorhinolaryngology – Head and Neck Surgery*, vol. **8**, pp. 1–10.

Shaffrey, C.I., Spotnitz, W.D., Shaffrey, M.E. and Jane, J.A. 1990, 'Neurosurgical applications of fibrin glue: augmentation of dural closure in 134 patients', *Neurosurgery*, vol. **26**, no. 2, pp. 207–210.

Sharma, A., Kaur, R., Kumar, S., Gupta, P., Pandav, S., Patnaik, B. and Gupta, A. 2003, 'Fibrin glue versus N-butyl-2-cyanoacrylate in corneal perforations', *Ophthalmology*, vol. **110**, no. 2, pp. 291–298.

Singh, A., Hosseini, M. and Hariprasad, S.M. 2010, 'Polyethylene glycol hydrogel polymer sealant for closure of sutureless sclerotomies: a histologic study', *American Journal of Ophthalmology*, vol. **150**, no. 3, pp. 346–351.e2.

Smith, D. 2004, 'Adhesives and sealants, in biomaterials science', in B. Ratner, F. Schoen, A. Hoffman and J. Lemons (eds), *Biomaterials Science: An Introduction to Materials in Medicine*, Elsevier Academic Press, Amsterdam; Boston.

Spotnitz, W.D. 1996, 'History of tissue adhesives, in surgical adhesives and sealants', in D.H. Sierra and R. Saltz (eds), *Surgical Adhesives and Sealants: Current Technology and Applications*, Technomic Pub. Lancaster, PA.

Spotnitz, W.D. and Burks, S. 2010, 'State-of-the-art review: hemostats, sealants, and adhesives II: update as well as how and when to use the components of the surgical toolbox', *Clinical and Applied Thrombosis/Hemostasis*, vol. **16**, no. 5, pp. 497–514.

Thavarajah, D., De Lacy, P., Hussain, R. and Redfern, R.M. 2010, 'Postoperative cervical cord compression induced by hydrogel (DuraSeal): q possible complication', *Spine*, vol. **35**, no. 1, pp. E25–E26.

© Woodhead Publishing Limited, 2013

Tissuemed. 2012, *TissuePatch 3 Instructions for Use*, Tissuemed Limited.

Wain, J.C., Kaiser, L.R., Johnstone, D.W., Yang, S.C., Wright, C.D., Friedberg, J.S., Feins, R.H., Heitmiller, R.F., Mathisen, D.J. and Selwyn, M.R. 2001, 'Trial of a novel synthetic sealant in preventing air leaks after lung resection', *The Annals of Thoracic Surgery*, vol. **71**, no. 5, pp. 1623–1628; discussion 1628–1629.

Wang, M., Mattson, M.S., Tirrell, D.A. and Kornfield, J.A. 2010, 'Tissue adhesive using engineered proteins', US 2010/0160960 A1.

Wathier, M.C., Carnahan, M.A., Jung, P.J., Kim, T. and Grinstaff, M.W. 2005, 'Dendrimer hydrogels as new alternative for the repair of clear corneal incisions', *Investigative Ophthalmology & Visual Science*, vol. **46**, no. 5, p. 4993.

Wathier, M. and Grinstaff, M. 2010, 'Hydrogel sealants for wound repair in ophthalmic surgery', in T. Chirila (ed.), *Biomaterials and Regenerative Medicine in Ophthalmology*, CRC Press; Woodhead, Boca Raton, FL; Oxford.

Webster, I. and West, P. 2002, 'Adhesives for medical applications', in S. Dumitriu (ed.), *Polymeric Biomaterials*, 2nd edn, Marcel Dekker, Inc., New York.

Wheat, J.C. and Wolf, J.S. 2009, 'Advances in bioadhesives, tissue sealants, and hemostatic agents', *Urologic Clinics of North America*, vol. **36**, no. 2, pp. 265–275.

Wong, S.C., Bachinsky, W., Cambier, P., Stoler, R., Aji, J., Rogers, J.H., Hermiller, J., Nair, R., Hutman, H. and Wang, H. 2009, 'A randomized comparison of a novel bioabsorbable vascular closure device versus manual compression in the achievement of hemostasis after percutaneous femoral procedures: the ECLIPSE (Ensure's Vascular Closure Device Speeds Hemostasis Trial)', *JACC: Cardiovascular Interventions*, vol. **2**, no. 8, pp. 785–793.

Wright, N.M., Kim, K.D., Cosgrove, R., Tew, J.M., Kaiser, M.G., McCormick, P.C., Chestnut, R., Ellenbogen, R.G., Van Loveren, H.R., Vale, F.L., Shaffrey, M.E., Chen, T.C., Wang, M.Y., Mayberg, M.R., Sharan, A.D., Gerszten, P.C., Welch, W.C., Graham, R.S., Brown, F.D., Fessler, R.G., Deutsch, H., Shah, M.V., McCutcheon, I.E., Karahalios, D.G., Long, D.M., Hopkins, L.N., Jallo, J., Delashaw, J.B., Ondra, S.L. and Gross, R.E. 2009, 'DuraSeal spinal sealant as an adjunct to sutured dural repair in the spine', *Neurosurgery*, vol. **65**, no. 2, p. 410.

© Woodhead Publishing Limited, 2013

17

Antibacterial adhesives for bone and tooth repair

E. A. ABOU NEEL, King Abdulaziz University, Saudi Arabia, Tanta University, Egypt and University College London, UK
and A. M. YOUNG, University College London, UK

DOI: 10.1533/9780857096425.4.491

Abstract: Bonding and repair of damaged tooth and bone directly *in vivo* is a more complicated problem than joining and assembly in the laboratory or factory. This is due to the requirement for the restorative material to be of low toxicity but capable of rapid set at body temperature and in the presence of bodily fluids and other tissues. Furthermore, bacteria and enzymes that penetrate the interface between adhesive materials and tissue can break down the latter and degrade any bond. In addition to having mechanical properties comparable with the tissue they replace, set formulations must preferably therefore be antibacterial and aid repair of damaged tissue. This chapter provides a general description of commercially available *in vivo* setting materials, cements and adhesives for tooth and bone repair and their current major drawbacks. It subsequently explores how these materials are being modified to reduce recurrent infections and encourage better surrounding tissue repair.

Key words: bonding to tooth and bone, infections affecting teeth and bone, fluoride/antibacterial-releasing dental materials, re-mineralising bone cements/adhesives.

17.1 Introduction to tooth repair

A high proportion of the world's population is affected by dental caries. It is caused by acid production by bacteria present in dental plaque on tooth surfaces. These acids dissolve the mineral content (hydroxyapatite) of enamel and dentine. Enzymes can subsequently degrade any demineralised collagen within the dentine that remains. Carious tooth can be repaired if the damage has not progressed to total tooth loss or other more complicated infections. This repair requires removal of infected enamel and dentine followed by insertion of biocompatible filling materials. The first part of this chapter will deal with current commercially available materials and then discuss the development of new antibacterial and collagen re-mineralising materials that can potentially reduce effects of the disease.

© Woodhead Publishing Limited, 2013

17.1.1 Materials currently used for tooth repair

Amalgam

For many years, amalgam was the material of choice for restoration of teeth. It consists of liquid mercury and silver–tin alloy powder. Reaction between these components gives a hard silvery-grey material. Nowadays, with increasing concern about restoration aesthetics and mercury toxicity, alternative polymer-based, tooth-coloured materials such as composites, or glass ionomer cements, and hybrids of the two, have been brought into the market. These, unlike classical amalgam restorations, are bonded to the excavated tissue. The ability to bond to dentine has meant that less tissue needs to be removed. Additionally, larger cavities can be successfully restored as the bonded material provides support for the remaining tooth structure. A major problem, however, if the bond fails is that, unlike silver and mercury, polymers are not generally antibacterial.

Composites

Dental composites consist of a resin matrix (mostly high molecular weight, hydrophobic, dimethacrylate monomers), silane-treated inorganic fillers (often silica based) and an initiator/activator (typically camphorquinone and dimethylparatoluidine) system. Upon exposure to a blue light (e.g. from an LED source), the highly filled composite pastes placed within a tooth structure set via free radical initiated polymerisation. This produces a cross-linked three-dimensional network and a material with suitable strength and wear characteristics to replace lost tissues. Gaining a strong, resilient bond between the composite and dentine can, however, be difficult. It generally requires a number of complex dentine pre-treatment steps and use of additional more hydrophilic methacrylate resin adhesives (see below).

A major problem with dental composites is polymerisation shrinkage during set. This causes stress on the bond between the material and tooth structure leading to gap generation at their interface. Additionally, differences in thermal expansion coefficients of the material and tooth can mean changes in temperature widen these gaps. This problem is then further exacerbated by cyclic loading. Water and enzyme penetration ('nanoleakage') at the material/dentine interface may weaken the adhesive and break down collagen, respectively. Ultimately 'bacterial microleakage' through widened gaps of micron dimension can occur. This can lead to staining around the restoration margins, breakdown of adhesion, recurrence of caries, inflammation of the tooth pulp and also postoperative pain (Hersek *et al.,* 2002; Murrey *et al.,* 2002).

Recurrent caries is considered the major contributing factor responsible for tooth restoration failure. Attempts made to reduce the polymerisation

© Woodhead Publishing Limited, 2013

shrinkage by modifying the composite composition (e.g. increasing the filler loading, using a high molecular weight methacrylate monomer or pre-cured resin as filler) and stress on the tooth by placement of the material in thin consecutive layers have been only partially successful. Additionally, in modern dentistry, there is a drive to remove less of the disease damaged tissue (Splieth *et al.*, 2001). In this situation, there is greater possibility of residual bacteria within the tooth cavity and so development of materials with some antibacterial action is becoming ever more crucial.

Glass ionomer cements (GICs)

Glass ionomer cements are self-adhesive, aesthetic filling materials. They consist of fluoroalumino silicate glass and an aqueous solution of polyacid, mostly polyacrylic. GICs set by acid–base reaction between the glass filler and the polyacid in the presence of water. GIC restorations have significantly reduced bacterial microleakage compared with those of composites for a number of reasons. Firstly, provided they do not dehydrate, GICs are dimensionally more stable during setting. Additionally, the polyacid in GICs associates with calcium ions of hydroxyapatite in enamel and dentine providing a mechanism for chemical bonding to tooth structure. There is therefore no need for the complex dentine pre-treatment procedures required with composite adhesion. Instead, simple conditioning of the excavated tooth surface with a polyacrylic acid solution is generally all that is required prior to material application. Although initial bond strengths of GICs are lower than those for composites, experimentally and clinically they have been found to be more durable.

Furthermore, GICs exhibit an initial burst fluoride release upon set. The acid/base setting process additionally leads to fluoride within the polymer matrix phase of the set cement which can subsequently be gradually released over a prolonged period (Forsten, 1990; De Moor *et al.*, 1996). GICs also take up fluoride, for example from toothpaste, and re-release it over time. Fluoride can react with hydroxyapatite and form a more acid-resistant fluroapatite (De Bruyne and De Moor, 2004; Wiegand *et al.*, 2007). At high concentration, it will inhibit bacterial metabolism and growth (Hamilton, 1990; Forss *et al.*, 1991). Initial moisture sensitivity, poorer wear resistance and in particular low flexural strength of GICs, however, limit their application to low-load-bearing clinical situations. This has lead therefore to the development, by many companies, of GIC/composite hybrid materials.

Hybrids of composites and GICs

Polyacid-modified composite resins (compomers) contain all the components of composites but in addition methacrylate monomers with acidic functional

© Woodhead Publishing Limited, 2013

groups. They also have some reactive glass powder of a similar type to that used in GICs. After setting by polymerisation, these fillers attract water (2–3.5% by mass) from their surroundings. The water can elicit a surface acid–base reaction between the acidic monomer and the reactive glass filler providing some fluoride release (Nicholson, 2007). Fluoride release is, however, often limited (Meyer *et al.*, 1998) and water uptake can cause decline in mechanical properties. Additionally, polymerisation shrinkage and the need for composite adhesives remain a major concern of compomers.

Resin modified glass ionomers (RMGICs) are a further hybrid of dental composites and GICs but unlike compomers they have significant water content in the original formulation. This enables them to set via both polymerisation and acid–base reaction. They often contain the hydrophilic monomer hydroxyl ethyl methacrylate (HEMA) in addition to all GIC components (Smith, 1998; Xie *et al.*, 2004). The hydrophilicity of HEMA can aid spreading and penetration of these formulations into dentine. Additionally, the polyacid gives a chemical bonding mechanism to tooth structure. Furthermore, RMGICs show a comparable level of early fluoride release and recharging capability to GICs (Xu and Burgess, 2003). Modern RMGICs can have much improved flexural strength compared with conventional GICs (Xie *et al.*, 2000). Low surface hardness and wear resistance, however, remain potential problems (Peutzfeldt, 1997; Xie *et al.*, 2000). Clinically, to overcome these limitations, GICs and RMGIC are often used as a base or liner beneath stronger composites but there is still room for further dental material improvement.

Resin adhesives

Resin adhesives are used to enhance retention of both composites and compomers to tooth structure and hence prevent bacterial microleakage (Van Meerbeek *et al.*, 2001). There are a wide range of different formulations but they generally consist of the components of RMGICs and composites but with much lower levels of filler to improve fluidity. Preparation of enamel for bonding is relatively straightforward requiring just partial etching of its hydroxyapatite crystals with 35% phosphoric acid gel for ~30 s followed by rinsing and drying. This produces a microscopically roughened surface into which methacrylate monomers can penetrate and bond by micromechanical retention (Van Landuyt *et al.*, 2007).

The heterogeneous structure and high water content of dentine (~22% by volume) makes it less compatible with hydrophobic methacrylate resin adhesives than enamel. Currently the most reproducible dentine bonding systems comprise an etchant, primer and adhesive resin. The etchant (commonly phosphoric acid gel) is required to remove any cutting debris left by excavation of carious tissue and additionally a surface layer of hydroxyapatite. This

© Woodhead Publishing Limited, 2013

leaves a mat of collagen fibrils into which the primer can subsequently penetrate. The primer is often an aqueous or ethanolic solution of largely hydrophilic monomers (e.g. HEMA) which can aid penetration of a low-viscosity adhesive methacrylate resin into demineralised collagen. Upon drying and cure a hybrid layer of resin modified collagen is formed within which the resin and collagen are micromechanically interlocked. Subsequent bonding between the hybrid layer and composite restoration is chemical in nature and achieved by copolymerisation of methacrylate groups in the primer, adhesive and composite. A major drive in modern dental adhesive technology has been to simply the procedure but this has often been at the expense of bonding reliability (Yoshida *et al.*, 2004).

17.1.2 Experimental dental materials

To help re-mineralise carious or acid etched dentine and stabilise the adhesive bond making the tooth and restoration as one assembly, calcium-phosphate fillers have recently been included in various dental composites and adhesives. In a further attempt to reduce bacterial microleakage and adhesion breakdown, a number of alternative antimicrobial components other than fluoride have also been added. Current research in this area is summarised below.

Calcium phosphate-releasing materials

Calcium and phosphate ions released into collagen from filler particles embedded within methacrylate composites can reprecipitate as hydroxyapatite. Release kinetics of these ions from the set composite depends strongly upon both the methacrylate hydrophilicity and the calcium-phosphate filler chemistry/aqueous solubility. Calcium phosphates vary in solubility according to the Ca/P ratio as well as the surrounding pH. The solubility of calcium phosphates generally increases as the Ca/P ratio decreases. Under neutral conditions, the solubility increases in the following order: fluroapatite [FA,$Ca_{10}(PO_4)_6F_2$], <hydroxyapatite [HA,$Ca_{10}(PO_4)_6OH_2$], <tricalcium phosphate [TCP), $Ca_3(PO_4)_2$] ~ amorphous calcium phosphate [ACP, $Ca_xH_y(PO_4)_{6-x}{\cdot}nH_2O$] <dicalcium phosphate [DCP, $CaHPO_4$], <monocalcium phosphate [MCP, $Ca(H_2PO_4)_2$] (Bohner, 2000a; Dorozhkin, 2008). Calcium-phosphate solubility also tends to increase as the pH is reduced. It is potentially possible therefore to produce 'responsive' composite materials that release higher levels of calcium and phosphate when surrounding bacteria produce acid.

Amorphous calcium phosphate (ACP) has been included in various methacrylate monomers (Regnault *et al.*, 2008), and proven to give levels of calcium and phosphate release sufficient to promote mineral re-deposition

© Woodhead Publishing Limited, 2013

(O'Donnell *et al.*, 2006). ACP composites have recently been commercialised as a cement, adhesive (Aegis Ortho) and sealant. The ACP adhesive formulation has been observed to have shear bond strength comparable with that of a commercial RMGIC adhesive (Foster *et al.*, 2008). Further work is still required, however, to assess if continuing release of calcium phosphate can make the ACP adhesive bond more durable under cyclic stress, thermal loading and ultimately *in vivo* as observed with GIC bonding.

Nanoparticles of dicalcium phosphate (DCP) have also been combined with silicon-carbide whiskers and added to dental resins. Chemical curing formulations were developed and proven to have calcium and phosphate release comparable with that of ACP composites (Xu *et al.*, 2006, 2007). The small size of the filler particles may have limited the filler loading capacity (60 wt%) but this problem may be overcome through use of reactive fillers such as MCP and TCP that produce DCP as below. Although calcium phosphate-releasing materials have proved to be successful in re-mineralising defective tooth structure, they have no antibacterial action.

Antibacterial monomer-containing materials

The antibacterial monomer, 12-methacryloyloxydodecyl-pyridinium bromide, MDPB has been included in some methacrylate composites and adhesives. This can be achieved without adverse effect on mechanical strengths because after polymerisation the MDPB is copolymerised with the resin phase and immobilised. Incorporation of this monomer can increase the size of bacterial inhibition zones around composite samples in agar diffusion tests. Moreover, it can reduce surface bacterial growth. The antibacterial action of this monomer, however, is not considered as effective as might be achieved with a free leaching antibacterial agent as it can only affect bacteria in close proximity to the composite surface (Imazato *et al.*, 1994, 1999; Imazato and McCabe, 1994; Imazato, 2003). Despite this limitation a product containing MDPB (Clearfil Protect Bond) has been commercialised.

Antibacterial filler-containing materials

An alternative antibacterial approach has been to introduce silver into dental composite fillers. Implantation of silver ions into conventional composite silica fillers has been shown to produce antibacterial action (Yamamoto *et al.*, 1996). In more recent studies, colourless silver containing silica fillers more suitable for aesthetic dental composites were produced. In short-term studies, dental composites produced using these fillers were found to be highly effective against bacterial suspensions (Kawashita *et al.*, 2000). Antibacterial silver and zinc have also been included in some calcium-phosphate fillers. When included in composite restorations these fillers were found to reduce

© Woodhead Publishing Limited, 2013

bacterial microleakage *in vitro*. This action could have been due to formation of antibacterial complexes that render the resin surface less prone to bacterial adhesion or adsorption of the leached chemicals onto the bacterial surface hence reducing its adhesion tendency, or reducing the metabolism of bacteria (Syafiuddin *et al*., 1997). The next stage for these materials would be an *in vivo* animal model before human trial and commercialisation.

Chlorhexidine-releasing materials

Chlorhexidine is a highly effective, broad spectrum antimicrobial agent that also has anti-fungal activity. At low concentration, it affects the integrity of the bacterial membrane and reduces their growth, but at high concentration, it kills bacteria (McDonnell and Russell, 1999). Chlorhexidine is used in mouth washes (e.g. Corsodyl™) (Wirthlin *et al*., 2005) and a wide range of devices to control oral infection and recurrence of caries (Patel *et al*., 2001). It additionally binds to enamel and reduces bacterial adherence to teeth (Dols-Lafargue *et al*., 2008). Furthermore this agent can inhibit proteins that break down demineralised collagen.

Chlorhexidine can be easily incorporated into materials as different salt forms. It may also be present as a powder or fully dissolved in the fluid phase of composite pastes (Jedrychowski *et al*., 1983; Leung *et al*., 2005). The level of chlorhexidine release can be varied by changing its form and concentration. For example, in one study, the less water soluble acetate form enabled more sustained release than the highly water soluble gluconate salt (Anusavice *et al*., 2006). The drug-release kinetics is also, however, strongly affected by the material type.

Early chlorhexidine-containing dental composites, developed by simple addition of chlorhexidine diacetate, showed good antibacterial action but only for a few days (Takemura *et al*., 1983). More recently, upon addition of hydrophilic HEMA to chlorhexidine-containing hydrophobic dental composites, increased water sorption was observed and a concomitant enhanced release of drug (Leung *et al*., 2005). The level of early chlorhexidine release was sufficient to have much greater antibacterial action against oral bacteria within a biofilm grown on the material surface than fluoride release from GICs. Additionally, the chlorhexidine-releasing composites were highly successful at preventing bacterial microleakage in an *in vitro* model designed to quantify this problem. Associated with enhanced water sorption and release of chlorhexidine, however, could be a substantial decline in material strength.

In a further study (Mehdawi *et al*., 2009), chlorhexidine diacetate was added to dental adhesive methacrylate monomers filled with a mixture of water-soluble monocalcium phosphate monohydrate (MCPM) and less soluble β-tricalcium phosphate (β-TCP). As with hydrophilic monomers, the

© Woodhead Publishing Limited, 2013

MCPM could increase water sorption to promote both chlorhexidine and calcium-phosphate release. The β-TCP, however, can subsequently react with remaining MCPM within the polymer and any water absorbed and then re-precipitate within the polymer as dicalcium phosphate dihydrate (DCPD also known as brushite). This provides a mechanism for limiting the reduction in resin strength that can occur upon water sorption or component release. At the present time, these systems are only experimental as further work is required to simultaneously optimise both mechanical and antibacterial properties.

17.1.3 Summary

Having been used for many years amalgam provides a strong restoration with antibacterial action but is not suitable for aesthetic applications. Composites and GICs otherwise are well accepted for aesthetic restorations, but bacterial microleakage and low mechanical properties remain the main disadvantages respectively. Complex adhesive procedures may also be required particularly with composites. Although hybrid restorative materials have overcome some of these limitations they are still not ideal. Calcium phosphate and antibacterial component-releasing materials can potentially lead to more ideal solutions but they require further work.

17.2 Introduction to bone repair

Bone defects can result from a wide range of causes including congenital abnormalities, traumatic injury, surgery required due to cancer and arthritis in addition to bacterial infections. Osteomyelitis and periodontitis are the most prevalent bacterial infections of the skeleton. The former can be life threatening and is characterised by inflammation and destructive bone loss primarily in the leg or vertebra (Varoga *et al*., 2008). Periodontitis is a broad term used to describe bacteria induced inflammatory conditions that can cause progressive loss of alveolar bone and ultimately tooth loss (Needleman *et al*., 2008). When bone loss is high, grafts may be used to fill defects and membranes are applied in periodontal treatments but if greater stabilisation is required screws and plates or injectable cements are needed.

Bone cements are extensively used in joint surgery for fixation of implants including prosthetic hip, knee and shoulder. By conforming to the shape and bonding to both implant and tissues they help in proper distribution of load. In vertebral surgery, they have been used to stabilize fractures or fill bony defects (Kim *et al*., 2004). They can also be employed for prevention of vertebral fracture or stabilisation of osteoporosis (Li *et al*., 2000). Any such reconstructive surgery, however, is associated with risk of (re)-infection

© Woodhead Publishing Limited, 2013

and hence high failure rate (Sutherland *et al*., 1997). Many devices for bone repair therefore contain antibacterial agents.

17.2.1 Materials currently used for bone repair

Bone grafts

Bone grafting may include surgical transfer of relevant tissue from healthy parts of a patient (autogenous grafts) or from a donor of same species (allografts) but material supply is a major problem. Grafts may additionally be from another species (xenografts, e.g. hydroxyapatite extracted from bovine bone) or synthetic (alloplasts). Synthetic hydroxyapatite and tricalcium phosphate (TCP) particles have both been used to fill bone defects (Komlev *et al*., 2002). Bone may re-grow in the spaces between particles as they are remodelled but if greater mechanical support is required then calcium-phosphate cements (see below) may be more suitable.

Guided tissue-regeneration (GTR) membranes

A guided tissue-regeneration membrane acts as a barrier preventing fast-growing soft tissue from invading space required to be filled with new bone. Degradable polymeric (e.g. polylactide or glycolide) or natural (e.g. collagen) membranes are often used. Many of these membranes have been formulated with antibiotics, the most common of which have been from the tetracycline family (Zarkesh *et al*., 1999). In addition to its antibiotic action, tetracycline reduces *in vivo* degradation of collagen within bone. Antibacterial chlorhexidine (Chen *et al*., 2003) and zinc (Giertsen *et al*., 1989; Chou *et al*., 2007), however, have also been included. Generally, drug-release kinetics is dependent on drug concentration and membrane porosity and hydrophilicity. Provided drug-release kinetics is well controlled, antibacterial agents can have significant beneficial clinical effects.

In various studies drug has been incorporated into GTR membranes by simple dropping of drug solution onto the material or by membrane immersion in the drug solution for a controlled period of time. The first method has been shown to provide good impregnation of GTR membranes with tetracyclines (Hung *et al*., 2005). Upon placement of the membrane back into water, however, most of the drug was released within 24 h. To improve both the loading efficiency and provide more sustained drug release, various authors have modified the surfaces of GTR membranes for example with carbohydrate derivatives (Lepretre *et al*., 2007; Tabary *et al*., 2007), tridodecylmethylammonium (Hung *et al*., 2005), or with a dense polymeric layer (Lee *et al*., 2008). Significant drug release for 80 days has been made possible in some cases through such modifications (Lepretre *et al*., 2007).

© Woodhead Publishing Limited, 2013

Of concern is that antibacterial drugs can affect other cell growth in addition to the bacteria. In one study, for example, viability of periodontal ligament (PDL) cells grown on tissue culture plastic and treated with various chlorhexidine concentrations (0–50 μg/mL of cell growth media) was observed to decline by 50% when using 15 μg/mL of chlorhexidine (Chen *et al*., 2003). Although cells grown on tissue culture plastic may be less protected and therefore more sensitive to drugs than those *in vivo*, it should be appreciated that 15 μg/mL of chlorhexidine are orders of magnitude lower than currently used in mouthwashes. In order to understand the full implication of this result for chlorhexidine-releasing devices *in vivo*, fluid flow around any specific site must be fully appreciated so that length of time of tissue exposure to the drug can additionally be estimated.

It should be noted that bone can only grow if provided with space to do so. On the other hand, thin polymeric membranes, beyond holding back soft tissue, provide no significant mechanical support during bone healing. For greater mechanical strength, a polymeric adhesive or calcium-phosphate cement is required. In this case bone can only replace the material if/when they degrade. Gaining bone cement degradation at a rate commensurate with possible bone repair is a significant challenge.

Poly(methyl) methacrylate bone cements

Poly(methyl) methacrylates (PMMAs) were first introduced as bone cements in the 1960s by Charnley and Smith (Dalby *et al*., 2002). PMMA cements consist of a resin matrix (mostly methyl methacrylate monomer), contrast agent (often barium sulfate) and initiator/activator (typically benzoyl peroxide/dimethylparatoluidine) system. Upon mixing PMMA components and injection into the defect, they set chemically via free radical initiated polymerisation. This produces long entangled polymer chains and a material with high-strength characteristics. PMMAs mainly depend on micromechanical not chemical interaction with the surrounding bone for adhesion (Clarkin *et al*., 2010).

Modern commercially available PMMA formulations are usually loaded with antibiotics, commonly gentamicin (a broad spectrum antibiotic that can withstand the high temperature produced during PMMA setting). Drug loading is typically 1.25–2.5 wt% to prevent infection (Ensing *et al*., 2008) and 2.5–10 wt% to treat an existing infection (Dunne *et al*., 2007). Gentamicin release, however, is generally not high. A maximum of 15% of the total amount of the drug may be released within the first few days. The release can be enhanced by increasing the actual amount of the drug (Dunne *et al*., 2007), or adding a release modulator such as lactose (Virtoa *et al*., 2003). If the drug release is too fast, however, the antibiotic may be

© Woodhead Publishing Limited, 2013

washed away from the wound site and at effective concentrations for too short a period of time (Wroblewski *et al.*, 1986; Dunne *et al.*, 2008).

A major problem with PMMA cements is polymerisation shrinkage during set. This causes stress on the bond between PMMA and surrounding bone and may lead to gap generation at their interface (as observed with dental composites bonded to dentine). Tissue fluid, enzyme penetration and ultimately 'bacterial microleakage' at this interface may subsequently weaken any adhesive bond and break down collagen. Additionally, the mismatch in rigidity of PMMA and bone may also lead to bond deterioration upon loading (Clarkin *et al.*, 2010). Often PMMA undergoes wear that may elicit long-term inflammatory response upon formation of particulates (Peter *et al.*, 1999). The use of PMMA is also complicated by the possibility of both thermal and chemical necrosis of the surrounding tissues and nerve ending as a result of the release of heat and residual monomer respectively (Donkerwolcke *et al.*, 1998). Furthermore, PMMA cements are non-degradable and cannot remodel or integrate into the surrounding tissues (Lieberman *et al.*, 2005).

Calcium-phosphate cements

The first calcium-phosphate cements (CPCs) were developed in the late 1980s to help in remineralisation of tooth structure destroyed by dental caries (Ishikawa *et al.*, 1995). These consisted of equimolar tetracalcium phosphate [TTCP, $Ca_4(PO_4)_2O$] and dicalcium phosphate anhydrous [DCPA, $CaHPO_4$] or dicalcium phosphate dihydrate [DCPD, $CaHPO_4{\cdot}2H_2O$]. They were subsequently, in 1996, FDA approved for cranial defect repair (David *et al.*, 2004). Nowadays, there are several commercially available formulations employed for maxillofacial and orthopaedic applications (Cuisinier *et al.*, 2004, Tamimi *et al.*, 2009). Generally, these formulations consist of a powder and liquid phase. The powder usually contains two or more calcium-phosphate compounds {tetracalcium phosphate [TTCP, $Ca_4(PO_4)_2O$]/dicalcium phosphate [DCP, $CaHPO_4$] or monocalcium phosphate [MCP, $Ca(H_2PO_4)_2$]/tricalcium phosphate [TCP), $Ca_3(PO_4)_2$]/calcium carbonate [$CaCO_3$] or amorphous calcium phosphate [ACP, $Ca_xH_y(PO_4)_{6-x}{\cdot}nH_2O$]/MCP/DCP}, while the liquid can be water, saline or sodium-phosphate solution.

Upon mixing the powder and liquid, a paste that can be easily injected and set *in situ* is formed. The setting reaction is a dissolution–precipitation reaction, that is, dissolution of soluble calcium phosphates from the powder and then precipitation of less soluble forms. Dependent upon the initial composition and pH, the final precipitated forms can be brushite [DCPD, $CaHPO_4{\cdot}2H_2O$] or apatite {hydroxyapatite [HA, $Ca_{10}(PO_4)_6OH_2$] or carbonated apatite [CA, $Ca_{10}(PO_4)_6OH_2\ CO_3$] (Gerhart *et al.*, 1988; Miyamoto

© Woodhead Publishing Limited, 2013

et al., 1995). For instance, TCP tends to form brushite under acidic conditions, but hydroxyapatite at neutral pH. Brushite cements can be faster setting and more resorbable than hydroxyapatite forming formulations but also of lower compressive strength.

Although, CPCs have been proven to be successful for bone repair, they have no antibacterial action. They are therefore usually loaded with antibiotics (Stallmann *et al*., 2006; Tamimi *et al*., 2008; Hofmann *et al*., 2009), particularly gentamicin sulfate. Antibiotic addition has been proven effective in reducing the number of *Staphylococcus aureus* and methicillin-resistant *Staphylococcus aureus* (MRSA) in experimental chronic osteomyelitis models (Stallmann *et al*., 2004; Joosten *et al*., 2005) and clinically been used to both prevent and treat infection.

Gentamicin release kinetics is commonly diffusion controlled, that is, cumulative release is proportional to the square root of time. From diffusion theory, release percentage from flat discs is expected additionally to be inversely proportional to specimen thickness. For samples of the order 1 mm thick, total release is typically a few days. Gentamicin release is also dependent on the cement type (brushite or hydroxyapatite), porosity and drug form (e.g. Bohner *et al*., 1997).

The relatively fast diffusion-controlled drug release from CPCs compared with that from polymers such as PMMA is primarily due to the high cement porosity. Porosity can be reduced and cement mechanical properties increased by reduction in the cement liquid component but only to a limited extent. Various authors have therefore attempted to add polymers into the aqueous phase to bind drugs and slow their release. For example, it has been proven that polyacrylic acid can hinder release of positively charged antibacterial agents such as gentamicin and chlorhexidine presumably due to its dissociation in water and production of COO^- groups (Bohner *et al*., 1997, 2000b; Young, unpublished data). Polyacrylic acid has also the potential to enhance the durability of the adhesive bond between the cement and the surrounding bone due to its known ability to chelate with calcium in hydroxyapatite. In a further study, prior mixing of gentamicin with polylactide powder enabled effective gentamicin release from HA cement over a period of weeks instead of days (Sasaki and Ishii, 1999).

Upon incorporation of some antibiotics into CPCs, the handling characteristics (consistency, setting time and injectability) and mechanical properties can both be affected. Tetracylcine, for example, has tended to increase the setting time and reduce the compressive strength of the apatite forming CPCs (Ratier *et al*., 2001) but gentamicin sulfate can have the opposite effect on brushite forming cements (Bohner *et al*., 1997; Joosten *et al*., 2005). Major problems with CPCs, however, include sensitivity of the setting process to the presence of blood and tissue fluid, difficulty in degradation rate

© Woodhead Publishing Limited, 2013

control and low mechanical strength. Their application is therefore limited to small defects and non-weight bearing situations.

17.2.2 Experimental bone cements

Injectable degradable polymers

The following will focus upon injectable poly(anhydrides), poly(ester) dimethacrylates and poly(propylene) fumarates. With these types of polymer, degradation rates can be more readily controlled than with CPCs. The polymer degradation products can be eliminated safely in the body but might be considered less biocompatible than calcium phosphate as they are not required for tissue repair. The anhydrides and poly(ester) dimethacrylates are relatively small fluid molecules with methacrylate groups on both ends. They can be rapidly cross-linked at body temperature using either light or chemical cure means. Cross-linking of poly(propylene) fumarate, however, is achieved through the use of dimethacrylate diluents. Cross-linking/polymerisation reactions provide a micromechanical means for the polymer to bond rapidly to roughened structure such as bone. When drugs are incorporated into these polymers, they can be slowly released over several weeks upon polymer degradation. In some cases water sorption may enhance drug release. Water sorption and acid production in the bulk of materials may additionally, however, cause the polymer to degrade catastrophically instead of via a surface erosion mechanism.

Poly(anhydrides)

Poly(anhydrides) are generally surface eroding polymers with a hydrophobic backbone and hydrolytic anhydride linkage (Muggli *et al.*, 1999). Surface erosion is potentially advantageous for drug-delivery applications as then both polymer loss and drug release may be linear with time. This assumes diffusion-controlled drug release to be much slower than the polymer degradation. With diffusion control the level of drug release per second declines with time. More seriously, however, with polymers undergoing bulk degradation a sudden dose dumping effect may be observed. The anhydride links within the cross-linked polymer can degrade rapidly in the presence of water potentially providing materials for short-term drug-release applications (Gopferich and Tessmar, 2002). The degradation time of these polymers may, however, be increased from days to years by increasing their hydrophobicity.

Photo-polymerisable polyanhydrides prepared from monomers of sebacic acid (SA) alone, or copolymers of SA and 1,3-bis(*p*-carboxyphenoxy) propane (CPP), or 1,6-bis(*p*-carboxyphenoxy) hexane (CPH) have been

© Woodhead Publishing Limited, 2013

formulated for bone repair (Chiu *et al.*, 2002). These polymers have also had Food and Drug Administration (FDA) approval as delivery devices of antibiotic for the treatment of chronic bone infections (Septacin™ implant) (Jain *et al.*, 2005). More recently, an injectable degradable poly(sebacic-co -ricinoleic-ester-anhydride) loaded with gentamicin (10–20 wt%) was also developed. This was shown to provide constant drug release (up to 20–80% depending on the molecular weight of the polymer and the drug concentration) over 28 days and to be effective when injected subcutaneously (Krasko *et al.*, 2007) or in an experimental bone model (Brin *et al.*, 2008).

A potential problem associated with the high reactivity of the anhydride group, however, may be difficulties in synthesis and purification.

Poly(propylene fumarates) (PPFs)

Injectable, biodegradable, poly(propylene fumarate) (PPF) formulations have been produced using unsaturated polyesters synthesised by reaction between fumaric acid and propylene glycol. The repeating units in PPF contain one double bond that can be cross-linked by any other C = C containing monomer. The PPF units also contain two ester groups that enable subsequent hydrolytic degradation of cross-linked polymers into fumaric acid and propylene glycol (He *et al.*, 2001). PPF formulations largely undergo bulk degradation; the degradation time is dependent on polymer structure but has generally been of the order of several months (Gunatillake and Adhikari, 2003).

PPF has been extensively studied as potential bone cement (Peter *et al.*, 1999; Jayabalan *et al.*, 2001; Choll *et al.*, 2007). One problem with these polymers, however, may be their low modulus. Although β-TCP addition can increase the material modulus there is concern that other mechanical properties may also be too low and with some formulations *in vivo* degradation was too fast for many orthopaedic applications (Mano *et al.*, 2004; Ginebra *et al.*, 2006). A possible partial explanation for low mechanical properties and fast degradation could be steric hindrance around the double bond in the fumarate systems limiting polymerisability.

Poly(ester) methacrylates

With methacrylates in non-degradable PMMA bone cements incomplete monomer conversion is a common observation. Greater and faster polymerisation of injectable triblock poly(propylene glycol-co-lactide) dimethacrylate monomers at body temperature, however, has been observed. In one study, for example, complete monomer conversion was achieved with some formulations using light cure initiators and less than 60 s of light exposure. Upon decreasing molecular weight of the monomer, polymerisation

© Woodhead Publishing Limited, 2013

rate was raised. The complete polymerisation is made possible by the high flexibility of the final cross-linked polymer chains. Whereas high conversion in dental composites and PMMA bone cement causes significant polymerisation shrinkage and heat generation, this is not the case with the studied formulations due to their high monomer molecular weight and therefore low reactive group (C=C) density.

The degradation rate of the cross-linked poly(propylene glycol-co-lactide) dimethacrylates can increase substantially upon reducing the length of the propylene glycol blocks (from months to weeks) providing a means to match degradation with bone re-growth (typically four–six months) (Ho and Young, 2006). Of additional importance, however, is the mechanism of polymer degradation (surface or water sorption and acid catalysed bulk). By reducing the molecular weight of these monomers there is a concomitant increase in cross-linking density of the resultant polymers and reduction in the probability of high water sorption and bulk sudden potentially catastrophic degradation.

When chlorhexidine diacetate particles (2.5–10 wt %) were incorporated into the above polymers, the release was primarily via a diffusion mechanism. At ten weeks the level released from 2-mm thick discs, varied between 15% and 82%, being greater with lower polymer cross-link density and higher initial drug concentration or particle size. The results were consistent with negatively charged degradation products within the polymer associating with the positively charged chlorhexidine delaying both polymer erosion and drug release (Young and Ho, 2008).

The modulus (rigidity) of the above cross-linked polymers was proportional to the inverse monomer molecular weight, but as a result of the high flexibility of poly(propylene glycol), they have much lower modulus than bone. A further problem was the acidic products associated with the polymer degradation. The section below will demonstrate how these problems might be solved.

Injectable degradable composites

Recently, it has been shown that using an equimolar mixture of monocalcium phosphate (MCPM)/β-tricalcium phosphate (β-TCP) as filler for poly(propylene glycol-co-lactide) dimethacrylate and upon placement in water, the modulus of the fully polymerised composite increased 10-fold in 24 h. After 1–10 weeks in water, the composite modulus was between 40 and 100 times that of the equivalent unfilled polymer. This increase in modulus was attributed to water sorption catalysed filler conversion to finer dispersed brushite crystals. Furthermore, the polymer degradation rate increased upon addition of this reactive filler mixture. Upon composite degradation both organic and inorganic components were released simultaneously. The acidic

© Woodhead Publishing Limited, 2013

organic degradation products, however, were neutralised by the inorganic ions thereby reducing the possibility of adverse *in vivo* reactions as well as bulk catalysed polymer degradation (Young *et al.*, 2009).

When loaded with 10 wt% chlorhexidine diacetate, these composites released 50–80% of drug via diffusion over a period of 10 weeks. Early release levels were proven sufficient to inhibit the growth of both *S. aureus* and *MRSA in vitro*. The level of release could also be tailored by adjusting the mass fraction of calcium-phosphate fillers; the higher the filler fraction, the faster the release (Young, unpublished data). Further work is now required to optimise these formulations for specific bone-repair applications.

17.2.3 Summary

Although autografts and allografts are often considered the gold standard for bone repair, for extensive injuries/defects their use is not feasible. In addition, these grafts, other particulate fillers and membranes (unlike bone cement) provide limited mechanical support. Ideally bone cement should degrade to enable full repair of surrounding tissue but during this period they must continue to provide any mechanical support that the newly forming tissue requires. Due to the difficulties involved in achieving this goal, non-degradable PMMA bone cements are still extensively employed.

With bone repair infection is a major concern, so many cements are supplied with antibacterial agents such as chlorhexidine, gentamicin and tetracyclines. Drug-release kinetics from set calcium-phosphate cement or polymeric adhesive depends upon both the material and drug structure. It can increase with raising material porosity but be decreased by material/drug interactions. The drug release must be sufficiently low so as to prevent adverse reactions but high enough to keep levels in surrounding fluids sufficient during any period during which infection is likely to occur. To achieve this, mechanisms of drug release need to be understood as well as fluid flow dynamics within the specific site that cement is employed.

17.3 Future trends

Despite many improvements in oral-health hygiene, dental caries is likely to remain one of the most common diseases of man in the foreseeable future. The complexity and dynamics of the oral environment and high demands on restorative material mechanical and biological characteristics, however, mean that as yet no commercial tooth restorative material is ideal for all clinical situations. There are therefore still many challenges for scientists and companies to overcome in the dental restorative material field. A major goal of many companies is the production of a self-adhesive formulation with high-mechanical properties, good aesthetics, low toxicity

© Woodhead Publishing Limited, 2013

and in addition the ability to prevent bacterial microleakage. Materials that furthermore could encourage tooth re-mineralisation and repair have been described within academic literature but further material development and optimisation followed by company commercialisation is still required.

Many advances in tooth repair have been extended for use in bone fixation and similar trends are likely to occur in the future. Developing an ideal adhesive for bone repair can be more complicated than for the tooth due to the fact that complete bone repair can only occur if the set adhesive degrades. Additionally, development of drug-releasing materials without loss of mechanical properties is challenging. Although data on many new degradable bone cements and adhesives have been published in recent years there remain many weaknesses in the formulations. Through exploitation of new techniques and greater fundamental understanding of how both micro and macroscopic properties of materials affect biological responses, we expect many new bone cements/adhesives will become available within the next ten years.

17.4 Acknowledgment

The authors would like to thank the Engineering and Physical Sciences Research Council (EPSRC).

17.5 References

Anusavice, K. J., Zhang, N. Z. and Shen, C. (2006), 'Controlled release of chlorhexidine from UDMA-TEGDMA resin', *Journal of Dental Research*, **85**, 950–954.

Bohner, M., Lemaître, J., Van Landuyt, P., Zambelli, P., Merkle, H. and Gander, B. (1997), 'Gentamicin-loaded hydraulic calcium phosphate bone cement as antibiotic delivery system', *Journal of Pharmacology Science*, **86**, 565–572.

Bohner, M. (2000a), 'Calcium orthophosphates in medicine: from ceramics to calcium phosphate cements', *Injury-International Journal of the Care of the Injured*, **31**, S37–S47.

Bohner, M., Lemaître, J., Merkle, H. P. and Gander B (2000b), 'Control of gentamicin release from a calcium phosphate cement by admixed poly(acrylic acid)', *Journal of Pharmaceutical Sciences*, **89**, 1262–1270.

Brin, Y. S., Golenser, J., Mizrahi, B., Maoz, G., Domb, A. J., Peddada, S., Tuvia, S., Nyska, A. and Nyska, M. (2008), 'Treatment of osteomyelitis in rats by injection of degradable polymer releasing gentamicin', *Journal of Controlled Release*, **131**, 121–127.

Chiu, L. L., Deng, J., Stephens, D. (2002), 'Polyanhydride implant for antibiotic delivery – from the bench to the clinic', *Advanced Drug Delivery Reviews*, **54**, 963–986.

Chen, Y.-T., Hung, C.-L., Lin, L.-W., Chi, L.-Y. and Ling, L.-J. (2003), 'Attachment of periodontal ligament cells to chlorhexidine-loaded guided tissue regeneration membranes', *Journal of Periodontology*, **74**, 1652–1659.

© Woodhead Publishing Limited, 2013

Choll, K, Andrew, M., Andrew, P., Jennifer, M., Lichun, L., Brad, C. and Michael, J. Y. (2007), 'Biomechanical evaluation of an injectable radiopaque polypropylene fumarate cement for kyphoplasty in a cadaveric osteoporotic vertebral compression fracture model', *Journal of Spinal Disorders*, **8**, 604–609.

Chou, A. H. K., LeGeros, R. Z., Chen, Z. and Li, Y. (2007), 'Antibacterial effect of zinc phosphate mineralized guided bone regeneration membranes', *Implant Dentistry*, **16**, 89–100.

Clarkin, O., Boyd, D. and Towler M. R. (2008), 'Strontium-based glass polyalkenoate cements for luting applications in the skeleton', *Journal of Biomaterials Applications*, **24**(6), 483–502.

Cuisinier, F., Schaaf, J., Van Landuyt, P., Roth, H., Lemaître, J. and Tenenbaum, H. (2004), 'Immediate implant placement using injectable calcium phosphate hydraulic cement in dogs', *Journal of Applied Biomaterials & Biomechanics*, **2**, 88–95.

Dalby, M. J., Silvio, L. D., Harper, E. J. and Bonfield, W. (2002), 'Increasing hydroxyapatite incorporation into poly(methylmethacrylate) cement increases osteoblast adhesion and response', *Biomaterials*, **23**, 569–576.

David, A., Nussbaum, M. S., Gailloud, P. and Murphy, K (2004), 'The chemistry of acrylic bone cements and implications for clinical use in image-guided therapy', *Journal of Vascular and Interventional Radiology*, **15**, 121–126.

De Bruyne, M. A. A., De Moor, R. J. G. (2004), 'The use of glass ionomer cements in both conventional and surgical endodontics', *International Endodontic Journal*, **37**, 91–104.

De Moor, R. J., Verbeeck, R. M. and De Maeyer, E A (1996), 'Fluoride release profiles of restorative glass ionomer formulations', *Dental Materials*, **12**, 88–95.

Dols-Lafargue, F. M., Heyraud, A., Chambat, G., Lonvaud-Funel, A. and Badet, C (2008), 'Effect of antiplaque compounds and mouthrinses on the activity of glucosyltransferases from Streptococcus sobrinus and insoluble glucan production', *Oral Microbiology Immunology*, **23**, 391–400.

Donkerwolcke, M., Burny, F. and Muster, D (1998), 'Tissues and bone adhesives – historical aspects', *Biomaterials*, **19**, 1461–1466.

Dorozhkin, S. V. (2008), 'Calcium orthophosphate cements for biomedical application', *Journal of Materials Science*, **43**, 3028–3057.

Dunne, N. J., Hill, J., McAfee, P., Kirkpatrick, R., Patrick, S. and Tunney, M. (2008), 'Incorporation of large amounts of gentamicin sulphate into acrylic bone cement: effect on handling and mechanical properties, antibiotic release, and biofilm formation', *Proceedings of the Institution of Mechanical Engineers, Part H, Journal of Engineering in Medicine*, **222**, 355–365.

Dunne, N., Hill, J., McAfee, P., Todd, K., Kirkpatrick, R., Tunney, M. and Patrick S (2007), 'In vitro study of the efficacy of acrylic bone cement loaded with supplementary amounts of gentamicin: effect on mechanical properties, antibiotic release, and biofilm formation', *Acta Orthopaedica*, **78**, 774–785.

Ensing, G. T., ven Horn, J. R., van der Mei, H. C., Busscher, H. J. and Neut, D. (2008), 'Copal bone cement is more effective in preventing biofilm formation than palacos R-G', *Clinical Orthopaedics and Related Research*, **466**, 1492–1498.

Forss, H., Jokinen, J., Spets-Happonen, S., Seppa, L. and Luoma, H (1991), 'Fluoride and mutans streptococci in plaque grown on glass ionomer and composite', *Caries Research*, **25**, 454–458.

© Woodhead Publishing Limited, 2013

Forsten, L. (1990), 'Short- and long-term fluoride release from glass ionomers and other fluoride-containing filling materials in vitro', *Scandinavian Journal of Dental Research*, **98**, 179–185.

Foster, J. A., Berzins, D. W. and Bradley, T. G. (2008), 'Bond strength of an amorphous calcium phosphate-containing orthodontic adhesive', *Angle Orthodontist*, **78**, 339–344.

Gerhart, T. N., Roux, R. D., Horowitz, G., Miller, R. L., Hanff, P. and Hayes, W. C. (1988), 'Antibiotic releases from an experimental biodegradable bone cement', *Journal of Orthopaedic Research*, **6**, 585–592.

Giertsen, E., Scheie, A. A. and Rølla, G. (1989), 'Dose-related effects of ZnCl2 on dental plaque formation and plaque acidogenicity in vivo', *Caries Research*, **23**, 272–277.

Ginebra, M. P., Traykova, T. and Planell, J. A. (2006), 'Calcium phosphate cements as bone drug delivery systems', *Journal of Controlled Release*, **113**, 102–110.

Gopferich, A. and Tessmar, J. (2002), 'Polyanhydride degradation and erosion', *Advanced Drug Delivery Reviews*, **54**, 911–931.

Gunatillake, P. A. and Adhikari, R. (2003), 'Biodegradable synthetic polymers for tissue engineering', *European Cells and Materials*, **5**, 1–16.

Hamilton, I. R. (1990), 'Biochemical effects of fluoride on oral bacteria', *Journal of Dental Research*, **69**, 660–667.

He, S., Timmer, M. D., Yaszemski, M. J., Yasko, A. W., Engel, P. S. and Mikos, A. G. (2001), 'Synthesis of biodegradable poly(propylene fumarate) networks with poly(propylene fumarate)-diacrylate macromers as crosslinking agents and characterisation of their degradation products', *Polymer*, **42**, 1251–1260.

Hersek, N., Canay, S., Akc, K. and Iftc, Y. C. (2002), 'Comparison of microleakage properties of three different filling materials: an autoradiographic study', *Journal of Oral Rehabilitation*, **29**, 1212–1217.

Ho, S. M. and Young, A. M. (2006), 'Synthesis, polymerisation and degradation of Poly(lactide-co-propylene glycol) dimethacrylate adhesives', *European Polymer Journal*, **42**, 1775–1785.

Hofmann, M. H., Mohammed, A. R., Perrie, Y., Gbureck, U., and Barralet, J. E. (2009), 'High-strength resorbable brushite bone cement with controlled drug-releasing capabilities', *Acta Biomaterialia*, **5**, 43–49.

Hung, S.-L., Lin, Y.-W., Chen, Y.-T. and Ling, L.-J. (2005), 'Attachment of periodontal ligament cells onto various antibiotics-loaded GTR membranes', *International Journal of Periodontics & Restorative Dentistry*, **25**, 265–275.

Imazato, S. (2003), 'Antibacterial properties of resin composites and dentine bonding systems', *Dental Materials*, **19**, 449–457.

Imazato, S. and McCabe, J. F. (1994), 'Influence of incorporation of antibacterial monomer on curing behavior of a dental resin composite', *Journal of Dental Research*, **73**, 1641–1645.

Imazato, S., Tarumi, H., Kato, S. and Ebisu. S. (1999), 'Water sorption and colour stability of composites containing the antibacterial monomer MDPB', *Journal of Dentistry*, **27**, 279–283.

Imazato, S., Torii, M., Tsuchitani, Y., McCabe, J. F. and Russell, R. R. B. (1994), 'Incorporation of bacterial inhibitor into resin composite', *Journal of Dental Research*, **73**, 1437–1443.

© Woodhead Publishing Limited, 2013

Ishikawa, K., Miyamoto, Y., Kon, M., Nagayama, M. and Asaoka, K. (1995), 'Non-decay type fast-setting calcium phosphate cement: composite with sodium alginate', *Biomaterials*, **16**, 527–532.

Jain, J. P., Modi, S., Domb, A. J. and Kumar, D. (2005), 'Role of polyanhydrides as localized drug carriers', *Journal of Controlled Release*, **103**, 541–563.

Jayabalan, M., Thomas, V. and Rajesh, P. N. (2001), 'Polypropylene fumarate/phloroglucinol triglycidyl methacrylate blend for use as partially biodegradable orthopaedic cement', *Biomaterials*, **22**, 2749–2757.

Jedrychowski, J. R., Caputo, A. A., Kerper, S. (1983), 'Antibacterial and mechanical properties of restorative materials combined with chlorhexidines', *Journal of Oral Rehabilitation*, **10**, 373–381.

Joosten, U., Joist, A., Frebel, T., Brandt, B., Diederichs, S. and Von Eiff, C. (2005), 'Evaluation of an in situ setting injectable calcium phosphate as a new carrier material for gentamicin in the treatment of chronic osteomyelitis: studies in vitro and in vivo', *Biomaterials*, **25**, 4287–4295.

Kawashita, M., Tsuneyama, S., Miyaji, F., Kokubo, T., Kozuka, H. and Yamamoto, K. (2000), 'Antibacterial silver-containing silica glass prepared by sol gel method', *Biomaterials*, **21**, 393–398.

Kim, S. B., Kim, Y. J., Yoon, T. L., Park, S. A., Cho, I. H., Kim, E. G., Kim, I. A. and Shin, J.-W. (2004), 'The characteristics of a hydroxyapatite–chitosan–PMMA bone cement', *Biomaterials*, **25**, 5715–5723.

Komlev, V. S., Barinov, S. M. and Koplik, E. V. (2002), 'A method to fabricate porous spherical hydroxyapatite granules intended for time-controlled drug release', *Biomaterials*, **23**, 3449–3454.

Krasko, M. Y., Golenser, J., Nyska, A., Nyska, M., Brin, Y. S. and Domb, A. J. (2007), 'Gentamicin extended release from an injectable polymeric implant', *Journal of Controlled Release*, **117**, 90–96.

Lee, S.-B., Lee, D.-Y., Lee, Y.-K., Kim, K.-N., Choib, S.-H. and Kima, K.-M. (2008), 'Surface modification of a guided tissue regeneration membrane using tetracycline-containing biodegradable polymers', *Surface and Interface Analysis*, **40**, 192–197.

Lepretre, S., Boschin, F., Tabary, N., Bria, M., Martel, B., Blanchemain, N., Hildebrand, H. F., Morcellet, M. and Delcourt-Debruyne, E. (2007), 'Guided tissue regeneration membranes with controlled delivery properties of chlorhexidine by their functionalization with cyclodextrins', *Journal of Inclusion Phenomena and Macrocyclic Chemistry*, **57**, 297–302.

Leung, D., Spratt, D. A., Pratten, J., Gulabivala, K., Mordan, N. J., Young, A. M. (2005), 'Chlorhexidine-releasing methacrylate dental composite materials', *Biomaterials*, **26**, 7145–7153.

Li, Y. W., Leong, J., Lu, W. W. (2000), 'A novel injectable bioactive bone cement for spinal surgery: a developmental and preclinical study', *Journal of Biomedical Materials Research*, **52**, 164–170.

Lieberman, I. H., Togawa, D., Kayanja, M. M. (2005), 'III. Kyphoplasty and Nucleus Pulposus Prosthesis. Vertebroplasty and kyphoplasty: Filler materials', *The Spine Journal*, **5**, 305S–316S.

Mano, J. F., Sousa, R. A., Boesel, L. F., Neves, N. M. and Reis, R. L. (2004), 'Bioinert, biodegradable and injectable polymeric matrix composites for hard tissue

© Woodhead Publishing Limited, 2013

replacement: state of the art and recent developments', *Composites Science and Technology*, **64**, 789–817.

McDonnell, G, and Russell, A. D. (1999), 'Antiseptics and disinfectants: activity, action, and resistance', *Clinical Microbiology Reviews*, **12**, 147–179.

Mehdawi, I., Abou Neel, E. A., Valappil, S., Palmer, G., Salih, V., Pratten, J., Spratt, D. and Young, A. (2009), 'Development of remineralising antibacterial dental materials', *Acta Biomaterialia*, **5**, 2525–2539

Meyer, J. M., Cattani-Lorente, M. A. and Dupuis, V. (1998), 'Compomers: between glass-ionomer cements and composites', *Biomaterials*, **19**, 529–539.

Miyamoto, Y., Ishikawa, K., Fukao, H., Sawada, M., Nagayama, M., Kon, M. and Asaoka, K (1995), 'In vivo setting behaviour of fast-setting calcium phosphate cement', *Biomaterials*, **16**, 855–860.

Muggli, D. S., Burkoth, A. K. and Anseth, K. S. (1999), 'Crosslinked polyanhydrides for use in orthopedic applications: degradation behavior and mechanics', *Journal of Biomedical Materials Research*, **46**, 271–278.

Murrey, P. E., Hafez, A. A., Smith, A. J. and Cox, C. F. (2002), 'Bacterial microleakage and pulp inflammation associated with various restorative materials', *Dental Materials*, **18**, 470–478.

Needleman, I., Worthington, H. V., Giedrys-Leeper, E. and Tucker, R. (2008), 'Guided tissue regeneration for periodontal infra-bony defects', *Cochrane Database of Systematic Reviews*, **4**, 1–37.

Nicholson, J. W. (2007), 'Polyacid-modified composite resins ("compomers") and their use in clinical dentistry', *Dental Materials*, **2**(3), 615–622.

O'Donnell, J. N. R., Skrtic, D. and Antonucci, J. M. (2006), 'Amorphous calcium phosphate composites with improved mechanical properties', *Journal of Bioactive and Compatible Polymers*, **21**, 169–184.

Patel, M. P., Cruchley, A. T., Coleman, D. C., Swai, H., Braden, M. and Williams, D. M. (2001), 'A polymeric system for the intra-oral delivery of an anti-fungal agent', *Biomaterials*, **22**, 2319–2324.

Peter, S. J., Kim, P., Yasko, A. W., Yaszemski, M. J. and Mikos, A. G. (1999), 'Crosslinking characteristics of an injectable poly(propylene fumarate)/beta-tricalcium phosphate paste and mechanical properties of the crosslinked composite for use as a biodegradable bone cement', *Journal of Biomedical Materials Research*, **44**, 314–321.

Peutzfeldt, A. (1997), 'Resin composites in dentistry: the monomer systems', *European Journal of Oral Sciences*, **105**, 97–116.

Ratier, Gibson, I. R., Best, S. M., Freche, M., Lacout, J. L. and Rodriguez, F. (2001), 'Setting characteristics and mechanical behaviour of a calcium phosphate bone cement containing tetracycline', *Biomaterials*, **22**, 897–901.

Regnault, W. F., Icenogle, T. B., Antonucci, J. M., and Skrtic, D. (2008), 'Amorphous calcium phosphate/urethane methacrylate resin composites. I. Physicochemical characterization', *Journal of Materials Science-Materials in Medicine*, **19**, 507–515.

Sasaki, S. and Ishii, Y. (1999), 'Apetite cement containing antibiotics: efficacy in treating osteomylities', *Journal of Orthopaedic Science*, **4**, 361–369.

Smith, D. C. (1998), 'Development of glass-ionomer cement systems', *Biomaterials*, **19**, 467–478.

© Woodhead Publishing Limited, 2013

Splieth, C., Rosin, M. and Gellissen, B. (2001), 'Determination of residual dentine caries after conventional mechanical and chemomechanical caries removal with cariosolv', *Clinical Oral Investigations*, **5**, 250–253.

Stallmann H. P., Faber, C., Bronckers, A. L. J. J., Amerongen, A. V. N., Wuisman, P. I. J. M. (2004), 'Osteomyelitis prevention in rabbits using antimicrobial peptide hLF1–11 – or gentamicin-containing calcium phosphate cement', *Journal of Antimicrobial Chemotherapy*, **54**, 472–476.

Stallmann, H. P., Faber, C., Bronckers, A. J. J., Amerongen, A. V. N. and Wuisman, P. I. J. M. (2006), 'In vitro gentamicin release from commercially available calcium-phosphate bone substitutes influence of carrier type on duration of the release profile', *BMC Musculoskeletal Disorders*, **7**, 1–8.

Sutherland, A. G., Raafat, A., Yates, P. and Hutchison, J. D. (1997), 'Infection associated with the use of allograft bone from the northeast Scotland Bone Bank', *Journal of Hospital Infection*, **35**, 215–220.

Syafiuddin, T., Hisamitsu, H., Toko, T., Trashi, T., Goto, N., Fujishima, A. and Miyazaki, T. (1997), 'In vitro inhibition of caries around a resin composite restoration containing antibacterial filler', *Biomaterials*, **18**, 1051–1057.

Tabary, N., Lepretre, S., Boschin, F., Blanchemain, N., Neut, C., Delcourt-Debruyne, E., Martel, B., Morcellet, M. and Hildebrand, H. F. (2007), 'Functionalization of PVDF membranes with carbohydrate derivates for the controlled delivery of chlorhexidin', *Biomolecular Engineering*, **24**, 472–476.

Takemura, K., Sakamoto, Y., Staninec, M., Kobayashi, S., Suehiro, K. and Tsuchitani, Y. (1983), 'Antibacterial activity of a BIS-GMA based composite resin and antibacterial effect of chlorhexidine incorporation', *Japanese Journal Conservative* Dentistry, **26**, 540–547.

Tamimi, F., Torres, J., Lopez-Cabarcos, E., Bassett, D. C., Habibovic, P., Luceron, E. and Barralet, J. E. (2009), 'A minimally invasive maxillofacial vertical bone augmentation using brushite based cements', *Biomaterials*, **30**, 208–216.

Tamimi, F., Torres, J., Bettini, R., Ruggera, F., Rueda, C., López-Ponce, M. and Lopez-Cabarcos, N. (2008), 'Doxycycline sustained release from brushite cements for the treatment of periodontal diseases', *Journal of Biomedical Materials Research*, **85A**, 707–714.

Van Landuyt, K. L., Snauwaert, J., De Munck, J., Peurnans, M., Yoshida, Y., Poitevin, A., Coutinho, E., Suzuki, K., Lambrechtsa, P. and Van Meerbeek, B. (2007), 'Systematic review of the chemical composition of contemporary dental adhesives', *Biomaterials*, **28**, 3757–3785.

Van Meerbeek, B., Vargas, M., Inoue, S., Yoshida, Y., Peumans, M., Lambrechtsa, P. and Vanherle G. (2001) 'Adhesives and cements to promote preservation dentistry', *Operative Dentistry*, (Suppl. **6)**, 119–144.

Varoga, D., Wruck, C. J., Tohidnezhad, M., Brandenburg, L., Paulsen, F., Mentlein, R,. Seekamp, A., Besch, L. and Pufe, T. (2008), 'Osteoblasts participate in the innate immunity of the bone by producing human beta defensin-3', *Histochemistry and Cell Biology*, **131**(2), 207–218.

Virtoa, M. R., Frutosa, P., Torradoa, S. and Frutos, G. (2003), 'Gentamicin release from modified acrylic bone cements with lactose and hydroxypropylmethylcellulose', *Biomaterials*, **24**, 79–87.

Wiegand, A., Buchalla, W. and Attin, T. (2007), 'Review on fluoride-releasing restorative materials – fluoride release and uptake characteristics, antibacterial activity and influence on caries formation', *Dental Materials*, **2**(3), 343–362.

© Woodhead Publishing Limited, 2013

Wirthlin, M. R., Chen, P. K. and Hoover, C. I. (2005), 'A laboratory model biofilm fermenter: Design and initial trial on a single species biofilm', *Journal of Periodontology*, **76**, 1443–1449.

Wroblewski, B. M., Esser, M. and Srigley, D. W. (1986), 'Release of gentamicin from bone cement: an ex-vivo study', *Acta Orthopaedica Scandinavica*, **57**, 413–414.

Xie, D., Brantley, W. A., Culbertson, B. M. and Wang, G. (2000), 'Mechanical properties and microstructures of glass-ionomer cements', *Dental Materials*, **16**, 129–138.

Xie, D., Wu, W., Puckett, A., Farmer, B. and Mays, J. W. (2004), 'Novel resin modified glass-ionomer cements with improved flexural strength and ease of handling', *European Polymer Journal*, **40**, 343–351.

Xu, H. H. K., Sun, L., Weir, M. D., Antonucci, J. M., Takagi, S., Chow, L. C. and Peltz, M. (2006), 'Nano DCPA-whisker composites with high strength and Ca and PO4 release', *Journal of Dental Research*, **85**, 722–727.

Xu, H. H. K., Sun, L. M., Weir, M. D., Takagi, S., Chow, L. C. and Hockey, B. (2007), 'Effects of incorporating nanosized calcium phosphate particles on properties of whisker-reinforced dental composites', *Journal of Biomedical Materials Research Part B-Applied Biomaterials*, **81B**, 116–125.

Xu, X. M. and Burgess, J. O. (2003), 'Compressive strength, fluoride release and recharge of fluoride-releasing materials', *Biomaterials*, **24**, 2451–2461.

Yamamoto, K., Ohashil, S., Aonol, M., Kokuboz, T., Yamada, I., Yamauchid, J. (1996), 'Antibacterial activity of silver ions implanted in SiO2 filler on oral streptococci', *Dental Materials*, **12**, 227–229.

Yoshida, Y., Nagakane, K., Fukuda, R., Nakayama, Y., Okazaki, M., Shintani, H., Inoue, S., Tagawa, Y., Suzuki, K., De Munck, J., Van Meerbeek, B. (2004), 'Comparative study on adhesive performance of functional monomers', *Journal of Dental Research*, **83**, 454–548.

Young, A. M., Ho, S. M. (2008), 'Drug release from injectable biodegradable polymeric adhesives for bone repair', *Journal of Controlled Release*, **127**, 162–172.

Young, A. M., Ho, S. M., Abou Neel, E. A., Ahmed, I., Barralet, J. E., Knowles, J. C. and Nazhat, S. N. (2009), 'Chemical characterization of a degradable polymeric bone adhesive containing hydrolysable fillers and interpretation of anomalous mechanical properties', *Acta Biomaterialia*, **5**, 2072–2083.

Zarkesh, N., Nowzari, H., Morrison, J. L. and Slots, J. (1999), 'Tetracyclicne-coated polytetrafluroethylene barrier membranes in the treatment of intraosseous periodontal lesions', *Journal of Periodontology*, **70**, 1008–1016.

© Woodhead Publishing Limited, 2013

18

Testing bond strength: the case of dental biomaterials

R. VAN NOORT, University of Sheffield, UK

DOI: 10.1533/9780857096425.4.514

Abstract: The collection of laboratory data is often perceived as being driven by a desire to use such data as a predictor of clinical performance. Some experiments are designed to test the fundamental behavioural characteristics of a material and other experiments are designed to study their performance when in function. In this chapter, the various approaches to the laboratory-based assessment of dental adhesives will be explored. The chapter will take a critical look at the design of the experimental methods and clarify issues in relation to our ability to assess the performance of an adhesive.

Key words: adhesive, bond strength, enamel, dentine, shear, micro-tensile, peel, modelling, structural integrity.

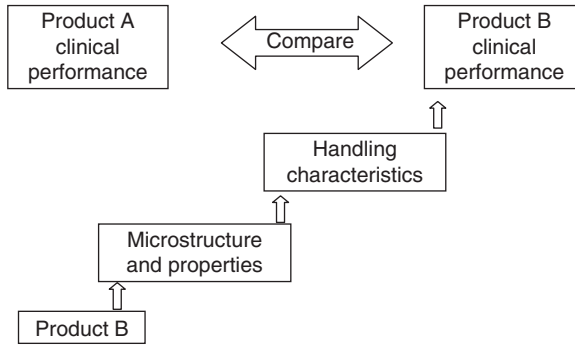
Note: This chapter has been previously published in *Dental biomaterials: imaging testing and modelling,* ed. R. V. Curtis and T. S. Watson (Chapter 11 'Modelling bond strength in dental biomaterials' by R. Van Noort), Woodhead Publishing Limited, 2008, ISBN: 978-1-84569-296-4.

18.1 Introduction

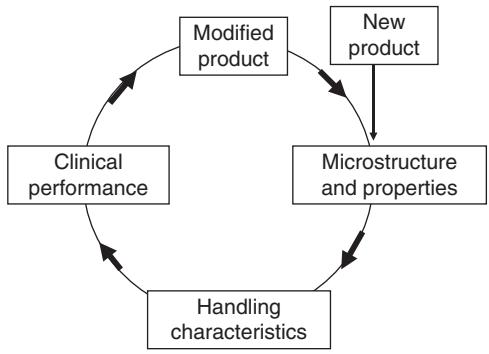
A considerable number of years ago, when I first joined the Dental School in Sheffield, I raised the question as to which was the best resin composite on the market. The only feedback I could get at the time was some comments about the relative merits of different materials based on personal experience and personal interpretation of a limited array of laboratory data about the products then on the market. In my naivety it seemed that a clinical study should be able to answer that question without too much difficulty. Ten years later I realized that things were not quite as straightforward as I imagined. By the time the work was published (van Noort and Davis, 1993), most of the materials that had been selected for the study no longer existed and thus, although it answered the fundamental question as to which material was best, the question itself had become irrelevant.

The presumption with an evidence-based approach to the selection of dental materials is that a material is developed and tried clinically and in

© Woodhead Publishing Limited, 2013



18.1 The product life cycle as often assumed in definitions of evidence-based medicine.



18.2 The product life cycle of a dental material as it goes through repeated numbers of iterations.

time we receive feedback on its clinical performance. In the meantime, a new material comes along and as we receive clinical feedback on its performance we can then compare one with the other material and decide which is the better of the two (Fig. 18.1) (see www.cebm.utoronto.ca). In reality the life span of a dental material is probably no more than 3–4 years before it is modified in the light of clinical experience and with each change the gathering of an evidence base of performance has to start all over again (Fig. 18.2). The extrapolation of data from one material to its supposed improved version is fraught with danger and the path to better dental materials is littered with casualties where the new improved version did not live up to expectation. Thus, by the time we have the clinical data it is too late to use it in our decision making as the material has changed or disappeared from the market.

© Woodhead Publishing Limited, 2013

My reason for recounting this story is that as a consequence of the short life span of a dental material, enormous emphasis is placed on the properties of a dental material that can be measured in the research laboratory as the gathering of clinical evidence takes such a long time. Thus, the collection of laboratory data is often perceived as being driven by a desire to use such data as a predictor of clinical performance. It is important that this point is appreciated from the outset as this puts quite a different complexion on the reasons why many laboratory-based experiments are carried out on dental materials. Whereas the research of the clinically oriented scientist seeks to establish a link between experiments carried out in the laboratory and the potential clinical performance of a material, the materials scientist's view of laboratory experiments is, generally speaking, quite different from this. The materials scientist will carry out experiments in the laboratory in order to understand how a material behaves and what factors control its behaviour. This allows the scientist to identify ways and means of improving the properties of a material. From their perspective, whether or not the material will meet the needs of a certain application may only be a secondary consideration. For example, the laboratory-based scientists may improve the properties of a fibre-reinforced resin composite but they would not even attempt to claim that this would make the 'improved' material suitable for making dentures or dental bridges. The point I am seeking to make is that some experiments are designed to test the fundamental behavioural characteristics of a material and other experiments are designed to study their performance when in function. It is important that we differentiate between these two types of experiments. For example, a micro-tensile bond strength test is designed to assess the fundamental behavioural characteristics of materials, whereas a microleakage test examines the performance of a material during function. The latter can generally be regarded as an attempt to test the material in a situation that simulates the clinical application of the material. One distinct difference between the two approaches is that, in the former, the variables can be reasonably carefully controlled, whereas in the case of the latter one has to deal with a multitude of variables that contribute to the outcome.

In this chapter, the various approaches to the laboratory-based assessment of dental adhesives will be explored. We will take a critical look at the design of the experimental methods and clarify issues in relation to our ability to assess the performance of an adhesive.

18.2 Rationale for bond strength testing

It is not unreasonable to take the point of view that if a material is to be used as an adhesive then one should test its adhesive qualities. However, that does not necessarily mean that we only need to look at the ability of the adhesive to bond to a surface, be it soft tissue, bone, enamel, dentine or any

© Woodhead Publishing Limited, 2013

man-made material. One factor that is often overlooked is the requirement for the adhesive to act as a means of transferring load from one part of a structure to another. This generates stresses and strains within the adhesive and it is important that the adhesive has the necessary mechanical properties to withstand these stresses and strains. For example, one might happily use Blu-Tack to stick bits of paper to the wall but one would not do the same with a framed picture. The ability of the Blu-Tack to stick to the wall or the picture is not really the issue here, but its inability to carry load is a problem and is fundamentally the reason why it would fail as an adhesive. Thus, the assessment of an adhesive should be based not merely on its ability to stick but also its ability to carry load; that is, more often than not, the adhesive has to be able to contribute to the structural integrity of the whole unit. This requires one to differentiate carefully between the need to assess the integrity of an adhesive bond, on the one hand, and the requirement for a structure to carry load, on the other. Some experiments are designed to do the former, while others are designed to test the latter. Those designed to test structural integrity can be recognized as experiments that seek to simulate the clinical situation. Thus shear or micro-tensile bond strength tests are experiments that test the integrity of the adhesive bond, while the enamel debonding test for an orthodontic bracket is an experiment seeking to simulate the clinical situation.

When one sets out to design a research project, the starting point is always to define the question one is seeking to address. Once one knows the question to ask one can then design the experiment that will seek to answer that question. This may all seem very obvious but it is noticeable in the ways that data are manipulated and presented that this fundamental point is often overlooked. When one considers this in the context of bond strength testing then it is important to appreciate that most bond strength tests are designed and conducted to answer a specific question. For example, a bond strength experiment may be conducted to determine the quality of the adhesion of a particular bonding system by examining the bond strength, and perhaps more importantly the mode of failure. Based on the information obtained it may be possible to suggest a means of improving the adhesion by overcoming any weaknesses that have been identified. You will note that this experiment would not provide an answer as to the clinical performance of the adhesive since that wasn't the question that was addressed. Nevertheless we regularly see attempts to try to extrapolate from bond strength data to clinical performance. If one wants to ask the question: 'What is the relationship between bond strength and clinical performance?', then one must design quite a different experiment to answer that question. Conducting only bond strength tests will not answer that question. Thus, it needs to be made clear from the outset what is the purpose of the experiment being conducted. In summary, one can look upon adhesive interface testing as addressing

© Woodhead Publishing Limited, 2013

different issues depending on how the experiment is designed. It is vitally important that the experiment undertaken matches the question asked such that one does not fall into the trap of making unjustified extrapolations to situations that the original question was not meant to address and for which the experiment was not designed.

18.3 Classification of dental adhesive testing techniques

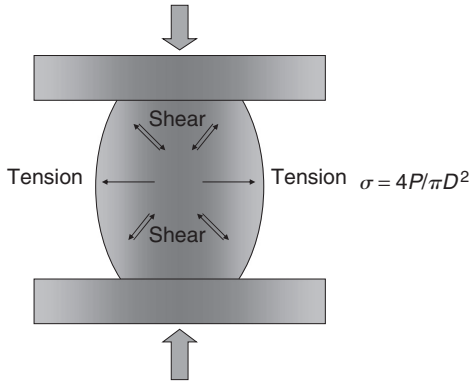
The types of laboratory experiments that can be conducted on dental adhesives can be classified into two types, namely behavioural tests and structural integrity tests. In the behavioural tests one seeks to establish the fundamental material behavioural properties. Examples of the sorts of things one might measure are tensile strength, elastic modulus, fracture toughness, coefficient of thermal expansion and translucency. In structural integrity tests, one sets out to provide an experimental arrangement that simulates the usage of the materials. Typical examples of such tests in dentistry include strength and fatigue testing of crowns and bridges, wear tests and microleakage tests. It is important to appreciate the distinction between these two approaches to materials testing.

18.3.1 Behavioural tests

In the behavioural tests the focus is on understanding how the material behaves and how one might be able to change the properties of the material by changing such things as its composition. The critical feature of the design of these experiments is that one needs to ensure that the data gathered are correct and appropriate, otherwise they can very easily be misinterpreted and the wrong conclusion may be drawn. For example, in the compressive strength test of a cylinder, the failure of the materials is in fact a combination of shear and tension, and the calculation of the compressive strength by dividing the stress at failure by the cross-sectional area of the cylinder is actually not valid (Fig. 18.3).

If one simply uses the test as a means of monitoring the setting process over time of a material such as a glass ionomer cement, or monitoring whether the compressive strength of the material is improved or made worse by a change in formulation, this does not matter, but if one were to try to extrapolate the data from the compressive strength test to a clinical compressive loading situation then this would be an erroneous use of this property of the material, since the stresses and strains generated under clinical loading conditions will be quite different from those in a compressive strength test.

© Woodhead Publishing Limited, 2013



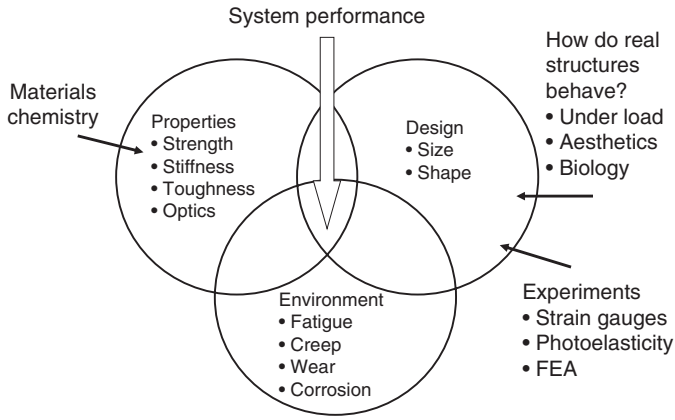
18.3 Complex tensile and shear stresses generated in a compressive strength test; σ, stress; P, load; D, diameter.

18.3.2 Structural integrity tests

In structural integrity tests, the material is being applied in a situation in an attempt to provide some insight into how the material might respond to a clinical environment and to learn what makes the structure fail. This will be a complex interaction between material, design and environment. Thus, the structural integrity test is seeking to establish a link between the material and its performance in a clinical situation. How effective this is depends on the quality of the design of the structural integrity test and there will be a need to validate the simulation.

The testing of crowns and bridges under various loading conditions is an example of structural integrity testing. Some of these tests are designed to answer the question as to whether or not the structural integrity is compromised by a change in materials or design, of which a typical example is the so-called 'crunch the crown' experiment. Often such experiments are criticized for their lack of clinical relevance, but one has to remember that these experiments are designed to assess the complex interaction between materials and design. The question being addressed in such experiments is whether or not the structural integrity of the structure has been compromised to such a degree that there is little point in carrying out the much more complex and time-demanding experiments that test the durability of the structure. If one now adds the ingredient of environment along with those of materials and design, then the experimental design needs to reflect that and issues such as cyclic loading and corrosion become much more important (Fig. 18.4). One sees this for example in wear tests, which try to examine simultaneously the complex interaction between different loading conditions and environments, and where the validity of the clinical wear simulation will determine

© Woodhead Publishing Limited, 2013



18.4 The factors influencing the performance of dental materials in the oral environment (FEA, finite element analysis).

the popularity of the wear tester in terms of its ability to predict the clinical performance of a material or a device.

As the experimental design becomes more concerned with asking questions about the potential performance in the clinical situation, so the experiments make a paradigm shift from the evaluation of the physical and behavioural characteristics of materials to what is more accurately described as system performance. It is important that this distinction is appreciated, otherwise one may fall into the trap of thinking that one is undertaking a test to determine fundamental materials properties whereas in fact one is conducting a structural integrity test. For example, the testing of the bond strength of orthodontic brackets is a structural integrity test, not a test of behavioural characteristics, and is potentially open to misunderstanding if one is unaware of this distinction (Eliades and Brantley, 2000).

It is important that the distinction between a behavioural test and a structural integrity test does not become blurred as the danger is that the experiment will not be able to provide valuable answers. Thus, the focus in the behavioural test must be on ensuring that the measurements undertaken provide genuine and reliable information on the behavioural characteristics of the material, while the structural integrity test must be so designed to provide a worthwhile simulation of the structure to be tested.

18.4 Behavioural adhesive tests

Next, I will explore some examples of what I consider to be behavioural tests and address some of the issues that arise in relation to how these tests are designed and conducted. However, before proceeding it is worth reiterating that in my view these experiments are not designed to assess the

© Woodhead Publishing Limited, 2013

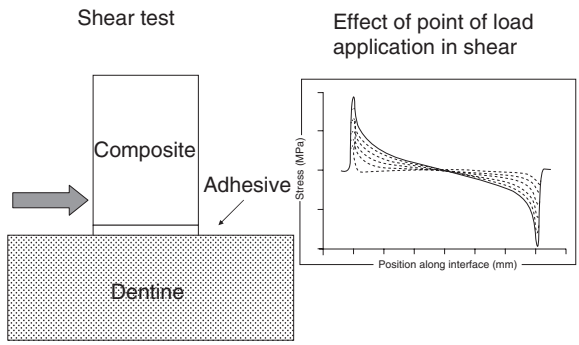
clinical performance of the materials used. Thus, it is pointless to enter into a discussion as to the clinical relevance of these experiments. What is important is that the experiments are designed such that the information obtained can be understood and is open to the correct interpretation. The focus of this discussion will be the methods used to assess the quality of adhesion between dentine and resins, although there are obviously other examples of fundamental tests of adhesion such as bone bonding to implants (Lin and Yen, 2004), resin bonding to fibre posts (Ferrari *et al.*, 2006) or resin bonding to ceramics (Kern and Wegner, 1998; Della Bona *et al.*, 2000).

18.4.1 Shear bond strength test

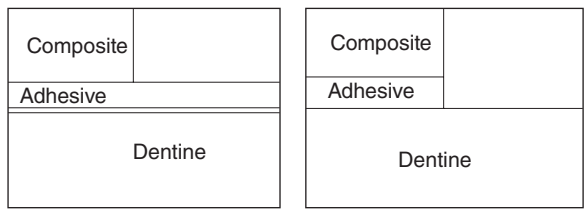
Of all the adhesive tests used in dentistry, the shear bond strength test has been one of the most popular bonding experiments ever devised. Its popularity has much to do with the simplicity with which this experiment can be conducted. When this experimental design was first introduced the quality of the dentine bonding agents was quite poor relative to the bonding agents available today. In those initial experiments the bond strength was so poor that failure would generally occur at the adhesive interface such that the bond strength, reported as a shear stress based on the ratio of load to bonding area, could be used as a measure of the quality of the adhesion achieved. As the quality of the adhesive bond improved then one would expect this to be reflected in an increase in the shear bond strength. However, it should be noted that this calculation of failure stress is in fact erroneous. The experimental design of the specimen and the manner of loading are such that the stresses experienced at the adhesive interface are extremely complex, as shown in Fig. 18.5. Failure is more likely to be due to interfacial tensile stresses generated as a consequence of the bending action rather than genuine shear (van Noort *et al.*, 1989). In addition, these tensile stresses can be considerably higher than the calculated shear stress. When bond strength values were low this was not a problem and as long as the experimental design used was consistent in terms of size, shape and load application, different adhesives could be compared by calculating the nominal shear bond strength.

Where one has to be really careful is in comparing shear bond strength data from experiments carried out in different laboratories. Minor modifications in the method used can potentially have a profound influence on the outcome of the experiment, such as, for example, the mode of application of the adhesive. Quite different results can be obtained if the adhesive is applied liberally over the dentine surface as compared with when it is constrained to the adhesive interface (van Noort *et al.*, 1991). This problem is exacerbated by all the other variables that can come into play when bonding to dentine (Al-Salehi and Burke, 1997; Tay and Pashley, 2004).

© Woodhead Publishing Limited, 2013



18.5 Interfacial stress distribution of the vertical stresses (σ_{yy}) for a shear bond strength test arrangement, showing high levels of tensile stress below the point of load application and compressive stresses on the side opposite to the point of load application.



18.6 Finite element analysis of the stress distribution for an unconstrained adhesive interface and a constrained adhesive interface.

Figure 18.6 shows that, for the unconstrained adhesive interface situation, the maximum stresses tend to occur at the adhesive/composite interface, while for the constrained condition the maximum stresses are at the dentine/adhesive interface, which invariably will produce different results. Thus, while it is reasonable to compare the adhesive performance of different dentine bonding agents within a laboratory, the comparison of data from different laboratories is fraught with danger, unless one can be sure that exactly the same experimental conditions were used.

As dentine bonding agents improved so another problem came to light, namely fractures no longer occurred at the adhesive interface but would tend to be cohesive in nature, more often than not involving the dentine. The reason for this is that the stresses generated by the bending action will predispose any crack that forms to deviate into the dentine when confronted with a strong adhesive bond. In shear bond strength tests this deviation of

© Woodhead Publishing Limited, 2013

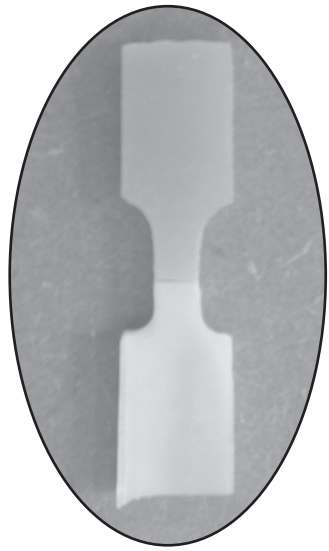
the fracture mode from the interface into the dentine tends to occur at a nominal shear stress of some 20 MPa. This has led some people to suggest that the bond strength exceeds the cohesive strength of the dentine and that the maximum bond strength that can be achieved to dentine is of the order of 20 MPa, which seriously misunderstands the actual situation. This interpretation does not fit comfortably with the observation that the ultimate tensile strength of dentine may be as high as 100 MPa (Bouillaguet *et al*., 2001). It is much more likely that the transition from an interfacial failure to a cohesive failure of the dentine is as much a consequence of the improved adhesion as it is of the design of the experiment. A similar problem arises with shear bond strength testing of resins to ceramics, where fractures are frequently cohesive in the ceramic (Blatz *et al*., 2004), which has been shown to be an experimental artefact (Della Bona and van Noort, 1995). The correct way to interpret the situation is that when cohesive failure of the dentine becomes the dominant mode of failure, it is no longer possible to differentiate between the different dentine bonding agents and an alternative test needs to be used. One such test that is gaining in popularity is the micro-tensile bond strength test.

18.4.2 Micro-tensile bond strength

The micro-tensile bond strength test has been gaining in popularity since it was first introduced in the early 1990s (van Meerbeek *et al*., 2003). The most important difference between the micro-tensile test design and the shear test design is the potential ability for the micro-tensile bond strength test to be able to calculate the average tensile stress at the adhesive interface. The concept is the same as one that has been used in engineering for decades whereby the stress–strain behaviour of a material is assessed using a dumbbell specimen design (Fig. 18.7). The idea behind this design is that all measurements are taken in the central part of the specimen, well away from the clamping site, such that a uniform stress field is generated and the local tensile stress can be calculated simply from the load divided by the cross-sectional area. The wider section of the specimen at each end is there to ensure that the specimen could be easily gripped and to avoid failure within the clamping zone as this would invalidate the experiment.

What this means is that it is then possible to assess the quality of the adhesion by comparing the tensile stress at failure for different bonding agents, evaluate the mode of failure and maybe identify the weakest link in the system, without this being influenced by geometric design features. The two notable differences that should strike one immediately when examining micro-tensile bond strength data: firstly, the 20 MPa ceiling observed for

© Woodhead Publishing Limited, 2013



18.7 Dumbell specimen design.

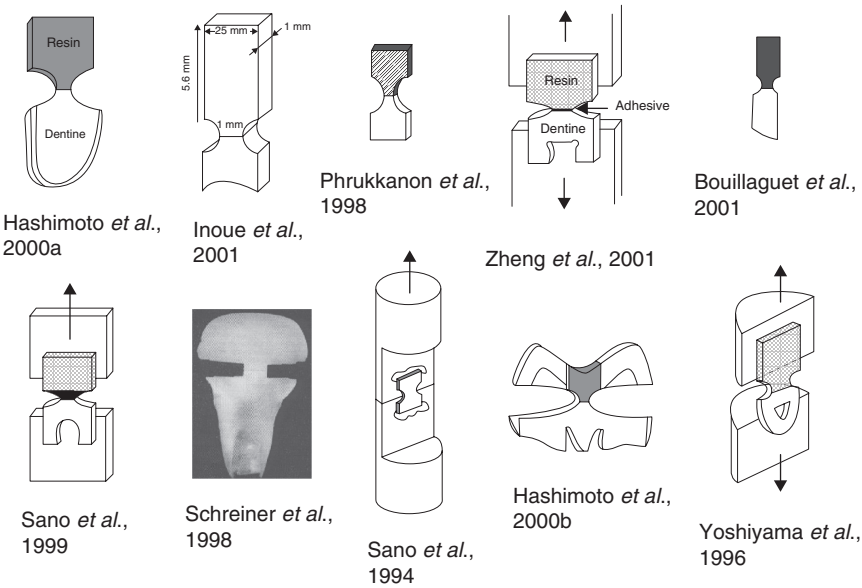
the shear bond strength test has disappeared and tensile bond strengths in excess of 40 MPa can be achieved; secondly, cohesive failure of the dentine is a much less common occurrence. Thus, the constraints imposed by the design of the shear bond-strength test have been removed.

As with all new tests, within a very short time of its introduction, various forms of the micro-tensile bond strength test have appeared (Fig. 18.8). There is a danger with these alternative designs that the original premise of producing a uniform stress at the interface is lost. The sorts of designs now used include the simple stick, dumbbell and various re-entrant designs. It is the latter that have become the main area of concern, since the interfacial stress will be affected by the degree of the re-entrant design. This means that we could again find ourselves in the situation where it becomes impossible to compare the results from different laboratories because of the use of different specimen designs.

Recently published work has shown that the micro-tensile bonds strength for the stick, dumbbell and parabolic designs are pretty much the same, but that sharp re-entrant shapes underestimate the stress at failure due to the stress-concentrating effect of such designs, which would suggest that one might as well use the stick specimen design since it is the easiest to produce (Betamar *et al.*, 2007a, b).

However, using the same design is not yet the complete answer to producing results that can be compared from one laboratory to another. There is also the issue of size and results will not be comparable if widely different

© Woodhead Publishing Limited, 2013



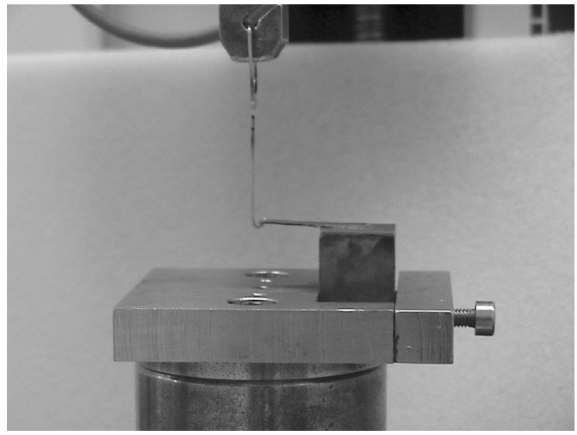
18.8 Various designs used in micro-tensile bond strength tests.

specimen sizes are used, despite them having the same shape. Since the days of Griffith's experiment on glass fibres it has been known that smaller specimens are stronger and that this is simply a consequence of the reduction and removal of inherent flaws in the system (Gordon, 1968). The same applies to the specimens used in the micro-tensile bond strength tests and a valid comparison is only possible if specimens are of a similar size or, better still, of the same cross-sectional area (Sano *et al*., 1994).

18.5 Structural adhesive tests

It is important to appreciate the distinction between a behavioural adhesive test as described above and a structural adhesive test. Whenever a dental device is used in an experimental design that mimics its use clinically this is a structural integrity test. For example, pull-out tests for fibre posts (Giachetti *et al*., 2004), debonding of orthodontic brackets (Vicente *et al*., 2006), debonding of resin-bonded bridges (van Dalen *et al*., 2005) and crown retention tests (Palacios *et al*., 2006) are all structural integrity tests. The experiment involves the testing of the whole system and thus one is looking at a system response. A consequence of this is that it generally turns into a multi-factorial problem that needs very careful analysis. If appropriately constructed in terms of the question the test is trying to address then such tests can be very enlightening. One obvious concern with structural

© Woodhead Publishing Limited, 2013



18.9 Design of a simple peel test for a cantilever bridge.

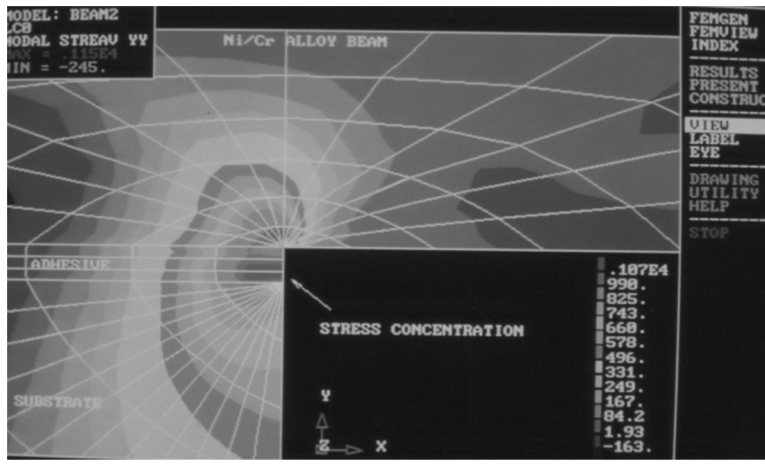
integrity tests is the validity of the experimental design used and its ability to answer the question it is seeking to address.

18.5.1 Structural integrity tests for cantilever resin-bonded bridges

As an illustration of how a structural integrity test can be used to acquire useful information on the behaviour of a complex system, I would like to take a closer look at the cantilever resin-bonded minimum preparation bridge. Numerous shear and tensile bond strength tests have been conducted with bond strengths typically being in the region of 30–40 MPa. This would suggest that a debonding force of some 300–700 N would be required to debond a cantilever resin-bonded bridge if based simply on the area of bonding provided, which obviously is absurd (van Noort, 2005). Thus it was proposed that a peel test along the lines shown in Fig. 18.9 would be more realistic for the assessment of the adhesion of the bridge.

The debonding force for the beams was found to be no more than 25 N in this experimental design, which is considerably more realistic (Northeast *et al.*, 1994). Perhaps this is not surprising since the design produces a highly significant stress concentration at the point where the beam attaches to the base, as shown in the finite element analysis (FEA) of the system in Fig. 18.10. One concern in such a test is always whether or not the correct loading condition has been considered. Further experiments were conducted to assess the failure load in what would be the occlusal direction and it was found that the failure loads for occlusal loading were some seven times higher than

© Woodhead Publishing Limited, 2013



18.10 FEA model of the local stress distribution for the vertical tensile stress (σ_{yy}) for a cantilever beam.

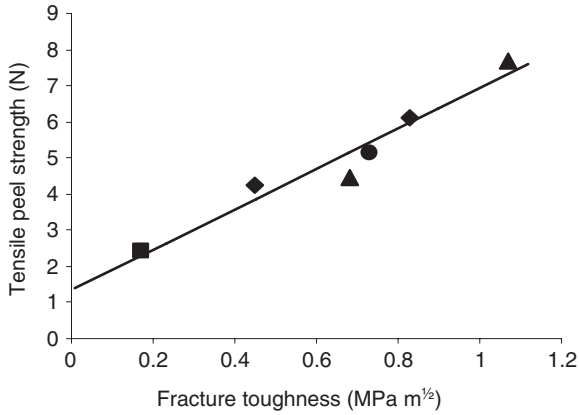
Table 18.1 Effect of elastic modulus on the maximum stress for the peel test arrangement

Material	Elastic modulus (GPa)	Maximum σ_{yy} (MPa)
Adhesive	10	74
	5	54
	1	30
Beam	200	54
	100	75

those for the peeling condition (Bhakta *et al*., 2006). Similar observations have been reported by van Dalen *et al*. (2005) and thus it is reasonable to assume that failure is most likely to occur by a peeling action.

The benefit of combining the experimental work with FEA modelling is that it provides an opportunity to interrogate the system and get an idea of what would happen if certain parameters were changed. For example, one can change the elastic modulus of the adhesive or the beam and see how this influences the peak stress in the system. The results for such an analysis are shown in Table 18.1, which would indicate that a combination of a high-stiffness beam material and a low-stiffness adhesive would provide the best outcome. This idea that a low elastic modulus adhesive provides a better resistance to failure by peeling forces deserves further study, especially since this fundamental material property has not previously been considered as a parameter for the selection of a resin-bonded bridge adhesive.

© Woodhead Publishing Limited, 2013

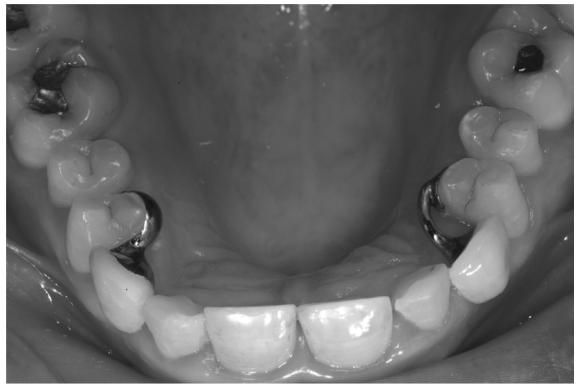


18.11 The relationship between tensile peel strength and fracture toughness of a range of luting agents.

Another material parameter that may have an influence on the outcome is the fracture toughness of the adhesive, which is based on the observation that the fracture is initiated in the adhesive. As it happens, Knobloch *et al*. (2000) had carried out a series of experiments on the fracture toughness of luting agents and so this afforded us the opportunity to compare the peel strength of these adhesives with their fracture toughness. The results of this comparison are shown in Fig. 18.11 and there appears to be a very close correlation between fracture toughness and peel strength (Al-Ghananeem and van Noort, 2004). This would suggest that a combination of low elastic modulus and high fracture toughness is required for an adhesive for cantilever resin-bonded bridges. Thus, it may be possible to link the material's fundamental behavioural properties to those of the system and point us to a possible solution to a problem.

An alternative approach that can help to improve the performance of the system is to consider a change in design. The fundamental weakness is the stress concentration that arises at the point of attachment of the tooth. One way of dealing with this is to change the position of the attachment, as shown in the clinical case study in Fig. 18.12. A comparison of the peel force between the cantilever and lingual bar designs showed a peel force for the old design of 7 N as compared with 38 N for the new design (Bhakta *et al*., 2006). There is no doubt that there are potential problems with the proposed design, but the important point that I wish to illustrate with this example is that sometimes we need to take a step back and consider the whole system and how we may change its behaviour rather than focusing on the materials that make up that system.

© Woodhead Publishing Limited, 2013



18.12 Suggested alternative design for a cantilever resin-bonded bridge.

18.6 Future trends

It seems to me that there are a number of avenues that still need to be trodden before we can make the connection with clinical performance. With regard to the assessment of the fundamental behavioural properties of adhesive interfaces, there is more we can do. In the case of dentine bonding, with the micro-tensile bond strength test we have an effective means of assessment of the tensile bond strength of resins to enamel and dentine and the technique can be applied to a variety of other materials. However, it is generally accepted that failure in shear occurs at lower stresses than failure in tension and therefore we could do with a shear bond strength test that genuinely assesses the resistance of the adhesive interface to shear stresses and would be as widely accepted as the micro-tensile bond strength test. Perhaps the push-out test deserves closer examination (Dhert *et al.*, 1992) or some form of torsional shear test. Also a fracture mechanics approach to the assessment of adhesive interfaces can potentially provide more insight (Lin and Douglas, 1994; Tantbirojn *et al.*, 2000; Armstrong *et al.*, 2001; Della Bona *et al.*, 2006).

Another aspect of the performance of dental adhesives that requires more attention is the durability of the bond under the aggressive conditions of the oral environment. This could range from examining the effects of long-term storage in water, or perhaps some more aggressive medium such as artificial saliva, in order to test hydrolytic stability (Carrilho *et al.*, 2005; De Munck *et al.*, 2006), to cyclic fatigue loading of the interface (Attia and Kern, 2004; De Munck *et al.*, 2005).

Structural integrity tests can play an important role in the identification of potential weaknesses in a system. However, by their nature such tests are

© Woodhead Publishing Limited, 2013

more complex and thus the results are generally speaking more difficult to interpret and also more prone to misinterpretation. Thus, it is important that these tests are designed in such a way as to be able to address the question that is being asked, and no more or no less.

Alongside the experimental testing of the structural integrity of a system, computational modelling of the system is gaining more popularity, be it an implant replacing a missing tooth (Pilliar *et al*., 2006), an orthodontic bracket (Katona, 1997), a veneer (Magne and Douglas, 1999) or a filling (Borkowski *et al*., 2006). One can approach this from the concept of benign design, by which I mean how the interfacial stresses can be minimized (Richardson *et al*., 2001; Bhakta *et al*., 2006). This is hard enough and an even greater challenge is to try to link the data from behavioural tests, such as the micro-tensile bond strength test, to the interfacial behaviour of a bonded structure under load (Fennis *et al*., 2005). This would provide us with the potential to make a prediction as to where and at what load an adhesive interface in a dental structure, such as a restored tooth, will fail and what we may have to do to prevent this from happening. If that were possible then we would have a seamless transition of understanding from the fundamental laboratory test to the clinical performance of our dental adhesives and we would begin to bridge the gap between dental engineering and the other engineering disciplines.

18.7 Conclusion

We have a challenge to develop behavioural and structural tests for dental adhesives that are relevant to their clinical application (van Meerbeek *et al*., 2003). If we are prepared to accept that our starting point is to use such tests to understand better how the materials we use and the structures we create work in practice, then such understanding and knowledge can be used to improve the system behaviour. In due course we may begin to move closer to the goal of being able to carry out laboratory-based experiments that will inform the clinical performance of the materials and systems being evaluated.

18.8 References

Al-Ghananeem, M.M. and van Noort, R. (2004) Tensile peel strength versus fracture toughness of luting cements. BSDR Annual Meeting, Birmingham, UK, April 2004 (abstract).

Al-Salehi, S. and Burke, F.J.T. (1997) Methods used in dentin bonding tests: An analysis of 50 investigations on bond strength. *Quintessence Int.* **28**: 717–723.

Armstrong, S.R., Keller, J.C. and Boyer, D.B. (2001) The influence of water storage and C-factor on the dentin–resin composite microtensile bond strength and

© Woodhead Publishing Limited, 2013

debond pathway utilizing a filled and unfilled adhesive resin. *Dent. Mater.* **17**: 268–276.

Attia, A. and Kern, M. (2004) Influence of cyclic loading and luting agents on the fracture load of two all-ceramic crown systems. *J. Prosthet. Dent.* **92**: 551–556.

Betamar, N., Cardew, G. and van Noort, R. (2007a) Influence of specimen designs on the microtensile bond strength to dentin. *J. Adhesive Dent.* **9**(2): 159–168.

Betamar, N., Cardew, G. and van Noort, R. (2007b) The effect of variations in hour glass specimen design on the microtensile bond strength to dentin. *J. Adhes. Dent.* **9**(5): 427–436.

Bhakta, S., van Noort, R. and Cardew, G. (2006) Improved retention of anterior cantilever resin bonded fixed partial dentures by design alteration: An experimental and finite element study. *J. Prosthet. Dent.* **95**: 209–217.

Blatz, M.B., Sadan, A., Maltezos, C., Blatz, U., Mercante, D. and Burgess, J.O. (2004) In vitro durability of the resin bond to feldspathic ceramics. *Am. J. Dent.* **17**: 169–172.

Borkowski, K., Kotousov, A. and Kahler, B. (2006) Effect of material properties of composite restoration on the strength of the restoration – dentine interface due to polymerization shrinkage, thermal and occlusal loading. *Med. Eng. Phys.* **29**: 671–676.

Bouillaguet, S., Gysi, P., Wataha, J.C., Ciucchi, B., Cattani, M., Godin, C. and Meyer, J.M. (2001) Bond strength of composite to dentin using conventional, one-step, and self-etching adhesive systems. *J. Dent.* **29**: 55–61.

Carrilho, M.R., Carvalho, R.M., Tay, F.R., Yiu, C. and Pashley, D.H. (2005) Durability of resin-dentin bonds related to water and oil storage. *Am. J. Dent.* **18**: 315–319.

Della Bona, A., Anusavice, K.J. and Mecholsky, J.J. Jr. (2006) Apparent interfacial fracture toughness of resin/ceramic systems. *J. Dent. Res.* **85**: 1037–1041.

Della, A., Anusavice, K.J. and Shen, C. (2000) Microtensile strength of composite bonded to hot-pressed ceramics. *J. Adhes. Dent.* **2**: 305–313.

Della Bona, A. and van Noort, R. (1995) Shear versus tensile bond strength of resin composite bonded to ceramic. *J. Dent. Res.* **74**: 1591–1596.

De Munck, J., Braem, M., Wevers, M., Yoshida, Y., Inoue, S., Suzuki, K., Lambrechts, P. and van Meerbeek, B. (2005) Micro-rotary fatigue of tooth-biomaterial interfaces. *Biomaterials* **26**: 1145–1153.

De Munck, J., Shirai, K., Yoshida, Y., Inoue, S., van Landuyt, K., Lambrechts, P., Suzuki, K., Shintani, H. and van Meerbeek, B. (2006) Effect of water storage on the bonding effectiveness of 6 adhesives to Class I cavity dentin. *Oper. Dent.* **31**: 456–465.

Dhert, W.J.A., Verheyen, C.C.P.M., Braak, L.H., De Wijn, J.R., Klein, C.P., De Groot, K. and Rozing, P.M. (1992) A finite element analysis of the push-out test: influence of test conditions. *J. Biomed. Mater. Res.* **26**: 119–130.

Eliades, T. and Brantley, W.A. (2000) The inappropriateness of conventional orthodontic bond strength assessment protocols. *Eur. J. Orthod.* **22**: 13–23.

Fennis, W.M., Kuijs, R.H., Barink, M., Kreulen, C.M., Verdonschot, N. and Creugers, N.H. (2005) Can internal stresses explain the fracture resistance of cusp-replacing composite restorations? *Eur. J. Oral. Sci.* **113**: 443–448.

Ferrari, M., Goracci, C., Sadek, F.T., Monticelli, F. and Tay, F.R. (2006) An investigation of the interfacial strengths of methacrylate resin-based glass fiber post-core buildups. *J. Adhes. Dent.* **8**: 239–245.

© Woodhead Publishing Limited, 2013

Giachetti, L., Scaminaci Russo, D., Bertini, F. and Giuliani, V. (2004) Translucent fiber post cementation using a light-curing adhesive/composite system: SEM analysis and pull-out test. *J. Dent.* **32**: 629–634.

Gordon, J.E. (1968) *The New Science of Strong Materials*, 1st edn, Princeton, NJ: Princeton University Press.

Hashimoto, M., Ohno, H., Kaga, M., Endo, K., Sano, H. and Oguchi, H. (2000a) In vivo degradation of resin–dentine bonds in humans over 1 to 3 years. *J. Dent. Res.* **79**: 1385–1391.

Hashimoto, M., Ohno, H., Endo, K., Kaga, M., Sano, H. and Oguchi, H. (2000b) The effect of hybrid layer thickness on bond strength: Demineralized dentine zone of the hybrid layer. *Dent. Mater.* **16**: 406–411.

Inoue, S., Vargas, M., Abe, Y., Yoshida, Y., Lamberchts, P., Vanherle, G., Sano, H. and van Meerbeek, B (2001) Microtensile bond strength of eleven contemporary modern adhesives to dentine. *J. Adhes. Dent.* **3**: 237–234.

Katona, T.R. (1997) Stresses developed during clinical debonding of stainless steel orthodontic brackets. *Angle Orthod.* **67**: 39–46.

Kern, M. and Wegner, S.M. (1998) Bonding to zirconia ceramic: Adhesion methods and their durability. *Dent. Mater.* **14**: 64–71.

Knobloch, L.A., Kerby, R.E., Seghi, R., Berlin, J.S. and Lee, J.S. (2000) Fracture toughness of resin-based luting cements. *J. Prosthet. Dent.* **83**: 204–209.

Lin, C.M. and Yen, S.K. (2004) Characterization and bond strength of electrolytic HA/TiO_2 double layers for orthopedic applications. *J. Mater. Sci. Mater. Med.* **15**: 1237–1246.

Lin, C.P. and Douglas, W.H. (1994) Failure mechanisms at the human dentin-resin interface: A fracture mechanics approach. *J. Biomech.* **27**: 1037–1047.

Magne, P. and Douglas, W.H. (1999) Porcelain veneers: Dentin bonding optimization and biomimetic recovery of the crown. *Int. J. Prosthodont.* **12**: 111–121.

Northeast, S.E., van Noort, R. and Shaglouf, A.S. (1994) Tensile peel failure of resin-bonded Ni/Cr beams: An experimental and finite element study. *J. Dent.* **22**: 252–256.

Palacios, R.P., Johnson, G.H., Phillips, K.M. and Raigrodski, A.J. (2006) Retention of zirconium oxide ceramic crowns with three types of cement. *J. Prosthet. Dent.* **96**: 104–114.

Phrukkanon, S., Burrow, M.F. and Tyas, M.J. (1998) The influence of cross-sectional shape and surface area on the microtensile bond test. *Dent. Mater.* **14**: 212–221.

Pilliar, R.M., Sagals, G., Meguid, S.A., Oyonarte, R. and Deporter, D.A. (2006) Threaded versus porous-surfaced implants as anchorage units for orthodontic treatment: Three-dimensional finite element analysis of peri-implant bone tissue stresses. *Int. J. Oral, Maxillofac. Implants.* **21**: 879–889.

Richardson, C.J., van Noort, R. and Howard, I.C. (2001) The influence of elastic modulus of restorative materials on the stress distribution in a canine tooth with an abrasion-erosion lesion. In *Computer Methods in Biomechanics and Biomedical Engineering – 3*, J. Middleton *et al*. (eds), London: Gordon and Breach Science Publishers, pp. 595–604.

Sano, H., Shono, T., Sonoda, H., Takatsu, T., Ciucchi, B., Carvalho, R. and Pashley, D.H. (1994) Relationship between surface area for adhesion and tensile bond strength – evaluation of a micro-tensile bond test. *Dent Mater* **10**: 236–240.

© Woodhead Publishing Limited, 2013

Sano, H., Yoshikawa, T., Pereira, P.N.R., Kanemura, N., Morigami, M., Tagami, J. and Pashley, D.H. (1999) Long-term durability of dentine bonds made with a self-etching primer, in vivo. *J. Dent. Res.* **78**: 906–911.

Schreiner, R.F., Chappell, R.P., Glaros, A.G. and Eick, J.D. (1998) Microtensile testing of dentine adhesives. *Dent. Mater.* **14**: 194–201.

Tantbirojn, D., Cheng, Y.S., Versluis, A., Hodges, J.S. and Douglas, W.H. (2000) Nominal shear or fracture mechanics in the assessment of composite-dentin adhesion? *J. Dent. Res.* **79**: 41–48.

Tay, F.R. and Pashley, D.H. (2004) Resin bonding to cervical sclerotic dentine: A review. *J. Dent.* **32**: 173–196.

van Dalen, A., Feilzer, A.J. and Kleverlaan, C.J. (2005) The influence of surface treatment and luting cement on in vitro behavior of two-unit cantilever resin-bonded bridges. *Dent. Mater.* **21**: 625–632.

van Meerbeek, B., De Munck, J., Yoshida, Y., Inoue, S., Vargas, M., Vijay, P., van Landuyt, K., Lambrechts, P. and Vanherle, G. (2003) Buonocore memorial lecture. Adhesion to enamel and dentin: current status and future challenges. *Oper. Dent.* **28**: 215–235.

van Noort, R. (2005) An overview of the clinical use of resin-to-metal bonding. In *Adhesive Technology for Restorative Dentistry*, J.-F. Roulet and G. Vanherle (eds), London: Quintessence Publishing Co., pp. 153–169.

van Noort, R. and Davis, L.G. (1993) A prospective study of the survival of chemically activated resin composite restorations in general dental practice: Five year results. *J. Dent.* **21**: 209–215.

van Noort, R., Cardew, G.E., Howard, I.C. and Noroozi, S. (1991) The effect of local interfacial geometry on the measurement of the tensile bond strength to dentin. *J. Dent. Res.* **70**: 889–893.

van Noort, R., Noroozi, S., Howard, I.C. and Cardew, G.E. (1989) A critique of bond strength measurements. *J. Dent.* **17**: 61–76.

Vicente, A., Navarro, R., Mena, A. and Bravo, L.A. (2006) Effect of surface treatments on the bond strength of brackets bonded with a compomer. *Am. J. Dent.* **19**: 271–274.

Yoshiyama, M., Carvalho, R., Sano, H., Horner, J.A., Brewer, P.D. and Pashley, D.H. (1996) Regional bond strengths of resins to human root dentine. *J. Dent.* **24**: 435–442.

Zheng, L., Pereira, P.N.R., Nakajima, M., Sano, H. and Tagami, J. (2001) Relationship between adhesive thickness and microtensile bond strength. *Oper. Dent.* **26**: 97–104.

© Woodhead Publishing Limited, 2013

Index

abdominal aortic aneurysm (AAA), 363
acetal, 117
acrylic polymers, 114
acrylonitrile butadiene styrene (ABS), 117
active brazing joining techniques, 423–43
  in vitro testing, 432–5
  industrial processing, 435–9
    arrangement of cylindrical samples within the fixture before brazing, 437
    centre of a joint brazed with filler metal, 438
    compositional EDS dot mapping of brazed joint, 439
    edge of a joint brazed with filler metal, 438
    EDS spectra of joint brazed with filler metal, 440
    graphite-heating-elements vacuum brazing furnace, 436
    temperature brazing cycle for filler metal number 39, 437
    typical active brazing conditions, 436
  knee prosthesis, 439–43
  mechanical characterisation, 430–2
    correspondence between test batches and filler metals, 431
    four-point-bending fatigue strengths of brazed specimens, 432
    four-point-bending static strengths of brazed specimens, 431
  metallurgy, 423–30
    chemical composition, melting, wetting behaviour and hardness of fillers, 425–6
    four-point-bending-strength of coupons with filler metals, 427
    quantitative SEM analysis at Ti6Al4V filler–metal interface, 428
    quantitative SEM analysis of filler metal number 39, 428
    residual stress management across Ti6Al4V and ZrO_2 joint, 430
    SEM image of actively brazed Ti6Al4V-ZrO_2 joint with filler metal, 427, 428, 429
    specimens of four-point-bending test, 430
active device test, 184
additives, 269, 307
adherend, 454
Adherus, 472–4
  Adherus Spine in use, 474
Adherus Dural Sealant, 473
Adherus Spinal Sealant, 473
adhesion, 388–94, 454
  hydrophobic recovery, 393–4
    graph depicting water contact angles and O/C ratios measured by XPS, 39
  interfacial entanglements diagram, 391
  promotion, 395–7
    chemical diagram of silane coupling agent, 397
    diagram of adhesive joint incorporating primer film, 397
  weak boundary layers, 394
  wettability and surface energy, 390–2
    contact angle diagram formed by drop of liquid on solid surface, 392
    water droplet on uncleaned and cleaned moulded connector module, 392

© Woodhead Publishing Limited, 2013

Adhesion Durability Tester (ADT), 378
adhesive bonding, 29, 32, 33, 41–5
  medical device adhesives benefits, limitations and typical applications, 42
adhesive failure, 454
adhesive forces, 375
adhesives, 454
  bonding strategies for joining medical polymers, 370–402
    adhesion mechanism, 388–94
    adhesion promotion, 395–7
    adhesive types used in medical devices, 397–401
    joint design with adhesive, 371–88
air overpressure (AOP), 92
alloys, 267–8, 309
amalgam, 492
amorphous calcium phosphate (ACP), 495–6, 501
amorphous polymers
  compared with semicrystalline, 306–7
    glass transition temperature and melting temperature, 308
    shear modulus and loss tangent of amorphous polymers, 306
    shear modulus and loss tangent of semicrystalline polymers, 307
AngioSeal, 472
  after implantation, 473
antibacterial adhesives
  bone and tooth repair, 491–507
    future trends, 506–7
arc suppression, 337
arc welding, 31
arcing, 337
Arrhenius equation, 386, 387
Arrhenius relationship, 419
ASTM F746, 75, 188, 196, 199
ASTM F2129, 75, 188, 190, 191, 196, 199
ASTM F1980–02, 386
ASTM G1, 199
ASTM G5, 188, 196, 199
ASTM G16, 198
ASTM G46, 187
ASTM G59, 188, 189
ASTM G61, 188, 196, 199
ASTM G71, 75, 193, 196
ASTM G100, 188
ASTM G102, 187
austenitic stainless-steel alloys, 155–6
autoclaving *see* steam sterilisation
autogenous welding, 213

β-tricalcium phosphate (β-TCP), 497–8, 505
barium sulphate, 500
base material (BM)
  thermal effects, 156–7
    microhardness tests, 157
beam delivery, 353–5
  curtain laser, 354
  laser beam and workpiece manipulation, 353
  moving laser, 353–4
  moving workpiece, 353
  scanning laser, 354–5
  simultaneous welding, 354
behavioural tests, 518–19
  adhesive, 520–5
    micro-tensile bond strength, 523–5
    shear bond strength test, 521–3
  tensile and shear stresses in compressive strength test, 519
bioburden, 83
biocompatibility, 21–3
BioGlue, 453, 478–9
  usage, 479
biological surgical G.R.F, 477–8
biomaterials
  advanced metal–ceramic joining techniques, 407–46
    active brazing, 423–43
    challenges, 409–15
    direct and indirect bonded, 418–23
    future trends, 443–5
    mechanical, 415–17
bioresorption, 463–4
blend polymer, 309
blow hole, 228
  schematic diagram, 229
bond, 454
bond strength, 454
  modelling in dental adhesives, 514–30
    behavioural adhesive tests, 520–5

© Woodhead Publishing Limited, 2013

classification of testing techniques, 518–20
future trends, 529–30
rationale for testing, 516–18
structural adhesive tests, 525–9
bone grafts, 499
bone repair
antibacterial adhesives, 498–506
experimental bone cements, 503–6
materials used for repair, 499–503
bore *see* conical female cavity
brasing, 30, 31, 212
brushite *see* dicalcium phosphate dihydrate
bubble test, 250
buffers, 337–8
burst test, 295
butt joint, 271
butyl, 117

calcium carbonate, 501
calcium phosphate, 495–6
calcium-phosphate cements, 501–3
cantilever resin-bonded bridges
structural integrity tests, 526–9
carbon dioxide lasers, 352
catheters, 362
laser and infrared bonding (welding) technology, 288–91
application for balloon and catheter bonding, 290
cell-adhesion analysis, 433
cell spreading, 16
cellulose acetate butyrate, 116
cellulose acetate propionate, 116
cellulose esters, 116
ceramics, 120–1
chemical vapour deposition (CVD), 418
chemical vapour dry-heat steriliser, 84
chlorhexidine, 497–8, 500
circular projection welding, 212
clamping, 355–6
system for through-transmission laser welding, 355
cleaning, 395–6
Clearfil Protect Bond, 496
Clearweld, 347, 363
cleavage, 373
CO_2 laser, 34–6, 277
cochlear implants, 58
coefficient of thermal expansion (CTE), 418
cohesive failure, 454
cohesive forces, 375
colourants, 269, 307
combustion synthesis (CS), 408
commercial biostable bio-derived sealants, 477–9
BioGlue, 478–9
biological surgical G.R.F (MicroVal), 477–8
tissue adhesives and sealants, 478
commercial resorbable bio-derived sealants, 475–7
fibrin sealants, 475–6
usage, 476
PEG/albumin, 476–7
clinical study of sealant applied over sutures, 477
tissue adhesives and sealants, 475
compatible combinations, 357
conical female cavity, 417
conical male cone, 416
continuous-conveyer process, 305
continuous seam sealing, 365
continuous welding, 305
cooling, 266, 302
copolymers, 267–8
corrosion
current direct measurements, 187–96
data gathering, 196–8
surface-condition sample variables affecting weld-corrosion risk, 198
test specimen considerations, 197
data interpretation, 204–5
future trends, 206–7
instrumentation and equipment, 201–2
electrical test cell components, functions, and requirements, 203
electrical three-electrode corrosion test cell, 202
measurements, 183–7
environmental variables affecting weld-corrosion risk and implant conditions, 185

© Woodhead Publishing Limited, 2013

corrosion (*cont.*)
immersion tests, 184
mitigations, 205–6
weld-corrosion prevention strategies and considerations, 205
overview, 178–83
assessment goals, 183
medical device welds, 181–3
sample on a single metal piece, 180
types, 179–81
performance evaluation of metal medical device welds, 178–207
test sample preparation, 198–201
standardised test electrode and holder, 200
corrosion current
direct measurements, 187–96
EIS equivalent circuits, 195
galvanic corrosion test cell configuration, 193
impedance data sample, 195
polarisation resistance plot, 190
polarisation scan for a 304SST sample, 189
polarisation scans to predict the risk and rate of galvanic corrosion, 192
Tafel plot, 191
variables and effects of galvanic corrosion, 192
corrosion resistance
welding effect, 158–9
welded joints between feed through terminals and lead connector, 159
Corsodyl, 497
CoSeal Surgical Sealant, 471
cracking, 229–30
schematic diagram, 230
crossed-wire joint, 159–60
joint-quality characterisation, 159–60
common methods for measuring joint breaking force, 162
previous crossed-wire microwelding studies, 161
RMW and LMW of 316 LVM, 160
'crunch the crown' experiment, 519
cutting, 70–1
cyanoacrylates, 479–80
tissue adhesives and sealants, 480

defibrillators, 59–64
resistance weld between Ti and MP35N wire, 63
weld between Ti and MP35N, 63
welds and mechanical joints in a bradycardia or pacing lead, 62
welds and mechanical joints in a high-voltage tachycardia, 61
degating, 320
degradation rate, 458
dental adhesives
classification of testing techniques, 518–20
behavioural tests, 518–19
structural integrity tests, 519–20
modelling bond strength, 514–30
behavioural adhesive tests, 520–5
product life cycle in evidence-based medicine, 515
product life cycle of a dental material, 515
rationale for testing, 516–18
dental composites, 492–3
dentine, 522–3
design for manufacturing and assembly (DFM/DFA), 269, 313
dicalcium phosphate anhydrous (DCPA), 501
dicalcium phosphate (DCP), 496, 501
dicalcium phosphate dihydrate (DCPD), 498, 501
die design, 333–6
non-planar and three dimensional complex, 334–5
die set design with two potential switching circuits, Plate VI
seal sample contains both flat seal and ring seal, 335
tear seal, 335–6
dielectric (RF) welding, 283
dielectric sealing, 327–8
diffusion brasing (DFB), 39
diffusion welding (DFW), 39
diode lasers, 277, 351

© Woodhead Publishing Limited, 2013

mounted on robot arm, 352
dipole polarisation, 324, 325–6
direct bonding techniques, 418–21
plot of diffusion bond strength vs CTE for various alumina combinations, 420
solid-phase bonding stage illustration of metals to ceramic, 419
double pulse resistance microwelding, 165–7
Pt-10% Ir to 316 LVM SS crossed-wire joints, 168
welding schedule, 167
down speed, 304
drawn-filled-tube (DFT), 56
drilling, 70–1
dry-heat sterilisation, 81–4, 118
commercial dry-heat steriliser, 84
microbial inactivation kinetics-death value, 83
schematic diagram, 82
dumbbell specimen design, 523
DuraSeal Dural Sealant System, 465–7
application to an incision, 467
schematic diagram, 468
dynamic mechanical analysis (DMA), 383
dynamic recrystallisation, 149

e-beam, 90
radiation sterilisation, 287
elastic modulus, 384
electrochemical impedance spectroscopy (EIS), 188, 194, 196
electron-beam welding (EBW), 212, 408, 445
electronic enclosures
hermetic sealing, 68–70
laser seam weld in a thin-walled titanium enclosure, 71
laser welding application showing surface tension effects, 70
overlap condition requirement to achieve full hermetic weld, 69
joint designs, 244–9
304 SS plate with partial penetration welds with helium–argon cover gas, 249
304 SS plate with partial penetration welds without cover gas, 249
overlap pulse requirement and penetration, 246
poor hermetic seam due to poor joint fit-up, 247
schematic diagram, 245
well-formed and polished hermetic seam, 248
electronic polarisation, 324
electrostatic bonding, 420–1
enclosure stress state, 257
energy director, 281, 283
Energy Dispersion Spectrum (EDS), 437
entanglement, 390
epoxy, 116
epoxy adhesives, 399
etchant, 494
ethylene oxide, 96–100
sterilisation, 84–6, 118, 287
prehumidification ethylene oxide (EO) sterilisation cycle, 86
schematic diagram, 85
ethylene propylene diene monomer (EPDM), 117
Euro-cone, 416
excimer lasers, 35
Exoseal, 472
PLGA plug for vascular closure, 473
external heating, 263, 271–9
extrusion welding, 279
heat sealing/welding (impulse sealer), 272–3
impulse heat sealing process, 273
hot-gas welding, 278
schematic diagram, 279
hot-plate welding, 272
infrared welding, 273–7
extracellular matrix (ECM), 17
extrusion welding, 279

fatigue test, 432
Fenton's reaction, 460–1
fibre lasers, 35, 351–2

© Woodhead Publishing Limited, 2013

fibrin sealants, 475–6
filler materials, 308
filters, 268
finite element analysis (FEA), 526–7
finite element method (FEM), 309
fluoropolymers, 288
fluorinated polymers, 115
FocalSeal L, 460, 467–9
  usage, 468
FocalSeal S, 469
focused laser beams, 222–5
  power density distribution of a high power Nd:YAG laser, 224
  schematic diagram, 223
  transverse electromagnetic mode of laser beam, 224
fracture toughness, 528
Fresnel absorption, 215
friction-stir welding (FSW), 37–8
friction welding, 36–8
  friction-stir welding, 37
  schematic diagram, 37
frictional heating, 280
functional graded material (FGM), 408, 444
fusion welding, 30

gamma irradiation, 90
gamma radiation sterilisation, 287
gas flow, 243
gas shielding, 33–4
gel time, 457–8
gelatin-resorcinol-formaldehyde-glutaraldehyde (GRFG), 477–8
gelatin resorcinol formaldehyde (GRF), 453
gentamicin, 500, 502
glass, 120–1
glass ionomer cements (GICs), 493
globular protein, 15
Gluetiss, 478
Gomori's method, 433
grade, 309
guided tissue-regeneration membrane, 499–500

Hagen–Ruben relation, 216–17
heat-affected zone (HAZ), 157
heat sealing/welding, 272–3
heat sterilisation, 80
  effect polymers, 100–5
heat welding, 123–4
heating, 324–7
  dipole polarisation, 325–6
    molecules exposed to the alternating electric field, 325
    overall schematic of RF sealing process, 325
  effects of frequency and temperature, 327
    dielectric properties at different temperature and 30MHz frequency, 327
  joint surface, 300–1
helium, 232
helium mass spectrometer, 232, 251–2
hermetic seal
  electronic enclosures, 68–70
    laser seam weld in a thin-walled titanium enclosure, 71
    laser welding application showing surface tension effects, 70
    overlap condition requirement to achieve full hermetic weld, 69
  leak rate determination based on helium content, 252–7
  leak rate measurement, 249–52
  physics of leak rate, 237–49
  validation in welded metallic implantable medical devices, 236–57
horn design, 309–12
  amplitude of vibration changes along the stack, 310
  near-field and far-field ultrasonic welding, 312
  resonant length and amplitude relationship (amplitude gain), 311
  vibration mechanism of an ultrasonic-welding system, 311
  vibration mode for larger horn, Plate V
hot-bar welding, 40–1
hot-gas welding, 278
hot-plate welding, 40–1, 272
Howell–Mann rate calculations, 254–5

© Woodhead Publishing Limited, 2013

calculation of helium leak rate based on air leak rate, 255
change in scaled helium leak rate *vs.* helium content, 256
hydrogen peroxide, 94–6
sterilisation, 86–8, 119
effect on polymers, 105, 107–8
schematic diagram, 87
hydrophobic recovery, 393–4
hydroxyl ethyl methacrylate (HEMA), 494
Hytrel, 365

image-analysis system, 433
immersion test, 184
immunohistochemistry, 433
implant heating, 263
implant welding, 283–7
induction-implant welding, 284–5
IR/laser-implant welding, 286
microwave-implant welding, 285–6
resistive-implant welding, 285
implantable medical devices
hermetic seal validation in welded metallic, 236–57
leak rate determination based on helium content, 252–7
leak rate measurement, 249–52
physics of leak rate, 237–49
laser hermetic welding, 211–35
focused laser beams, 222–5
future trends, 233–5
hermetic-sealing technique, 212–14
laser conduction welding, 214–22
parameters, 225–8
requirements, 228–33
impulse sealer welding, 272–3
in vitro testing, 432–5
adhering cells on sample brazed with filler metal, 434
filler metals ranking, 435
indirect bonding techniques, 421–3
liquid-phase bonding stages to metals and ceramics, 422
induction-implant welding, 284–5
schematic diagram, 284
induction welding, 40
inductively coupled plasma–atomic emission spectroscopy (ICP–AES), 187
inductively coupled plasma–mass spectroscopy (ICP–MS), 187
industrial processing, 435–9
inflatable devices, 365
prototype neck brace undergoing testing, 366
infrared welding, 273–7
IR heating absorption efficiency of polyethylene with carbon black levels, 276
IR lamp near infrared wavelength transmission of transparent polymers, 275
non-contact, 274
single and modified multiple focusable IR spot lamps, Plate III
through-transmission infrared welding of plastics, 276
typical wavelength distribution for quartz halogen IR lamp, 274
injectable degradable composites, 505–6
injectable degradable polymers, 503
insertion, 318–19
interfacial free energy, 9
interfacial surface tension, 8
intermetallic compound (IMC), 140–1, 142, 157–8
intermolecular diffusion, 266, 302
intermolecular forces, 389
internal heating, 263, 279–83
dielectric (RF) welding, 283
spin welding, 280
ultrasonic welding, 281–3
schematic diagram, 282
vibration welding, 280–1
Invibio®, 366
ionic polarisation, 324
ionisation, 6
ionising radiation, 88
IR/laser-implant welding, 286

joining methods
adhesive bonding, 41–3
applications samples, 43–5

© Woodhead Publishing Limited, 2013

joining methods (*cont.*)
laser welding in intraocular lenses, 43
laser welding of surgical parts, 44
laser welding of dissimilar joints in knee prostheses, 45
laser welding of endoscopes, 44
medical applications, 28–45
overview, 28–33
welding process classification, 30
platinum alloy and stainless steel wires for electronic medical devices, 154–74
crossed-wire joint, 159–60
future trends, 174
material joining challenges, 156–9
material properties, 155–6
material properties (annealed condition), 155
processes, 162–73
welding processes, 33–41
joint breaking force (JBF), 145
joint design, 314–17, 359
accelerated testing of adhesive joints, 386–8
load generated for joint testing, 388
adhesive, 371–88
loading conditions for adhesive joint, 372
adhesive joint failure, 374
considerations, 314–15
designs suitable for transmission laser welding, 359
energy director, 315–16
cross-section of joint interface from an energy director joint design, 316
tongue and groove joint design, 315
general guideline on dimension and tolerance, 314
measuring work of adhesion (G_0), 375–82
acetoxy cured silicone medical adhesive, 376
adhesive bond loaded at 45° peel load, 379
ADT test measures the crack growth rate over time, 379
cohesive and adhesive failure sample, 382
configuration for flexible medical adhesive bonded to rigid substrate, 378
failure force as failure rate function for two epoxy system, 381
testing of adhesive bond between stiff epoxy and titanium disc, 380
shear (interference), 316
cross section of joint interface, 317
typical design, 317
textured surface, 316–17
viscoelasticity of polymers and adhesives, 382–5
stress-strain curve for polymeric adhesive, 383
thermo mechanical spectra of two crosslinked epoxy systems, 385
Young's and elastic modulus, 384
joint testing, 294–5

Kapton film, 273
knee prosthesis, 439–43
longitudinal section across brazed joint, 442
semi-finished metal-ceramic knee prostheses, 443
transverse section across brazed joint, 441
Knudsen number, 241

lap joint, 271
laser-beam welding (LBW), 33, 408, 444–5
laser conduction welding, 214–22
focused laser beam impinges on a metallic surface, 215
laser energy, 225
absorption, 215–18
absorptivity of laser beam at room and melting temperature, 217
laser welds by conduction and keyhole welding, 216
laser hermetic welding
focused laser beams, 222–5

© Woodhead Publishing Limited, 2013

future trends, 233–5
hermetic-sealing technique, 212–14
hermetically welded pacemaker, 214
implantable medical devices, 211–35
laser conduction welding, 214–22
parameters, 225–8
laser pulse, 226
overlap of pulse laser seam weld, 227
seam weld joint cross-section, 227
requirements, 228–33
Butt joint design, 231
temperature cycle, 232
laser melting, 218–22
semi-infinite substrate under laser irradiation, 219
times to melt and vaporise under Nd:YAG laser irradiation, 222
laser micro-welding (LMW), 138–44, 168–74
bonding mechanism, 170–2
crossed-wire NITi, 170
overwelded LMW Pt-10% Ir to 316 LVM SS crossed-wire joints, 173
effects on mechanical performance, 138–40
deformation, 141
multiple plateaus in processed samples, 140
tensile curves for varying peak power input, 139
effects on NiTi microstructure and phase transformation, 140–4
base and re-solidified material cross section, 142
DSC scans for base and CO_2 laser-welded metal, 144
DSC scans for base and Nd:YAG laser-welded metal, 144
EDS line scan across weld region, 142
fusion zone microstructure at the top of weld-fusion zone, 143
fixtures for crossed-wire welding, 169
joint breaking force, 171
Pt-10% Ir to 316 LVM SS crossed-wire joints, 172
pulsed profile, 171
wire orientation, 172–4
cross-section of Pt-10% Ir to 316 LVM SS crossed-wire LMW joint, 173
laser-seam welding, 69–70
laser welding, 33–6, 122–3, 247, 277–8, 350–6
beam delivery, 353–5
clamping, 355–6
laser types, 350–3
carbon dioxide, 352
diode, 351
fibre, 351–2
2.0μm wavelength lasers, 352–3
Nd:YAG, 351
welding plastics usage, 351
process configurations, 278
schematic diagram, 34
leak path, 240–44
air conductance *vs.* tube diameter, 244
dimensionless Reynolds and Knudsen number, 241
leak rate
determination based on helium content, 252–7
flow rate detection, 257
package volumes and specification, 252
variable definitions, 253
measurement, 249–52
weight loss, 250–1
physics, 237–49
commonly used desiccants and getters for internal moisture controls, 239
electronic enclosures joint designs, 244–9
internal moisture content *vs.* dew point temperature, 238
suppression capability of various gases, 239
leak test, 232–3, 295
Lewis acid, 6
interaction, 8–9, 14

© Woodhead Publishing Limited, 2013

Lewis base, 6
interaction, 8–9, 14
Lifshitz–van der Waals force, 6, 7, 11
interaction, 8
light curable adhesives, 401
linear continuous conveyer automatic machine, 331–2
Keifel high throughput linear continuous automatic RF welding system, 334
linear viscoelasticity (LVE), 383
liquid-phase indirect bonding techniques, 421

Maxwell-Wagner polarisation, 324
mean-free path, 241–2
mechanical forces, 388–9
mechanical interlock, 454–5
mechanical joining, 29, 415–17
conical female cavity (bore), 417
conical male cone (trunnion), 416
medical devices
adhesive types, 397–401
epoxy dispense pattern on pacemaker titanium shield, 399
RTV silicone dispensed onto device to prevent fluid ingress, 398
corrosion performance evaluation of metal welds, 178–207
current direct measurements, 187–96
data gathering, 196–8
data interpretation, 204–5
future trends, 206–7
instrumentation and equipment, 201–2
measurements, 183–7
mitigations, 205–6
overview, 178–83
test sample preparation, 198–201
microwelding, 47–76
future trends, 76–7
joint design and process selection, 65–73
materials challenges, 49–56
testing and verification, 73–6
medical materials
anatomy of interaction, 10–20
interface between an artificial implant and biological tissue, 19
living cells, 16–18
protein dissolved in biofluid, 16
protein molecule, 13–16
tissues, 18–19
tribology, 19–20
variation of interfacial free energy with separation, 12
biological interactions, 3–24
drug delivery materials, 20–1
future trends, 24
hierarchy of interactions determining biocompatibility, 23
metrology of biocompatibility, 21–3
overview, 3–10
concept system, 4
definition, 4–5
importance of materials used in implanted device, 5
interaction changed due to welding and joining, 10
nature of interaction, 5–7
ontology, 4
surface attributes, 5
surface free energy, 7–10
sterilisation, 79–128
effects on different materials, 96–121
methods, 80–96
overview, 79–80
suitable method selection, 126–7
medical plastics
fundamental processes, 263–7
diffusion process, 266
key parameters, 266–7
modulus vs temperature for amorphous and semicrystalline polymers, 265
squeeze flow model at joint interface, Plate II
thermoplastics vs thermosets, 264
welding of plastics based on heating techniques, 265
radio frequency (RF) and dielectric welding, 323–43
dielectric heating fundamentals, 324–7

© Woodhead Publishing Limited, 2013

key factors affecting sealing process and seal quality, 333–8
RF welding process advantage limitations and future trends, 341–3
sealing process description and process parameters, 327–33
testing approaches for seals and dielectric sealing process, 338–41
weldability, 338
transmission laser welding strategies, 344–68
advantages and limitation, 344–5
applications, 360
equipment forms, 350–6
joint designs, 359
main welding parameters and effects, 349–50
monitoring and quality control, 360
process description, 345–9
weldable materials, 356–9
ultrasonic welding, 296–322
advantages and limitations, 321–2
fundamental processes, 297–302
horn design, 309–12
other specific applications, 318–20
parameters and control, 302–5
part and joint design, 313–17
process optimisation, 317–18
troubleshooting, 320–1
weldability, 306–9
weldability, 267–9
alloys and copolymers, 267–8
moisture, 269
plastics with filters or regrind, 268
special additives and colourants, 269
table for thermoplastics, 268
testing, 269
welding methods, 261–95
external heating processes, 271–9
implant welding processes, 283–7
internal heating processes, 279–83
part and joint design, 269–71
potential impacts from other manufacturing processes, 286–7
special welding applications, 287–95
medical polymers
bonding strategies and adhesives, 370–402
adhesion mechanism, 388–94
adhesion promotion, 395–7
adhesive types used in medical devices, 397–401
joint design with adhesive, 371–88
melt depth, 220
melting time, 221
metal-ceramic joining techniques
biomaterials, 407–46
active brazing, 423–43
direct and indirect bonded, 418–23
mechanical, 415–17
challenges, 409–15
ceramic cup and femoral ball, 412
friction and wear of Al_2O_3-Al_2O_3 hip joint vs metal polyethylene prosthesis, 411
mechanical properties of most popular orthopaedic biomaterials, 410
most common orthopaedic biomaterials with their primary uses, 409
properties of bioceramics vs some metals, 414
relative rates of bioreactivity for ceramic implants materials, 411
time dependence of formation of bone bonding, 412
future trends, 443–5
schematic illustration of FGM joint between a metal and ceramic, 444
metal to glass sealing, 212
metals
sterilisation effects, 118–21
12-methacryloyloxydodecyl-pyridinium bromide (MDPB), 496
methyl methacrylate monomer, 500
micro-plasma welding, 212
micro-resistance spot welding (MRSW), 147–51
micro-tensile bond strength, 523–5
various design, 525
micro-TIG, 212

© Woodhead Publishing Limited, 2013

microelectromechanical systems (MEMS), 360, 362
microfluidic devices, 360, 362
microwave-implant welding, 285–6
  schematic diagram, 286
microwelding
  future trends, 76–7, 151–2
  joint design and process selection, 65–73
  materials challenges, 49–56
    base metal and laser welds fracture surfaces, 55
    base metal and laser welds made with oxygen content in argon shielding gas, 54
    implantable materials, 49
    laser weld between Ti and Pt alloys, 56
    metallic material properties, 52–3
    weldability matrix for metals, 51
    weldability matrix for plastics, 50
  medical components and devices, 47–76
  Nitinol (NiTi), 134–8, 138–51
  shape-memory alloys, 133–52
  testing and verification, 73–6
    test and loading condition effect on measured weld strength, 75
2.0μm wavelength lasers, 352–3
modelling
  bond strength of dental biomaterials, 514–30
    behavioural adhesive tests, 520–5
    bond strength testing rationale, 516–18
    dental adhesive testing techniques classification, 518–20
    future trends, 529–30
    product life cycle in definitions of evidence-based medicine, 515
    product life cycle of dental material, 515
    structural adhesive tests, 525–9
modulus, 458
moisture, 269
monocalcium phosphate (MCP), 501
monocalcium phosphate monohydrate (MCPM), 497–8, 505
Morse taper coupling, 415–16
Mynx vascular closure system (VCS), 471–2
  arteriotomy, 472

nanoleakage, 492
Nd:YAG lasers, 34–6, 351
neodymium yttrium aluminium garnet *see* Nd:YAG lasers
neurostimulators, 59–64
  spinal nerve stimulation implant, Plate I
Nitinol (NiTi), 364
  fundamentals, 134–8
    phase diagram, 135
  microwelding, 138–51
nitrile, 117
non-planar complex die design, 334–5
non-uniform corrosion, 179

Ocular Therapeutix *see* ReSure Ocular Bandage
OcuSeal Liquid Ocular Bandage, 469
  OcuSeal applicator after assembly and ready to apply, 470
olefin polymers, 113–14
optical waveguide lightmode interferometry (OWLI), 22
optical waveguide lightmode spectroscopy (OWLS), 22
orbital-vibration welding, 281
osteomyelitis, 498
overlap rate, 226
ozone, 94–6
  sterilisation, 93–6, 120
    commercial ozone steriliser, 95
    effects on polymers, 110–13
    schematic diagram, 94

pacemakers, 59–64
  manufacturing microjoining processes, 60
  typical implanted cardiac leads, Plate I
part design, 313–14
  near-field vs far-field, 313
  parallel and uniform contact, 313
  resonance effects, 314
    thin-wall welding application, 312
  stress risers, 313

© Woodhead Publishing Limited, 2013

PEEK-OPTIMA, 366
peel, 373
peel testing, 74
PEG, 458–63
  crosslinking reaction of PEG SS end groups with primary amines, 462
  four-armed PEG functionalised with N-hydroxy-succinimidylsuccinate, 460
  four-armed PEG synthesis, 459
  schematic of hydrogel structure, 462
percutaneous transluminal coronary angioplasty (PTCA), 289
periodontitis, 498
phenolics, 116
physical vapour deposition (PVD), 418
pin and strap technology, 376
pinhole, 229
  schematic diagram, 230
plasma-seam welding, 69
plasma welding, 246
plastics, 96–113, 113–18, 263
  different sterilisation modalities effect, 113–18
  ethylene oxide effects, 96–100
    polymers compatible with the ethylene oxide technique, 97–9
  heat sterilisation effect on polymers, 100–5
    polymer compatibility for dry heat and steam sterilisation techniques, 102–5
    polymers and materials compatible with dry-heat sterilisation technique, 106
  hydrogen-peroxide sterilisation effect on polymers, 105, 107–8
    compatibilities of some polymers with hydrogen peroxide, 107
  irradiation effects on polymers, 108–10
    compatibilities of some polymers for irradiation, 110
  ozone sterilisation effects on polymers, 110–13
    compatibility of some polymers for ozone sterilisation technique, 111–12
platinum alloy
  crossed-wire joint, 159–60
  future trends, 174
  joining processes, 162–73
  joining to stainless steel wires for electronic medical devices, 154–74
  material joining challenges, 156–9
    intermetallic formation, 157–8
    material properties effect on joint formation, 156
    thermal effects on based materials, 156–7
    welding effect on corrosion resistance, 158–9
  material properties, 155–6
plunge welding, 305
point of greatest vulnerability (PGV), 204
Poiseuille equation, 243, 244
polarisation test, 188
poly terephthalate copolymer, 116
polyacid-modified composite resins, 493–4
polyacrylic, 117
polyacrylic acid, 502
polyamides, 115
poly(anhydrides), 503–4
polyaryletherketone, 116
polycarbonate, 117
polychlorophrene, 118
polyester, 116
poly(ester) methacrylates, 504–5
polyetheretherketone (PEEK), 116, 365–8
  cross-section of laser weld between carbon-black filled and natural parts, 367
  cross-section of laser weld between two carbon-black filled parts, 367
  transmission laser welding to carbon pigmented moulded material, 366
polyimide, 116
polyketones, 116
polymer bags, 73
polymer enclosures, 73
polymer tube-to-solid pin assembly, 72–3
polymer tube-to-tube assembly, 72

© Woodhead Publishing Limited, 2013

polymers
heat sterilisation effect, 100–5
hydrogen peroxide sterilisation effect, 105, 107–8
irradiation effects, 108–10
ozone sterilisation effects, 110–13
poly(methyl) methacrylate bone cements, 500–1
poly(propylene fumarate) (PPF), 504
polyurethane, 117, 398–9
practical adhesion, 375
pressure, 295
application, 264, 266, 302
pressure sensitive adhesives (PSA), 400
primary forces, 390
primers, 396–7, 495
process control, 303
weld collapse distance, 303
weld energy, 303
weld time, 303
process optimisation, 317–18
ProGEL Surgical Sealant, 476
pseudoelasticity, 136–8
stress–strain curve for pseudoelastic NiTi alloy, 137
pull testing, 74
pulse repetition, 226
pulse width, 226
pumps, 58

radiation sterilisation, 88–90, 119
automatic tote box irradiator, 89
irradiation, 89
radiation welding
fluoropolymers, 288
through-transmission IR principle with black PFA at joint interface, Plate IV
radio frequency (RF)/dielectric welding
heating fundamentals, 324–7
heating mechanisms, 324–7
key factors affecting sealing process and seal quality, 333–8
die temperature, 330
hold time, 330
interdependency of process parameters, 329
power input, 329
power requirement, 328–9
single vs double cycle process, simultaneous vs sequential, 330
weld pressure/collapse distance, 329
weld/seal time, 329
radio frequency (RF) welding of medical plastics, 323–43
testing approaches for seals and dielectric sealing process, 338–41
weldability, 338
RF welding process advantage limitations and future trends, 341–3
future trend, 342–3
RF sealing vs conventional heat sealing, 342
sealing process description and process parameters, 327–33
key process requirements and parameters, 328–31
sealing-process automation, 331–3
radioactive seed implants, 64
radioactive tracer gas, 251
radiofrequency welding (RFW), 40, 124–5
random sequential addition (RSA), 13
regrind plastics, 309
residual gas analysis (RGA), 233
resin adhesives, 494–5
resin modified glass ionomers (RMGICs), 494
resistance microwelding (RMW), 144–51, 162–8
bonding mechanism, 167–8
crossed-wire RMW process, 163
joint breaking force for single pulse RMW, 166
mechanical properties and failure mechanism, 145–7
effects of welding current on joint breaking force and set-down, 145
failure modes with increasing weld current, 147
fracture surfaces of joint welded at different welding currents, 146
micro-resistance spot welding (MRSW) on NiTi microstructure and phase transformation, 147–51

© Woodhead Publishing Limited, 2013

DSC heating and cooling curves of annealed wire, 151
hardness traces along cross-section of welds, 149
joints welded at different welding currents, 148
stages of the bonding mechanism, 150
RMW crossed-wire joints, 165
setdown in crossed-wire joining, 164
resistance-seam welding, 69
resistive-implant welding, 285
schematic diagram, 285
ReSure Ocular Bandage, 469–71
covering a corneal incision one day after cataract surgery, 470
Reynolds number, 241
ring-to-ring assembly, 71–2
roll-processing method, 347
room temperature vulcanised (RTV), 398–9
rotary table process, 305

saturated steam, 90
scan welding
schematic diagram, 320
scanning ion conduction microscopy (SICM), 23
sealants, 454
tissue adhesives for surgical applications, 449–80
application methods, 456–7
bonding mechanism, 454–6
commercial biostable bio-derived sealants and adhesives, 477–9
commercial biostable synthetic sealants and adhesives, 479–80
commercial resorbable bio-derived sealants and adhesives, 475–7
commercial resorbable synthetic sealants and adhesives, 464–74
definitions and general considerations, 454
principles, 450–3
synthetic bioresorbable sealants, 457–64
sealed bags, 365
self-propagating high temperature synthesis (SHS), 408, 444
semi-automatic manual loading machine, 331
RF machine, 332
sensors, 58
Septacin, 504
shape-memory alloys
micro-welding, 133–52
future trends, 151–2
laser welded microisotopes made from Nitinol, 134
Nitinol (NiTi), 134–8, 138–51
shape-memory effect (SME), 136
shear bond strength test, 521–3
FEM of stress distribution, 522
interfacial stress distribution of vertical stresses, 522
shear joint, 271, 283
shear loading, 372–3
silica fillers, 496
silicone adhesives, 398
silicone medical adhesive, 376
Silly Putty, 382
siloxane, 394
small-diameter tubing
longitudinal seam weld, Plate VIII
soldering, 30, 32
solid-phase diffusion welding, 418
solid-phase indirect bonding techniques, 421
solid state bonding process, 418–19
solid state welding, 30, 32, 212
solvent bonding/welding, 291–4
compatible polymers with solvents for bonding, 293
solvent selection for bonding amorphous polymers, 292
solvent welding, 399–400
spin welding, 280
spot welding, 319
stacking, 318
schematic diagram, 319
stainless steel
crossed-wire joint, 159–60
future trends, 174
joining processes, 162–73
joining to platinum alloy wires for electronic medical devices, 154–74
material joining challenges, 156–9

© Woodhead Publishing Limited, 2013

stainless steel (*cont.*)
intermetallic formation, 157–8
material properties effect on joint formation, 156
thermal effects on based materials, 156–7
welding effect on corrosion resistance, 158–9
material properties, 155–6
steam autoclave, 92–3
steam sterilisation, 90–3, 119–20, 287
dynamic evacuation pulsing steam sterilisation cycle, 92
dynamic gravity pulsing sterilisation cycle curve, 92
schematic diagram, 91
steam–air mixtures (SAM), 92
steam–formaldehyde, 93
step joint, 271
sterilisation
effects on different materials, 96–121
different modalities effect on plastics, 113–18
metals, 118–21
plastics, 96–113
effects on medical materials and welded devices, 79–128
effects on welded joints, 121–5
miscellaneous effects, 125
methods, 80–96
overview, 79–80
suitable method selection, 126–7
sterility assurance level (SAL), 127
strength, 458
stress-induced martensite (SIM), 137–8
stress–strain curve, 136–8
pseudoelastic NiTi alloy, 137
structural integrity tests, 519–20
adhesive, 525–9
alternative design for cantilever resin-bonded bridge, 529
cantilever resin-bonded bridges, 526–9
effect of elastic modulus on maximum stress, 527
FEA model of local stress distribution, 527
simple peel test for a cantilever bridge, 526
tensile peel strength and fracture toughness, 528
factors influencing performance of dental materials, 520
stud welding, 319
Stumbo method, 82
styrene polymers, 114
substrate, 454
SuperGlue, 400
surface energy, 390–3
surface free energy, 7–10
medical materials that interact repulsively and attractively with the host, 10
surface tension parameters of some artificial and biological materials, 9
surface roughening, 395
surgery
principles of tissue adhesives and sealants, 450–3
placement over incision to provide apposition, 451
polymerisation of cyanoacrylate, 453
resorbable tissue adhesive maybe placement, 451
tissue adhesives and sealants, 449–80
application methods, 456–7
bonding mechanism, 454–6
commercial biostable bio-derived sealants and adhesives, 477–9
commercial biostable synthetic sealants and adhesives, 479–80
commercial resorbable bio-derived sealants and adhesives, 475–7
commercial resorbable synthetic sealants and adhesives, 464–74
definitions and general considerations, 454
synthetic bioresorbable sealants, 457–64
swaging, 320
swelling, 458
synthetic bioresorbable sealants, 452–3, 457–64
chemical structure of focalSeal L macromonomer, 461
light activated polymerisation of FocalSeal L lung sealant, 461

© Woodhead Publishing Limited, 2013

synthetic hydrogel sealants bioresorption, 463–4
hydrogel sealants swell, soften and weaken after implantation, 464
hydrolysis reaction of PEG succinate linkages, 463
resorption of FocalSeal S rat subcutaneous implants, 465

Tafel extrapolation method, 189–90
tear seal die design, 335–6
bottom flat seal and die seal and attached to aluminium base plate, 336
set of dies with flat and tear seal, 336
Teflon, 288
temperature-induced transformation, 135–6
shape-memory effect (SME) behaviour of Nitinol SMA, 137
volume transformed as a function of temperature, 136
tensile loading, 372
tetracalcium phosphate (TTCP), 501
tetracylcine, 502
textiles, 358–9
protective clothing with seams welded and hence sealed using laser welding, 358
thermal modelling, 347–8
finite element thermal model, Plate VII
thermoplastics, 263
thermosets, 263
three dimensional complex die design, 334–5
through-transmission infrared welding, 72
time of flight secondary ion mass spectrometry (ToF SIMS), 393
Tisseel, 453, 475
tissue adhesives
bonding mechanism, 454–6
stained tissue section showing FocalSeal S sealant, 456
tissue surface, 455
sealants for surgical applications, 449–80
application methods, 456–7
commercial biostable bio-derived sealants and adhesives, 477–9
commercial biostable synthetic sealants and adhesives, 479–80
commercial resorbable bio-derived sealants and adhesives, 475–7
commercial resorbable synthetic sealants and adhesives, 464–74
definitions and general considerations, 454
principles, 450–3
synthetic bioresorbable sealants, 457–64
TissuePatch, 474
tongue and groove joint, 271
tooth repair
antibacterial adhesives, 491–8
experimental dental materials, 495–8
materials used for repair, 492–5
total joint arthroplasty (TJA), 409
transmission laser welding strategies
applications, 360, 362–8
catheters and small-diameter tubing, 362
microfluidic devices and microelectromechanical systems (MEMS), 360, 362
polyetheretherketone (PEEK) film and implants, 365–8
sealed bags and inflatable devices, 365
textiles and vascular graft, 362–5
medical plastics, 344–68
equipment forms, 350–6
joint designs, 359
main welding parameters and effects, 349–50
monitoring and quality control, 360
summary of features of optical monitoring methods, 361
process description, 345–9
advantages and disadvantages, 346
beam manipulation with scanning optics, 348
colour independence, 348–9
diagram showing beam movement over work piece, 347

© Woodhead Publishing Limited, 2013

transmission laser welding strategies (*cont.*)
laser-welded transparent medical devices, 349
modelling, 347–8
weldable materials, 356–9
compatible combinations, 357
textiles, 358–9
transmission properties, 356–7
weld compatibility between different plastics, 357
weldable plastics, 356
transmission properties, 356–7
Transverse Electromagnetic Mode (TEM), 223
travel speed, 226
trigger force, 304
trunnion *see* conical male cone
tube-to-tube assembly, 71–2
tubing, small-diameter, 362
turntables indexing, 331
RF welding systems, 333

ultrasonic bonding, 124
ultrasonic welding (USW), 38–9, 124, 281–3
fundamental processes, 297–302
boosters and horns for 40kHz ultrasonic machine, 299
components of an ultrasonic-welding machine, 298
converter booster and horn assembly for 20kHz ultrasonic machine, 299
heating and welding with energy director at joint interface, 301
main components, 297
storage vs loss modulus, 301
typical bench-top ultrasonic-welding equipment from various venders, 298
welding machine characteristics based on operation frequencies, 300
medical plastics, 296–322
advantages and limitations, 321–2
horn design, 309–12
part and joint design, 313–17
process optimisation, 317–18
weldability, 306–9
other specific applications, 318–20
degating, 320
insertion, 318–19
sewing, slitting, sealing scan welding, 320
spot welding, 319
stacking, 318
stud welding, 319
swaging, 320
parameters and control, 302–5
other process parameters, 303–4
plunge or continuous welding, 305
power requirement, 302
process control, 303
rotary table or continuous-conveyer process, 305
welding process operation, 305
schematic diagram, 39
troubleshooting, 320–1
alignment, 321
material issues, 321
part and joint design, 321
part-dimension consistency, 321
process parameters, 321
uniform corrosion, 179
uniformity, 336–7

vaporising time, 221
vascular devices, 57–8
balloon catheter joined to lumen expanding a laser cut stent, 58
guidewire for catheter applications, 57
laser cut stent, 59
vascular graft textile, 362–5
cross-sectional view of laser weld between polyester fabric and polyester film, 364
schematic illustration of abdominal aortic aneurysm along with Anaconda endovascular device, 363
vibration amplitude, 303–4
vibration welding, 280–1
orbital-vibration, 282
schematic diagram, 281

© Woodhead Publishing Limited, 2013

Vicryl, 453
vinyl polymers, 115
void in weld, 229–30
  schematic diagram, 229
von Kossa staining method, 433

weak boundary layers, 394
Wein's law, 275
weld discolouration, 230–1
weld force, 304
weld pressure, 304
weldability, 267–9, 306–9, 338
  material structure and properties, 306–9
    additives, 307
    amorphous vs semicrystalline, 306–7
    colourants, 307
    filler materials, 308
    grade/alloy/blend, 309
    moisture, 308–9
    regrind, 309
  PVC RF sealing seal cross-section with weld bead, 340
  RF welding weldability for different plastics, 339–40
WeldControl system, 367–8
welded devices
  sterilisation, 79–128
    effects on welded joints, 121–5
    methods, 80–96
    overview, 79–80
    suitable method selection, 126–7
welding, 29, 33–41, 262–3
  adhesive bonding, 262
  fundamental processes of plastics welding, 263–7
    based on heating techniques, 265
    diffusion processes (chain entanglement), 266
    key parameters, 266–7
    modulus vs temperature for amorphous and semicrystalline polymers, 265
    thermoplastics vs thermosets, 264
  mechanical fastening, 262
  medical plastics, 261–95
    external heating processes, 271–9
    implant welding processes, 283–7
    internal heating processes, 279–83
    potential impacts from other manufacturing processes, 286–7
    weldability, 267–9
  part and joint design, 269–71
    typical joint design, 271
  process operation, 305
  special welding applications, 287–95
wettability, 390–3
wire-to-pin assemblies, 66–8
  laser welding of small diameter coil, 68
  resistance spot weld of titanium wire to Ti6Al4V terminal block, 67
wire-to-wire assembly, 65–6
  tip forming of a catheter wire, 66
work of adhesion, 375

X-ray, 90
X-ray diffraction, 429
X-ray photoelectron spectroscopy (XPS), 393
X-ray stress analyser, 429
X-rays analysis, 439–40

YAG laser, 277
Young's modulus, 384

© Woodhead Publishing Limited, 2013